frontiers | Research Topics

Cross-talk and interaction between endocrinology and urology: Challenges and opportunities

Edited by
Xiao-qiang Liu, Yuxuan Song and Caigan Du

Published in
Frontiers in Endocrinology

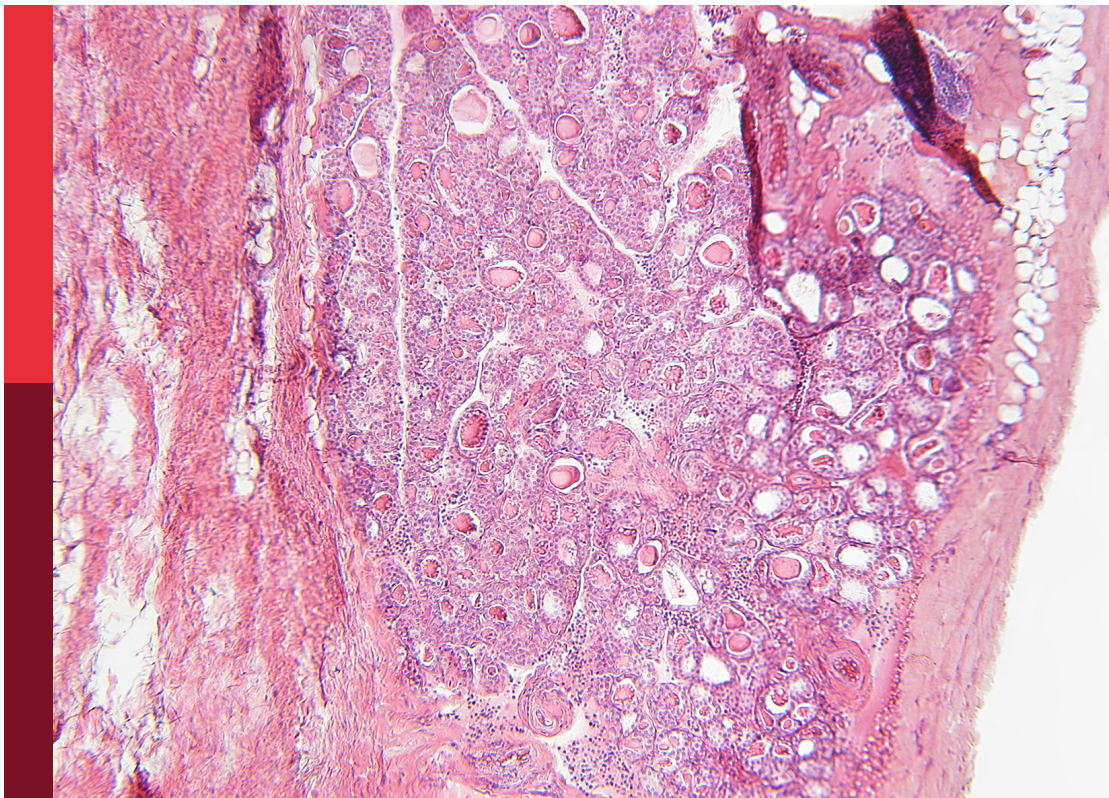

ISSN 1664-8714
ISBN 978-2-8325-3684-1
DOI 10.3389/978-2-8325-3684-1

About Frontiers

Frontiers is more than just an open access publisher of scholarly articles: it is a pioneering approach to the world of academia, radically improving the way scholarly research is managed. The grand vision of Frontiers is a world where all people have an equal opportunity to seek, share and generate knowledge. Frontiers provides immediate and permanent online open access to all its publications, but this alone is not enough to realize our grand goals.

Frontiers journal series

The Frontiers journal series is a multi-tier and interdisciplinary set of open-access, online journals, promising a paradigm shift from the current review, selection and dissemination processes in academic publishing. All Frontiers journals are driven by researchers for researchers; therefore, they constitute a service to the scholarly community. At the same time, the *Frontiers journal series* operates on a revolutionary invention, the tiered publishing system, initially addressing specific communities of scholars, and gradually climbing up to broader public understanding, thus serving the interests of the lay society, too.

Dedication to quality

Each Frontiers article is a landmark of the highest quality, thanks to genuinely collaborative interactions between authors and review editors, who include some of the world's best academicians. Research must be certified by peers before entering a stream of knowledge that may eventually reach the public - and shape society; therefore, Frontiers only applies the most rigorous and unbiased reviews. Frontiers revolutionizes research publishing by freely delivering the most outstanding research, evaluated with no bias from both the academic and social point of view. By applying the most advanced information technologies, Frontiers is catapulting scholarly publishing into a new generation.

What are Frontiers Research Topics?

Frontiers Research Topics are very popular trademarks of the *Frontiers journals series*: they are collections of at least ten articles, all centered on a particular subject. With their unique mix of varied contributions from Original Research to Review Articles, Frontiers Research Topics unify the most influential researchers, the latest key findings and historical advances in a hot research area.

Find out more on how to host your own Frontiers Research Topic or contribute to one as an author by contacting the Frontiers editorial office: frontiersin.org/about/contact

Cross-talk and interaction between endocrinology and urology: Challenges and opportunities

Topic editors

Xiao-qiang Liu — Tianjin Medical University General Hospital, China
Yuxuan Song — Peking University People's Hospital, China
Caigan Du — University of British Columbia, Canada

Citation

Liu, X.-q., Song, Y., Du, C., eds. (2023). *Cross-talk and interaction between endocrinology and urology: Challenges and opportunities*. Lausanne: Frontiers Media SA. doi: 10.3389/978-2-8325-3684-1

Table of contents

frontiers | Frontiers in Endocrinology

TYPE Editorial
PUBLISHED 21 August 2023
DOI 10.3389/fendo.2023.1269484

OPEN ACCESS

EDITED AND REVIEWED BY
Henrik Falhammar,
Karolinska Institutet (KI), Sweden

*CORRESPONDENCE
Yuxuan Song
yuxuan_song2013@163.com

RECEIVED 30 July 2023
ACCEPTED 14 August 2023
PUBLISHED 21 August 2023

CITATION
Song Y, Du C and Liu X (2023) Editorial: Cross-talk and interaction between endocrinology and urology: challenges and opportunities.
Front. Endocrinol. 14:1269484.
doi: 10.3389/fendo.2023.1269484

Editorial: Cross-talk and interaction between endocrinology and urology: challenges and opportunities

Yuxuan Song[1]*, Caigan Du[2] and Xiaoqiang Liu[3]

[1]Department of Urology, Peking University People's Hospital, Beijing, China, [2]Department of Urological Sciences, University of British Columbia, Vancouver, BC, Canada, [3]Department of Urology, Tianjin Medical University General Hospital, Tianjin, China

KEYWORDS

endocrinology, urology, andrology, prostate, adrenal

Editorial on the Research Topic

Cross-talk and interaction between endocrinology and urology: challenges and opportunities

The urinary and reproductive systems are closely interconnected with the endocrine System (1, 2). Some of the urinary and reproductive organs themselves function as endocrine organs. If these organs undergo pathological changes, it can affect the endocrine system (3). Conversely, when the endocrine system experiences metabolic disorders, the urinary system can also be affected (4, 5).

In recent decades, there have been rapid advances in the diagnosis and treatment of endocrine and urological diseases. Therefore, this Research Topic aims to study the endocrine metabolic disorders in patients with urinary and reproductive system diseases and their pathophysiological mechanisms. Through this interaction, we hope to promote cooperation and communication among experts in the fields of urinary and reproductive systems and endocrinology, and to carry out meaningful collaborative research, thereby proposing new ideas for diagnosis and treatment.

Liu et al. investigates the impact of steroid hormones on retinal neurodegenerative diseases (RND) using genetic variations as instrumental variables. Glaucoma risk was found to be influenced by testosterone/17β-estradiol (T/E2) (OR = 1.11, 95% CI, 1.01–1.22, P = 0.03), which was validated by multiple methods. However, no impact of other steroid hormones (aldosterone, androstenedione, progesterone, and 17-hydroxyprogesterone) was observed on diabetic retinopathy (DR) and age-related macular degeneration (AMD) risk. The study suggests that T/E2 may have a suggestive effect on glaucoma risk, but further research is needed to explore steroid hormones as targets for prevention and treatment.

An et al. investigates the relevance of metabolic syndrome (MetS) and metabolic scores to metastatic prostate cancer (PCa) occurrence, progression, and prognosis. Patients with MetS had higher T stage, Gleason score, and tumor load, with shorter time to progression to castration-resistant PCa stage. The median survival time was significantly shorter in the MetS group. Metabolic score correlated with survival time. The study concludes that MetS may promote metastatic PCa progression and affect prognosis, suggesting its role as a risk factor in metastatic PCa outcomes.

Li et al. evaluates the outcome and safety of retroperitoneal laparoscopic partial adrenalectomy in treating nonfunctional unilateral adrenal tumors in the day surgery mode. The surgery was performed on 19 patients, and the results showed that retroperitoneal laparoscopic partial adrenalectomy is safe when strict selection criteria and perioperative management are followed. The procedure potentially shortens the hospital stay and reduces hospitalization costs.

Patients with PCa develop resistance to vinblastine, and Chen et al. aims to explore the genetic alterations underlying this resistance. The study identified CCNB1 and AURKA as critical genes for PCa progression and castration-resistant PCa resistant to vinblastine. The findings provide insights into the mechanisms of resistance and potential therapeutic targets for patients with PCa.

Zhou et al. explores the relationship between C-reactive protein (CRP) levels and PCa prognosis. Elevated CRP levels were associated with worse overall survival, cancer-specific survival, and progression-free survival in prostate cancer patients. The study suggests that CRP levels could serve as a prognostic marker for PCa outcomes, though further validation is needed.

Li et al. compares the efficacy and safety of conservative treatment and surgery for patients with small nonfunctional adrenal incidentalomas. The results indicate that surgical treatment is more effective for 1-3cm nonfunctional adrenal incidentaloma, but conservative treatment is safer and more economical. Follow-up after both treatments is essential.

Li et al. compares tumor control in patients with PCa with oligometastasis following combined robot-assisted radical prostatectomy and androgen deprivation with androgen deprivation therapy alone using PSA percentage decline rate. The study concludes that both treatments provide effective tumor control, with combined therapy showing a significant advantage in PSA percentage decline rate without compromising urinary continence.

Li et al. identifies hub genes related to bicalutamide resistance in prostate cancer and constructs a prognostic model for patient prognosis. Genetic alterations associated with resistance to bicalutamide are explored, providing potential targets for endocrine therapy resistance in prostate cancer patients.

You et al. investigates the efficacy and safety of bipolar androgen therapy in patients with castration-resistant PCa following resistance to abiraterone or enzalutamide. The review finds that bipolar androgen therapy is safe and effective, resensitizing patients to subsequent endocrine therapy and potentially improving overall survival and quality of life.

Wang et al. discusses surgical management strategies for complicated pheochromocytomas/paragangliomas based on case reports. The goal is to provide insights into the safe and effective surgical management of these tumors.

Yan et al. investigates whether intravenous volume expansion is necessary after preoperative α-blocker administration for adrenal pheochromocytoma. Analysis indicates that abandonment of intravenous volume expansion is not an independent risk factor for intraoperative hemodynamic instability. Tumor size is identified as an independent risk factor.

Liao et al. reports a rare case of adult bilateral pure androgen-secreting adrenal tumors (PASATs) and conducts a systematic review on adult PASATs. Characteristics of PASATs are summarized, including patient demographics, symptoms, androgen levels, tumor size, and malignancy features.

Li et al. compares the advantages and disadvantages of robot-assisted laparoscopic adrenalectomy with retroperitoneal laparoscopic adrenalectomy. robot-assisted laparoscopic adrenalectomy is found to reduce intraoperative blood loss and accelerate postoperative gastrointestinal recovery but has longer operation time, higher hospitalization expense, and different pathological types compared to retroperitoneal laparoscopic adrenalectomy.

Ren et al. aimed to develop a metabolic syndrome-related prognostic index (MSRPI) to predict biochemical recurrence-free survival (BFS) in patients with PCa and identify cold and hot tumors for personalized treatment. The researchers analyzed data from the Cancer Genome Atlas and Gene Expression Omnibus databases to identify prognostic metabolic syndrome-related genes and potential tumor subtypes. Using the LASSO algorithm and multivariate Cox regression, they constructed the MSRPI based on seven metabolic syndrome-related genes. The high-risk MSRPI was associated with poor BFS, validated internally and externally. The MSRPI also helped differentiate between cold and hot tumors, providing potential for precision therapy in patients with PCa.

Enzalutamide, a second-generation endocrine therapy drug for PCa, was analyzed to identify an enzalutamide-induced signature (ENZ-sig) for predicting progression and relapse-free survival in PCa by Feng et al. Candidate markers were derived from single-cell RNA sequencing analysis, and a 10-gene prognostic model (ENZ-sig) was constructed based on these markers. ENZ-sig was validated in multiple datasets, demonstrating its robust predictability. Biological enrichment analysis revealed that high ENZ-sig patients were more sensitive to cell cycle-targeted drugs, suggesting potential combination therapy strategies for PCa.

Gao et al. aimed to differentiate between adrenal Cushing syndrome (adrenal CS) and Cushing disease (CD) using serum steroid profiles. Liquid chromatography with tandem mass spectrometry was used to analyze 11 serum steroids in patients with adrenal CS or CD. The results showed distinct serum steroid profiles between adrenal CS and CD, with dehydroepiandrosterone sulfate, dehydroepiandrosterone, and androstenedione ratios identified as biomarkers for discrimination. The study highlights the diagnostic value of serum steroid profiles in distinguishing between adrenal CS and CD.

Du et al. aimed to explore how sex hormones affect the association between 25-hydroxyvitamin D [25(OH)D] and osteoporosis using a two-step Mendelian randomization (MR) analysis. The results showed that 25(OH)D and total testosterone (TT) had a causal effect on osteoporosis, while other sex hormones (A4, E2, and T/E2) did not show significant associations. The study provides evidence that TT mediates the causal effect of 25(OH)D on osteoporosis, suggesting that interventions targeting TT could reduce the burden of osteoporosis related to high 25(OH)D.

Huang et al. used MR analysis to explore the causal genetic association between thyroid function and benign prostatic diseases (BPDs). Genetic variations in thyroid function and BPDs were analyzed, and the results showed that TSH, subclinical hypothyroidism, and overt hypothyroidism had a significant effect

on genetic susceptibility to benign prostate hyperplasia and prostatitis. However, hyperthyroidism and FT4 levels did not show significant effects. The study sheds light on the potential causal relationship between thyroid function and BPDs.

Liu et al. discusses the potential role of aldosterone, a mineralocorticoid hormone, in the pathogenesis of diabetic retinopathy (DR). Aldosterone may influence DR through its effects on oxidative stress, vascular regulation, and inflammatory mechanisms. The article highlights the value of aldosterone as a potential diagnostic and treatment target for DR, though further research is needed to fully understand the association between mineralocorticoids and DR.

Zhang et al. discusses the use of PARP inhibitors in PCa treatment. PARP inhibitors have shown promising results in patients with BRCA mutations. The article explores the potential of extending the use of PARP inhibitors to other populations, such as those with "BRCAness" tumors. Additionally, the interaction between androgen receptor signaling and PARP inhibitors is explored, providing insights into potential combination therapies for PCa.

Qin et al. investigated the impact of androgen deprivation therapy (ADT) on the tumor immune microenvironment in PCa. The analysis of single-cell transcriptomes from PCa tumors before and after ADT revealed a weakened killing effect of immune cells on tumors and reduced interaction between immune cells and tumor cells. The study also observed an increase in immunosuppressive cells (MDSC and Treg) after ADT. These findings suggest that ADT induces an immunosuppressive environment in the PCa tumor microenvironment, providing implications for combining ADT with immunotherapy.

Gao et al. aimed to establish and validate the cut-off values of estimated glomerular filtration rate (eGFR) and urinary albumin-to-creatinine ratio (UACR) for diabetic kidney disease (DKD). The study involved 374 patients with type 2 diabetes with baseline eGFR ≥60 mL/min/1.73 m2 and UACR <30 mg/g. The results showed that eGFR ≤84.8 mL/min/1.73 m2 or UACR ≥15.5 mg/g in the normal range may be effective cut-off values for predicting DKD.

Zhou et al. proposed a standardized scoring system, the ADRENAL score, to quantify the functional and anatomical characteristics of adrenal tumors. The score was based on six parameters, including functional status, tumor size, relationship to adjacent organs, intratumoral enhancement on CT, nearness to major vessels, and body mass index. The ADRENAL score was found to be a valid predictor of surgical outcomes in adrenal surgery, providing a common reference for preoperative risk assessment and comparative analysis of different surgical techniques and approaches.

Author contributions

YS: Conceptualization, Writing – original draft, Writing – review & editing. CD: Writing – original draft. XL: Conceptualization, Writing – original draft, Writing – review & editing.

Conflict of interest

The authors declare that the research was conducted in the absence of any commercial or financial relationships that could be construed as a potential conflict of interest.

Publisher's note

References

1. Grollman A. Modern endocrinology in urologic practice. *J Urol* (1948) 60(2):357–62. doi: 10.1016/S0022-5347(17)69245-0

2. Steiner MM. Modern concepts of urologic endocrinology. *J Urol* (1959) 81(1):1–12. doi: 10.1016/S0022-5347(17)65959-7

3. Liang G, Song Y, Liu L, Zhou K, Tian J, Li J, et al. Association of hypogonadism symptoms and serum hormones in aging males. *Andrologia* (2021) 53(5):e14013. doi: 10.1111/and.14013

4. Liang G, Song Y, Wang X, Li J, Shi H, Zhu Q, et al. Serum sex hormone-binding globulin is associated with symptomatic late-onset hypogonadism in aging rural males: a community-based study. *Sex Health* (2021) 18(2):156–61. doi: 10.1071/SH20201

5. Song Y, Qin C, Zhang C, Peng Y, Yang W, Du Y, et al. Gnrh family genes contributed to gender-specific disparity of bladder cancer prognosis through exerting opposite regulatory roles between males and females. *J Cancer Res Clin* (2023) 149 (10):6827–40. doi: 10.1007/s00432-023-04640-2

frontiers | Frontiers in Endocrinology

TYPE Original Research
PUBLISHED 24 November 2022
DOI 10.3389/fendo.2022.1073082

OPEN ACCESS

EDITED BY
Yuxuan Song,
Peking University People's Hospital, China

REVIEWED BY
Zhen Liang,
Peking Union Medical College Hospital (CAMS), China
Shangren Wang,
Tianjin Medical University, China

*CORRESPONDENCE
Gongxian Wang
wanggx-mr@126.com
Daniel Eun
Daniel.Eun@tuhs.temple.edu
Yaoliang Deng
dylkf317@163.com

†These authors have contributed equally to this work

SPECIALTY SECTION
This article was submitted to Adrenal Endocrinology, a section of the journal Frontiers in Endocrinology

RECEIVED 18 October 2022
ACCEPTED 09 November 2022
PUBLISHED 24 November 2022

CITATION
Zhou X, Li X, Fu B, Liu W, Zhang C, Xia Y, Gong H, Zhu L, Lei E, Kaplan J, Deng Y, Eun D and Wang G (2022) The ADRENAL score: A comprehensive scoring system for standardized evaluation of adrenal tumor. *Front. Endocrinol.* 13:1073082. doi: 10.3389/fendo.2022.1073082

The ADRENAL score: A comprehensive scoring system for standardized evaluation of adrenal tumor

Xiaochen Zhou[1†], Xuwen Li[1†], Bin Fu[1†], Weipeng Liu[1], Cheng Zhang[1], Yu Xia[1], Honghan Gong[2], Lingyan Zhu[3], Enjun Lei[4], Joshua Kaplan[5], Yaoliang Deng[6*], Daniel Eun[5*] and Gongxian Wang[1*]

[1]Department of Urology, The First Affiliated Hospital of Nanchang University, Nanchang, Jiangxi, China, [2]Department of Radiology, The First Affiliated Hospital of Nanchang University, Nanchang, Jiangxi, China, [3]Department of Endocrinology, The First Affiliated Hospital of Nanchang University, Nanchang, Jiangxi, China, [4]Department of Anesthesiology, The First Affiliated Hospital of Nanchang University, Nanchang, Jiangxi, China, [5]Department of Urology, Temple University Hospital, Philadelphia, PA, United States, [6]Department of Urology, The First Affiliated Hospital of Guangxi Medical University, Nanning, Guangxi, China

Objectives: To propose an original and standardized scoring system to quantify the functional and anatomical characteristics of adrenal tumor.

Materials and methods: Four groups of consecutive adrenalectomies (n = 458) with heterogeneity in tumor characteristics and surgical approaches, including 212 laparoscopic cases (Group 1) and 105 robotic cases (Group 2) from The First Affiliated Hospital of Nanchang University, 28 robotic cases from Temple University Hospital (Group 3) and 113 laparoscopic cases from The First Affiliated Hospital of Guangxi Medical University (Group 4). All patients were followed up for 4.5 to 5.5 years. Six parameters including functional status or suspicion of malignancy, tumor size, relationship to adjacent organs, intratumoral enhancement on CT, nearness of the tumor to major vessels and body mass index were assessed and scored on a 0, 1 and 2 points scale. Correlation between the sum of the 6 scores and tumor laterality (ADRENAL score) verse operative time (OT), estimated blood loss (EBL), perioperative complications, transfusion, conversion and length of hospital stay was analyzed.

Results: ADRENAL score was a strong predictor of both OT and EBL in all four groups ($p < 0.05$ for all tests). In Group 2 and 4, higher ADRENAL score seemed to correlate with longer hospital stay. No statistically significant correlation between ADRENAL score and complication, transfusion or conversion was noted yet.

Conclusions: ADRENAL score appears to be a valid predictor of surgical outcomes. It may provide a common reference for adrenal surgery training program, preoperative risk assessment and stratified comparative analysis of adrenal surgeries *via* different techniques and approaches.

KEYWORDS

adrenal tumor, treatment, surgical risks, scoring system, the ADRENAL score

Introduction

The overall frequency of adrenal tumors is as high as 8.7% on autopsy (1) with adrenal incidentaloma being reported in 4% of patients receiving abdominal CT scans (2, 3). While small non-functioning incidentaloma (< 4 cm) with benign appearance can be managed by active surveillance, adrenal lesions that require surgical resection still spans a large spectrum of benign and malignant indications (4). Since the initial report of laparoscopic transperitoneal (5) and retroperitoneal adrenalectomy (6), minimally invasive surgery has been popularized and become the standard of care for benign adrenal lesions (7). With the increase in experience and introduction of da Vinci robotic system (8), even large (up to 8 cm) (9) or organ-confined malignant adrenal tumor can be safely removed *via* minimally invasive technique with comparable outcomes (10).

The functional status and diversity in size and pathology make the adrenal surgery a unique challenge for both urologists and anesthesiologists. The functional status (11), pheochromocytoma (12) and malignancy (13), tumor size (14) and body mass index (BMI) (15) are documented risk factors for adrenal surgery. However, the characterization of these factors is currently descriptive and lacks standardization and integration. Beyond these established risk factors, other anatomical features of the adrenal tumor are routinely considered in surgical planning. In particular, the relationship between the tumor and adjacent organs or major vessels may greatly affect the resectability of the lesion and contribute to surgical risks. A comprehensive scoring system integrating these established risk factors and anatomical features may help in evaluating the difficulty of surgery and assessing intraoperative risks. It may also provide a common reference for training programs and stratified analysis of adrenal surgeries *via* different techniques and approaches.

The objectives of this study were (a) to propose a standardized and original scoring system of adrenal tumors (designated as the ADRENAL Score) for preoperative assessment based on routinely performed endocrinological, oncological and radiological studies; (b) and to evaluate the correlation between the ADRENAL Score verse surgical outcomes and complications.

Materials and methods

Patients and tumors

Four groups of patients (n = 458) treated with minimally invasive adrenalectomy were evaluated retrospectively or prospectively. Data of Group 1 consisting of 212 consecutive laparoscopic retroperitoneal adrenalectomy cases performed by Dr.Wang's team from January 2010 to December 2014 was retrospectively evaluated. Data of group 2 consisting of 105 consecutive robotic retroperitoneal adrenalectomy cases performed by the same surgical team from February 2015 to June 2016 were prospectively collected and evaluated. Group 3 consisting of 28 consecutive cases of robotic transperitoneal adrenalectomy cases performed by Dr.Eun's team from January 2014 to April 2016 and Group 4 consisting of 113 laparoscopic retroperitoneal adrenalectomy cases performed by Dr.Deng's team from January 2014 to December 2016 was retrospectively evaluated. All patients were followed up for 4.5 to 5.5 years. Patient demographics in each group were listed in Table 1. In summary, 74 (34.91%), 46 (43.81%), 16 (57.14%) and 47 (41.59%) patients were male in Group 1 to 4, respectively. The average age was 47.13 ± 13.03, 48.01 ± 12.20, 60.79 ± 10.64 and 45.50 ± 12.64 yr, respectively. The average body mass index

TABLE 1 Patient demographics.

Group (n)		Group 1 (212)	Group 2 (105)	Group 3 (28)	Group 4 (113)
Demographics	Male, n (%)	74 (34.91%)	46 (43.81%)	16 (57.14%)	47 (41.59%)
	Age, yr	47.13±13.03	48.01±12.20	60.79±10.64	45.50±12.64
	BMI, kg/m^2	22.90±3.40	23.67±3.66	28.42±6.93	23.33±4.08

Group 1: laparoscopic retroperitoneal adrenalectomy; Group 2: robotic retroperitoneal adrenalectomy; Group 3: robotic transperitoneal adrenalectomy; Group 4: laparoscopic retroperitoneal adrenalectomy. BMI, body mass index. Values expressed as mean ± SD.

(BMI) was 22.90 ± 3.40, 23.67 ± 3.66, 28.42 ± 6.93 and 23.33 ± 4.08, respectively.

Preoperatively, all patients underwent routine laboratory test for differential diagnosis of adrenal lesions including but not limited to blood potassium, aldosteronism test, urine and plasma cortisol, plasma catecholamines and urine vanillylmandelic acid. The presence and anatomical characteristics of adrenal masses were confirmed by non-contrast- and contrast-enhanced computed tomography (CT).

ADRENAL score

The ADRENAL score consists of 7 components that describe critical endocrinological, oncological and anatomical features of an adrenal mass as well as the patient body mass index. Each component in the ADRENAL score is designated by an English letter, forming the acronym ADRENAL: (A)ldosterone/cortisol/catecholamine secretion or suspicion of malignancy based on endocrinological and radiological study, (D)imension (tumor size as the maximal diameter), (R)elationship to adjacent organs, (E)nhancement on computerized tomography, (N)earness of the tumor to major vessels, (A)dipose (patient habitus as body mass index), and a (L)aterality descriptor. Of the 7 components, 6 (A.D.R.E.N.A.) are scored on a 0, 1 or 2-point scale. The 7th descriptor is a suffix which describes the laterality of the mass, either left (l) or right (r). The scoring criteria were described in Table 2 and illustrated in Figures 1, 2 and Supplemental Figure 1.

Data collection and scoring

>In authors' institute, a team including three urologists, one endocrinologist, one radiologist and one anesthesiologist were assigned to the collection and revision of patient data. Two urologist independently recorded "(D)imension", "(R)elationship to adjacent organs", "(E)nhancement on enhanced CT scan", "(N)earness of the tumor to major vessels", "(A)dipose: BMI" and "(L)aterality" of the tumor which were verified by the 3rd urologist and an radiologist if any discrepancy noted. The endocrinologist and radiologist were responsible for the evaluation and scoring of "(A)ldosterone/cortisol/catecholamine/malignancy". Age-adjusted Charlson comorbidity score and ASA (American Society of Anesthesiologists) score of the patients were assessed and reviewed by an urologist with on-line Charlson comorbidity score calculator (http://www.touchcalc.com/calculators/cci_js) and an anesthesiologist, respectively. Tumor characteristics and average ADRENAL score in each group were listed in Table 3. In summary, the average tumor size was 3.36 ± 1.95, 4.07 ± 2.72, 5.13 ± 3.94 and 2.97 ± 1.67 cm in Group 1 to 4, respectively. 110 (51.89%), 49 (46.67%), 10 (35.71%) and 58 (51.33%) tumors were located on the left side, respectively. The independently assessed ADRENAL score was 2.52 ± 1.89 (1 to 8), 3.26 ± 2.45 (1 to 9), 4.32 ± 2.50 (2 to 9) and 5.16 ± 1.83 (1 to 9), respectively.

Statistical analysis

Data are shown as the mean plus or minus standard deviation (SD). Statistical difference in ASA score and age-adjusted Charlson comorbidity score among different ADRENAL score groups were analyzed by one-way ANOVA test. The correlation analysis of the ADRENAL score and each component verse operative time (OT) and estimated blood loss (EBL) was performed by Pearson correlation test. The correlation of the ADRENAL score and OT or EBL was tested in linear regression model, in which an R^2 of greater than 0.5 was considered a significant correlation. Statistical difference in OT

TABLE 2 Components and criteria of the ADRENAL score.

ADRENAL score	0 pt	1 pt	2 pts
(A)ldosterone/cortisol/catecholamine/malignancy	Non-functional incidentaloma: including myelolipoma, cystic mass, etc	Suspicion of PA, CS	Suspicion of PCC or malignancy
(D)imension	≤ 4 cm	> 4 cm but < 7 cm	≥ 7 cm
(R)elationship to adjacent organs	A clear tumor boundary without signs of local invasion	< 50% tumor edge with unclear boundary, but no signs of local invasion	≥ 50% tumor edge with unclear boundary, suspicious invasion to adjacent organs
(E)nhancement on CT scan	Highest intratumoral CT numbers on contrast-enhanced CT scan < 10 HU	Highest intratumoral CT numbers on contrast-enhanced CT scan ≥ 10 HU but < 85 HU	Highest intratumoral CT numbers on contrast-enhanced CT scan ≥ 85 HU
(N)earness of the tumor to major vessels	≥ 7 mm	< 7 mm but not pressing against a major vessel	Pressing against a major vessel
(A)dipose: BMI (kg/m^2)	≤ 25	> 25 but < 30	≥ 30
(L)aterality	No points given. Assigned a descriptor of L (left) or R (right).		

PA, primary aldosteronism; CS, Cushing's syndrome; PCC, pheochromocytoma.

10.3389/fendo.2022.1073082

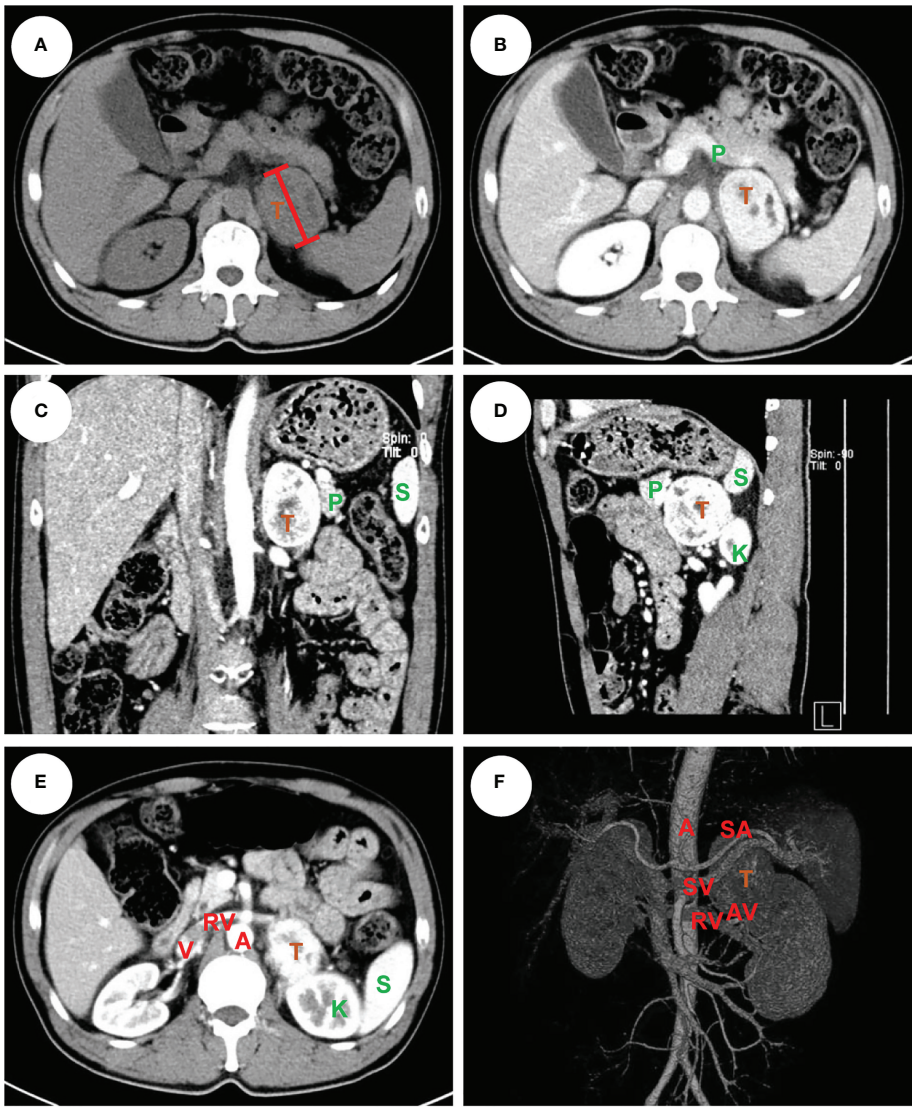

FIGURE 1
An example of left pheochromocytoma. The male patient had a 6 cm pheochromocytoma arising from the left adrenal gland **(A)** with 110 HU on contrast-enhanced CT **(B)**. A clear tumor boundary was observed on transverse **(B)**, coronal **(C)** and sagittal **(D)** section which revealed a close relationship between the tumor and ipsilateral kidney, spleen and pancreas. A venous phase section **(E)** showed the left renal vein travelled to the vena cava underneath the tumor, which was further confirmed by a 3-D vessel reconstruction based on arterial-venous phase CT scan demonstrating the relative location of the tumor to surrounding major abdominal vessels **(F)**. The tumor was removed robotically *via* retroperitoneal approach. The patient had an ADRENAL score of $2_A + 1_D + 2_R + 2_E + 2_N + 0_A + L_L = 9L$. T: tumor, P: pancreas, K: kidney, S: spleen, A: aorta, V: (inferior) vena cava, RV: renal vein, SA: splenic artery, SV: splenic vein, AV: adrenal vein.

and EBL among Grade I, Grade II and Grade III groups were analyzed by Student t test. Pearson chi-square test was used to calculate the odds ratio. All data were analyzed with the Statistical Package for Social Science Software, v.16.0 (SPSS Inc., Chicago, IL, USA) and a p-value of less than 0.05 was considered statistically significant. Graphs were plotted in GraphPad Prism v.7 (GraphPad Software Inc., La Jolla, CA, USA) or Microsoft Excel 2010 (Microsoft Corp., Redmond, WA, USA).

Results

Surgical outcomes

Surgical outcomes of the four groups of patients were listed in Table 4. In summary, the average operative time was 130.27 ± 50.30, 149.64 ± 72.64, 208.04 ± 120.65 and 106.96 ± 49.16 min in Group 1 to 4, respectively. To note that the operative time for both laparoscopic and robotic surgery was defined as from the

10.3389/fendo.2022.1073082

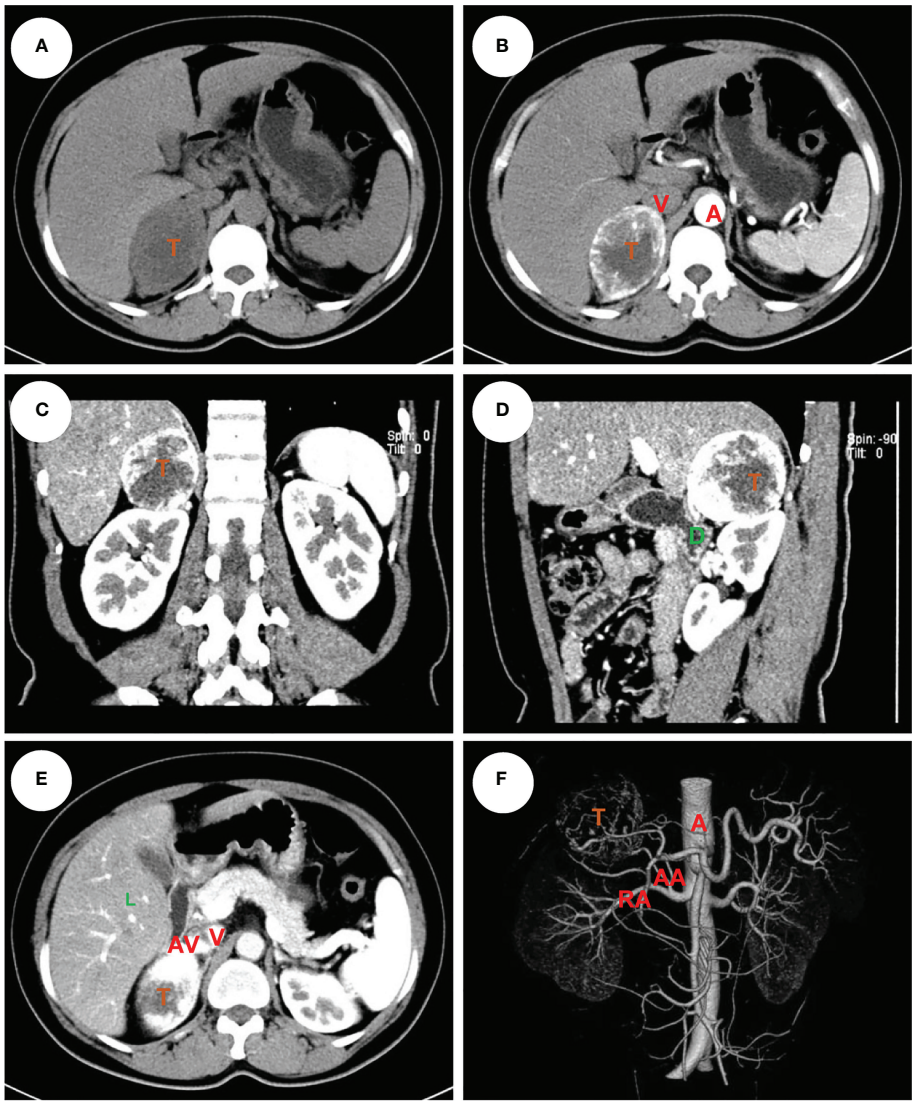

FIGURE 2
An example of right pheochromocytoma. The female patient had a 6 cm pheochromocytoma arising from the right adrenal gland **(A)** with 120 HU on contrast-enhanced CT **(B)**. A clear tumor boundary was observed on transverse **(B)**, coronal **(C)** and sagittal **(D)** section which revealed a close relationship between the tumor and ipsilateral kidney, right hepatic lobe and duodenum. An arterial-venous phase section **(E)** showed a short adrenal vein draining directly into the vena cava. The 3-D vessel reconstruction based on arterial phase CT scan demonstrated the relative location of the tumor to surrounding major abdominal vessels **(F)**. The tumor was removed robotically *via* retroperitoneal approach. The patients had an ADRENAL score of $2_A + 1_D + 0_R + 2_E + 1_N + 1_A + R_L = 7R$. T, tumor; L, liver; D, duodenum; A, aorta; V, (inferior) vena cava; RA, renal artery; AA, (middle) adrenal artery; AV, adrenal vein.

first incision to the closure of all incisions. The average estimated blood loss was 134.96 ± 101.71, 85.14 ± 155.60, 261.60 ± 570.47 and 93.85 ± 153.49 ml, respectively. One case in Group 1, another case in Group 2 and 5 cases in Group 4 were converted to open surgery due to significant adhesion or excessive bleeding. No conversion was observed in Group 3. One case in Group 1, another case in Group 2 and 2 cases in Group 3 were reported to have positive surgical margin. Surgical margin was negative for all cases in Group 4. The average hospital stay was 15.70 ± 6.88, 15.34 ± 4.68, 3.46 ± 3.54 and 15.75 ± 8.18 days, respectively. Overall complication rate was 9.91% (n = 21), 3.81% (n = 4), 7.14% (n = 2) and 25.66% (n = 29), respectively. No patient death was observed during perioperative period in all series. Postoperative pathological study (Table 3) revealed cortical adenoma [146 (68.87%), 63 (60.00%), 11 (39.29%) and 81 (71.68%) cases in Group 1 to 4, respectively] as the most common indication, followed by pheochromocytoma [45 (21.23%), 21 (20.00%), 6 (21.43%) and

10.3389/fendo.2022.1073082

TABLE 3 Tumor characteristics.

		Group 1 (n = 212)	Group 2 (n = 105)	Group 3 (n = 28)	Group 4 (n = 113)
Tumor Characteristics	Tumor size, cm	3.36±1.95	4.07±2.72	5.13±3.94	2.97±1.67
	Left, n (%)	110 (51.89%)	49 (46.67%)	10 (35.71%)	58 (51.33%)
	Pathology, n (%)				
	Cortical adenoma	146 (68.87%)	63 (60.00%)	11 (39.29%)	81 (71.68%)
	Pheochromocytoma	45 (21.23%)	21 (20.00%)	6 (21.43%)	22 (19.47%)
	Malignancy	6 (2.83%)	2 (1.90%)	9 (32.14%)	4 (3.54%)
	Other	15 (7.08%)	19 (18.10)	2 (7.14%)	6 (5.31%)
ADRENAL score		**2.52±1.89**	**3.26±2.45**	**4.32±2.50**	**5.16±1.83**

Group 1: laparoscopic retroperitoneal adrenalectomy; Group 2: robotic retroperitoneal adrenalectomy; Group 3: robotic transperitoneal adrenalectomy; Group 4: laparoscopic retroperitoneal adrenalectomy. ADRENAL score: refer to Table 2 for details on the scoring system. Values expressed as mean ± SD.

22 (19.47%), respectively] and other pathologies including cyst, hematoma, angioleiomyolipoma, myelolipoma, and rarely B-cell lymphoma. Malignancy of the adrenal gland was rare [Group 1: 6 (2.83%); Group 2: 2 (1.90%); Group 4: 4 (3.54%)] but accounted for 32.14% (n = 9) in Group 3 due to selection of patients.

Validation of the ADRENAL score

The ADRENAL score was applied to all patients according the scoring criteria as demonstrated previously (Table 2 and Supplemental Table 1). Patients were grouped according to ADRENAL score in each series. The variance in age-adjusted Charlson comorbidity score (11) and ASA (American Society of Anesthesiologists) score (16), two reported risk factors of adrenal surgery, was first tested (Supplemental Figure 2). Results showed that the difference in comorbidity and ASA score was statistically significant in Group 3 (p = 0.0119), but not in Group 1 (p = 0.4137), Group 2 (p = 0.2251) or Group 4 (p = 0.7208). A significant difference in ASA score was found in Group 4 (p = 0.0019), but not in Group 1 (p = 0.2721), Group 2 (p = 0.7546) or Group 3 (p = 0.2251). Keeping these in mind, we proceeded to validation of correlation between ADRENAL score and OT and EBL, two quantifiable major surgical outcomes.

We first tested the correlation between each of the 7 components in ADRENAL score verse OT and EBL (Table 5). Based on the scoring criteria of ADRENAL score, a 0, 1 or 2 points was assigned to tumor function and malignancy (A), tumor size (D), relationship with adjacent organs (R), intratumoral enhancement (E), distance to major vessels (N) and BMI (A). Correlation between the scored value of the above 6 components and the actual value of tumor size (D) and BMI (A) verse OT and EBL was evaluated by Pearson correlation test. Results showed that these 6 components seemed to inconsistently correlate with OT and EBL in all 4 groups. The exact *p* values were listed in Table 5. No significant difference was found in either OT or EBL between left and right tumors in either group by Student t test. Due to the selection of patients, we did not include tumors with local invasion in the indication of our laparoscopic adrenalectomy (Group 1). The (R) score was therefore 0 for all cases in Group 1 and cannot be analyzed.

Next, we analyzed the correlation between ADRENAL score verse OT and EBL. The correlation between the numeric value of ADRENAL score verse OT and EBL was consistently and statistically significant in all groups by Pearson correlation test (Table 5). To further evaluate the value of ADRENAL score in predicting surgical outcomes, we tested ADRENAL score in linear regression model to see whether higher ADRENAL score correlated with longer OT or greater EBL (Figure 3). Indeed, the

TABLE 4 Surgical outcomes.

		Group 1 (n = 212)	Group 2 (n = 105)	Group 3 (n = 28)	Group 4 (n = 113)
Outcomes	OT, min	130.27±50.30	149.64±72.64	208.04±120.65	106.96±49.16
	EBL, ml	134.96±101.71	85.14±155.60	261.60±570.47	93.85±153.49
	Conversion, n (%)	1 (0.47%)	1 (0.95%)	0	5 (4.42%)
	PSM, n (%)	1 (0.47%)	1 (0.95%)	2 (7.14%)	0
	LHS, day	15.70±6.88	15.43±4.59	3.46±3.54	15.75±8.18
	Overall Complications, n (%)	21 (9.91%)	4 (3.81%)	2 (7.14%)	29 (25.66%)

Group 1: laparoscopic retroperitoneal adrenalectomy; Group 2: robotic retroperitoneal adrenalectomy; Group 3: robotic transperitoneal adrenalectomy; Group 4: laparoscopic retroperitoneal adrenalectomy. OT, operative time; EBL, estimated blood loss; LHS, length of hospital stays. Values expressed as mean ± SD.

TABLE 5 Correlation analysis of each single components in ADRENAL score, ADRENAL score and a Grade classification verse OT and EBL.

Group (n)	Surgical outcomes	*p* value								
		(A)[c]	(D)[b,c]	(R)[c]	(E)[c]	(N)[c]	(A)[b,c]	(L)[d]	ADRENAL score[c]	Grade classification based on ADRENAL score[e]
Group 1[a] (212)	OT	NS	0.0014 <0.0001	N/A	0.0012	0.0005	0.0127 NS	NS	<0.0001	0.0006
	EBL	NS	NS NS	N/A	0.0101	NS	NS NS	NS	0.0090	0.0427
Group 2 (105)	OT	NS	0.0069 0.0100	NS	0.0152	NS	NS NS	NS	0.0024	0.0147
	EBL	NS	0.0045 0.0108	<0.0001	0.0018	0.0003	NS NS	NS	0.0004	<0.0001
Group 3 (28)	OT	NS	0.0404 0.0165	0.0026	NS	NS	NS NS	NS	0.0203	0.0404
	EBL	NS	0.0477 0.0120	<0.0001	NS	0.0460	NS NS	NS	0.0072	0.0279
Group 4 (113)	OT	0.0023	0.0160 0.0004	NS	NS	0.0002	NS NS	NS	<0.0001	0.0009
	EBL	0.0121	0.0098 0.0006	NS	0.0126	0.0015	NS NS	NS	<0.0001	0.0080

Group 1: laparoscopic retroperitoneal adrenalectomy; Group 2: robotic retroperitoneal adrenalectomy; Group 3: robotic transperitoneal adrenalectomy; Group 4: laparoscopic retroperitoneal adrenalectomy. OT, operative time; EBL, estimated blood loss; NS, not significant ($p > 0.05$); N/A, not available.
[a]All tumors in Group 1 had clear boundary without signs of local invasion. Therefore, (R) score is 0 for all cases in Group 1 and cannot be analyzed.
[b]Upper p value: correlation between the scored value of (D) or (A) verse OT or EBL; lower p value: correlation between the actual value of (D) or (A) verse OT or EBL.
[c]Pearson correlation test.
[d]Student t test.
[e]One-way ANOVA.

numeric value of ADRENAL score verse OT and EBL fitted well in linear regression model as indicated by an R^2 of greater than 0.5 (R^2 was 0.8477 for OT and 0.8150 for EBL in Group 1; 0.6013 for OT and 0.7973 for EBL in Group 2; 0.8040 for OT and 0.8359 for EBL in Group 3; 0.7869 for OT in Group 4). However, the R^2 for ADRENAL score verse EBL in Group 4 was 0.4805.

Validation of a grading system based on the ADRENAL score

For more practical use of the ADRENAL score, we proposed a 4-grade classification for adrenal masses based on the ADRENAL score. Grade 0: ADRENAL score = 0; Grade I: ADRENAL score < 4 (1-3); Grade II: ADRENAL score ≥ 4 but ≤ 7 (4-7); Grade III: ADRENAL score > 7 (8-12). Grade 0 adrenal masses or tumors assigned with an ADRENAL score of 0 were not indicated for surgery and managed by watchful waiting in all authors' institutions, and therefore not included in this study. Percentage of Grade I, Grade II and Grade III tumors in each group were listed in Supplemental Figure 3. Student t test was performed to determine any statistical difference in OT or EBL between any two grades in each group (Figure 4). Indeed, both OT and EBL in Grade III verse Grade I was consistently statistically significant in all 4 groups (OT: p values for Grade I verse Grade III in Group 1 to Group 4 were 0.0428, 0.0116, 0.037 and 0.0033, respectively; EBL: 0.0322, < 0.0001, 0.0236 and 0.0013, respectively). However, OT or EBL of Grade I verse Grade II or Grade II verse Grade III in the 4 groups was not consistently statistically significant (OT: p values for Grade I verse Grade II in Group 1 to Group 4 were 0.0004, NS, NS and NS, respectively; Grade II verse Grade III: NS, NS, NS and 0.0011, respectively; EBL: p values for Grade I verse Grade II in Group 1 to Group 4 were NS, 0.0003, NS and NS, respectively; Grade II verse Grade III: NS, 0.024, NS and 0.013, respectively; NS: not significant), despite the fact that higher grade correlated with longer OT and larger EBL in all 4 groups (Supplemental Tables 2, 3).

Surgeries of Group 1 and Group 2 patients were performed by the same surgical team using conventional laparoscopy and da Vinci robotic system, respectively, both *via* retroperitoneal approach. By comparing the surgical outcomes of these two groups stratified by the 4-grade classification based on the ADRENAL score, which we believe was more reasonable than an overall comparison, we could determine whether robotic surgery was indeed superior to laparoscopic surgery eliminating any bias from different surgical techniques and approaches. We first did a non-stratified analysis of the difference in overall OT and EBL between Group 1 (laparoscopic) and Group 2 (robotic). Robotic surgery seemed to take a slightly longer time than laparoscopic surgery (146.21 ± 64.75 vs 130.89 ± 50.46 min) but with a significant *p* value of 0.0215, while the blood loss was significantly lower in robotic group than laparoscopic group (101.06 ± 138.88 vs 151.69 ± 94.14 ml, $p = 0.0020$). Stratified by

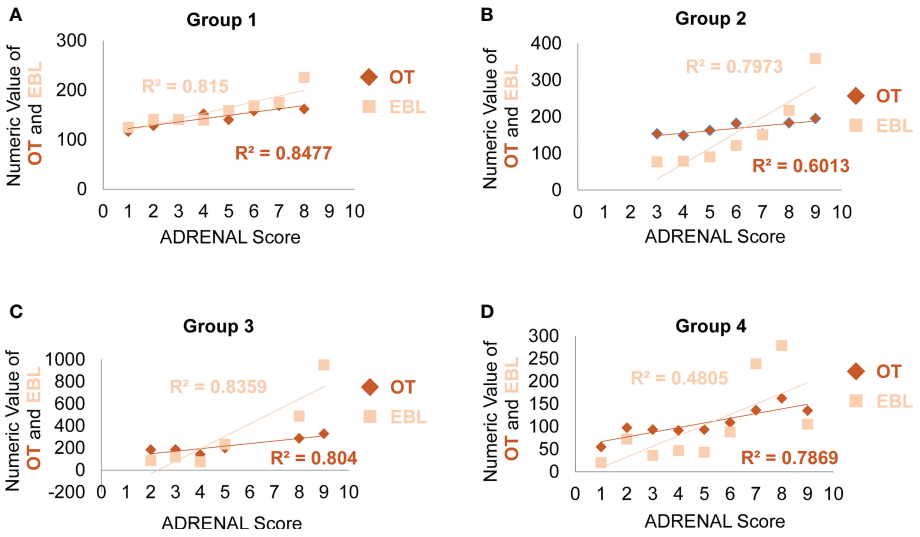

FIGURE 3
Analysis of the correlation between the ADRENAL score verse OT and EBL. In linear regression model, the correlation between the ADRENAL score and OT or EBL was tested in Group 1 **(A)**, Group 2 **(B)** and Group 3 **(C)** and Group 4 **(D)**. An $R^2 > 0.5$ was considered a significant correlation.

the 4-grade classification based on the ADRENAL score (Figure 4), no significant difference was found in OT between robotic and laparoscopic group in Grade I, Grade II, nor Grade III tumors. However, robotic surgery seemed to correlate with significantly lower EBL than laparoscopic group in both Grade I and Grade II tumors ($p < 0.0001$ and $p = 0.0129$, respectively), but not in Grade III tumors.

Complication, conversion, transfusion and length of hospital stay

In terms of perioperative complications (Group 1: number of complications/number of cases = 21/212, overall complication rate: 9.91%; Group 2: 4/105, 3.81%; Group 3: 2/28, 7.14%; Group 4: 28/113, 24.78%), most were Clavien-Dindo Grade I including fever and vomiting managed with antipyretics and antiemetics, respectively. 9 patients in Group 1, 1 patient in Group 2 and 2 patients in Group 3 had postoperative infection and managed with antibiotics. 1 patient in Group 1, 2 patients in Group 2 and 1 patient in Group 2 had abnormal blood pressure and managed with vasoactive drugs accordingly. 1 patient in Group 2 and 1 patient in Group 3 converted to open surgery due to excessive adhesion and received blood transfusion. No Grade III to Grade V complication was encountered in patients included in this study. Overall, patients with Grade II and Grade III tumor seemed to have a higher, but not statistical significant, risk of perioperative complication rate than those bearing Grade I tumor (Supplemental Table 4).

Conversion to open surgery was only observed in 1 Grade II case in Group 1, 1 Grade III case in Group 2, 1 Grade III case in Group 3, 2 Grade II cases and 3 Grade III cases in Group 4, due to significant adhesion (Supplemental Table 5). All conversion was observed in Grade II or Grade III tumors, while none in Grade I tumors in all 4 groups. 2 Grade II cases in Group 1, 1 Grade III case in Group 2, 1 Grade III case in Group 3, 1 Grade I case, 3 Grade II cases and 3 Grade III cases in Group 4 received intraoperative transfusion due to excessive bleeding (Supplemental Table 6).

Length of hospital stay was listed in Supplemental Table 7. To note that the length of hospital stay in Group 1, 2 and 4 (Chinese hospitals), which was defined as from the first day of administration to the day of discharge, appeared to be significantly longer than that in Group 3 (US hospital) due to different policies for inpatient management. Results showed that patients bearing Grade III tumor had significantly prolonged hospital stay in Group 2 and Group 4, compared with patients with Grade I tumor in each respective group.

Discussion

Adrenal tumor is a common indication of surgery in urology. The functional status and suspicion of malignancy (fast growing, large size, signs of local invasion or metastatic lesion) are considered to be the two most important factors when deciding if an adrenal tumor should be removed. As far as surgery is concerned, the functional status (11), pheochromocytoma (12) and malignancy

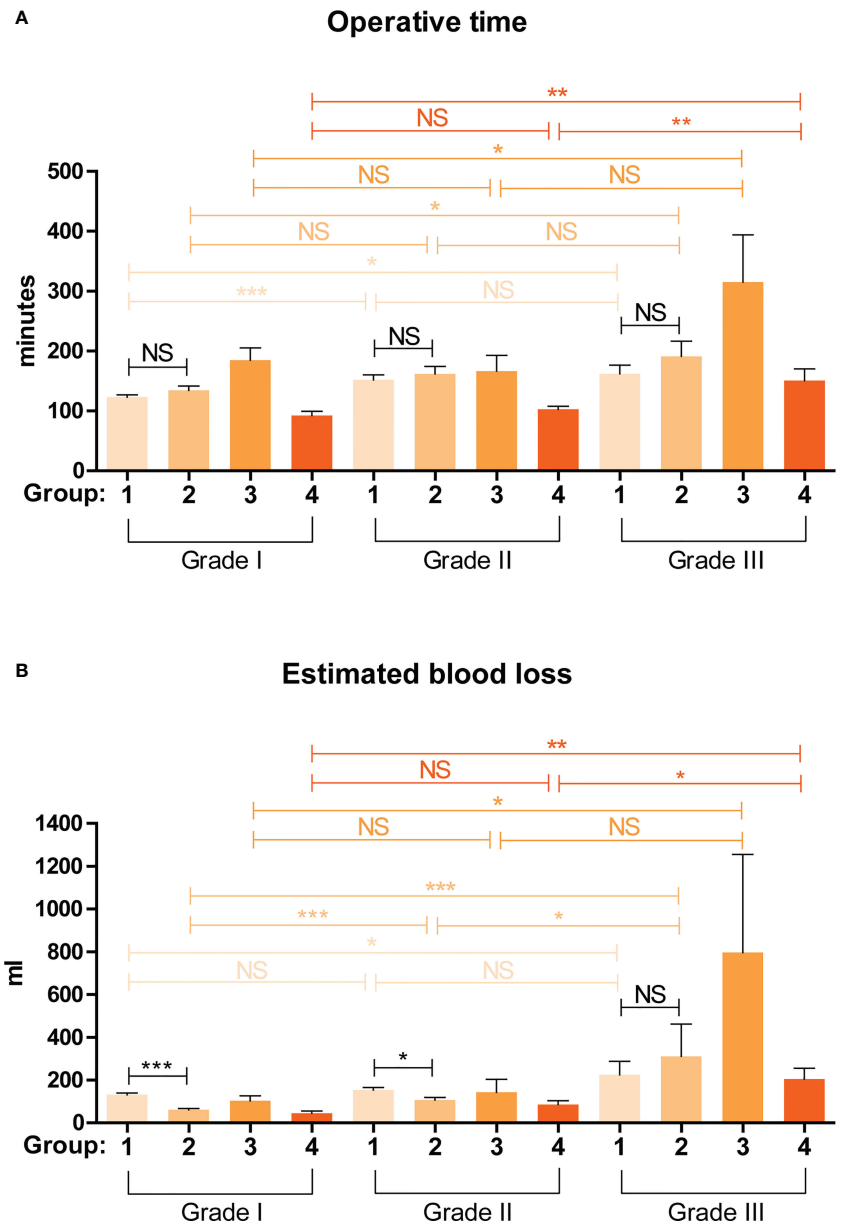

FIGURE 4
Validation of the predictive value of a grading system based on the ADRENAL score in OT and EBL. A 4-grade classification for adrenal masses was proposed based on the ADRENAL score. Grade 0: ADRENAL score = 0; Grade I: ADRENAL score < 4 (1-3); Grade II: ADRENAL score ≥ 4 but ≤ 7 (4-7); Grade III: ADRENAL score > 7 (8-12). Student t test was performed to analyze the difference in OT and EBL. A p value <0.05 was considered statistically significant. (*p < 0.05; **p < 0.01; ***p < 0.001; NS, not significant).

(13), tumor size (14) and BMI (15) are all documented as risk factors. In particular, while most adrenal tumors are small, large tumor still spans a significant portion (136 out of 458 adrenal tumors included in this study were greater than 4 cm, among which 37 tumors were greater than 7 cm). As such, the relationship between the tumor and surrounding structures (large vessels and organs) may pose a unique challenge and needs to be reviewed before surgery.

It is the goal of both the patient and the surgeon to ensure that the adrenal tumor can be safely and completely removed. Achieving this goal relies on an accurate assessment of the patient's risk before surgery. After all, high-risk patients are more likely to be in danger during surgery. However, due to the complex and diverse risk factors affecting surgery, how to establish an evaluation system that incorporates various factors is a problem for urologists to think about. Some relevant

evaluation systems, such as the weiss scoring system (17), the pheochromocytoma of the adrenal gland scaled score (PASS), the grading system for adrenal pheochromocytoma and paraganglioma (GAPP) (18, 19), and the utrecht score (20), have some reference significance, but they are mostly based on postoperative pathology to predict expected survival rather than surgical risk assessment. Only Caiazzo (21) provided an adrenalectomy risk score. There has been little research on surgical risk assessment systems for patients with adrenal tumors, which is why we conducted this study.

In this study, we proposed an original and standardized preoperative scoring system, designated as the ADRENAL score, which integrates these established risk factors and tumor anatomy for adrenal masses. This scoring system quantitatively describes the nature and anatomical characteristics of adrenal masses based on multidisciplinary assessment that are routinely performed in the clinical practice, looking to provide an overall estimation of the clinical significance of the tumor and the risk of surgery. In the clinical practice, endocrinologists and urologists may be assisted by this 0 to 12 scoring system coupled with a laterality indicator when making any clinical decision on the indication of surgery, preoperative preparation and assessment, intraoperative precautions, postoperative management and follow-up. As far as surgery is concerned, the ADRENAL score has been shown in this study to predict the operative time and estimated blood loss in minimally invasive adrenal surgeries. By comparative analysis, our data suggested that the integrated scoring system may be more accurate and comprehensive in predicting operative time (OT) and estimated blood loss (EBL) than a single risk factor. ADRENAL score seemed to be positively, but not statistical significantly related with complication, transfusion and conversion. Larger sample size is required to establish the possible correlation. Further, patients with higher ADRENAL score were subjected to significantly longer hospital stay, which may be explained by higher (but not statistically significant) complication, transfusion and conversion rate, and a longer time required for a definitive diagnosis before surgery (for Group 1, 2 and 4).

Our current data suggested a possible predictive role of ADRENAL score in various surgical outcomes. As such, besides preoperative risk assessment, the ADRENAL score may serve as a valid grading system in risk-stratified designing of adrenalectomy training programs for the training of young doctors and safety of patients. For conducting clinical research, the ADRENAL score could be a valuable tool for more scientific evaluation of a surgeon's learning curve, and comparative studies on adrenal surgeries *via* different techniques and approaches.

Design of study

In this study, we included 4 groups of patients treated with laparoscopic or robotic adrenalectomy *via* retroperitoneal or transperitoneal approach, aiming to achieve an unbiased validation of the ADRENAL score. To improve the quality of the analysis, doctors involved in the data collection and scoring process were all blinded to the final outcome of statistical analysis; and a single or the same group of doctors was assigned to the scoring of a specific component in the ADRENAL score for each group. The rational of including the 7 components in the ADRENAL score was given in Supplemental Materials.

Limitations of study

One potential limitation of this study is the lack of stratified evaluation of complications based on Clavien-Dindo classification (22). Further studies are required to establish a possible correlation between the ADRENAL score and the grade of complications. We also noted a significant variance ($p = 0.0119$) in age-adjusted Charlson comorbidity score among patients assigned with different ADRENAL score from Group 3. As such, the possible interference of patients comorbidity cannot be ruled out in all statistical analysis in Group 3. Another limitation is that we did not include open surgery in our study, which is still the standard of care for adrenal malignancy. Further external validation of the ADRENAL score is required.

Conclusions

The ADRENAL score of adrenal mass is a comprehensive scoring system which integrates established risk factors and the most important anatomical features of the tumor. It can be assessed retrospectively and prospectively by routinely performed endocrinological, oncological and radiological studies of adrenal mass. Our study demonstrated that the ADRENAL score seems to correlate with surgical outcomes. Therefore, it may provide a common reference for adrenal surgery training program, preoperative risk assessment and stratified comparative analysis of adrenal surgeries *via* different techniques and approaches. Validation of this system in other institutions is currently on-going.

Data availability statement

The original contributions presented in the study are included in the article/Supplementary Material. Further inquiries can be directed to the corresponding authors.

Ethics statement

The studies involving human participants were reviewed and approved by The Ethical Committee of The First Affiliated Hospital of Nanchang University. The patients/participants provided their written informed consent to participate in this study.

Author contributions

Conceived and designed the experiments: XZ, BF, DE, and GW. Console surgeon: DE, GW and YD. Collected and analyzed the data: XL, WL, CZ, YX, HG, LZ, EL, JK. Wrote the paper: XZ and XL. All authors contributed to the article and approved the submitted version.

Funding

Fund programs: Key Research and Development Program of Jiangxi Province (20171ACB20029 to XZ).

Conflict of interest

The authors declare that the research was conducted in the absence of any commercial or financial relationships that could be construed as a potential conflict of interest.

Publisher's note

Supplementary material

The Supplementary Material for this article can be found online at: https://www.frontiersin.org/articles/10.3389/fendo.2022.1073082/full#supplementary-material

References

1. Stefanidis D, Goldfarb M, Kercher KW, Hope WW, Richardson W, Fanelli RD, et al. SAGES guidelines for minimally invasive treatment of adrenal pathology. *Surg Endosc* (2013) 27(11):3960–80. doi: 10.1007/s00464-013-3169-z

2. Bovio S, Cataldi A, Reimondo G, Sperone P, Novello S, Berruti A, et al. Prevalence of adrenal incidentaloma in a contemporary computerized tomography series. *J Endocrinol Invest* (2006) 29(4):298–302. doi: 10.1007/BF03344099

3. Kebebew E. Adrenal incidentaloma. *N Engl J Med* (2021) 384(16):1542–51. doi: 10.1056/NEJMcp2031112

4. Young WF Jr. Clinical practice. the incidentally discovered adrenal mass. *N Engl J Med* (2007) 356(6):601–10. doi: 10.1056/NEJMcp065470

5. Gagner M, Pomp A, Heniford Bt, Pharand D, Lacroix A. Laparoscopic adrenalectomy: Lessons learned from 100 consecutive procedures. *Ann Surg* (1997) 226(3):238–46. doi: 10.1097/00000658-199709000-00003

6. Walz MK, Peitgen K, Walz MV, Hoermann R, Saller B, Giebler RM, et al. Posterior retroperitoneoscopic adrenalectomy: Lessons learned within five years. *World J Surg* (2001) 25(6):728–34. doi: 10.1007/s00268-001-0023-6

7. Fiori C, Checcucci E, Amparore D, Cattaneo G, Manfredi M, Porpiglia F, et al. Adrenal tumours: open surgery versus minimally invasive surgery. *Curr Opin Oncol* (2020) 32(1):27–34. doi: 10.1097/CCO.0000000000000594

8. Horgan S, Vanuno D. Robots in laparoscopic surgery. *J Laparoendosc Adv Surg Tech A* (2001) 11(6):415–9. doi: 10.1089/10926420152761950

9. Agcaoglu O, Aliyev S, Karabulut K, Mitchell J, Siperstein A, Berber E. Robotic versus laparoscopic resection of large adrenal tumors. *Ann Surg Oncol* (2012) 19 (7):2288–94. doi: 10.1245/s10434-012-2296-4

10. Zhao J, Ma W, Xie J, Dai J, Huang X, Fang C, et al. Laparoscopic treatment of Large adrenal tumor is safe and effective? a single center experiences. *J Invest Surg* (2021) 34(9):957–62. doi: 10.1080/08941939.2020.1719243

11. Gupta PK, Natarajan B, Pallati PK, Gupta H, Sainath J, Fitzgibbons RJ Jr, et al. Outcomes after laparoscopic adrenalectomy. *Surg Endosc* (2011) 25(3):784–94. doi: 10.1007/s00464-010-1256-y

12. Conzo G, Pasquali D, Colantuoni V, Circelli L, Tartaglia E, Gambardella C. Current concepts of pheochromocytoma. *Int J Surg* (2014) 12(5):469–74. doi: 10.1016/j.ijsu.2014.04.001

13. Hauch A, Al-Qurayshi Z, Kandil E. Factors associated with higher risk of complications after adrenal surgery. *Ann Surg Oncol* (2015) 22(1):103–10. doi: 10.1245/s10434-014-3750-2

14. Constantinides VA, Christakis I, Touska P, Meeran K, Palazzo F. Retroperitoneoscopic or laparoscopic adrenalectomy? a single-centre UK experience. *Surg Endosc* (2013) 27(11):4147–52. doi: 10.1007/s00464-013-3009-1

15. Dancea HC, Obradovic V, Sartorius J, Woll N, Blansfield JA. Increased complication rate in obese patients undergoing laparoscopic adrenalectomy. *JSLS* (2012) 16(1):45–9. doi: 10.4293/108680812X13291597715862

16. Permpongkosol S, Link RE, Su LM, Romero FR, Bagga HS, Pavlovich CP, et al. Complications of 2,775 urological laparoscopic procedures: 1993 to 2005. *J Urol* (2007) 177(2):580–5. doi: 10.1016/j.juro.2006.09.031

17. Wong CL, Fok CK, Chan YK, Tam VH, Fung LM. Was it an adrenocortical adenoma or an adrenocortical carcinoma? limitation of the Weiss scoring system in determining the malignant potential of adrenocortical tumor: Report on two cases. *Case Rep Endocrinol* (2022) 2022:7395050. doi: 10.1155/2022/7395050

18. Wachtel H, Hutchens T, Baraban E, Schwartz LE, Montone K, Baloch Z, et al. Predicting metastatic potential in pheochromocytoma and paraganglioma: A comparison of PASS and GAPP scoring systems. *J Clin Endocrinol Metab* (2020) 105(12):e4661–4670. doi: 10.1210/clinem/dgaa608

19. Thompson LD. Pheochromocytoma of the adrenal gland scaled score (PASS) to separate benign from malignant neoplasms: a clinicopathologic and immunophenotypic study of 100 cases. *Am J Surg Pathol* (2002) 26(5):551–66. doi: 10.1097/00000478-200205000-00002

20. Sanders K, Cirkel K, Grinwis GCM, Teske E, van Nimwegen SA, Mol JA, et al. The Utrecht score: A novel histopathological scoring system to assess the prognosis of dogs with cortisol-secreting adrenocortical tumours. *Vet Comp Oncol* (2019) 17(3):329–37. doi: 10.1111/vco.12474

21. Caiazzo R, Marciniak C, Lenne X, Clément G, Theis D, Ménégaux F, et al. Adrenalectomy risk score: An original preoperative surgical scoring system to reduce mortality and morbidity after adrenalectomy. *Ann Surg* (2019) 270(5):813–9. doi: 10.1097/SLA.0000000000003526

22. Clavien Pa, Barkun J, DE Oliveira ML, Vauthey JN, Dindo D, Schulick RD, et al. The clavien-dindo classification of surgical complications: five-year experience. *Ann Surg* (2009) 250(2):187–96. doi: 10.1097/SLA.0b013e3181b13ca2

frontiers | Frontiers in Endocrinology

TYPE Original Research
PUBLISHED 24 November 2022
DOI 10.3389/fendo.2022.1055826

OPEN ACCESS

EDITED BY
Xiao-qiang Liu,
Tianjin Medical University General Hospital, China

REVIEWED BY
Jiadi Gan,
Sun Yat-sen University Cancer Center (SYSUCC), China
Yongbiao Huang,
Tongji Hospital, China

*CORRESPONDENCE
Yiqing Du
175247106@qq.com
Tao Xu
xutao@pkuph.edu.cn

†These authors have contributed equally to this work

SPECIALTY SECTION
This article was submitted to Reproduction, a section of the journal Frontiers in Endocrinology

RECEIVED 28 September 2022
ACCEPTED 31 October 2022
PUBLISHED 24 November 2022

CITATION
Qin C, Wang J, Du Y and Xu T (2022) Immunosuppressive environment in response to androgen deprivation treatment in prostate cancer. *Front. Endocrinol.* 13:1055826. doi: 10.3389/fendo.2022.1055826

Immunosuppressive environment in response to androgen deprivation treatment in prostate cancer

Caipeng Qin[1†], Jing Wang[2†], Yiqing Du[1*] and Tao Xu[1*]

[1]Department of Urology, Peking University People's Hospital, Beijing, China, [2]Department of Urologic Oncology, The First Affiliated Hospital of University of Science and Technology of China (USTC), Division of Life Sciences and Medicine, University of Science and Technology of China, Hefei, China

Rationale: To invest the role of androgen deprivation therapy (ADT) on the tumor immune microenvironment of prostate cancer.

Methods: Here we have profiled the transcriptomes of 19,227 single cells from 4 prostate tumors, including two cases who received ADT. To validated the single-cell analysis we use another group of patients receiving neoadjuvant ADT.

Results: After receiving ADT treatment, the killing effect of prostate cancer immune cells on tumors is weakened, the interaction between immune cells and tumor cells is weakened, and the proportion of immunosuppressive cells Myeloid-derived suppressor cell (MDSC) and Regulatory T cells (Treg) cells increases.

Conclusions: Our results highlight that ADT induces immunosuppressive in the prostate tumor microenvironment. These data have important implications for combining ADT with immunotherapy.

KEYWORDS

prostate cancer, single cell RNAseq, ADT, immune microenvironment, immunotherapy

Introduction

Prostate cancer is the most common malignancy in men worldwide (1), and androgen deprivation therapy (ADT) has become the standard treatment for locally advanced or metastatic prostate cancer (2, 3). In these patients, ADT forces changes in the tumor biology that result in distinct molecular profiles. Such as ADT treatment induces the up-regulated expression of Nuclear receptor coactivator 2(NCoA2), which could activate the PI3K signaling pathway to promote prostate cancer metastasis and CRPC (4). After receiving ADT treatment, the negative regulation of ZBTB46 by AR is

abolished, and the up-regulated ZBTB46 transcriptionally activates the expression of SNAI1, a key initiator of epithelial-to-mesenchymal transition (EMT) (5). GRB10 is transcriptionally repressed by AR and mediates the activation of AKT to prompt the progress of prostate cancer after receive ADT (6). Future more, prostate cancer cells are surrounded by a complex tumor immune microenvironment, and tumor immune response to the ADT, remains elusive. Others have previously highlighted that ADT induces a complex immune response within the prostate tumor microenvironment (7, 8).Single-cell RNA-sequencing (scRNA-seq) technology enables the complexity of the TME to be revealed. Furthermore, scRNA-seq provides unique opportunities to assess the regulation, and interaction of individual cell, especial between the tumor cells and immune cells. In this Article, we have performed scRNA-seq on 4 prostate tumors with 2 cases receive ADT and obtained transcriptomic profiles for 11,367 cells. We have uncovered the effects of ADT on the immune microenvironment of prostate cancer.

Results

Single-cell RNA sequencing uncovers the cellular diversity of prostate cancer

To study the cellular composition of prostate cancers, we collected 4 tissue samples from 4 patients (2 patients receive neoadjuvant ADT) and performed unsorted single-cell RNA sequencing (scRNA-seq). After standard data processing and quality control procedures, yielding high-quality transcriptomic profiles for 19,227 cells (7,570 untreated cells VS 11,657 ADT treated cells). Analysis and visualization by Uniform Manifold Approximation and Projection (UMAP) showed that single-cell transcriptomes of different patients intermingled in many clusters. Further, we analyzed the expression of immune, stromal, and epithelial marker genes to annotate the clusters. We next subset and analyzed 8 subclusters (Figures 1A–D).

The tumor immune microenvironment exhibits immunosuppressive signature after ADT

We analyzed the gene expression of 1,1367 T cells of the prostate tumor microenvironment. We identified CD4, CD8 and NKT clusters (Figure 2A) based on typical marker genes (Figures 2A, B) and gene signatures. Cytotoxicity-related genes GNLY, NKG7, GZMB and GZMA were downregulated in both tumor-derived CD4+ and CD8+ T cells (Figures 3A, B). Furthermore, Regular T cells in tumors showed lower expression levels of immune regulator LGALS3, Chemokine ligands CCL4, exhaustion markers LAG3, which suggesting a suppressor immune microenvironment after ADT (Figure 3C). Compared with treatment naïve tissues, the gene expression results of tumor-derived CD4+ and CD8+ T cells after ADT treatment, showed downregulated in similar pathways, among which IFN response related pathways ranked high in both groups (Figures 3D, E). In comparison GSVA bar plots comparing the activities of 50 hallmarks between tumor-derived and nonmalignant tissue-derived CD4+ and CD8+ T cells.

We analyzed the transcriptomes of myeloid cells, acquired 1307 macrophages based on the expression of canonical markers and their tissue origins(Figure 4A), We calculated an M1 score and M2 score for each cell based on previously reported markers (9). Similarly, we found that the M1 signatures weaker compared with M2 signature stronger (Figure 4B). This result indicates that macrophage inactivation in the tumor microenvironment (TME) after ADT.

To future investigate potential influence of ADT on TME of prostate cancer, cell-cell communication analysis was performed using CellPhoneDB with or without ADT, respectively. A publicly available repository of curated receptors and ligands and their interactions is available (10). Broadcast ligands for which cognate receptors were detected demonstrated extensive communication between cells. We found immune interactions between tumor cells and T cells decreased after ADT (Figure 5A), including PVR-CD226, similarly, capacity to attract cytotoxic T cell (CXCL12-CXCR4) weakened (Figure 5B).

ADT induces myeloid-derived suppressor cell (MDSC) infiltration and increases the distance between cytotoxic T cells and epithelial cells in the prostate cancer microenvironment

Multi-IHC staining was performed with matched pairs of pre-ADT and post-ADT samples from additional 5 patients received neoadjuvant ADT (Figure 6A), Siglec15 was used to marker epithelial cell, results showed significantly increased intratumoral MDSC cell density by IHC as compared to untreated matched samples (Figures 6B–D). MDSC may mediate prostate tumor cell immune escape.

Each phenotyped cells was assigned an identification number with x and y coordinates to determine their relationship to adjacent other cells (Figure 7A). Using R software phenoptr, the distance between epithelial cells and cytotoxic T cells were calculated for each high-power fields of tissue and the mean separation was determined, cytotoxic T cells located further away from ADT treated epithelial cells compared

10.3389/fendo.2022.1055826

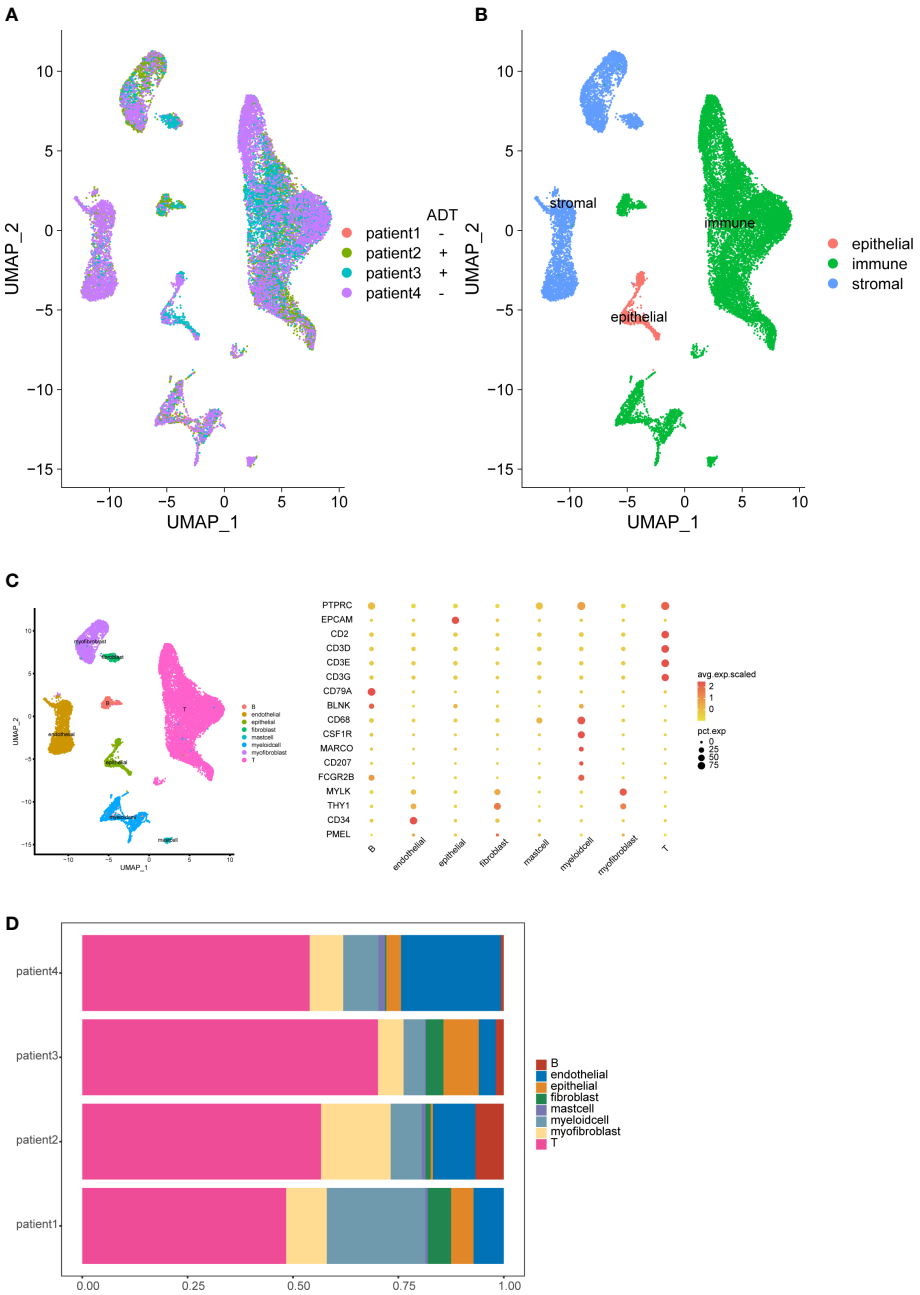

FIGURE 1
Overview of the single-cell landscape for prostate cancer. UMAPs of all single-cell transcriptomes after filtering, color-coded by patient **(A)** and quantification of main cell types per patient and UMAP of all single-cell transcriptomes color-coded by main cell type **(B)**. UMAPs of all single-cell transcriptomes color-coded by cell cluster; Marker gene expression for each cell type, where dot size and color represent percentage of marker gene expression (pct. exp) and the averaged scaled expression (avg. exp. scale) value, respectively **(C)**. Cell composition distribution for each patient sample **(D)**.

with naïve epithelial at 111.07μm and 67.73μm ($p = 0.0046$), respectively (Figures 7B, C).

To evaluate cellular engagement within prostate cancer environment, a circular area with a radius of 30μm was selected around each cytotoxic T cell, and the number of epithelial cells were recorded, results show that the number of engaged epithelial cell decreased after ADT ($p = 0.038$) (Figures 7D, E).

10.3389/fendo.2022.1055826

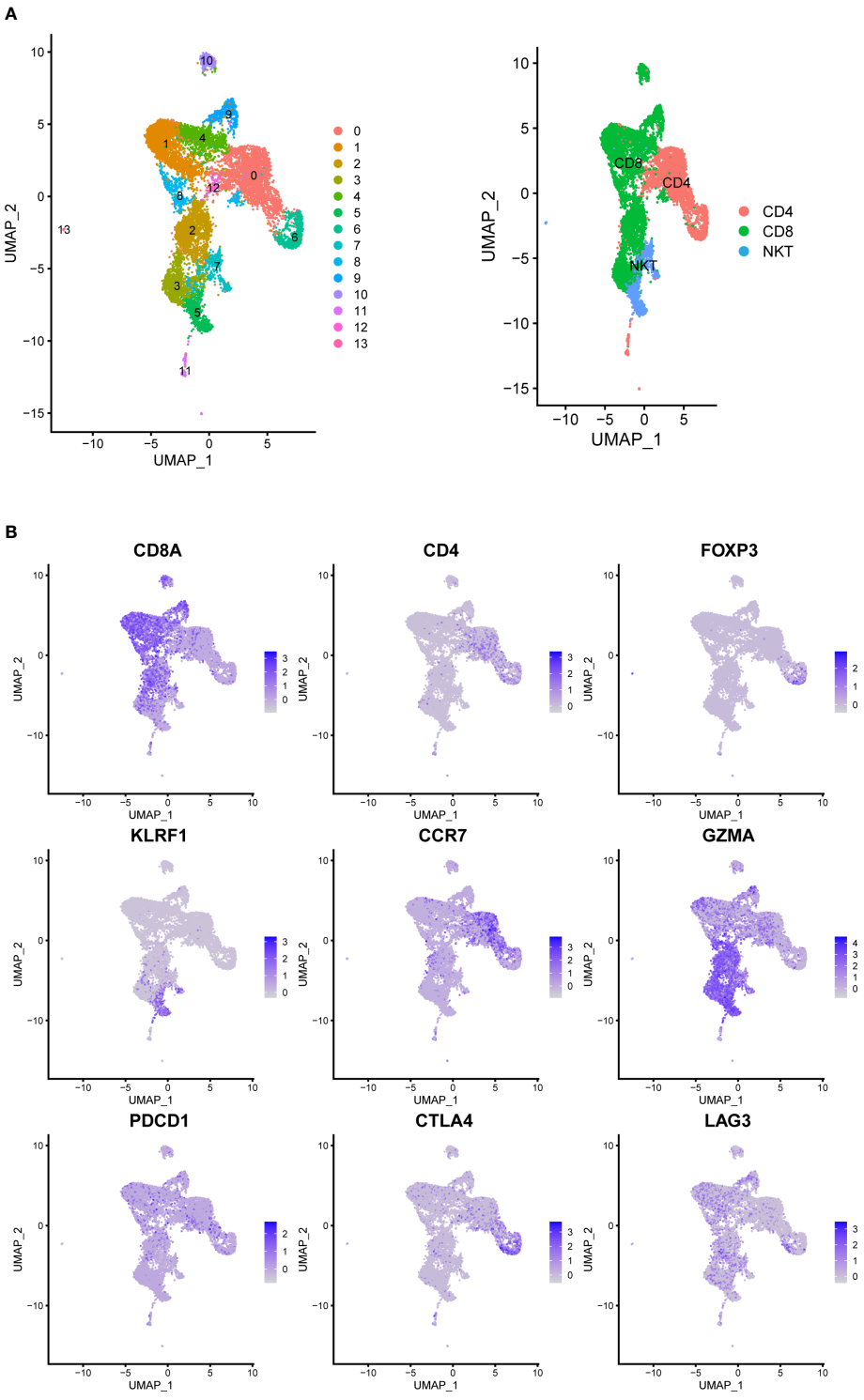

FIGURE 2
Prostate Cancer Contains Canonical T Cell. **(A)** UMAP of T-cells labeled by different cell types obtained from prostate tumors tissue with or without ADT (N = 4 patients). Phenotypic clusters are represented in distinct colors. **(B)** Relative intensity of expression of select genes superimposed on the UMAP projections.

10.3389/fendo.2022.1055826

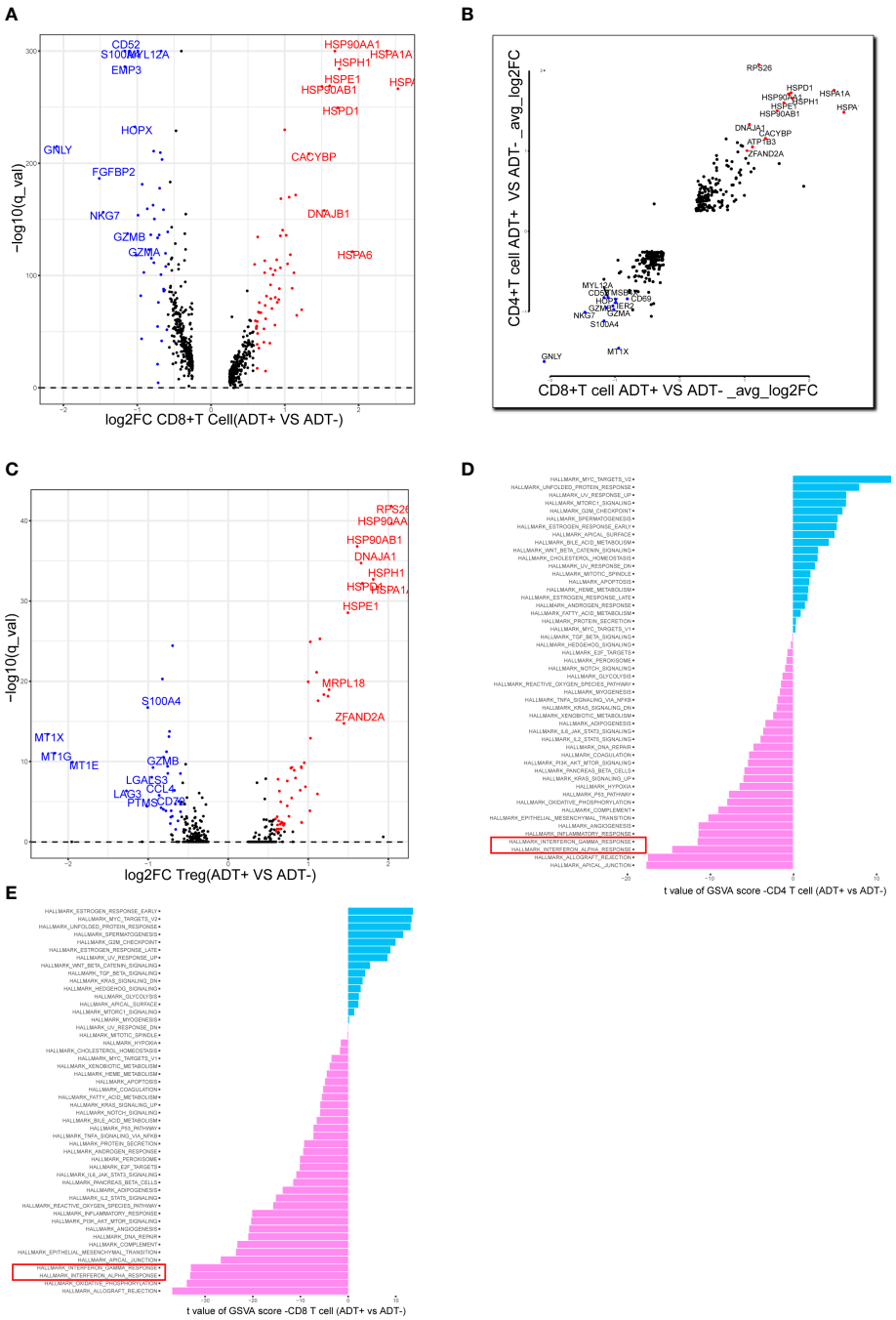

FIGURE 3
Assessing the functional states of tumor-infiltrating T cells in prostate cancer. **(A)** Volcano plot showing DEGs in ADT-derived cytotoxic T cells in comparison with those derived from without ADT tissues. Representative genes are labeled. **(B)** Scatterplot showing DEGs in ADT-derived CD8+ and CD4+ T cells in comparison with those derived from without ADT tissues. Representative genes are labeled. **(C)** Volcano plot showing DEGs in ADT-derived Treg cells in comparison with those derived from without ADT tissues. Representative genes are labeled. **(D, E)** GSVA bar plots comparing the activities of 50 hallmarks between tissue with and without ADT-derived CD4+ and CD8+ T cells.

10.3389/fendo.2022.1055826

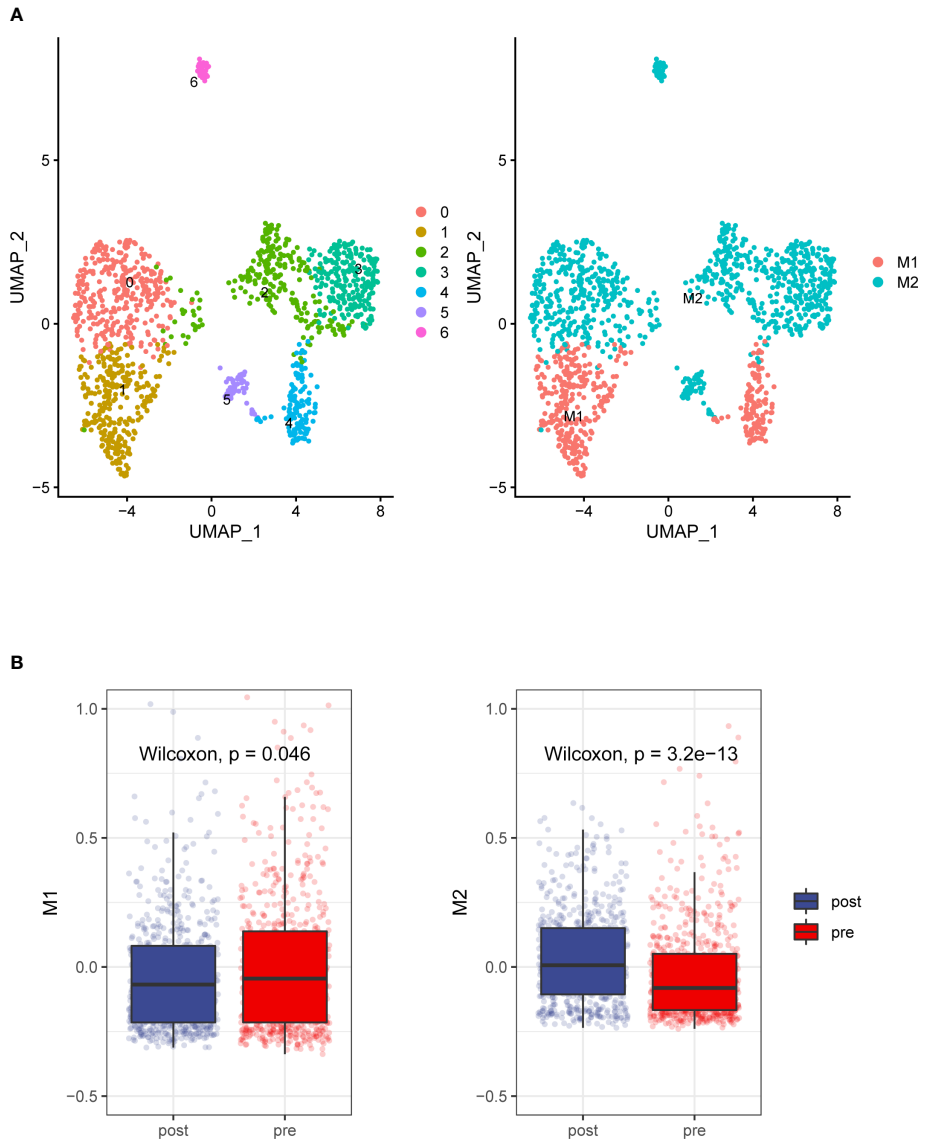

FIGURE 4
Detailed characterization of macrophage cells. **(A)** UMAP plot showing 7 clusters of macrophage cells. According to gene signature of M1 and M2, Macrophages grouped into two categories **(B)**. Compare to the prostate tumors tissue without ADT, prostate cancer tissue with ADT shows more M2 signatures and less M1 signature.

Discussion

Typically, males are more prone to develop cancer in nearly every organ type (11). The sporadic mechanistic researches on sexual dimorphisms in cancer have been almost focused on cancer genetics (12–16). Moreover, Gonadal hormones have a significant influence on immune function (17), which may be associated with sex-biased incidence and mortality of various cancers arising in non-reproductive organs. However, Pertinent contributions by sex hormones in the tumor immune microenvironment are poorly understood.

CD8+ T cells in the tumor immune microenvironment have an enormous potential to recognize and eliminate tumor cells. On the other hand, the tumor immune microenvironment also contains cellular and molecular entities, such as regulatory T cells (18), myeloid-derived suppressor cells (19), Tumor

10.3389/fendo.2022.1055826

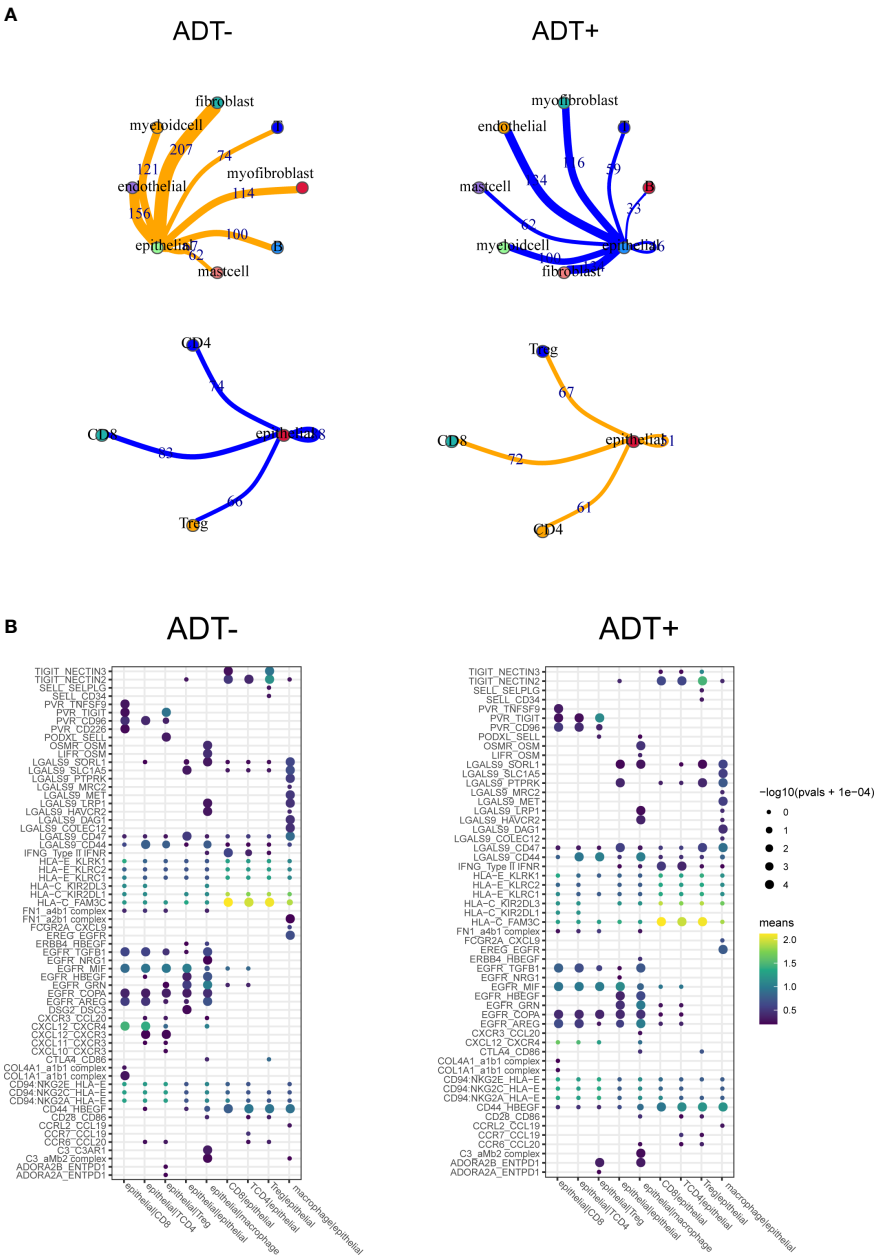

FIGURE 5
Composition and cell-cell interactions of the prostate cancer microenvironment. **(A)** View of the ligands expressed by epithelial cell and the other cells expressing the cognate receptors primed to receive the signal. Numbers indicate the quantity of ligand–receptor pairs for each intercellular link. **(B)** Summary of selected ligand-receptor interactions between epithelial cell and the other cell types. P-values (permutation test) are represented by the size of each circle. The color gradient indicates the level of interaction.

associated macrophage (20), immune checkpoint ligands and receptors (21), inhibitory cytokines (22), and metabolic challenges (23), which promote T cell dysfunction.

Previous studies have highlighted androgen cell signal as a novel T cell intrinsic regulator prompting CD8+ T cell exhaustion, by transactivating Tcf7 to regular in CD8+ progenitor exhausted T cells (24).

Here, we try to describe the role of androgen on the prostate tumor immune microenvironment. For ADT has become the standard treatment for locally advanced or metastatic prostate cancer, but despite initial responses, recurrent castration-resistant prostate cancer (CRPC) eventually occurs (25), Multiple mechanisms have been proposed to explain the development of CRPC. The well-established dependency of

10.3389/fendo.2022.1055826

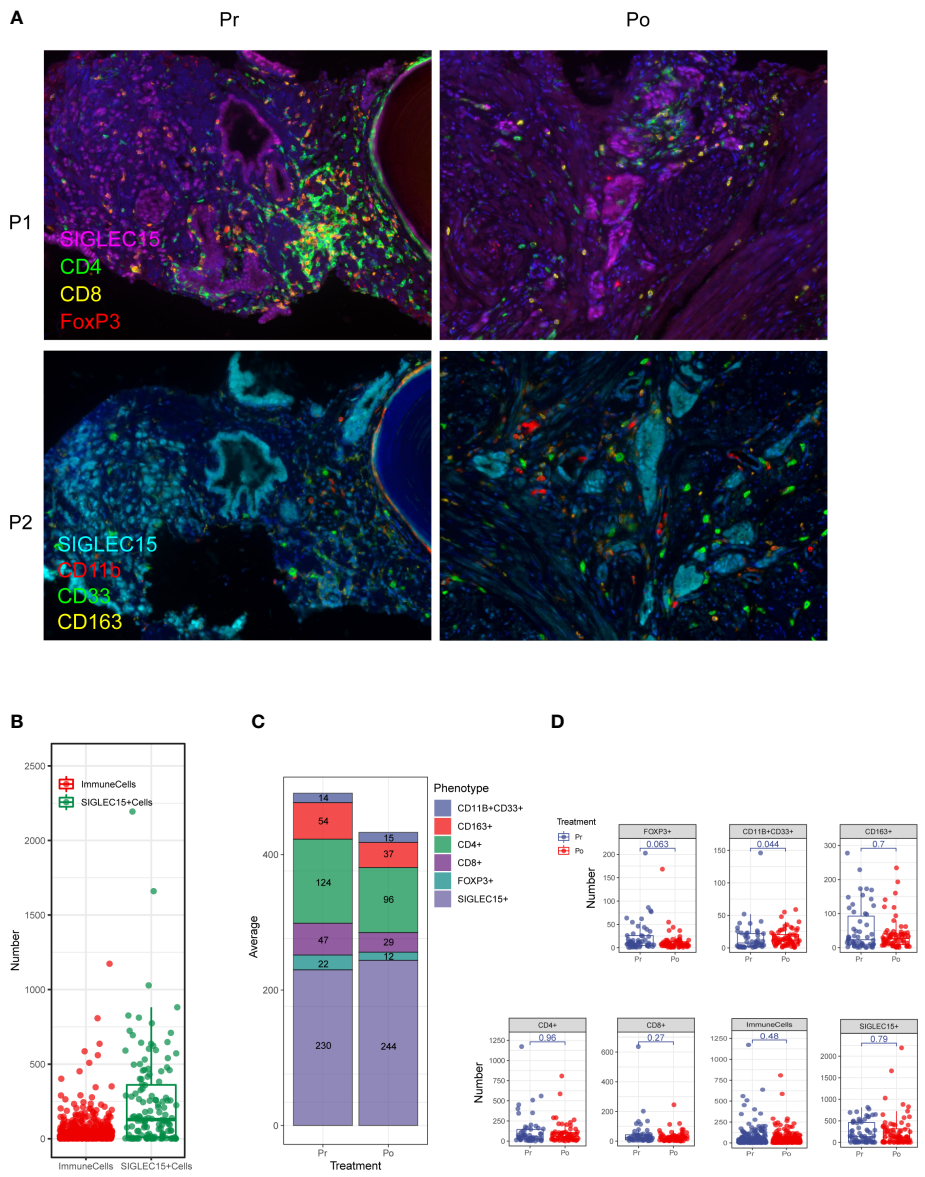

FIGURE 6
Multiplex fluorescent immunohistochemistry allows phenotyping of 6 unique cell types in the prostate cancer microenvironment. **(A)** A composite image was created incorporating all of the fluorophores present in a single tissue slide after multispectral imaging (Pr, pre-ADT; Po, post-ADT; P1, panel 1; P2, panel 2). **(B–D)** Counts of immune cells and epithelial cells per field. **(C)** The effect of ADT on the number of every cell type.

cancer cells on the tumor microenvironment suggests that it might control the emergence of CRPC. Thus, our current study examines change of tumor immune microenvironment after ADT in prostate cancer.

Although ADT was associated with significantly higher levels of ICOS+ and GrB+ cells, which may represent an activated T cell subset, greater immune cell infiltration is not found in prostate tumors after ADT (8). Another study shows that ADT could lead to significant increases in intra tumoral CD8+ T cell infiltration as compared to a cohort of untreated, matched controls. However, the CD8+ T cell infiltrate is accompanied by a proportional increase in regulatory T cells (Treg), suggesting that adaptive Treg resistance may dampen the immunogenicity of ADT (26).Thus, Effects of ADT on the tumor immune microenvironment of prostate cancer remain elusive.

Previous studies have mostly used immunohistochemistry or flow cytometry to evaluate the proportion and phenotype of immune cells, With the application of single-cell transcriptome technology, a comprehensive assessment of immune cell function has become possible. To systematically survey the

10.3389/fendo.2022.1055826

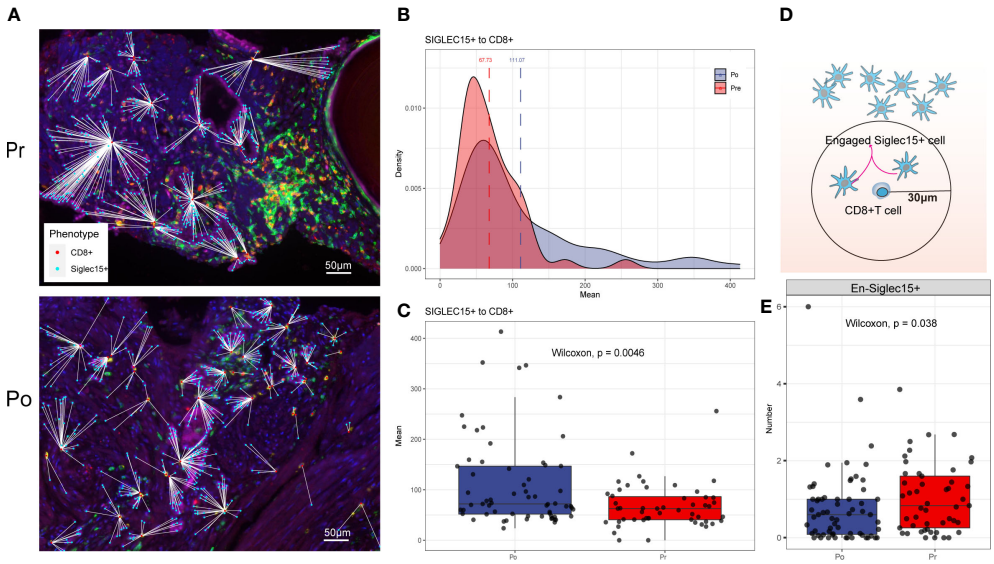

FIGURE 7
(A–C) ADT is associated with greater distance to cytotoxic T lymphocytes from epithelial cells. **(D, E)** ADT is associated with less cytotoxic T lymphocytes engaged epithelial cells.

impact of ADT on the prostate cancer microenvironment, we perform scRNA-seq on 11,367 cells from 4 prostate cancer samples with two cases received ADT.

In our study, we compared the expression profiles of ADT treatment tissue-derived and treatment naïve tissue-derived CD8+ T cells, CD4+ T cells. T cells in ADT treatment tissue showed lower expression levels of cytotoxicity-related genes GNLY, NKG7, GZMB and GZMA (both CD4+ and CD8+ T cells), Interestingly, ADT treatment-derived Tregs showed a lower expression level of LGALS3 (27), which was reported to mediate Tregs, chemokine CCL4 and exhaustion markers LAG3. Meanwhile, the gene expression results of ADT treatment-derived CD4+ and CD8+ T cells, showed enrichment in similar pathways, among which IFN response-related pathways are significantly downregulated, which shows the immunosuppressive signature after ADT.

Finally, we investigate specific ligand-receptor interactions between tumor cells and the other cell type in the TME. We identified immune interactions between tumor cells and T cells decreasing, especially the immune promotion related pairs such as PVR-CD226 and CXCL12-CXCR4, which may mediate tumor cell immune escape despite heavy lymphocyte infiltration. On the other hand, spatial characterization of tumor environment analysis shows that CD8+T cells/Tumor cells engagement are decreased and accompanied by greater distance between CD8+T cells and tumor cells.

Much like classic M1 and M2 polarization models (28), macrophage activation in ADT tissue follows an M1-down and M2-up coupled pattern, in which M1 and M2 are discrete states, and coupled programs. This also remind the immune suppress effect of ADT on the prostate cancer microenvironment.

In our study we find that the proportion of myeloid-derived suppressor cells (MDSCs) increase in the prostate tissue after ADT. Former study identifies MDSCs as a driver of CRPC by activating the androgen receptor pathway in prostate tumor cells, promoting cell survival and proliferation in androgen deprived conditions (29).

In the present study, this study demonstrates that ADT promotes immunosuppressive environment in prostate cancer including the inhibition of killing capacity of T cell, M1-down and M2-up coupled pattern in the macrophage, proportion increasing of MDSCs and spatial characterization of immune cells.

Material and methods

Human specimens

The prostate cancer samples used were collected from patients who undergone radical prostatectomy at Peking University People`s Hospital. The study was approved by the Peking University people`s Hospital Institutional Review Board, and all patients provided informed consent. Fresh tissue samples were immediately dissected into fractions for (1) flash freezing, (2) fixation in 4% paraformaldehyde solution followed by paraffin embedding and (3) enzymatic digestion into single cells as described below.

Preparation of single-cell suspension

Freshly collected tissue samples were used for single-cell isolation kept in MACS tissue storage solution (Miltenyi Biotec) until processing. Tissue samples were cut into ~1-mm cubic pieces in the RPMI-1640 medium (Invitrogen) with 10% fetal bovine serum (FBS, Gibco), and enzymatically digested with MACS tumor Dissociation Kit (Miltenyi Biotec, NO. 130-095-929) for 30~40 min at 37°C on a rotor, according to manufacturer's instruction. The dissociated cells were subsequently passed through a 40 mm Cell-Strainer (Corning) and centrifuged at ~300–500g for 8 min. After the supernatant was removed, the pelleted cells were suspended in red blood cell lysis buffer and incubated for 2 min to lyse red blood cells. After washing twice with PBS (Invitrogen), the cell pellets were re-suspended in sorting buffer (PBS supplemented with 1% FBS).

Single-cell 3′ mRNA sequencing library preparation

The 10x barcoding and complementary DNA (cDNA) synthesis were performed using 10x chromium 3′ scRNA-seq V2 chemistry according to the manufacturer's instructions. Briefly, Single cells were sorted into 1.5 mL tubes (Eppendorf) and counted manually under the microscope. The concentration of single cell suspensions was adjusted to 300-350 cells/ul. Cells were loaded between 7,000 and 10,000 cells/chip position using the Chromium Single cell 30 Library, Gel Bead & Multiplex Kit and Chip Kit (103 Genomics, V2 barcoding chemistry) according to the manufacturer's instructions. All the subsequent steps were performed following the standard manufacturer's protocols. Purified libraries were analyzed by an Illumina Hiseq 4000 sequencer with 150-bp paired-end reads.

Multi-color immunohistochemistry of human tissues

Multiplex immunofluorescence staining was obtained using PANO7-plex IHC kit, cat 0004100100 (Panovue, Beijing, China). Mouse anti-human Siglec15(Abcam, ab198684, 1:100), rabbit anti-human CD4(Abcam, ab133616, 1:500), mouse anti-human CD8A (CST, CST70306, 1:200), mouse anti-human FoxP3(Abcam, ab20034, 1:50), rabbit anti-human CD11b (CST, CST49420, 1:200), rabbit anti-human CD33 (Abcam, ab199432, 1:100), rabbit anti-human CD163(CST, CST93498, 1:500) were sequentially applied, followed by horseradish peroxidase-conjugated secondary antibody incubation and tyramide signal amplification.

The Mantra System (PerkinElmer, Waltham, Massachusetts, US) were used to scan the stained slides to obtain multispectral images. the scans were combined to build a single stack image.

Single-stained and unstained sections of images were used to extract the spectrum of autofluorescence of tissues and each fluorescein, respectively, which were further used to establish a spectral library required for multispectral unmixing by inform image analysis software (PerkinElmer, Waltham, Massachusetts, US). We obtained reconstructed images of sections with the autofluorescence removed by using this spectral library. For each patient, a total of 8-15 high-power fields were taken based on their tumor sizes.

Data availability statement

The original contributions presented in the study are included in the article/supplementary material. Further inquiries can be directed to the corresponding authors.

Ethics statement

The study was approved by the Peking University People's Hospital Institutional Review Board, and all patients provided informed consent.

Author contributions

Conceptualization, data curation, and writing, CQ. Software and visualization, JW. Review and editing, YD and TX. All authors contributed to the article and approved the submitted version.

Funding

This study was supported by the Peking University Medicine Fund of Fostering Young Scholars' Scientific (BMU2022PYB016) and Technological Innovation and the Fundamental Research Funds for the Central Universities.

Conflict of interest

The authors declare that the research was conducted in the absence of any commercial or financial relationships that could be construed as a potential conflict of interest.

Publisher's note

References

1. Siegel RL, Miller KD, Fuchs HE, Jemal A. Cancer statistics, 2022. *CA: Cancer J Clin* (2022) 72(1):7–33. doi: 10.3322/caac.21708

2. Huggins C, Stevens R, Hodges CV. Studies on prostatic cancer: II. the effects of castration on advanced carcinoma of the prostate gland. *Arch Surg* (1941) 43 (2):209–23. doi: 10.1098/rstb.2016.0146

3. Sharifi N, Gulley JL, Dahut WL. Androgen deprivation therapy for prostate cancer. *Jama* (2005) 294(2):238–44. doi: 10.1001/jama.294.2.238

4. Qin J, Lee H-J, Wu S-P, Lin S-C, Lanz RB, Creighton CJ, et al. Androgen deprivation–induced NCoA2 promotes metastatic and castration-resistant prostate cancer. *J Clin Invest* (2014) 124(11):5013–26. doi: 10.1172/JCI76412

5. Chen W, Tsai Y, Siu M, Yeh H, Chen C, Yin J, et al. Inhibition of the androgen receptor induces a novel tumor promoter, ZBTB46, for prostate cancer metastasis. *Oncogene* (2017) 36(45):6213–24. doi: 10.1038/onc.2017.226

6. Hao J, Ci X, Xue H, Wu R, Dong X, Choi SYC, et al. Patient-derived hormone-naive prostate cancer xenograft models reveal growth factor receptor bound protein 10 as an androgen receptor-repressed gene driving the development of castration-resistant prostate cancer. *Eur Urol* (2018) 73(6):949–60. doi: 10.1016/j.eururo.2018.02.019

7. Obradovic AZ, Dallos MC, Zahurak ML, . Partin AW, Schaeffer EM, Ross AE, et al. Chapman: T-cell infiltration and adaptive treg resistance in response to androgen deprivation with or without vaccination in localized prostate cancer. *Clin Cancer Res* (2020) 26(13):3182–92. doi: 10.1158/1078-0432.CCR-19-3372

8. Gao J, Ward JF, Pettaway CA, Shi LZ, Subudhi SK, Vence LM, et al. VISTA is an inhibitory immune checkpoint that is increased after ipilimumab therapy in patients with prostate cancer. *Nat Med* (2017) 23(5):551–5. doi: 10.1038/nm.4308

9. Azizi E, Carr AJ, Plitas G, Cornish AE, Konopacki C, Prabhakaran S, et al. Single-cell map of diverse immune phenotypes in the breast tumor microenvironment. *Cell* (2018) 174(5):1293–308.e36. doi: 10.1016/j.cell.2018.05.060

10. Vento-Tormo R, Efremova M, Botting RA, Turco MY, Vento-Tormo M, Meyer KB, et al. Single-cell reconstruction of the early maternal–fetal interface in humans. *Nature* (2018) 563(7731):347–53. doi: 10.1038/s41586-018-0698-6

11. Bray F, Ferlay J, Soerjomataram I, Siegel RL, Torre LA, Jemal A. Global cancer statistics 2018: GLOBOCAN estimates of incidence and mortality worldwide for 36 cancers in 185 countries. *CA: Cancer J Clin* (2018) 68(6):394–424. doi: 10.3322/caac.21492

12. Li CH, Haider S, Shiah Y-J, Thai K, Boutros PC. Sex differences in cancer driver genes and biomarkers. *Cancer Res* (2018) 78(19):5527–37. doi: 10.1158/0008-5472.CAN-18-0362

13. Yuan Y, Liu L, Chen H, Wang Y, Xu Y, Mao H, et al. Comprehensive characterization of molecular differences in cancer between male and female patients. *Cancer Cell* (2016) 29(5):711–22. doi: 10.1016/j.ccell.2016.04.001

14. Li Z, Tuteja G, Schug J, Kaestner KH. Foxa1 and Foxa2 are essential for sexual dimorphism in liver cancer. *Cell* (2012) 148(1-2):72–83. doi: 10.1016/j.cell.2011.11.026

15. Robertson AG, Kim J, Al-Ahmadie H, Bellmunt J, Guo G, Cherniack AD, et al. Comprehensive molecular characterization of muscle-invasive bladder cancer. *Cell* (2017) 171(3):540–556.e25. doi: 10.1016/j.cell.2017.09.007

16. Dunford A, Weinstock DM, Savova V, Schumacher SE, Cleary JP, Yoda A, et al. Tumor-suppressor genes that escape from X-inactivation contribute to cancer sex bias. *Nat Genet* (2017) 49(1):10–6. doi: 10.1038/ng.3726

17. Klein SL, Flanagan KL. Sex differences in immune responses. *Nat Rev Immunol* (2016) 16(10):626–38. doi: 10.1038/nri.2016.90

18. Sawant DV, Yano H, Chikina M, Zhang Q, Liao M, Liu C, et al. Adaptive plasticity of IL-10+ and IL-35+ treg cells cooperatively promotes tumor T cell exhaustion. *Nat Immunol* (2019) 20(6):724–35. doi: 10.1038/s41590-019-0346-9

19. Gabrilovich DI, Ostrand-Rosenberg S, Bronte V. Coordinated regulation of myeloid cells by tumours. *Nat Rev Immunol* (2012) 12(4):253–68. doi: 10.1038/nri3175

20. Shimura S, Yang G, Ebara S, Wheeler TM, Frolov A, Thompson TC. Reduced infiltration of tumor-associated macrophages in human prostate cancer: association with cancer progression. *Cancer Res* (2000) 60(20):5857–61.

21. Okazaki T, Chikuma S, Iwai Y, Fagarasan S, Honjo T. A rheostat for immune responses: the unique properties of PD-1 and their advantages for clinical application. *Nat Immunol* (2013) 14(12):1212–8. doi: 10.1038/ni.2762

22. Yi JS, Cox MA, Zajac AJ. T-Cell exhaustion: characteristics, causes and conversion. *Immunology* (2010) 129(4):474–81. doi: 10.1111/j.1365-2567.2010.03255.x

23. Le Bourgeois T, Strauss L, Aksoylar H-I, Daneshmandi S, Seth P, Patsoukis N, et al. Targeting T cell metabolism for improvement of cancer immunotherapy. *Front Oncol* (2018) 8:237. doi: 10.3389/fonc.2018.00237

24. Kwon H, Schafer JM, Song N-J, Kaneko S, Li A, Xiao T, et al. Androgen conspires with the CD8+ T cell exhaustion program and contributes to sex bias in cancer. *Sci Immunol* (2022) 7(73):1–20. doi: 10.1126/sciimmunol.abq2630

25. Karantanos T, Corn PG, Thompson TC. Prostate cancer progression after androgen deprivation therapy: mechanisms of castrate resistance and novel therapeutic approaches. *Oncogene* (2013) 32(49):5501–11. doi: 10.1038/onc.2013.206

26. Obradovic AZ, Dallos MC, Zahurak ML, . Partin AW, Schaeffer EM, Ross AE, et al. Chapman: T-cell infiltration and adaptive treg resistance in response to androgen deprivation with or without vaccination in localized prostate CancerImmune response to ADT and GVAX in localized prostate cancer. *Clin Cancer Res* (2020) 26(13):3182–92. doi: 10.1158/1078-0432.CCR-19-3372

27. Fermino ML, Dias FC, Lopes CD, Souza MA, Cruz Â.K, Liu FT, et al. Galectin-3 negatively regulates the frequency and function of CD 4+ CD 25+ f oxp3 + regulatory T cells and influences the course of l eishmania major infection. *Eur J Immunol* (2013) 43(7):1806–17. doi: 10.1002/eji.201343381

28. Hu W, Li X, Zhang C, Yang Y, Jiang J, Wu C. Tumor-associated macrophages in cancers. *Clin Trans Oncol* (2016) 18(3):251–8. doi: 10.1007/s12094-015-1373-0

29. Calcinotto A, Spataro C, Zagato E, Di Mitri D, Gil V, Crespo M, et al. IL-23 secreted by myeloid cells drives castration-resistant prostate cancer. *Nature* (2018) 559(7714):363–9. doi: 10.1038/s41586-018-0266-0

frontiers | Frontiers in Endocrinology

TYPE Original Research
PUBLISHED 06 December 2022
DOI 10.3389/fendo.2022.1090763

OPEN ACCESS

EDITED BY
Yuxuan Song,
Peking University People's Hospital, China

REVIEWED BY
Savio Domenico Pandolfo,
Federico II University Hospital, Italy
Biagio Barone,
University of Naples Federico II, Italy
Xiaoxue Liu,
Wuhan University, China

*CORRESPONDENCE
Ning Tao
38518412@qq.com

†These authors have contributed equally to this work and share first authorship

SPECIALTY SECTION
This article was submitted to Reproduction, a section of the journal Frontiers in Endocrinology

RECEIVED 06 November 2022
ACCEPTED 18 November 2022
PUBLISHED 06 December 2022

CITATION
An H, Ma D, Mei Y, Wang L, Maimaitiyiming A, Zhuo T, Aihaiti R, Bu K, Huang X, Zhang K, Yao M, Ling C, Li W and Tao N (2022) Metabolic syndrome and metastatic prostate cancer correlation study, a real-world study in a prostate cancer clinical research center, Xinjiang, China.
Front. Endocrinol. 13:1090763.
doi: 10.3389/fendo.2022.1090763

Metabolic syndrome and metastatic prostate cancer correlation study, a real-world study in a prostate cancer clinical research center, Xinjiang, China

Hengqing An[1,2,3†], Dongsheng Ma[1,2†], Yujie Mei[4†], Lulu Wang[1†], Abudukeyoumu Maimaitiyiming[1†], Tao Zhuo[1,2], Renaguli Aihaiti[1,2], Ke Bu[4], Xin Huang[1,2], Kaige Zhang[1,2], Miao Yao[1,2], Chenyang Ling[1], Weizun Li[1] and Ning Tao[5*]

[1]The First Affiliated Hospital, Xinjiang Medical University, Urumqi, China, [2]Department of Urology, The First Affiliated Hospital of Xinjiang Medical University, Urumqi, China, [3]Xinjiang Clinical Research Center of Urogenital Diseases, Urumqi, China, [4]College of Public Health, Xinjiang Medical University, Urumqi, China, [5]Department of Epidemiology and Health Statistics, College of Public Health, Xinjiang Medical University, Urumqi, China

Objective: The aim of this study was to investigate the relevance of metabolic syndrome (MetS) and metabolic scores to the occurrence, progression and prognosis of metastatic prostate cancer (mPCA), assessing the definition of the variables of metabolic syndrome, and the potential mechanisms of MetS and mPCA.

Methods: Data were obtained from the database of prostate cancer follow-up at the Urology Centre of the First Affiliated Hospital of Xinjiang Medical University (N=1303). After screening by inclusion and exclusion criteria, clinical data of 190 patients diagnosed with mPCA by pathology and imaging from January 2010 to August 2021 were finally included, including 111 cases in the MetS group and 79 cases in the Non-MetS group.

Results: The MetS group was higher than the Non-MetS group: T stage, Gleasson score, initial PSA, tumor load, PSA after 7 months of ADT (P<0.05), with a shorter time to progression to CRPC stage(P<0.05)[where the time to progression to CRPC was relatively shorter in the high metabolic score subgroup of the MetS group than in the low subgroup (P<0.05)].Median survival time was significantly shorter in the MetS group than in the Non-MetS group (P<0.05),and there was a correlation with metabolic score, with the higher metabolic score subgroup having a lower survival time than the lower metabolic score subgroup (P<0.05).

Conclusion: Those with mPCA combined with MetS had lower PSA remission rates, more aggressive tumors, shorter time to progression to CRPC and shorter median survival times than those with mPCA without MetS.Tumour

progression and metabolic score showed a positive correlation, predicting that MetS may promote the progression of mPCA, suggesting that MetS may be a risk factor affecting the prognosis of mPCA.

KEYWORDS

metabolic syndrome, metastatic prostate cancer, central obesity, insulin resistance, androgen deprivation therapy, novel endocrine therapy

Introduction

Metabolic syndrome (MetS) is a group of clinical syndromes characterised by the aggregation of multiple disease states, including abdominal obesity, persistent hypertension, dyslipidaemia, abnormalities of glucose metabolism (1).MetS can significantly affect the occurrence, development and prognosis of other related diseases, increase the incidence of cardiovascular accidents and cancer, and result in increased hospitalization, surgical complications and mortality compared to non-MetS patients. The National Cholesterol Education Program Adult Treatment Panel III (NCEP ATP III) defines MetS in a way that is widely accepted by the academic community, and considers that patients who meet three of the five criteria of abdominal obesity, hyperlipidaemia, hypertension, elevated fasting glucose levels and decreased HDL cholesterol levels are diagnosed with MetS. In 2017, the Chinese Guidelines for the Prevention and Treatment of Type 2 Diabetes published in China revised and published the diagnostic criteria for MetS in China based on this diagnostic criteria, with reference to the definition of abdominal obesity and hyperglycaemia in China. The MetS was first proposed as a risk-related compound factor in 2004, and middle-aged men with metabolic syndrome are more likely to develop prostate cancer (PCA) (2). Given the presence of complex hormonal and metabolic changes in MetS, and the prostate as a specific endocrine and reproductive organ in men, it is predicted that there may be a relationship between MetS and PCA (3).There are differences between populations of different ethnicities and regions. The prevalence of MetS in Latin American countries is 15.5% (23.1% in men and 12.2% in women) (4). The prevalence of MetS in European and American countries is 24.3% (23.9% in men and 24.6% in women) (5). In China, recent surveys in different age and regional populations have found that the prevalence of MetS varies from approximately 3.6 to 50.1%, with significant gender and regional differences (6–8). The relationship between MetS and PCA is still not fully established. However, studies that use rigorous and uniform criteria to define the metabolic syndrome in homogeneous ethnic groups are necessary to further elucidate the link between the metabolic syndrome and prostate cancer outcomes (9).No epidemiological studies related to high-quality MetS have been reported in Xinjiang, China, but the high-fat dietary structure characteristics of Xinjiang may lead to a higher prevalence than the Chinese average, which is also corroborated by the high prevalence characteristics of diabetes, hypertension, hyperlipidemia and other related diseases in Xinjiang. As people's material life has become richer in recent years, unhealthy and irregular diet and lifestyle habits have increased the incidence of MetS year by year, and the risk of cardiovascular and cerebrovascular accidents has gradually emerged. Metabolic syndrome and cardiovascular disease are closely related and there is a significant dose-response relationship between the components of MetS and the risk of cardiovascular disease (10). Metabolism and cancer are closely related and there is a correlation between many solid tumors such as endometrial, colorectal, gastric, liver, bladder and prostate cancers (11–13). Metabolic dysfunction is associated with the risk and mortality of colorectal, pancreatic, postmenopausal breast and bladder cancers (14). PCA is currently the most prevalent malignancy of the male reproductive system worldwide, with the 2nd and 5th highest incidence and mortality rates of malignancies in men, respectively (15). Due to its high prevalence in middle-aged and elderly men and its insidious onset, patients are often in the middle to advanced stages at the time of first presentation, with metastatic prostate cancer (mPCA) being an important stage of disease that severely affects patient prognosis. In the European and American populations, mPCA accounts for only 5%-6% of new diagnosed PCA, with an overall 5-year survival rate of approximately 30% (16).The MetS component is associated with an age-specific increase in the incidence of PCA, and a history of MetS is associated with a high prevalence of PCA (17, 18).The prevalence of MetS may be higher in Xinjiang, China, than in other parts of China due to dietary habits and lifestyle.The prevalence of prostate cancer is higher in Xinjiang, China, but the treatment situation is not optimistic. While previous literature aimed to explore the relationship between MetS and the risk of PCA in different populations, this study focused on the correlation between MetS and the occurrence, progression

and prognosis of mPCA in Xinjiang, China.It is expected to inform the development of scientific and effective public health policies and clinical treatment protocols.

Materials and methods

Data sources and descriptions

The study collected clinical data of 1303 prostate cancer patients from January 2010 to August 2021 from the prostate cancer follow-up database of the Urology Center of the First Affiliated Hospital of Xinjiang Medical University. 1018 cases were excluded according to the inclusion and exclusion criteria, 67 cases were lost in the follow-up process and 28 cases refused to be included in the study. 190 cases were finally screened and included in the study, all of which were diagnosed with mPCA by pathology and imaging, including 111 cases in the MetS group and 79 cases in the Non-MetS group.According to the clinical study design requirements, the group of mPCA patients with combined MetS was set up as the observation group and the group of mPCA patients with Non-MetS was set up as the control group. See Figure 1.

Biochemical indicators

(1) Endocrine-related indicators

Glycerin trilaurate (TG), high density lipoprotein cholesterol (HDL), fasting blood-glucose (FBG).

(2) Prostate cancer tumor-related indicators

Prostate specific antigen (PSA), serum testosterone (TE), Gleason score, tumor staging.

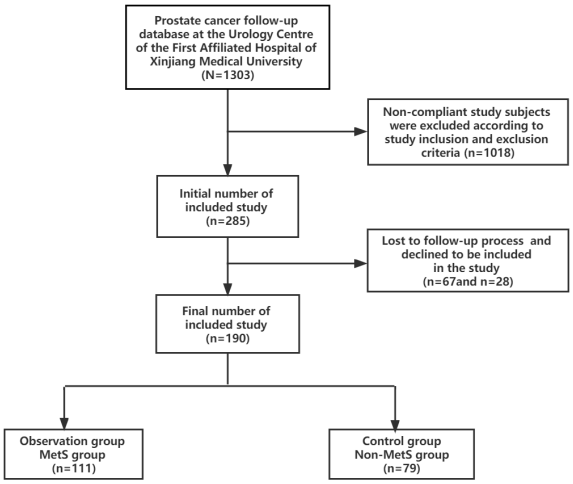

FIGURE 1
The process for study participants.

Blood pressure

Because of its fluctuating nature and the transient rise in blood pressure that can be caused by emotional or physical activity, is diagnosed when the patient's blood pressure is elevated on at least two different days at rest. If the patient has a clear previous history of hypertension, this may also be considered to meet the criteria for MetS iv.

Blood glucose and lipid levels

Blood was collected from the elbow vein in the morning on an empty stomach or during an 8-hour fast, and FBG and TG levels were measured.

Body mass index

BMI= Body weight divided by height squared(kg/m^2)

Measurement of serum PSA and testosterone levels

Serum PSA and testosterone levels were measured by electrochemiluminescence in the early morning on an empty stomach, and the maximum values of PSA were determined by the department of urology of the First Affiliated Hospital of Xinjiang Medical University or the external medical institutions.

Gleason pathology score

The highest total Gleason score in the normative standard pathology report after the puncture is used.

TNM staging of tumors

The TNM stage of the tumor was determined in conjunction with the patient's clinical data and the histopathology of the prostate puncture/electrodectomy.

Imaging

Adome-pelvic enhanced computed tomography (CT), Prostate Diffusion Weighted Imaging (PDWI-MRI), Emission Computed Tomography (ECT).

Definitions covered in this study

(1) In this study, the term PCA progression refers to the development of metastatic hormone sensitive prostate cancer (mHSPC) to Castration Resistant Prostate Cancer (CRPC). mHSPC progression to CRPC is defined as the interval between the initiation of androgen stripping therapy and the diagnosis of CRPC.

CRPC: serum testosterone (T) , T<50ng/dL or T<1.7nmol/L) under castration; with one of the following conditions: (i) Biochemical progression: PSA reviewed at 1 week intervals for 3 consecutive biochemical progression,two of which are >50% higher than the lowest value and the absolute PSA increase is >2ng/ml; (ii) Imaging progression: two or more new bone metastases or more than one soft tissue lesions on bone scan (19).

(2) Based on the CHAARTED study (20), mHSPC can be classified into two categories: high tumor load and low tumor load. High tumor load is defined as≥4 bone metastases (≥1 bone metastasis located outside the pelvis or spine) or the presence of visceral metastases; low tumor load is defined as the absence of high load factors.

(3) The definition of MetS is based on the 2009 edition published by the International Diabetes Federation, the American Heart Association and the American Heart, Lung and Blood Institute (NHLBI) (21). (i) Obesity is defined as a BMI≥25 Kg/m^2; (ii) a TG level of at least 150 mg/dL (1.7 mmol/L) or medication for elevated TG; (iii) HDL-C less than 40 mg/dL (1.0 mmol/L) or medication for reduced HDL-C; (iv) elevated blood pressure (systolic blood pressure (SBP) ≥130 mmHg and/or diastolic blood pressure (DBP) ≥85 mmHg in patients with a history of hypertension or antihypertensive medication; (v) FBG of at least 100 mg/dL (5.6 mmol/L) or medication. A score of 1 is assigned for each of the above criteria, and a metabolic score of ≥3 is diagnostic of MetS.

Inclusion and exclusion criteria

Inclusion criteria

(1) Patients who have been diagnosed with metastatic prostate malignancy (not limited to adenocarcinoma, intraductal prostate cancer, etc.) at the initial diagnosis and who have been clinically diagnosed with metastatic prostate malignancy in combination with imaging and biochemical indices, and who have been staged using the American Joint Committee on Cancer (AJCC) criteria; (2) Patients who have not received any androgen deprivation thearpy (ADT), new endocrine therapies (e.g.abiraterone acetate, docetaxel, bicalutamide, etc.) in the past or at the start of the study that may affect the observational parameters.

Exclusion criteria

(1) patients with other malignancies at the time of initial diagnosis (e.g. lymphatic malignancies, gastrointestinal malignancies, etc.); (2) patients with combined cardiopulmonary disease (e.g. severe coronary syndromes, acute and chronic lung disease, etc.); (3) those with incomplete clinical data and missing general information at the beginning of the study; (4) loss of follow-up.

Ethical review

This study complies with the principles of the Declaration of Helsinki, Ethics Committee: Ethics Committee of the First Affiliated Hospital of Xinjiang Medical University, Approval date: 1 March 2021, No. (20210301-92).

All prostate tissue samples required for pathological diagnosis were intraoperative surgical tissue samples with the informed and consent of the patients. All patients signed the informed consent form for surgery and the consent form for surgical sample collection.Informed consent of subjects: Clinical information of patients was used in this study and informed consent was obtained from all subjects by telephone or in writing.

Medical follow up observation

①For regular inpatient or outpatient follow-up patients, data can be collected by medical record browsing ②For patients who cannot come to the hospital for treatment, the form of telephone or door-to-door return visits can be used, but due to objective factors resulting in the inability to complete the specified corresponding examination, an appropriate amount of postponement or coupling of adjacent data can be used. ③For late follow-up missing, there are two categories: data missing and outcome missing; for data missing, recall or statistical processing can be used, for outcome missing the remaining indicators are chosen instead, e.g. the end time of follow-up as survival time, and the outcome is marked. The ideal frequency and duration of follow-up is a full assessment every six months after diagnosis of prostate cancer, with a minimum outpatient registration visit and PSA test completed every month, with fluctuations of no more than 50% of the respective follow-up cycle time. The study follow-up deadline is August 2022.

Cross-sectional analysis using baseline data

Description and comparison of baseline characteristics of the study population.

Age, Ethnicity, Smoking and Alcoholism were consistent at baseline (P>0.05), see Table 1.

Statistical methods

The data were analyzed using SPSS version 26.The relationship between general information and clinical information in the Non-MetS group and MetS group was first assessed by univariate analysis; Comparisons between groups were made using the t-test, count data were described as rates, comparisons between groups were made using the ^{2}test, rank data were described as rates, and comparisons between groups were made using the rank sum test.After applying covariance diagnosis to exclude problems of multiple covariance, regression models were developed using multifactorial logistic regression

10.3389/fendo.2022.1090763

TABLE 1 Analysis of the general data between the Non-MetS group and MetS group.

Groups	Non-MetS group (N = 79)	MetS group (N = 111)	χ^2	*P*
Age (years), n (%)			2.507	0.113
≤65	13 (16.45)	29 (26.13)		
>65	66 (83.55)	82 (73.87)		
Ethnic group,n (%)			0.158	0.691
Han	45 (56.96)	60 (54.05)		
Others	34 (43.04)	51 (45.95)		
Smoking,n (%)			0.033	0.857
Yes	31 (39.24)	45 (40.54)		
No	48 (60.76)	66 (59.46)		
Alcoholism,n (%)			0.267	0.605
Yes	10 (12.66)	17 (15.32)		
No	69 (87.34)	94 (84.68)		

analysis to assess risk factors in patients with metastatic prostate cancer combined with MetS. Next, the relationship between MetS and time to progression to CRPC was compared using t-test and one-way ANOVA. Overall survival (OS) time at 3-year follow-up and 5-year follow-up were selected as prognostic indicators. One-way COX regression analysis was used to test the association between variables related to MetS and OS in mPCA patients, and variables with statistically significant initial screening were included in a multi-factor COX proportional risk regression model to calculate Hazard ratios (HR) and 95% confidence intervals (CI) for the variables. Survival time was calculated in months from the time of treatment after diagnosis, with those lost to follow-up or alive at the follow-up cut-off considered as truncated data. 3-year and 5-year survival curves were plotted using the Kaplan-Meier method, and Logrank tests were performed to determine whether there was a statistical difference. The test levels for the above statistical analyses were all two-sided $\alpha = 0.05$, with a statistical difference $P< 0.05$.

Results

Inter-group comparison

Based on the definition of MetS, patients with metastatic prostate cancer were divided into two groups: MetS group (Observation group)/Non-MetS group (Control group). Comparison between the groups in Table 1 shows that there was no statistical difference between the two groups in terms of age (*P*=0.113), ethnic classification (*P*=0.691), and history of smoking and alcohol consumption (*P*=0.857) and (*P*=0.605) between the Non-MetS group and MetS group. See Table 1.

Comparative analysis between groups showed that testosterone levels were significantly higher in the MetS group (14.46±6.36) than in the Non-MetS group (11.81±5.923), with a statistically significant difference between the two groups (*P*=0.004). There was no significant correlation between the two groups in the presence of visceral metastases and neurological invasion (*P*=0.820, *P*=0.683). The relationship between the metrics of mPCA patients,initial PSA, PSA after 7 months of ADT, tumor load, Gleason score,prostate volume and T-stage was also investigated. The results showed that there was no statistical difference between the presence or absence of combined MetS and prostate volume in mPCA patients (*P*=0.098), while there was a significant correlation between high initial PSA levels (≥100ng/ml), high pathological Gleason score (≥8), PSA after 7 months of ADT , high tumor load and high T-stage (≥4) (*P*<0.05).mPCA patients with combined MetS having a more advanced tumor stage, a higher number of bone metastases, relative insensitivity to ADT treatment, a higher degree of malignancy and a poorer prognosis. See Table 2.

Logistic regression

The presence or absence of combined MetS in patients with metastatic prostate cancer was used as the dependent variable, and factors that were statistically significant in the univariate analysis were included as independent variables (T-stage, Gleasson score, Initial PSA, Tumour load, PSA after 7 months of ADT) in a multifactorial Logistic regression analysis model with a forward stepwise method of independent variable screening.No multicollinearity among variables.The multi-factor logistic regression analysis revealed tumor load is risk factors for MetS with mPCA patients (*P*=0.007). See Table 3

MetS in relation to mPCA progression to the CRPC stage

The two study populations were followed up until August 2021 according to the CRPC definition. we found the time to

10.3389/fendo.2022.1090763

TABLE 2 Analysis of the clinical data between the Non-MetS group and MetS group.

Groups	Non-MetS group (N=79)	MetS group (N=111)	χ^2	*P*
T-Stage,n (%)			8.692	0.003
<4	47 (59.49)	42 (37.84)		
≥4	32 (40.51)	69 (62.16)		
Gleason Score,n (%)			7.433	0.006
<8	14 (17.72)	6 (5.41)		
≥8	65 (82.28)	105 (94.59)		
Initial PSA (ng/ml),n (%)			4.566	0.033
<100	29 (36.71)	25 (22.52)		
≥100	50 (63.29)	86 (77.48)		
Prostate volume(ml),n (%)			4.641	0.098
<66	61 (78.21)	70 (63.06)		
≥66	17 (21.79)	40 (36.94)		
Alkaline phosphatase(U/L),n (%)			1.475	0.478
≤126	33 (42.31)	49 (44.14)		
>126	45 (57.69)	62 (55.86)		
Tumor load,n (%)			20.255	<0.001
High	37 (46.84)	87 (78.38)		
Low	42 (53.16)	24 (21.62)		
Nerve invasion,n (%)			0.762	0.683
Yes	35 (44.30)	47 (42.34)		
No	44 (55.70)	63 (57.66)		
Visceral metastasis,n (%)			0.052	0.820
Yes	16 (20.25)	24 (21.62)		
No	63 (79.75)	87 (78.38)		
PSA after 7 months of ADT (ng/ml),n (%)			12.323	0.002
<0.2	33 (41.77)	21 (18.92)		
≥0.2	46 (58.23)	89 (81.08)		
Testosterone (nmol/l), $\overline{\chi} \pm s$	11.81±5.923	14.46±6.36	-2.910	0.004

progression to CRPC being significantly shorter in the MetS group than in the Non-MetS group (*P*=0.008).We consider that: mPCA patients with the combined MetS are more likely to progress to the CRPC stage of the disease. See Table 4.

The relationship between the various subgroups of the MetS and the time to progression to CRPC, as defined by Mets, was explored and the results are shown in Table 5. ANOVA showed a statistically significant difference between time to progression to CRPC and the MetS scores (*P*=0.032).

MetS in relation to survival time

The survival function curve visually shows that mPCA patients with non-MetS have a higher 5-year survival curve than those with combined MetS.The median survival time estimates for mPCA patients with non-MetS and with MetS were 58 months and 27 months respectively. The Log Rank test for overall comparison of survival curves between the two groups (*P*=0.044). It can be concluded that there is a difference

TABLE 3 Multifactorial Logistic Regression Analysis of mPCA Combined with MetS.

Variable	Regression coefficient	Standard error	*Wald*^{2}	Exp(B)	*P*
T-Stage	0.346	0.347	0.998	1.414	0.318
Gleasson score	0.709	0.569	1.548	2.031	0.213
Initial PSA	0.033	0.391	0.007	1.033	0.933
Testosterone	0.048	0.028	2.995	1.049	0.084
Tumor load	0.977	0.363	7.247	2.655	0.007
PSA after 7 months of ADT	0.522	0.387	1.820	1.686	0.177
Constant	-2.109	0.661	10.177	0.121	0.001

TABLE 4 Time of progression to CRPC between the Non-MetS group and MetS group (month, M).

	Non-MetS group (N=79) ($\overline{X} \pm S$)	MetS group (N=111) ($\overline{X} \pm S$)	t	*P*
Time to CRPC (months, M)	21.61 ± 10.873	17.50 ± 7.718	2.717	0.008

TABLE 5 Time of MetS score subgroup progression to CRPC (month, M).

	0	1	2	3	4	5	F	*P*
Time to CRPC (months, M)	20.57 ± 7.763	20.25 ± 10.779	23.34 ± 11.847	17.05 ± 8.048	17.52 ± 6.976	18.75 ± 8.172	2.510	0.032

in survival between mPCA patients with MetS and non-MetS, with mPCA patients with non-MetS having a higher survival rate than with MetS. See Figure 2.

Survival function curves visually show that the 5-year survival curves of patients with metastatic prostate cancer with MetS score ≦ 2 are higher than those of patients with metastatic prostate cancer with MetS score > 2.The median survival time estimates for mPCA patients with MetS score ≦2, MetS score =3 and MetS score ≧4 were 58 months, 31 months and 25 months respectively. The Log Rank test results for the overall comparison of the three groups of survival curves (*P*=0.005),two-way comparison show the results the overall comparison of the survival curves between the MetS score ≦ 2 and MetS score ≧ 4 (*P*<0.001).It can be concluded that there was a difference in the survival rate between the mPCA atients with MetS score ≦ 2 and MetS score ≧ 4. Survival rates for mPCA patients with MetS score ≦ 2 were higher than those with MetS score ≧ 4. See Figure 3.

The estimated median 3-year survival times for mPCA patients with non-MetS and those with combined MetS were 33 months and 26 months, respectively. The Log Rank test for the overall comparison of the 3-year survival curves between the two groups (*P*=0.011), showed differences in survival between mPCA patients with combined MetS and non-MetS, possibly indicating that mPCA patients with non-MetS have a higher survival rate than those with MetS. See Figure 4.

The 3-year median survival time estimates for mPCA patients with MetS score ≦ 2, MetS score = 3 and MetS score ≧ 4 were 33 months, 26 months and 24 months respectively. The Log Rank test for the overall comparison of the survival curves of the three groups resulted (*P*=0.033), and there was a difference in the 3-year survival rate for the three groups of mPCA patients. The results of the two-by-two comparison showed the results of the Log Rank test for the overall comparison of the survival curves of the three groups with MetS score ≦ 2, MetS score = 3 and MetS score ≧ 4 (*P*<0.05).It can be concluded that there was a difference in the survival rate of mPCA patients with MetS score ≦ 2 and MetS score = 3 and MetS score ≧ 4. The survival rate of prostate cancer patients with MetS score ≦ 2 was higher than that of The survival rate of mPCA patients with MetS score=3 as well as MetS score≧4. See Figure 5.

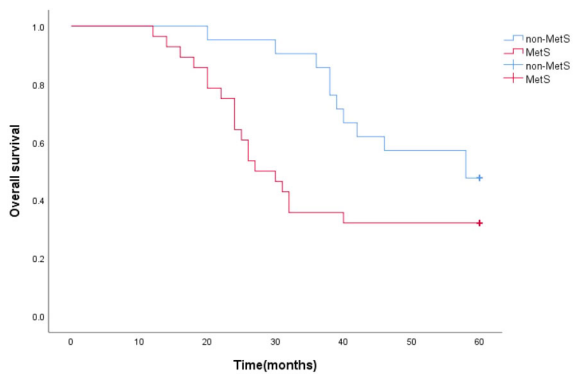

FIGURE 2
5-year survival curves for mPCA patients with MetS and non-MetS.

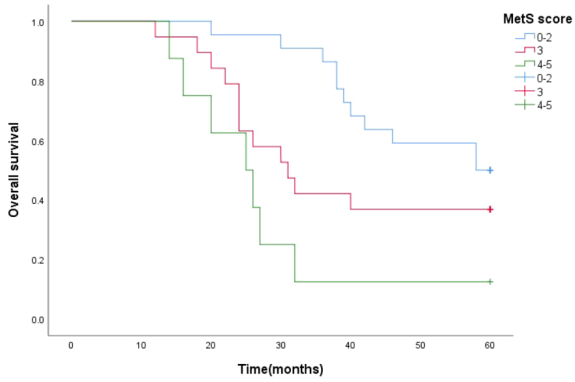

FIGURE 3
5-year survival curves for mPCA patients with different MetS scores.

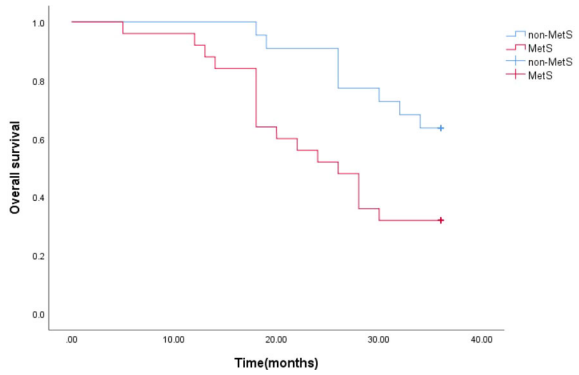

FIGURE 4
3-year survival curves for mPCA patients with MetS and non-MetS.

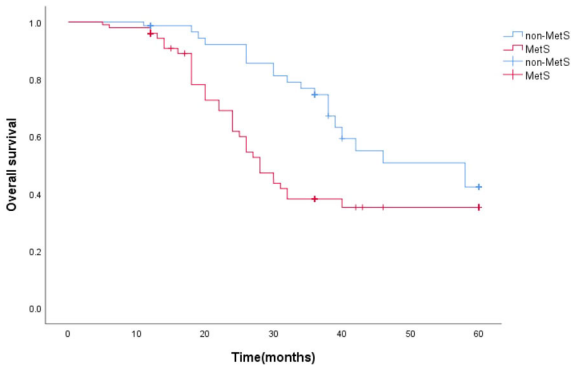

FIGURE 6
Overall survival curves for mPCA patients with MetS and non-MetS.

The survival function curves visually show that the overall survival curve was higher in the non-MetS group than in the MetS group. The overall median survival time estimates for mPCA patients with non-MetS and those with combined MetS were 58 months and 28 months, respectively. The Log Rank test for overall comparison of survival curves between the two groups (P=0.005). It can be concluded that mPCA Patients with non-MetS have a higher survival rate than those with the MetS. See Figure 6.

The median survival time estimates for mPCA patients with MetS score ≦ 2, MetS score = 3 and MetS score ≧ 4 were 58 months, 30 months and 26 months respectively. The Log Rank test for the overall comparison of the overall survival curves of the three groups (P=0.002), meaning that there was a difference in the overall survival of the three groups of mPCA patients. See Figure 7.

Univariate analysis and multi-factor cox regression

Univariate cox regression analysis in this study, it was found that Diabetes, BMI, T-stage, Initial PSA, Tumour load, MetS, MetS score and PSA after 7 months of ADT, HDL were found to be associated with prognosis in mPCA patients (P<0.05). See Table 6. The covariates with statistically significant from the univariate analysis results were included in the multifactorial cox regression analysis (the forward stepwise method). The results showed that in the mPCA population,Patients with MetS score of 4-5 have 2.826-fold the risk of death compared to those with a score of 0-2, Patients with MetS score of 3 have 1.454-fold the risk of death compared to patients with a score of 0-2,and the risk of death from a high tumor load was 2.381-fold higher than from a low tumor load.

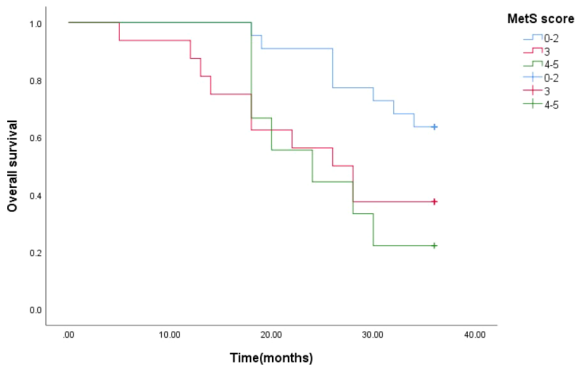

FIGURE 5
3-year survival curves for mPCA patients with different MetS scores.

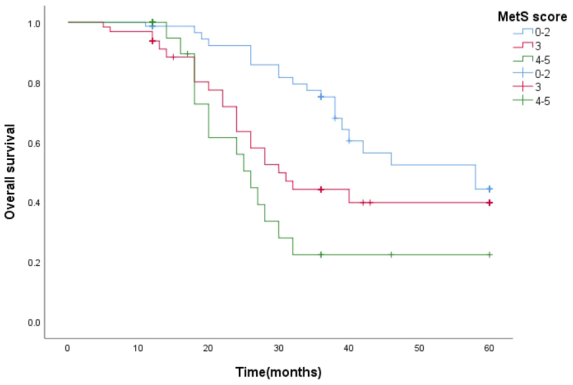

FIGURE 7
Overall survival curves for mPCA patients with different MetS scores.

10.3389/fendo.2022.1090763

TABLE 6 Univariate analysis and multi-factor cox regression analysis.

Variable	Univariate cox regression analysis		Multivariate cox regression analysis	
	HR (95%CI)	*P*	HR (95%CI)	*P*
T-stage				
<4	1*		1*	
≥4	1.963 (1.139, 3.386)	0.015	–	0.139
Gleason score				
<8	1*		1*	
≥8	1.097 (0.470, 2.557)	0.831	–	–
Initial PSA(ng/ml)				
<100	1*		1*	
≥100	2.467 (1.275, 4.775)	0.007	–	0.054
FBG×TG(mmol/l)2				
≤8.69	1*		1*	
>8.69	1.227 (0.715, 2.104)	0.457	–	–
Hypertension				
No	1*		1*	
Yes	1.019 (0.600, 1.731)	0.945	–	–
Diabetes				
No	1*		1*	
Yes	2.052 (1.215, 3.466)	0.007	–	0.287
TG(mmol/l)				
<1.70	1*		1*	
≥1.70	1.022 (0.550, 1.899)	0.945	–	–
HDL(mmol/l)				
<1.0	1*		1*	
≥1.0	0.522 (0.308, 0.886)	0.016	–	0.158
BMI(kg/m2)				
<25	1*		1*	
≥25	1.787 (1.061, 3.009)	0.029	–	0.431
PSA after 7 months of ADT(ng/ml)				
<0.2	1*		1*	
≥0.2	1.902 (1.050, 3.446)	0.034	–	0.202
Tumor load				
Low	1*		1*	
High	2.675 (1.459, 4.904)	0.001	2.381 (1.264, 4.483)	0.007
Mets				
No	1*		1*	
Yes	2.140 (1.238, 3.699)	0.006	–	0.329
Mets score		0.004		0.015
0-2	1*		1*	
3	1.982 (1.086, 3.614)	0.026	1.454 (0.774, 2.729)	0.244
4-5	3.127 (1.561, 6.261)	0.001	2.826 (1.396, 5.724)	0.004

1* reference standard, - not statistically significant.

Discussion

MetS is influenced by a variety of factors such as diet, genetics and ethnicity. With the development of people's modern urban lifestyle and a dramatic increase in morbidity, MetS has become a public health issue of increasing concern.PCA is a common genitourinary malignancy in men and is clinically characterised by a year-on-year increase in incidence and a diversification and complexity of treatment modalities. There are complex and precise hormonal mechanisms of action and clinical metabolic alterations in MetS, and as the prostate is a specific endocrine and reproductive organ in men, there may be a link between MetS and

PCA risk, disease progression, and tumor invasion.As research on PCA biology continues to evolve, we understand the deep interactions between autophagy and apoptosis in prostate cancer cells. Depending on the cellular microenvironment, the complexity and multidirectionality of autophagy in tumor cells, there may be some influence in the mPCA combined with MetS (22).There are no large sample, long follow-up, retrospective study on the relationship between MetS and mPCA in China,This study is the first real-world study to report the relationship between mPCA and MetS in Xinjiang, China, and even in the Northwest.

Gacci M et al (23) Meta-analysis showed that MetS was strongly associated with poorer tumor outcomes in prostate cancer, including high-grade prostate cancer (Gleason score ≥8), seminal vesicle infiltration and risk of biochemical recurrence.However, Harding J et al (24) concluded that MetS is a protective factor for prostate cancer and that men with MetS are less likely to develop prostate cancer. Large number of studies have continued to explore the relationship between MetS and the development and aggressiveness of PCA, while relatively few studies have explored the association between mPCA and MetS. Our findings are consistent with those of Gacci, M, and DeNunzio C et al (23, 25) that patients with metastatic prostate cancer combined with MetS have a higher degree of tumor malignancy. The proportion of T ≥ 4 was higher in the observation group than in the group without combined MetS when comparing the T< 4 and T ≥ 4 subgroups of clinical T staging. The difference between the high and low tumor load groups in the Non-MetS and MetS groups was also statistically significant (p<0.001), while often a higher number of bone metastases at the time of initial diagnosis predicted a more aggressive tumor and a poor prognosis. This also suggests whether we can consider MetS as a risk factor for promoting early metastasis of prostate cancer.Although patients with MetS may have elevated initial serum testosterone levels and high PSA, they also present a number of problems for follow-up treatment such as a shortened treatment window and treatment insensitivity. Also as the evaluation of the effect of receiving ADT is usually based on the PSA level (0.2-4 ng/ml) after 7 months of ADT as an important reference point, then the indirect augmentation effect of MetS should be taken into account when deciding on the subsequent treatment regimen. After giving endocrine therapy to patients with metastatic prostate cancer, the difference in PSA levels after 7 months of endocrine therapy between the Non-MetS and MetS groups was statistically significant (p=0.002). The first may be due to the fact that the same dose of ADT was administered during ADT treatment, however, due to the larger body surface area of the combined obese patients, the ideal dose of administration was not achieved and testosterone suppression was insufficient, resulting in a slow decrease in PSA. Secondly, in patients with combined MetS, the Hypothalamic-pituitary-gonadal axis/ adrenal axis causes hormonal disorders in the body, and endocrine therapy in these patients can increase the degree of pre-existing metabolic components. Smith MR and Braga-Basaria M (26, 27) also showed that endocrine therapy in prostate cancer patients significantly increases the incidence of MetS and subgroups, which may ultimately lead to a reduction in PSA remission rates.Since PSA levels can be influenced by many factors, Tarantino G et al,studied the effects of obesity, smoking habits, alcohol abuse and chronic obstructive pulmonary disease on PSA levels in men with pathologically histologically confirmed prostate cancer, showed that only smoking was associated with PSA levels (28), but this finding has not been verified in our study.

In this study, the time to progression to CRPC was significantly shorter in the MetS group than in the Non-MetS group, with a statistically significant difference (17.50±7.718 months vs 21.61 ±10.873 months, P=0.008), which may be related to the fact that MetS leads to more aggressive prostate cancer, i.e. prostate cancer patients with combined MetS have more rapid disease progression to the CRPC stage, which is also consistent with the existing study (29). However, when the relationship between MetS score and progression of metastatic prostate cancer was further investigated, a statistical difference was found between time to progression to CRPC and MetS score between 0, 1, 2, 3, 4 and 5 (P=0.032). For prostate cancer patients with MetS scores of 3 and above, we hypothesise that the higher the MetS score, the faster the disease progression. This may be due to the interaction between the MetS components and the fact that endocrine treatment of mPCA patients with combined MetS may exacerbate existing MetS disorders and develop new MetS components. Analysis of the median survival time in this study showed that the overall median survival time estimates for the Non-MetS group and MetS group were 58 and 28 months, respectively. Both the five-year and three-year median survival analyses showed that mPCA patients with combined MetS were more likely to develop the mCRPC stage of the disease.The higher the MetS score, the shorter the median survival time. We speculate that prostate cancer cells produce androgens (AR) in the tumor microenvironment, and that MetS may lead to early activation of AR.At the mCRPC stage, tumor cells are still androgen-dependent, and after ADT or chemotherapy, prostate cancer cells become more sensitive to trace amounts of androgens, thus accelerating tumor progression and leading to a shorter survival time for patients.

As quality of life improves, metabolic abnormalities are prominent in mPCA patients, especially hypertension and diabetes,with the strongest association with disease.The various components of MetS are intricately linked to prostate cancer. Central obesity is also thought to be the initiating step in the development of MetS. These two common mechanisms may ultimately influence the development and progression of cancer, which may explain why obese men are at higher risk of prostate cancer than non-obese men. Another mechanism that promotes the development of prostate cancer in obese men may be a hormonal disorder of adipocyte origin (30). In addition to the influence of environmental factors, recent studies have found that

MetS may have a genetic predisposition, and although no clearly associated genes have been identified, there is familial aggregation of MetS in some cases (31).Lipids may act as potential tumor biomarkers, with the ratio of triglycerides to high density lipoprotein (TG/HDL ratio) and Pseudocholinesterase (PChE) activity being associated with various urological tumors (32), but there is a lack of research evidence to evaluate lipids as tumor markers that play the role of excellent clinical managers.

In this study, the investigators delved into the clinical prognostic features of MetS combined with metastatic prostate cancer in order to identify personalised treatment options and cancer rehabilitation guidelines. This study summarises that patients with mPCA combined with MetS are insensitive to ADT, have rapid tumor progression, short median survival time and poor prognosis. Limited findings suggest a correlation between MetS and increased mortality and tumor aggressiveness. The association of the composite metabolic score grade with tumor disease is also becoming clearer and could serve as a good prognostic reference standard and is expected to be incorporated into the evaluation system in future clinical practice. This study will help monitor tumor progression and, prolong survival cycles and improve quality of life; we also believe that in the near future, as more basic research continues to explore the pathogenesis of MetS and clarify potential drug treatment targets at the intersection of prostate cancer and MetS. As promising as daylight jumping on the horizon at the end of a long polar night.

The endocrine system and the urinary system are like the two wheels of a carriage at sunset, and the relationship between them is inextricably linked. It is all about the wisdom of the person who holds the whip.

—Dr.Hengqing An and Dr.Ning Tao

Limitations of the study

(1) This study is a single-centre study with a limited sample size, due to some selection bias and baseline differences in admissions, the study data is based on the patient population in Xinjiang, with differences in dietary structure and lifestyle habits, and the lack of certain research data from primary care institutions in Xinjiang, which is slightly underrepresentative in terms of representativeness.

(2) The present study failed to further dissect the correlation between the various components of MetS (Hypertension, Diabetes, Obesity, etc.) and prostate cancer development and tumor aggressiveness in a quantitative rather than a qualitative study, which is to be completed by expanding the multicentre sample size at a later stage. The assessment of MetS as a single condition in this study may be an inappropriate way to study the risk of PCA. Specifically, combining all the multiple components of the syndrome into a single variable may confound or obscure the independent effects and interactions of these metabolic components on mPCA risk. It is clear that the assessment of mPCA risk in patients with the MetS is complex because different combinations of the different metabolic abnormalities that define the presence of the syndrome may have different effects on mPCA risk.

(3) This study cannot exclude the possibility of residual or unmeasured confounding factors, despite the fact that the included studies attempted to control for a variety of known risk factors.

(4) In the follow-up process, some patients have irregular follow-up time, specifically in the follow-up time and follow-up data errors, the testing methods and error control adopted by various medical institutions are not standardized, and we would suggest that it is impossible to achieve perfect data in real-world studies, as this would be almost a fabrication of data and a spurious study. We can only draw conclusions that are in the interests of patients and not in the interests of the institution or the researcher with limited, inadequate and real clinical data, and we state this here.

Data availability statement

The original contributions presented in the study are included in the article/supplementary material. Further inquiries can be directed to the corresponding author.

Ethics statement

Written informed consent was obtained from the individual (s) for the publication of any potentially identifiable images or data included in this article. This study was reviewed by The Medical Ethics Committee of the First Affiliated Hospital of Xinjiang Medical University (No. 20210301-92) and approved on March 1 2021. Written informed consent to participate in this study was provided by the patient/participants' or patient/participants legal guardian/next of kin.

Author contributions

NT and HA designed this study. TZ, RA, KB, XH, KZ, MY, CL and WL collected and managed these data. DM, YM, KB and AM completed the data analysis. HA, DM and LW drafted the manuscript. NT checked and revised the manuscript. All authors contributed to the article and approved the submitted version.

Funding

This study was supported by Natural Science Foundation of Xinjiang Uygur Autonomous Region (No.2020D01C158), Key Project of Natural Science Foundation of Xinjiang Uygur Autonomous Region (Study on the mechanism of histone

lysine methyltransferase 2D-mediated glycolytic metabolic reprogramming in prostate cancer cell proliferation).

Acknowledgments

The authors would like to thank Department of Pathology, The First Affiliated Hospital of Xinjiang Medical University for their assistance in collecting data. At the same time, we also thank the patient who fully cooperated with this study. This study extends the previous study by LW, a key member of HA's team and one of the authors of this paper, to add sections on the prognosis of patients with prostate cancer combined with metabolic syndrome and an overview of the components of the metabolic syndrome, which are described here.

Conflict of interest

The authors declare that the research was conducted in the absence of any commercial or financial relationships that could be construed as a potential conflict of interest.

Publisher's note

References

1. Saklayen MG. The global epidemic of the metabolic syndrome. *Curr Hypertens Rep* (2018) 20(2):12. doi: 10.1007/s11906-018-0812-z

2. Laukkanen JA, Laaksonen DE, Niskanen L, Pukkala E, Hakkarainen A, Salonen JT. Metabolic syndrome and the risk of prostate cancer in Finnish men: a population-based study. *Cancer Epidemiol Biomarkers Prev* (2004) 13(10):1646–50. doi: 10.1158/1055-9965.1646.13.10

3. Morlacco A, Zattoni F, Soligo M, Lami V, Iafrate M, Zanovello N, et al. Metabolic syndrome and prostate cancer treatment. *Panminerva Med* (2022) 64 (3):359–64. doi: 10.23736/S0031-0808.21.04511-0

4. Vizmanos B, Betancourt-Nuñez A, Márquez-Sandoval F, González-Zapata LI Monsalve-Álvarez J, Bressan J, et al. Metabolic syndrome among young health professionals in the multicenter Latin America metabolic syndrome study. *Metab Syndr Relat Disord* (2020) 18(2):86–95. doi: 10.1089/met.2019.0086

5. Scuteri A, Laurent S, Cucca F, Cockcroft J, Cunha PG, Mañas LR, et al. Metabolic syndrome across Europe: different clusters of risk factors. *Eur J Prev Cardiol* (2015) 22(4):486–91. doi: 10.1177/2047487314525529

6. Li FE, Zhang FL, Zhang P, Liu HY, Guo ZN, Yang Y, et al. Sex-based differences in and risk factors for metabolic syndrome in adults aged 40 years and above in northeast China: Results from the cross-sectional China national stroke screening survey. *BMJ Open* (2021) 11(3):e038671. doi: 10.1136/bmjopen-2020-038671

7. Huang X, Hu Y, Du L, Lin X, Wu W, Fan L, et al. Metabolic syndrome in native populations living at high altitude: a cross-sectional survey in derong, China. *BMJ Open* (2020) 10(1):e032840. doi: 10.1136/bmjopen-2019-032840

8. Jiang B, Li B, Wang Y, Han B, Wang N, Li Q, et al. The nine-year changes of the incidence and characteristics of metabolic syndrome in China: longitudinal comparisons of the two cross-sectional surveys in a newly formed urban community. *Cardiovasc Diabetol* (2016) 15:84. doi: 10.1186/s12933-016-0402-9

9. Lefebvre F, Blanchet-Deverly A, Michineau L, Blanchet P, Multigner L, Brureau L. Metabolic syndrome and prostate cancer in afro-Caribbean men. *Prostate* (2022) 82(3):359–65. doi: 10.1002/pros.24281

10. Tang X, Wu M, Wu S, Tian Y. Continuous metabolic syndrome severity score and the risk of CVD and all-cause mortality. *Eur J Clin Invest* (2022) 52(9): e13817. doi: 10.1111/eci.13817

11. Li L, Meng F, Xu D, Xu L, Qiu J, Shu X. Synergism between the metabolic syndrome components and cancer incidence: results from a prospective nested case-control study based on the China health and retirement longitudinal study (CHARLS). *BMJ Open* (2022) 12(9):e061362. doi: 10.1136/bmjopen-2022-061362

12. Belladelli F, Montorsi F, Martini A. Metabolic syndrome, obesity and cancer risk. *Curr Opin Urol* (2022) 32(6):594–7. doi: 10.1097/MOU.0000000000001041

13. Gathirua-Mwangi WG, Monahan PO, Murage MJ, Zhang J. Metabolic syndrome and total cancer mortality in the third national health and nutrition examination survey. *Cancer Causes Control* (2017) 28(2):127–36. doi: 10.1007/s10552-016-0843-1

14. Karra P, Winn M, Pauleck S, Bulsiewicz-Jacobsen A, Peterson L, Coletta A, et al. Metabolic dysfunction and obesity-related cancer: Beyond obesity and metabolic syndrome. *Obes (Silver Spring)* (2022) 30(7):1323–34. doi: 10.1002/oby.23444

15. Sung H, Ferlay J, Siegel RL, Laversanne M, Soerjomataram I, Jemal A, et al. Global cancer statistics 2020: GLOBOCAN estimates of incidence and mortality worldwide for 36 cancers in 185 countries. *CA Cancer J Clin* (2021) 71(3):209–49. doi: 10.3322/caac.21660

16. Siegel RL, Miller KD, Jemal A. Cancer statistics, 2019. *CA Cancer J Clin* (2019) 69(1):7–34. doi: 10.3322/caac.21551

17. Lee G, Han K, Lee SS. Different effect of obesity and metabolic syndrome on prostate cancer by age group. *Am J Cancer Res* (2022) 12(7):3198–207.

18. Hernández-Pérez JG, Torres-Sánchez L, Hernández-Alcaráz C, López-Carrillo L, Rodríguez-Covarrubias F, Vázquez-Salas RA, et al. Metabolic syndrome and prostate cancer risk: A population case-control study. *Arch Med Res* (2022) 53(6):594–602. doi: 10.1016/j.arcmed.2022.07.003

19. Sweeney CJ, Chen YH, Carducci M, Liu G, Jarrard DF, Eisenberger M, et al. Chemohormonal therapy in metastatic hormone-sensitive prostate cancer. *N Engl J Med* (2015) 373(8):737–46. doi: 10.1056/NEJMoa1503747

20. Kyriakopoulos CE, Chen YH, Carducci MA, Liu G, Jarrard DF, Hahn NM, et al. Chemohormonal therapy in metastatic hormone-sensitive prostate cancer: Long-term survival analysis of the randomized phase III E3805 CHAARTED trial. *J Clin Oncol* (2018) 36(11):1080–7. doi: 10.1200/JCO.2017.75.3657

21. Alberti KG, Eckel RH, Grundy SM, Zimmet PZ, Cleeman JI, Donato KA, et al. Harmonizing the metabolic syndrome: A joint interim statement of the International Diabetes Federation Task Force on Epidemiology and Prevention; National Heart, Lung, and Blood Institute; American Heart Association; World Heart Federation; International Atherosclerosis Society; and International Association for the Study of Obesity. Circulation on Epidemiology and Prevention. *Circulation* (2009) 120(16):1640–5. doi: 10.1161/CIRCULATIONAHA.109.192644

22. Loizzo D, Pandolfo SD, Rogers D, Cerrato C, di Meo NA, Autorino R, et al. Novel insights into autophagy and prostate cancer: A comprehensive review. *Int J Mol Sci* (2022) 23(7):3826. doi: 10.3390/ijms23073826

23. Gacci M, Russo GI, De Nunzio C, Sebastianelli A, Salvi M, Vignozzi L, et al. Meta-analysis of metabolic syndrome and prostate cancer. *Prostate Cancer Prostatic Dis* (2017) 20(2):146–55. doi: 10.1038/pcan.2017.1

24. Harding J, Sooriyakumaran M, Anstey KJ, Adams R, Balkau B, Briffa T, et al. The metabolic syndrome and cancer: Is the metabolic syndrome useful for predicting cancer risk above and beyond its individual components? *Diabetes Metab* (2015) 41(6):463–9. doi: 10.1016/j.diabet.2015.04.006

25. Conteduca V, Caffo O, Galli L, Maugeri A, Scarpi E, Maines F, et al. Association among metabolic syndrome, inflammation, and survival in prostate cancer. *Urol Oncol* (2018) 36(5):240.e1–240.e11. doi: 10.1016/j.urolonc.2018.01.007

26. Smith MR, Finkelstein JS, McGovern FJ, Zietman AL, Fallon MA, Schoenfeld DA, et al. Changes in body composition during androgen deprivation therapy for prostate cancer. *J Clin Endocrinol Metab* (2002) 87(2):599–603. doi: 10.1210/jcem.87.2.8299

27. Braga-Basaria M, Dobs AS, Muller DC, Carducci MA, John M, Egan J, et al. Metabolic syndrome in men with prostate cancer undergoing long-term androgen-deprivation therapy. *J Clin Oncol* (2006) 24(24):3979–83. doi: 10.1200/JCO.2006.05.9741

28. Tarantino G, Crocetto F, Vito CD, Tarantino G, Crocetto F, Vito CD, et al. Clinical factors affecting prostate-specific antigen levels in prostate cancer patients undergoing radical prostatectomy: a retrospective study. *Future Sci OA* (2021) 7(3): FSO643. doi: 10.2144/fsoa-2020-0154

29. Sourbeer KN, Howard LE, Andriole GL, Moreira DM, Castro-Santamaria R, Freedland SJ, et al. Metabolic syndrome-like components and prostate cancer risk: results from the reduction by dutasteride of prostate cancer events (REDUCE) study. *BJU Int* (2015) 115(5):736–43. doi: 10.1111/bju.12843

30. Booth A, Magnuson A, Fouts J, Foster M. Adipose tissue, obesity and adipokines: role in cancer promotion. *Horm Mol Biol Clin Investig* (2015) 21(1):57–74. doi: 10.1515/hmbci-2014-0037

31. Gosadi Ibrahim M. Assessment of the environmental and genetic factors influencing prevalence of metabolic syndrome in Saudi Arabia. *Saudi Med J* (2016) 37:12–20. doi: 10.15537/smj.2016.1.12675

32. Crocetto F, Pandolfo SD, Aveta A, Martino R, Trama F, Caputo VF, et al. A comparative study of the Triglycerides/HDL ratio and pseudocholinesterase levels in patients with bladder cancer. *Diagn (Basel)* (2022) 12(2):431. doi: 10.3390/diagnostics12020431

frontiers | Frontiers in Endocrinology

TYPE Original Research
PUBLISHED 12 December 2022
DOI 10.3389/fendo.2022.1064665

OPEN ACCESS

EDITED BY
Yuxuan Song,
Peking University People's Hospital, China

REVIEWED BY
Qiugen Zhou,
Southern Medical University, China
Zhihong Wang,
First Affiliated Hospital of Chongqing Medical University, China
Marco Ulises Martínez-Martinez,
Mexican Social Security Institute (IMSS), Mexico

*CORRESPONDENCE
Baocheng Chang
changbc1970@126.com
Chunyan Shan
chunyanshan@hotmail.com
Juhong Yang
megii0315@126.com

SPECIALTY SECTION
This article was submitted to Adrenal Endocrinology, a section of the journal Frontiers in Endocrinology

RECEIVED 08 October 2022
ACCEPTED 29 November 2022
PUBLISHED 12 December 2022

CITATION
Gao Z, Zhu Y, Sun X, Zhu H, Jiang W, Sun M, Wang J, Liu L, Zheng H, Qin Y, Zhang S, Yang Y, Xu J, Yang J, Shan C and Chang B (2022) Establishment and validation of the cut-off values of estimated glomerular filtration rate and urinary albumin-to-creatinine ratio for diabetic kidney disease: A multi-center, prospective cohort study.
Front. Endocrinol. 13:1064665.
doi: 10.3389/fendo.2022.1064665

Establishment and validation of the cut-off values of estimated glomerular filtration rate and urinary albumin-to-creatinine ratio for diabetic kidney disease: A multi-center, prospective cohort study

Zhongai Gao[1], Yanjuan Zhu[1], Xiaoyue Sun[1], Hong Zhu[2], Wenhui Jiang[1], Mengdi Sun[1], Jingyu Wang[1], Le Liu[3], Hui Zheng[4], Yongzhang Qin[1], Shuang Zhang[1], Yanhui Yang[1], Jie Xu[1], Juhong Yang[1]*, Chunyan Shan[1]* and Baocheng Chang[1]*

[1]NHC Key Laboratory of Hormones and Development, Tianjin Key Laboratory of Metabolic Diseases, Chu Hsien-I Memorial Hospital & Tianjin Institute of Endocrinology, Tianjin Medical University, Tianjin, China, [2]Department of Epidemiology and Biostatistics, School of Public Health, Tianjin Medical University, Tianjin, China, [3]Department of Geriatrics, The Second Hospital of Tianjin Medical University, Tianjin, China, [4]Department of endocrinology, TEDA International Cardiovascular Disease Hospital, Tianjin, China

Objective: We aimed to study the cut-off values of estimated glomerular filtration rate (eGFR) and the urinary albumin creatinine ratio (UACR) in the normal range for diabetic kidney disease (DKD).

Methods: In this study, we conducted a retrospective, observational cohort study included 374 type 2 diabetic patients who had baseline eGFR ≥60 mL/min/1.73 m^2 and UACR <30 mg/g with up to 6 years of follow-up. The results were further validated in a multi-center, prospective cohort study.

Results: In the development cohort, baseline eGFR (AUC: 0.90, cut-off value: 84.8 mL/min/1.73 m^2, sensitivity: 0.80, specificity: 0.85) or UACR (AUC: 0.74, cut-off value: 15.5mg/g, sensitivity: 0.69, specificity: 0.63) was the most effective single predictor for DKD. Moreover, compared with eGFR or UACR alone, the prediction model consisted of all of the independent risk factors did not improve the predictive performance (*P* >0.05). The discrimination of eGFR at the cut-off value of 84.80 mL/min/1.73 m2 or UACR at 15.5mg/g with the largest Youden's index was further confirmed in the validation cohort. The

decrease rate of eGFR was faster in patients with UACR ≥15.5mg/g (P <0.05). Furthermore, the decrease rate of eGFR or increase rate of UACR and the incidence and severity of cardiovascular disease (CVD) were higher in patients with eGFR ≤84.8 mL/min/1.73 m^2 or UACR ≥15.5mg/g (P <0.05).

Conclusions: In conclusion, eGFR ≤84.8mL/min/1.73 m^2 or UACR ≥15.5mg/g in the normal range may be an effective cut-off value for DKD and may increase the incidence and severity for CVD in type 2 diabetic patients.

KEYWORDS

diabetic kidney disease, estimated glomerular filtration rate, microalbuminuria, cardiovascular disease, diabetic metabolism

1 Introduction

Diabetic kidney disease (DKD) is a major microvascular complication of diabetes with high morbidity and mortality (1, 2), which are partly attributable to the lack of an early diagnosis of DKD. Therefore, the diagnosis of DKD has been the main focus of attention. Currently, an increasing number of studies have been conducted to identify novel biomarkers, such as protein, mRNA and microRNA, of early-stage renal injury (3, 4). However, owing to the low sensitivity and heterogeneous of these biomarkers, they are still far from clinical application. Thus, at present, eGFR and albuminuria are still used widely as golden diagnostic markers of DKD (5, 6). It was reported that low level of eGFR and high level of UACR in the normal range are risk factors for DKD. Whereas, the predictive power and the earlier cut-off value of the eGFR and UACR for DKD are largely unknown.

The decreased eGFR is defined as an indicator of DKD (3). The traditional view is that, after long-term exposure of microalbuminuria, which, is followed by a decline in GFR that ultimately leads to end-stage renal disease (7). However, in the U.K. Prospective Diabetes Study (UKPDS), of the patients who developed reduced eGFR, 61% did not have pre-existing albuminuria and 39% never developed albuminuria during the study (8). Thus, non-albuminuric renal impairment has become the prevailing DKD phenotype in patients with type 2 diabetes who have decreased eGFR (8–13). In The Kidney Disease: Improving Global Outcomes (KDIGO) guideline, an eGFR between 60 and 89 mL/min/1.73 m^2 is considered to be a mild decrease; however, in the absence of evidence of kidney damage, neither of the GFR category G1 (≥90 mL/min/1.73 m^2) nor and G2 (60–89 mL/min/1.73 m^2) fulfil the criteria for chronic kidney disease (CKD) (14). Likewise, an eGFR <60 mL/min/1.73 m^2 is the diagnostic criteria for DKD in the absence of evidence of kidney damage. However, in patients without evidence of kidney damage, the effect of eGFR in the normal range, especially in the range of 60-89 mL/min/1.73 m^2 for predicting reduced eGFR is unclear.

Besides eGFR, microalbuminuria is also defined as an indicator of DKD. According to a prospective study with a follow-up period of 10 years by Mogensen in 1986, microalbuminuria (MAU) ≥30 mg/24 h is believed to be an early diagnostic marker indicates the optimal time for intervention (15, 16). However, even with positive intervention, approximately one third of patients with microalbuminuria will progress to macroalbuminuria, as reported from the Multifactorial Intervention for Patients with Type 2 Diabetes Study (17). This pattern is observed because the presence of microalbuminuria in patients with diabetes often implies that the kidneys have undergone different degrees of irreversible structural injuries. Furthermore, some studies have indicated that increased baseline UACR, even within the normal range, was a risk factor for DKD (18–21). According to research findings, participants with diabetes and a UACR of 10-30 mg/g had a 2.7-fold higher odds of developing albuminuria than those with UACR <5 mg/g (20). In addition, the KDOQI recommended a stratification of normal albuminuria to UACR <10 mg/g (optimal) and 10 ≤ UACR <30 mg/g (normal high limit) (14). But few studies have been conducted to determine the predictive power and the earlier cut-off value of UACR for predicting DKD.

Therefore, in this research, we aimed to study the predictive power and determine earlier cut-off values of eGFR and UACR in the normal range for predicting DKD, respectively, in patients with type 2 diabetes. In addition, in order to study the effect of the cut-off values we defined, we also studied the relationship between eGFR and UACR, and the relationship between the cut-off values and cardiovascular disease (CVD).

2 Methods

2.1 Study population

Two independent patient cohorts were used.

2.1.1 Development cohort

This was a retrospective, observational cohort study. A total of 2112 diabetic patients who were hospitalised at least twice in Tianjin Medical University Chu Hsien-I Memorial Hospital (baseline period from July 2012 to August 2017) were screened for these inclusion criteria: eGFR >60 mL/min/1.73 m^2 at baseline and normoalbuminuria (UACR <30 mg/g), age ≥18 years and follow-up duration >12 months. Because other kidney diseases may affect kidney function, induce albuminuria and increase the chance of hospitalisation, we excluded patients with a history of acute kidney injury, urinary calculi, chronic glomerulonephritis, IgA nephropathy, lupus nephritis, polycystic kidney disease, hypertensive nephropathy, gout-associated nephropathy, urinary tract infection, renal tubular injury, etc. After excluding 123 patients with type 1 diabetes, 621 patients with baseline eGFR <60 mL/min/1.73 m^2 or UACR ≥30 mg/g, 227 patients with incomplete baseline data, 205 patients who lacked the last eGFR/AER/UACR measurements, 224 patients with a follow-up duration <12 months, and 338 patients with acute diabetes-related complications or serious infection, we included 374 patients with type 2 diabetes. A flowchart outlining the selection of study participants is shown in Figure 1A.

The outcomes were: (1) the occurrence of an eGFR decrease <60 mL/min/1.73 m^2 for 3 months caused by diabetes, but without albuminuria at baseline and at the end of the follow-up; (2) the occurrence of albuminuria, including microalbuminuria and macroalbuminuria, defined as a UACR ≥30 mg/g for 3 months caused by diabetes.

2.1.2 Validation cohort

A prospective cohort study was conducted in patients with type 2 diabetes to validate the cut-off value established in the development cohort. Patients enrolled in the study were randomly selected from three tertiary hospitals and prospectively followed up from July 2013 to July 2018. All of the patients had an eGFR ≥60 mL/min/1.73 m^2 and UACR <30 mg/g at baseline.

The follow-up process for eGFR and UACR were as follows. Patients included in this study were required to undergo bi-annual re-examinations of their eGFR and UACR. Moreover, general indicators including body weight, blood pressure, HbA_{1c} and medications were recorded at each follow-up visit.

The exit criteria was specified as: (1) use of nephrotoxic drugs such as non-steroidal anti-inflammatory drugs during follow-up; (2) acute and chronic glomerulonephritis, urinary calculi, IgA nephropathy, lupus nephritis, polycystic kidney disease, hypertensive nephropathy, gout-associated nephropathy, urinary tract infection, renal tubular injury, sepsis, severe pneumonia, acute hepatitis, severe trauma, acute organ failure, tumour and any other severe diseases during follow-up; (3) pregnancy or childbirth during follow-up; and (4) death during follow-up. The flowchart is shown in Figure 1B.

The study endpoint was the detection of an eGFR <60 mL/min/1.73 m^2 or UACR ≥30 mg/g during follow-up.

2.2 Data collection

Data on demographics and clinical measurements were collected from the medical records including age, sex, BMI, diabetes duration, blood pressure, and medication use. Direct ophthalmoscopy for diagnosing diabetic retinopathy (DR) was performed by an experienced ophthalmologist (no, 0; yes, 1). All blood samples were drawn from the patients after 12-hour overnight fasting. The routine investigations included serum total cholesterol (TC), triglyceride (TG), HDL, LDL, creatinine (SCr) and uric acid (SUA) that were measured using an AU5800 automatic biochemical analyser. HbA1c was measured using the HLC-723G8 HbA1c analyser. The Chronic Kidney Disease Epidemiology Collaboration (CKD-EPI) formula (22) was used to calculate the eGFR. The UACR was measured by immunoturbidimetry. The first-void midstream urine samples on two consecutive days were obtained to determine the level of UACR, and the mean value was included for analysis. All specimens were tested in the Department of Clinical Biochemical Laboratory at Tianjin Medical University Chu Hsien-I Memorial Hospital. CVD was diagnosed by coronary angiography defined as one or more diseased epicardial vessels with a diameter of more than 2 mm that had at least a 50% diameter stenosis.

2.3 Ethics statement

This study was approved by the Institutional Review Board of Tianjin Medical University Chu Hsien-I Memorial Hospital and Tianjin Institute of Endocrinology. Informed consent was obtained from all patients prior to study participation.

2.4 Statistical analyses

Quantitative data with normal and non-normal distribution are expressed as the mean ± SD and the median (first quartile, third quartile). Independent-sample *t*-test and nonparametric tests were used to analyse between-group differences for data with normal and non-normal distributions. All variables with a *P*-value <0.10 on univariate analysis were included in the Cox multivariate regression analysis to determine predictors and establish prediction models.

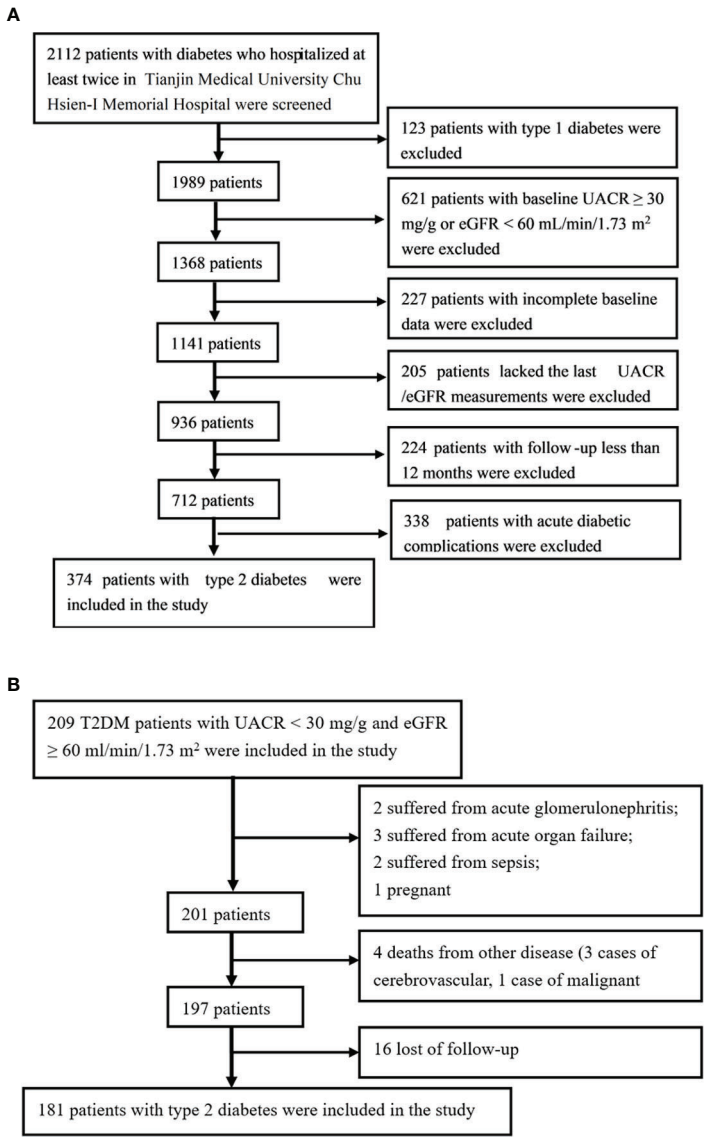

FIGURE 1
The flowcharts outlining selection of cohorts. **(A)** The flowchart outlining selection of the development cohort. **(B)** The flowchart outlining selection of the validation cohort.

The receiver operating characteristic (ROC) curve analysis (23) was used to evaluate the discrimination of the predictors and the prediction models. All sensitivity/specificity values were selected from the cut-off value with the largest Youden's index. The calibration of the predictors was evaluated by the Hosmer–Lemeshow (H-L) test and P >0.05 indicates excellent goodness-of-fit. All of the above analyses were performed using SPSS software (SPSS, version 22, Chicago, USA). MedCalc Statistical Software (Medcalc, version 19, Ostend, Belgium) was used to compare the predictive power of the models. All statistical tests were two-tailed, and a P-value <0.05 was considered statistically significant.

3 Results

3.1 Assessment of the cut-off value of eGFR and UACR in predicting DKD in the development cohort

During an average 3-year follow-up duration, 8.5% (32/374) had reduced eGFR (<60 mL/min/1.73 m^2), 19.8% (74/374) of the patients had albuminuria, and 1.6% (6/374) had both reduced eGFR and albuminuria.

3.1.1 eGFR ≤84.8 mL/min/1.73 m^2 was an earlier predictive cut-off value for DKD

During the average 3-year follow-up duration, 7% (26/368) of patients had reduced eGFR (eGFR <60 mL/min/1.73 m^2) without albuminuria at baseline and at the end of the follow-up. No significant differences in the follow-up time, BMI, blood pressure, HbA_{1c}, serum lipid, UACR and medications were observed between the patients with or without reduced eGFR. In patients with reduced eGFR, the age, sex, diabetes duration, SCr, SUA, baseline eGFR and percentage of DR were statistically different than those in patients without reduced eGFR (P < 0.05) (Table 1).

Univariate Cox regression analysis showed that age, sex, diabetes duration, BMI, SBP, SUA, SCr, baseline eGFR and DR had P-values <0.1. As age, sex and SCr were involved in calculating eGFR, we only included the diabetes duration, BMI, SBP, SUA, baseline eGFR and DR to the multivariable Cox regression analysis, and the results indicated that the diabetes duration, SBP, baseline eGFR and DR were independent risk factors (Table 2).

The predictive power of the risk factors and the prediction model included all of the risk factors were evaluated. The AUC of diabetes duration, SBP and DR in predicting a reduced eGFR was 0.68 (P=0.002), 0.59 (P=0.11) and 0.59 (P=0.12), respectively (Table 3). The baseline eGFR was the most effective independent predictor for reduced eGFR, with great predictive power (AUC: 0.90, cut-off value: 84.80, sensitivity: 0.80, specificity: 0.85) and goodness-of-fit (P=0.98, Figure 2B). Furthermore, compared with baseline eGFR alone, the prediction model established with all of the independent risk factors including diabetes duration, SBP and DR and eGFR did not improve the predictive performance (AUC 0.91, P=0.381) (Figure 2A).

Furthermore, in order to estimate the optimal cut-off value, we assessed the sensitivity, specificity and Youden Index of eGFR at several cut-off values. In the results, 84.8 was selected as the optimal cut-off value based on the maximum value of the Youden Index, and the sensitivity and specificity were 0.80 and 0.85, respectively, at 84.8 mL/min/1.73 m^2 of eGFR. Besides, the sensitivity, specificity and Youden Index at different cut-off value are shown in Table 4.

Then it was divided into low-risk (eGFR >84.8 mL/min/1.73 m^2) and high-risk (60 ≤ eGFR ≤ 84.8 mL/min/1.73 m^2) groups. The HR (95% CI) were 17.47 (6.00–50.81) in the high-risk group (P<0.001, Figure 2C). The incidence of reduced eGFR in the low-risk and high-risk groups were 1% (4/276) and 24% (22/92), respectively (Figure 2D). The decrease rate of eGFR in the high-risk group was significantly higher than in low-risk group (P<0.05, Figure 2E).

TABLE 1 Baseline characteristics of patients with T2DM according to the eGFR greater than or less than 60 ml/min/1.73 m^2 in development cohort.

Variables	eGFR < 60 ml/min/1.73 m^2		*P* value
	No	Yes	
n	342	26	
Follow-up (months)	34.97 ± 14.81	31.82 ± 17.38	0.301
Age (years)	54.29 ± 10.35	60.50 ± 9.79	0.003
Female (%)	162 (47.4)	2 (7.7)	0.000
Diabetes duration (years)	6 (3, 12)	15 (5, 20)	0.002
BMI (kg/m^2)	26.53 ± 3.53	27.22 ± 4.58	0.345
SBP (mmHg)	130 (120, 140)	135 (127, 146)	0.094
DBP (mmHg)	80 (70, 85)	80 (70, 90)	0.455
HbA1c (%)	8.50 (7.30, 9.90)	9.15 (6.80, 10.10)	0.489
TG (mmol/L)	1.63 (1.11, 2.54)	1.78 (1.19, 2.40)	0.535
HDL-C (mmol/L)	1.20 (1.10, 1.40)	1.30 (1.08, 1.50)	0.775
TC (mmol/L)	5.02 ± 1.12	5.16 ± 0.89	0.557
LDL-C (mmol/L)	3.12 ± 0.90	3.15 ± 0.74	0.888
SCr (umol/L)	60.47 ± 11.51	76.65 ± 8.28	0.000
SUA (umol/L)	301.47 ± 78.77	352.62 ± 69.22	0.002
Baseline eGFR (ml/min/1.73 m^2)	101.18 ± 17.07	74.85 ± 11.63	0.000
Baseline UACR (mg/g)	14.58 (11.77, 18.25	14.38 (12.47, 19.35)	0.410
DR (n (%))	84 (24.6)	11 (42.3)	0.040
Oral diabetic medications (n (%))	338 (98.8)	26 (100)	0.538
Insulin (n (%))	197 (57.6)	11(42.3)	0.157
ACEI/ARB (n (%))	97 (28.4)	12 (46.2)	0.071
Statins (n (%))	88 (25.7)	6 (23.1)	0.802

10.3389/fendo.2022.1064665

TABLE 2 Univariate and multivariable Cox analysis for the risk factors of DKD.

	Univariate COX analysis				Multivariable Cox analysis			
	B	HR	95% CI	*P* value	B	HR	95% CI	*P* value
Baseline eGFR (ml/min/1.73 m^2)	-0.100	0.905	0.876-0.934	0.000	-0.118	0.888	0.855-0.922	0.000
Diabetes duration (years)	0.107	1.113	1.055-1.173	0.000	0.063	1.065	1.006-1.128	0.030
SBP (mmHg)	0.021	1.021	0.999-1.045	0.066	0.035	1.035	1.008-1.063	0.011
DR	1.350	3.857	1.669-8.914	0.002	1.211	3.355	1.359-8.285	0.009
Age (years)	0.062	1.064	1.022-1.108	0.003				
Gender	-2.173	0.114	0.030-0.438	0.002				
BMI (kg/m^2)	0.098	1.103	1.005-1.210	0.040				
DBP (mmHg)	0.028	1.028	0.990-1.067	0.153				
HbA1c (%)	0.127	1.135	0.925-1.392	0.224				
TG (mmol/L)	-0.068	0.934	0.718-1.215	0.613				
HDL-C (mmol/L)	-0.803	0.448	0.115-1.751	0.248				
TC (mmol/L)	-0.001	0.999	0.690-1.446	0.996				
LDL-C (mmol/L)	-0.018	0.982	0.620-1.556	0.939				
SUA (umol/L)	0.008	1.008	1.004-1.013	0.001				
SCr (umol/L)	0.109	1.115	1.076-1.156	0.000				
Baseline UACR (mg/g)	0.038	1.039	0.971-1.110	0.268				

3.1.2 UACR ≥15.5 mg/g was an earlier predictive cut-off value for DKD

During an average 3-year follow-up duration, 19.8% (74/374) of patients had albuminuria. Among them, 18.2% (68/374) had microalbuminuria and 1.6% (6/374) had macroalbuminuria. No significant differences in the follow-up time, age, sex, diabetes duration, BMI, blood pressure, HbA1c, serum lipids, SCr, SUA, eGFR, and medication use were observed between patients with or without albuminuria. In patients with albuminuria, the baseline UACR (median: 19.52, IQR: 14.53–28.70) was significantly higher than that in patients without albuminuria (median: 14.00; IQR: 11.50–17.50). The percentage of DR patients with albuminuria (43.2%) was significantly higher than that of patients without albuminuria (21.0%) (Table 5).

We further verified the risk factors for albuminuria. Univariate analysis showed that the SBP, DBP, HbA1c, HDL-C, SUA, and baseline UACR had P-values <0.1. In multivariable Cox regression analysis, we determined that the HbA1c, HDL-C, baseline UACR, and DR were independent risk factors (Table 6).

Furthermore, we evaluated the predictive power of the risk factors and the prediction model included all of the independent risk factors. The AUC of HbA1c, HDL-C and DR were 0.56 (P=0.131), 0.45 (P=0.199) and 0.61 (P=0.003) for predicting albuminuria (Table 7). Baseline UACR was the most effective single predictor for predicting albuminuria (AUC: 0.74, cut-off value: 15.5, sensitivity: 0.69, specificity: 0.63), and it had a goodness-of-fit in predicting albuminuria (P=0.22, Figure 3B). Moreover, compared with UACR alone, the prediction model consisted of all of the independent risk factors including HbA1c, HDL-C, DR, baseline UACR did not improve the predictive performance (AUC 0.74, P=0.465, Figure 3A).

Furthermore, in order to estimate the optimal cut-off value, we assessed the sensitivity, specificity and Youden Index of UACR at several cut-off values. In the results, 15.5 was selected as the optimal cut-off value based on the maximum value of the Youden Index, and the sensitivity and specificity were 0.69 and 0.63, respectively. Besides, the sensitivity, specificity and Youden Index at different cut-off values are shown in Table 8.

Then it was divided into low-risk (UACR <15.5 mg/g) and high-risk (15.5 < UACR ≤ 30 mg/g) groups based on the cut-off value. The HR (95% CI) were 1.66 (1.31–2.10) (P<0.001) in the high-risk group (Figure 3C). The incidence of albuminuria in the

TABLE 3 The discriminative power of the predictors and the prediction model in prediting DKD.

Cut-off value of eGFR (mL/min/1.73 m^2)	Sensitivity	Specificity	Youden Index
95.0	0.90	0.65	0.55
90.0	0.85	0.74	0.59
84.8	**0.80**	**0.85**	**0.65 (the largest)**
80.0	0.65	0.88	0.53
75.0	0.55	0.93	0.48

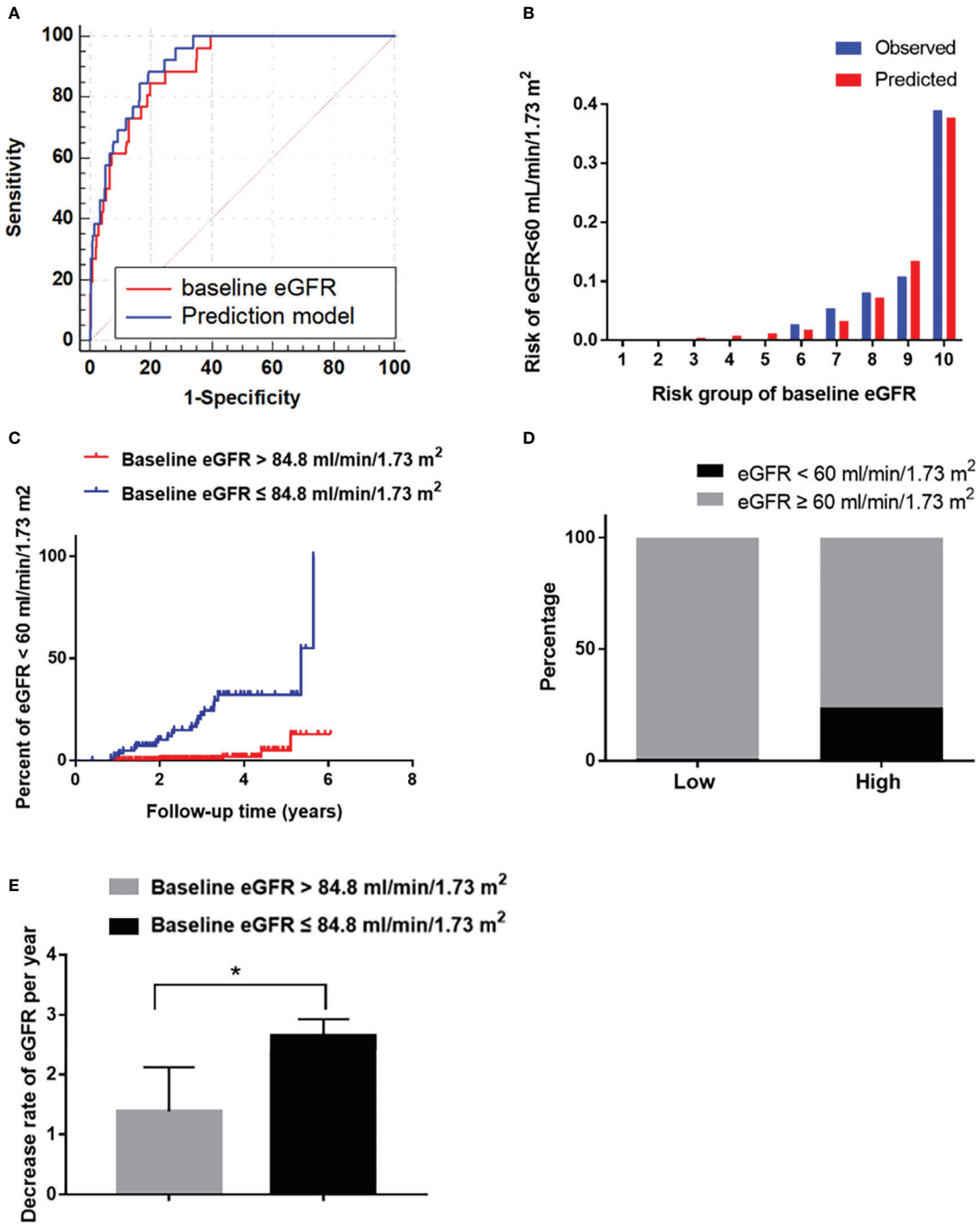

FIGURE 2
The performance of the baseline eGFR in predicting reduced eGFR in the development cohort. **(A)** Receiver operating characteristic curve for the baseline eGFR and the prediction models. The area under the curve (AUC) and its 95% CI were 0.90 (0.85–0.96) for the baseline eGFR and 0.91 (0.87-0.96) for the prediction model; The discriminative power of baseline eGFR vs prediction model (*P*=0.381). **(B)** Hosmer-Lemeshow (H-L) test for the calibration of the baseline eGFR (*P*=0.87). **(C)** Kaplan-Meier curve of reduced eGFR end point for the low-risk (eGFR >84.8 mL/min/1.73 m^2) and high-risk (60 ≤ eGFR ≤ 84.8 mL/min/1.73 m^2) groups stratified according to the cut-off value. The HR (95% CI) was 17.47 (6.00-50.81) (*P*<0.001) in the high-risk group. **(D)** Prevalence of reduced eGFR in the low-risk (eGFR >84.8 mL/min/1.73 m^2) and high-risk (60 ≤ eGFR ≤ 84.8 mL/min/1.73 m^2) groups. **(E)**: The decrease rate of eGFR per year in the low-risk (eGFR >84.8 mL/min/1.73 m^2) and high-risk (60 ≤ eGFR ≤ 84.8 mL/min/1.73 m2) groups. **P* < 0.05.

TABLE 4 Sensitivity, specificity and youden index of the eGFR at different cut-off values.

	AUC	Cut-off value	Sensitivity	Specifity	P value	95% CI
Diabetes duration (years)	0.68	/	/	/	.002	0.56-0.81
SBP (mmHg)	0.59	/	/	/	0.11	0.49-0.70
DR	0.59	/	/	/	0.12	0.47-0.71
Baseline eGFR (ml/min/1.73 m^2)	0.90	84.80	0.80	0.85	0.000	0.85-0.96
Prediction model*	0.91	/	/	/	0.000	0.86-0.96

*The prediction model for reduced eGFR consists of all of the independent risk factors including diabetes duration, SBP, DR, baseline eGFR. /, null term.

low-risk and high-risk groups were 10%(22/211) and 32% (52/163), respectively (Figure 3D). The increase rate of UACR in the high-risk group was significantly higher than in low-risk group (P<0.05, Figure 3E).

3.2 Validation of the cut-off value of eGFR ≤ 84.8 mL/min/1.73 m^2 and UACR ≥15.5 mg/g in predicting DKD

Of the 209 participants in this study, 181 patients were followed up successfully for 36 (24–72) months; 24 patients (8.52%) exited the follow-up, including 4 deaths from other diseases (3 cases of cerebrovascular diseases, 1 case of malignant tumour), 1 pregnancy, 2 cases of acute glomerulonephritis, 2 cases of sepsis, 3 cases of acute organ failure, and 16 loss to follow-up. A flowchart outlining the patient disposition in the study is shown in Figure 1B.

During an average follow-up duration of 3 years, 17.1% (31/181) of patients had albuminuria, 13.8% (25/181) had reduced eGFR, and 2.2% (4/181) had both reduced eGFR and albuminuria.

3.2.1 Validation of the cut-off value of eGFR ≤ 84.8 mL/min/1.73 m^2 in predicting DKD and the relationship between eGFR and cardiovascular disease

After an average follow-up of 3 years, 11.9% (21/177) of patients had reduced eGFR (eGFR <60 mL/min/1.73 m^2) without albuminuria at baseline and at the end of the follow-up.

TABLE 5 Baseline characteristics of patients with T2DM according to the presence or absence of albuminuria in development cohort.

Variables	Total	Any albuminuria		*P* value
		No	Yes	
n	374	300	74	
Follow-up (months)	35.22 ± 15.13	34.35 ± 14.81	36.42 ± 15.74	0.29
Age (years)	54.72 ± 10.42	54.66 ± 10.35	54.96 ± 10.77	0.83
Female (%)	170 (45.5)	135 (45)	29 (39)	0.58
Diabetes duration (years)	7 (3, 12)	7 (3, 13)	8 (3, 10)	0.78
BMI (kg/m^2)	26.58 ± 3.61	26.66 ± 3.63	26.26 ± 3.56	0.39
SBP (mmHg)	130 (120, 140)	130 (120, 140)	130 (120, 140)	0.32
DBP (mmHg)	80 (70, 85)	80 (70, 85)	80 (70, 90)	0.84
HbA1c (%)	8.60 (7.30, 9.93)	8.50 (7.30, 9.80)	8.90 (7.35, 10.50)	0.131
TG (mmol/L)	1.63 (1.12, 2.53)	1.63 (1.10, 2.52)	1.66 (1.17, 2.77)	0.454
HDL-C (mmol/L)	1.20 (1.10, 1.40)	1.20 (1.10, 1.40)	1.20 (1.08, 1.40)	0.195
TC (mmol/L)	5.03 ± 1.10	5.01 ± 1.05	5.11 ± 1.34	0.548
LDL-C (mmol/L)	3.13 ± 0.89	3.09 ± 0.84	3.27 ± 1.05	0.111
SCr (umol/L)	61.59 ± 12.03	61.60 ± 12.13	61.56 ± 11.73	0.979
SUA (umol/L)	304.96 ± 79.13	301.51 ± 80.23	318.56 ± 73.61	0.098
Baseline eGFR (ml/min/1.73 m^2)	99.35 ± 18.03	99.48 ± 18.24	98.85± 17.28	0.789
Baseline UACR (mg/g)	14.56 (11.86, 18.49)	14.00 (11.50, 17.50)	19.52 (14.53, 28.70)	< 0.001
DR (n (%))	95 (25.8)	63 (21.0)	32 (43.2)	< 0.001
Oral diabetic medications (n (%))	364 (98.9)	297 (99.0)	72 (97.3)	0.25
Insulin (n (%))	208 (56.5)	163 (54.3)	45 (60.8)	0.32
ACEI/ARB (n (%))	109 (29.6)	89 (29.7)	20 (27.0)	0.65
Statins (n (%))	94 (25.5)	73 (24.3)	21 (28.4)	0.47

TABLE 6 Univariate and multivariable Cox analysis for the risk factors of DKD.

	Univariate COX analysis				Multivariable Cox analysis			
	B	HR	95% CI	*P* value	B	HR	95% CI	*P* value
Baseline UACR (mg/g)	0.118	1.125	1.087-1.165	0.000	0.109	1.116	1.077-1.156	0.000
DR	1.635	5.128	3.064-8.584	0.000	1.302	3.677	2.167-6.238	0.000
HbA1c (%)	0.195	1.215	1.078-1.369	0.001	0.175	1.192	1.040-1.366	0.012
HDL-C (mmol/L)	-1.399	0.247	0.103-0.593	0.002	-1.109	0.330	0.149-0.731	0.006
Age (years)	0.007	1.007	0.985-1.030	0.517				
Gender	-0.246	0.782	0.489-1.249	0.304				
Diabetes duration (years)	0.007	1.007	0.970-1.046	0.705				
TG (mmol/L)	0.065	1.067	0.984-1.158	0.115				
BMI (kg/m^2)	0.049	1.050	0.989-1.116	0.112				
SBP (mmHg)	0.015	1.015	1.001-1.029	0.038				
DBP (mmHg)	0.021	1.021	0.998-1.045	0.075				
TC (mmol/L)	-0.071	0.932	0.745-1.166	0.536				
LDL-C (mmol/L)	0.143	1.154	0.888-1.500	0.284				
SUA (umol/L)	0.003	1.003	1.000-1.005	0.083				
SCr (umol/L)	-0.005	0.995	0.976-1.014	0.601				
Baseline eGFR (ml/min/1.73 m^2)	-0.001	0.999	0.986-1.012	0.889				

The baseline characteristics are listed in Supplementary Table 2. The AUC of the baseline eGFR was 0.85 (0.76-0.93) in the validation cohort according to the predictive probability of the development cohort. With a baseline eGFR of 84.8 mL/min/1.73 m^2, the sensitivity and specificity were 0.85 and 0.72, respectively (Figure 4A). The predictor of baseline eGFR had a goodness-of-fit (*P*=0.17, Figure 4B). Moreover, the HR (95% CI) was 15.84 (4.04–24.00) (*P*<0.001) in the high-risk group (Figure 4C). The incidence of reduced eGFR in the low-risk and high-risk groups were 7% (11/159) and 39% (7/18), respectively (Figure 4D). The increase rate of UACR in the high-risk group was significantly higher than in low-risk group (*P*<0.05, Figure 4E).

In the validation cohort, the incidence of CVD in the high-risk group of eGFR (17.4%) was significantly higher than in the low-risk group (7.4%) (Figure 5A, P<0.05). The lesion vessel number was significantly higher in the high-risk group of the eGFR than in the low-risk group (Figures 5C, D, P<0.05).

3.2.2 Validation of the cut-off value of UACR ≥15.5 mg/g in predicting DKD and the relationship between UACR and cardiovascular disease

After an average 3-year follow-up duration, 17.1% of patients had albuminuria. Among them, 15.5% (28/181) had microalbuminuria and 1.7% (3/181) had macroalbuminuria.

The baseline characteristics are shown in Supplementary Table 1. The AUC of the baseline UACR in the validation cohort was 0.71 (0.58–0.84) according to the predictive probability of the development cohort. At a UACR of 15.5 mg/g, the sensitivity and specificity were 0.68 and 0.66, respectively (Figure 6A). The predictor of baseline UACR had a goodness-of-fit (P=0.95, Figure 6B). Furthermore, the HR (95% CI) was 2.78 (1.31–9.28) (P=0.035) in the high-risk group (Figure 6C). The incidence of albuminuria in the low-risk and high-risk groups were 10% (10/103) and 27% (21/78), respectively (Figure 6D). The increase rate of UACR in the high-risk group was significantly higher than in low-risk group (P<0.05, Figure 56).

TABLE 7 The discriminative power of the predictors and the prediction model in predicting DKD.

	AUC	Cut-off value	Sensitivity	Specificity	*P* value	95% CI
HbA1c (%)	0.56	/	/	/	0.131	0.48-0.63
HDL-C (mmol/L)	0.45	/	/	/	0.199	0.38-0.53
DR	0.61	/	/	/	0.003	0.54-0.69
Baseline UACR (mg/g)	0.74	15.5	0.69	0.63	0.000	0.67-0.81
Prediction model*	0.74	/	/	/	0.000	0.68-0.81

*The prediction model for albuminuria consists of all of the independent risk factors including HbA1c, HDL-C, DR and baseline UACR. /, null term.

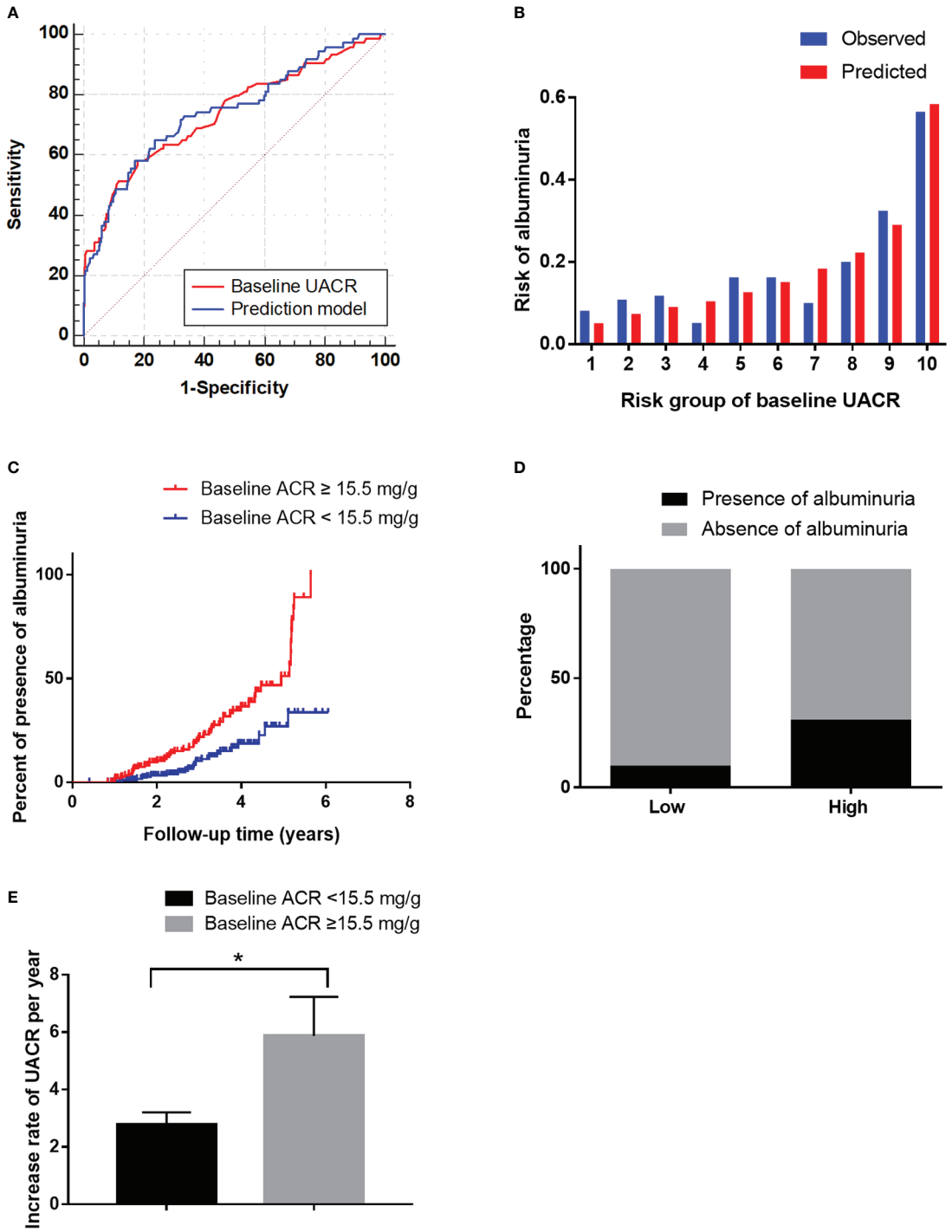

FIGURE 3
The performance of the baseline UACR in predicting albuminuria in the development cohort. **(A)**: Receiver operating characteristic curve for the baseline UACR and the prediction models. The area under the curve (AUC) and its 95% CI were 0.74 (0.67–0.81) for the baseline UACR and 0.74 (0.68-0.81) for the prediction model. The discriminative power of baseline UACR vs the prediction model (P=0.465). **(B)**: Hosmer-Lemeshow (H-L) test for the calibration of the baseline UACR (P=0.22). **(C)**: Kaplan-Meier curve of albuminuria end point for the low-risk (UACR < 15.5 mg/g) and high-risk groups (30 > UACR ≥ 15.5 mg/g) according to the cut-off value. The HR (95% CI) was 1.66 (1.31-2.10) (P < 0.001) in the high-risk group. **(D)**: Prevalence of albuminuria in the low-risk (UACR <15.5 mg/g) and high-risk (30 > UACR ≥ 15.5 mg/g) groups. **(E)**: The increase rate of UACR per year in the low-risk (UACR < 15.5 mg/g) and high-risk groups (30 > UACR ≥ 15.5 mg/g) according to the cut-off value. *$P < 0.05$.

10.3389/fendo.2022.1064665

TABLE 8 Sensitivity, specificity and youden index of the UACR at different cut-off values.

Cut-off value ofUACR (mg/g)	Sensitivity	Specificity	Youden Index
5.0	1	0.02	0.02
10.0	0.93	0.16	0.09
15.5	**0.69**	**0.63**	**0.32(the largest)**
20.0	0.31	0.89	0.20
25.0	0.28	0.96	0.24

In the validation cohort, the incidence of CVD in the high-risk group of UACR (43.5%) was significantly higher than in the low-risk group (25.7%) (Figure 5B, P<0.05). The lesion vessel number was significantly higher in the high-risk group of the UACR than in the low-risk group (Figure 5C, D, P<0.05).

3.3 The relationship between eGFR and UACR

In the validation cohort, we further investigated the relationship between eGFR and UACR at the cut-off value metioned above. In the subgroup of eGFR ≤ 84.80 ml/min/1.73 m^2, the endpoint eGFR was lower and the decline rate of eGFR was faster in the group of baseline UACR ≥ 15.5 mg/g than in the group of baseline UACR < 15.5 mg/g. In the subgroup of eGFR > 84.80 ml/min/1.73 m^2, the eGFR and the decline rate of eGFR was not statistically different between the two groups (Table 9). Besides, the endpoint UACR had no significant difference in patients with eGFR lower or higher than 84.80 ml/min/1.73 m^2 (Supplementary Table 3).

4 Discussion

In this study, we identified that the eGFR and UACR in the normal range had the most predictive power for predicting DKD. The prediction models did not improve significantly by addition of further variables. Furthermore, we defined that eGFR at 84.8 mL/min/1.73 m^2 or UACR at 15.5 mg/g with the largest Youden's index were an earlier cut-off value for DKD. Patients with eGFR at 60–84.8 mL/min/1.73 m^2 or UACR at 15.5-30 mg/g were more likely to develop DKD than patients with eGFR >84.8 mL/min/1.73 m^2 or UACR <15.5 mg/g. Patients who had eGFR ≤84.80 ml/min/1.73 m^2 or UACR ≥15.5 mg/g may had higher incidence and severity for CVD.

It was reported that eGFR and albuminuria were the most important factors to predict onset and progression of early CKD in individuals with type 2 diabetes, and inclusion of demographic, clinical, and other laboratory predictors barely improved predictive performance (24). Consistent with this study, the results in our study indicated that baseline eGFR was effective enough to predict DKD, and UACR was effective enough to predict DKD. In addition, adding other risk factors into the predictive model will not substantially improve risk prediction. This by no means negates the importance of the other risk factors such as hyperglycemia (25–27) and hyperlipidemia (28) as modifiable factors in the progression of DKD, because ability to predict the progression of the disease should not be equated with causality. On the contrary, it provides the simplest and most effective way to predict DKD.

The eGFR is the most important indicator that reflects renal function. Once the process of renal function decline begins, it will irreversibly progress to end-stage renal disease. Recent studies have shown that the decreased eGFR within the normal range may be a risk factor for DKD (29, 30). However, as the single predictor, the predictive performance of baseline eGFR was unclear. In this study, all of the patients had normal albuminuria at baseline, and in order to strictly exclude the patients with pre-existing kidney damage, we excluded patients with UACR ≥30 mg/g at the end of the follow-up. Our results demonstrated that the baseline eGFR as a single predictor is effective enough to identify patients at high risk for DKD with an AUC of 0.91. Furthermore, we determined the optimal cut-off value of eGFR at 84.8 mL/min/1.73 m^2. In the validation cohort, at the eGFR of 84.8 mL/min/1.73 m^2, the sensitivity and specificity were 85% and 72%, respectively. This added to the evidence base that the eGFR cut-off value of 84.8 mL/min/1.73 m^2 was effective enough to distinguish high-risk from low-risk patients. Compared with participants in the low-risk group, those in the high-risk group had a 15.84-fold increase in the odds of DKD, and the decrease rate of eGFR was higher in patients with eGFR ≤84.80 ml/min/1.73 m^2 than in patients with eGFR >84.80 ml/min/1.73 m2. Considering that eGFR is strongly influenced by age, we divided our patients into four groups according to quartiles: >61, 55-61, 48-55, or <48. We found that in each group, the cut-off of 84.8 had very consistent sensitivity and specificity. In addition, we included age in the multivariate COX regression analysis, and found that the inclusion of age either in the prediction model that included all risk factors with statistical differences or in the models that only included age and eGFR, could not improve the predictive value of the model. All these results support that the cut-off value is reliable across age. We also included gender into multivariable Cox analysis, but no statistical difference was found. Therefore, we believe that the cut-off value of eGFR at 84.8 mL/min/1.73 m^2

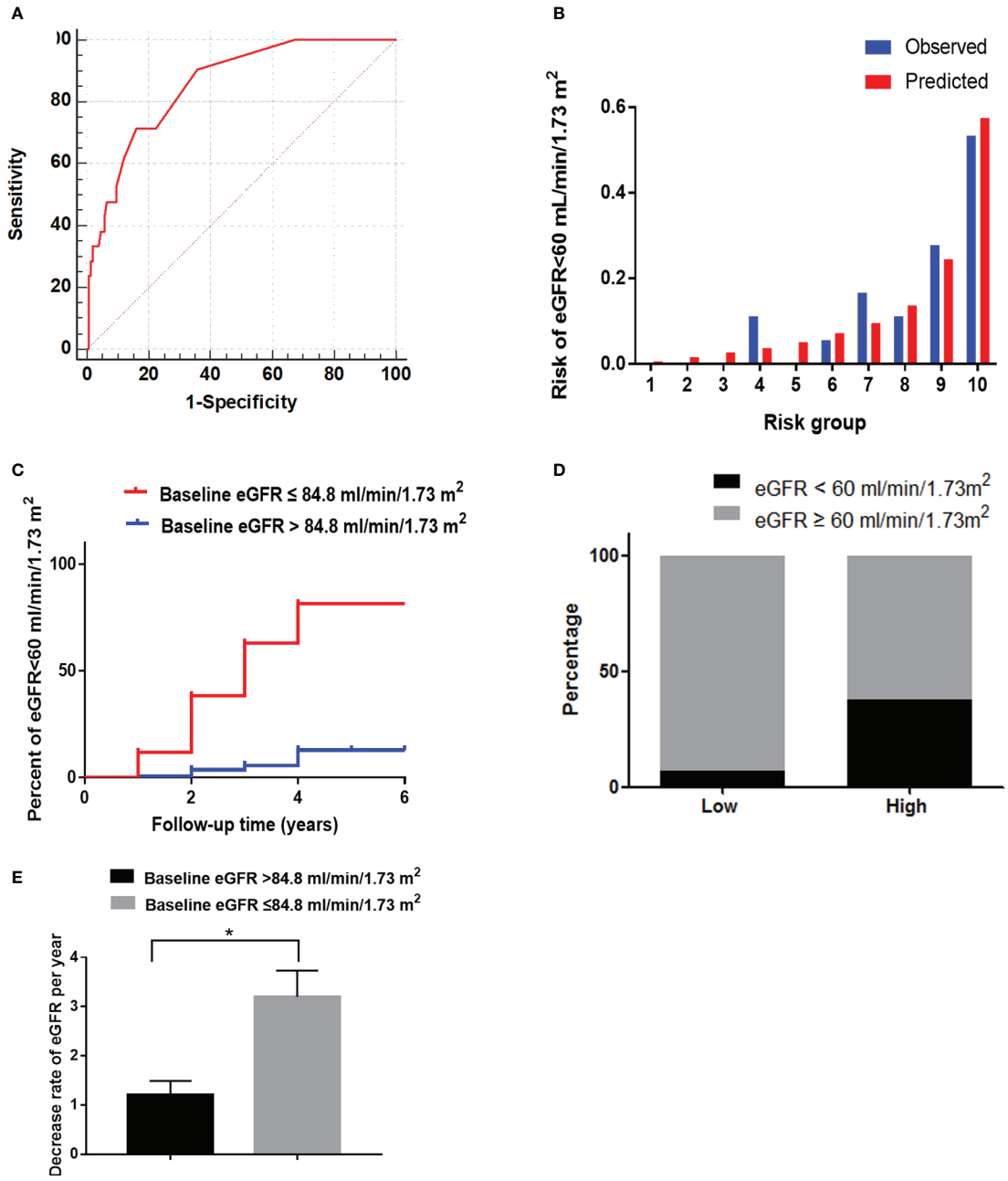

FIGURE 4
The performance of the baseline eGFR in predicting reduced eGFR in the validation cohort. **(A)** Receiver operating characteristic curve of baseline eGFR in predicting reduced eGFR. The area under the curve (AUC) and its 95%CI were 0.85(0.76-0.93). The sensitivity and specificity were 0.85 and 0.72, respectively, at 84.8 mL/min/1.73 m^2 of eGFR. **(B)** Hosmer-Lemeshow (H-L) test for the calibration of the baseline eGFR(P=0.17). **(C)** Kaplan-Meier curve of reduced eGFR end point for the low-risk (eGFR >84.8 mL/min/1.73 m^2) and high-risk (60 ≤ eGFR ≤ 84.8 mL/min/1.73 m^2) groups. The HR (95% CI) was 15.84 (4.04-24.00) (P < 0.001) in the high-risk group. **(D)** Prevalence of reduced eGFR in the two risk groups. **(E)** The decrease rate of eGFR per year in the low-risk (eGFR > 84.8 mL/min/1.73 m^2) and high-risk (60 ≤ eGFR ≤ 84.8 mL/min/1.73 m2) groups. *P < 0.05.

can effectively predict the development of DKD. At the same time, we calculated the difference in eGFR between the groups at baseline and at the end of follow-up, and the results showed that patients with eGFR ≤84.8 had a greater eGFR decline than those with eGFR >84.8 even after the correction of follow-up time. These results suggest that patients with eGFR ≤ 84.8 have a faster decline of renal function. Thus we conclude that in the absence of albuminuria and other evidence of kidney damage, the

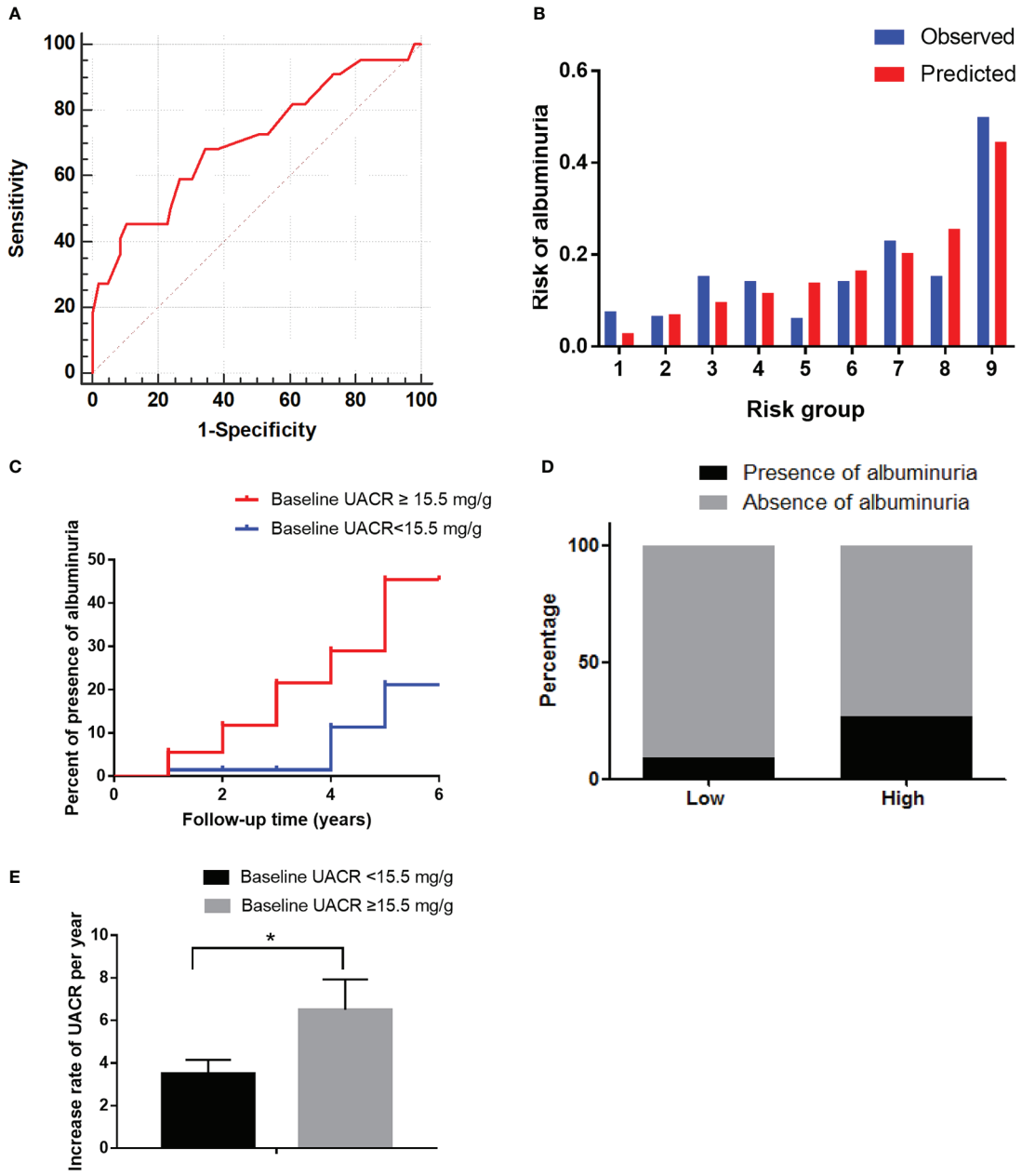

FIGURE 5
The performance of the baseline UACR in predicting albuminuria and baseline eGFR in predicting reduced eGFR in the validation cohort. **(A)**: Receiver operating characteristic curve of baseline UACR in predicting albuminuria. The area under the curve (AUC) and its 95% CI were 0.71(0.58-0.84). The sensitivity and specificity were 0.68 and 0.66, respectively, at 15.5mg/g of UACR. **(B)**: Hosmer-Lemeshow (H-L) test for the calibration of the baseline UACR (P=0.95). **(C)**: Kaplan-Meier curve of albuminuria end point for the low-risk (UACR < 15.5 mg/g) and high-risk (30 > UACR ≥ 15.5 mg/g) groups. The HR (95% CI) was 2.78 (1.31-9.28) (P = 0.035) in the high-risk group. **(D)**: Prevalence of albuminuria in the two risk groups. **(E)**: The increase rate of UACR per year in the low-risk (UACR < 15.5 mg/g) and high-risk groups (30 > UACR ≥ 15.5 mg/g) according to the cut-off value. *$P < 0.05$.

progressive decline in renal function may already exist in patients with an eGFR of 60–84.8 mL/min/1.73 m^2.

It is well known that hyperfiltration is one major feature of early DKD. Besides, in a follow-up study of patients with diabetic nephropathy, researchers at the Joslin Diabetes Center found that there was a progressive decline in eGFR before reaching the stage of less than 60 (31). Therefore, both hyperfiltration and a mild decrease in the normal range of eGFR may predict DKD. They may exist in different periods before the onset of DKD. In a meta-analysis including 23 studies, it was found that patients

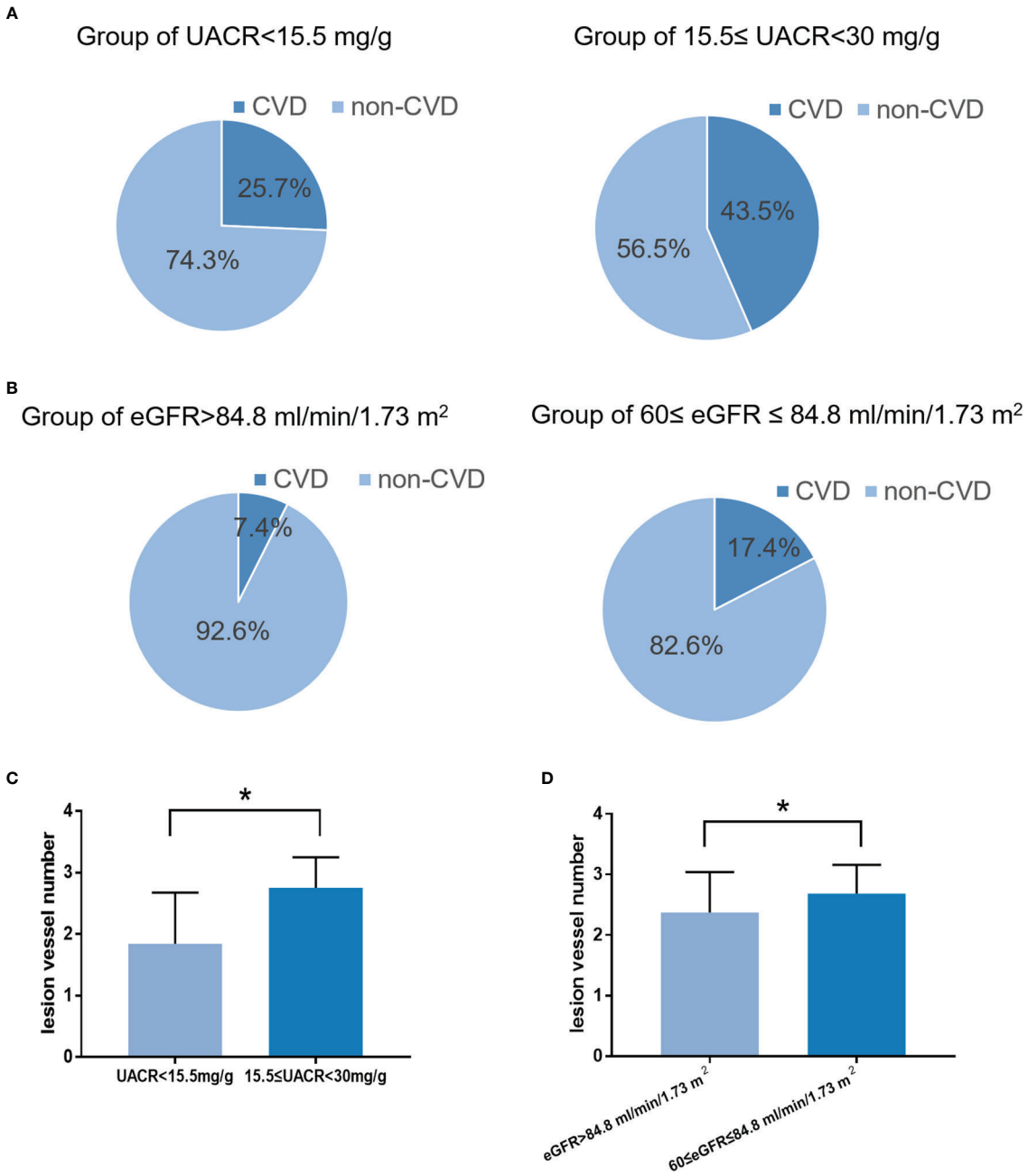

FIGURE 6
The incidence and severity of CVD in the low-risk and high-risk groups. **(A)**: The incidence and severity of CVD in the low-risk and high-risk groups according to the cut-off value of the UACR ($P < 0.05$). **(B)**: The incidence and severity of CVD in the low-risk and high-risk groups according to the cut-off value of the eGFR ($P < 0.05$). **(C)**: The severity of CVD in the low-risk and high-risk groups according to the cut-off value of the UACR ($P < 0.05$). **(D)**: The severity of CVD in the low-risk and high-risk groups according to the cut-off value of the eGFR ($P < 0.05$). *$P < 0.05$.

with hyperfiltration may need up to 10 years to develop DKD (32); However, in our study, the average time for patients with eGFR ≤84.80 ml/min/1.73 m^2 to develop DKD is about 3 years. Therefore, eGFR ≤84.80 ml/min/1.73 m^2 may be a more recent predictor of DKD compared with hyperfiltration. In addition, it is currently believed that there is a considerable proportion of non-albuminuria DKD in patients with DKD. These patients do not necessarily experience the classic Mogensen staging: hyperfiltration phase, intermittent microalbuminuria, persistent microalbuminuria phase, macroalbuminuria phase and failure of kidney function, and they may develop directly into the decline of renal function. Therefore, our study have

10.3389/fendo.2022.1064665

TABLE 9 The subgroup analysis of eGFR and eGFR decline rate in the normal and high-normal group of UACR according to the cut-off value of 15.5mg/g.

Indicators	Baseline eGFR > 84.80 mL/min/1.73 m^2			Baseline eGFR ≤ 84.80 mL/min/1.73 m^2		
	Baseline ACR <15.5	Baseline ACR ≥ 15.5	*P*	Baseline ACR <15.5	Baseline ACR ≥ 15.5	*P*
Baseline eGFR	103.65 ± 16.93	99.80 ± 15.87	0.11	76.36 ± 7.65	75.38 ± 7.37	0.63
Endpoint eGFR	103.08 ± 16.88	99.91 ± 15.90	0.17	77.94 ± 17.10	69.45 ± 15.06	0.04
eGFR decline rate (per month)	0.13 (0.01, 0.33)	0.16 (0.02, 0.44)	0.15	-0.11 (-0.41, 0.13)	0.12 (-0.05, 0.41)	0.02

suggested that eGFR ≤84.80 ml/min/1.73 m^2 may provide a new clue for those who are at increased risk of developing non-albuminuria DKD.

UACR is a widely used indicator for diagnosing early DKD (33, 34). Previous studies have demonstrated that an increased baseline UACR, even within the normal range, was a risk factor for developing albuminuria (18–21). Participants with diabetes and a UACR of 10-30 mg/g had a 2.7-fold higher odds of developing albuminuria than those with UACR <5 mg/g (20). In addition, the KDOQI recommended a stratification of normal albuminuria to UACR <10 mg/g (optimal) and 10 ≤ UACR <30 mg/g (normal high limit) (14). Thus higher UACR in the normal range is indeed a risk factor for DKD. In this study, we assessed the predictive power of the baseline UACR and found that it was the most effective single predictor for predicting DKD with an AUC of 0.74. Furthermore, we determined that the optimal cut-off value of UACR is 15.5 mg/g. In the validation cohort, at an UACR cut-off value of 15.5 mg/g, the sensitivity and specificity were 0.68 and 0.66, respectively. In addition, compared with participants in the low-risk group, those in the high-risk groups had 2.78 fold increases in the odds of DKD, and the increase rate of UACR was higher in patients with UACR ≥15.5 mg/g than in patients with UACR <15.5 mg/g. Therefore, UACR at 15.5 mg/g may be a simple and effective cut-off value to distinguish high-risk patients from other populations. The increase of UACR in the normal range may reflect earlier abnormalities of glomerular haemodynamics and permselectivity (19) or the reabsorption dysfunction of the renal tubules (35). On the other hand, albuminuria may not simply be an indicator of damage in the glomerular filtration barrier, or as a predictor of DKD progression, because albuminuria in itself can be toxic to the kidney and affect pathological processes (36), such as causing tubulointerstitial inflammation, oxidative stress, fibrosis and tubular cell injury and death by activating a series of signalling pathways in proximal tubular cells (37–39). Therefore, the early prevention and treatment of UACR may prevent associated tubular injury and delay the progression of albuminuria.

It has been reported that elevated ACR, even within the normal range, is associated with a faster decline in eGFR in diabetic patients (40). Consistent with the previously reported literature, in this study, it was found that in the subgroup of the baseline eGFR lower than 84.80 ml/min/1.73 m^2, the level of eGFR was lower and the decline rate of eGFR was faster in the patients with UACR ≥15.5 mg/g than in patients with UACR <15.5 mg/g. Thus we concluded that on the basis of eGFR at lower level in the normal range, UACR ≥ 15.5 mg/g may effectively indicate faster decline in eGFR.

The eGFR and UACR are independent predictors of cardiovascular events in type 2 diabetes mellitus (41, 42). Numerous studies have confirmed that renal function decline, defined as eGFR <60 mL/min/1.73 m^2, was independently associated with an increased risk of cardiovascular events in patients with diabetes (43–45). We found that the incidence and severity of CVD in patients with eGFR of 60–84.8 mL/min/1.73 m^2 was higher than in patients with eGFR >84.8 mL/min/1.73 m^2, so we suggested that the range of 60-84.8 ml/min/1.73 m^2 of eGFR may already increase the risk for CVD. Albuminuria is believed to reflect endothelial injury that extends from the glomerulus to the arterial circulation at large, thus linking this marker to both kidney disease and cardiovascular disease (CVD) (46–50). A study showed that participants with UACR median value of ≥3.9 mg/g for men, and ≥7.5 mg/g for women experienced a nearly 3-fold higher risk of CVD than those with UACR below the median (51). Consistent with this study, we also found that the incidence and severity of CVD were significantly higher in high-risk patients (UACR at 15.5-30 mg/g) than in low-risk patients (UACR <15.5 mg/g). This adds to the growing body of evidence that challenges the notion that UACR <30 mg/g indicates “normal” albumin excretion.

We have several limitations. First, our samples size was not large enough. To overcome this, we randomly selected patients from three tertiary hospital in the validationn cohort. This may enhance the effectiveness of the study. However, a more comprehensive analysis of the relationship between eGFR ≤84.8 mL/min/1.73 m2 or UACR ≥15.5 mg/g and CVD are needed. Secondly, we did not obtain the general data such as blood biochemistry except UACR and eGFR after follow-up. Our focus was to study the impact of the general data of the baseline on the outcome in order to find the risk factors leading to DKD. Therefore, we did not record the general data of the patient at the end of follow-up except UACR and eGFR. In addition, we believe that the general data at the end of follow-up and the outcome events occur at the same time, therefore they may have limited impact on our research results.

In conclusion, eGFR ≤84.8 mL/min/1.73 m^2 or UACR ≥15.5 mg/g in the normal range may be an effective cut-off value for DKD. Paying attention to the decrease of eGFR and increase of UACR within the normal range and providing early and reasonable intervention may prevent or delay the development of DKD. In addition, patients who had eGFR lower than or equal to the cut-off value or UACR higher than or equal to the cut-off value may had higher incidence and severity for CVD.

Data availability statement

The raw data supporting the conclusions of this article will be made available by the authors, without undue reservation.

Ethics statement

This study was approved by the Institutional Review Board of Tianjin Medical University Chu Hsien-I Memorial Hospital and Tianjin Institute of Endocrinology. Informed consent was obtained from all patients prior to study participation.

Author contributions

ZG and YZ performed the research, analyzed the data and wrote the manuscript and they are co-first authors and contributed equally to this study. XS, WJ, MS, JW, LL, HuZ, YQ, SZ, YY, JX performed the research and acquired data. HoZ contributed to statistical analyses. JY, CS and BC designed the study and revised the manuscript, and they are co-corresponding authors and contributed equally to this study, and they take full responsibility for the work and approved the final version to be published. All authors contributed to the article and approved the submitted version.

Funding

This work was supported by the National Natural Science Foundation of China): 82074253, 82274299; Tianjin Key Medical Discipline (Specialty) Construction Project (TJYXZDXK-032A).

Conflict of interest

The authors declare that the research was conducted in the absence of any commercial or financial relationships that could be construed as a potential conflict of interest.

Publisher's note

Supplementary material

The Supplementary Material for this article can be found online at: https://www.frontiersin.org/articles/10.3389/fendo.2022.1064665/full#supplementary-material

References

1. Cho NH, Shaw JE, Karuranga S, Huang Y, da Rocha Fernandes JD, Ohlrogge AW. Et al, IDF diabetes atlas: Global estimates of diabetes prevalence for 2017 and projections for 2045. *Diabetes Res Clin Pract* (2018) 138:271–81. doi: 10.1016/j.diabres.2018.02.023

2. Molitch ME, Adler AI, Flyvbjerg A, Nelson RG, So WY, Wanner C, et al. Diabetic kidney disease: a clinical update from kidney disease: Improving global outcomes. *Kidney Int* (2015) 87(1):20–30. doi: 10.1038/ki.2014.128

3. Colhoun HMMarcovecchio ML. Biomarkers of diabetic kidney disease. *Diabetologia* (2018) 61(5):996–1011. doi: 10.1007/s00125-018-4567-5

4. Lin CH, Chang YCChuang LM. Early detection of diabetic kidney disease: Present limitations and future perspectives. *World J Diabetes* (2016) 7(14):290–301. doi: 10.4239/wjd.v7.i14.290

5. Hallan SI, Ritz E, Lydersen S, Romundstad S, Kvenild KOrth SR. Combining GFR and albuminuria to classify CKD improves prediction of ESRD. *J Am Soc Nephrol* (2009) 20(5):1069–77. doi: 10.1681/ASN.2008070730

6. Gansevoort RT, Matsushita K, van der Velde M, Astor BC, Woodward M, Levey AS, et al. Lower estimated GFR and higher albuminuria are associated with adverse kidney outcomes. a collaborative meta-analysis of general and high-risk population cohorts. *Kidney Int* (2011) 80(1):93–104. doi: 10.1038/ki.2010.531

7. Williams ME. Diabetic nephropathy: the proteinuria hypothesis. *Am J Nephrol* (2005) 25(2):77–94. doi: 10.1159/000084286

8. Penno G, Solini A, Orsi E, Bonora E, Fondelli C, Trevisan R, et al. Non-albuminuric renal impairment is a strong predictor of mortality in individuals with type 2 diabetes: the renal insufficiency and cardiovascular events (RIACE) Italian multicentre study. *Diabetologia* (2018) 61(11):2277–89. doi: 10.1007/s00125-018-4691-2

9. Williams ME. Diabetic chronic kidney disease: when the other shoe drops. *Med Clin North Am* (2013) 97(1):xi–xii. doi: 10.1016/j.mcna.2012.11.005

10. Porrini E, Ruggenenti P, Mogensen CE, Barlovic DP, Praga M, Cruzado JM, et al. Non-proteinuric pathways in loss of renal function in patients with type 2 diabetes. *Lancet Diabetes Endocrinol* (2015) 3(5):382–91. doi: 10.1016/S2213-8587(15)00094-7

11. Kramer HJ, Nguyen QD, Curhan GHsu CY. Renal insufficiency in the absence of albuminuria and retinopathy among adults with type 2 diabetes mellitus. *Jama* (2003) 289(24):3273–7. doi: 10.1001/jama.289.24.3273

12. Retnakaran R, Cull CA, Thorne KI, Adler AIHolman RR. Risk factors for renal dysfunction in type 2 diabetes: U.K. prospective diabetes study 74. *Diabetes* (2006) 55(6):1832–9. doi: 10.2337/db05-1620

13. Perkins BA, Ficociello LH, Roshan B, Warram JHKrolewski AS. In patients with type 1 diabetes and new-onset microalbuminuria the development of advanced chronic kidney disease may not require progression to proteinuria. *Kidney Int* (2010) 77(1):57–64. doi: 10.1038/ki.2009.399

14. Levey AS, de Jong PE, Coresh J, El Nahas M, Astor BC, Matsushita K. Et al, the definition, classification, and prognosis of chronic kidney disease: a KDIGO controversies conference report. *Kidney Int* (2011) 80(1):17–28. doi: 10.1038/ki.2010.483

15. Viberti GC, Hill RD, Jarrett RJ, Argyropoulos A, Mahmud UKeen H. Microalbuminuria as a predictor of clinical nephropathy in insulin-dependent diabetes mellitus. *Lancet* (1982) 1(8287):1430–2. doi: 10.1016/S0140-6736(82)92450-3

16. Mogensen CE, Chachati A, Christensen CK, Close CF, Deckert T, Hommel E, et al. Microalbuminuria: an early marker of renal involvement in diabetes. *Uremia Invest* (1985) 9(2):85–95. doi: 10.3109/08860228509088195

17. Gaede P, Tarnow L, Vedel P, Parving HHPedersen O. Remission to normoalbuminuria during multifactorial treatment preserves kidney function in patients with type 2 diabetes and microalbuminuria. *Nephrol Dial Transplant* (2004) 19(11):2784–8. doi: 10.1093/ndt/gfh470

18. Gall MA, Hougaard P, Borch-Johnsen KParving HH. Risk factors for development of incipient and overt diabetic nephropathy in patients with non-insulin dependent diabetes mellitus: prospective, observational study. *Bmj* (1997) 314(7083):783–8. doi: 10.1136/bmj.314.7083.783

19. Hovind P, Tarnow L, Rossing P, Jensen BR, Graae M, Torp I, et al. Predictors for the development of microalbuminuria and macroalbuminuria in patients with type 1 diabetes: inception cohort study. *Bmj* (2004) 328(7448):1105. doi: 10.1136/bmj.38070.450891.FE

20. Xu J, Lee ET, Devereux RB, Umans JG, Bella JN, Shara NM, et al. A longitudinal study of risk factors for incident albuminuria in diabetic American indians: the strong heart study. *Am J Kidney Dis* (2008) 51(3):415–24. doi: 10.1053/j.ajkd.2007.11.010

21. Tanaka S, Tanaka S, Iimuro S, Yamashita H, Katayama S, Akanuma Y, et al. Predicting macro- and microvascular complications in type 2 diabetes: the Japan diabetes complications study/the Japanese elderly diabetes intervention trial risk engine. *Diabetes Care* (2013) 36(5):1193–9. doi: 10.2337/dc12-0958

22. Levey AS, Stevens LA, Schmid CH, Zhang YL, Castro AF3rd, Feldman HI, et al. A new equation to estimate glomerular filtration rate. *Ann Intern Med* (2009) 150(9):604–12. doi: 10.7326/0003-4819-150-9-200905050-00006

23. Cook NR. Use and misuse of the receiver operating characteristic curve in risk prediction. *Circulation* (2007) 115(7):928–35. doi: 10.1161/CIRCULATIONAHA.106.672402

24. Dunkler D, Gao P, Lee SF, Heinze G, Clase CM, Tobe S, et al. Risk prediction for early CKD in type 2 diabetes. *Clin J Am Soc Nephrol* (2015) 10(8):1371–9. doi: 10.2215/CJN.10321014

25. Ismail-Beigi F, Craven T, Banerji MA, Basile J, Calles J, Cohen RM, et al. Effect of intensive treatment of hyperglycaemia on microvascular outcomes in type 2 diabetes: an analysis of the ACCORD randomised trial. *Lancet* (2010) 376 (9739):419–30. doi: 10.1016/S0140-6736(10)60576-4

26. Zoungas S, Chalmers J, Ninomiya T, Li Q, Cooper ME, Colagiuri S, et al. Association of HbA1c levels with vascular complications and death in patients with type 2 diabetes: evidence of glycaemic thresholds. *Diabetologia* (2012) 55(3):636–43. doi: 10.1007/s00125-011-2404-1

27. Forsblom CM, Groop PH, Ekstrand A, Tötterman KJ, Sane T, Saloranta C, et al. Predictors of progression from normoalbuminuria to microalbuminuria in NIDDM. *Diabetes Care* (1998) 21(11):1932–8. doi: 10.2337/diacare.21.11.1932

28. Russo GT, De Cosmo S, Viazzi F, Pacilli A, Ceriello A, Genovese S, et al. Plasma triglycerides and HDL-c levels predict the development of diabetic kidney disease in subjects with type 2 diabetes: The AMD annals initiative. *Diabetes Care* (2016) 39(12):2278–87. doi: 10.2337/dc16-1246

29. Takagi M, Babazono TUchigata Y. Differences in risk factors for the onset of albuminuria and decrease in glomerular filtration rate in people with type 2 diabetes mellitus: implications for the pathogenesis of diabetic kidney disease. *Diabetes Med* (2015) 32(10):1354–60. doi: 10.1111/dme.12793

30. Low S, Tai ES, Yeoh LY, Liu YL, Liu JJ, Tan KH, et al. Onset and progression of kidney disease in type 2 diabetes among multi-ethnic Asian population. *J Diabetes Complications* (2016) 30(7):1248–54. doi: 10.1016/j.jdiacomp.2016.05.020

31. Krolewski AS, Bonventre JV. High risk of ESRD in type 1 diabetes: new strategies are needed to retard progressive renal function decline. *Semin Nephrol* (2012) 32(5):407–14. doi: 10.1016/j.semnephrol.2012.07.002

32. Magee GM, Bilous RW, Cardwell CR, Hunter SJ, Kee F, Fogarty DG. Is hyperfiltration associated with the future risk of developing diabetic nephropathy? a meta-analysis. *Diabetologia.* (2009) 52(4):691–7. doi: 10.1007/s00125-009-1268-0

33. Warram JH, Gearin G, Laffel LKrolewski AS. Effect of duration of type I diabetes on the prevalence of stages of diabetic nephropathy defined by urinary albumin/creatinine ratio. *J Am Soc Nephrol* (1996) 7(6):930–7. doi: 10.1681/ASN.V76930

34. KDOQI. Clinical practice guidelines and clinical practice recommendations for diabetes and chronic kidney disease. *Am J Kidney Dis* (2007) 49(2 Suppl 2):S12–154. doi: 10.1053/j.ajkd.2006.12.005

35. Chen Y, Zelnick LR, Wang K, Hoofnagle AN, Becker JO, Hsu CY, et al. Kidney clearance of secretory solutes is associated with progression of CKD: The CRIC study. *J Am Soc Nephrol* (2020) 31(4):817–27. doi: 10.1681/ASN.2019080811

36. Remuzzi G, Benigni ARemuzzi A. Mechanisms of progression and regression of renal lesions of chronic nephropathies and diabetes. *J Clin Invest* (2006) 116(2):288–96. doi: 10.1172/JCI27699

37. Ohse T, Inagi R, Tanaka T, Ota T, Miyata T, Kojima I, et al. Albumin induces endoplasmic reticulum stress and apoptosis in renal proximal tubular cells. *Kidney Int* (2006) 70(8):1447–55. doi: 10.1038/sj.ki.5001704

38. Morigi M, Macconi D, Zoja C, Donadelli R, Buelli S, Zanchi C, et al. Protein overload-induced NF-kappaB activation in proximal tubular cells requires H(2)O (2) through a PKC-dependent pathway. *J Am Soc Nephrol* (2002) 13(5):1179–89. doi: 10.1097/01.ASN.0000013304.48222.02

39. Li X, Pabla N, Wei Q, Dong G, Messing RO, Wang CY, et al. PKC-delta promotes renal tubular cell apoptosis associated with proteinuria. *J Am Soc Nephrol* (2010) 21(7):1115–24. doi: 10.1681/ASN.2009070760

40. Babazono T, Nyumura I, Toya K, Hayashi T, Ohta M, Suzuki K, et al. Higher levels of urinary albumin excretion within the normal range predict faster decline in glomerular filtration rate in diabetic patients. *Diabetes Care* (2009) 32(8):1518–20. doi: 10.2337/dc08-2151

41. Ninomiya T, Perkovic V, de Galan BE, Zoungas S, Pillai A, Jardine M, et al. Albuminuria and kidney function independently predict cardiovascular and renal outcomes in diabetes. *J Am Soc Nephrol* (2009) 20(8):1813–21. doi: 10.1681/ASN.2008121270

42. Drury PL, Ting R, Zannino D, Ehnholm C, Flack J, Whiting M, et al. Estimated glomerular filtration rate and albuminuria are independent predictors of cardiovascular events and death in type 2 diabetes mellitus: the fenofibrate intervention and event lowering in diabetes (FIELD) study. *Diabetologia* (2011) 54(1):32–43. doi: 10.1007/s00125-010-1854-1

43. Freeman RV, Mehta RH, Al Badr W, Cooper JV, Kline-Rogers EEagle KA. Influence of concurrent renal dysfunction on outcomes of patients with acute coronary syndromes and implications of the use of glycoprotein IIb/IIIa inhibitors. *J Am Coll Cardiol* (2003) 41(5):718–24. doi: 10.1016/S0735-1097(02)02956-X

44. Sørensen CR, Brendorp B, Rask-Madsen C, Køber L, Kjøller ETorp-Pedersen C. The prognostic importance of creatinine clearance after acute myocardial infarction. *Eur Heart J* (2002) 23(12):948–52. doi: 10.1053/euhj.2001.2989

45. Nag S, Bilous R, Kelly W, Jones S, Roper NConnolly V. All-cause and cardiovascular mortality in diabetic subjects increases significantly with reduced estimated glomerular filtration rate (eGFR): 10 years' data from the south Tees diabetes mortality study. *Diabetes Med* (2007) 24(1):10–7. doi: 10.1111/j.1464-5491.2007.02023.x

46. Borch-Johnsen K, Feldt-Rasmussen B, Strandgaard S, Schroll MJensen JS. Urinary albumin excretion. an independent predictor of ischemic heart disease. *Arterioscler Thromb Vasc Biol* (1999) 19(8):1992–7. doi: 10.1161/01.ATV.19.8.1992

47. Yuyun MF, Khaw KT, Luben R, Welch A, Bingham S, Day NE, et al. A prospective study of microalbuminuria and incident coronary heart disease and its prognostic significance in a British population: the EPIC-Norfolk study. *Am J Epidemiol* (2004) 159(3):284–93. doi: 10.1093/aje/kwh037

48. Hillege HL, Fidler V, Diercks GF, van Gilst WH, de Zeeuw D, van Veldhuisen DJ, et al. Urinary albumin excretion predicts cardiovascular and noncardiovascular mortality in general population. *Circulation* (2002) 106 (14):1777–82. doi: 10.1161/01.CIR.0000031732.78052.81

49. Romundstad S, Holmen J, Kvenild K, Hallan HEllekjaer H. Microalbuminuria and all-cause mortality in 2,089 apparently healthy individuals: a 4.4-year follow-up study. the nord-trøndelag health study (HUNT), Norway. *Am J Kidney Dis* (2003) 42(3):466–73. doi: 10.1016/s0272-6386(03)00742-x

50. Dinneen SF, Gerstein HC. The association of microalbuminuria and mortality in non-insulin-dependent diabetes mellitus. a systematic overview of the literature. *Arch Intern Med* (1997) 157(13):1413–8. doi: 10.1001/archinte.1997.00440340025002

51. Arnlöv J, Evans JC, Meigs JB, Wang TJ, Fox CS, Levy D, et al. Low-grade albuminuria and incidence of cardiovascular disease events in nonhypertensive and nondiabetic individuals: the framingham heart study. *Circulation* (2005) 112 (7):969–75. doi: 10.1161/CIRCULATIONAHA.105.538132

frontiers | Frontiers in Endocrinology

TYPE Original Research
PUBLISHED 19 December 2022
DOI 10.3389/fendo.2022.1106175

OPEN ACCESS

EDITED BY
Xiao-qiang Liu,
Tianjin Medical University General Hospital, China

REVIEWED BY
Shaochuan Liu,
Tianjin Medical University, China
Bosen You,
Harbin Medical University, China

*CORRESPONDENCE
Duocheng Qian
qiandc666@126.com
Chao Li
chaoli1979@126.com
Chengdang Xu
xuchengdang1990@163.com

†These authors have contributed equally to this work and share first authorship

SPECIALTY SECTION
This article was submitted to Adrenal Endocrinology, a section of the journal Frontiers in Endocrinology

RECEIVED 23 November 2022
ACCEPTED 06 December 2022
PUBLISHED 19 December 2022

CITATION
Chen X, Ma J, Wang X'a, Zi T, Qian D, Li C and Xu C (2022) *CCNB1* and *AURKA* are critical genes for prostate cancer progression and castration-resistant prostate cancer resistant to vinblastine.
Front. Endocrinol. 13:1106175.
doi: 10.3389/fendo.2022.1106175

CCNB1 and *AURKA* are critical genes for prostate cancer progression and castration-resistant prostate cancer resistant to vinblastine

Xi Chen[1†], Junjie Ma[2†], Xin'an Wang[1†], Tong Zi[1], Duocheng Qian[3*], Chao Li[1*] and Chengdang Xu[1*]

[1]Department of Urology, Tongji Hospital, School of Medicine, Tongji University, Shanghai, China, [2]Department of Urology, The Second Affiliated Hospital of Jiaxing University, Jiaxing, Zhejiang, China, [3]Department of Urology, Shanghai Fourth People's Hospital, Affiliated to Tongji University School of Medicine, Shanghai, China

Background: Prostate cancer (PCa) is a common malignancy occurring in men. As both an endocrine and gonadal organ, prostate is closely correlated with androgen. So, androgen deprivation therapy (ADT) is effective for treating PCa. However, patients will develop castration-resistant prostate cancer (CRPC) stage after ADT. Many other treatments for CRPC exist, including chemotherapy. Vinblastine, a chemotherapeutic drug, is used to treat CRPC. However, patients will develop resistance to vinblastine. Genetic alterations have been speculated to play a critical role in CRPC resistance to vinblastine; however, its mechanism remains unclear.

Methods: Various databases, such as Gene Expression Omnibus (GEO), The Cancer Genome Atlas (TCGA) and Chinese Prostate Cancer Genome and Epigenome Atlas (CPGEA), were used to collect the RNA-sequence data of PCa and CRPC patients and vinblastine-resistant PCa cells. Using online tools, Metascape and TIMER, the pathways and immune infiltration associated with vinblastine resistance-related genes in PCa were analyzed. The function of these genes was verified in clinical samples and CRPC cells.

Results: Using GSE81277 dataset, we collected the RNA-sequence data of vinblastine sensitive and resistant LNCaP cells and found nine genes (*CDC20*, *LRRFIP1*, *CCNB1*, *GPSM2*, *AURKA*, *EBLN2*, *CCDC150*, *CENPA* and *TROAP*) that correlated with vinblastine resistance. Furthermore, *CCNB1*, *GPSM2* and *AURKA* were differently expressed between normal prostate and PCa tissues, even influencing PCa progression. The GSE35988 dataset revealed that *CCNB1* and *AURKA* were upregulated in PCa and CRPC samples. Various genes were also found to affect the survival status of PCa patients based on TCGA. These genes were also related to immune cell infiltration. Finally, we verified the function of *CCNB1* and *AURKA* and observed that they were upregulated in PCa

and CRPC clinical samples and increased the sensitivity of CRPC cells to vinblastine.

Conclusion: *CCNB1* and *AURKA* are central to CRPC resistance to vinblastine and affect PCa progression.

KEYWORDS

vinblastine resistant, CCNB1, AURKA, castration-resistant prostate cancer, cancer development, bioinformatic analysis

1 Introduction

Prostate cancer (PCa) is a common disease occurring in older men and has the highest incidence and second-highest mortality rate in the USA (1). In China, the morbidity and mortality rates of PCa have been increasing rapidly (2). To date, many effective methods have been used to treat PCa, including surgical intervention, androgen deprivation therapy (ADT) and chemotherapy (3). As a hormone-sensitive endocrine and gonadal organ, the progression of PCa is closely related with androgen. This is also the reason that ADT is the first-line therapy method for treating PCa; however, patients undergoing ADT progress to the castration-resistant PCa (CRPC) stage (4). Moreover, chemotherapy, a second-line treatment, can be used in treating both hormone-sensitive PCa (HSPC) and CRPC (5). However, patients with chemotherapy also develop resistance to the treatment. The mechanism of resistance to chemotherapy in patients with CRPC remains unclear.

Vinblastine is a type of chemotherapeutic drug that can regulate spindle microtubule formation and inhibit nuclear division at metaphase. Additionally, it can also inhibit the viability of the RNA synthesis enzyme, thereby killing the cells in the G1 phase (6). Vinblastine has been widely used in the treatment of many solid cancers, such as lung, breast and ovarian cancers. Vinblastine is also used in HSPC and CRPC treatments (7–9). However, vinblastine treatment eventually, in most cases, leads to vinblastine resistance in patients. Genetic alteration is hypothesised to be one of the main reasons for the development of vinblastine resistance in patients with PCa and CRPC; however, its underlying mechanism remains unknown.

Hence, this study aims to identify the specific gene alterations in patients with CRPC who show resistance to vinblastine. In this study, we used a gene dataset, GSE81277, to identify the differentially expressed genes between normal and vinblastine-resistant PCa LNCaP cells. Furthermore, the role of these genes in affecting the PCa development was analyzed and immune cell infiltration in PCa were also analyzed. We found two key genes, *CCNB1* and *AURKA* were upregulated in PCa and CRPC samples and influenced the sensitivity of CRPC cells to vinblastine. So, we thought that *CCNB1* and *AURKA* may play an important role in CRPC resistant to vinblastine.

2 Materials and methods

2.1 Data sourcing

We collected three gene datasets, GSE81277, GSE21034 and GSE35988, from the Gene Expression Omnibus (GEO) database (http://www.ncbi.nlm.nih.gov/geo/). GSE81277 included the RNA sequence data of LNCaP PCa cells resistant to vinblastine. Three vinblastine sensitive and three resistant samples were obtained from GSE81277. Furthermore, GSE21034 and GSE35988 included the RNA and clinical data of patients with PCa. Additionally, the clinical data of patients with PCa were collected from both The Cancer Genome Atlas (TCGA) (http://cancergenome.nih.gov/) and Chinese Prostate Cancer Genome and Epigenome Atlas (CPGEA) (http://www.cpgea.com) databases.

2.2 Data handing

The primary RNA-sequence data obtained from different databases were normalized using R software (version 4.0.3). Based on the document comments, the expression matrix including probe ID was substituted by the corresponding gene ID. The genes with $|\log2FC > 1|$ and $P < 0.05$ were considered as critical genes. The genes were reflected in volcano map made by R software "Enhancedvolcano" package. Additionally, the clinical data from different databases were downloaded for further study.

2.3 Pathways analysis and protein-protein interaction network

The pathways of the enriched hub genes were analyzed using the online tool Metascape (http://metascape.org/), and the

bubble map was constructed using R software "ggplot2" package. Furthermore, the PPI network was constructed using STRING (https://cn.string-db.org/).

2.4 Online tool

Online tools, such as UALCAN (http://ualcan.path.uab.edu/), gene expression profiling interactive analysis (GEPIA) (http://www.gepia.cancer-pku.cn/) and Tumour Immune Estimation Resource (TIMER) (https://cistrome.shinyapps.io/timer/) were used for analysis.

2.5 Tumour stage and survival analysis

Based on the clinical data from different databases, the expression of hub genes in different tumour stages was analyzed. Additionally, using GEPIA the hub genes that influence overall survival (OS) and disease-free survival (DFS) in patients with PCa were also analyzed.

2.6 Immune immersion analysis

The correlation and mutation type of the identified hub genes and immune cells in PCa were analyzed using TIMER.

2.7 Clinical specimen collection

Clinical PCa and CRPC specimens were collected from Tongji Hospital, School of Medicine, Tongji University. The collection method was approved by the Ethics Committee of Tongji Hospital, School of Medicine, Tongji University (SBKT-2021-220). Patients who provided the samples were informed of the experiment and gave informed consent.

2.8 Cell culture and drug treatment

PCa cell lines were purchased from the Chinese Academy of Science Cell Bank (Shanghai, China). The human CRPC cell lines C4-2 and 22Rv1 were cultured in Roswell Park Memorial Institute (RPMI) 1640 medium (Catalog No. R8758, Sigma, Darmstadt, Germany) containing 10% fetal bovine serum (FBS) (Catalog No. 10091, Gibco, Thermo Fisher Scientific, Waltham, MA, USA). The cells were cultured in a humid environment with 5% CO2 and 95% air at 37°C. Vinblastine (Catalog No. S4505) was purchased from SelleckChem (Houston, TX, USA). The CRPC cells were treated with vinblastine (3.25 nmol/L) for 24 h.

2.9 Cell transfection and lentivirus production

Cell transfection assays were performed with Lipofectamine 2000 (Catalog No. 11668019, Thermo Fisher Scientific). shRNA lentivirus was constructed for specific gene knockdowns. The shRNAs were purchased from the Youze Biotechnology Company. Additionally, blank control lentivirus (shControl) without knockdown specific genes was also constructed by the Youze Biotechnology Company. The shRNA sequence was as follows: shCCNB1: GCAGCACCTG GCTAAGAATGCAGCACCTGGCTAAGAAT and shAURKA: CCGGCCTGTCTTACTGTCATTCGAACTCGAGTTCGAA TGACAGTAAGCAGGTTTTTG.

2.10 RNA extraction and qRT-PCR

The total RNA was extracted from CRPC cell lines utilizing TRIzol Reagent (Sigma–Aldrich, St. Louis, MO, USA, Catalog No. T9424). cDNA was transcribed using the reverse transcription kit (Advantage® RT-for-PCR Kit, Takara Bio Inc., Kusatsu, Japan, Catalog No. 639505). Finally, we measured the volume of cDNA using a real-time PCR kit (TB Green® Premix Ex Taq™ II, Takara Bio Inc., Catalog No. RR420A) according to the manufacturer's instructions. The primers of CCNB1, AURKA and GAPDH are shown in Table 1. The $2^{-\Delta\Delta Ct}$ method was used to quantify mRNA expression levels.

2.11 Antibodies

Rabbit monoclonal anti-CCNB1 antibody (Catalog No. ab156447), anti-AURKA antibody (Catalog No. ab108353) and anti-GAPDH antibody (Catalog No. ab9485) were purchased from Abcam (Abcam UK, Cambridge, UK).

2.12 Western blot

Tissue samples and cell line proteins were extracted with RIPA lysis buffer. Protein samples were treated with Dual Colour Protein

TABLE 1 Primers used for the qRT-PCR.

Gene Name	Primer sequence
CCNB1	Forward: 5′-GCACTTTCCTCCTTCTCA-3′
	Reverse: 5′-CGATGTGGCATACTTGTT-3
AURKA	Forward: 5′-ACAGGTCTGGCTGGCCGTTGGC-3′
	Reverse: 5′-GGCGCACACCGCGCGCAGGCG-3′
GAPDH	Forward: 5-GGAGCGAGATCCCTCCAAAAT-3′
	Reverse: 5′-GGCTGTTGTCATACTTCTCATGG-3′

Loading Buffer (Thermo Fisher Scientific, Waltham, MA, USA). Sodium dodecyl-sulfate polyacrylamide gel electrophoresis (10%) was used to separate proteins, which were then transferred to nitrocellulose membranes (Merck KGaA, Darmstadt, Germany). Protein-Free Rapid Blocking Buffer (Thermo Fisher Scientific) was utilized to block the membranes. Then, the membranes were incubated at 4°C overnight with primary antibodies against CCNB1 (1:1000), AURKA (1:1000) and GAPDH (1:1000) (Abcam UK, Cambridge, UK). On the second day, the membranes were washed thrice using 1×TBST (10 min/cycle). Then, the membranes were incubated at normal temperature for 1.5 h with a matched secondary antibody (Catalog No. A0208, HRP-labeled Goat Anti-Human IgG (H+L), Beyotime Biotechnology, Shanghai, China). Finally, the membranes were exposed to X-ray film.

2.13 Cell proliferation assay

Cell proliferation ability was detected using Cell counting kit-8 (CCK-8) (Dojindo, Japan). Briefly, cells were placed in 96-well plates (3000 cells/well) and cultured with 200 μL RPMI 1640 + 10% FBS for 0 h, 24 h, 48 h or 72 h. After culturing, cells were detected using CCK-8, following the manufacturer's instructions. Absorbance at 450 nm was measured using a spectrophotometer (LD942, Beijing, China).

2.14 Statistical analysis

The matrix data were analyzed using R version 4.0.3 (Institute for Statistics and Mathematics, Vienna, Austria; https://www.r-project.org). Comparisons between two groups were performed using the Wilcoxon test, and the Kruskal–Wallis test was employed for comparisons between more than two groups. Hazard ratios (HRs), 95% confidence interval (95% CI) and P values were used as statistical metrics. Twotailed,$P < 0.05$ was deemed as statistically significant.

3 Results

3.1 Nine hub genes correlated with vinblastine resistance in LNCaP PCa cells

The potential hub genes that correlated with PCa resistance to vinblastine were identified. In the GEO database, we found a gene dataset, GSE81277, which included the RNA-sequence data of both vinblastine-sensitive and -resistant LNCaP cells. Subsequently, the volcano map revealed nine hub genes (*CDC20*, *LRRFIP1*, *CCNB1*, *GPSM2*, *AURKA*, *EBLN2*, *CCDC150*, *CENPA* and *TROAP)* from LNCaP PCa cell samples that correlated with vinblastine resistance (Figure 1A). Further, we constructed a heat map to reflect the specific expression of each hub gene in the GSE81277 dataset (Figure 1B).

3.2 The pathways and PPI network of the enriched nine hub genes

The potential pathways and the correlation of each hub gene were analyzed using Metascape. The pathways enriched by the hub genes are illustrated in a bubble map. We found these genes mainly enriched in "microtubule cytoskeleton organization involved in mitosis" (Figure 2A). Then, using STRING, we constructed the PPI network to find the correlation between each hub gene. The network revealed that apart from *EBLN2* and *CCDC150*, each hub gene correlated with other genes (Figure 2B).

3.3 Vinblastine resistance-related hub gene expressions in PCa samples

After identifying the nine hub genes that were associated with vinblastine resistance in PCa, we examined the expression of these genes in PCa. We collected the sequence data of patients with PCa from different databases, such as TCGA, CPGEA and GEO. In TCGA, apart from *LRRFIP1*, all other gene expressions changed in PCa. Moreover, only *GPSM2* was downregulated whereas other genes were upregulated in PCa (Figure 3A). As the TCGA data included samples from Western populations, we further tested the expression of these hub genes in different populations, including the Asian population. Using the CPGEA database, we collected the RNA-sequence data of the Chinese population. The data revealed a change in the expressions of these nine genes in Chinese patients with PCa. Furthermore, *GPSM2* and *EBLN2* were downregulated whereas other hub genes were upregulated (Figure 3B). Finally, the GSE21034 dataset was used to verify the results. In GSE21034, we found that the expression of *LRRFIP1*, *CCNB1*, *GPSM2* and, *AURKA* changed in PCa samples, with *GPSM2* being downregulated (Figure 3C). As methylation level can affect the function of genes, we further examined the methylation level of these nine genes in the TCGA database. However, data on *EBLN2* could not be found and thus, only the methylation level of eight genes was tested. The methylation level of *GPSM2*, *EBLN2*, *CCDC150* and *TROAP* showed a statistically significant change compared to the other genes (Figure S1).

3.4 Vinblastine resistance-related hub genes affect PCa progression

As vinblastine resistance-related hub genes have been reported to influence PCa occurrence, we further evaluated these genes' role in PCa progression. As the Tumour-Node-

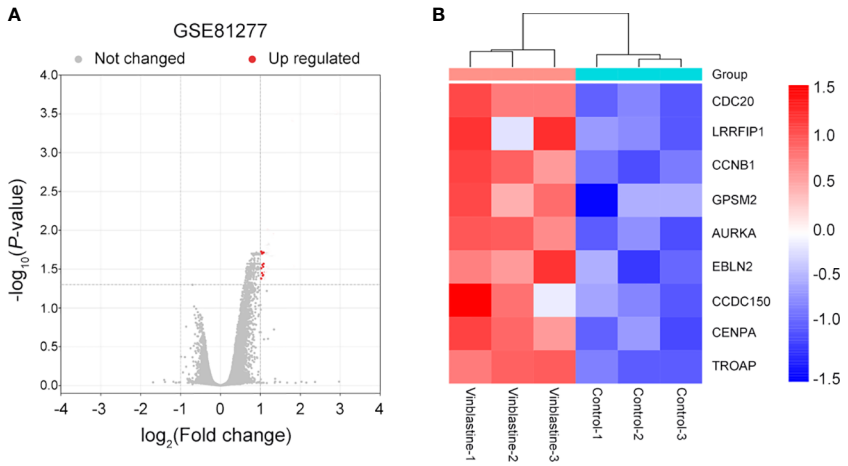

FIGURE 1
Nine vinblastine resistance-related genes were found from GSE81277. **(A)** The volcano map reflects the differently expressed genes in GSE81277. **(B)** The heatmap reflected the expression of nine hub genes in different datasets of GSE81277.

Metastasis (TNM) staging has been widely used to determine the severity of PCa (10), we evaluated the expression of these nine hub genes in different TNM tumour stages. Depending on the clinical data from different databases, the function of these vinblastine resistance-related hub genes in PCa progression was analyzed. In the TCGA database, we found that *GPSM2* expression was downregulated when PCa progressed from the T2 stage to the T3 stage (Figure 4A). As *LIRRFIP1* was not differentially expressed between normal and tumour tissues, *LIRRFIP1* was not included in the study. However, the other genes did not significantly affect the primary tumour (T) stage (Figure 4A). In Chinese patients with PCa, the nine genes also did not show a significant effect on the T stage (Figure S2A). Furthermore, the nine genes also did not significantly influence node metastasis (Figures S2B, C). Then, using the clinical data from GSE21034, we classified the patients with PCa into a primary tumour group and metastasis group based on the occurrence of distant metastasis. *CDC20*, *CCNB1*, *AURKA*, *CDCC150* and *TROAP* were observed to influence distant metastasis (Figure 4B).

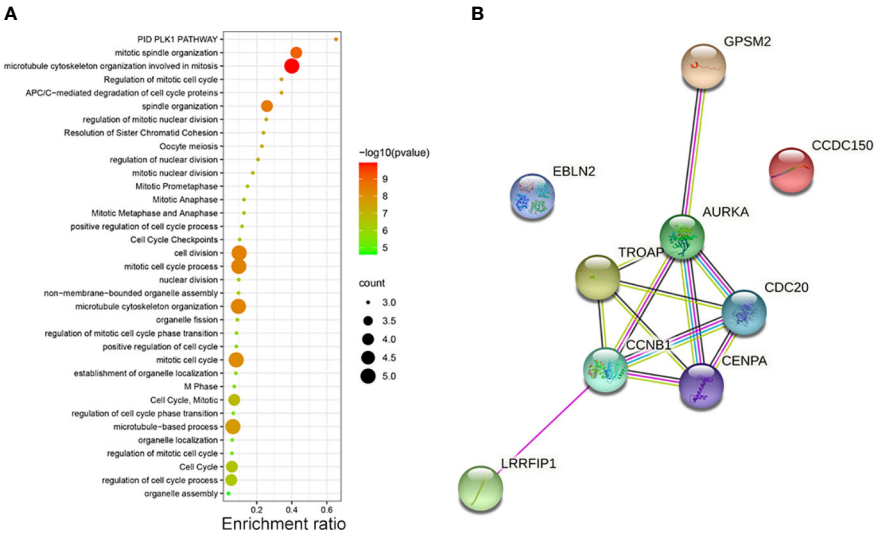

FIGURE 2
(A) The pathways of vinblastine resistance-related genes depending on Metascape. **(B)** The PPI network reflects the association between each hub genes.

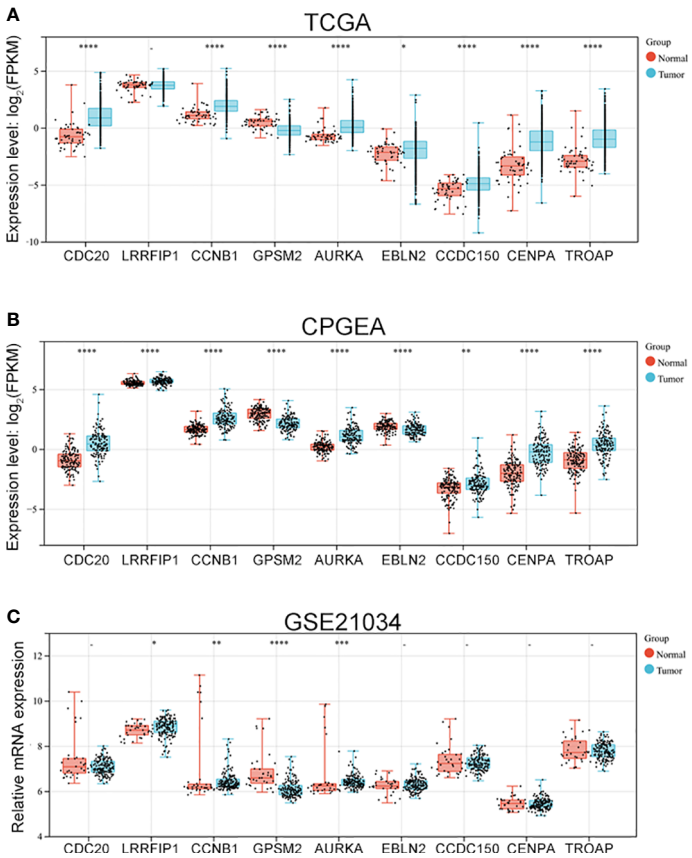

FIGURE 3
The expression of vinblastine resistance-related genes in PCa patients from different databases. Expression of nine vinblastine resistance-related hub genes in PCa patients from TCGA **(A)** database, CPGEA **(B)** database, and GSE21034 **(C)** dataset. – represents no statistical differences. * represents $P<0.05$, ** represents $P<0.01$, *** represents $P<0.001$, **** represents $P<0.0001$.

3.5 Verification of the expression of vinblastine resistance-related genes in CRPC samples

The GSE35988 dataset was used to verify the above results. In GSE35988, apart from *LRRFIP1*, all other genes influenced PCa occurrence (Figure 5A). Further, using the GSE35988 dataset, we classified patients with PCa into a primary tumour group and a CRPC group. Apart from *GPSM2*, other genes were upregulated in the CRPC samples (Figure 5B).

3.6 Vinblastine resistance-related hub genes affect survival status in patients with PCa

The influence of the eight hub genes on the survival status of patients with PCa was evaluated using GEPIA. *LRRFIP1* did not significantly affect PCa occurrence; therefore, it was excluded from the study process. Apart from *GPSM2* and *EBLN2*, all other genes were observed to influence the DFS of patients with PCa (Figure 6). Furthermore, *CDC20* and *CDCC150* influenced the OS of patients with PCa (Figure S3).

3.7 Association of vinblastine resistance-related hub genes with immune infiltration in PCa

Immune infiltration has been reported to play an important role in PCa (11). Hence, the correlation between these vinblastine resistance-related hub genes and immune cells in PCa was analyzed using TIMER. However, *EBLN2* could not be identified using TIMER, thereby excluding it from the study. Apart from *LRRFIP1* and *TROAP*, all other gene mutation types were associated with immune cell infiltrations in PCa (Figure S4).

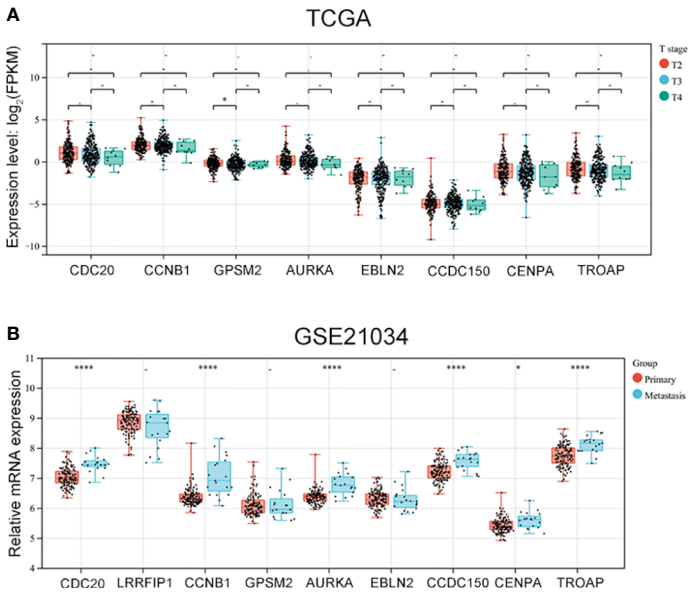

FIGURE 4
The expression of vinblastine resistance-related genes in different tumor stage from different databases. **(A)** The expression of eight vinblastine resistance-related genes in different T stage from TCGA database. **(B)** The expression of nine vinblastine resistance-related hub genes in primary and metastasis PCa patients from GSE21034 datasets. – represents no statistical differences. * represents $P<0.05$, **** represents $P<0.0001$.

Next, the specific correlation between these gene expressions and immune cells in PCa was evaluated. *LRRFIP1* was not observed to be associated with CD4+T cells in PCa (Figure 7B). Moreover, *AURKA* was not correlated with Purity cell, and CD8+T cell in PCa (Figure 7E). Furthermore, *CCDC150* was not correlated with CD4+T cell, CD8+T cell and Macrophage cell in PCa (Figure 7F). Additionally, *TROAP* was not correlated with CD4+T cells and Macrophage cells in PCa

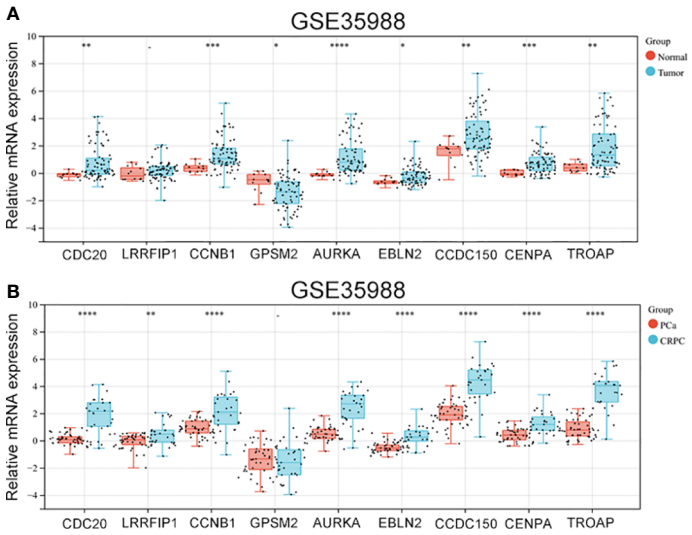

FIGURE 5
The expression of vinblastine resistance-related genes in GSE35988 datasets. **(A)** The expression of nine vinblastine resistance-related hub genes between normal and tumor samples from GSE35988. **(B)** The expression of nine vinblastine resistance-related hub genes between PCa and CRPC samples from GSE35988. – represents no statistical differences. * represents $P<0.05$, ** represents $P<0.01$, *** represents $P<0.001$, **** represents $P<0.0001$.

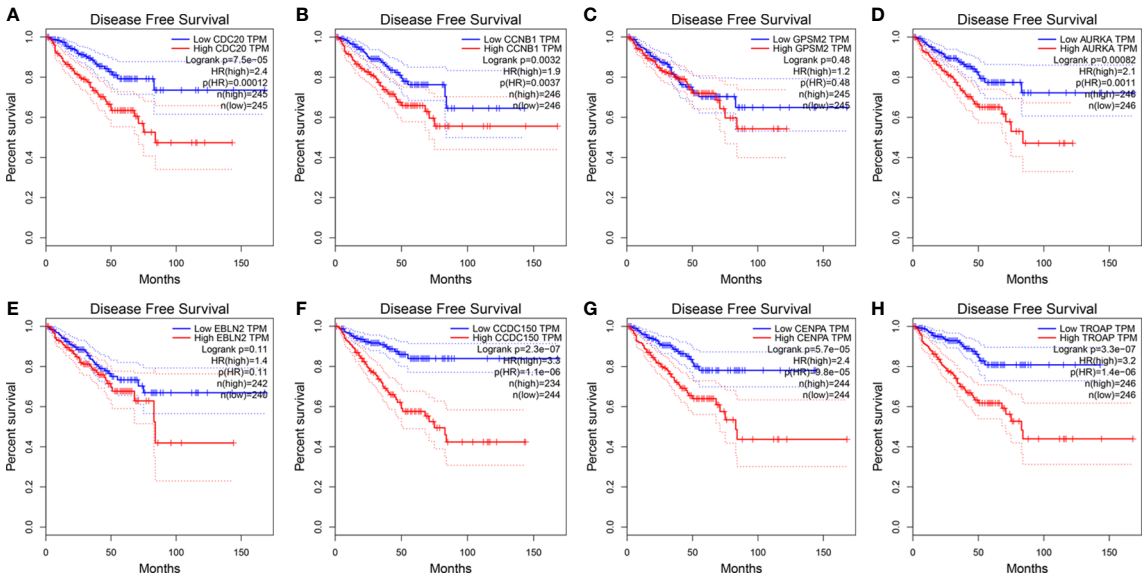

FIGURE 6
The expression of vinblastine resistance-related genes with PCa patients DFS status from TCGA database. **(A)** *CDC20* **(B)** *CCNB1* **(C)** *GPSM2* **(D)** *AURKA* **(E)** *EBLN2* **(F)** *CCDC150* **(G)** *CENPA* **(H)** *TROAP*.

(Figure 7G). However, other genes showed a correlation with all immune cells in PCa (Figure 7).

3.8 Validation of the expression and function of vinblastine resistance-related hub genes in CRPC samples and cells

Finally, the function of these hub genes was verified using clinical samples and PCa cells. Depending on that the above results, *CCNB1* and *AURKA* were upregulated in vinblastine-resistant PCa cells, PCa samples and CRPC samples. Additionally, they also affected the patient's survival status, and even PCa progression. hence, they were selected as the study objectives and thought they may critical for CRPC resistant to vinblastine. C4-2 PCa cells, which were cultured from LNCaP cells and grown in an environment without androgen, were considered as a cell line model of CRPC and another PCa cell line: 22Rv1 which can also growth without androgen were used in the study (12). Further, these two types of cells are sensitive to vinblastine.

The protein levels of CCNB1 and AURKA were analyzed in clinical normal prostate tissues, primary PCa samples and CRPC samples. These genes were found to be upregulated in tumour tissues and highly expressed in CRPC samples (Figures 8A, B), indicating their role in the occurrence of both PCa and CRPC. Next, we constructed CCNB1 and AURKA knockdown CRPC cell lines. The knockdown lentivirus decreased the expression of CCNB1 and AURKA at both mRNA and protein levels in C4-2 cells (Figures 8C–E) and can also inhibit the expression of CCNB1 and AURKA protein in 22Rv1 cells (Figure S5A). Then, the C4-2 and 22Rv1 cell lines were treated with vinblastine for 24 h to determine their proliferation ability. We observed that vinblastine decreased cell proliferation of C4-2 (Figure 8F). Further same results were observed in 22Rv1 cells (Figure S5B). Next, we transfected the specific knockdown lentivirus into C4-2 and 22Rv1 cells to determine the influence of the two genes on CRPC cells proliferation ability with vinblastine treatment. CCNB1 and AURKA knockdown decreased the proliferation ability of the C4-2 cells (Figures 8G, H) and 22Rv1 cells (Figure S5C, D). Thus, CCNB1 and AURKA have a potential role in the occurrence of PCa and CRPC and can influence CRPC resistant to vinblastine.

4 Discussion

With the increase in life span, the incidence of PCa among men is increasing rapidly (2). The progression of PCa is correlated with androgen closely and this is the reason that ADT can treat PCa effectively. As the first-line therapy method, ADT can effectively prolong the life span of patients with PCa (13). However, ADT treatment eventually leads to the progression of primary PCa tumours to the CRPC stage (14). Moreover, chemotherapy can also be used in the treatment of

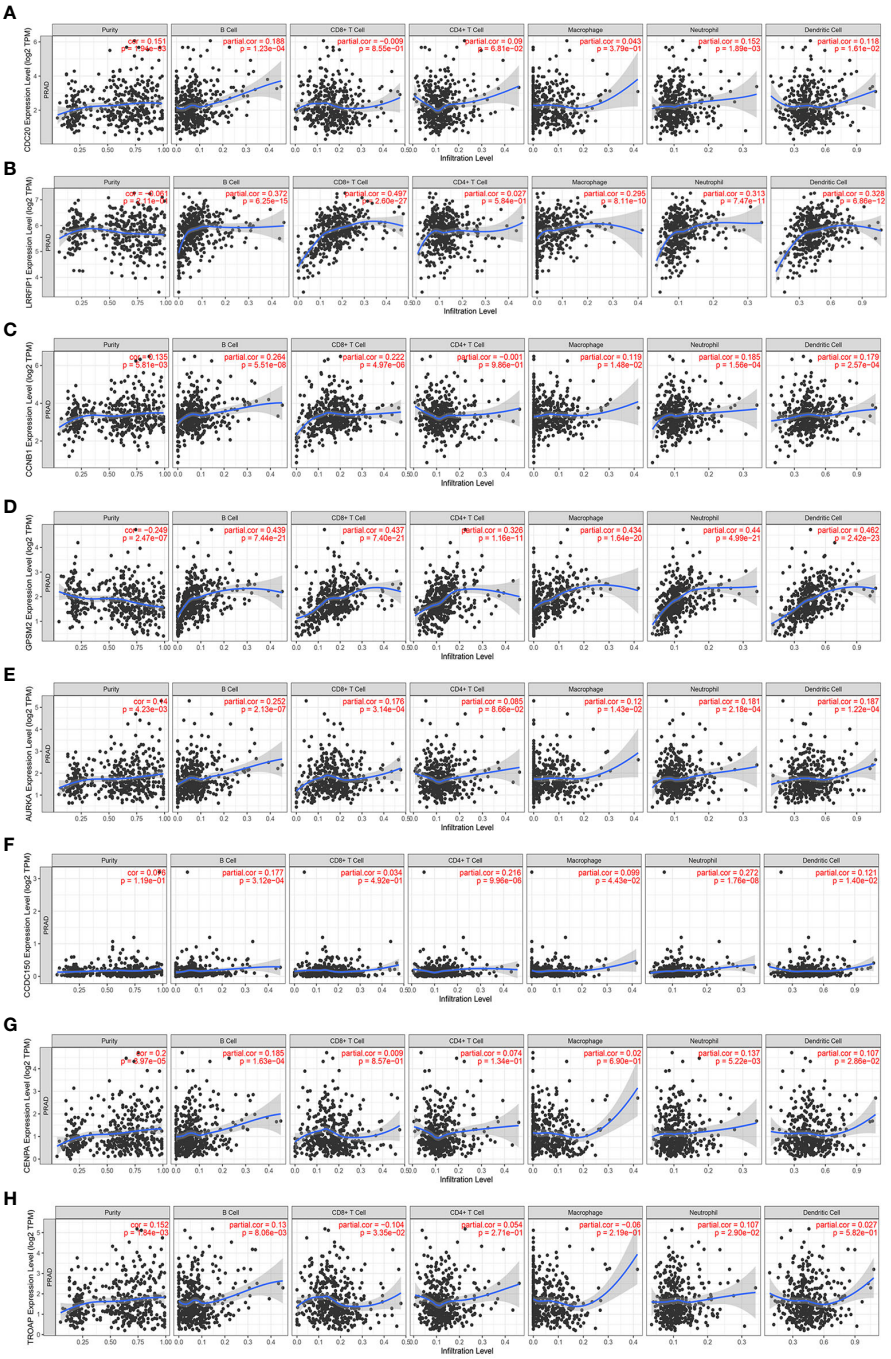

FIGURE 7
The correlation between the expression of vinblastine resistance-related genes and immune cell infiltration from TIMER webtool. **(A)** *CDC20* **(B)** *LRRFIP1* **(C)** *CCNB1* **(D)** *GPSM2* **(E)** *AURKA* **(F)** *CCDC150* **(G)** *CENPA* **(H)** *TROAP*.

PCa and CRPC (6). Some chemotherapy drugs like docetaxel and vinblastine have been reported to be useful in treating PCa, achieving good curative effects (5). Hence, elucidating the mechanism of chemotherapeutic resistance to chemotherapy drugs is of clinical importance in CRPC treatment.

In 1999, a Phase II clinical trial reported that vinblastine improved the symptoms in patients with advanced PCa and had a good tolerance (15). Furthermore, vinblastine was also reported to improve the effect of Estramustine phosphate in treating PCa (16). Additionally, vinblastine has also been used to treat CRPC (5, 7,

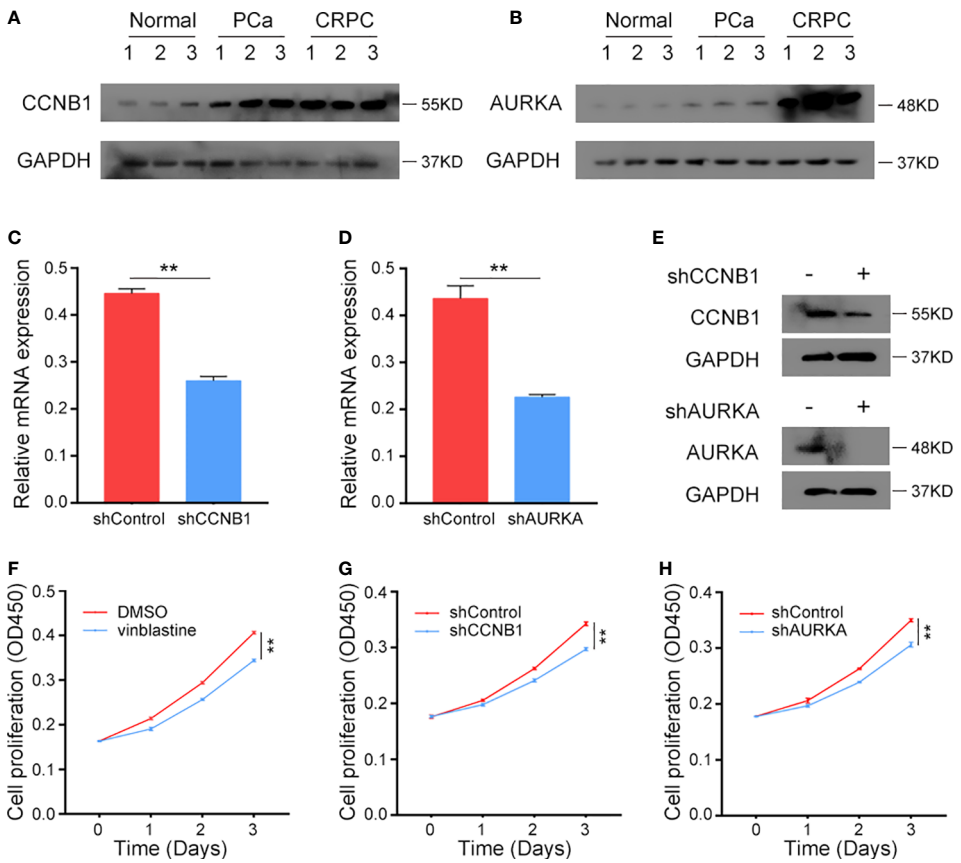

FIGURE 8
The expression *CCNB1* and *AURKA* in clinical samples and the function of *CCNB1* and *AURKA* to C4-2 cells in vinblastine. **(A, B)** The protein level of CCNB1 **(A)** and AURKA **(B)** in normal, primary PCa, and CRPC samples. **(C, D)** The mRNA level of CCNB1 **(C)** and AURKA **(D)** when different lentivirus transfected into C4-2 CRPC cells. **(E)** The protein level of CCNB1 and AURKA when different lentivirus transfected into C4-2 CRPC cells. **(F)** The cell proliferation level of C4-2 cells when C4-2 cells treated by DMSO or vinblastine. **(G, H)** The cell proliferation level of C4-2 cells after different lentivirus transfected into C4-2 CRPC cells with vinblastine treatment. **(G)** shCCNB1 **(H)** shAURKA. ** represents $P<0.01$.

17). It improves the effects of the various drugs used in CRPC treatment. Studies have reported that vinblastine improves the function of docetaxel and prednisone in treating CRPC (8, 18, 19). Moreover, vinblastine treatment of PCa and CRPC has also been reported *in vitro*. It decreases the proliferation and induces the apoptosis of PCa cell lines, such as LNCaP and DU145 (20, 21). Thus, vinblastine effectively treats PCa and CRPC; however, resistance to vinblastine eventually occurs.

Genetic alterations could play a vital role in CRPC resistance to vinblastine. Hence, in this study, we aimed to identify the potential genes that correlated with CRPC resistance to vinblastine. Nine hub genes were found to be upregulated in vinblastine-resistant LNCaP cells. Moreover, on examining their expression and clinical value, two hub genes, *CCNB1* and *AURKA*, were upregulated in vinblastine-resistant CRPC cells, PCa clinical samples and CRPC samples. This indicates that these two hub genes are not only important to vinblastine resistance but also in CRPC. Finally, functional analyses of *CCNB1* and *AURKA* revealed that these two genes affected the sensitivity of CRPC cells to vinblastine, indicating their role in the occurrence of PCa and resistance to drugs. Therefore, these two genes' alterations may be the reason for CRPC resistant to vinblastine.

Cyclin B1 (*CCNB1*), which is essential for cell cycle progression through mitosis, is overexpressed in various cancers compared with normal cells and tissues like breast cancer and non-small cell lung cancer (22–24). The overexpression of *CCNB1* has also been indicated as a poor outcome in some patients with cancer (24, 25). In patients with PCa, high *CCNB1* expression often occurred with a high tumour grade (26). Additionally, some studies also reported that patients with a high *CCNB1* expression are likely to experience tumour metastasis and have a poor prognosis (27, 28). Consistent with previous results, this study also observed that *CCNB1* affected

PCa progression and prognosis. Similarly, another study reported that the high expression of *CCNB1* could be a potential reason for PCa resistance to docetaxel (29). Similar to *CCNB1*, Aurora kinase A (*AURKA*) is also a cell cycle-regulated kinase that is involved in microtubule formation or stabilization at the spindle pole during chromosome segregation (30). Genetic analysis reveals that *AURKA* is upregulated in PCa tissues, especially in neuroendocrine PCa tissues (31). In PCa, *AURKA* is considered an oncogene. Its oncogenic function has been correlated with N-myc (32, 33). Furthermore, a Phase II study reported that an *AURKA* inhibitor, Alisertib, could treat PCa (34). Moreover, Alisertib has also been reported to enhance the effect of docetaxel in PCa treatment (35). Additionally, *AURKA* is considered a critical factor for solid tumour resistance to chemotherapy drugs (36). In this study, we also proved that these two genes were important in CRPC and even CRPC resistant to vinblastine.

However, this study has many limitations. First, the nine hub genes identified are from LNCaP PCa cells. Although LNCaP is a PCa cell line cultured from metastasis node tissues obtained from patients with PCa (37), it is less representative than clinical samples. Therefore, results observed in PCa cells may differ from those in clinical samples. Second, although the expression and function of the two hub genes could be important in the occurrence of both PCa and CRPC clinical samples and PCa cell lines, the study size was small hence, the results cannot be generalised. Therefore, further experiments with large samples are required to validate our findings. Third, although vinblastine can be used to treat CRPC, it is not commonly used in clinical. So, the clinical value of this study is limited. However, this study still contributes to defining CRPC resistant to vincristine. To the best of our knowledge, this study is the first to identify the potential genetic alterations that occur in CRPC resistance to vinblastine.

5 Conclusion

Nine hub genes (*CDC20*, *LRRFIP1*, *CCNB1*, *GPSM2*, *AURKA*, *EBLN2*, *CCDC150*, *CENPA* and *TROAP)* that may play a vital role in PCa resistance to vinblastine were identified and they also corelated with PCa progression. Furthermore, two hub genes, *CCNB1* and *AURKA* are important factors for CRPC resistant to vinblastine.

Data availability statement

The original contributions presented in the study are included in the article/supplementary material. Further inquiries can be directed to the corresponding authors.

Ethics statement

The studies involving human participants were reviewed and approved by Ethic committee of Tongji Hospital, School of Medicine, Tongji University. The patients/participants provided their written informed consent to participate in this study.

Author contributions

XC and JM put forward the idea of the article, wrote the manuscript and analyzed the data. TZ collected the data from public database. XW finished the RT-qPCR, Western blot and CCK-8 experiments. CL help collecting the clinical specimens. DQ and CX revised the manuscript. All authors contributed to the article and approved the submitted version.

Funding

This study was supported by Natural Science Foundation of Shanghai Municipal Science and Technology Committee (NO.22ZR1456800, NO.21ZR1458300), National Natural Science Foundation of China (NO.82001610), Clinical Research Plan of SHDC (NO. SHDC2020CR3074B) and New Frontier Technology Joint Research Project of Shanghai Municipal Hospital (NO. SHDC12019112), The Shanghai Science and Technology Innovation Action Plan (NO. 20Y11904400).

Acknowledgments

We thank Bullet Edits Limited for the linguistic editing and proofreading of the manuscript.

Conflict of interest

The authors declare that the research was conducted in the absence of any commercial or financial relationships that could be construed as a potential conflict of interest.

Publisher's note

Supplementary material

The Supplementary Material for this article can be found online at: https://www.frontiersin.org/articles/10.3389/fendo.2022.1106175/full#supplementary-material

References

1. Siegel RL, Miller KD, Fuchs HE, Jemal A. Cancer statistics, 2021. *CA Cancer J Clin* (2021) 71(1):7–33. doi: 10.3322/caac.21654

2. Chen X, Ma J, Xu C, Wang L, Yao Y, Wang X, et al. Identification of hub genes predicting the development of prostate cancer from benign prostate hyperplasia and analyzing their clinical value in prostate cancer by bioinformatic analysis. *Discovery Oncol* (2022) 13(1):54. doi: 10.1007/s12672-022-00508-y

3. Chen X, Wu Y, Wang X, Xu C, Wang L, Jian J, et al. CDK6 is upregulated and may be a potential therapeutic target in enzalutamide-resistant castration-resistant prostate cancer. *Eur J Med Res* (2022) 27(1):105. doi: 10.1186/s40001-022-00730-y

4. Heidenreich A, Bastian PJ, Bellmunt J, Bolla M, Joniau S, van der Kwast T, et al. EAU guidelines on prostate cancer. part II: Treatment of advanced, relapsing, and castration-resistant prostate cancer. *Eur Urol* (2014) 65(2):467–79. doi: 10.1016/j.eururo.2013.11.002

5. Arsov C, Winter C, Rabenalt R, Albers P. Current second-line treatment options for patients with castration resistant prostate cancer (CRPC) resistant to docetaxel. *Urol Oncol* (2012) 30(6):762–71. doi: 10.1016/j.urolonc.2010.02.001

6. Nader R, El Amm J, Aragon-Ching JB. Role of chemotherapy in prostate cancer. *Asian J Androl* (2018) 20(3):221–9. doi: 10.4103/aja.aja_40_17

7. Oudard S, Caty A, Humblet Y, Beauduin M, Suc E, Piccart M, et al. Phase II study of vinorelbine in patients with androgen-independent prostate cancer. *Ann Oncol* (2001) 12(6):847–52. doi: 10.1023/A:1011141611560

8. Koletsky AJ, Guerra ML, Kronish L. Phase II study of vinorelbine and low-dose docetaxel in chemotherapy-naive patients with hormone-refractory prostate cancer. *Cancer J* (2003) 9(4):286–92. doi: 10.1097/00130404-200307000-00011

9. Sweeney CJ, Monaco FJ, Jung SH, Wasielewski MJ, Picus J, Ansari RH, et al. A phase II Hoosier oncology group study of vinorelbine and estramustine phosphate in hormone-refractory prostate cancer. *Ann Oncol* (2002) 13(3):435–40. doi: 10.1093/annonc/mdf029

10. Paner GP, Stadler WM, Hansel DE, Montironi R, Lin DW, Amin MB. Updates in the eighth edition of the tumor-Node-Metastasis staging classification for urologic cancers. *Eur Urol* (2018) 73(4):560–9. doi: 10.1016/j.eururo.2017.12.018

11. Strasner A, Karin M. Immune infiltration and prostate cancer. *Front Oncol* (2015) 5:128. doi: 10.3389/fonc.2015.00128

12. Zegarra-Moro OL, Schmidt LJ, Huang H, Tindall DJ. Disruption of androgen receptor function inhibits proliferation of androgen-refractory prostate cancer cells. *Cancer Res* (2002) 62(4):1008–13.

13. Culig Z, Santer FR. Androgen receptor signaling in prostate cancer. *Cancer Metastasis Rev* (2014) 33(2-3):413–27. doi: 10.1007/s10555-013-9474-0

14. Ross RW, Xie W, Regan MM, Pomerantz M, Nakabayashi M, Daskivich TJ, et al. Efficacy of androgen deprivation therapy (ADT) in patients with advanced prostate cancer: association between Gleason score, prostate-specific antigen level, and prior ADT exposure with duration of ADT effect. *Cancer* (2008) 112(6):1247–53. doi: 10.1002/cncr.23304

15. Fields-Jones S, Koletsky A, Wilding G, O'Rourke M, O'Rourke T, Eckardt J, et al. Improvements in clinical benefit with vinorelbine in the treatment of hormone-refractory prostate cancer: a phase II trial. *Ann Oncol* (1999) 10 (11):1307–10. doi: 10.1023/A:1008315106697

16. Hudes G, Einhorn L, Ross E, Balsham A, Loehrer P, Ramsey H, et al. Vinblastine versus vinblastine plus oral estramustine phosphate for patients with hormone-refractory prostate cancer: A Hoosier oncology group and fox chase network phase III trial. *J Clin Oncol* (1999) 17(10):3160–6. doi: 10.1200/JCO.1999.17.10.3160

17. Morant R, Hsu Schmitz SF, Bernhard J, Thurlimann B, Borner M, Wernli M, et al. Vinorelbine in androgen-independent metastatic prostatic carcinoma–a phase II study. *Eur J Cancer* (2002) 38(12):1626–32. doi: 10.1016/S0959-8049(02)00145-4

18. Robles C, Furst AJ, Sriratana P, Lai S, Chua L, Donnelly E, et al. Phase II study of vinorelbine with low dose prednisone in the treatment of hormone-refractory metastatic prostate cancer. *Oncol Rep* (2003) 10(4):885–9. doi: 10.3892/or.10.4.885

19. Tralongo P, Bollina R, Aiello R, Di Mari A, Moruzzi G, Beretta G, et al. Vinorelbine and prednisone in older cancer patients with hormone-refractory metastatic prostate cancer. a phase II study. *Tumori* (2003) 89(1):26–30. doi: 10.1177030089160308900106

20. Hossein G, Zavareh VA, Fard PS. Combined treatment of androgen-independent prostate cancer cell line DU145 with chemotherapeutic agents and lithium chloride: Effect on growth arrest and/or apoptosis. *Avicenna J Med Biotechnol* (2012) 4(2):75–87.

21. Levrier C, Rockstroh A, Gabrielli B, Kavallaris M, Lehman M, Davis RA, et al. Discovery of thalicthuberine as a novel antimitotic agent from nature that disrupts microtubule dynamics and induces apoptosis in prostate cancer cells. *Cell Cycle* (2018) 17(5):652–68. doi: 10.1080/15384101.2017.1356512

22. Pines J. Mitosis: a matter of getting rid of the right protein at the right time. *Trends Cell Biol* (2006) 16(1):55–63. doi: 10.1016/j.tcb.2005.11.006

23. Kawamoto H, Koizumi H, Uchikoshi T. Expression of the G2-m checkpoint regulators cyclin B1 and cdc2 in nonmalignant and malignant human breast lesions: immunocytochemical and quantitative image analyses. *Am J Pathol* (1997) 150(1):15–23.

24. Soria JC, Jang SJ, Khuri FR, Hassan K, Liu D, Hong WK, et al. Overexpression of cyclin B1 in early-stage non-small cell lung cancer and its clinical implication. *Cancer Res* (2000) 60(15):4000–4.

25. Hassan KA, Ang KK, El-Naggar AK, Story MD, Lee JI, Liu D, et al. Cyclin B1 overexpression and resistance to radiotherapy in head and neck squamous cell carcinoma. *Cancer Res* (2002) 62(22):6414–7.

26. Kallakury BV, Sheehan CE, Rhee SJ, Fisher HA, Kaufman RPJr., Rifkin MD, et al. The prognostic significance of proliferation-associated nucleolar protein p120 expression in prostate adenocarcinoma: a comparison with cyclins a and B1, ki-67, proliferating cell nuclear antigen, and p34cdc2. *Cancer* (1999) 85(7):1569–76. doi: 10.1002/(SICI)1097-0142(19990401)85:7<1569::AID-CNCR19>3.0.CO;2-M

27. LaTulippe E, Satagopan J, Smith A, Scher H, Scardino P, Reuter V, et al. Comprehensive gene expression analysis of prostate cancer reveals distinct transcriptional programs associated with metastatic disease. *Cancer Res* (2002) 62(15):4499–506.

28. Glinsky GV, Berezovska O, Glinskii AB. Microarray analysis identifies a death-from-cancer signature predicting therapy failure in patients with multiple types of cancer. *J Clin Invest* (2005) 115(6):1503–21. doi: 10.1172/JCI23412

29. Gomez LA, de Las Pozas A, Reiner T, Burnstein K, Perez-Stable C. Increased expression of cyclin B1 sensitizes prostate cancer cells to apoptosis induced by chemotherapy. *Mol Cancer Ther* (2007) 6(5):1534–43. doi: 10.1158/1535-7163.MCT-06-0727

30. Du R, Huang C, Liu K, Li X, Dong Z. Targeting AURKA in cancer: molecular mechanisms and opportunities for cancer therapy. *Mol Cancer* (2021) 20(1):15. doi: 10.1186/s12943-020-01305-3

31. Beltran H, Rickman DS, Park K, Chae SS, Sboner A, MacDonald TY, et al. Molecular characterization of neuroendocrine prostate cancer and identification of new drug targets. *Cancer Discovery* (2011) 1(6):487–95. doi: 10.1158/2159-8290.CD-11-0130

32. Otto T, Horn S, Brockmann M, Eilers U, Schuttrumpf L, Popov N, et al. Stabilization of n-myc is a critical function of aurora a in human neuroblastoma. *Cancer Cell* (2009) 15(1):67–78. doi: 10.1016/j.ccr.2008.12.005

33. Mosquera JM, Beltran H, Park K, MacDonald TY, Robinson BD, Tagawa ST, et al. Concurrent AURKA and MYCN gene amplifications are harbingers of lethal treatment-related neuroendocrine prostate cancer. *Neoplasia* (2013) 15(1):1–10. doi: 10.1593/neo.121550

34. Beltran H, Oromendia C, Danila DC, Montgomery B, Hoimes C, Szmulewitz RZ, et al. A phase II trial of the aurora kinase a inhibitor alisertib for patients with castration-resistant and neuroendocrine prostate cancer: Efficacy and biomarkers. *Clin Cancer Res* (2019) 25(1):43–51. doi: 10.1158/1078-0432.CCR-18-1912

35. Graff JN, Higano CS, Hahn NM, Taylor MH, Zhang B, Zhou X, et al. Open-label, multicenter, phase 1 study of alisertib (MLN8237), an aurora a kinase inhibitor, with docetaxel in patients with solid tumors. *Cancer* (2016) 122 (16):2524–33. doi: 10.1002/cncr.30073

36. Miralaei N, Majd A, Ghaedi K, Peymani M, Safaei M. Integrated pan-cancer of AURKA expression and drug sensitivity analysis reveals increased expression of AURKA is responsible for drug resistance. *Cancer Med* (2021) 10(18):6428–41. doi: 10.1002/cam4.4161

37. Namekawa T, Ikeda K, Horie-Inoue K, Inoue S. Application of prostate cancer models for preclinical study: Advantages and limitations of cell lines, patient-derived xenografts, and three-dimensional culture of patient-derived cells. *Cells* (2019) 8(1). doi: 10.3390/cells8010074

frontiers | Frontiers in Endocrinology

TYPE Original Research
PUBLISHED 20 December 2022
DOI 10.3389/fendo.2022.1099818

OPEN ACCESS

EDITED BY
Yuxuan Song,
Peking University People's Hospital, China

REVIEWED BY
Xiang Dai,
Peking University People's Hospital, China
Jingjing Guan,
Sun Yat-sen University, China

*CORRESPONDENCE
Xiaochen Zhou
mo_disc@126.com
Gongxian Wang
urowgx@126.com

†These authors have contributed equally to this work

SPECIALTY SECTION
This article was submitted to Adrenal Endocrinology, a section of the journal Frontiers in Endocrinology

RECEIVED 16 November 2022
ACCEPTED 07 December 2022
PUBLISHED 20 December 2022

CITATION
Li X, Xi H, Yu Y, Liu W, Zhu X, Gong Z, Fu B, Wang G and Zhou X (2022) Retroperitoneal laparoscopic partial adrenalectomy (RLPA) for 20-40 mm nonfunctional adrenal tumors in the day surgery mode.
Front. Endocrinol. 13:1099818.
doi: 10.3389/fendo.2022.1099818

Retroperitoneal laparoscopic partial adrenalectomy (RLPA) for 20-40 mm nonfunctional adrenal tumors in the day surgery mode

Xuwen Li[1†], Haibo Xi[1†], Yue Yu[1†], Wei Liu[1], Xiaoping Zhu[2], Zhixian Gong[2], Bin Fu[1], Gongxian Wang[1*] and Xiaochen Zhou[1*]

[1]Department of Urology, The First Affiliated Hospital of Nanchang University, Nanchang, China, [2]Department of Day Ward, The First Affiliated Hospital of Nanchang University, Nanchang, China

Objectives: To investigate the outcome and safety of retroperitoneal laparoscopic partial adrenalectomy in the treatment of nonfunctional unilateral adrenal tumors in the day surgery mode.

Methods: Nineteen patients bearing nonfunctional unilateral 20-40 mm adrenal tumors were prospectively enrolled and underwent retroperitoneal laparoscopic partial adrenalectomy in the day surgery unit of our hospital between June 2021 and March 2022. All patients were diagnosed with non-functional adrenal tumors as outpatients before being admitted to the day surgery unit with their consent. Patient demographics and perioperative data were prospectively documented. The patients were followed up by telephone on day 1, 3 and 7 after discharge and followed up for 6 months.

Results: The patient's age was 50.5 ± 11.9 yr (range from 19.0 - 69.0). Seven patients were female. Twelve patients underwent surgery on the left side. The maximal diameter of tumor was 28.3 ± 5.7 mm (20.0 - 40.0 mm). Operation time was 72.1 ± 14.9 min (58.0 - 120.0 min). Mean blood loss was 64.7 ± 50.4 ml (30.0 - 200.0 ml). The gastrointestinal function recovery time was 9.7 ± 2.6 h (6.0 - 16.0 h). Retroperitoneal drainage was removed 24.8 ± 13.3 h (range 18.0 - 72.0) after surgery. Four patients were transferred to the general ward for postoperative management, while others were discharged within 24 hours after surgery. Length of hospital stay was 48.8 ± 13.1 h (38.0 - 85.0h). Hospitalization expense was 24168.4 ± 2910.3 RMB¥ (20844.3 - 34369.8 RMB¥). Postoperative pathology revealed 17 cortical adenoma, 1 pheochromocytoma and 1 lymphatic duct tumor.

Conclusion: Retroperitoneal laparoscopic partial adrenalectomy for nonfunctional unilateral adrenal tumors in the day surgery mode is safe when strict selection criteria and perioperative management protocol are followed, which has the potential to shorten length of hospital stay and reduce lower hospitalization costs.

KEYWORDS

adrenal tumor, retroperitoneal laparoscopic partial adrenalectomy, day surgery mode, hospital stay, hospitalization cost

1 Introduction

Adrenal tumors are common, affecting 8.7% of the population (1). Although most adrenal tumors are benign, the management protocol of adrenal tumors always requires thorough urological and endocrinological studies due to their potential to overproduce hormones that affect organs throughout the body (2). Surgical excision of adrenal tumors ≥ 20 mm has become a consensus among urologists (3). Retroperitoneal laparoscopic adrenalectomy (RLA) is currently the first-line choice to remove benign adrenal tumors (4, 5). However, a growing number of researchers believe that for small (20-40 mm) adrenal tumors, it is preferable to preserve some healthy adrenal tissue in the aim of lowering the risk of postoperative adrenal insufficiency (6, 7).

Day surgery mode is a new surgery management mode proposed by the famous British surgeon Nicoll (8, 9), which means that within 24 h, patients who meet the inclusion criteria are arranged to complete the admission, operation and discharge in a pre-planned protocol. Under special circumstances, patients with delayed hospitalization should not stay longer than 48 hours. "Day surgery mode" is a treatment mode favored by surgeons in Europe and America because it can significantly reduce the length of hospital stay for patients and effectively make use of scarce medical resources (10). In our country, day surgery management mode is in the stage of development and exploration for many types of surgical interventions, including adrenalectomy.

At present, RLA in day surgery mode has been reported in some developed countries and large hospitals in China (11, 12). However, due to the potential bleeding risk of partial adrenalectomy, there have been no reports of retroperitoneal laparoscopic partial adrenalectomy (RLPA) in this mode. As such, we conducted this study to investigate the efficacy and safety of RLPA in the treatment of 20-40 mm nonfunctional unilateral adrenal tumors in the day surgery mode.

2 Materials and methods

The study was approval of by institutional review board and ethics committee of the First Affiliated Hospital of Nanchang University. Documentation of medical history, laboratory studies and non-contrast/contrast enhanced adrenal CT were performed prior to administration in the day surgery unit. Patients bearing non-functional unilateral adrenal tumor ranged from 20 to 40mm were enrolled after multidisciplinary discussion of urologists, endocrinologists, and anesthesiologists. Patients with ASA score > 2, younger than 18 yr or older than 70 yr were excluded. Prior to surgery, all candidates were re-evaluated and informed of the surgical and perioperative management plan by a urologist. A signed consent form was obtained from each candidate.

All surgeries were performed by the same experienced urologist. Patient was anesthetized and placed on flank position for a standard retroperitoneal laparoscopic partial adrenalectomy. Only the tumor was removed and hemostasis was achieved by a combination of bipolar and hem-o-locs. A drainage tube was placed through a trocar site at the end of surgery. Two hundred mg hydrocortisone was given during surgery to minimize the risk of adrenal crisis. On the first and second day after surgery, 100 mg and 50 mg hydrocortisone were given, respectively for the same reason.

Postoperative vital signs were closely monitored and postoperative rehabilitation education was conducted. Patients were encouraged to ambulate as soon as possible. The recovery time of gastrointestinal function and the status of drainage fluid were observed. Urethral catheter was removed 8 hours after surgery and drainage tube was removed when discharge was negligible or < 20 ml. Patients were discharged after all tubes were removed. Patients with inconformity or drainage tube not removed within 48h were then transferred to the general ward for further management. All patients were followed up by telephone 1,3 and 7 days after discharge. All patients were followed up for at least 6 months.

Patient demographic and perioperative data were prospectively documented, including tumor size, laterality, operation time, blood loss, gastrointestinal function recovery time, drainage tube placement time, complications, hospital stay and hospitalization expense were recorded. The operation time was defined as the time from first incision to all incisions were closed. Gastrointestinal function recovery time was defined as the time between leaving the operating room and the first passage of gas or defecation.

Quantitative variables were expressed as mean ± SD and qualitative variables were expressed as categorical variables (i.e., yes or no). SPSS V25.0 software was used to perform all the statistical analyses.

3 Results

During June 2021 to March 2022, 19 patients were enrolled. The demographic and preoperative data were summarized in Table 1. The patient's age (mean ± SD) was 50.5 ± 11.9 yr (19.0 - 69.0). Seven patients were female. Mean BMI was 24.4 ± 3.6 kg/m^2 (17.8 - 33.9). Twelve patients underwent surgery on the left side. The tumor maximal diameter was 28.3 ± 5.7 mm (20.0 - 40.0).

Laparoscopic partial adrenalectomy was performed in all patients successfully. As summarized in Table 2, the operation time was 72.1 ± 14.9 min (58.0 - 120.0). Mean blood loss was 64.7 ± 50.4 ml (30.0 - 200.0). The gastrointestinal function recovery time was 9.7 ± 2.6 h 6.0 - 16.0), and the drainage tube placement time was 24.8 ± 13.3 h (18.0 - 72.0). Four patients were transferred to the general inpatient unit for extended hospitalization: one patient suffered from postoperative fever, two patients had prolonged drainage, and one patient needed longer observation for concerning vitals. Despite the delay, these 4 patients were all discharged within 85 h. The mean Hospital stay was 48.8 ± 13.05 h (38.0 - 85.0). And hospitalization expense was 24168.4 ± 2910.25 RMB¥ (20844.3 - 34369.8). Pathological study revealed 17 cortical adenomas, 1 pheochromocytoma and 1 lymphatic duct tumor. Telephone follow-up on days 1,3 and 7 after discharge were performed and found no significant concerns. Other complications were not noted during a minimal follow-up of 6 month.

After removing the 4 delayed discharged patients from the 19-patient data set, we analyzed the 15 patients who were discharged following day surgery mode protocol again and summarized the data in Table 3, 4. The patient's age was 50.1 ± 13.0 yr (29.0.0 - 69.0). Six patients were female. Mean BMI was 24.5 ± 3.7 kg/m^2 (17.8 - 33.9). Ten patients underwent surgery on the left side. The tumor maximal diameter was 25.9 ± 3.7 mm (20.0 - 32.0). The operation time was 66.1 ± 5.0 min (58.0 - 75.0). Mean blood loss was 45.3 ± 11.9 ml (30.0 - 70.0). The gastrointestinal function recovery time was 9.3 ± 2.6 h (6.0 - 16.0). Drainage tube placement time was 20.0 ± 2.3 h (18.0 - 24.0). The mean Hospital stay was 42.9 ± 2.6 h (38.0 - 48.0). Hospitalization expense was 23097.7 ± 1171.12 RMB¥ (20844.3 - 24832.5). Pathological study revealed all tumors were cortical adenomas.

4 Discussion

With the development of the concept of minimally invasive surgery, the surgical treatment of adrenal tumors has evolved from open surgery to laparoscopic surgery, from total resection to partial resection. Michael Gagner performed the first laparoscopic resection of the adrenal gland in 1992 (13). Since then, the technique has been perfected by urologists from all over the world. Twenty years later, laparoscopic adrenalectomy *via* retroperitoneal approach was proposed, with significantly faster postoperative recovery (14). This was confirmed in later studies (15). From that standing ground, researchers shifted

TABLE 1 Demographics and preoperative data.

	n = 19
Age (yr), mean (SD), range	50.5 (11.9), 19.0 - 69.0
Weight (kg), mean (SD), range	67.6 (13.9), 41.0 - 93.0
BMI (kg/m^2), mean (SD), range	24.4 (3.6), 17.8 - 33.9
Gender, n (%)	
Female	7 (36.8%)
Male	12 (63.2%)
Laterality, n (%)	
L	12 (63.2%)
R	7 (36.8%)
Tumor maximal diameter (mm), mean (SD), range	28.3 (5.7), 20.0 - 40.0

TABLE 2 Intraoperative and postoperative data.

	n = 19
Operation time (min), mean (SD), range	72.1 (14.9), 58.0 - 120.0
Blood loss (ml), mean (SD), range	64.7 (50.4), 30.0 - 200.0
Gastrointestinal function recovery time (h), mean (SD), range	9.7 (2.6), 6.0 - 16.0
Drainage tube placement time (h), mean (SD), range	24.8 (13.3), 18.0 - 72.0
Transfer to general ward, n (%)	4 (21.1%)
Reasons for changing wards, n (%)	
Fever	1 (5.3%)
Not meet extubation standards	2 (10.5%)
Watchful waiting	1 (5.3%)
Hospital stay (h), mean (SD), range	48.8 (13.0), 38.0 - 85.0
Hospitalization expense (RMB¥), mean (SD), range	24168.4 (2910.3), 20844.3 - 34369.8
Pathologic, n (%)	
Cortical adenomas	16 (84.2%)
Pheochromocytoma	2 (10.5%)
Lymphatic duct tumor	1 (5.3%)

TABLE 3 Demographics and preoperative data.

	n = 15
Age (yr), mean (SD), range	50.1 (13.0), 29.0 - 69.0
Weight (kg), mean (SD), range	67.2 (13.8), 41.0 - 93.0
BMI (kg/m^2), mean (SD), range	24.5 (3.7), 17.8 - 33.9
Gender, n (%)	
Female	6 (40.0%)
Male	9 (50.0%)
Laterality, n (%)	
L	10 (66.7%)
R	5 (33.3%)
Tumor maximal diameter (mm), mean (SD), range	25.9 (3.7), 20.0 - 32.0

TABLE 4 Intraoperative and postoperative data.

	n = 15
Operation time (min), mean (SD), range	66.1 (5.0), 58.0 - 75.0
Blood loss (ml), mean (SD), range	45.3 (11.9), 30.0 - 70.0
Gastrointestinal function recovery time (h), mean (SD), range	9.3 (2.6), 6.0 - 16.0
Drainage tube placement time (h), mean (SD), range	20.0 (2.3), 18.0 - 24.0
Transfer to general ward, n (%)	0 (0%)

(Continued)

TABLE 4 Continued

	n = 15
Reasons for changing wards, n (%)	
Fever	–
Drainage of fluid more	–
Watchful waiting	–
Hospital stay (h), mean (SD), range	42.9 (2.6), 38.0 - 48.0
Hospitalization expense (RMB¥), mean (SD), range	23097.7 (1171.1), 20844.3 - 24832.5
Pathologic, n (%)	
Adenoma sebaceum	15 (100.0%)
Pheochromocytoma	0 (0%)
Lymphatic duct tumor	0 (0%)

their focus on whether or not preserving the healthy adrenal tissue when resecting an adrenal tumor. Not surprisingly, preservation of normal functional adrenal tissue significantly reduced the risk of postoperative adrenal insufficiency (6, 16). To date, retroperitoneal laparoscopic partial adrenalectomy (RLPA) for benign lesions was accepted by the majority.

Day surgery mode has been favored by surgeons since it was proposed by the famous British surgeon Nicoll (9). Its rapid hospitality-operation-discharge mode can effectively alleviate the problem of hospital bed shortage. This is especially important in developing countries with limited medical resources. In addition, the development of minimally invasive surgery technology provides a guarantee for the operation of the day surgery mode. After minimally invasive surgery, patients suffer less injury and recover more rapidly, making administration-discharge within 24-48 hours possible. At the same time, the natural development of minimally invasive surgery also has the tendency to shift to the day surgery or outpatient surgery mode (17).

Laparoscopic adrenalectomy has been reported to be successfully performed in the day surgery or outpatient surgery mode (11, 18–20). Although partial adrenalectomy is preferable to total adrenalectomy for benign lesions, the potential risk of bleeding should be noted and hemostasis should be ensured during surgery (5). Nevertheless, a successful implantation of day surgery mode in partial adrenalectomy must be based on the premise of patient safety and surgical outcomes, which largely depend on thorough preoperative assessment and delicate surgical techniques. As such, we developed a management protocol based on the experience of our own and others (21) (Figure 1).

To ensure patient safety, we strictly selected patients with non-functional small tumors for RLPA in day surgery mode. For postoperative management, we tended to take personalized management on each patient based on intraoperative findings, including the amount of dissection, blood loss, vitals, and gross section view of the resected tumor. Under the pressure of Covid

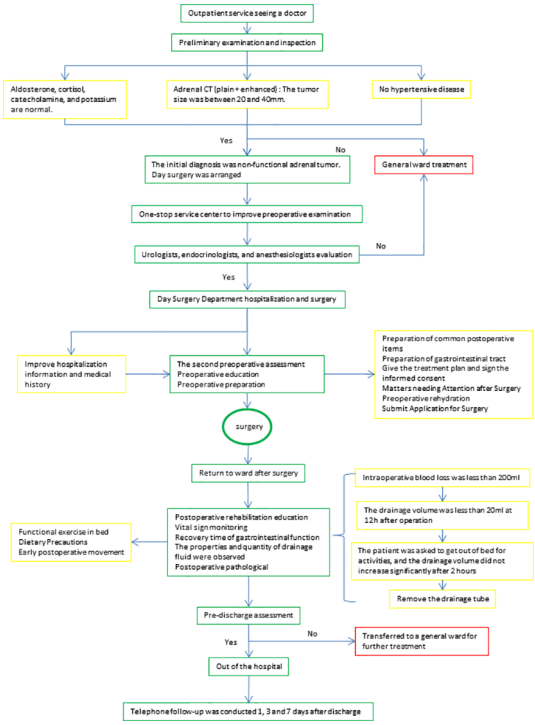

FIGURE 1
Diagnosis and treatment Procedures. After the initial selection, the patients were assigned to a one-stop service center to complete the preoperative examination. Hospitalization and surgery in the day surgery unit after assessment by the urologist, endocrinologist and anesthesiologist. After surgery, the choice of removal of the drainage tube and discharge was evaluated.

pandemic, we established a telephone follow-up system to detect early discomfort after discharge.

Except the 4 patients who were transferred to the general ward for extended observation and management, other patients were all discharged within 48 hours. During the postoperative telephone follow-up, there were no complaints or discomfort from any of the patients. This is similar to the results reported by Mohammad (12) for laparoscopic adrenalectomy, suggesting that the day surgery mode of RLPA is safe.

Another advantage of RLPA in the day surgery mode lies in the hospitalization cost. The cost of hospitalization for a patient admitted in a general ward is around 33,498.3 RMB¥ (counted from patients administered during the same period of time), which is almost 40% higher than the average of 24,168.4 RMB¥ in our group of patients. The average length of stay for a patient in a general ward is 7 days, which is much longer than our group of patients as well.

The major limitations of our study were its nonrandomized design and relatively small sample size. Further studies are required to establish the safety and outcomes of RLPA in day surgery mode.

Conclusions

Retroperitoneal laparoscopic partial adrenalectomy for 20-40 mm nonfunctional unilateral adrenal tumors in the day surgery mode seems to be a safe strategy, that significantly reduce the cost and time of hospitalization.

Data availability statement

The original contributions presented in the study are included in the article/Supplementary Material. Further inquiries can be directed to the corresponding authors.

Ethics statement

The studies involving human participants were reviewed and approved by the Ethical Committee of The First Affiliated Hospital of Nanchang University. The patients/participants provided their written informed consent to participate in this study.

Author contributions

Conception and design: XCZ and GW. Surgeons: GW and HX. Acquisition of data: WL and YY. Preparation of tools: XPZ and ZG. Analysis and interpretation of data: XL and YY. Drafting of the manuscript and statistical analysis: XL and XCZ. Critical revision: BF and XPZ. Obtaining funding: XCZ and HX. All authors contributed to the article and approved the submitted version.

Funding

Key Research and Development Program of Jiangxi Province (20171ACB20029 to XCZ). Applied Research and Cultivation Program of Jiangxi Province (20212BAG70001 to HX).

Acknowledgments

Thank BF and XPZ for providing suggestions for the writing of the article.

Conflict of interest

The authors declare that the research was conducted in the absence of any commercial or financial relationships that could be construed as a potential conflict of interest.

Publisher's note

Supplementary material

The Supplementary Material for this article can be found online at: https://www.frontiersin.org/articles/10.3389/fendo.2022.1099818/full#supplementary-material

References

1. Brunt LM. SAGES guidelines for minimally invasive treatment of adrenal pathology. *Surg Endosc* (2013) 27(11):3957–9. doi: 10.1007/s00464-013-3168-0

2. Bancos I, Prete A. Approach to the patient with adrenal incidentaloma. *J Clin Endocrinol Metab* (2021) 106(11):3331–53. doi: 10.1210/clinem/dgab512

3. Mazzaglia PJ, Varghese J, Habra MA. Evaluation and management of adrenal neoplasms: endocrinologist and endocrine surgeon perspectives. *Abdom Radiol (NY)* (2020) 45(4):1001–10. doi: 10.1007/s00261-020-02464-z

4. Yip L, Duh QY, Wachtel H, Jimenez C, Sturgeon C, Lee C, et al. American Association of endocrine surgeons guidelines for adrenalectomy: Executive summary. *JAMA Surg* (2022) 157(10):870–7. doi: 10.1001/jamasurg.2022.3544

5. Kwak J, Lee KE. Minimally invasive adrenal surgery. *Endocrinol Metab (Seoul)* (2020) 35(4):774–83. doi: 10.3803/EnM.2020.404

6. Bhambhvani HP, Daneshvar MA, Peterson DJ, Ball MW. Partial versus total adrenalectomy for pheochromocytoma: a population-based comparison of outcomes. *Int Urol Nephrol* (2021) 53(12):2485–92. doi: 10.1007/s11255-021-03004-4

7. Najah H, Gaye D, Haissaguerre M. Laparoscopic transperitoneal left partial adrenalectomy for familial pheochromocytoma (with video). *J Visc Surg* (2020) 157 (5):437–8. doi: 10.1016/j.jviscsurg.2020.08.007

8. Detmer DE, Buchanan-Davidson DJ. Ambulatory surgery. *Surg Clin North Am* (1982) 62(4):685–704. doi: 10.1016/S0039-6109(16)42788-X

9. Nicoll JH. The surgery of infancy-II. *Pediatr Anesth* (1998) 8(4):344–44. doi: 10.1046/j.1460-9592.1998.00260.x

10. Martinussen PE, Midttun L. Day surgery and hospital efficiency: empirical analysis of Norwegian hospitals, 1999-2001. *Health Policy* (2004) 68(2):183–96. doi: 10.1016/j.healthpol.2003.09.003

11. Gill IS, Hobart MG, Schweizer D, Bravo EL. Outpatient adrenalectomy. *J Urol* (2000) 163(3):717–20. doi: 10.1016/S0022-5347(05)67790-7

12. Mohammad WM, Frost I, Moonje V. Outpatient laparoscopic adrenalectomy: a Canadian experience. *Surg Laparosc Endosc Percutan Tech* (2009) 19(4):336–7. doi: 10.1097/SLE.0b013e3181b05dcc

13. Gagner M, Lacroix A, Bolté E. Laparoscopic adrenalectomy in cushing's syndrome and pheochromocytoma. *N Engl J Med* (1992) 327(14):1033. doi: 10.1056/NEJM199210013271417

14. Hisano M, Vicentini FC, Srougi M. Retroperitoneoscopic adrenalectomy in pheochromocytoma. *Clinics (Sao Paulo)* (2012) 67 Suppl 1(Suppl 1):161–7. doi: 10.6061/clinics/2012(Sup01)27

15. Tuncel A, Langenhuijsen J, Erkan A, Mikhaylikov T, Arslan M, Aslan Y, et al. Comparison of synchronous bilateral transperitoneal and posterior retroperitoneal laparoscopic adrenalectomy: results of a multicenter study. *Surg Endosc* (2021) 35(3):1101–7. doi: 10.1007/s00464-020-07474-y

16. Kaouk JH, Matin S, Bravo EL, Gill IS. Laparoscopic bilateral partial adrenalectomy for pheochromocytoma. *Urology* (2002) 60(6):1100–3. doi: 10.1016/S0090-4295(02)02013-7

17. Ramírez-Plaza CP, Perales JL, Camero NM, Rodríguez-Cañete A, Bondía-Navarro JA, Santoyo-Santoyo J, et al. Outpatient laparoscopic adrenalectomy: a new step ahead. *Surg Endosc* (2011) 25(8):2570–3. doi: 10.1007/s00464-011-1588-2

18. Gartland RM, Fuentes E, Fazendin J, Fong ZV, Stephen A, Porterfield JR Jr, et al. Safety of outpatient adrenalectomy across 3 minimally invasive approaches at 2 academic medical centers. *Surgery* (2021) 169(1):145–9. doi: 10.1016/j.surg.2020.03.026

19. Moughnyeh M, Lindeman B, Porterfield JR, Dream S. Outpatient robot-assisted adrenalectomy: Is it safe? *Am J Surg* (2020) 220(2):296–7. doi: 10.1016/j.amjsurg.2020.04.037

20. Pigg RA, Fazendin JM, Porterfield JR, Chen H, Lindeman B, et al. Patient satisfaction is equivalent for inpatient and outpatient minimally-invasive adrenalectomy. *J Surg Res* (2022) 269:207–11. doi: 10.1016/j.jss.2021.08.019

21. Fazendin JM, Gartland RM, Stephen A, Porterfield JR Jr, Hodin R, Lindeman B, et al. Outpatient adrenalectomy: A framework for assessment and institutional protocol. *Ann Surg* (2022) 275(2):e541–2. doi: 10.1097/SLA.0000000000004977

frontiers | Frontiers in Endocrinology

TYPE Original Research
PUBLISHED 10 January 2023
DOI 10.3389/fendo.2022.1088557

OPEN ACCESS

EDITED BY
Xiao-qiang Liu,
Tianjin Medical University General Hospital, China

REVIEWED BY
Qi-Chen Yang,
Sichuan University, China
Shuo Zhang,
Beijing Tongren Hospital, Capital Medical University, China

*CORRESPONDENCE
Zhipeng You
yzp74@sina.com

SPECIALTY SECTION
This article was submitted to Reproduction, a section of the journal Frontiers in Endocrinology

RECEIVED 03 November 2022
ACCEPTED 02 December 2022
PUBLISHED 10 January 2023

CITATION
Liu K, Fan H, Hu H, Cheng Y, Liu J and You Z (2023) Genetic variation reveals the influence of steroid hormones on the risk of retinal neurodegenerative diseases. *Front. Endocrinol.* 13:1088557. doi: 10.3389/fendo.2022.1088557

Genetic variation reveals the influence of steroid hormones on the risk of retinal neurodegenerative diseases

Kangcheng Liu, Huimin Fan, Hanying Hu, Yanhua Cheng, Jingying Liu and Zhipeng You*

Jiangxi Province Division of National Clinical Research Center for Ocular Diseases, Jiangxi Clinical Research Center for Ophthalmic Disease, Jiangxi Research Institute of Ophthalmology and Visual Science, Affiliated Eye Hospital of Nanchang University, Nanchang, China

It is difficult to get evidence from randomized trials of a causal relationship between steroid hormones produced by the adrenal gland and gonad and retinal neurodegenerative disorders (RND). In this study, genetic variations of aldosterone (Aldo), androstenedione (A4), progesterone (P4), hydroxyprogesterone (17-OHP), and testosterone/17β-estradiol (T/E2) were obtained from genome-wide association studies as instrumental variables. Mendelian randomization (MR) analysis was used to assess the impact on the risk of RND, including glaucoma (8,591 cases and 210,201 controls), diabetic retinopathy (DR, 14,584 cases and 202,082 controls) and age-related macular degeneration (AMD, 14,034 cases and 91,214 controls). As the main method, inverse variance weighted results suggest that the increased glaucoma risk was affected by T/E2 (OR = 1.11, 95% CI, 1.01–1.22, P = 0.03), which was further validated by other methods (P_{WM}= 0.03, P_{MLE}= 0.03, $P_{MR\text{-}RAPS}$= 0.03). In the replicated stage, the causal relationship between T/E2 and glaucoma was verified based on the MRC-IEU consortium (P = 0.04). No impact of Aldo, A4, P4, 17-OHP, and T/E2 was observed for the risk of DR (P > 0.05) and AMD (P > 0.05). The heterogeneity test (P > 0.05) and pleiotropy test (P > 0.05) verified the robustness of the results. Our results suggest that T/E2 has a suggestive effect on the glaucoma risk. However, the genetic evidence based on a large sample does not support the effect of steroid hormones on DR and AMD risk. Further studies are vital to assess the possibility of steroid hormones as targets for prevention and treatment.

KEYWORDS

steroid hormones, retinal neurodegenerative disease, Mendelian randomization, causality, glaucoma

1 Introduction

Steroid hormones, including aldosterone (Aldo), androstenedione (A4), progesterone (P4), hydroxyprogesterone (17-OHP), testosterone (T), and 17β-estradiol (E2), are produced primarily by the adrenal gland and gonads (1). As regulators of various physiological processes, their biological synthesis originates from cholesterol (2). 17-OHP is transformed from progesterone into A4, T, and Aldo. Moreover, androgens (such as A4 and T) are precursors for E2. The levels of these steroid hormones are in dynamic balance in the body and affect the body's inflammation, metabolism, cell proliferation, and other physiological activities. When the adrenal gland or gonad is in a disease state (such as primary aldosteronism (PA), prostate cancer (PC), or ovarian tumor), steroid hormone levels will change significantly and further affect other organs (such as the heart) of the body.

Notably, steroid hormone receptors have been found throughout eye structures, including the retina (3, 4). These findings revealed that steroid hormones could likely influence visual processing and retinal neurodegenerative diseases (RND) risk. Some studies believe that changes in steroid hormone homeostasis will damage the retina, leading to glaucoma, age-related macular degeneration (AMD), diabetic retinopathy (DR), and other RND (5–7). The study of the rat model shows that Aldo can affect the retinal ischemic damage caused by glaucoma through the Renin-Angiotensin-Aldo System (8, 9). After systemic administration of Aldo, Nitta et al. (10) found progressive loss of retinal ganglion cells (RGCs) without elevated intraocular pressure (IOP), which means that PA will increase the glaucoma risk. Ohshima et al. compared 137 glaucoma patients with PA and 177 controls and found no difference in the prevalence of glaucoma optic disc appearance between the two groups (11). Hao et al. found that E2 can protect RGCs under a high glucose environment through the mitochondrial pathway (12). However, Siddiqui et al.'s study on 255 subjects suggested that E2 was not related to DR risk (13). Lin et al.'s cohort study found that elevated androgen levels in PC patients increased the AMD risk (14). POLA study monitored several steroid hormones in serum and found no correlation between T, E2, and AMD. From these contradictory results, it can be found that the steroid hormones' effect on RND is still unclear. Clarifying the causal relationship between the steroid hormones and RND helps define the strategic approach of steroid hormone benefits, potentially valuable for RND.

However, due to the complexity of the steroid hormone system, many confounders affect the evaluation of randomized controlled studies. It is difficult for researchers to determine the effect of a single steroid hormone on the RND risk. To obtain more reliable results with large samples, the Mendelian randomization (MR) study provides an alternative method to explore the influence of various factors on RND risk through genetic variation (15, 16). M. Verbanck et al. used MR to analyze the influence of testosterone on prostate cancer, hypertension, and other diseases (17). Pott et al. (18) also found the sex-specific causal networks of steroid hormones and obesity through MR research. These studies provide additional possibilities for exploring the effects of steroid hormones on disease risk.

Therefore, to better explore the role of steroid hormones on the risk of RND, we performed a two-sample MR study in which we simultaneously obtained four different instrumental variables (IVs) of steroid hormones from genome-wide association studies (GWASs) of large samples. Through exploring causality, we hope to increase the understanding of the risk of steroid hormones affecting RND. Moreover, it provides a more theoretical basis for reducing the RND risk caused by changes in steroid hormone levels.

2 Methods

2.1 Design of the two-sample MR study

To investigate the effect of steroid hormone levels on the risk of RND (glaucoma, DR, and AMD), we conducted an MR study. Considering the winners' curses and weak instruments, we chose a two-sample MR instead of a one-sample MR (19). According to Mendel's laws of inheritance, single nucleotide polymorphisms (SNPs) are inherited independently and circumvented reverse causality. In addition, this two-sample MR study follows the MR-STROBE guidance (20).

2.2 Exposure: Genetic predictors for steroid hormones

In our study, steroid hormones mainly included Aldo, A4, P4, 17-OHP, and T/E2. Single nucleotide polymorphisms (SNPs) predicting levels of five steroid hormones were obtained from the GWAS by Pott et al. (18). This GWAS used data from LIFE-Adult (males/females: 863/618) (21) and LIFE-Heart (males/females: 1357/711) (22). In LIFE-Adult and LIFE-Heart, A4, P4, and 17-OHP were measured by liquid chromatography-tandem mass spectrometry (LC—MSMS). For T and E2, the electrochemiluminescence immunoassay was used for measurement in LIFE-Adult, and LC—MSMS was used for measurement in LIFE-Heart. At the same time, this GWAS based on two Life studies has adjusted age, sex, and log-transformed BMI and was imputed using 1000 Genomes (Phase 3) reference panel.

2.3 Outcome: summary-level data of RND

To explore the influence of steroid hormones on RND risk, we selected glaucoma, DR, and AMD as the main subjects in the discovery stage. The summary-level data of glaucoma and DR were obtained from FinnGen biobank (218,792 subjects; browser: r5.finngen.fi) (23). The GWASs from FinnGen biobank analyzed 16,962,023 variables and adjusted age, sex, genetic relatedness, genotyping batch, and first 10 principal components (PCs). Detailed information on glaucoma and DR on the GWASs is provided in Table 1. The summary-level data of AMD were obtained from the GWAS by Winkler et al. (24). This GWAS included 14,034 AMD patients and 91,214 controls through 11 data sources (Table 1). All data sources of the GWAS by Winkler et al. were processed through a standardized quality-control pipeline (25) and adjusted age, population stratification, DNA source, and two PCs.

In the replicated stage, we chose the largest sample size, GWAS (ID: ukb-b-8398), as the replication outcome of glaucoma. Based on the MRC-IEU consortium (26), this GWAS analyzed 9,851,867 SNPs from 150,642 European samples. This GWAS was obtained from the MR base database (27), which contains 4,737 glaucoma cases and 458,196 controls (as of October 31, 2022) (Table 1).

2.4 IVs selection and assumption

To obtain reliable results, MR analysis needs to satisfy the following three assumptions (Figure 1): (1) Each SNP as IV is associated with each steroid hormone; (2) All IVs that passed quality selection should not be associated with confounders; (3) The effects of the IVs on the risk of each steroid hormone are only mediated by RND.

Since there are too few IVs obtained by selecting the threshold of 5×10^{-8} (genome-wide significance), $P < 1\times10^{-5}$ (locus-wide significance) is selected as the threshold to obtain higher statistical power for obtaining IVs, similar to other MR studies, this threshold is acceptable (28). A threshold ($R^2 < 0.001$) and clumping distance (10,000 kb) were set for IVs to attenuate linkage disequilibrium (LD) by referring to the European-based 1,000 Genome Projects. Remove palindromic SNPs and use MR-Steiger filtering (29) to clarify the causality direction of each IV between steroid hormones and RND.

TABLE 1 GWAS samples of retinal neurodegenerative diseases used in MR study.

Stage	Outcome	Cases	Controls	Population	Reference
Discovery	glaucoma	8,591	210,201	European	FinnGen biobank (22)
Discovery	DR	14,584	202,082	European	FinnGen biobank (22)
Discovery	AMD	14,034	91,214	European	Winkler et al (23)
Replicated	glaucoma	4,737	458,196	European	MRC-IEU consortium (25)

DR, Diabetic retinopathy; AMD, Age-related macular degeneration.

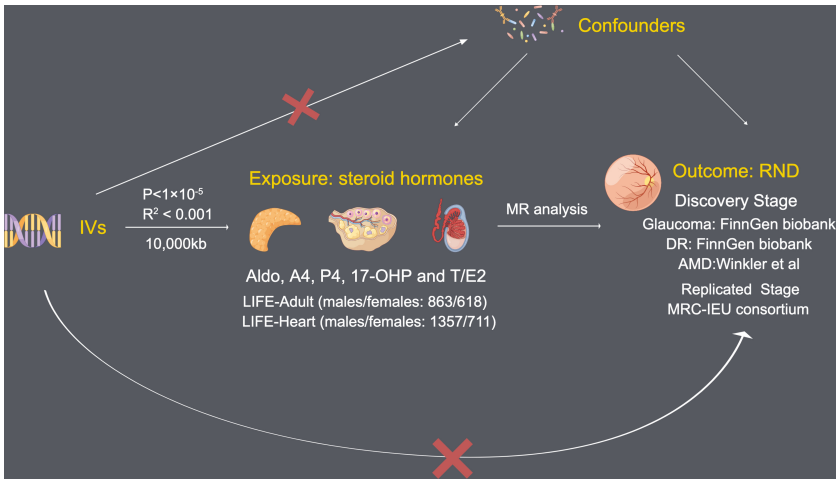

FIGURE 1
Assumptions of Mendelian randomization analysis between steroid hormone and RND.

2.5 Methods of MR analysis

2.5.1 Causal effect estimation

MR analysis of only one SNP was performed using the Wald ratio (WR) method. For causal estimation of multiple SNPs, inverse variance weighted (IVW) is the main evaluation method for MR analysis (30). At the same time, four additional methods are used to verify the results of IVW with causality between steroid hormones and RND: (1) MR-Egger (31): Even if most IVs have pleiotropy, it can provide effective estimates. However, compared with the other 4 methods, the causal estimates of MR-Egger may be biased; (2) Weighted median (32): The weighted median of the WR estimate is calculated to obtain a relatively robust causal estimate; (3) Maximum likelihood estimator (MLE) (33): the results assume the linear correlation of RND and each steroid hormone with jointly normal distribution and allow for uncertainty in both gene–steroid hormone and gene–RND associations; (4) MR robust adjusted profile score (MR-RAPS) (34): Even if there are weak IVs, the method can also provide robust causal estimates.

2.5.2 Sensitivity analysis

MR Egger expression and MR-PRESSO tested the pleiotropy of MR results. Moreover, MR-PRESSO can also be used to remove outliers (35). Cochrane's Q method tested the heterogeneity of MR results between steroid hormones and RND. At the same time, SNPs were deleted one by one by using the Leave-one-out method to evaluate whether they drove the causal effect between steroid hormones and RND.

2.6 Statistical analysis

All statistical analyses were completed in R software environment of version 2.22. R packages "TwoSampleMR" and "MR-PRESSO" were used to analyze the causality between steroid hormones and RND. F statistics < 10 is considered a weak IV ($F = \frac{R^2(n-k-1)}{k(1-R^2)}$; R^2: GM taxa variance explained by SNPs; n: sample size; k: the number of included IVs) (36). The effect estimates of IVs predicted steroid hormones on RND were presented as odds ratio (OR) with a 95% confidence interval (CI). $P < 0.05$ was considered suggestive of significance and a potential causal effect.

3 Results

3.1 Causal associations between steroid hormones and glaucoma (discovery stage)

After data harmonization of GWAS data, 17 SNPs related to Aldo, 16 SNP s related to A4, 28 SNPs related to P4, 11 SNPs related to 17-OHP, and 15 SNPs related to T/E2 were used as IVs for MR analysis (Supplementary Table S1). All IVs are strong instruments (F, 19.52 to 85.15) (Supplementary Table S1).

As the most important method, IVW results found that the increased risk of glaucoma was affected by T/E2 (OR = 1.11, 95% CI, 1.01–1.22, $P = 0.03$) (Figure 2 and Table 2). The results of WM ($P = 0.03$), MLE ($P = 0.03$), and MR-RAPS ($P = 0.03$) also verified this discovery (Figure 2 and Table 2). The results of Aldo (P_{IVW}= 0.25, $P_{MR\text{-}Egger}$ = 0.35, P_{WM}= 0.88, P_{MLE}= 0.65, $P_{MR\text{-}RAPS}$= 0.66), A4 (P_{IVW}= 0.35, $P_{MR\text{-}Egger}$ = 0.98, P_{WM}= 0.99, P_{MLE}= 0.55, $P_{MR\text{-}RAPS}$= 0.57), P4 (P_{IVW}= 0.93, $P_{MR\text{-}Egger}$ = 0.50, P_{WM}= 0.82, P_{MLE}= 0.85, $P_{MR\text{-}RAPS}$= 0.85) and 17-OHP (P_{IVW}= 0.77, $P_{MR\text{-}Egger}$ = 0.25, P_{WM}= 0.82, P_{MLE}= 0.51, $P_{MR\text{-}RAPS}$= 0.52) did not suggest a significant causal relationship with glaucoma (Figure 2 and Table 2).

The heterogeneity test used Cochrane's Q method to confirm that there was no heterogeneity in MR results (IVW: all $P > 0.62$; MR-Egger: all $P > 0.56$) (Figure 2 and Table 2). MR-Egger regression confirmed that the results did not have level pleiotropy (all $P > 0.14$) and was further verified by MR-PRESSO (all $P > 0.67$) (Figure 2 and Table 2). More details are shown in Supplementary Table S2. Meanwhile, there was no significant difference in causal estimations of each steroid hormone on glaucoma by the leave-one-out analysis (Supplementary Figure S1).

3.2 Causal associations between steroid hormones and DR (discovery stage)

After quality control, the same number of SNPs as glaucoma was used as strong IVs (F, 19.52 to 85.15) for MR analysis (Supplementary Table 1).

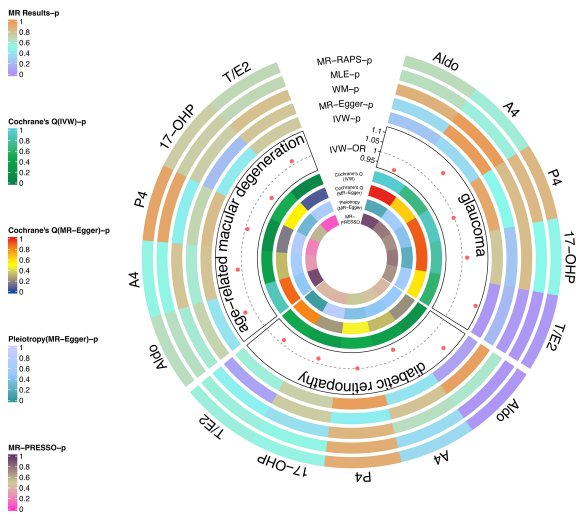

FIGURE 2
Causal analysis of steroid hormone and RND based on MR analyses and sensitivity analyses in the discovery stage.

TABLE 2 MR results and sensitivity analyses between steroid hormones and glaucoma.

	P (MR results)					*P* (Cochrane's Q)		*P* (Pleiotropy)	
	IVW	MR-Egger	WM	MLE	MR-RAPS	IVW	MR-Egger	MR-Egger regression	MR-PRESSO
Discovery stage									
Aldo	0.25	0.35	0.88	0.65	0.66	0.97	0.99	0.14	0.918
A4	0.35	0.98	0.99	0.55	0.57	0.68	0.64	0.59	0.767
P4	0.93	0.51	0.82	0.85	0.85	0.91	0.91	0.41	0.698
17-OHP	0.77	0.25	0.82	0.51	0.52	0.82	0.91	0.19	0.769
T/E2	0.03	0.19	0.04	0.03	0.03	0.62	0.57	0.58	0.679
Replicated stage									
Aldo	0.93	0.20	0.67	0.75	0.76	0.81	0.95	0.20	0.735
A4	0.35	0.75	0.80	0.32	0.35	0.87	0.81	0.66	0.935
P4	0.17	0.16	0.06	0.69	0.67	0.17	0.47	0.11	0.057
17-OHP	0.43	0.45	0.07	0.55	0.55	0.09	0.08	0.49	0.133
T/E2	0.04	0.44	0.11	0.04	0.05	0.65	0.77	0.29	0.675

MR, Mendelian randomization; IVW, Inverse variance weighted; WM, Weighted median; MLE, maximum likelihood estimator; MR-RAPS, MR robust adjusted profile score; Aldo, aldosterone; A4, androstenedione; P4, progesterone; 17-OHP, hydroxyprogesterone; T/E, Testosterone_Estradiol_Ratio.

The results of MLE (OR = 1.10, 95% CI, 1.05–1.14, $P = 0.02$) and MR-RAPs (OR = 1.10, 95% CI, 1.05–1.15, $P = 0.02$) found that Aldo had a potential causal relationship with cataract (Figure 2 and Table 3). The main results for IVW were close to significant differences ($P = 0.07$) (Figure 2 and Table 3). Heterogeneity tests (IVW: $P = 0.23$; MR-Egger: $P = 0.21$) and pleiotropy tests (MR-Egger regression: $P = 0.49$; MR-PRESSO: $P = 0.408$) verified the robustness of the results (Figure 2 and Table 3).

There was no significant causal association between these 4 steroid hormones (A4, P4, 17-OHP, and T/E2) and DR (all $P > 0.05$) (Figure 2 and Table 3). The Cochrane's Q test confirmed no heterogeneity in these results (P, 0.23 to 0.48) (Figure 2 and Table 3). MR-Egger regression and MR-PRESSO test confirmed that there was no pleiotropy in these results (A4, P4, and 17-OHP: all $P > 0.05$) (Figure 2 and Table 3). The results of T/E2 had pleiotropy by MR-Egger regression ($P = 0.04$), which is contrary to MR- PRESSO ($P = 0.412$). More details are shown in Supplementary Table S2. Additionally, the leave-one-out method was used to further validate data robustness between each steroid hormone and DR (Supplementary Figure S2).

3.3 Causal associations between steroid hormones and AMD (discovery stage)

After data harmonization of GWAS data, 18 SNPs related to Aldo, 15 SNP s related to A4, 28 SNPs related to P4, 12 SNPs related to 17-OHP, and 15 SNPs related to T/E2 were used as IVs, and the details of all IVs can be found in Supplementary Table S1. The 5 steroid hormones did not show a significant

TABLE 3 MR results and sensitivity analyses between steroid hormones and DR in the discovery stage.

	P (MR results)					*P* (Cochrane's Q)		*P* (Pleiotropy)	
	IVW	MR-Egger	WM	MLE	MR-RAPS	IVW	MR-Egger	MR-Egger regression	MR-PRESSO
Aldo	0.07	0.97	0.60	0.02	0.02	0.23	0.21	0.49	0.408
A4	0.39	0.79	0.64	0.35	0.34	0.35	0.32	0.45	0.464
P4	0.98	0.44	0.86	0.91	0.91	0.48	0.47	0.38	0.513
17-OHP	0.73	0.75	0.37	0.53	0.53	0.31	0.24	0.82	0.386
T/E2	0.56	0.08	0.46	0.56	0.56	0.47	0.82	0.04	0.412

MR, Mendelian randomization; IVW, Inverse variance weighted; WM, Weighted median; MLE, maximum likelihood estimator; MR-RAPS, MR robust adjusted profile score; Aldo, aldosterone; A4, androstenedione; P4, progesterone; 17-OHP, hydroxyprogesterone; T/E, Testosterone_Estradiol_Ratio.

effect on AMD risk (all $P > 0.05$) (Figure 2 and Table 4). The results of sensitivity analysis confirmed the absence of significant heterogeneity (all $P > 0.05$) and pleiotropy (all $P > 0.05$) (Figure 2 and Table 4). More details are shown in Supplementary Table S2. Additionally, the leave-one-out method was used to further validate data robustness between each steroid hormone and AMD (Supplementary Figure S3).

3.4 Causal associations between steroid hormones and glaucoma (replicated stage)

For the causal relationship between T/E2 and glaucoma found in the discovery stage, we verified it in the replicated stage. Based on the GWAS from the MRC-IEU consortium, eight SNPs related to Aldo, seven SNP s related to A4, six SNPs related to P4, five SNPs related to 17-OHP, and six SNPs related to T/E2 were used as IVs (Supplementary Table S1).

In the replicated stage, the results of IVW verified the findings at the discovery stage, that is, T/E2 was causally associated with the risk of glaucoma (P = 0.04), while Aldo (P=0.93), A4 (P = 0.35), P4 (P = 0.17) and 17-OHP (P = 0.43) were not significantly causally associated with glaucoma (Figure 3 and Table 2). Similarly, the results of MLE showed the effect of T/E2 on glaucoma risk (P = 0.04) (Figure 3, Supplementary Table S2). Furthermore, MR- RAPS results showed an association between T/E2 and glaucoma that approached statistical difference (P = 0.05) (Figure 3 and Table 2). More details are shown in Supplementary Table S2. At the same time, the results of Leave-on-out did not show that a single IV drove the causal relationship between each steroid hormone and glaucoma (Supplementary Figure S4).

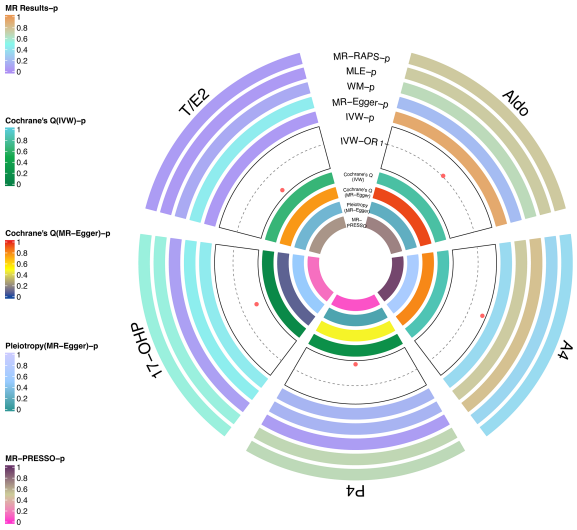

FIGURE 3
Causal analysis of steroid hormone and glaucoma based on MR analyses and sensitivity analyses in the replicated stage.

4 Discussion

Our study systematically assessed the causal correlation of steroid hormone and RND (glaucoma, DR, and AMD) using the data from large-scale GWAS. Our study's observational and IVW results supported the T/E2 effect on glaucoma to a certain extent, which was further validated by the WM, MLE, and MR-RAPS results. At the same time, this discovery was verified in the replicated stage. This means that glaucoma risk is affected by T and E2. The increase of the T level or the decrease of the E2 level will increase the value of T/E2, indicating that the risk of glaucoma increases. Therefore, T/E2 may be a biomarker to assess glaucoma risk. However, gene data based on a large sample did not show the effect of steroid hormones on DR and AMD risk.

Dewundara et al. reported that age at menarche and menopause, using oral contraceptives or bilateral ovariectomy would increase the glaucoma risk by reducing the duration of E2 exposure (37). In a *post hoc* analysis from a clinical trial, the intervention of E2 may become a protective factor of glaucoma

TABLE 4 MR results and sensitivity analyses between steroid hormones and AMD in the discovery stage.

	P (MR results)					*P* (Cochrane's Q)		*P* (Pleiotropy)	
	IVW	MR-Egger	WM	MLE	MR-RAPS	IVW	MR-Egger	MR-Egger regression	MR-PRESSO
Aldo	0.39	0.71	0.58	0.64	0.65	0.89	0.89	0.46	0.920
A4	0.79	0.59	0.79	0.52	0.53	0.38	0.33	0.63	0.271
P4	0.82	0.70	0.45	0.94	0.94	0.18	0.15	0.74	0.196
17-OHP	0.43	0.21	0.74	0.73	0.74	0.51	0.54	0.29	0.564
T/E2	0.75	0.78	0.81	0.68	0.68	0.07	0.06	0.67	0.066

MR, Mendelian randomization; IVW, Inverse variance weighted; WM, Weighted median; MLE, maximum likelihood estimator; MR-RAPS, MR robust adjusted profile score; Aldo, aldosterone; A4, androstenedione; P4, progesterone; 17-OHP, hydroxyprogesterone; T/E, Testosterone_Estradiol_Ratio.

by reducing IOP (38). Moreover, Nakazawa et al. showed that E2 could activate the ERK-c-Fos pathway, thereby reducing the death of RGC and exerting neuroprotective effects (39). In contrast, Estradiol regulates nitric oxide signaling and enhances ocular blood flow, thereby lowering IOP. From the genetic perspective, Magalhães et al. also mentioned that the NOS3 gene coding for endothelial nitric oxide (NO) synthase is associated with glaucoma (40). Mookherjee et al. (41) also suggested that E2 may play a role in the pathogenesis of glaucoma. When CYP1B1 is mutated, the metabolic activity of E2 may be affected, leading to the upregulation of Myocilin and affecting the development of primary open-angle glaucoma (POAG) (41). A cohort study of 63 women with POAG also found a correlation between E2 and POAG, confirming that a decreased level of E2 is a risk factor for POAG (42). Our results also verify this conclusion to some extent: reduced E2 levels increased susceptibility to glaucoma.

Notably, the control of IOP is closely related to glaucoma progress. Through pathway analysis, Youngblood et al. identified E2 as an upstream regulator of IOP-related genes such as TES (43). Jojua et al. (44) examined the levels of E2 and gonadotropins in 71 patients with POAG and the results confirmed the role of E2 and gonadotropins in IOP regulation. Therefore, we speculate that the effect of E2 on glaucoma risk may lie in the effect of E2 on IOP.

T and E2 are in dynamic balance in the body, and their imbalance may affect the risk of disease (45). This means that the effect of steroid hormones may not be limited to the change of E2. There is a gap in current research on T's role in the glaucomatous process. A cohort study in Korea showed that the use of androgen deprivation therapy was associated with a decreased risk of POAG patients with prostate cancer (46). Bailey et al. confirmed the association between the gene variant set of T and glaucoma at the genetic level (47). Kang et al. evaluated the postmenopausal sex hormone levels of 189 POAG patients and 189 controls and found a suggestive association between elevated T levels and increased IOP and glaucoma risk (48). Our results are consistent with the above studies' conclusions and reflect that elevated T levels will increase the risk of glaucoma. Lee et al. believed that T inhibits the activity of endothelial NO synthase in the trabecular meshwork, thereby reducing the outflow of aqueous humor and increasing IOP, which aggravates the RGCs damage. However, additional research is required to corroborate this viewpoint.

Takasago et al. administered Aldo (40, 80, or 160 μg/kg/day) to rats and found that the RGC number was significantly reduced (49). Different from the animal experiment, compared with the control group, the patients with aldosteronism have no significant difference in their prognosis of glaucomatous optic disc appearance (11). Our MR results also found no causal relationship between aldosterone and glaucoma. Due to the species differences between animal models and humans, the effects of aldosterone on the eyes are also different. Moreover, the effect of Aldo is not only in itself but, more importantly, in the Renin-Angiotensin-Aldo System's co-regulation.

Further limitations include that our study does not support the effect of steroids on DR and AMD risk, even though we chose 1×10^{-5} (locus-wide significance) as the threshold for the IVs. Typically, a more stringent threshold (genome-wide significance threshold) should be chosen, which will further reduce the number of IVs eligible for quality control. Therefore, the effect of T/E2 on glaucoma risk still deserves to be studied in depth. In future studies, the GWAS sample size needs to be expanded to obtain more valid IVs for further validation to obtain more rigorous conclusions. Also, since there are many different types of glaucoma (e.g., POAG, primary angle closure glaucoma), we will further explore the effect of T/E2 on the risk of different types of glaucoma in the future study. On the other hand, we exclusively examined the effect of serum steroid hormones on the risk of RND. Local steroid hormone levels in the eye could be a more visual response to the effect on RND. Due to the lack of a GWAS for ocular local steroid hormone levels, further studies are needed to obtain IVs that can be used for evaluation. In addition, since the genetic variation of steroid hormones originates from the European population, the conclusions still need to be generalized with caution to extend the conclusion to Asian races.

Through MR analysis, we found a causal relationship between T/E2 and glaucoma, which provides new genetic evidence for glaucoma prevention and risk assessment. However, there is still a lack of strong evidence for the effect of steroids on DR and AMD. Further research is needed to confirm their relationship.

Data availability statement

The original contributions presented in the study are included in the article/Supplementary Material. Further inquiries can be directed to the corresponding author.

Ethics statement

To ensure that the individual information of the subject will not be disclosed, all summary-level data are from de-identified genome-wide association studies (GWASs) and can be used without restriction. All GWASs (including GWASs of steroid hormone as exposure and GWASs of RND as outcomes) were performed following the declaration of Helsinki and were approved by the ethics committee of the affiliated institution.

The ethical approval for each study can be found in the original publication.

Author contributions

KL and ZY designed the study. KL and ZY analyzed the data and drew the figures. All authors critically revised the manuscript. All authors read and approved the final manuscript.

Funding

This work was supported by grants from the National Natural Science Foundation of China (81860175, 8226040184) and, Science and Technology Innovation Base Construction - Clinical Medicine Research Centre Project (20221ZDG02012) to ZY; the postgraduates innovation special fund project of Jiangxi province (YC2022—B051) and a grant from the Talent Development project of the Affiliated Eye Hospital of Nanchang University (No.2022X05) and to KL. The funders had no role in the study design, data collection, data analysis, interpretation, or writing of the report.

Acknowledgments

We want to acknowledge the participants and investigators of the GWAS from Pott et al. (18), FinnGen study (https://finngen.gitbook.io/documentation/), the GWAS from Winkler et al. (24) and MRC-IEU consortium for sharing the genetic data. We thank Figdraw (www.figdraw.com) for expert assistance in Figure 1. We thank Home for Researchers editorial team (www.home-for-researchers.com) for language editing service.

Conflict of interest

The authors declare that the research was conducted in the absence of any commercial or financial relationships that could be construed as a potential conflict of interest.

Publisher's note

Supplementary material

The Supplementary Material for this article can be found online at: https://www.frontiersin.org/articles/10.3389/fendo.2022.1088557/full#supplementary-material

SUPPLEMENTARY FIGURE 1
The leave-one-out results of steroid hormone for glaucoma in the discovery stage.

SUPPLEMENTARY FIGURE 2
The leave-one-out results of steroid hormone for DR in the discovery stage.

SUPPLEMENTARY FIGURE 3
The leave-one-out results of steroid hormone for AMD in the discovery stage.

SUPPLEMENTARY FIGURE 4
The leave-one-out results of steroid hormone for glaucoma in the replicated stage.

References

1. Holst JP, Soldin OP, Guo T, Soldin SJ. Steroid hormones: relevance and measurement in the clinical laboratory. *Clin Lab Med* (2004) 24:105–18. doi: 10.1016/j.cll.2004.01.004

2. Sanderson JT. The steroid hormone biosynthesis pathway as a target for endocrine-disrupting chemicals. *Toxicol Sci* (2006) 94:3–21. doi: 10.1093/toxsci/kfl051

3. Cascio C, Deidda I, Russo D, Guarneri P. The estrogenic retina: The potential contribution to healthy aging and age-related neurodegenerative diseases of the retina. *Steroids* (2015) 103:31–41. doi: 10.1016/j.steroids.2015.08.002

4. Jain A, Wordinger RJ, Yorio T, Clark AF. Role of the alternatively spliced glucocorticoid receptor isoform GRβ in steroid responsiveness and glaucoma. *J ocular Pharmacol Ther* (2014) 30:121–7. doi: 10.1089/jop.2013.0239

5. Fourgeux C, Bron A, Acar N, Creuzot-Garcher C, Bretillon L. 24S-hydroxycholesterol and cholesterol-24S-hydroxylase (CYP46A1) in the retina: from cholesterol homeostasis to pathophysiology of glaucoma. *Chem Phys Lipids* (2011) 164:496–9. doi: 10.1016/j.chemphyslip.2011.04.006

6. Suzuki R, Lee K, Jing E, Biddinger SB, McDonald JG, Montine TJ, et al. Diabetes and insulin in regulation of brain cholesterol metabolism. *Cell Metab* (2010) 12:567–79. doi: 10.1016/j.cmet.2010.11.006

7. Toops KA, Tan LX, Jiang Z, Radu RA, Lakkaraju A. Cholesterol-mediated activation of acid sphingomyelinase disrupts autophagy in the retinal pigment epithelium. *Mol Biol Cell* (2015) 26:1–14. doi: 10.1091/mbc.e14-05-1028

8. Fujita T, Hirooka K, Nakamura T, Itano T, Nishiyama A, Nagai Y, et al. Neuroprotective effects of angiotensin II type 1 receptor (AT1-r) blocker *via* modulating AT1-r signaling and decreased extracellular glutamate levels. *Invest Ophthalmol Vis Sci* (2012) 53:4099–110. doi: 10.1167/iovs.11-9167

9. Fukuda K, Hirooka K, Mizote M, Nakamura T, Itano T, Shiraga F. Neuroprotection against retinal ischemia-reperfusion injury by blocking the angiotensin II type 1 receptor. *Invest Ophthalmol Vis Sci* (2010) 51:3629–38. doi: 10.1167/iovs.09-4107

10. Nitta E, Hirooka K, Tenkumo K, Fujita T, Nishiyama A, Nakamura T, et al. Aldosterone: a mediator of retinal ganglion cell death and the potential role in the

pathogenesis in normal-tension glaucoma. *Cell Death Dis* (2013) 4:e711. doi: 10.1038/cddis.2013.240

11. Ohshima Y, Higashide T, Sakaguchi K, Sasaki M, Udagawa S, Ohkubo S, et al. The association of primary aldosteronism with glaucoma-related fundus abnormalities. *PLoS One* (2020) 15:e0242090. doi: 10.1371/journal.pone.0242090

12. Hao M, Li Y, Lin W, Xu Q, Shao N, Zhang Y, et al. Estrogen prevents high-glucose-induced damage of retinal ganglion cells *via* mitochondrial pathway. *Graefes Arch Clin Exp Ophthalmol* (2015) 253:83–90. doi: 10.1007/s00417-014-2771-7

13. Siddiqui K, George TP, Alosaimi J, Bukhari KO, Rubeaan KA. Level of hormones in menopause in relation to diabetic retinopathy among type 2 diabetic women. *Health Care Women Int* (2021) 42:58–66. doi: 10.1080/07399332.2020.1798962

14. Lin SY, Lin CL, Chang CH, Wu HC, Lin CH, Kao CH. Risk of age-related macular degeneration in patients with prostate cancer: a nationwide, population-based cohort study. *Ann Oncol* (2017) 28:2575–80. doi: 10.1093/annonc/mdx402

15. Liu K, Zou J, Fan H, Hu H, You Z. Causal effects of gut microbiota on diabetic retinopathy: A mendelian randomization study. *Front Immunol* (2022) 13:930318. doi: 10.3389/fimmu.2022.930318

16. Thanassoulis G, O'Donnell CJ. Mendelian randomization: nature's randomized trial in the post-genome era. *JAMA* (2009) 301:2386–8. doi: 10.1001/jama.2009.812

17. Mohammadi-Shemirani P, Chong M, Pigeyre M, Morton RW, Gerstein HC, Paré G. Effects of lifelong testosterone exposure on health and disease using mendelian randomization. *Elife* (2020) 9:e58914. doi: 10.7554/eLife.58914

18. Pott J, Horn K, Zeidler R, Kirsten H, Ahnert P, Kratzsch J, et al. Sex-specific causal relations between steroid hormones and obesity-a mendelian randomization study. *Metabolites* (2021) 11:738. doi: 10.3390/metabo11110738

19. Lawlor DA, Harbord RM, Sterne JA, Timpson N, Davey Smith G. Mendelian randomization: using genes as instruments for making causal inferences in epidemiology. *Stat Med* (2008) 27:1133–63. doi: 10.1002/sim.3034

20. Skrivankova VW, Richmond RC, Woolf BAR, Yarmolinsky J, Davies NM, Swanson SA, et al. Strengthening the reporting of observational studies in epidemiology using mendelian randomization: The STROBE-MR statement. *JAMA* (2021) 326:1614–21. doi: 10.1001/jama.2021.18236

21. Loeffler M, Engel C, Ahnert P, Alfermann D, Arelin K, Baber R, et al. The LIFE-Adult-Study: objectives and design of a population-based cohort study with 10,000 deeply phenotyped adults in Germany. *BMC Public Health* (2015) 15:691. doi: 10.1186/s12889-015-1983-z

22. Scholz M, Henger S, Beutner F, Teren A, Baber R, Willenberg A, et al. Cohort profile: The Leipzig research center for civilization diseases-heart study (LIFE-heart). *Int J Epidemiol* (2020) 49:1439–1440h. doi: 10.1093/ije/dyaa075

23. Kurki MI, Karjalainen J, Palta P, Sipilä TP, Kristiansson K, Donner K, et al. FinnGen: Unique genetic insights from combining isolated population and national health register data. *medRxiv* (2022) 2022:03.03.22271360. doi: 10.1101/2022.03.03.22271360

24. Winkler TW, Grassmann F, Brandl C, Kiel C, Günther F, Strunz T, et al. Genome-wide association meta-analysis for early age-related macular degeneration highlights novel loci and insights for advanced disease. *BMC Med Genomics* (2020) 13:120. doi: 10.1186/s12920-020-00760-7

25. Winkler TW, Day FR, Croteau-Chonka DC, Wood AR, Locke AE, Mägi R, et al. Quality control and conduct of genome-wide association meta-analyses. *Nat Protoc* (2014) 9:1192–212. doi: 10.1038/nprot.2014.071

26. Ruth Mitchell E, Mitchell R, Raistrick CA, Paternoster L, Hemani G, Gaunt TR. (2019) 2. MRC IEU UK Biobank GWAS pipeline version.

27. Hemani G, Zheng J, Elsworth B, Wade KH, Haberland V, Baird D, et al. The MR-base platform supports systematic causal inference across the human phenome. *Elife* (2018) 7:e34408. doi: 10.7554/eLife.34408

28. Sanna S, van Zuydam NR, Mahajan A, Kurilshikov A, Vich Vila A, Võsa U, et al. Causal relationships among the gut microbiome, short-chain fatty acids and metabolic diseases. *Nat Genet* (2019) 51:600–5. doi: 10.1038/s41588-019-0350-x

29. Hemani G, Tilling K, Davey Smith G. Orienting the causal relationship between imprecisely measured traits using GWAS summary data. *PloS Genet* (2017) 13:e1007081. doi: 10.1371/journal.pgen.1007081

30. Burgess S, Scott RA, Timpson NJ, Davey Smith G, Thompson SG. Using published data in mendelian randomization: a blueprint for efficient identification of causal risk factors. *Eur J Epidemiol* (2015) 30:543–52. doi: 10.1007/s10654-015-0011-z

31. Bowden J, Del Greco MF, Minelli C, Davey Smith G, Sheehan NA, Thompson JR. Assessing the suitability of summary data for two-sample mendelian randomization analyses using MR-egger regression: the role of the I2 statistic. *Int J Epidemiol* (2016) 45:1961–74. doi: 10.1093/ije/dyw220

32. Bowden J, Davey Smith G, Haycock PC, Burgess S. Consistent estimation in mendelian randomization with some invalid instruments using a weighted median estimator. *Genet Epidemiol* (2016) 40:304–14. doi: 10.1002/gepi.21965

33. Nguyen LT, Schmidt HA, von Haeseler A, Minh BQ. IQ-TREE: a fast and effective stochastic algorithm for estimating maximum-likelihood phylogenies. *Mol Biol Evol* (2015) 32:268–74. doi: 10.1093/molbev/msu300

34. Zhao Q, Chen Y, Wang J, Small DS. Powerful three-sample genome-wide design and robust statistical inference in summary-data mendelian randomization. *Int J Epidemiol* (2019) 48:1478–92. doi: 10.1093/ije/dyz142

35. Verbanck M, Chen CY, Neale B, Do R. Detection of widespread horizontal pleiotropy in causal relationships inferred from mendelian randomization between complex traits and diseases. *Nat Genet* (2018) 50:693–8. doi: 10.1038/s41588-018-0099-7

36. Burgess S, Davies NM, Thompson SG. Bias due to participant overlap in two-sample mendelian randomization. *Genet Epidemiol* (2016) 40:597–608. doi: 10.1002/gepi.21998

37. Dewundara SS, Wiggs JL, Sullivan DA, Pasquale LR. Is estrogen a therapeutic target for glaucoma? *Semin Ophthalmol* (2016) 31:140–6. doi: 10.3109/08820538.2015.1114845

38. Newman-Casey PA, Talwar N, Nan B, Musch DC, Pasquale LR, Stein JD. The potential association between postmenopausal hormone use and primary open-angle glaucoma. *JAMA Ophthalmol* (2014) 132:298–303. doi: 10.1001/jamaophthalmol.2013.7618

39. Nakazawa T, Takahashi H, Shimura M. Estrogen has a neuroprotective effect on axotomized RGCs through ERK signal transduction pathway. *Brain Res* (2006) 1093:141–9. doi: 10.1016/j.brainres.2006.03.084

40. Magalhães da Silva T, Rocha AV, Lacchini R, Marques CR, Silva ES, Tanus-Santos JE, et al. Association of polymorphisms of endothelial nitric oxide synthase (eNOS) gene with the risk of primary open angle glaucoma in a Brazilian population. *Gene* (2012) 502:142–6. doi: 10.1016/j.gene.2012.04.047

41. Mookherjee S, Acharya M, Banerjee D, Bhattacharjee A, Ray K. Molecular basis for involvement of CYP1B1 in MYOC upregulation and its potential implication in glaucoma pathogenesis. *PloS One* (2012) 7:e45077. doi: 10.1371/journal.pone.0045077

42. Qiu Y, Yu J, Tang L, Ren J, Shao M, Li S, et al. Association between sex hormones and visual field progression in women with primary open angle glaucoma: A cross-sectional and prospective cohort study. *Front Aging Neurosci* (2021) 13:756186. doi: 10.3389/fnagi.2021.756186

43. Youngblood HA, Parker E, Cai J, Perkumas K, Yu H, Sun J, et al. Identification of estrogen signaling in a prioritization study of intraocular pressure-associated genes. *Int J Mol Sci* (2021) 22:10288. doi: 10.3390/ijms221910288

44. Jojua T, Sumbadze TS, Papava M. Secretion of sex hormones in patients with open angle glaucoma. *Georgian Med News* (2005), (124–125):33–7. Available at: https://pubmed.ncbi.nlm.nih.gov/16148373/.

45. Dai W, Ming W, Li Y, Zheng HY, Wei CD, Rui Z, et al. Synergistic effect of a physiological ratio of estradiol and testosterone in the treatment of early-stage atherosclerosis. *Arch Med Res* (2015) 46:619–29. doi: 10.1016/j.arcmed.2015.11.003

46. Ahn HK, Lee HS, Park JY, Kim DK, Kim M, Hwang HS, et al. Androgen deprivation therapy may reduce the risk of primary open-angle glaucoma in patients with prostate cancer: a nationwide population-based cohort study. *Prostate Int* (2021) 9:197–202. doi: 10.1016/j.prnil.2021.05.001

47. Bailey JNC, Gharahkhani P, Kang JH, Butkiewicz M, Sullivan DA, Weinreb RN, et al. Testosterone pathway genetic polymorphisms in relation to primary open-angle glaucoma: An analysis in two Large datasets. *Invest Ophthalmol Vis Sci* (2018) 59:629–36. doi: 10.1167/iovs.17-22708

48. Kang JH, Rosner BA, Wiggs JL, Pasquale LR. Sex hormone levels and risk of primary open-angle glaucoma in postmenopausal women. *Menopause* (2018) 25:1116–23. doi: 10.1097/GME.0000000000001120

49. Takasago Y, Hirooka K, Nakano Y, Kobayashi M, Ono A. Elevated plasma aldosterone levels are associated with a reduction in retinal ganglion cell survival. *J Renin Angiotensin Aldosterone Syst* (2018) 19:1470320318795001. doi: 10.1177/1470320318795001

frontiers | Frontiers in Endocrinology

TYPE Original Research
PUBLISHED 01 February 2023
DOI 10.3389/fendo.2023.1119251

OPEN ACCESS

EDITED BY
Yuxuan Song,
Peking University People's Hospital, China

REVIEWED BY
Jiaxiang Liu,
Chinese Academy of Medical Sciences and Peking Union Medical College, China
Xiao-qiang Liu,
Tianjin Medical University General Hospital, China

*CORRESPONDENCE
Xiaochen Zhou
mo_disc@126.com
Gongxian Wang
urowgx@163.com
Haibo Xi
13870834578@163.com

†These authors have contributed equally to this work

SPECIALTY SECTION
This article was submitted to Adrenal Endocrinology, a section of the journal Frontiers in Endocrinology

RECEIVED 08 December 2022
ACCEPTED 19 January 2023
PUBLISHED 01 February 2023

CITATION
Li X, Xiao S, Zhan X, Yu Y, Zhang C, Xi H, Wang G and Zhou X (2023) For small (1-3cm) nonfunctional adrenal incidentaloma (NFAI), which option is more appropriate for conservative treatment or surgery? *Front. Endocrinol.* 14:1119251. doi: 10.3389/fendo.2023.1119251

For small (1-3cm) nonfunctional adrenal incidentaloma (NFAI), which option is more appropriate for conservative treatment or surgery?

Xuwen Li†, Song Xiao†, Xiangpeng Zhan†, Yue Yu, Cheng Zhang, Haibo Xi*, Gongxian Wang* and Xiaochen Zhou*

Department of Urology, The First Affiliated Hospital of Nanchang University, Nanchang, China

Objective: To compare the efficacy and safety between conservative treatment and surgery for the patients with small (1-3cm) nonfunctional adrenal incidentaloma (NFAI).

Methods: The patients with small (1-3cm) NFAI who received conservative treatment or surgery in our hospital from November 2018 to December 2019 were retrospectively collected. A total of 83 patients were included in this study. They were divided into two groups according to the treatment methods: the surgery group (n=51) and the conservative treatment group (n=32).Then patients' demographics, tumor characteristics, functional indicators and complications were compared. Statistical analysis was performed using t-test for continuous variables and Pearson chi-square test or Fisher's exact test for categorical variables.

Results: At the time of diagnosis, after 3 months, after 6 months, after 12 months, and after 24 months, we found that there was no significant difference between the two groups in systolic blood pressure, diastolic blood pressure, serum potassium levels, and hormone levels. 51 patients chose to have surgery, of which 41 patients chose RLA and 10 patients chose RARLA. RARLA group patients had the highest total cost and conservative treatment group patients had the lowest cost, and the difference was significant ($P < 0.001$). There was no significant difference in tumor size in the conservative treatment group between at the time of diagnosis and after 24 months ($P = 0.305$).

Conclusion: Surgical treatment is more effective for 1-3cm NFAI, but conservative treatment is safer and more economical. Follow-up after conservative or surgical treatment is necessary.

KEYWORDS

nonfunctional adrenal incidentaloma, conservative treatment, surgery, efficacy, safety

1 Introduction

Adrenal incidentaloma (AI) refers to the adrenal tumor whose diameter ≥ 1cm is accidentally found by imaging examination during physical examination or diagnosis and treatment of other non-adrenal diseases (1, 2). AI is a common disease, accounting for 8.7% of the autopsy population (3). And as people aged, the incidence in the elderly population increased to 10% (4). Approximately 80% of AI are benign and have no endocrine function, while 20% are malignant and have endocrine function (5). Nonfunctional adrenal incidentaloma (NFAI) is adrenal tumor that has no endocrine function at the time of diagnosis, accounting for roughly 75% of all AI (5). Almost all patients with NFAI have no symptoms, but one study found a 41% long-term incidence of hypertension in patients with NFAI (6). Due to the fact that NFAI is mostly benign, and considering the trauma and risk of surgery, a basic consensus in the past has been to recommend conservative treatment for tumors between 1 and 3cm with no endocrine function (1, 7). However, with the development of minimally invasive concept and the progress of surgical technology and equipment, the trauma and risk of surgery gradually decreased (8, 9). Doctors and patients are becoming increasingly concerned about the tumor's malignant potential, the potential for hormone secretion, and the potential close relationship with hypertension. Patients with small adrenal tumors discovered in an outpatient clinic are increasingly requesting or being recommended surgical treatment. However, for these small NFAI, conservative treatment or surgical treatment is still being discussed by endocrinologists and urologists.

In order to compare the efficacy and safety of conservative treatment and surgical treatment for these patients with small NFAI, we carried out this study. We hope to provide new data for the treatment of these patients through this study.

2 Materials and methods

2.1 Data source and ethics statement

Our prospectively maintained database was retrospectively scrutinized to acquire details regarding the baseline demographic and clinical information after obtaining the approval of the institutional review board and ethics committee of the First Affiliated Hospital of Nanchang University.

2.2 Patient selection

The patients with small (1-3cm) NFAI who received conservative treatment or surgery in our hospital from November 2018 to December 2019 were retrospectively collected. The patients were included in this analysis according to the following inclusion criteria: [1] Patients diagnosed as adrenal tumor; [2] The tumor size was 1-3 cm; [3] Unilateral tumor; [4] At the initial diagnosis, the serum potassium was between 3.5-5.5 mmol/L; [5] the levels of aldosterone, cortisol and VMA were within the normal range. The exclusion criteria were as follows: [1] During hospitalization, other operations other than adrenalectomy were performed; [2] systolic blood pressure exceeded 140 mmHg at initial diagnosis; [3] diastolic blood pressure exceeded 90 mmHg at initial diagnosis; [4] accompanied by other serious complications.

2.3 Technical considerations

Patients in the conservative treatment group did not receive any medical or lifestyle interventions. All the patients in the surgery group were operated by the same medical team, and the surgical methods were divided into retroperitoneal laparoscopic adrenalectomy (RLA) and robot assisted laparoscopic adrenalectomy (RARLA) according to the characteristics of the tumor. All patients underwent follow-up examinations at 3, 6, 12 and 24 months after diagnosis or surgery. All patients were asked to sign an informed consent form.

2.4 Variables and endpoints

Variables in the study include demographic characteristics (age, sex, body mass index (BMI)), serum potassium level, blood pressure level, hormone level (aldosterone, cortisol, Urine Vanilla Amygdalic Acid (VMA)), tumor characteristics (tumor size, tumor site), treatment methods (surgical treatment, waiting for observation), and other variables (total cost).

The primary end points of this study were to compare the average differences in tumor size, blood pressure and hormone levels between the surgery group and the conservative treatment group at the time of diagnosis, after 3 months, after 6 months, after 12 months, and after 24 months. The secondary endpoint was the total cost of the two groups, which was defined as the cost of hospitalization and outpatient services.

2.5 Statistical analysis

Means and standard deviations were determined for the normally distributed continuous variables, while those with nonnormal distribution were presented as median and interquartile range. Categorical variables were presented as frequencies and their proportions. The Student's t-test was performed for the normally distributed continuous variables. The Mann-Whitney test was employed to analyze VMA between the surgery group and the conservative treatment group. Analysis of variance was used to compare the total cost among conservative treatment, Retroperitoneal laparoscopic adrenalectomy (RLA) and Robot assisted laparoscopic adrenalectomy (RARLA) groups. All categorical variables were compared with the Chi square test. SPSS 26.0 (IBM Corp, Armonk, NY) was utilized for all statistical analysis with a two-sided p value < 0.05 denoting statistical significance.

3 Results

According to the inclusion and exclusion criteria, 81 patients were included in this study from November 2018 to December 2019. Thirty-two patients with unilateral nonfunctioning adrenal

10.3389/fendo.2023.1119251

incidentaloma chose conservative treatment, while 51 patients chose to undergo surgery, of which 41 patients chose RLA, and 10 patients chose RARLA. There was no significant difference in baseline characteristics between the two groups (Table 1).

By comparing the average difference between the two groups of patients at the time of diagnosis, after 3 months, after 6 months, after 12 months, and after 24 months, we found that there was no significant difference between the two groups in systolic blood pressure, diastolic blood pressure, serum potassium levels, and hormone levels (Table 2). After 24 months, only 2 (3.9%) patients in the surgery group had an increase in aldosterone, while the conservative treatment group was 3 (9.4%). However, 2 (3.9%) patients in the surgery group had increased cortisol, compared with 4 (12.5%) in the conservative treatment group.

51 patients chose to have surgery, of which 41 patients chose RLA and 10 patients chose RARLA. We compared the total cost of conservative treatment, RLA and RARLA groups and found that RARLA groups patients had the highest total cost and conservative treatment groups patients had the lowest cost, and the difference was significant ($P < 0.001$) (Figure 1). There was no significant difference in tumor size in the conservative treatment group between at the time of diagnosis and after 24 months ($P = 0.305$) (Figure 2).

4 Discussion

Physical examination has become a service item accepted by an increasing number of people as people pay more attention to their health. The growing popularity of physical examinations, as well as the accompanying increase in imaging, is a major reason for the rising incidence of adrenal incidentaloma (AI) year after year (10). Nonfunctional adrenal incidentaloma (NFAI) are adrenal tumors that have no endocrine function at the time of diagnosis, accounting for roughly 75% of all adrenal incidentaloma (5).

TABLE 1 Baseline demographical and clinicopathological characteristics of patients.

Variables	Adrenalectomy (n=51)	Watchful Waiting (n=32)	*P*
Age, year, mean (SD)	49.3(10.6)	49.6(11.1)	0.912
Gender, n (%)			0.790
Male	19(37.3%)	11(34.4%)	
Female	32(62.7%)	21(65.6%)	
BMI, kg/m^2, mean (SD)	23.9(3.1)	24.8(3.1)	0.221
Tumor size, cm, mean (SD)	2.1(0.5)	2.0(0.5)	0.237
Tumor site, n (%)			0.849
Left	25(49.0%)	15(46.9%)	
Right	26(51.0%)	17 (53.1%)	

SD, standard deviation; BMI, body mass index.

TABLE 2 Comparison of follow-up results of adrenalectomy group and watchful waiting group.

Variables	Adrenalectomy (n=51)	Watchful Waiting (n=32)	*P*
Systolic pressure, mmHg, mean (SD)			
At diagnosis	119.63(12.92)	118.53(14.85)	0.723
After 3 months	114.80(10.90)	114.34(9.23)	0.835
After 6 months	118.57(8.50)	117.00(7.50)	0.395
After 12 months	121.10(5.26)	120.88(4.09)	0.839
After 24 months	122.12(7.30)	122.06(9.66)	0.976
Diastolic pressure, mmHg, mean (SD)			
At diagnosis	78.51(10.53)	77.47(12.19)	0.681
After 3 months	72.29(6.06)	72.47(5.35)	0.894
After 6 months	76.90(6.90)	75.94(5.60)	0.508
After 12 months	76.16(4.97)	75.31(4.93)	0.452
After 24 months	75.39(10.96)	77.88(7.69)	0.230
Serum potassium, mmol/L, mean (SD)			
At diagnosis	3.88(0.25)	3.94(0.31)	0.301
After 3 months	3.81(0.25)	3.77(0.21)	0.509
After 6 months	3.94(0.34)	3.94(0.41)	0.978
After 12 months	4.21(0.28)	4.16(0.24)	0.462
After 24 months	4.36(0.37)	4.22(0.48)	0.160
Increased aldosterone, n (%)			
At diagnosis	0	0	–
After 3 months	0	0	–
After 6 months	0	1(3.1%)	0.386
After 12 months	0	3(9.4%)	0.105
After 24 months	2(3.9%)	3(9.4%)	0.588
Increased cortisol, n (%)			
At diagnosis	0	0	–
After 3 months	0	0	–
After 6 months	0	2(6.3%)	0.146

(Continued)

10.3389/fendo.2023.1119251

TABLE 2 Continued

Variables	Adrenalectomy (n=51)	Watchful Waiting (n=32)	*P*
After 12 months	2(3.9%)	3(9.4%)	0.588
After 24 months	2(3.9%)	4(12.5%)	0.301
VMA, mg, median (25th–75th percentile)			
At diagnosis	9.04(6.83-12.82)	7.37(3.78-11.11)	0.064
After 3 months	8.90(6.52-11.39)	7.08(3.90-11.36)	0.086
After 6 months	7.79(6.70-9.62)	6.75(5.97-9.96)	0.091
After 12 months	7.25(5.45-9.47)	6.54(4.72-9.62)	0.405
After 24 months	8.50(4.24-12.21)	9.45(6.60-11.76)	0.446

SD, standard deviation; VMA, Urine Vanilla Amygdalic Acid.

Although most NFAI are benign and non-functional, with no obvious clinical symptoms, it has become an important disease affecting human health, attracting the long-term attention of endocrinologists and urologists due to its relatively high incidence in the population and the potential for malignant lesions (3, 4, 11). Endocrinologists and urologists share the goal of finding an effective, safe, and cost-effective treatment.

Previously, the general consensus was to surgically resect NFAI larger than 3cm and to treat tumors smaller than 3cm conservatively (7). Of course, as with other types of tumors, size is not the sole determinant of treatment. Another general agreement is that when a NFAI becomes functional or significantly grows in size during conservative treatment, surgical treatment is a better option than conservative treatment (10, 12).

However, as research on NFAI progresses, its potential impact on people's health becomes clearer. NFAI, on the one hand, are thought to be risk factors for cardiovascular disease. Tuna (13) compared the prevalence of hypertension in the general population to patients with NFAI in one study. The study's findings revealed that the incidence of hypertension in patients with NFAI was significantly higher than in the general population. Furthermore, Cansu and his colleagues revealed in a paper that NFAI can increase patients' cardiovascular risk, and that this effect may be related to carotid intima media thickness (CIMT), pulse wave velocity (PWV), augmentation index (AIx) (14). This viewpoint was supported by Emral's research (15). NFAI, on the other hand, are thought to be closely related to metabolic disorders. Ribeiro Cavalari (16) compared the prevalence of metabolic syndrome in NFAI to that of the general population in one study. The incidence of NFAI was 69.2% versus 31.0% in the general population, indicating a significant difference between the two. In another study, patients with NFAI were found to have a higher risk of insulin resistance and diabetes (17). Furthermore, NFAI can

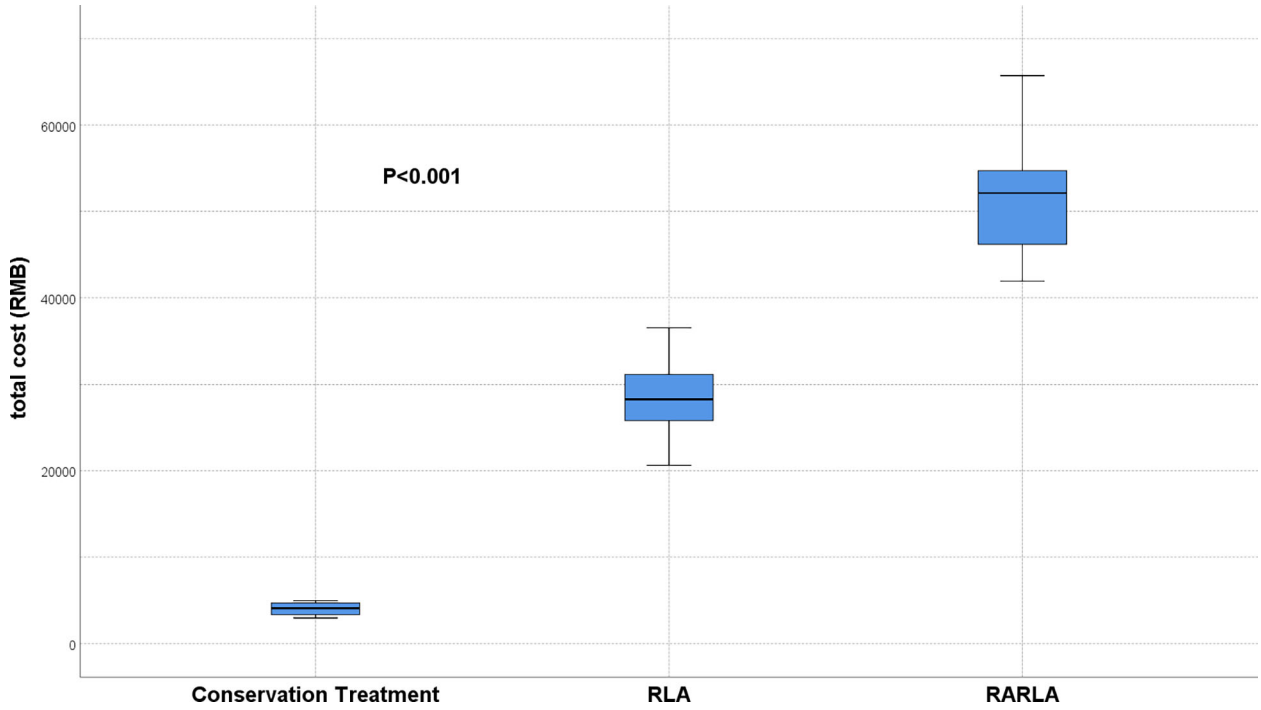

FIGURE 1
Comparison of total costs in the conservative treatment, LPA and RALPA groups. The total costs of conservative treatment was the least, while RALPA was the most.

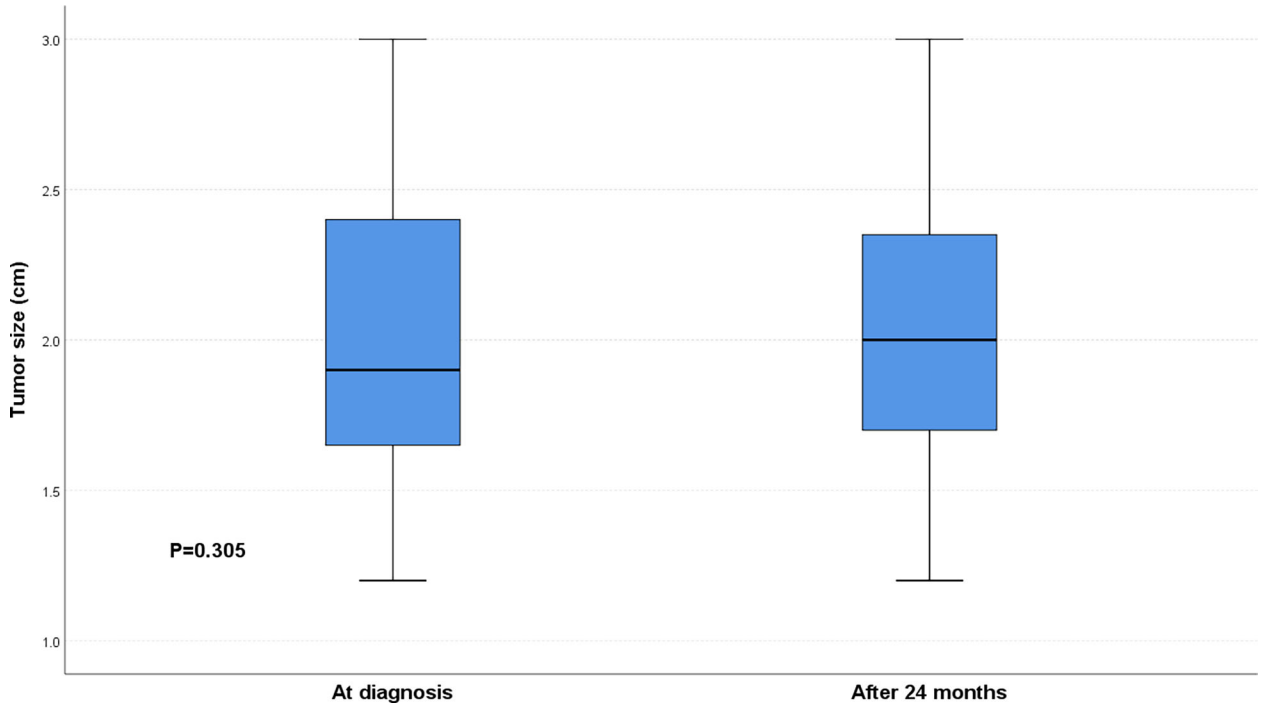

FIGURE 2
Comparison of tumor size at diagnosis and 24 months later in the conservative treatment group. Within 24 months, patients in the conservative treatment group showed no significant tumor growth.

cause a decrease in serum adiponectin levels as well as an (17) increase in blood lipid levels, affecting bone metabolism (18) and the appearance of periodontal disease (19).

According to the above studies, even if the NFAI does not have significant cortisol and aldosterone overproduction, it can still have a negative impact on our health in a variety of ways. This appears to imply that early surgical treatment for patients with NFAI can prevent further damage. Our findings appear to support this viewpoint, with increased aldosterone and cortisol occurring in 3.9% of the surgery group after 2 years, compared to 9.4% and 12.5% in the conservative group, respectively. Although our findings did not indicate hypertension in the conservative treatment group, this could be due to the shorter follow-up period.

Safety and cost are also important considerations in treatment selection. Conservative treatment for small NFAI was previously recommended because it was safer and less expensive than surgery. However, with the introduction of laparoscopic (8) and Da Vinci surgical robots (9), the risk of surgery has decreased significantly. That is one of the reasons why an increasing number of patients are undergoing surgery. Of course, the risk of surgery remains higher than the risk of conservative treatment; after all, surgery is a traumatic procedure. Our findings show that conservative treatment is more cost-effective, whereas patients undergoing robot-assisted abdominal surgery as part of the surgical approach face greater financial strain.

In conclusion, for patients with 1-3cm NFAI, surgical treatment is more appropriate in terms of therapeutic effect. Conservative treatment may be an option if safety or economic factors are taken into account; after all, as our study demonstrated, conservative treatment did not significantly increase the size of the tumor within two years.

5 Conclusions

Surgical treatment is more effective for 1-3cm NFAI, but conservative treatment is safer and more economical. Follow-up after conservative or surgical treatment is necessary.

Data availability statement

The original contributions presented in the study are included in the article/Supplementary Material. Further inquiries can be directed to the corresponding authors.

Ethics statement

The studies involving human participants were reviewed and approved by the Ethical Committee of The First Affiliated Hospital of Nanchang University. The patients/participants provided their written informed consent to participate in this study.

Author contributions

Conception and design: GW and XCZ. Surgeons: GW and XCZ. Acquisition of data: SX and XPZ. Preparation of tools: YY and CZ. Analysis and interpretation of data: XL and XPZ. Drafting of the

manuscript and statistical analysis: XL and SX. Critical revision: GW and HX. Obtaining funding: XCZ and HX. All authors contributed to the article and approved the submitted version.

Funding

Key Research and Development Program of Jiangxi Province (20171ACB20029 to XZ). Applied Research and Cultivation Program of Jiangxi Province (20212BAG70001 to HX).

Acknowledgments

Thanks to HX and GW for providing suggestions for the writing of the article.

Conflict of interest

The authors declare that the research was conducted in the absence of any commercial or financial relationships that could be construed as a potential conflict of interest.

Publisher's note

References

1. Fassnacht M, Arlt W, Bancos I, Dralle H, Newell-Price J, Sahdev A, et al. Management of adrenal incidentalomas: European society of endocrinology clinical practice guideline in collaboration with the European network for the study of adrenal tumors. *Eur J Endocrinol* (2016) 175(2):G1–g34. doi: 10.1530/EJE-16-0467

2. Suradi HH, Amarin JZ, Zayed AA. Adrenal incidentaloma. *N Engl J Med* (2021) 385 (8):768. doi: 10.1056/NEJMc2108550

3. Brunt LM. Sages guidelines for minimally invasive treatment of adrenal pathology. *Surg Endosc* (2013) 27(11):3957–9. doi: 10.1007/s00464-013-3168-0

4. Podbregar A, Janez A, Goricar K, Jensterle M. The prevalence and characteristics of non-functioning and autonomous cortisol secreting adrenal incidentaloma after patients' stratification by body mass index and age. *BMC Endocr Disord* (2020) 20(1):118. doi: 10.1186/s12902-020-00599-0

5. Bernardi S, Calabrò V, Cavallaro M, Lovriha S, Eramo R, Fabris B, et al. Is the adrenal incidentaloma functionally active? an approach-To-The-Patient-Based review. *J Clin Med* (2022) 11(14):4064. doi: 10.3390/jcm11144064

6. Graham DJ, Mchenry CR. The adrenal incidentaloma: guidelines for evaluation and recommendations for management. *Surg Oncol Clin N Am* (1998) 7(4):749–64. doi: 10.1016/S1055-3207(18)30243-6

7. Cambos S, Tabarin A. Management of adrenal incidentalomas: Working through uncertainty. *Best Pract Res Clin Endocrinol Metab* (2020) 34(3):101427. doi: 10.1016/j.beem.2020.101427

8. Baba S, Iwamura M. Retroperitoneal laparoscopic adrenalectomy. *BioMed Pharmacother* (2002) 56(Suppl 1):113s–9s. doi: 10.1016/s0753-3322(02)00225-1

9. Ye C, Yang Y, Guo F, Wang F, Zhang C, Yang B, et al. Robotic enucleation of adrenal masses: technique and outcomes. *World J Urol* (2020) 38(4):853–8. doi: 10.1007/s00345-019-02868-7

10. Jason DS, Oltmann SC. Evaluation of an adrenal incidentaloma. *Surg Clin North Am* (2019) 99(4):721–9. doi: 10.1016/j.suc.2019.04.009

11. Müller A, Ingargiola E, Solitro F, Bollito E, Puglisi S, Terzolo M, et al. May an adrenal incidentaloma change its nature? *J Endocrinol Invest* (2020) 43(9):1301–7. doi: 10.1007/s40618-020-01219-3

12. Kebebew E. Adrenal incidentaloma. *N Engl J Med* (2021) 384(16):1542–51. doi: 10.1056/NEJMcp2031112

13. Tuna MM, Imga NN, Doğan BA, Yılmaz FM, Topçuoğlu C, Akbaba G, et al. Non-functioning adrenal incidentalomas are associated with higher hypertension prevalence and higher risk of atherosclerosis. *J Endocrinol Invest* (2014) 37(8):765–8. doi: 10.1007/s40618-014-0106-5

14. Cansu GB, SARI R, Yilmaz N, Özdem S, Çubuk M. Markers of subclinical cardiovascular disease in nonfunctional adrenal incidentaloma patients without traditional cardiovascular risk factors. *Exp Clin Endocrinol Diabetes* (2017) 125(1):57–63. doi: 10.1055/s-0042-109866

15. Emral R, Aydoğan B, Köse AD, Demir Ö, Çorapçıoğlu D. Could a nonfunctional adrenal incidentaloma be a risk factor for increased carotid intima-media thickness and metabolic syndrome. *Endocrinol Diabetes Nutr (Engl Ed)* (2019) 66(7):402–9. doi: 10.1016/j.endinu.2019.01.007

16. Ribeiro Cavalari EM, De Paula MP, Arruda M, Carraro N, Martins A, de Souza K, et al. Nonfunctioning adrenal incidentaloma: A novel predictive factor for metabolic syndrome. *Clin Endocrinol (Oxf)* (2018) 89(5):586–95. doi: 10.1111/cen.13822

17. Akkus G, Evran M, Sert M, Tetiker T. Adipocytokines in non-functional adrenal incidentalomas and relation with insulin resistance parameters. *Endocr Metab Immune Disord Drug Targets* (2019) 19(3):326–32. doi: 10.2174/1871530318666181009112042

18. Francucci CM, Caudarella R, Rilli S, Fiscaletti P, Ceccoli L, Boscaro M. Adrenal incidentaloma: effects on bone metabolism. *J Endocrinol Invest* (2008) 31(7 Suppl):48–52.

19. Rodrigues MO, Moraes AB, De Paula MP, Pereira VA, Leão ATT, Vieira Neto L. Adrenal incidentaloma as a novel independent predictive factor for periodontitis. *Endocrinol Invest* (2021) 44(11):2455–63. doi: 10.1007/s40618-021-01557-w

frontiers | Frontiers in Endocrinology

TYPE Systematic Review
PUBLISHED 03 February 2023
DOI 10.3389/fendo.2023.1111277

OPEN ACCESS

EDITED BY
Yuxuan Song,
Peking University People's Hospital, China

REVIEWED BY
Donghui Jin,
Chinese Academy of Medical Sciences and Peking Union Medical College, China
Yahang Liang,
The First Affiliated Hospital of Nanchang University, China

*CORRESPONDENCE
Baoluo Ma
zkc7312976@163.com

†These authors have contributed equally to this work and share first authorship

This article was submitted to Reproduction, a section of the journal Frontiers in Endocrinology

SPECIALTY SECTION
RECEIVED 29 November 2022
ACCEPTED 06 January 2023
PUBLISHED 03 February 2023

CITATION
Zhou K, Li C, Chen T, Zhang X and Ma B (2023) C-reactive protein levels could be a prognosis predictor of prostate cancer: A meta-analysis.
Front. Endocrinol. 14:1111277.
doi: 10.3389/fendo.2023.1111277

C-reactive protein levels could be a prognosis predictor of prostate cancer: A meta-analysis

Kechong Zhou[1†], Chao Li[2†], Tao Chen[1], Xuejun Zhang[1] and Baoluo Ma[1*]

[1]Department of Urology, Xiangyang Central Hospital, Affiliated Hospital of Hubei University of Arts and Science, Xiangyang, Hubei, China, [2]Department of Orthopedics, Xiangyang Central Hospital, Affiliated Hospital of Hubei University of Arts and Science, Xiangyang, Hubei, China

Background: The relationship between the C-reactive protein (CRP) and prognosis in prostate cancer (PCa) has been widely discussed over the past few years but remains controversial.

Material and methods: In our meta-analysis, we searched 16 reliable studies in the PubMed, Embase, and Cochrane Library databases. Otherwise, we have successfully registered on the INPLASY. We also performed random- and fixed-effects models to evaluate the hazard ratio (HR) and 95% confidence interval (CI), respectively.

Result: The result of our meta-analysis shows that elevated CRP levels were related to worse overall survival (OS) (HR = 1.752, 95% CI = 1.304–2.355, p = 0.000), cancer-specific survival (CSS) (HR =1.823, 95%CI = 1.19-2.793, P = 0.006), and progression-free survival (PFS) (HR = 1.663, 95% CI = 1.064–2.6, p = 0.026) of PCa patients. There was significant heterogeneity, so we performed a subgroup analysis according to the staging of the disease and found the same result. Furthermore, the heterogeneity was also reduced, and no statistical significance.

Conclusion: Our study shows that the level of CRP could reflect the prognosis of prostate cancer patients. We find that PCa patients with high levels of CRP often have worse OS, CSS, and PFS, although the stages of the patients' disease are different. More studies are needed to verify this idea.

KEYWORDS

meta-analysis, C-reactive protein, prostate cancer, prognosis, survival, crp

1 Introduction

Prostate cancer (PCa) is one of the most common cancers, with a mortality rate that is among the top five worldwide. Moreover, it is the second most frequently diagnosed cancer among men (1). Most PCa patients are diagnosed when the disease is only localized, which means that many patients could be curable if the disease is detected in the early stages. In

contrast, approximately 30% of patients will have cancer recurrence. Therefore, it is important to find more accurate prognoses and predictive markers for the treatment of PCa.

Before that, many indicators have been shown to be closely related to the prognosis of prostate cancer. For example, Gleason score, metastases, pain phosphatase, alkaline, and albumin were prognostic factors for several survival indicators of PCa (2–5). Moreover, systemic inflammation was discussed as a predictive factor for the survival of PCa patients in some studies (6). Some studies also showed that anti-inflammatory drugs had a protective effect on PCa patients (7).

C-reactive protein (CRP) is mainly produced by the liver as a typical acute-phase protein, which is one of the most common markers of systemic inflammation and is routinely measured (8). The elevation of CRP level was discussed as a prognostic indicator for many cancers, such as lung cancer, breast cancer, and colorectal cancer (9). It is also associated with the prognosis of urological cancers such as renal cell carcinoma (10, 11).

In the past few years, the relationship between CRP levels and the prognosis of prostate cancer patients remains controversial. Some studies suggested that PCa patients with elevated CRP levels often had worse survival (12, 13). Some other studies had different views and believed that there was no significant correlation between the CRP level and the prognosis of prostate cancer patients (14–16). The results of these studies were different, and due to their small sample size, the results were not very reliable. Therefore, we performed this meta-analysis by summarizing all credible articles to explore the relationship between C-reactive protein levels and prognosis in prostate cancer. Then, subgroup analysis was performed by staging the disease.

2 Materials and methods

2.1 Search strategy

We independently and systematically searched the Embase, PubMed, and Cochrane Library databases, and assessed the relationship between C-reactive protein levels and survival of prostate cancer patients up to October 2019. We used the following search terms: “Prostate Cancer”, “PCa”, “CRP”, and “C reactive protein”. Otherwise, we have successfully registered on the INPLASY, and our registration number was “INPALSY202060061”. There was no restriction on the type of study or the sample size.

2.2 Inclusion and exclusion criteria

Those who met the following conditions were eligible for inclusion in this study: 1) the studies discussed the relationship between CRP and the prognosis in PCa patients; 2) the study design was prospective, randomized controlled trials (RCTs) or retrospective studies; 3) contain data on hazard ratio (HR) and 95% confidence interval (CI) or include the survival curves of CRP in PCa patients. Studies were excluded based on the following criteria: 1) data cannot be obtained even after contacting the author; 2) the type of study was abstract, review, and comment; 3) duplicate studies.

2.3 Data abstraction

We gathered the following information for inclusion in the study by carefully reading and sifting through the retrieved titles and abstracts: 1) the basic characteristics of the study including the family name of the lead author, time of publication, nationality of patients, size of the sample, age, and staging of the disease; 2) time of follow-up, CRP cutoff values, and median follow-up; 3) HR, p-value, and 95% CIs of elevated CRP for all prognostic indicators, such as overall survival (OS), disease-specific survival (DSS), cancer-specific survival (CSS), recurrence-free survival (RFS), progression-free survival (PFS), and disease-free survival (DFS). It was worth mentioning that we have combined some similar prognostic indicators to make the study feasible. For example, CSS and DSS were considered to be CSS; PFS, RFS, and DFS were considered to be PFS. In order to ensure the effectiveness of the results, all results we have extracted were from multivariate analysis. When there was no exact HR reported, we extracted the data from its survival curve and calculated HR. We used the Newcastle–Ottawa Scale (NOS) to evaluate the quality of all included articles (17), and we also evaluated the selection, exposure, and comparability of these studies.

2.4 Statistical analysis

All statistical analyses were performed using Stata 12.0 software. Egger’s test and Begg’s funnel plot were used to assess the publication bias (18). The HR and 95% CIs were calculated to evaluate the correlation between C-reactive protein levels and the survival of PCa patients. We checked the heterogeneity among the included studies by using the chi-square test, and when $p < 0.05$, we considered the result significant. The higher the value of I^2, the higher the heterogeneity. We recognized that there was no significant heterogeneity when $I^2 <$ 50%. The fixed-effects model (Mantel–Haenszel method) was adopted when no significant heterogeneity was detected ($p > 0.05$ and $I^2 <$ 50%) (19). Otherwise, the random-effects model (DerSimonian and Laird method) was used (20). We also performed subgroup analyses when patients had different stages.

3 Results

3.1 Data retrieval

A total of 639 potentially relevant studies were identified from the aforementioned databases. As shown in Figure 1, the full text of 73 studies on the association between C-reactive protein levels and prognosis in prostate cancer was retrieved after screening the titles. A total of 57 studies were excluded after screening the abstract: 23 were about the association between C-reactive protein levels and the risk of prostate cancer; 14 were reviews; 5 were comments and

10.3389/fendo.2023.1111277

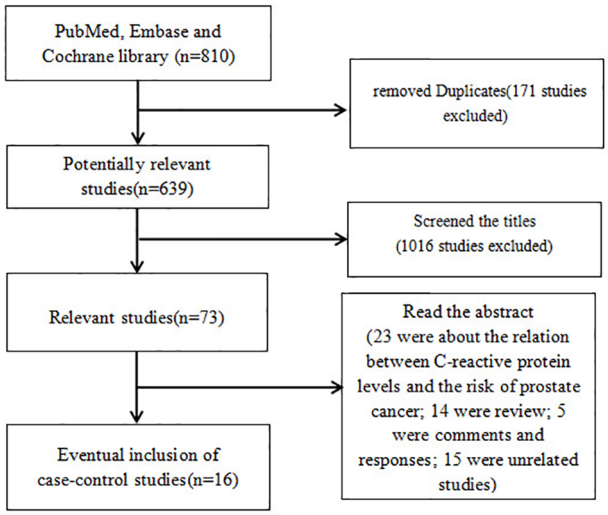

FIGURE 1
Flowchart illustrating the search strategy for CRP and prognosis in prostate cancer. CRP, C-reactive protein.

responses; 15 were unrelated studies. Finally, 16 studies were pooled in the final meta-analysis, which contained 13,555 PCa patients.

3.2 Study characteristics

The main features of all included studies are presented in Table 1. The patients were from the United Kingdom, Russia, Japan, Canada, Austria, Sweden, China, and the United States. The research population was also different: five were metastatic prostate cancer (mPCa) patients, four were localized PCa patients, and the remaining were not clearly stated. Otherwise, CRP values were analyzed by different techniques in each study that we included. A total of 12 studies used a dichotomous variable to analyze CRP with different cutoff values. Only one study dealt with trichotomous variables and compared the survival between the highest tertile and the lowest tertile. CRP was considered a continuous variable in the remaining three studies, in which HR was calculated as a unit change on a log scale. All studies showed the values of HR and confidence interval (Table 2). Significantly,

TABLE 1 Main characters of studies included in this meta-analysis.

First author	Year	Country	Sample size	Age	Treatment	Cutoff (mg/L)	Median follow-up
McArdle PA	2006	UK	62	NR	NR	10	62 m
Beer TM	2008	USA and Canada	160	68.0 (45–92)	Endocrine	8	NR
Nakashima J	2008	Japan	126	NR	NR	1.5	39.7 m (1–144)
Stark JR	2009	USA	601	68.6	NR	1.7	NR
McArdle PA	2010	UK	98	NR	NR	3.10	10 y
McArdle PA	2010	UK	98	NR	NR	3.10	10 y
Ito M	2011	Japan	80	NR	Docetaxel	5	9.4 m (1–31)
McCall P	2012	UK	61	70 (63–75)	NR	IHC	8.4 y (5.7–11)
Pond GR	2012	Russia and USA	110	NR	Docetaxel–prednisone	Log	18
Pond GR	2012	Russia and USA	110	NR	Docetaxel–prednisone	Log	18
Prins RC	2012	USA	119	71.9 (45.8–91.5)	NR	Log	19.7 m (0.9–98.5)
Hall WA	2013	USA	54	45–74	RP	Log	NR
Hall WA	2013	USA	152	43–83	RT	Log	NR
Matsuyama H	2014	Japan	279	71 (48–91)	Docetaxel	3.2	94 m (81–101)
Thurner E	2015	Austria	261	67.9	NR	8.6	80 m (76.3–83.7)
Thurner E	2015	Austria	261	67.9	NR	8.6	80 m (76.3–83.7)
Thurner E	2015	Austria	261	67.9	NR	8.6	80 m (76.3–83.7)
Xu LY	2015	China	135	NR	NR	10	NR
Liao SG	2016	China	115	74.8	NR	8	NR
Liao SG	2016	China	115	74.8	NR	8	NR
Sevcenco S	2016	European and American	7,205	61 (57–66)	NR	5	27 m (19–48)
Aryhur R	2018	Swedish	779	NR	NR	10	NR
Aryhur R	2018	Swedish	1,741	NR	NR	10	NR

RP, radical prostatectomy; RT, radiotherapy; IHC, immunohistochemistry; m, months; y, years; NR, not reported.

TABLE 2 Main data of studies included in this meta-analysis.

First author	Year	Disease	Survival analysis	Multivariate analysis	*p*
				HR (95% CI)	
McArdle PA	2006	mPCa	CSS	1.97 (0.99–3.92)	0.052
Beer TM	2008	mAIPCa	OS	1.405 (1.199–1.647)	<0.0001
Nakashima J	2008	mPCa	DSS	1.884 (1.028–3.454)	0.0404
Stark JR	2009	PCa	CSS	1.48 (0.83–2.66)	0.08
McArdle PA	2010	Localized PCa	OS	1.60 (1.03–2.47)	0.036
McArdle PA	2010	Localized PCa	CSS	1.88 (1.01–3.52)	0.048
Ito M	2011	CRPCa	OS	1.95 (1.33–2.96)	<0.001
McCall P	2012	Hormone-naive advanced prostate cancer	DSS	4.3 (1.5–12.4)	0.009
Pond GR	2012	mCRPCa	OS	1.38 (1.12–1.70)	0.003
Pond GR	2012	mCRPCa	PFS	1.44 (1.17–1.77)	< 0.001
Prins RC	2012	CRPCa	OS	1.106 (1.022–1.197)	0.013
Hall WA	2013	Localized PCa	RFS	1.48 (0.68–3.21)	0.325
Hall WA	2013	Localized PCa	RFS	2.03 (1.19–3.47)	0.009
Matsuyama H	2014	CRPCa	OS	1.94 (1.08–3.55)	0.0268
Thurner E	2015	Localized PCa	OS	3.24 (1.84–5.71)	<0.001
Thurner E	2015	Localized PCa	CSS	4.31 (1.22–15.1)	0.023
Thurner E	2015	Localized PCa	DFS	2.07 (1.02–4.17)	0.043
Xu LY	2015	mPCa	OS	2.39 (1.56–3.69)	<0.001
Liao SG	2016	CRPCa	OS	2.003 (1.285–3.121)	0.002
Liao SG	2016	CRPCa	PFS	2.184 (1.401–3.403)	0.001
Sevcenco S	2016	Localized PCa	RFS	1.23 (1.04–1.45)	NR
Aryhur R	2018	PCa	CSS	1.00 (0.92–1.10)	NR
Aryhur R	2018	PCa	OS	0.97 (0.89–1.06)	NR

HR, hazard ratio; CI, credibility interval; mPCa, metastatic prostate cancer; mAIPCa, metastatic androgen-independent prostate cancer; PCa, prostate cancer; CRPCa, castration-resistant prostate cancer; OS, overall survival; CSS, cancer-specific survival; DSS, disease-specific survival; PFS, progression free survival; RFS, recurrence-free survival; DFS, disease free survival; NR, not report.

all data with multivariate analysis were collected to ensure the credibility of the results.

3.3 Meta-analysis

By analyzing all studies, we found that there was a significant correlation between C-reactive protein levels and prognosis in PCa patients (Figures 2, 3). According to the high heterogeneity (I^2 > 50%), the random-effects model was carried out to calculate the pooled HR and their 95% CI. Otherwise, the subgroup analyses were also performed as follows to reduce heterogeneity.

3.3.1 Overall survival

For OS, there was significant heterogeneity between studies of categorized CRP (I^2 = 0.888, p = 0.000), and log CRP (I^2 = 0.725, p = 0.057) has no significant heterogeneity. Elevated serum CRP level was significantly associated with the OS of PCa for categorized data (HR = 1.752, 95% CI = 1.304–2.355, p = 0.000) and log CRP (HR = 1.142, 95% CI = 1.059–1.232, p = 0.001) (Figures 2, 3).

3.3.2 Cancer-specific survival

For CSS, seven studies discussed the association between the high CRP level and worse CSS for categorized CRP, and the pooled HR was 1.823 (95% CI = 1.19–2.793, p = 0.006). There was also significant heterogeneity (I^2 = 0.752, p = 0.000). Only one study discussed log CRP (Figures 2, 3).

3.3.3 Progression-free survival

For PFS, there was also a significant association between the high CRP level and worse PFS for categorized CRP (HR = 1.663, 95% CI = 1.064–2.6, p = 0.026) and log CRP (HR = 1.504, 95% CI = 1.247–1.814, p = 0.000). Some heterogeneity was also found for categorized CRP (I^2 = 0.718, p = 0.029) (Figures 2, 3).

In summary, a high CRP level was proved to be associated with a worse OS, CSS, and PFS, which meant that serum CRP level could be a prognostic biomarker for the survival of PCa patients. However, there was also significant heterogeneity between the studies that we included. Therefore, we performed a subgroup analysis by the staging of the disease to find the sources of heterogeneity.

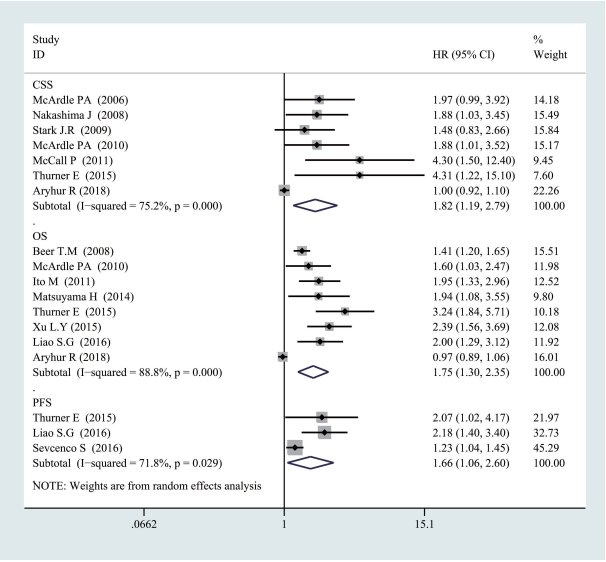

FIGURE 2
Forest plot of categorized CRP and prognosis in prostate cancer from random-effects analysis. CRP, C-reactive protein.

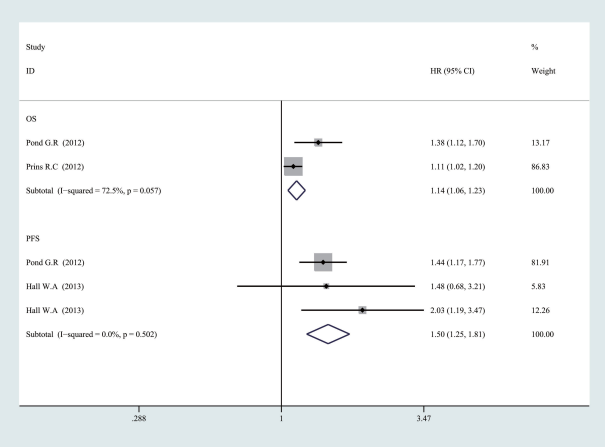

FIGURE 3
Forest plot of log CRP and prognosis in prostate cancer from fixed-effects analysis. CRP, C-reactive protein.

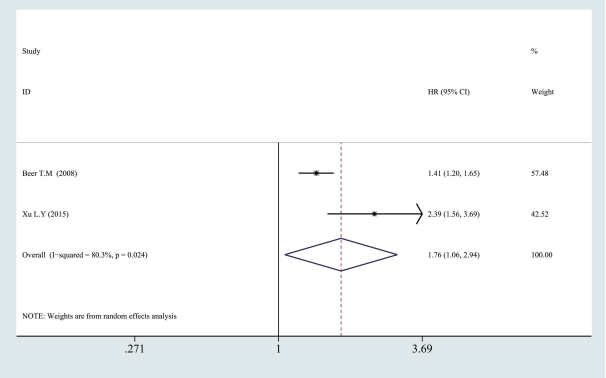

FIGURE 4
Relationship between categorized CRP and prognosis in mPCa. CRP, C-reactive protein; mPCa, metastatic prostate cancer.

3.3.4 Relationship between high CRP level and prognosis in mPCa

In the subgroup analysis, we also found a significant association between high CRP levels and worse OS in mPCa by pooled HR of two studies (HR = 1.765, 95% CI = 1.058–2.943, $p = 0.029$) (Figure 4).

3.3.5 Relationship between high CRP level and prognosis in localized PCa

As shown in Figure 5, a significant association also could be observed between elevated CRP levels and worse OS (HR = 2.083, 95% CI = 1.473–2.944, $p = 0.000$, $I^2 = 0.732$, $p = 0.053$), CSS (HR = 2.215, 95% CI = 1.266–3.874, $p = 0.005$, $I^2 = 0.000$, $p = 0.95$), and PFS (HR = 2.137, 95% CI = 1.839–2.484, $p = 0.000$, $I^2 = 0.254$, $p = 0.247$) in localized PCa for categorized CRP. Significantly, all heterogeneity between included studies was reduced, and there was no significant heterogeneity between studies on localized PCa ($p > 0.05$, $I^2 < 50\%$). It indicated that the staging of the disease was likely to be the source of heterogeneity.

3.4 Publication bias

As shown in Figure 6, we also used Egger's test and Begg's funnel plot to evaluate the publication bias. The results showed that there was no publication bias because of the symmetric shapes of all models ($p = 0.252$).

3.5 Sensitivity analysis

Sensitivity analysis was used to assess one study's effect on the total analytical results. Figure 7 shows the sensitivity analysis of the subgroup of CSS. No study impacted the pooled HRs significantly, which meant that our results were reliable.

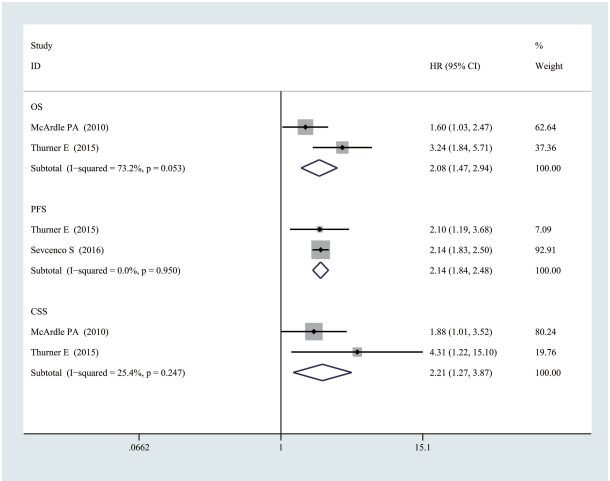

FIGURE 5
Relationship between categorized CRP and prognosis in localized PCa. CRP, C-reactive protein; PCa, prostate cancer.

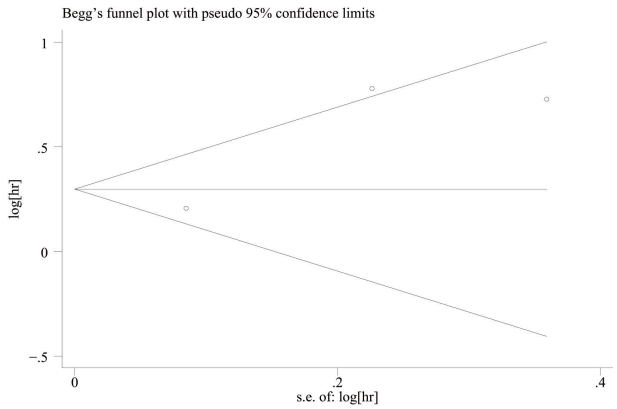

FIGURE 6
Funnel plot (categorized CRP and PFS in prostate cancer). CRP, C-reactive protein; PFS, progression-free survival.

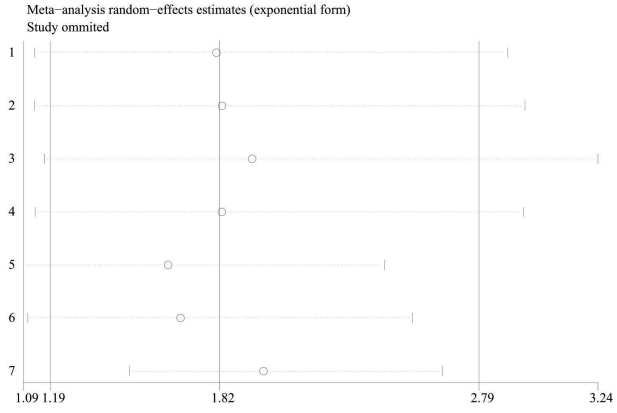

FIGURE 7
Sensitivity analysis (CSS in prostate cancer). CSS, cancer-specific survival.

4 Discussion

This was a meta-analysis of C-reactive protein levels and prognosis in prostate cancer. We found that PCa patients often had worse survival with high levels of CRP. The results further confirmed the study of Liu et al. (21). Moreover, we also performed subgroup analyses by staging the disease because of the bigger sample size. Our study also indicated that the level of CRP was related to the survival of both mPCa patients and localized PCa patients.

As prostate cancer is the most common malignancy in the male reproductive system, its treatment is varied. It could be roughly divided into wait and watch, active monitoring, surgical treatment, radiotherapy, androgen deprivation therapy (ADT), etc. (22). However, mPCa is still deadly, with a 5-year survival rate of approximately 30%, indicating the need for better treatment options. In recent years, there are also some new advances in the treatment of prostate cancer. Arpit et al. found that rucaparib and olaparib (poly-ADP-ribose polymerase (PARP) inhibitors) could be used as the targeted therapy option for patients with mPCa (23). Arnas et al. suggested that high-intensity focused ultrasound (HIFU) has a high control rate and safety in the treatment of local prostate cancer patients and should be promoted in clinical treatment (24). Jiang et al. also found that nanotechnology could create good synergy with radiotherapy, chemotherapy, thermotherapy, photodynamic therapy, and gene therapy, which could increase the effectiveness of treatment and reduce drug resistance (25). With the recent advances, the treatments of prostate cancer became varied, so it was particularly important to evaluate the prognosis of prostate cancer patients.

In recent years, diversified predictors have been confirmed for predicting the prognosis of PCa. One of the most commonly used prostate-specific antigens was the conventional measurement index in the treatment of all PCa patients. In addition, many studies found that epidermal growth factor receptor (EGFR), pAkt, nuclear factor-kappa B, macrophage inhibitory cytokine-1 (MIC-1), matrix metalloproteinase-1 (MMP-1), MMP-9 and tissue inhibitor of metalloproteinase-2 (TIMP-2), and macrophage inhibitory cytokine-1 were associated with the outcome of PCa patients (26, 27). However, in fact, all the above biomarkers must be tested in pathological tissues. This made it difficult for real-time monitoring of the prognosis of patients. Instead, the inflammation indicators were easy to examine from the blood. Brown et al. found that an inflammation-based prognostic score (Glasgow Prognostic Score) was associated with advanced lung and gastrointestinal cancers for the first time (28). After that, the Glasgow Prognostic Score was found to be related to many types of cancer. Recently, one study found that the prognostic value of the Glasgow Prognostic Score in PCa patients, the elevation of CRP (>10 mg/L), and hypoalbuminemia (<35 g/L) were related to worse prognoses of PCa patients (6). William Khalil et al. also summarized the hematological indicators related to the prognosis of prostate cancer, including collagenases, stromelysins, TIMP-1 and TIMP-2, MMP-13, osteopontin (OPN), MMP-2, MMP-9, and MMP-7 (29). Maria et al. also considered the following blood indicators to be associated with the prognosis of prostate cancer: prostate-specific antigen (PSA) + kallikrein antigen (KLK2), AKT, chromogranin A (CHGA), and early prostate cancer antigen (EPCA) (30). Katalin et al. also considered that the following blood-derived biomarkers played an important role in the prognosis of prostate cancer: circulating tumor cells, cellular and soluble immunological and inflammation-related blood markers, and extracellular vesicles and their microRNA content (31). However, the inflammation indicators could be more easily detected from the blood and are widely used in the clinical setting. CRP is the most common indicator of inflammation and has also been widely studied in recent years.

There are many possible mechanisms for the elevation of CRP with worse survival in cancer patients. Chronic inflammation could promote the growth of vascular endothelial cells, which was beneficial to the occurrence of tumors (32). On the one hand, the inflammatory reaction could be activated by the rapid growth of the tumor. Many inflammatory factors are released when the tumor is growing. On the other hand, inflammation also could provide a microenvironment for the growth of tumors, for example, survival factors and growth factors (33). Moreover, a significant negative correlation was recently found between the elevation of CRP and T-lymphocyte subset infiltration (34). Therefore, our study is necessary for the advancement in the treatment of PCa.

The level of CRP is also important for the outcome in PCa. Sevcenco et al. suggested that patients are more prone to experience biochemical recurrence (BCR) with high levels of CRP (35). Hall et al. performed multivariable analysis and found that a higher CRP level is an independent prognostic factor for BCR in patients with radiotherapy (36). According to the multivariate analysis of McArdle et al., a CRP level >10 mg dl^{-1} before a diagnosis is an independent prognostic factor for

both OS and CSS of PCa patients (37). Otherwise, Arthur et al. found that elevated CRP is associated with increased odds of both a high risk and metastatic PCa and high PSA levels, which means that the level of CRP would rise with the increase of tumor stage and disease progression for PCa patients (38). Sevcenco et al. also found that the patients with higher Gleason scores on biopsy, lymph node metastasis, seminal vesicle invasion, extracapsular extension, and positive surgical margins status often had a higher level of CRP compared with patients without these features (35). This further confirmed this conclusion, but more studies are needed to confirm the conclusions.

Firstly, we analyzed the association between the elevation of CRP and the prognosis of PCa patients. We found that CRP level could be a prognosis predictor of PCa in both categorized data and log data. The result showed that elevated CRP levels were associated with worse OS, CSS, and PFS in PCa patients. However, significant heterogeneity was observed; the heterogeneity might be due to many aspects, for example, basic characteristics, the staging of the disease, follow-up time, the difference in treatment, and the different cutoff values. Therefore, we chose a random-effects model to reduce the effect of these differences. Otherwise, we performed a subgroup analysis by the staging of the disease according to the characteristics of these studies and found that the heterogeneity was significantly reduced, which meant that the staging of the disease was likely to be the source of heterogeneity. The result further confirmed that CRP level could be a prognosis predictor for PCa.

For mPCa, we found a significant association between high CRP levels and worse OS in mPCa. For localized PCa, a significant association also could be observed between elevated CRP levels and worse OS, CSS, and PFS. Furthermore, we found that heterogeneity was significantly reduced, which indicated that the staging of the disease contributed to the source of heterogeneity. Our meta-analysis proved that an elevated CRP level is a strong prognosis predictor of PCa patients, which could be helpful for the treatment of PCa. It also could help doctors better monitor the progress of the disease.

Our research includes more new studies compared with the research of Liu et al. (21). Moreover, we also performed Begg's test to make our results more credible and the subgroup analysis by staging the disease, explored the relationship between CRP and the survival of patients with different stages of PCa, and found the source of heterogeneity.

However, our study also has some limitations. There is also a need for more credible studies to confirm our conclusions, although we have reviewed all the current literature. The heterogeneity was significant in our study, but we performed stratified analysis to reduce the heterogeneity, which made the results more credible. In addition, the techniques for detecting CRP were different, which made the results unreliable.

5 Conclusion

In general, our meta-analysis found that elevated CRP levels were related to worse OS, CSS, and PFS in PCa patients. Furthermore, we also observed the same relationship between CRP and the survival of localized PCa patients. Therefore, it can be indicated that the CRP level could be used as a prognosis predictor of prostate cancer. More studies are needed to confirm these conclusions.

Data availability statement

The original contributions presented in the study are included in the article/supplementary material. Further inquiries can be directed to the corresponding author.

Author contributions

i) Conception and design: KZ. ii) Administrative support: BM. iii) Provision of study materials or patients: KZ and XZ. iv) Collection and assembly of data: BM, CL and KZ. v) Data analysis and interpretation: KZ, CL and TC. vi) Manuscript writing: KZ and CL. All authors contributed to the article and approved the submitted version.

Funding

This work was supported by a research grant provided by Xiangyang Central Hospital (20160608).

Acknowledgments

We thank INPLASY for the permission for our meta registration (DOI number is "10.37766/inplasy2020.6.0061"). We also sincerely thank CL (Xiangyang Central Hospital) and Jun Cao (Xiangyang Central Hospital) for their help and support of the meta-analysis.

Conflict of interest

The authors declare that the research was conducted in the absence of any commercial or financial relationships that could be construed as a potential conflict of interest.

Publisher's note

References

1. Torre LA, Bray F, Siegel RL, Ferlay J, Lortet-Tieulent J, Jemal A. Global cancer statistics, 2012. *CA: A Cancer J Clin* (2015) 65:87. doi: 10.3322/caac.21262

2. Halabi S, Vogelzang NJ, Kornblith AB, Ou SS, Kantoff PW, Dawson NA, et al. Pain predicts overall survival in men with metastatic castration-refractory prostate cancer. *J Clin Oncol* (2008) 26:2544. doi: 10.1200/JCO.2007.15.0367

3. Armstrong AJ, Garrett-Mayer ES, Yang YC, de Wit R, Tannock IF, Eisenberger M. A contemporary prognostic nomogram for men with hormone-refractory metastatic prostate cancer: A TAX327 study analysis. *Clin Cancer Res* (2007) 13:6396. doi: 10.1158/1078-0432.CCR-07-1036

4. Halabi S, Small EJ, Kantoff PW, Kattan MW, Kaplan EB, Dawson NA, et al. Prognostic model for predicting survival in men with hormone-refractory metastatic prostate cancer. *J Clin Oncol* (2003) 21:1232. doi: 10.1200/JCO.2003.06.100

5. Smaletz O, Scher HI, Small EJ, Verbel DA, McMillan A, Regan K, et al. Nomogram for overall survival of patients with progressive metastatic prostate cancer after castration. *J Clin Oncol* (2002) 20:3972. doi: 10.1200/JCO.2002.11.021

6. Shafique K, Proctor MJ, McMillan DC, Qureshi K, Leung H, Morrison DS. Systemic inflammation and survival of patients with prostate cancer: Evidence from the Glasgow inflammation outcome study. *Prostate Cancer Prostatic Dis* (2012) 15:195. doi: 10.1038/pcan.2011.60

7. Mahmud S, Franco E, Aprikian A. Prostate cancer and use of nonsteroidal anti-inflammatory drugs: Systematic review and meta-analysis. *Br J Cancer* (2004) 90:93. doi: 10.1038/sj.bjc.6601416

8. Hurlimann J, Thorbecke GJ, Hochwald GM. The liver as the site of c-reactive protein formation. *J Exp Med* (1966) 123:365. doi: 10.1084/jem.123.2.365

9. Roxburgh CS, McMillan DC. Role of systemic inflammatory response in predicting survival in patients with primary operable cancer. *Future Oncol* (2010) 6:149. doi: 10.2217/fon.09.136

10. Saito K, Kihara K. Role of c-reactive protein in urological cancers: A useful biomarker for predicting outcomes. *Int J UROL* (2013) 20:161. doi: 10.1111/j.1442-2042.2012.03121.x

11. Wu Y, Fu X, Zhu X, He X, Zou C, Han Y, et al. Prognostic role of systemic inflammatory response in renal cell carcinoma: A systematic review and meta-analysis. *J Cancer Res Clin Oncol* (2011) 137:887. doi: 10.1007/s00432-010-0951-3

12. Beer TM, Lalani AS, Lee S, Mori M, Eilers KM, Curd JG, et al. C-reactive protein as a prognostic marker for men with androgen-independent prostate cancer. *CANCER-AM Cancer Soc* (2008) 112:2377. doi: 10.1002/cncr.23461

13. Thurner E, Krenn-Pilko S, Langsenlehner U, Stojakovic T, Pichler M, Gerger A, et al. The elevated c-reactive protein level is associated with poor prognosis in prostate cancer patients treated with radiotherapy. *Eur J Cancer* (2015) 51:610. doi: 10.1016/j.ejca.2015.01.002

14. McArdle PA, Mir K, Almushatat ASK, Wallace AM, Underwood MA, McMillan DC. Systemic inflammatory response, prostate-specific antigen and survival in patients with metastatic prostate cancer. *UROL Int* (2006) 77:127. doi: 10.1159/000093905

15. Stark JR, Li H, Kraft P, Kurth T, Giovannucci EL, Stampfer MJ, et al. Circulating prediagnostic interleukin-6 and c-reactive protein and prostate cancer incidence and mortality. *Int J Cancer* (2009) 124:2683. doi: 10.1002/ijc.24241

16. Elsberger B, Lankston L, McMillan DC, Underwood MA, Edwards J. Presence of tumoural c-reactive protein correlates with progressive prostate cancer. *Prostate Cancer Prostatic Dis* (2011) 14:122. doi: 10.1038/pcan.2011.5

17. Stang A. Critical evaluation of the Newcastle-Ottawa scale for the assessment of the quality of nonrandomized studies in meta-analyses. *Eur J Epidemiol* (2010) 25:603. doi: 10.1007/s10654-010-9491-z

18. Hayashino Y, Noguchi Y, Fukui T. Systematic evaluation and comparison of statistical tests for publication bias. *J Epidemiol* (2005) 15:235. doi: 10.2188/jea.15.235

19. DerSimonian R, Laird N. Meta-analysis in clinical trials revisited. *CONTEMP Clin TRIALS* (2015) 45:139. doi: 10.1016/j.cct.2015.09.002

20. Mantel N, Haenszel W. Statistical aspects of the analysis of data from retrospective studies of disease. *J Natl Cancer Inst* (1959) 22:719.

21. Liu Z, Chu L, Fang J, Zhang X, Zhao H, Chen Y, et al. Prognostic role of c-reactive protein in prostate cancer: A systematic review and meta-analysis. *Asian J ANDROL* (2014) 16:467. doi: 10.4103/1008-682X.123686

22. Achard V, Putora PM, Omlin A, Zilli T, Fischer S. Metastatic prostate cancer: Treatment options. *Oncology* (2022) 100:48. doi: 10.1159/000519861

23. Rao A, Moka N, Hamstra DA, Ryan CJ. Co-Inhibition of androgen receptor and PARP as a novel treatment paradigm in prostate cancer-where are we now? *Cancers (Basel)* (2022) 14(3):801. doi: 10.3390/cancers14030801

24. Bakavicius A, Marra G, Macek P, Robertson C, Abreu AL, George AK, et al. Available evidence on HIFU for focal treatment of prostate cancer: A systematic review. *Int Braz J UROL* (2022) 48:263. doi: 10.1590/s1677-5538.ibju.2021.0091

25. Zhao J, Zhang C, Wang W, Li C, Mu X, Hu K. Current progress of nanomedicine for prostate cancer diagnosis and treatment. *BioMed Pharmacother* (2022) 155:113714. doi: 10.1016/j.biopha.2022.113714

26. Mimeault M, Johansson SL, Batra SK. Pathobiological implications of the expression of EGFR, pAkt, NF-kappaB and MIC-1 in prostate cancer stem cells and their progenies. *PloS One* (2012) 7:e31919. doi: 10.1371/journal.pone.0031919

27. Ozden F, Saygin C, Uzunaslan D, Onal B, Durak H, Aki H. Expression of MMP-1, MMP-9 and TIMP-2 in prostate carcinoma and their influence on prognosis and survival. *J Cancer Res Clin Oncol* (2013) 139:1373. doi: 10.1007/s00432-013-1453-x

28. Brown DJF, Milroy R, Preston T, McMillan DC. The relationship between an inflammation-based prognostic score (Glasgow prognostic score) and changes in serum biochemical variables in patients with advanced lung and gastrointestinal cancer. *J Clin Pathol* (2007) 60:705. doi: 10.1136/jcp.2005.033217

29. El-Chaer WK, Moraes CF, Nóbrega OT. Diagnosis and prognosis of prostate cancer from circulating matrix metalloproteinases and inhibitors. *J Aging Res* (2018) 2018:1. doi: 10.1155/2018/7681039

30. Adamaki M, Zoumpourlis V. Prostate cancer biomarkers: From diagnosis to prognosis and precision-guided therapeutics. *Pharmacol THERAPEUT* (2021) 228:107932. doi: 10.1016/j.pharmthera.2021.107932

31. Balázs K, Antal L, Sáfrány G, Lumniczky K. Blood-derived biomarkers of diagnosis, prognosis and therapy response in prostate cancer patients. *J Personalized Med* (2021) 11:296. doi: 10.3390/jpm11040296

32. Xavier P, Belo L, Beires J, Rebelo I, Martinez-de-Oliveira J, Lunet N, et al. Serum levels of VEGF and TNF-α and their association with c-reactive protein in patients with endometriosis. *Arch GYNECOL OBSTET* (2006) 273:227. doi: 10.1007/s00404-005-0080-4

33. Hanahan D, Weinberg RA. Hallmarks of cancer: The next generation. *CELL* (2011) 144:646. doi: 10.1016/j.cell.2011.02.013

34. Canna K, McArdle PA, McMillan DC, McNicol AM, Smith GW, McKee RF, et al. The relationship between tumour T-lymphocyte infiltration, the systemic inflammatory response and survival in patients undergoing curative resection for colorectal cancer. *Br J Cancer* (2005) 92:651. doi: 10.1038/sj.bjc.6602419

35. Sevcenco S, Mathieu R, Baltzer P, Klatte T, Fajkovic H, Seitz C, et al. The prognostic role of preoperative serum c-reactive protein in predicting the biochemical recurrence in patients treated with radical prostatectomy. *Prostate Cancer Prostatic Dis* (2016) 19:163. doi: 10.1038/pcan.2015.60

36. Hall WA, Nickleach DC, Master VA, Prabhu RS, Rossi PJ, Godette K, et al. The association between c-reactive protein (CRP) level and biochemical failure-free survival in patients after radiation therapy for nonmetastatic adenocarcinoma of the prostate. *CANCER-AM Cancer Soc* (2013) 119:3272. doi: 10.1002/cncr.28185

37. McArdle PA, Qayyum T, McMillan DC. Systemic inflammatory response and survival in patients with localised prostate cancer: 10-year follow-up. *UROL Int* (2010) 85:482. doi: 10.1159/000320242

38. Arthur R, Williams R, Garmo H, Holmberg L, Stattin P, Malmstrom H, et al. Serum inflammatory markers in relation to prostate cancer severity and death in the Swedish AMORIS study. *Int J Cancer* (2018) 142:2254. doi: 10.1002/ijc.31256

frontiers | Frontiers in Endocrinology

TYPE Original Research
PUBLISHED 09 February 2023
DOI 10.3389/fendo.2023.1123934

OPEN ACCESS

EDITED BY
Yuxuan Song,
Peking University People's Hospital, China

REVIEWED BY
Zuyin Li,
Peking University People's Hospital, China
Octavian Sabin Tataru,
George Emil Palade University of Medicine, Pharmacy, Sciences and Technology of Târgu Mureş, Romania
Yu Xia,
Shanghai Jiao Tong University, China

*CORRESPONDENCE
Xiaochen Zhou
mo_disc@126.com
Gongxian Wang
urowgx@163.com

†These authors have contributed equally to this work

SPECIALTY SECTION
This article was submitted to Adrenal Endocrinology, a section of the journal Frontiers in Endocrinology

RECEIVED 14 December 2022
ACCEPTED 31 January 2023
PUBLISHED 09 February 2023

CITATION
Li X, Xi H, Cheng X, Yu Y, Zhang C, Wang G and Zhou X (2023) Assessment of oligometastasis status of prostate cancer following combined robot-assisted radical prostatectomy and androgen deprivation versus androgen deprivation therapy alone using PSA percentage decline rate. *Front. Endocrinol.* 14:1123934. doi: 10.3389/fendo.2023.1123934

Assessment of oligometastasis status of prostate cancer following combined robot-assisted radical prostatectomy and androgen deprivation versus androgen deprivation therapy alone using PSA percentage decline rate

Xuwen Li†, Haibo Xi†, Xiaofeng Cheng†, Yue Yu, Cheng Zhang, Gongxian Wang* and Xiaochen Zhou*

Department of Urology, The First Affiliated Hospital of Nanchang University, Nanchang, China

Objective: To compare the tumor control in prostate cancer patients with oligometastasis following combined robot-assisted radical prostatectomy and androgen deprivation versus androgen deprivation therapy alone based on total prostate-specific antigen (tPSA) assessment.

Methods: Medical data of a total of 18 prostate cancer patients with oligometastasis administered in The First Affiliated Hospital of Nanchang University from March 2017 to March 2018 were prospectively collected. 10 patients received a combined therapy of robot-assisted radical prostatectomy and pharmaceutical androgen deprivation (RARP+ADT group), while 8 patients received pharmaceutical androgen deprivation therapy alone (ADT group). Then demographic characteristics, prostate volume, tumor characteristics and tPSA data were analysised and compared. Statistical analysis was performed using t-test for continuous variables and Pearson chi-square test or Fisher's exact test for categorical variables.

Results: No significant difference was found in patients' age (p = 0.075), prostate volume (p = 0.134) and number of bone metastasis (p = 0.342). Pre-treatment Gleason score was significantly lower in RA group (p = 0.003). Patients in RARP+ADT group had significantly lower pre-treatment tPSA (p = 0.014), while no statistical difference was noted in reexamined tPSA (p = 0.140) on follow-up. No statistical difference was noted in tPSA decline rates (declined tPSA value per day) in RARP+ADT and ADT group (8.1 $\pm$ 4.7 verse 7.5 $\pm$ 8.0 ng/ml/d, p = 0.853). However, tPSA percentage decline rate (declined tPSA percentage per day) was significantly higher in RARP+ADT group (11.6 $\pm$ 1.5%/d verses 2.9 $\pm$ 2.2%/d, p< 0.001). Immediate urinary continence was achieved in 9 patients (90%) upon removal of urethral catheter on post-operative day 7 in RARP+ADT group.

Conclusion: ADT alone and in combination with RARP both provide effective tumor control in patients suffering from prostate cancer with oligometastasis. ADT combined with RARP exhibited significant advantage in PSA percentage decline rate without compromising patients' urinary continence. Long-term tumor control requires further follow-up.

KEYWORDS

oligometastatic prostate cancer, androgen deprivation therapy, tobot-assisted radical prostatectomy, TPSA, PSA percentage decline rate

1 Introduction

Prostate Cancer (PCa) is one of the most common malignant tumor of the male reproductive system, with one of the highest morbidity rate in European and American countries (1), and the second highest mortality rate, after lung cancer (2). The incidence of PCa has increased significantly in recent years in our country. Patients with localized PCa have an excellent prognosis after radical prostatectomy, whereas patients with metastatic PCa have an average survival time of only 42.1 months (3). Unfortunately, the proportion of patients with late partial or distant metastasis in our country is as high as 60 ~ 70% (4). As a result, improving tumor control in patients with metastatic PCa is a critical issue that must be addressed urgently in clinic.

In the mid-1990s, Hellman and Weichselbaum jointly proposed the concept of "oligometastases" in tumors, and described the oligometastases state as a period of mild tumor bioaggressivity, a transitional stage between localized disease and widespread metastasis. The number of metastatic tumors is limited and the metastatic organs are limited and qualitative, and have not been disseminated throughout the body (5). While androgen deprivation therapy (ADT) is considered the first-line treatment regimen in EAU guidelines for patients diagnosed with metastatic PCa for the first time, a number of studies have shown that patients with metastatic PCa who received both local treatment (including radical prostatectomy and radical radiotherapy) and ADT had significant advantages in overall survival, tumor-specific survival, progression-free survival, and progression to castration-resistant PCa (6–9). Nonetheless, in patients with metastatic PCa, local therapy combined with ADT is not part of the standard treatment protocol.

Therefore, we conducted this study to compare the short-term tumor control effects of robot-assisted radical prostatectomy combined with androgen deprivation therapy (RARP+ADT) versus ADT alone. We adopted total prostate-specific antigen (tPSA) as a reference indicator. We hope that this study will provide more data and evidence for the clinical value of local therapy in the control of oligometastatic PCa tumors.

2 Materials and methods

2.1 Data source and ethics statement

After obtaining the approval from the institutional review board and ethics committee of the First Affiliated Hospital of Nanchang University, we prospectively collected demographic and clinical data of patients with oligo-metastatic PCa admitted between March 2017 and March 2018.

2.2 Patient selection

Patients with elevated tPSA and suspected PCa were identified as potential candidates. All potential candidates underwent systemic imaging and prostate biopsy prior to treatment. Only when a prostate biopsy confirmed a prostate cancer and imaging examination suggested bone metastasis, these potential candidates were listed as official candidates. Patients over the age of 85 and those with radiographic evidence of visceral metastasis were excluded. Prior to treatment, candidates were informed of all treatment options including surgery and/or ADT. All candidates were informed that ADT was compulsory and strongly recommended. They were also told that concomitant RARP might yield better overall tumor control result than receiving ADT alone. Patients that agreed to RARP were then assigned to RARP +ADT group, while the otherwise were assigned to ADT group. Informed consent forms were obtained from all candidates prior to treatment. Eventually, a total of 18 patients with oligo-metastatic PCa were enrolled. Ten patients were treated with robot-assisted radical prostatectomy and androgen deprivation while 8 patients were managed by androgen deprivation therapy alone.

2.3 Technical considerations

In the combination treatment group, patients were scheduled to receive robot-assisted radical prostatectomy and androgen deprivation therapy (RARP+ADT). All patients received oral Bicalutamide (50 mg qd, AstraZeneca) from the day before surgery and subcutaneous Goserelin Acetate (3.6 mg qm, AstraZeneca) from the fifth day after surgery. All operations were performed by the same experienced medical team.

In the ADT group, Bicalutamide (50 mg qd, AstraZeneca) was taken orally from the first day of treatment, and Goserelin Acetate (3.6 mg qm, AstraZeneca) was injected subcutaneously 6 days later.

2.4 Objectives and data collection

2.4.1 Objectives

Primary objective of the study was to assess the PSA percentage decline rate between patients that received RARP+ADT and those treated by ADT alone,

which was calculated as $\frac{\text{pre-tPSA-pos-tPSA}}{\text{pre-tPSA}} \times 100\,\% \div \text{tPSA review interval}$. Pre-tPSA was the baseline total PSA obtained prior to treatment; pos-tPSA was the total PSA obtained after a certain time following treatment; tPSA review interval is the time gap between the time of initial treatment and the time of first tPSA following treatment. The secondary objective was to assess the tPSA decline rate between the two group of patients, which was calculated as $\frac{\text{pre-tPSA-pos-tPSA}}{\text{tPSA review interval}}$.

2.4.2 Data collection

Pre-treatment assessment included age, body mass index (BMI), prostate volume, tumor characteristics (Gleason score, bone metastasis and distant lymph node metastasis), urinary control (assessed by ICI-Q-SF) and pre-tPSA. The post-treatment assessment was the pos-tPSA data and interval at the first review. Both intraoperative and postoperative conditions (operation time, blood loss, complications, catheter removal time, urinary control) were also recorded in the RARP+ADT group.

2.5 Statistical analysis

Means and standard deviations were determined for the normally distributed continuous variables, while those with nonnormal distribution were presented as median and interquartile range. Categorical variables were presented as frequencies and their proportions. The Student's t-test was performed for the normally distributed continuous variables. All categorical variables were compared with the Chisquare test. SPSS 26.0 (IBM Corp, Armonk, NY) was utilized for all statistical analysis with a two-sided p value < 0.05 denoting statistical significance.

3 Results

A total of 18 candidates were included in the study between March 2017 and March 2018. These candidates were divided into two groups, the RARP+ADT group (n = 10) and the ADT group (n = 8). Demographic characteristics, prostate volume, and tumor characteristics are shown in Table 1. The age was 70.9 ± 6.9 yrs (mean ± SD) ranged from 61.0 to 82.0 yrs in ADT group versus 64.6 ± 7.0 yrs ranged from 56.0 to 77.0 yrs in RARP+ADT group, respectively (p = 0.075). The weight was 68.4 ± 6.2 kg ranged from 59.0 to 80.0 kg in ADT group versus 70.4 ± 7.4 kg ranged from 59.0 to 80.0 kg in RARP+ADT group, respectively (p = 0.545). The BMI was 25.7 ± 3.0 kg/m^2 ranged from 22.5 to 31.3 kg/m^2 in ADT group, while the RARP+ADT group was 25.1 ± 7.5 kg/m^2 ranged from 21.7 to 29.4 kg/m^2, respectively (p = 0.715). Prostate volume was 44.8 ± 21.9 cm^3 ranged from 20.5 to 91.1 cm^3 in ADT group versus 57.3 ± 11.4 cm^3 ranged from 41.4 to 72.4 cm^3 in RARP+ADT group, respectively (p = 0.134). Gleason score was 8.6 ± 0.9 ranged from 8.0 to 10.0 in ADT group, while the RARP+ADT group was 7.3 ± 0.7 ranged from 6.0 to 8.0, respectively (p = 0.003). The bone metastasis was 3.0 ± 1.1 ranged from 2.0 to 5.0 in ADT group, while 2.5 ± 1.1 ranged from 1.0 to 5.0 in RARP+ADT group, respectively (p = 0.342). All candidates had normal urine control before treatment.

Table 2 records the intraoperative and postoperative conditions of patients in RARP+ADT group. All operations were successfully completed. The operation time was 113.5 ± 14.7 min ranged from 90.0 to 140.0. The blood loss was 88.0 ± 53.5 ml ranged from 40.0 to 200.0 ml. Two patients developed fever and managed with antibotics (Clavien-Dindo Grade II). All patients had their catheters removed 7 days after surgery. One patient had urinary incontinence after catheter removal.

TABLE 1 Demographic characteristics, prostate volume and tumor characteristics.

	ADT (n = 8)	RARP+ADT (n = 10)	p
Age (yr), mean (SD), range	70.9 (6.9), 61.0 - 82.0	64.6 (7.0), 56.0 - 77.0	0.075
Weight (kg), mean (SD), range	68.4 (6.2), 59.0 - 80.0	70.4 (7.4), 59.0 - 80.0	0.545
BMI (kg/m^2), mean (SD), range	25.7 (3.0), 22.5 - 31.3	25.1 (7.5), 21.7 - 29.4	0.715
Prostate volume (cm^3), mean (SD), range	44.8 (21.9), 20.5 - 91.1	57.3 (11.4), 41.4 - 72.4	0.134
Gleason score, mean (SD), range	8.6 (0.9), 8.0 - 10.0	7.3 (0.7), 6.0 - 8.0	0.003
Bone metastasis, mean (SD), range	3.0 (1.1), 2.0 - 5.0	2.5 (1.1), 1.0 - 5.0	0.342
Distant lymph node metastasis, mean (SD), range	0	0	–
Urinary control, n (%)	8 (100.0%)	10 (100.0%)	–

All patients were monitored for tPSA before and after treatment and followed up for at least 4.5 years. The pre-tPSA was 235.3 ± 144.0 ng/ml ranged from 56.7 to 420.0 ng/ml in ADT group, which was significantly higher than RARP+ADT group (70.6 ± 42.9 ng/ml ranged from 18.3 to 134.6 ng/ml, p = 0.014). The pos-tPSA was 35.9 ± 42.4 ng/ml ranged from 0.2 to 129.6 ng/ml in ADT group versus 14.1 ± 12.4 ng/ml ranged from 1.3 to 43.8 ng/ml in RARP+ADT group, respectively (p = 0.140). The tPSA review interval was 44.0 ± 27.4 days ranged from 13.0 to 90.0 days in ADT group, while all patients in the RARP+ADT group received tPSA re-examination on the 7th day after surgery. The tPSA decline rate were comparable between two groups (7.5 ± 8.0 ng/ml/d vs. 8.1 ± 4.7 ng/ml/d, p = 0.853), while the PSA percentage decline rate was significantly different (2.9 ± 2.2%/d vs. 11.6 ± 1.5%/d, p< 0.001, Table 3).

4 Discussion

Genomic studies on oligometastatic PCa have indicated its unique biological characteristics, suggesting that it may be a special subtype of PCa (10–13). Although the concept of oligometastases was proposed as early as in the 1990s (5), there is no standard definition of the scope and number of lesions of oligometastases at present. Through literature search, we found that 6 papers defined the number and range of metastases of oligometastases: two of them took ≤ 5 metastases as the standard (14, 15), One paper was based on ≤ 4 metastases (16), and in three papers, the standard was ≤ 3

TABLE 2 Perioperative data of RARP+ADT group.

	RARP+ADT (n = 10)
Operation time (min), mean (SD), range	113.5 (14.7), 90.0 - 140.0
Blood loss (ml), mean (SD), range	88.0 (53.5), 40.0 - 200.0
Complications	
Fever, n (%)	2 (20.0%)
Leaking urine, n (%)	1 (10.0%)
Urinary control, n (%)	9 (90.0%)

metastases (17–19). Two studies limited the metastases to bone metastases and distant lymphatic metastases (17, 18).

Accumulating evidence suggested that patients with oligometastatic PCa might benefit from the surgical removal of the cancerous prostate gland. There have been several clinical studies on the surgical treatment of metastatic PCa. SWOG (Southwest Oncology Group) study No. 8894 reviewed 1286 patients with PCa with bone metastasis, and the results suggested that based on ADT, the overall survival rate of patients undergoing surgery was 1.55 times that of those without surgery (20). Heidenreich reported 61 cases of oligometastatic PCa with an average follow-up of > 40 months. The results showed that the overall survival rates of patients with surgery combined with ADT and ADT alone were 91.3% and 78.9%, respectively, and the tumor specific survival rates were 95.6% and 84.2%, respectively, with significant differences (8). Culp reviewed 8185 cases of metastatic PCa from the U.S. National Cancer Institute's SEER (Surveillance Epidemiology and End Results) database, followed for an average of 16 months. The overall survival rates of patients treated with ADT combined with surgery, ADT combined with radiotherapy and ADT alone were 64.7%, 62.6% and 22.5%, respectively, and the tumor-specific survival rates were 75.8%, 61.3% and 48.7%, respectively, suggesting that surgery and radiotherapy brought significant survival benefits to patients compared with no local therapy (6). Similar results were also obtained in the retrospective comparative analysis of 7858 patients with metastatic PCa by Antwi (7). Locally advanced and inoperable patients can be treated with radiotherapy for local tumor control. However, Gratzke et al. reviewed 1538 cases of metastatic PCa included in the Missouri Cancer Registry (MCR) database. The results suggest that surgery is significantly better than radiotherapy, ADT alone or other treatments in terms of overall survival (21). Similar results were also obtained in a retrospective analysis of 916 cases of metastatic PCa conducted by Taipei Medical University and New Jersey Cancer Institute (22). Only one prospective randomized controlled study evaluating the efficacy of surgical treatment for metastatic PCa has been reported, and the results showed that ADT combined with surgery has significant advantages over ADT alone in progression-free survival, overall survival, tumor-specific survival, and progression to castration-resistant PCa (8). There are two popular theories about the relationship between primary tumor and metastasis, namely "seed and soil" theory and "self-planting" theory. The former refers to the factors secreted by the tumor primary site, which can promote the microenvironment (soil) suitable for the growth of circulating tumor cells (seeds) in other parts of the body (23). The latter refers to the fact that tumor cells from distant metastases can be replanted in the primary site, leading to a vicious cycle between the primary site and the metastases (24, 25). Therefore, removal of the primary site may interrupt the complementary relationship between the primary site and the metastatic site, which is beneficial for tumor control.

Serum PSA is the preferred screening indicator for PCa and the main tumor marker for prognosis assessment. In addition to the PSA value itself, PSA dynamics is also of great value for diagnosis and prognosis assessment. Currently, PSA dynamics consists of three reference criteria, namely PSA velocity (PSAV), PSA doubling time (PSADT), and PSA flare phenomenon (PSAFP). The concept of PSAV is based on the linear relationship between PSA growth and time. The calculation formula of PSAV in AJCC Guide 2014 edition is PSAV = [(PSA2 - PSA1) + (PSA3 - PSA2)] ÷ 2, where PSA1, PSA2 and PSA3 are the results of three PSA tests within two years. Studies have shown that PSAV > 2 ng/ml/year indicates that surgical treatment may be necessary for patients (26). The concept of PSADT is based on the power function relationship between PSA growth and time, which is a descriptive indicator of the rate of PSA re-increase in PCa patients after treatment. It also contains two aspects of basic PSA level and PSAV information. The calculation formula is PSADT = (t2 - t1) lg2 ÷ (lgPSA2 - lgPSA1). A large retrospective study stratified PSADT by< 3 months, 3 to 8 months, 9 to 14 months, and > 15 months suggested a significant correlation between PSADT and tumor-specific and overall survival, and patients with PSADT< 9 months had a poor prognosis (27). The AJCC guidelines states that PSADT is useful for assessing local recurrence and distant metastasis. PSAFP refers to the abnormal rise of PSA in patients with advanced

TABLE 3 tPSA decline rate and tPSA percentage decline rate.

	ADT (n = 8)	RARP+ADT (n = 10)	*p*
pre-tPSA[a] (ng/ml), mean (SD), range	235.3 (144.0), 56.7 - 420.0	70.6 (42.9), 18.3 - 134.6	0.014
pos-tPSA[b] (ng/ml), mean (SD), range	35.9 (42.4), 0.2 - 129.6	14.1 (12.4), 1.3 - 43.8	0.140
tPSA review interval[c] (d), mean (SD), range	44.0 (27.4), 13.0 - 90.0	7.0	0.007
tPSA decline rate[d] (ng/ml/d), mean (SD), range	7.5 (8.0), 1.0 - 24.6	8.1 (4.7), 2.4 - 15.0	0.853
PSA percentage decline rate[e] (%/d), mean (SD), range	2.9 (2.2), 1.1 - 6.7	11.6 (1.5), 8.3 - 13.3	< 0.001

[a], baseline total PSA obtained prior to treatment.
[b], total PSA obtained after a certain time (tPSA review interval) following treatment.
[c], tPSA review interval: the time gap between the time of initial treatment and the time of first tPSA following treatment. tPSA was re-examined 7 days after surgery in all patients in RARP+ADT group.
[d], tPSA decline rate was calculated as $\frac{\text{pre-tPSA} - \text{pos-tPSA}}{\text{tPSA review interval}}$.
[e], PSA percentage decline rate (PSAPDR) = $\frac{\text{pre-tPSA} - \text{pos-tPSA}}{\text{pre-tPSA}} \times 100\,\% \div$tPSA review interval.

PCa after the start of second-line therapy (such as paclitaxel-based chemotherapy regimen and abiraterone endocrine therapy), which soon drops below the baseline level (28). There is increasing evidence that the occurrence of this phenomenon may indicate that patients are responding to treatment (29).

With the occurrence and development of prostate cancer, the PSA of patients usually keeps rising in a certain period of time. Following ADT and/or local therapy, PSA typically continues to decrease over time up to baseline levels that are correlated with the patient's tumor load and treatment, with some individualized variation. When treatment fails and the tumor continues to progress, PSA may show a trend of continuous increase (Figure 1). As mentioned above, PSAV, a concept based on the linear relationship between PSA growth and time, can be used to reflect the stage of tumor occurrence and development. From a mathematical point of view, this value normalized the time of two PSA reviews and the absolute value of PSA used to calculate PSAV. That is, on the assumption of a linear relationship between PSA growth and time, PSAV is still comparable among different patients, different initial PSA and different review time. The upper limit of reference value can be obtained through correlation studies (for example, PSAV > 2 ng/ml/year indicates that surgical treatment may be necessary for patients (26)). PSADT, a concept based on the power function relationship between PSA growth and time, is used to reflect the rise rate of PSA during the period of tumor progression after treatment. From a mathematical point of view, this value is also standardized for PSA interval time and absolute value of PSA used to calculate PSADT. PSADT values calculated by any two points on the left red line were the same (Figure 1). That is, PSADT was also comparable among different patients, different initial PSA and different review time based on the assumption that the change trend of PSA was a power function with time. The upper limit of reference value can also be obtained through correlation studies (for example, patients with PSADT< 9 months have poor prognosis (27)). However, there is currently a lack of reference indicators similar to PSAV and PSADT to describe the rate of PSA decline after treatment.

Considering that the time of PSA review after treatment may be different for different patients, and the initial PSA may be different, we proposed the PSA percentage decline rate (PSAPDR) based on the concept of a linear relationship between PSA decline and time. That is, the percentage of PSA decline in unit time (days as unit time), calculated by PSAPDR = [(initial PSA- reexamination PSA)] ÷ initial PSA × 100% ÷ days between two PSA examinations. PSAPDR normalized the initial PSA with "percentage" and the review time with "rate of decline". In other words, although the absolute value of PSA (green dot) and the review time might be different among patients, the PSAPDR values calculated at any two points on the green solid line are the same (Figure 1). That is, similar to PSAV and PSADT, PSAPDR also has comparability among different patients who has different initial PSA and different review time. It is possible to obtain a reference value through subsequent correlation studies to evaluate the effect of a treatment on tumor control, and even to predict the risk of tumor recurrence and timely intervention.

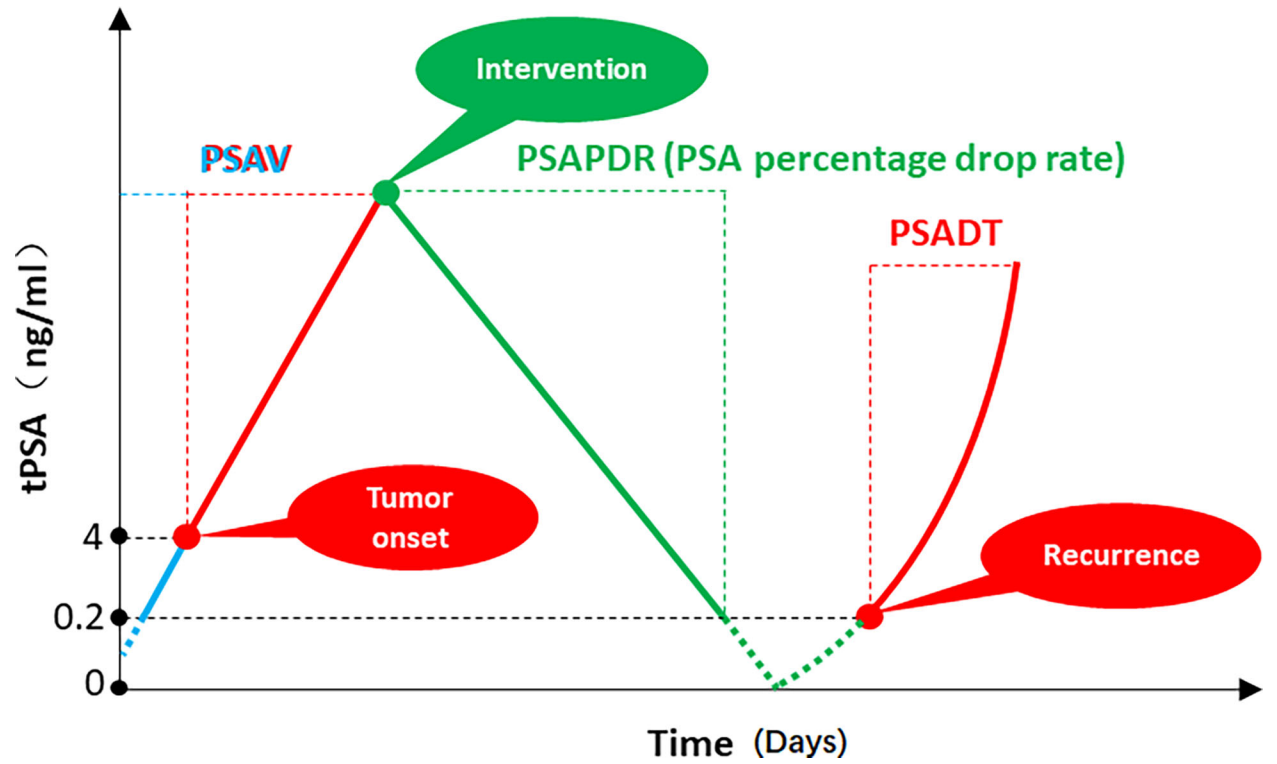

FIGURE 1
PSA velocity (PSAV), PSA doubling time (PSADT), and PSA percentage decline rate (PSAPDR). The concept of PSAV is based on the linear relationship between PSA growth and time. The calculation formula is [(PSA2 - PSA1) + (PSA3 - PSA2)] ÷ 2. The concept of PSADT is based on the power function relationship between PSA growth and time, which is a descriptive indicator of the rate of PSA re-increase in PCa patients after treatment. (t2 - t1) lg2 ÷ (lgPSA2 - lgPSA1). PSA percentage decline rate (PSAPDR) was defined as the percentage of PSA decline in unit time (days as unit time), which calculated as [(initial PSA- reexamination PSA)] ÷ initial PSA × 100% ÷ days between two PSA examinations.

In this study, PSAPDR in the RARP+ADT group and the ADT group were 11.6 ± 1.5%/d and 2.9 ± 2.2%/d, respectively, with significant statistical difference ($p< 0.001$), suggesting that the effect of surgery combined with ADT on PSA reduction was significantly higher than that of ADT alone. There was no significant difference in the tPSA decline rate between the RARP+ADT group and the ADT group, namely the absolute value of daily tPSA decline (8.1 ± 4.7 and 7.5 ± 8.0 ng/ml/d, respectively) (p = 0.853). This may be related to the significantly higher initial PSA in the ADT group than in the RARP+ADT group (235.3 ± 144.0 vs. 70.6 ± 42.9 ng/ml, p = 0.014).

In conclusion, robot-assisted radical prostatectomy combined with ADT and ADT alone are two effective treatments for oligometastatic PCa. Under the premise of strict control of surgical safety, taking PSAPDR (PSA percentage decline rate) as the reference index, surgery combined with ADT seems to have a better effect on the reduction of tPSA in patients than ADT alone. The main limitations of this study are the limited number of cases in the two groups involved and the short follow-up time. The clinical significance of PSAPDR in terms of patients' survival (overall survival, progression-free survival and etc) requires further investigation.

5 Conclusions

In conclusion, robot-assisted radical prostatectomy combined with ADT and ADT alone are two effective treatments for oligometastatic PCa. Under the premise of strict control of surgical safety, taking PSAPDR (PSA percentage decline rate) as the reference index, surgery combined with ADT seems to have a better effect on the reduction of tPSA in patients than ADT alone. The main limitations of this study are the limited number of cases in the two groups involved and the short follow-up time. The clinical significance of PSAPDR in terms of patients' survival (overall survival, progression-free survival and etc) requires further investigation.

Data availability statement

The original contributions presented in the study are included in the article/supplementary material. Further inquiries can be directed to the corresponding authors.

Ethics statement

The studies involving human participants were reviewed and approved by the Ethical Committee of The First Affiliated Hospital of Nanchang University. The patients/participants provided their written informed consent to participate in this study.

Author contributions

Conception and design: GW and XZ. Surgeons: GW and XZ. Acquisition of data: XL. Preparation of tools: YY and CZ. Analysis and interpretation of data: XC. Drafting of the manuscript and statistical analysis: XL. Critical revision: GW and HX. Obtaining funding: XZ and HX. All authors contributed to the article and approved the submitted version.

Funding

Key Research and Development Program of Jiangxi Province (20171ACB20029 to XZ). Applied Research and Cultivation Program of Jiangxi Province (20212BAG70001 to HX).

Acknowledgments

Thank HX and GW for providing suggestions for the writing of the article.

Conflict of interest

The authors declare that the research was conducted in the absence of any commercial or financial relationships that could be construed as a potential conflict of interest.

Publisher's note

Supplementary material

The Supplementary Material for this article can be found online at: https://www.frontiersin.org/articles/10.3389/fendo.2023.1123934/full#supplementary-material

References

1. Fouad TM. Trends in metastatic breast and prostate cancer. *N Engl J Med* (2016) 374(6):595. doi: 10.1056/NEJMc1515983

2. Siegel RL, Miller KD, Fuchs HE, Jemal A. Cancer statistics, 2021. *CA Cancer J Clin* (2021) 71(1):7–33. doi: 10.3322/caac.21654

3. PEYROMAURE M, Debré B, MAO K, Zhang G, Wang Y, Sun Z, et al. Management of prostate cancer in China: A multicenter report of 6 institutions. *J Urol* (2005) 174 (5):1794–7. doi: 10.1097/01.ju.0000176817.46279.93

4. Stamey TA, Caldwell M, Mcneal JE, Nolley R, Hemenez M, Downs J, et al. The prostate specific antigen era in the united states is over for prostate cancer: what happened in the last 20 years? *J Urol* (2004) 172(4 Pt 1):1297–301. doi: 10.1097/01.ju.0000139993.51181.5d

5. Hellman S, Weichselbaum RR. Oligometastases. *J Clin Oncol* (1995) 13(1):8–10. doi: 10.1200/JCO.1995.13.1.8

6. Culp SH, Schellhammer PF, Williams MB. Might men diagnosed with metastatic prostate cancer benefit from definitive treatment of the primary tumor? A SEER-based study. *Eur Urol* (2014) 65(6):1058–66. doi: 10.1016/j.eururo.2013.11.012

7. Antwi S, Everson TM. Prognostic impact of definitive local therapy of the primary tumor in men with metastatic prostate cancer at diagnosis: A population-based, propensity score analysis. *Cancer Epidemiol* (2014) 38(4):435–41. doi: 10.1016/j.canep.2014.04.002

8. Heidenreich A, Pfister D, Porres D. Cytoreductive radical prostatectomy in patients with prostate cancer and low volume skeletal metastases: results of a feasibility and case-control study. *J Urol* (2015) 193(3):832–8. doi: 10.1016/j.juro.2014.09.089

9. Wilt TJ, Brawer MK, Jones KM, Barry MJ, Aronson WJ, Fox S, et al. Radical prostatectomy versus observation for localized prostate cancer. *N Engl J Med* (2012) 367 (3):203–13. doi: 10.1056/NEJMoa1113162

10. Tamoto E, Tada M, Murakawa K, Takada M, Shindo G, Teramoto K, et al. Gene-expression profile changes correlated with tumor progression and lymph node metastasis in esophageal cancer. *Clin Cancer Res* (2004) 10(11):3629–38. doi: 10.1158/1078-0432.CCR-04-0048

11. Wuttig D, Baier B, Fuessel S, Meinhardt M, Herr A, Hoefling C, et al. Gene signatures of pulmonary metastases of renal cell carcinoma reflect the disease-free interval and the number of metastases per patient. *Int J Cancer* (2009) 125(2):474–82. doi: 10.1002/ijc.24353

12. Sonpavde G. The biology of prostate cancer metastases: does oligo differ from polymetastatic? *Curr Opin Urol* (2017) 27(6):542–6. doi: 10.1097/MOU.0000000000000434

13. Lussier YA, Xing HR, Salama JK, Khodarev NN, Huang Y, Zhang Q, et al. MicroRNA expression characterizes oligometastasis(es). *PloS One* (2011) 6(12):e28650. doi: 10.1371/journal.pone.0028650

14. Ahmed KA, Barney BM, Davis BJ, Park SS, Kwon ED, Olivier KR, et al. Stereotactic body radiation therapy in the treatment of oligometastatic prostate cancer. *Front Oncol* (2012) 2:215. doi: 10.3389/fonc.2012.00215

15. Tabata K, Niibe Y, Satoh T, Tsumura H, Ikeda M, Minamida S, et al. Radiotherapy for oligometastases and oligo-recurrence of bone in prostate cancer. *Pulm Med* (2012) 2012:541656. doi: 10.1155/2012/541656

16. Schick U, Jorcano S, Nouet P, Rouzaud M, Vees H, Zilli T, et al. Androgen deprivation and high-dose radiotherapy for oligometastatic prostate cancer patients with less than five regional and/or distant metastases. *Acta Oncol* (2013) 52(8):1622–8. doi: 10.3109/0284186X.2013.764010

17. Berkovic P, De Meerleer G, Delrue L, Lambert B, Fonteyne V, Lumen N, et al. Salvage stereotactic body radiotherapy for patients with limited prostate cancer metastases: Deferring androgen deprivation therapy. *Clin Genitourin Cancer* (2013) 11 (1):27–32. doi: 10.1016/j.clgc.2012.08.003

18. Decaestecker K, De Meerleer G, Lambert B, Delrue L, Fonteyne V, Claeys T, et al. Repeated stereotactic body radiotherapy for oligometastatic prostate cancer recurrence. *Radiat Oncol* (2014) 9:135. doi: 10.1186/1748-717X-9-135

19. Ost P, Jereczek-Fossa BA, As NV, Zilli T, Muacevic A, Olivier K, et al. Progression-free survival following stereotactic body radiotherapy for oligometastatic prostate cancer treatment-naive recurrence: A multi-institutional analysis. *Eur Urol* (2016) 69(1):9–12. doi: 10.1016/j.eururo.2015.07.004

20. Thompson IM, Tangen C, Basler J, Crawford ED. Impact of previous local treatment for prostate cancer on subsequent metastatic disease. *J Urol* (2002) 168 (3):1008–12. doi: 10.1016/S0022-5347(05)64562-4

21. Gratzke C, Engel J, Stief CG. Role of radical prostatectomy in metastatic prostate cancer: data from the Munich cancer registry. *Eur Urol* (2014) 66(3):602–3. doi: 10.1016/j.eururo.2014.04.009

22. Shao YH, Kim S, Moore DF, Shih W, Lin Y, Stein M, et al. Cancer-specific survival after metastasis following primary radical prostatectomy compared with radiation therapy in prostate cancer patients: results of a population-based, propensity score-matched analysis. *Eur Urol* (2014) 65(4):693–700. doi: 10.1016/j.eururo.2013.05.023

23. Psaila B, Lyden D. The metastatic niche: adapting the foreign soil. *Nat Rev Cancer* (2009) 9(4):285–93. doi: 10.1038/nrc2621

24. Comen E, Norton L, Massagué J. Clinical implications of cancer self-seeding. *Nat Rev Clin Oncol* (2011) 8(6):369–77. doi: 10.1038/nrclinonc.2011.64

25. Kim MY, Oskarsson T, Acharyya S, Nguyen DX, Zhang XH, Norton L, et al. Tumor self-seeding by circulating cancer cells. *Cell* (2009) 139(7):1315–26. doi: 10.1016/j.cell.2009.11.025

26. Scheerer J, Kahabka P, Altwein JE, Weißbach L. Unusually large numbers needed to treat for radical prostatectomy in prostate cancer patients with PSA velocity ≤2 ng/ml/year. *Urol Int* (2012) 89(2):155–61. doi: 10.1159/000339604

27. Teeter AE, Presti JCJr., Aronson WJ, Terris MK, Kane CJ, Amling CL, et al. Does PSADT after radical prostatectomy correlate with overall survival?–a report from the SEARCH database group. *Urology* (2011) 77(1):149–53. doi: 10.1016/j.urology.2010.04.071

28. Sella A, Sternberg CN, Skoneczna I, Kovel S. Prostate-specific antigen flare phenomenon with docetaxel-based chemotherapy in patients with androgen-independent prostate cancer. *BJU Int* (2008) 102(11):1607–9. doi: 10.1111/j.1464-410X.2008.07873.x

29. Wenisch JM, Mayr FB, Spiel AO, Radicioni M, Jilma B, Jilma-Stohlawetz P, et al. Androgen deprivation decreases prostate specific antigen in the absence of tumor: Implications for interpretation of PSA results. *Clin Chem Lab Med* (2014) 52(3):431–6. doi: 10.1515/cclm-2013-0535

frontiers | Frontiers in Endocrinology

TYPE Original Research
PUBLISHED 02 March 2023
DOI 10.3389/fendo.2023.1145820

OPEN ACCESS

EDITED BY
Yuxuan Song,
Peking University People's Hospital, China

REVIEWED BY
Barbara Seeliger,
Institue of Image-Guided Surgery, France
Weimin Zhou,
Jiangxi Cancer Hospital, China

*CORRESPONDENCE
Haibo Xi
13870834578@163.com
Gongxian Wang
urowgx@163.com
Xiaochen Zhou
mo_disc@126.com

†These authors have contributed equally to this work

SPECIALTY SECTION
This article was submitted to Adrenal Endocrinology, a section of the journal Frontiers in Endocrinology

RECEIVED 16 January 2023
ACCEPTED 21 February 2023
PUBLISHED 02 March 2023

CITATION
Li X, Xiao S, Yu Y, Liu W, Xi H, Wang G and Zhou X (2023) Robotic-assisted laparoscopic adrenalectomy (RARLA): What advantages and disadvantages compared to retroperitoneal laparoscopic adrenalectomy (RLA)?
Front. Endocrinol. 14:1145820.
doi: 10.3389/fendo.2023.1145820

Robotic-assisted laparoscopic adrenalectomy (RARLA): What advantages and disadvantages compared to retroperitoneal laparoscopic adrenalectomy (RLA)?

Xuwen Li†, Song Xiao†, Yue Yu, Wei Liu, Haibo Xi*, Gongxian Wang* and Xiaochen Zhou*

Department of Urology, The First Affiliated Hospital of Nanchang University, Nanchang, China

Objective: To explore the advantages and disadvantages of robot-assisted laparoscopic adrenalectomy compared with retroperitoneal laparoscopic adrenalectomy.

Methods: A total of 101 patients with adrenal tumors who received retroperitoneal laparoscopic adrenalectomy (RLA) (n=75) or robot-assisted laparoscopic adrenalectomy (RARLA) (n=26) in our hospital from January 2021 to December 2021 were retrospectively collected. Patients' demographics, tumor characteristics, and perioperative indicators were compared. Statistical analysis was performed using t-test for continuous variables and Pearson chi-square test or Fisher's exact test for categorical variables.

Results: We found that blood loss in the RARLA group was significantly less than that in the RLA group (66.9 ± 35.5 ml vs 91.5 ± 66.1 ml, $p = 0.020$). Gastrointestinal function recovery time in RARLA group was significantly less than that in RLA group (19.9 ± 6.9 hours vs 32.0 ± 9.0 hours, $p < 0.001$). However, the operation time, drainage tube placement time, post-operative hospital stay in the RARLA group were significantly longer compared with the RLA group (149.6 ± 53.4 mins vs 118.7 ± 41.2 mins, $p = 0.003$; 4.9 ± 2.0 days vs 3.6 ± 1.1 days, $p = 0.004$; 6.4 ± 1.8 days vs 4.6 ± 1.6 days, $p < 0.001$). The hospitalization expense in the RARLA group is significantly higher than that in the RLA group (59284 ± 8724 RMB¥ vs 39785 ± 10126 RMB¥, $p < 0.001$). We found that there was no significant difference in the incidence of postoperative complications between the two groups. However, the pathological types of the two groups were significantly different. Patients in the RLA group had a higher proportion of

adrenocortical adenoma, while patients in the RARLA group had a higher proportion of pheochromocytoma.

Conclusion: Compared with traditional laparoscopic adrenalectomy, robot-assisted laparoscopic adrenalectomy can significantly reduce intraoperative blood loss and accelerate postoperative gastrointestinal recovery. It is committed to studying how to reduce the hospitalization time and hospitalization cost of RARLA, which can make RARLA more widely used.

KEYWORDS

robot-assisted, laparoscopic, adrenalectomy, retroperitoneal, surgery

1 Introduction

Adrenal gland is an important endocrine organ, and adrenal tumor is the most common adrenal disease. Since Gagner et al. (1) first reported successful laparoscopic adrenalectomy in 1992, laparoscopic adrenalectomy has become the gold standard for the treatment of adrenal tumors (2). In recent years, with the development of Da Vinci surgical robot, Da Vinci robot has gradually appeared in urological surgery, such as radical prostatectomy, radical cystectomy, partial nephrectomy and so on (3, 4). Many scholars have also studied the application of robots in adrenalectomy. Some scholars thought that robot-assisted laparoscopy has no obvious advantage in the treatment of adrenal tumors compared with traditional laparoscopy, and its application value is controversial. Karen et al. found that the subjective benefits of robotic surgery include a three-dimensional surgical field of view, an ergonomically comfortable position, and the elimination of tremors in the surgeon. Robot-assisted laparoscopic surgery takes significantly longer, but patient outcomes are similar to laparoscopic techniques (5). However, some scholars found that robot-assisted adrenalectomy can safely and effectively shorten operation time. In addition, it also has the advantages of short hospital stay, less blood loss, and low incidence of postoperative complications compared with laparoscopic adrenalectomy (6). These findings seem to support the use of robotic minimally invasive surgery for adrenal tumors. This study compared and analyzed the effects of Da Vinci robot-assisted laparoscopic and retroperitoneal laparoscopic adrenalectomy (RLA) in the Department of Urology, the First Affiliated Hospital of Nanchang University, and explored the advantages and disadvantages of robot-assisted laparoscopic adrenalectomy (RARLA).

2 Materials and methods

2.1 Data source and ethics statement

This study was conducted with the approval of the Institutional Review Committee and the Ethics Committee of the First Affiliated Hospital of Nanchang University. We used the hospital database to collect the basic, clinical and pathological information of patients undergoing adrenalectomy.

2.2 Patient selection

The patients with adrenal tumors who received retroperitoneal laparoscopic adrenalectomy (RLA) or robot-assisted laparoscopic adrenalectomy (RARLA) in our hospital from January 2021 to December 2021 were retrospectively collected. The patients were included in this study according to the following inclusion criteria: [1] Patients diagnosed as adrenal tumor; [2] Unilateral tumor. The exclusion criteria were as follows: [1] During hospitalization, other operations other than adrenalectomy were performed; [2] accompanied by other serious comorbidity.

2.3 Technical considerations

After signing informed consent, patients received retroperitoneal laparoscopic adrenalectomy (RLA) or robot-assisted laparoscopic adrenalectomy (RARLA) (RLA and RARLA were both performed *via* the retroperitoneoscopic approach). All operations were performed by an experienced surgical team.

2.4 Variables and endpoints

Variables in the study include demographic characteristics [age, sex, body mass index (BMI)], tumor characteristics (tumor size, tumor site, pathologic type), treatment methods (RLA, RARLA), perioperative results (operation time, blood loss, gastrointestinal function recovery time, complication, drainage tube placement time, postoperative hospital stay), and other variable (hospitalization expense). Drainage tube was placed routinely for patients after adrenalectomy. When the postoperative drainage fluid is less than 30 ml per day, the doctors will consider removing the drainage tube according to the patient ‘s condition.

The end points of this study were to compare the average differences in operation time, blood loss, gastrointestinal function recovery time, complication, drainage tube placement time, postoperative hospital stay and hospitalization expense between RLA group and RARLA group.

2.5 Statistical analysis

Means and standard deviations were determined for the normally distributed continuous variables. Categorical variables were presented as frequencies and their proportions. The Student's t-test was performed for the normally distributed continuous variables. All categorical variables were compared with the Chisquare test. SPSS 26.0 (IBM Corp, Armonk, NY) was utilized for all statistical analysis with a two-sided p value < 0.05 denoting statistical significance.

3 Results

According to the inclusion and exclusion criteria, 101 patients were included in this study from January 2021 to December 2021. 75 patients chose to perform retroperitoneal laparoscopic surgery, while only 26 patients chose to perform robot-assisted laparoscopic surgery. No significant differences in terms of age ($p = 0.471$), sex ($p = 0.668$), BMI ($p = 0.909$), and tumor site ($p = 0.707$) was observed between two groups (all $p > 0.05$). However, tumor size in the RARLA group tended to be larger compared with RLA group (4.9 ± 2.9 cm vs 2.4 ± 1.1 cm, $p < 0.001$) (Table 1).

We found that blood loss in the RARLA group was significantly less than that in the RLA group (66.9 ± 35.5 ml vs 91.5 ± 66.1 ml, $p = 0.020$). Gastrointestinal function recovery time in RARLA group was significantly less than that in RLA group (19.9 ± 6.9 hours vs 32.0 ± 9.0 hours, $p < 0.001$). However, the operation time, drainage tube placement time, post-operative hospital stay in the RARLA group is significantly longer compared with the RLA group (149.6 ± 53.4 mins vs 118.7 ± 41.2 mins, $p = 0.003$; 4.9 ± 2.0 days vs 3.6 ± 1.1 days, $p = 0.004$; 6.4 ± 1.8 days vs 4.6 ± 1.6 days, $p < 0.001$). The hospitalization expense in the RARLA group is significantly higher than that in the RLA group (59284 ± 8724 RMB¥ vs 39785 ± 10126 RMB¥, $p < 0.001$). We found that there was no significant difference in the incidence of postoperative complications between the two groups (4.0% vs 3.8%). By the way, the four patients with complications in the retrospective cohort were classified as grade I according to the Clavien-Dindo classification. However, the pathological types of the two groups were significantly different. Patients in the RLA group had a higher proportion of adrenocortical adenoma (50.0% vs 88.0%), while patients in the RARLA group had a higher proportion of pheochromocytoma (11.5% vs 5.3%) (Table 2).

4 Discussion

With the development of minimally invasive technology, laparoscopy is more and more widely used in surgery. Laparoscopic adrenalectomy has become the preferred treatment for most adrenal tumors. Compared with open adrenalectomy, patients have better tolerance to laparoscopic adrenalectomy (7). In 2001, Horgan et al. (8) first used the Da Vinci robotic surgical system to complete unilateral adrenalectomy. They found that robotic surgery was a safe and effective alternative to traditional laparoscopic surgery. With the development of robotic surgery, many medical centers began to perform robot-assisted laparoscopic adrenalectomy, and the safety and effectiveness of this surgical method have been verified (9, 10).

There have been some comparative studies on robot-assisted laparoscopic adrenalectomy and traditional laparoscopic adrenalectomy. Agcaoglu et al. (11) have shown that for larger adrenal tumors, robot-assisted laparoscopic adrenalectomy can shorten the operation time and reduce the probability of conversion to open surgery. Robot-assisted laparoscopic adrenalectomy can be used as the preferred surgical method for larger adrenal tumors. However, in their study, only adrenal tumors larger than 5cm in diameter were included. Karabulut et al. (12) have shown that robot-assisted laparoscopic adrenalectomy has lower morbidity and shorter hospital stay after the robotic

TABLE 1 Baseline demographical and clinicopathological characteristics of patients.

Variables	RLA (n = 75)	RARLA (n = 26)	*P*
Age, year, mean (SD)	49.7 (12.9)	47.4 (15.3)	0.471
Sex, n (%)			0.668
Male	44.0 (58.7 %)	14.0 (53.8 %)	
Female	31.0 (41.3 %)	12.0 (46.2 %)	
BMI, kg/m^2, mean (SD)	24.1 (3.8)	24.0 (3.4)	0.909
Tumor size, cm, mean (SD)	2.4 (1.1)	4.9 (2.9)	< 0.001
Tumor site, n (%)			0.701
Left	35.0 (46.7 %)	11.0 (42.3 %)	
Right	40.0 (53.3 %)	15.0 (57.7 %)	

RLA, Retroperitoneal laparoscopic adrenalectomy; RARLA, Robot assisted laparoscopic adrenalectomy; SD, standard deviation; BMI, body mass index.

TABLE 2 Comparison of perioperative and pathological results.

Variables	RLA (n = 75)	RARLA (n = 26)	*P*
Operation time, min, mean (SD)	118.7 (41.2)	149.6 (53.4)	0.003
Blood loss, ml, mean (SD)	91.5 (66.1)	66.9 (35.5)	0.020
Gastrointestinal function recovery time, hour, mean (SD)	32.0 (9.0)	19.9 (6.9)	< 0.001
Complication, n (%)			1.000
Yes	3 (4.0 %)	1 (3.8 %)	
None	72 (96.0 %)	25 (96.2 %)	
Drainage tube placement time, day, mean (SD)	3.6 (1.1)	4.9 (2.0)	0.004
Postoperative hospital stay, day, mean (SD)	4.9 (1.6)	6.4 (1.8)	< 0.001
Hospitalization expense, RMB¥, mean (SD)	39785 (10126)	59284 (8724)	< 0.001
Pathologic types, n (%)			< 0.001
Adrenocortical adenoma	66 (88.0 %)	13 (50.0 %)	
Pheochromocytoma	4 (5.3 %)	3 (11.5 %)	
Others pathologic types	5 (6.7 %)	10 (38.5 %)	

RLA, Retroperitoneal laparoscopic adrenalectomy; RARLA, Robot assisted laparoscopic adrenalectomy; SD, standard deviation; BMI, body mass index.

procedures than traditional laparoscopic surgery. In their study, the operation time of different surgical approaches was also compared. The results showed that operation time was similar between the laparoscopic and robotic groups for both lateral transabdominal and posterior retroperitoneal approaches. However, some important perioperative indicators, such as the time of drainage tube removal and postoperative gastrointestinal recovery time, were not involved in their study (13, 14).

In this study, we found that robot-assisted laparoscopic adrenalectomy can significantly reduce intraoperative blood loss and accelerate postoperative gastrointestinal function recovery compared with traditional laparoscopic adrenalectomy. The reason for less bleeding in robot surgery may be that the anatomical structure is clearer when using the robot system, thus avoiding the damage of some small blood vessels. This is very helpful for the clarity of the surgical field (15). Consistent with our findings, Brunaud et al. prospectively evaluated 50 patients with RARLA and 59 patients with RLA, and they found that RARLA was associated with lower blood loss (49.0 vs 71.0 ml, $p < 0.001$) (16). Robotic surgery reduces the damage to surrounding tissues due to clear vision and accurate operation, reduces the damage to the gastrointestinal system, and accelerates the recovery of gastrointestinal function. Lin et al. (17) found that the intestinal recovery time of patients undergoing robotic surgery was faster than that of patients undergoing ordinary laparoscopic surgery, and the anal exhaust and defecation time was shorter. Robotic surgery causes less damage to the patient ‘s body and promotes the recovery of intestinal and other functions.

In the present study, the average operation time of the RARLA group was 30 minutes longer than that of the RLA group. It is generally accepted that the operation time of RARLA is longer than that of RLA in the initial stage of application (18). In fact, some studies have highlighted the docking procedure as the reason for the significant increase in RLA operation time (19). In addition, several variables (robotic operating room, robot platform preparation during anesthesia, and surgical team familiarity with robotic surgery) have a significant effect on the operation time (18). Studies have found that rich laparoscopic surgery experience and previous robotic surgery can significantly reduce the learning curve of RLA (18, 20). The length of hospital stay may be affected by differences in medical reimbursement systems, the distance of patients from referral centers, and cultural expectations. As a new technology, robotic surgery will cost more than traditional laparoscopic surgery, but with the emergence of domestic robots, it is believed that the cost of robotic surgery will be greatly reduced.

In addition, it is worth noting that the choice of surgical approach may also be a factor affecting the outcome of surgery. Previous studies have shown that the retroperitoneal approach has shorter operating time, less bleeding, and earlier recovery of gastrointestinal function compared to the anterior abdominal approach (21–23). Therefore, at present, most patients with adrenal tumors in our center are treated *via* retroperitoneal approach. The anterior abdominal approach is only used in a few large tumors. Based on our experience, we believe that the retroperitoneal approach can reach the adrenal gland with less tissue dissection and avoid peritoneal damage. This may be one reason for less bleeding and faster recovery of gastrointestinal function during operation. Of course, more research is needed.

The main limitation of the study is its retrospective, non-randomized design. The secondary limitation of the study is the small sample size. Due to the limitation of sample size, we cannot analyze the two surgical approaches of lateral transabdominal and posterior retroperitoneal simultaneously. We only study the posterior retroperitoneal approach. The robot system provides a three-dimensional display for surgeons, enhances depth perception, enables surgeons to operate in a comfortable sitting position, keeps eyes, hands and targets consistent, and the device contains a ‘ wrist ‘ joint to improve flexibility. We believe that the ability of robotic

surgery to restore hand-eye coordination and three-dimensional vision lost in laparoscopic surgery will enable us to perform complex surgeries with greater accuracy and confidence and better outcomes.

5 Conclusion

Compared with traditional laparoscopic adrenalectomy, robot-assisted laparoscopic adrenalectomy can significantly reduce intraoperative blood loss and accelerate postoperative gastrointestinal recovery. It is committed to studying how to reduce the hospitalization time and hospitalization cost of RARLA, which can make RARLA more widely used.

Data availability statement

The original contributions presented in the study are included in the article/Supplementary Material. Further inquiries can be directed to the corresponding authors.

Ethics statement

The studies involving human participants were reviewed and approved by the Ethical Committee of The First Affiliated Hospital of Nanchang University. The patients/participants provided their written informed consent to participate in this study. Written informed consent was obtained from the individual(s) for the publication of any potentially identifiable images or data included in this article.

Author contributions

Conception and design: GW and XZ. Surgeons: GW and XZ. Acquisition of data: SX. Preparation of tools: YY and WL. Analysis and interpretation of data: XL. Drafting of the manuscript and statistical analysis: XL and SX. Critical revision: GW and HX. Obtaining funding: XZ and HX. All authors contributed to the article and approved the submitted version.

Funding

Key Research and Development Program of Jiangxi Province (20171ACB20029 to XZ). Applied Research and Cultivation Program of Jiangxi Province (20212BAG70001 to HX).

Acknowledgments

Thank HX and GW for providing suggestions for the writing of the article.

Conflict of interest

The authors declare that the research was conducted in the absence of any commercial or financial relationships that could be construed as a potential conflict of interest.

Publisher's note

Supplementary material

The Supplementary Material for this article can be found online at: https://www.frontiersin.org/articles/10.3389/fendo.2023.1145820/full#supplementary-material

References

1. Gagner M, Lacroix A, Bolté E. Laparoscopic adrenalectomy in cushing's syndrome and pheochromocytoma. *New Engl J Med* (1992) 327(14):1033. doi: 10.1056/nejm199210013271417

2. Smith CD, Weber CJ, Amerson JR. Laparoscopic adrenalectomy: New gold standard. *World J Surg* (1999) 23(4):389–96. doi: 10.1007/pl00012314

3. Haglind E, Carlsson S, Stranne J, Wallerstedt A, Wilderäng U, Thorsteinsdottir T, et al. Urinary incontinence and erectile dysfunction after robotic versus open radical prostatectomy: A prospective, controlled, nonrandomised trial. *Eur Urol* (2015) 68 (2):216–25. doi: 10.1016/j.eururo.2015.02.029

4. Bochner BH, Dalbagni G, Sjoberg DD, Silberstein J, Keren Paz GE, Donat SM, et al. Comparing open radical cystectomy and robot-assisted laparoscopic radical cystectomy: A randomized clinical trial. *Eur Urol* (2015) 67(6):1042–50. doi: 10.1016/j.eururo.2014.11.043

5. Pineda-Solís K, Medina-Franco H, Heslin MJ. Robotic versus laparoscopic adrenalectomy: A comparative study in a high-volume center. *Surg endoscopy* (2013) 27(2):599–602. doi: 10.1007/s00464-012-2496-9

6. Brandao LF, Autorino R, Laydner H, Haber GP, Ouzaid I, De Sio M, et al. Robotic versus laparoscopic adrenalectomy: A systematic review and meta-analysis. *Eur Urol* (2014) 65(6):1154–61. doi: 10.1016/j.eururo.2013.09.021

7. Heger P, Probst P, Hüttner FJ, Gooßen K, Proctor T, Müller-Stich BP, et al. Evaluation of open and minimally invasive adrenalectomy: A systematic review and network meta-analysis. *World J Surg* (2017) 41(11):2746–57. doi: 10.1007/s00268-017-4095-3

8. Horgan S, Vanuno D. Robots in laparoscopic surgery. *J laparoendoscopic advanced Surg techniques Part A* (2001) 11(6):415–9. doi: 10.1089/10926420152761950

9. Brandao LF, Autorino R, Zargar H, Krishnan J, Laydner H, Akca O, et al. Robot-assisted laparoscopic adrenalectomy: Step-by-Step technique and comparative outcomes. *Eur Urol* (2014) 66(5):898–905. doi: 10.1016/j.eururo.2014.04.003

10. Gan L, Peng L, Li J, Meng C, Li K, Wu J, et al. Comparison of the effectiveness and safety of robotic-assisted and laparoscopic in adrenalectomy: A systematic review and meta-analysis. *Int J Surg (London England)* (2022) 105:106853. doi: 10.1016/j.ijsu.2022.106853

11. Agcaoglu O, Aliyev S, Karabulut K, Mitchell J, Siperstein A, Berber E. Robotic versus laparoscopic resection of Large adrenal tumors. *Ann Surg Oncol* (2012) 19 (7):2288–94. doi: 10.1245/s10434-012-2296-4

12. Karabulut K, Agcaoglu O, Aliyev S, Siperstein A, Berber E. Comparison of intraoperative time use and perioperative outcomes for robotic versus laparoscopic adrenalectomy. *Surgery* (2012) 151(4):537–42. doi: 10.1016/j.surg.2011.09.047

13. Niglio A, Grasso M, Costigliola L, Zenone P, De Palma M. Laparoscopic and robot-assisted transperitoneal lateral adrenalectomy: A Large clinical series from a single center. *Updates Surg* (2020) 72(1):193–8. doi: 10.1007/s13304-019-00675-8

14. De Crea C, Pennestrì F, Voloudakis N, Sessa L, Procopio PF, Gallucci P, et al. Robot-assisted vs laparoscopic lateral transabdominal adrenalectomy: A propensity score matching analysis. *Surg endoscopy* (2022) 36(11):8619–29. doi: 10.1007/s00464-022-09663-3

15. Makay O, Erol V, Ozdemir M. Robotic adrenalectomy. *Gland Surg* (2019) 8 (Suppl 1):S10–s6. doi: 10.21037/gs.2019.01.09

16. Brunaud L, Bresler L, Ayav A, Zarnegar R, Raphoz AL, Levan T, et al. Robotic-assisted adrenalectomy: What advantages compared to lateral transperitoneal laparoscopic adrenalectomy? *Am J Surg* (2008) 195(4):433–8. doi: 10.1016/j.amjsurg.2007.04.016

17. Lin Y, Zhang Y, Luo L, Zhang X. Clinical effect of robot-assisted radical cystectomy in bladder cancer. *Am J Trans Res* (2021) 13(9):10545–53.

18. Mihai R, Donatini G, Vidal O, Brunaud L. Volume-outcome correlation in adrenal surgery-an eses consensus statement. *Langenbeck's Arch Surg* (2019) 404 (7):795–806. doi: 10.1007/s00423-019-01827-5

19. Hyams ES, Stifelman MD. The role of robotics for adrenal pathology. *Curr Opin Urol.* (2009) 19(1):89–96. doi: 10.1097/MOU.0b013e32831b446c

20. Ludwig WW, Gorin MA, Pierorazio PM, Allaf ME. Frontiers in robot-assisted retroperitoneal oncological surgery. *Nat Rev Urol* (2017) 14(12):731–41. doi: 10.1038/nrurol.2017.149

21. Gavriilidis P, Camenzuli C, Paspala A, Di Marco AN, Palazzo FF. Posterior retroperitoneoscopic versus laparoscopic transperitoneal adrenalectomy: A systematic review by an updated meta-analysis. *World J Surg* (2021) 45(1):168–79. doi: 10.1007/s00268-020-05759-w

22. Conzo G, Tartaglia E, Gambardella C, Esposito D, Sciascia V, Mauriello C, et al. Minimally invasive approach for adrenal lesions: Systematic review of laparoscopic versus retroperitoneoscopic adrenalectomy and assessment of risk factors for complications. *Int J Surg (London England)* (2016) 28 Suppl 1:S118–23. doi: 10.1016/j.ijsu.2015.12.042

23. Lairmore TC, Folek J, Govednik CM, Snyder SK. Improving minimally invasive adrenalectomy: Selection of optimal approach and comparison of outcomes. *World J Surg* (2016) 40(7):1625–31. doi: 10.1007/s00268-016-3471-8

frontiers | Frontiers in Endocrinology

TYPE Original Research
PUBLISHED 16 March 2023
DOI 10.3389/fendo.2023.1148898

OPEN ACCESS

EDITED BY
Yuxuan Song,
Peking University People's Hospital, China

REVIEWED BY
Pengju Li,
The First Affiliated Hospital of Sun Yat-sen University, China
Cong Li,
Southern Medical University, China

*CORRESPONDENCE
Jianheng Ye
yejianheng1989@hotmail.com
Zhaodong Han
75028579@qq.com
Weide Zhong
zhongwd2009@live.cn

†These authors have contributed equally to this work

SPECIALTY SECTION
This article was submitted to Adrenal Endocrinology, a section of the journal Frontiers in Endocrinology

RECEIVED 20 January 2023
ACCEPTED 01 March 2023
PUBLISHED 16 March 2023

CITATION
Feng Y, Deng Y, Tang Z, Cai S, Li J, Liu R, Wan J, He H, Zeng G, Ye J, Han Z and Zhong W (2023) Prognostic implication of heterogeneity and trajectory progression induced by enzalutamide in prostate cancer.
Front. Endocrinol. 14:1148898.
doi: 10.3389/fendo.2023.1148898

Prognostic implication of heterogeneity and trajectory progression induced by enzalutamide in prostate cancer

Yuanfa Feng[1,2†], Yulin Deng[1†], Zhenfeng Tang[1†], Shanghua Cai[1,3], Jinchuang Li[2], Ren Liu[4], Jiaming Wan[2], Huichan He[1], Guohua Zeng[1], Jianheng Ye[2*], Zhaodong Han[2*] and Weide Zhong[1,2,3,4,5*]

[1]Urology Key Laboratory of Guangdong Province, The First Affiliated Hospital of Guangzhou Medical University, Guangzhou Medical University, Guangzhou, Guangdong, China, [2]Department of Urology, Guangdong Key Laboratory of Clinical Molecular Medicine and Diagnostics, Guangzhou First People's Hospital, School of Medicine, South China University of Technology, Guangzhou, Guangdong, China, [3]Guangzhou Medical University, Guangzhou Laboratory, Guangzhou, Guangdong, China, [4]Guangdong Provincial Institute of Nephrology, Nanfang Hospital, Southern Medical University, Guangzhou, Guangdong, China, [5]Macau Institute for Applied Research in Medicine and Health, Macau University of Science and Technology, Avenida Wai Long, Taipa, Macau, China

Background: Enzalutamide, as a second-generation endocrine therapy drug for prostate cancer (PCa), is prominent representative among the synthetic androgen receptor antagonists. Currently, there is lack of enzalutamide-induced signature (ENZ-sig) for predicting progression and relapse-free survival (RFS) in PCa.

Methods: Enzalutamide-induced candidate markers were derived from single-cell RNA sequencing analysis integrating three enzalutamide-stimulated models (0-, 48-, and 168-h enzalutamide stimulation). ENZ-sig was constructed on the basis of candidate genes that were associated with RFS in The Cancer Genome Atlas leveraging least absolute shrinkage and selection operator method. The ENZ-sig was further validated in GSE70768, GSE94767, E-MTAB-6128, DFKZ, GSE21034, and GSE70769 datasets. Biological enrichment analysis was used to discover the underlying mechanism between high ENZ-sig and low ENZ-sig in single-cell RNA sequencing and bulk RNA sequencing.

Results: We identified a heterogenous subgroup that induced by enzalutamide stimulation and found 53 enzalutamide-induced candidate markers that are related to trajectory progression and enzalutamide-stimulated. The candidate genes were further narrowed down into 10 genes that are related to RFS in PCa. A 10-gene prognostic model (ENZ-sig)—IFRD1, COL5A2, TUBA1A, CFAP69, TMEM388, ACPP, MANEA, FOSB, SH3BGRL, and ST7—was constructed for the prediction of RFS in PCa. The effective and robust predictability of ENZ-sig was verified in six independent datasets. Biological enrichment analysis revealed that differentially expressed genes in high ENZ-sig were more activated in cell cycle–related pathway. High–ENZ-sig patients were more sensitive to cell cycle–targeted drugs (MK-1775, AZD7762, and MK-8776) than low–ENZ-sig patients in PCa.

Conclusions: Our results provided evidence and insight on the potential utility of ENZ-sig in PCa prognosis and combination therapy strategy of enzalutamide and cell cycle–targeted compounds in treating PCa.

KEYWORDS

prostate cancer, enzalutamide, relapse-free survival, signature, endocrine therapy

1 Introduction

Prostate cancer (PCa), which represents 27% of all new cancer cases every year, is among the most common cancer in men (1). It has been reported that approximately 268,490 cancer cases were diagnosed as PCa and 34,500 deaths were estimated as PCa in the United States in 2022 (1). Despite that diverse treatments including radical prostatectomy, radiotherapy, chemotherapy, and endocrine therapy were leveraging to counter PCa, prognosis and treatment are still poor, especially for the patients who possess high-grade disease (2). As an androgen-dependent disease, endocrine therapy that targets androgens or androgen receptors (AR) had been the first-line therapy for those patients with PCa who did not benefit from surgery or radiation (3). However, whether the endocrine therapy targets the hypothalamic-pituitary negative feedback pathway, inhibits androgen synthesis, or blocks androgen receptors, long-term hormone deficiency would cause a series of side effects, such as hyperlipidemia, osteoporosis, insulin resistance, anemia, and sexual dysfunction (4). More importantly, in response to androgen deprivation, most PCa progresses to castrate-resistant PCa (CRPC), which is inevitable in endocrine treatment for PCa (2). Thus, it is highlighted that how to effectively address the limitations of endocrine therapy is essential to increase the therapeutic efficiency and improve prognosis of patients with PCa.

Enzalutamide, a prominent representative among synthetic AR antagonists, is a second-generation AR antagonist displaying effective antineoplastic by binding directly to the AR. However, sustained medicine with enzalutamide would inevitably progress to enzalutamide resistance and treatment failure (3). Therefore, it is especially significant to improve the therapeutic efficiency of enzalutamide treatment for shortening duration of enzalutamide treatment and prolonging survival. However, the underlying mechanism induced by enzalutamide is still unclear. It is reported that enzalutamide plays the part of agonist in transcriptional activity, inducing the expression of cancer-related genes in PCa cells (5). Moreover, it is noticed that PCa was reported as a heterogeneity tumor that result in distinct cellular phenotypes, and such inter-tumoral heterogeneity would generate different treatment response phenotypes (6, 7). Thus, exploring the enzalutamide-mediated transcription in single-cell resolution may contribute to understand the molecular mechanisms of enzalutamide, even the mechanisms of enzalutamide resistance, which could improve prognosis, and provide potentially strategy of combination treatment for PCa.

In this work, we explored the cell heterogeneity and transcriptional alteration that induced by enzalutamide and identified a heterogeneous cluster that resists enzalutamide-treatment by using single-cell RNA sequencing (scRNA-seq) analysis. Following the time trajectory analysis in 0-, 48-, and 168-h enzalutamide-stimulated models, time-dependent enzalutamide-induced gene sets were further discovered. Then, a prognostic model, named ENZ-sig, was built on the basis of 10 prognostic enzalutamide-induced markers for the prediction of relapse-free survival (RFS) in PCa. We examined the predicting ability and clinical significance of ENZ-sig in PCa from The Cancer Genome Atlas (TCGA-PRAD) and further validated in six independent cohorts (i.e., GSE70768, GSE94767, E-MTAB-6128, DFKZ, GSE21034, and GSE70769). Finally, pathway enrichment analysis revealed that patients in the high-risk group were more activated in cell cycle pathway, giving insight on the combination treatment strategy related to enzalutamide and cell cycle–targeted compounds for patients with PCa.

2 Materials and methods

2.1 Data sources and processes

The raw count data of scRNA-seq underlying enzalutamide-stimulated LNCap after 0, 48, and 168 h, respectively, were obtained from Taavitsainen et al. (8). The RNA sequencing data and clinical features from TCGA were downloaded and processed by GDCRNAtools (9). The clinical information and mRNA expression data from GSE70768, GSE94767, DFKZ, GSE21034, and GSE70769 datasets were acquired from Gene Expression Omnibus (GEO; https://www.ncbi.nlm.nih.gov/geo/), and data from E-MTAB-6128 were derived from ArrayExpress (https://www.ebi.ac.uk/arrayexpress/). The detailed information of above datasets is summarized in Table S1.

2.2 Single-cell RNA sequencing data processing and analysis

By using Seurat package (10), the raw count data were initialized and created as a Seurat object with the criteria of min.cells = 3 and min.features = 200. Then, quality control was performed to ensure that mitochondrial counts were less than 20% and that unique feature

counts were less than 5,000 and more than 200 in each cell. Furthermore, standard pre-processing workflow, including data normalization and scaling, and the detection of highly variable features were conducted in the three enzalutamide-induced models, separately. The joint analysis of these three models was further performed by FindIntegrationAnchors() and IntegrateData() with parameters of anchor.features = 2,000 and dims = 1:50. Selecting the top 50 principal components and a resolution of 0.2, the integrated object was clustered into different cell subgroup. Non-linear dimensional reduction was using to visualize and explore the integrated clusters. Differentially up-expressed markers in each cell subgroup were defined using FindAllMarkers() function with log [fold change (FC)] > 0.25 and adjusted p-value < 0.05. Differentially expressed genes (DEGs) in C7 were identified by FindMarkers() function with the cutoff criteria of log|FC|>0.25 and adjusted p-value < 0.05.

2.3 Cell trajectory analysis

Monocle R package (v2.24.0) was performed to explore the time trajectory of enzalutamide-induced cell in three stimulated models (DMSO, 48-h stimulation, and 168-h stimulation). The DEGs that derived from three stimulated models were defined as time trajectory features to ordering cells in pseudo-time. The time trajectory markers was obtained from the function of differential GeneTest() in Monocle (11).

2.4 Pathway enrichment analysis

To detect the biological changes in cell cluster, pathway score was measured by gene set variation analysis (GSVA) on the basis of the gene sets of "Hallmark" and "KEGG" obtained from MSigDB (12). Differential expression analysis was carried out to explore the DEGs between C7 and other clusters. The statistically significant DEGs with the threefold were identified and further fitted into "enrichR" package. Gene set enrichment analysis (GSEA) was conducted on the basis of the pre-ranking gene set that ordered by the FC from differentially expressed analysis.

2.5 Construction and validation of enzalutamide-induced signature

Candidate enzalutamide-induced genes were identified from the gene set that intersected with DEGs in C7 and markers in cell trajectory analysis. To select the key prognostic enzalutamide-induced features, least absolute shrinkage and selection operator (LASSO) method with 10-fold cross-validation was further performed to narrow down the significant enzalutamide-induced genes. Enzalutamide-induced signature (ENZ-sig) was calculated as follows: β(feature1) × expr (feature1) + β(feature2) × expr (feature2) + ··· + β (feature n) × expr (feature n), where β is the LASSO Cox coefficient of each feature in the regression model and expr is the expression value of the corresponding feature. This strategy was further utilized in six independent datasets to validated the efficiency and robustness of ENZ-sig in PCa.

2.6 Development and validation of nomogram

A predicting nomogram leverages the vital prognostic characteristics for predicting 3-, 5-, and 7-year RFS of patients with PCa in the TCGA-PRAD dataset. To determine the capability of the nomogram to predict 3-, 5-, and 7-year RFS outcomes, the calibration curves were developed by "rms" R package.

2.7 Scoring the activity of ENZ-sig in single cell

To estimate the activity of ENZ-sig for individual cells, R package AUCell was performed on the basis of the expression of 10 ENZ-sig genes (13). The area under the curve (AUC) that generated by AUCell represented the score activity of ENZ-sig in single cell. Cells were divided into two groups on the basis of optimal cutoff value evaluated by AUCell.

2.8 Statistical analysis

All statistical analyses in our study were performed in R (version 4.0.5). Kaplan–Meier survival analysis was performed using "survival" R package, and the optimal cutoff value was defined by "survminer". Wilcoxon signed-rank test, with two-tailed $P < 0.05$ being considered as statistical significance level. P-value adjustment was applied when multiple comparisons were necessary.

3 Results

3.1 Landscape of enzalutamide-induced cell heterogeneity and transcriptional alteration

After quality control and normalization, the dimension reduction on the three types of enzalutamide-derived models is shown in Figures 1A–C. The joint analysis of these three models was further performed to explore the characteristics of enzalutamide-induced cell heterogeneity or transcriptional alteration in PCa cell line. Eight clusters were obtained after scRNA-seq integration (Figure 1D). Interestingly, by comparing the proportion of originating cells and the number of cells in each cluster, we found that cluster 7 (C7) was mostly enriched in ENZ168 model (Figure 1E). Moreover, the top five differentially expressed markers of each cluster were displayed as a heatmap plot (Figure 1F). Biological pathway analysis indicates that the enrichment pathway in C7 was more activated in 39 of the 50 Hallmark gene sets compared with other clusters, such as fatty acid metabolism, TGF-β signaling, androgen response, epithelial–mesenchymal transition, and PI3K-AKT-MTOR signaling

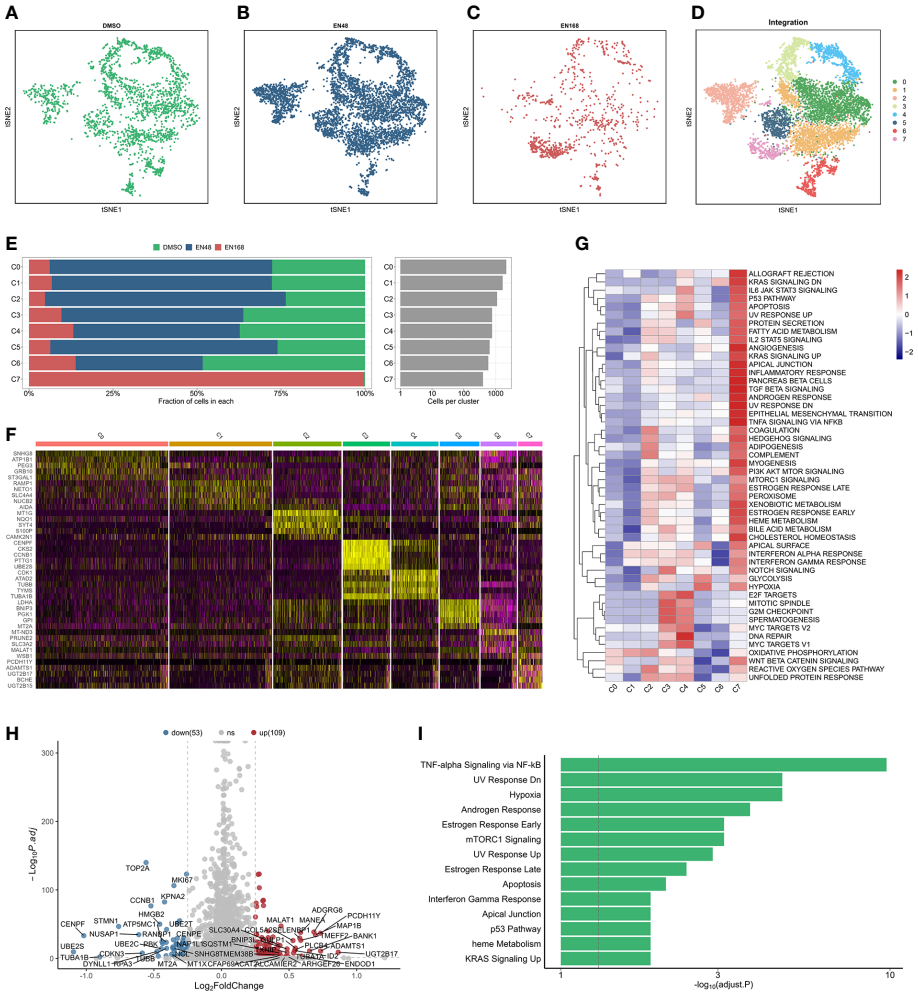

FIGURE 1
The landscape of integrated profiling induced by enzalutamide. The t-distributed stochastic neighbor embedding (tsne) diagram of cells stimulated: DMSO **(A)**, 48-h enzalutamide **(B)**, and 168-h enzalutamide **(C)**. **(D)** The tsne diagram of integrated analysis induced by enzalutamide in 0, 48, and 168 **(H, E)** The proportion and number of cells in each cluster. **(F)** Heatmap for the top five markers in each cluster. **(G)** Gene set variation analysis in each cluster using Hallmark gene set. **(H)** volcano plot for the differentially expressed genes (DEGs) between cluster 7 and other clusters. Red dots indicate upregulated genes with $\log_2$(fold change) > 0.25 and adjusted p-value < 0.05. Blue dots represent downregulated genes with $\log_2$(fold change) < −0.25 and adjusted p-value < 0.05. **(I)** Biological enrichment using the statistically significant genes from DEGs in cluster 7. Gray vertical dotted line indicates the threshold of adjusted p-value less than 0.05.

(Figure 1G). The differentially expressed analysis between C7 and other clusters was highlighted that 109 upregulated genes and 53 downregulated genes were significantly differentially expressed in C7 (Figure 1H). The upregulated genes were enriched in TNF-α signaling *via* NF-kB, hypoxia, androgen response, and mTORC1 signaling, indicating that C7 displayed strongly tumor-promoting progression under treating with enzalutamide (Figure 1I).

3.2 Identifying enzalutamide-induced pseudo-time trajectory

For exploring the enzalutamide-induced gene sets, we further conducted the pseudo-time trajectory analysis to construct a linear trajectory from 0-, 48-, to 168-h enzalutamide-stimulated models (Figures 2A, B). As shown in Figure 2C, we found that C7 was specifically located at the end of time-trajectory, indicating that C7 was heterogeneous cluster induced by enzalutamide-stimulated alone with trajectory-evolved. Next, 53 dysregulated genes based on the trajectory progression and enzalutamide-stimulated models were detected (Figure 2D). Five representative trajectory-related markers (IFRD1, COL5A2, TUB1A1, and CFAP69) show the upregulated expression tendency alone with enzalutamide-stimulated models and transferred cluster (Figure 2E).

3.3 Construction of enzalutamide-induced signature for predicting RFS in prostate cancer

Thirty-one enzalutamide-induced candidate genes were further generated by intersecting with DEGs in C7 and

10.3389/fendo.2023.1148898

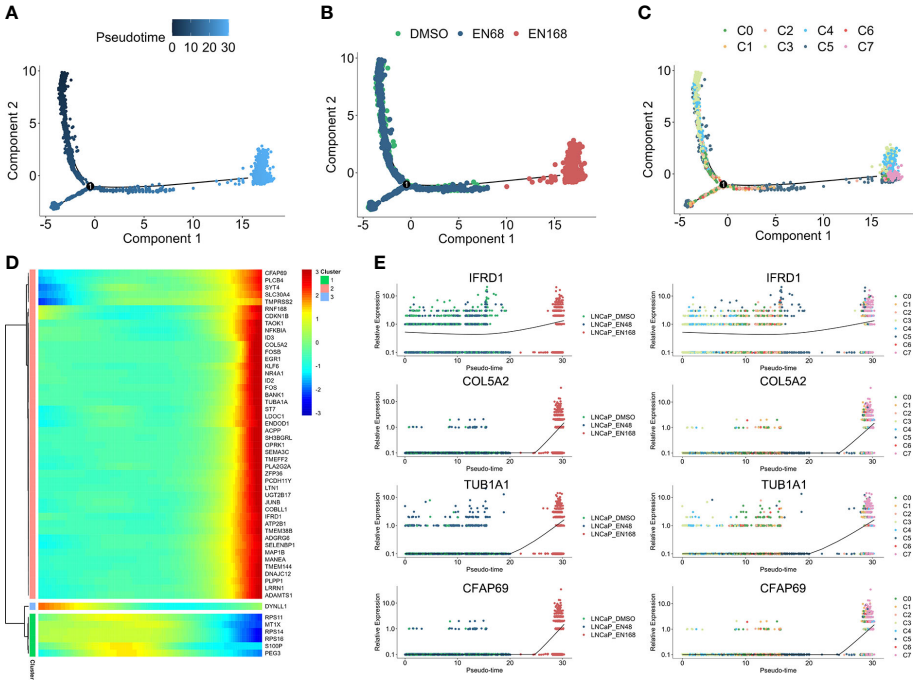

FIGURE 2
The progression trajectory of enzalutamide-induced and pseudo-time gene expression pattern. Pseudo-trajectory **(A)**, cell type **(B)**, and cell clusters **(C)** of enzalutamide-induced cells. **(D)** Heatmap for expression pattern of genes that induced by enzalutamide-stimulated alone with trajectory-evolved. **(E)** Expression tendency of representative genes in enzalutamide-induced model and cell clusters.

trajectory-related markers. Lasso algorithm was performed to screen the significantly prognostic genes that induced by enzalutamide in these candidate genes (Figure 3A). With the optimal lambda value of 0.025 based on minimal mean square error (Figure 3B), 10 genes [i.e., IFRD1, COL5A2, TUBA1A, CFAP69, TMEM38B, ACPP, MANEA, FOSB, SH3BGRL, and suppressor of tumorigenicity (ST7)] were identified as significantly enzalutamide-induced genes that are related to the prognosis of PCa RFS. Meanwhile, IFRD1, COL5A2, TUBA1A, and CFAP69 served as the risk factors (coefficient > 0), and TMEM388, ACPP, MANEA, FOSB, SH3BGRL, and ST7 served as protective factors (coefficient < 0) in PCa (Figure 3C). Then, an enzalutamide-related signature was constructed for the prediction of PCa RFS on the basis of 10 genes expression abundances and lasso Cox coefficient. The calculation formula is as follows: 0.316 × expression of IFRD1 + 0.211 × expression of COL5A2 +0.081 × expression of TUBA1A + 0.071 × expression of CFAP69 + (−0.020 × expression of TMEM38B) + (−0.076 × expression of APCC) + (−0.088 × expression of MANEA) + (−0.095 × expression of FOSB) + (−0.113× expression of SH3BGRL) + (−0.237 × expression of ST7). We divided the patients into high- and low-risk groups on the basis of the ENZ-sig and found that patients with higher ENZ-sig presented worse RFS than those with lower ENZ-sig ($p < 0.0001$, Figure 3D). Moreover, the distribution of the risk score and the RFS status are displayed in Figure 3E. It is clear that the higher the risk score, the more inclined to relapse. The ROC analysis indicated that the prognostic accuracy values for 3-, 5-, and 7-year RFS were 0.761, 0.706, and 0.742, respectively, for ENZ-sig (Figure 3F).

3.4 Evaluating the clinical relevance of ENZ-sig in prostate cancer

To explore the clinical relevance of ENZ-sig, we further investigated the relationship between ENZ-sig and clinicopathological features, including Gleason score, tumor stage, N stage, and metastasis. The result revealed that ENZ-sig was significantly positively correlated with Gleason score (Figure 3G), tumor stage (Figure 3H), N stage (Figure 3I), and metastasis (Figure 3J), indicating that the levels of ENZ-sig were significantly related to the progression of PCa. The univariate (Figure 3K) and multivariate (Figure 3L) Cox regression model were further performed to discover the prognostic value of ENZ-sig in PCa. We found that tumor stage (HR = 4.863; 95% CI 2.656 to 8.902; $p < 0.001$), Gleason score (HR = 4.299; 95% CI, 2.774 to 6.661; $p < 0.001$), and ENZ-sig (HR = 4.911; 95% CI, 3.303 to 7.303; $p < 0.001$) were significantly associated with PCa RFS. Moreover, tumor stage (HR = 2.621; 95% CI, 1.380 to 4.979; $p = 0.003$), Gleason score (HR = 2.079; 95% CI, 1.252 to 3.451; $p = 0.005$), and ENZ-sig (HR = 2.909; 95% CI, 1.805 to 4.688; $p < 0.001$) were the independent prognostic factors for predicting RFS in Pca, and its predicting abilities were unrestricted with the existing clinical variables, demonstrating the clinical utility of ENZ-sig for predicting RFS in PCa.

3.5 Validation of the enzalutamide-induced signature in independent datasets

Following the same calculation formula, we leveraged six independent datasets (GSE70768, GSE94767, E-MTAB-6128,

10.3389/fendo.2023.1148898

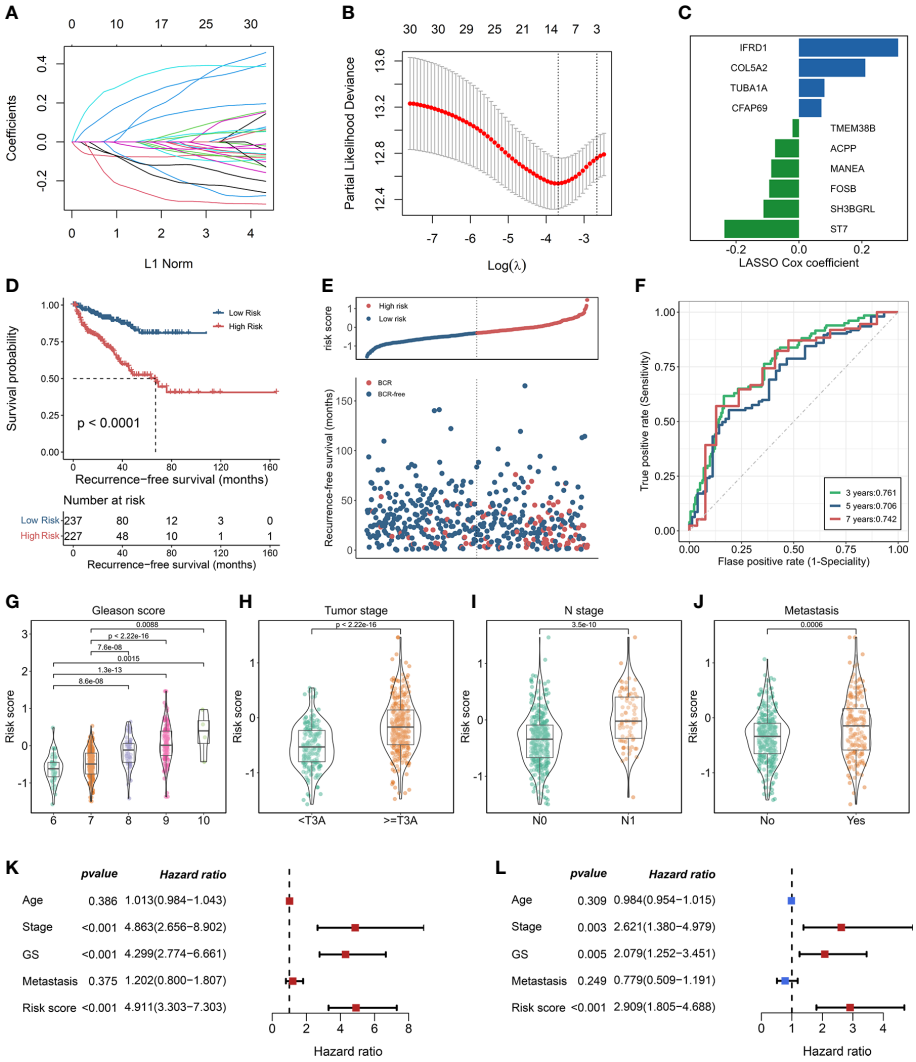

FIGURE 3
Construction of enzalutamide-induced signature and its clinical relevance. **(A)** Lasso cox regression coefficients of 31 candidate genes. **(B)** Partial likelihood deviance of candidate genes derived from lasso Cox regression analysis with 10-fold cross-validation. Two vertical dotted lines represent minimum mean cross-validation error and one standard error of the minimum, respectively. **(C)** The coefficients of 10 genes selected from lasso Cox regression model. **(D)** Kaplan–Meier curve in terms of RFS for high-risk and low-risk patients divided by enzalutamide-induced signature. **(E)** The risk score and recurrence-free survival status based on TCGA-PRAD cohort. **(F)** The receiver operating characteristics curve for the prediction of 3-, 5-, and 7-year RFS based on the risk score derived from enzalutamide-induced signature. The abundance of risk score calculated by enzalutamide-induced signature in different clinicopathological characteristics, including Gleason score **(G)**, tumor stage **(H)**, N stage **(I)**, and metastasis status **(J)**. Univariate Cox regression analysis **(K)** and multivariate Cox regression analysis **(L)** for enzalutamide-induced signature and clinical variables, including age, stage, Gleason score, and metastasis status.

DFKZ, GSE21034, and GSE70769) to verify the robustly predicting performance of ENZ-sig for PCa RFS (Figures 4A–F). As expected, PCa RFS was correlated with ENZ-sig, and patients with higher risk scores presented significantly worse RFS compared with those with lower risk scores in the six PCa datasets (GSE70768: HR = 3.77, p = 0.002; GSE94767: HR = 2.6, p = 0.00304; E-MTAB-6128: HR = 3.93, p = 0.0229; DKFZ: HR = 6.22, p = 2.25e-07; GSE21034: HR = 5.19, p = 8.37e-08; and GSE70769: HR = 5.15, p = 2.91e-07). Moreover, the multivariate Cox regression analysis revealed that ENZ-sig was a significantly independent prognostic factor in GSE70768 (HR = 2.84, p = 0.04), DKFZ (HR = 3.21, p = 0.01), GSE21034 (HR = 7.72, p = 0.02), and GSE70769 (HR = 2.80, p = 0.02) cohorts. Importantly, the ROC analysis showed a stable predicting ability of ENZ-sig for PCa RFS in these six cohorts, highlighting that ENZ-sig was a reliable and effective predictor for PCa RFS.

3.6 Development of the nomogram and evaluation of its clinical utility

On the basis of our findings that the ENZ-sig calculated by ENZ-sig as well as Gleason score and tumor stage are predictive of

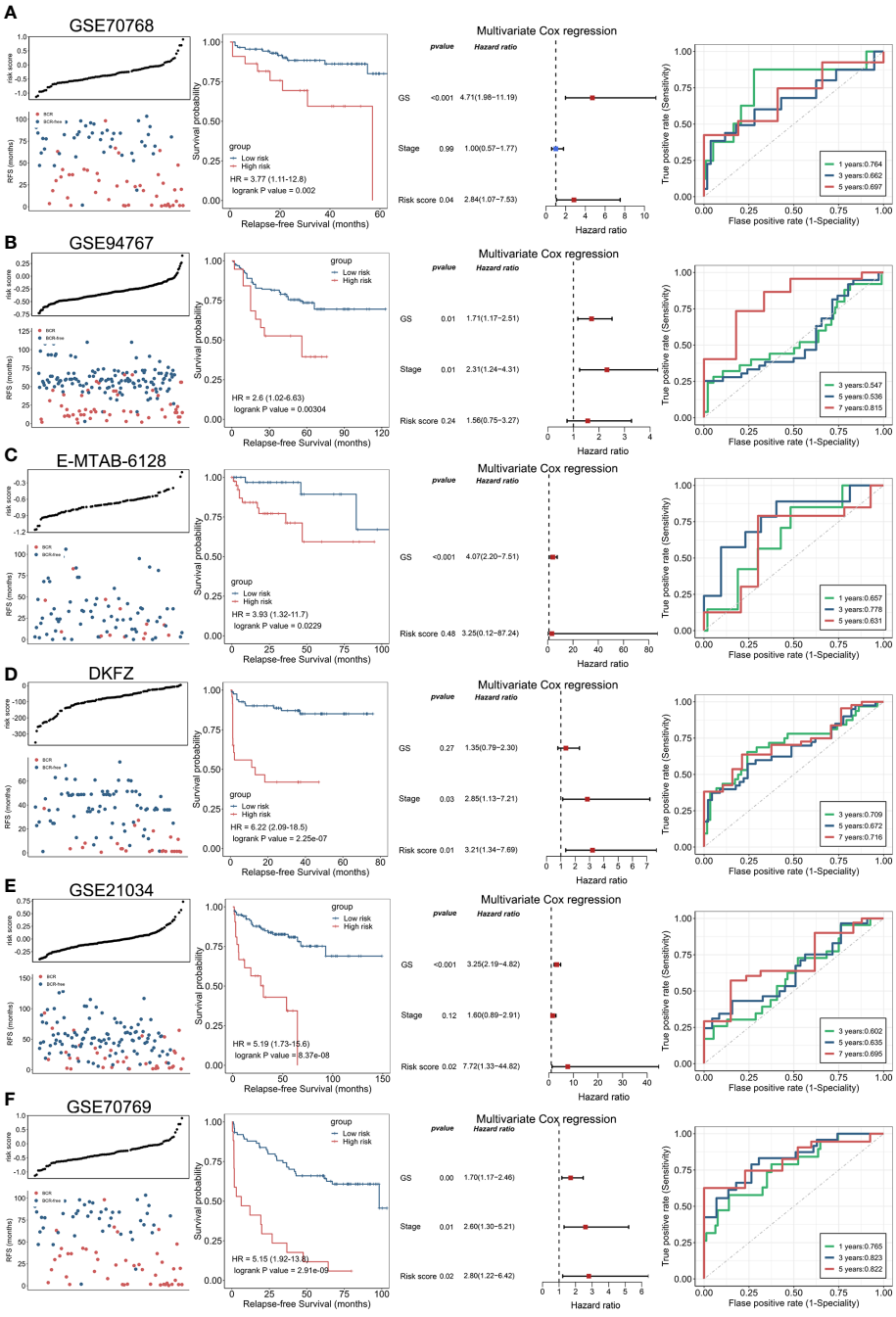

FIGURE 4
Validation of enzalutamide-induced signature in independent cohort. The plot of risk score and RFS status, Kaplan–Meier curve, multivariate Cox regression analysis, and receiver operating characteristics curve for evaluating the predicting ability of enzalutamide-induced signature in GSE70768 **(A)**, GSE94767 **(B)**, E-MTAB-6128 **(C)**, DFKZ **(D)**, GSE21034 **(E)**, and GSE70769 **(F)** cohorts, respectively.

PCa RFS, we constructed nomograms for predicting patients' 3-, 5-, and 7-year RFS, respectively (Figure 5A). Figure 5B shows that the AUC values of the nomograms were 0.791, 0.794, and 0.83 for 3-, 5-, and 7-year RFS, respectively. Nomogram showed higher AUC values than Gleason score, tumor stage, and ENZ-sig, indicating that the predictability of RFS was improved by integrating these prognostic features. In Figure 5C, the calibration curves suggested that the nomogram-predicted probability is relatively close to the actual RFS outcome (diagonal line).

3.7 Functional characteristics related to enzalutamide-induced signature

To discover the biological mechanisms involving the ENZ-sig, we first evaluated the ENZ-sig levels of each cell according to the expression of 10 ENZ-sig genes by AUCell method. It is noticed that AUCell, a scoring system, uses the AUC to measure the score of gene set. The histogram presented the distribution of ENZ-sig levels and cellular frequency (Figure 6A). With the optimal threshold

10.3389/fendo.2023.1148898

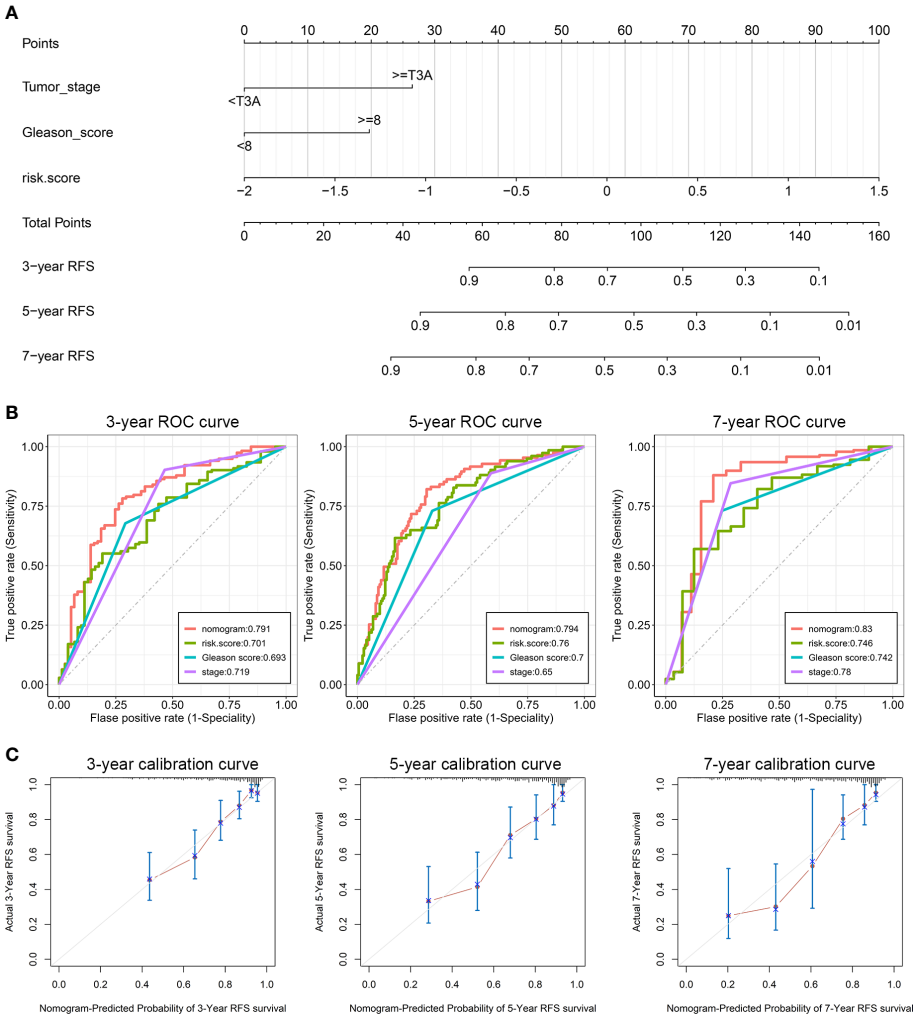

FIGURE 5
Clinical utilization of enzalutamide-induced signature. Nomograms **(A)**, including the ROC curves **(B)** and the calibration plots **(C)** for the prediction of relapse-free survival for patients with PCa at 3, 5, and 7 years, respectively.

estimated by AUCell, cells were divided into high–ENZ-sig and low–ENZ-sig groups. The distribution of the cells with AUC > 0.19 (Figure 6B) and ENZ-sig activity (Figure 6C) was shown on the t-distributed stochastic neighbor embedding diagram. As expected, the proportion of high–ENZ-sig group was higher in EN168 model and C7 than that in the other models or clusters (Figure 6D). Then, biological enrichment analysis was performed on the basis of the DEGs between high ENZ-sig and low ENZ-sig. As shown in Figure 6E, cell cycle–related pathways, i.e., E2F targets, G2M checkpoint, mitotic spindle, and Myc targets, were significantly enriched in the high–ENZ-sig group, demonstrating the strong relationship between ENZ-sig and cell cycle. We further conducted the GSVA analysis and compared the differential pathway score between the high-risk and low-risk patients in TCGA-PRAD. The result showed that patients with higher score of ENZ-sig were more activated in the cell cycle pathway than patients with lower score of ENZ-sig (Figure 6F). The GSEA was further verified the relation between ENZ-sig and cell cycle pathway. As shown in Figure 6G, cell cycle–related pathways, i.e., E2F targets (NES = 1.96, FDR = 8.33e-10), G2M checkpoint (NES = 1.77, FDR = 2.80e-06), and mitotic spindle (NES = 1.39, FDR = 0.014), were significantly enriched in the high-risk group. The correlation analysis revealed the significantly positive relation between ENZ-sig and cell cycle score in PCa [correlation coefficient (corr) = 0.256, p = 7.62e-09; Figure 6H], indicating that ENZ-sig mediated the activation of cell cycle pathway that contributed to increasing risk of progression and poor outcome for PCa. Moreover, cell cycle–related genes, e.g., CDC20, PLK1, CDC45, CDK1, CDKN2C, MCM2, E2F5, and E2F3, were significantly upregulated in high–ENZ-sig group (Figure 6I).

3.8 Ability of model in predicting drug sensitivity

Given the significantly prognostic value of ENZ-sig in the prediction of PCa RFS, we further explore the relationship between ENZ-sig and drug sensitivity. First, we measured the half-maximal inhibitory concentration (IC50) of each drug/

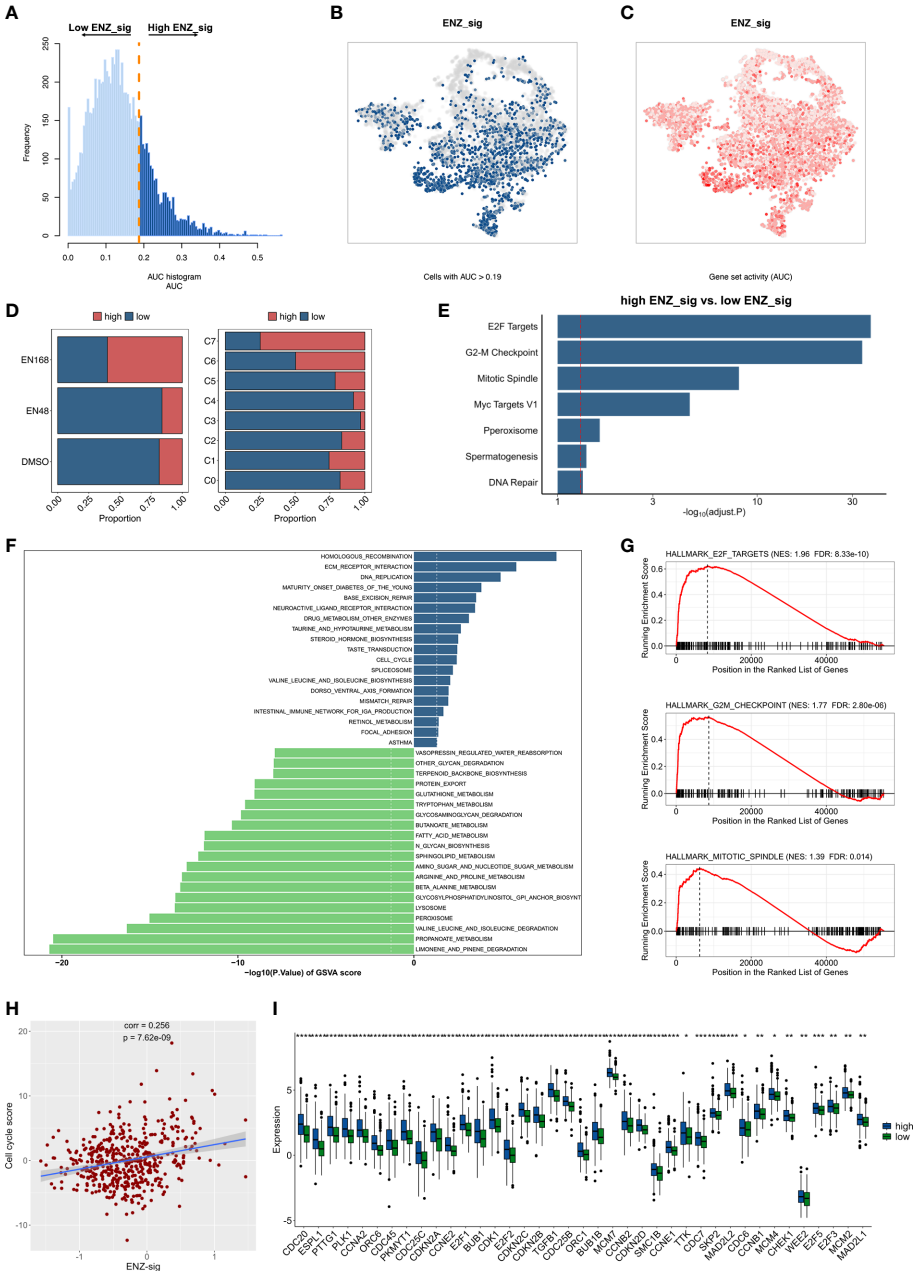

FIGURE 6
Biological pathway enrichment related to enzalutamide-induced signature. **(A)** The distribution of AUC and cell frequency. **(B)** AUC and cell frequency. **(B)** T-distributed stochastic neighbor embedding (Tsne) diagram for cells with AUC higher than selected threshold. Blue dots indicate cells with higher than 0.19, and gray dots indicates cells with less than 0.19. **(C)** Tsne diagram for ENZ-sig activity that colored by AUC. The deeper color represents a larger AUC. **(D)** The distribution of high ENZ-sig cells and low ENZ-sig cells in enzalutamide-stimulated models and clusters. **(E)** Bar plot for enrichment analysis based on the differentially expressed genes between high ENZ-sig and low ENZ-sig group. Red dotted line represents adjusted p-value less than 0.05. **(F)** Gene set variation analysis between high-risk and low-risk group stratified by enzalutamide-induced signature. Dotted line indicates p-value less than 0.05. **(G)** Gene set enrichment analysis in the high-risk group and the low-risk group. **(H)** Correlation between ENZ-sig and cell cycle score in PCa. **(I)** Box plot shows the statistically significant genes related to cell cycle pathway between the high-risk and low-risk groups. Statistical significance: *p < 0.05; **p < 0.01; ***p < 0.001; ****p < 0.0001.

compound in TCGA-PRAD dataset by "oncoPredict" package. Then, correlation analysis was performed between IC50 and ENZ-sig. The overview result is displayed in Figure 7A. We noticed that four cell cycle–targeted drugs, i.e., dinaciclib, MK-1775, AZD7762, and MK-8776, were significantly related to ENZ-sig. In detail, the sensitivity of dinaciclib was positively correlated with ENZ-sig (corr = 0.274, p = 5.30e-10; Figure 7B). The IC50 of dinaciclib was higher in high–ENZ-sig group than that in low–ENZ-sig group (p = 8.8e-06; Figure 7B). Moreover, in Figures 7C–E, MK-1775 (corr = −0.202, p = 5.62e-06), AZD7762 (corr = −0.339, p = 9.15e15), and MK-8776 (corr = −0.195, p = 1.19e-05) presented a significantly negative correlation with ENZ-sig. Furthermore, patients in the high–ENZ-sig group have lower IC50 of MK-1775 (p = 8.8e-05), AZD7762 (p = 2.8e-12), and MK-8776 (p = 0.00052)

10.3389/fendo.2023.1148898

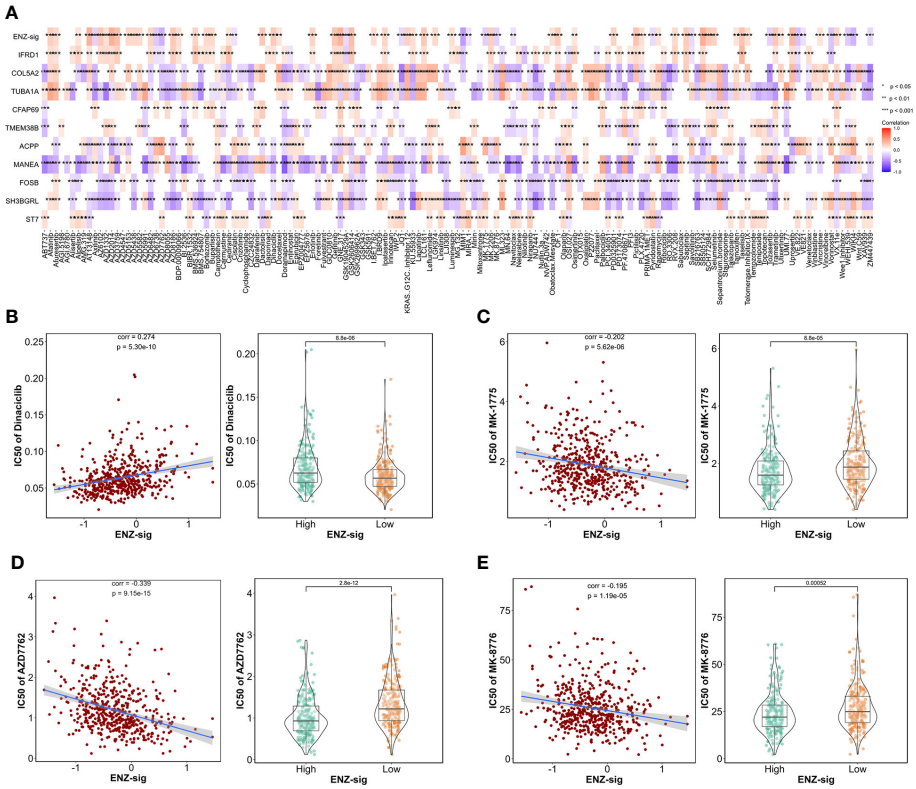

FIGURE 7
Ability of model in predicting drug sensitivity. **(A)** Heatmap plot indicates the correlation between drugs/compounds, ENZ-sig, and 10 ENZ-signature genes. Scatter diagram and box plot show the relationship between the sensitivity of dinaciclib **(B)**, MK-1775 **(C)**, AZD7762 **(D)**, MK-8776 **(E)**, and ENZ-sig.

than those in the low–ENZ-sig group, indicating that patients with higher ENZ-sig were more sensitive with cell cycle–targeted drug/compound in PCa.

4 Discussions

The extensive application of scRNA-seq technologies facilitates the comprehension of cell heterogeneity and genomic characteristics that mediated by drug treatment (14). However, enzalutamide-mediated transcriptional activity in scRNA-seq resolution has not been obtained. Leveraging scRNA-seq analysis, we integrated the three enzalutamide-simulated models (i.e., DMSO, ENZ-48, and ENZ-168) and distinguished eight subclusters. Notably, unlike other clusters, the proportion of cells in C7 was largely derived from ENZ-168 model. Furthermore, the underlying biological pathway in C7 was more activated in androgen response, epithelial–mesenchymal transition, fatty acid metabolism, and PI3K/AKT/MTOR signaling than those in the other cell clusters, indicating that C7 was a tumor-promoting cluster evoking by enzalutamide. For further exploring the related genes that induced by enzalutamide, time trajectory analysis was performed following the enzalutamide-stimulated timeline (0, 48, and 168 h). We identified several cancer-related genes that presented marked dynamic expression pattern corresponding to enzalutamide-stimulated timeline.

The intersected gene set between differentially expressed markers in C7 and dynamically changed genes in time trajectory analysis was further leveraged to constructed risk model. Thirty-one candidate genes were screened and selected by lasso Cox regression model, and 10 significant enzalutamide-induced genes (IFRD1, COL5A2, TUBA1A, CFAP69, TMEM388, ACPP, MANEA, FOSB, SH3BGRL, and ST7) related to PCa RFS were remained. It is reported that IFRD1 (known as interferon-related developmental regulator 1) encoded a protein related to interferon-γ and was significantly correlated with survival outcome in colon cancer (15). COL5A2 promotes proliferation and invasion in PCa and is related to the prediction of RFS for patients with PCa (16). Moreover, COL5A2 was identified as enzalutamide-resistant genes in CRPC cells *in vitro* (17). Wang et al. showed that TUBA1A, known as tubulin α 1a, was a potential prognostic marker and therapeutic target in gastric cancer (18). CFAP69 has been demonstrated to be a prognostic marker that is related to the survival of breast cancer patients (19). TMEM38B, as regulators of endoplasmic reticulum (ER) calcium storage, was induced by KLF9, contributing to the release of calcium from ER, aggravation of ER stress, and molecular death (20). ACPP (prostate acid phosphate) has shown to be a prognostic factor for predicting the RFS in PCa and to be correlated with CRPC bone metastases (21). MANEA is the sole endo-acting glucoside hydrolase related to N-glycan trimming and disrupting N-linked glycosylation as therapeutic agents for cancer (22). Barrett et al. reported that FOSB is required for migration and invasion in

PCa cells (23). Kwon et al. indicated that the declining expression of SH3BGRL was related to the aggressiveness of PCa (24). ST7 was demonstrated to function as tumor suppressor in PCa by remodeling tumor microenvironment (25). Collectively, except for the five genes (COL5A2, ACPP, FOSB, SH3BGRL, and ST7) that function as important biomarkers in PCa, the significant role of another five genes (IFRD1, TUBA1A, CFAP69, TMEM38B, and MANEA) in PCa is still not demonstrated, which needs further investigation. Whereas, all these 10 enzalutamide-induce genes likely play a significant role in PCa and may serve as biomarkers for prognosis of the disease. Interestingly, we noticed that IFRD1 presented the highest lasso Cox coefficient among these 10 genes, suggesting that IFRD1 was making the most vital contribution compared with other nine genes.

Given the vitally prognostic role of these 10 enzalutamide-induced genes, we constructed a predicting model, ENZ-sig, based on transcriptional expression and lasso Cox coefficient of each gene. ENZ-sig presented robust ability to classify patients into high-risk group and low-risk group with significantly different RFSs. Although several risk stratification signatures have been developed for predicting RFS of PCa. Hu et al. reported an overall survival (OS)–related signature for predicting PCa OS based on the expression levels of five autophagy-related genes (ARGs) and a disease-free survival (DFS)–related signature for the prediction of PCa DFS based on the expression of 22 ARGs (26). Mei et al. developed an m7G-related prognostic signature for the prediction of PCa RFS leveraging the data from TCGA and GEO (27). Feng et al. screened and selected 10 genes for establishing circadian clock related signature as a promising tool for the prediction of PCa RFS (28). However, the predicting accuracy and robustness of validation limited their clinical utilization, and, more importantly, enzalutamide-related signature for predicting PCa RFS has not been described yet. In our study, the ENZ-sig was effectively validated in six independent datasets (i.e., GSE70768, GSE94767, E-MTAB-6128, DFKZ, GSE21034, and GSE70769). In these datasets, ENZ-sig has successfully stratified patients into two groups, and the statistical significance in RFS between these two groups was found, strongly indicating the effective and robust prognostic ability of ENZ-sig for predicting PCa RFS.

We further extended the clinical utilization of ENZ-sig by examining the correlation between ENZ-sig and FDA-approved drugs for PCa. The result showed that ENZ-sig was significantly negatively correlated with the IC50 of three cell cycle–targeted drugs (i.e., MK-1775, AZD7762, and MK-8776), suggesting that patients with high ENZ-sig are more sensitive to these cell cycle–targeted drugs than those with low ENZ-sig. It is reported that the combination of enzalutamide and Chk1/2 inhibitor AZD7762 presented additive and synergistic therapeutic effects in xenograft and patient-derived tumor xenograft models *in vivo* (29). Moreover, MU380, a more effective analog of Chk1 inhibitors MK-8776, significantly enhances the sensitivity of human docetaxel-resistant PCa cells to gemcitabine through inducing mitotic catastrophe (30). Furthermore, Bridges et al. illustrated that MK-1775, a novel Wee1 kinase inhibitor, could promote the sensitivity of radiotherapy for p53-defective human tumor cells (30). Given the impressive role of these three cell cycle inhibitors in PCa treatment, ENZ-sig may serve as a clinical indicator not only for the prognosis in RFS but also for supporting the clinical evaluation of cell cycle–targeted drugs in combination therapy for PCa.

Our results provided evidence and insight on the potential utility of ENZ-sig in PCa prognosis and clinical use. However, there are some limitations in the current ENZ-sig model. More enzalutamide-induced genes ought to be discovered to optimize the ENZ-sig model. In addition, the 10 enzalutamide-induced markers identified in the study warrant further experimental investigation to unfold their vital functions in PCa and to explore new therapies targeting these molecules.

5 Conclusions

By integrating scRNA-seq and bulk RNA sequencing analysis, we demonstrated a heterogeneous sub-cluster that induced by enzalutamide and identified ENZ-sig for the prediction of PCa RFS in TCGA-PRAD. The effective and robust predictability of this model was validated in six independent datasets. Moreover, ENZ-sig showed a high correlation with cell cycle pathway, which may be utilized in clinic to accurately predict RFS and provided combination therapy strategies of patients with PCa.

Data availability statement

The original contributions presented in the study are included in the article/Supplementary Material. Further inquiries can be directed to the corresponding authors.

Author contributions

YF: software, formal analysis, investigation, writing—original draft, and visualization. ZT: methodology and resources. YD: visualization and resources. SC: data curation and writing—review and editing. RL: resources and data curation. JL: data curation and validation. JW: methodology and visualization. HH: formal analysis and resources. GZ: data curation. JY: investigation, resources, writing—original draft, and funding acquisition. ZH: conceptualization, methodology, project administration, writing—review and editing, and funding acquisition. WZ: conceptualization, supervision, project administration, writing—original draft, writing—review and editing, and funding acquisition. All authors contributed to the article and approved the submitted version.

Funding

This work was supported by grants from the National Natural Science Foundation of China 82072813 (WZ), Science and Technology Projects in Guangzhou 202201010726 (ZH), Science and Technology Development Fund of Macau SAR 0031/2021/A (WZ), Emergency Key Program of Guangzhou Laboratory EKPG21-04 (WZ), Guangdong Basic and Applied Basic Research Foundation

2020A1515110792, 2022A1515010342 (JY), and Guangdong Basic and Applied Basic Research Foundation 2022A1515110245 (YD).

Acknowledgments

We sincerely acknowledge the contributions from TCGA and GEO.

Conflict of interest

The authors declare that the research was conducted in the absence of any commercial or financial relationships that could be construed as a potential conflict of interest.

Publisher's note

Supplementary material

The Supplementary Material for this article can be found online at: https://www.frontiersin.org/articles/10.3389/fendo.2023.1148898/full#supplementary-material

References

1. Siegel RL, Miller KD, Fuchs HE, Jemal A. Cancer statistics, 2022. *CA: Cancer J Clin* (2022) 72(1):7–33. doi: 10.3322/caac.21708

2. Rebello RJ, Oing C, Knudsen KE, Loeb S, Johnson DC, Reiter RE, et al. Prostate cancer. *Nat Rev Dis Primers* (2021) 7(1):9. doi: 10.1038/s41572-020-00243-0

3. Desai K, McManus JM, Sharifi N. Hormonal therapy for prostate cancer. *Endocrine Rev* (2021) 42(3):354–73. doi: 10.1210/endrev/bnab002

4. Nguyen PL, Alibhai SM, Basaria S, D'Amico AV, Kantoff PW, Keating NL, et al. Adverse effects of androgen deprivation therapy and strategies to mitigate them. *Eur Urol* (2015) 67(5):825–36. doi: 10.1016/j.eururo.2014.07.010

5. Chen Z, Lan X, Thomas-Ahner JM, Wu D, Liu X, Ye Z, et al. Agonist and antagonist switch DNA motifs recognized by human androgen receptor in prostate cancer. *EMBO J* (2015) 34(4):502–16. doi: 10.15252/embj.201490306

6. Haffner MC, Zwart W, Roudier MP, True LD, Nelson WG, Epstein JI, et al. Genomic and phenotypic heterogeneity in prostate cancer. *Nat Rev Urol* (2021) 18 (2):79–92. doi: 10.1038/s41585-020-00400-w

7. Lim ZF, Ma PC. Emerging insights of tumor heterogeneity and drug resistance mechanisms in lung cancer targeted therapy. *J Hematol Oncol* (2019) 12(1):134. doi: 10.1186/s13045-019-0818-2

8. Taavitsainen S, Engedal N, Cao S, Handle F, Erickson A, Prekovic S, et al. Single-cell atac and rna sequencing reveal pre-existing and persistent cells associated with prostate cancer relapse. *Nat Commun* (2021) 12(1):5307. doi: 10.1038/s41467-021-25624-1

9. Li R, Qu H, Wang S, Wei J, Zhang L, Ma R, et al. Gdcrnatools: An R/Bioconductor package for integrative analysis of lncrna, mirna and mrna data in gdc. *Bioinf (Oxford England)* (2018) 34(14):2515–7. doi: 10.1093/bioinformatics/bty124

10. Hao Y, Hao S, Andersen-Nissen E, Mauck WM3rd, Zheng S, Butler A, et al. Integrated analysis of multimodal single-cell data. *Cell* (2021) 184(13):3573–87.e29. doi: 10.1016/j.cell.2021.04.048

11. Trapnell C, Cacchiarelli D, Grimsby J, Pokharel P, Li S, Morse M, et al. The dynamics and regulators of cell fate decisions are revealed by pseudotemporal ordering of single cells. *Nat Biotechnol* (2014) 32(4):381–6. doi: 10.1038/nbt.2859

12. Subramanian A, Tamayo P, Mootha VK, Mukherjee S, Ebert BL, Gillette MA, et al. Gene set enrichment analysis: A knowledge-based approach for interpreting genome-wide expression profiles. *Proc Natl Acad Sci United States America* (2005) 102 (43):15545–50. doi: 10.1073/pnas.0506580102

13. Aibar S, González-Blas CB, Moerman T, Huynh-Thu VA, Imrichova H, Hulselmans G, et al. Scenic: Single-cell regulatory network inference and clustering. *Nat Methods* (2017) 14(11):1083–6. doi: 10.1038/nmeth.4463

14. Zhang Y, Wang D, Peng M, Tang L, Ouyang J, Xiong F, et al. Single-cell rna sequencing in cancer research. *J Exp Clin Cancer Res CR* (2021) 40(1):81. doi: 10.1186/s13046-021-01874-1

15. Lewis MA, Sharabash N, Miao ZF, Lyons LN, Piccirillo J, Kallogjeri D, et al. Increased Ifrd1 expression in human colon cancers predicts reduced patient survival. *Digestive Dis Sci* (2017) 62(12):3460–7. doi: 10.1007/s10620-017-4819-0

16. Ren X, Chen X, Fang K, Zhang X, Wei X, Zhang T, et al. Col5a2 promotes proliferation and invasion in prostate cancer and is one of seven Gleason-related genes that predict recurrence-free survival. *Front Oncol* (2021) 11:583083. doi: 10.3389/fonc.2021.583083

17. Kohrt SE, Awadallah WN, Phillips RA3rd, Case TC, Jin R, Nanda JS, et al. Identification of genes required for enzalutamide resistance in castration-resistant prostate cancer cells in vitro. *Mol Cancer Ther* (2021) 20(2):398–409. doi: 10.1158/1535-7163.Mct-20-0244

18. Wang D, Jiao Z, Ji Y, Zhang S. Elevated Tuba1a might indicate the clinical outcomes of patients with gastric cancer, being associated with the infiltration of macrophages in the tumor immune microenvironment. *J gastrointestinal liver diseases: JGLD* (2020) 29(4):509–22. doi: 10.15403/jgld-2834

19. Tian Y, Wang J, Wen Q, Gao A, Huang A, Li R, et al. The significance of tumor microenvironment score for breast cancer patients. *BioMed Res Int* (2022) 2022:5673810. doi: 10.1155/2022/5673810

20. Fink EE, Moparthy S, Bagati A, Bianchi-Smiraglia A, Lipchick BC, Wolff DW, et al. Xbp1-Klf9 axis acts as a molecular rheostat to control the transition from adaptive to cytotoxic unfolded protein response. *Cell Rep* (2018) 25(1):212–23.e4. doi: 10.1016/j.celrep.2018.09.013

21. Larson SR, Chin J, Zhang X, Brown LG, Coleman IM, Lakely B, et al. Prostate cancer derived prostatic acid phosphatase promotes an osteoblastic response in the bone microenvironment. *Clin Exp metastasis* (2014) 31(2):247–56. doi: 10.1007/s10585-013-9625-2

22. Sobala ŁF, Fernandes PZ, Hakki Z, Thompson AJ, Howe JD, Hill M, et al. Structure of human endo-α-1,2-Mannosidase (Manea), an antiviral host-glycosylation target. *Proc Natl Acad Sci United States America* (2020) 117(47):29595–601. doi: 10.1073/pnas.2013620117

23. Barrett CS, Millena AC, Khan SA. Tgf-β effects on prostate cancer cell migration and invasion require fosb. *Prostate* (2017) 77(1):72–81. doi: 10.1002/pros.23250

24. Kwon OK, Ha YS, Lee JN, Kim S, Lee H, Chun SY, et al. Comparative proteome profiling and mutant protein identification in metastatic prostate cancer cells by quantitative mass spectrometry-based proteogenomics. *Cancer Genomics Proteomics* (2019) 16(4):273–86. doi: 10.21873/cgp.20132

25. Hooi CF, Blancher C, Qiu W, Revet IM, Williams LH, Ciavarella ML, et al. St7-mediated suppression of tumorigenicity of prostate cancer cells is characterized by remodeling of the extracellular matrix. *Oncogene* (2006) 25(28):3924–33. doi: 10.1038/sj.onc.1209418

26. Hu D, Jiang L, Luo S, Zhao X, Hu H, Zhao G, et al. Development of an autophagy-related gene expression signature for prognosis prediction in prostate cancer patients. *J Trans Med* (2020) 18(1):160. doi: 10.1186/s12967-020-02323-x

27. Mei W, Jia X, Xin S, Liu X, Jin L, Sun X, et al. A N(7)-Methylguanine-Related gene signature applicable for the prognosis and microenvironment of prostate cancer. *J Oncol* (2022) 2022:8604216. doi: 10.1155/2022/8604216

28. Feng D, Xiong Q, Zhang F, Shi X, Xu H, Wei W, et al. Identification of a novel nomogram to predict progression based on the circadian clock and insights into the tumor immune microenvironment in prostate cancer. *Front Immunol* (2022) 13:777724. doi: 10.3389/fimmu.2022.777724

29. Karanika S, Karantanos T, Li L, Wang J, Park S, Yang G, et al. Targeting DNA damage response in prostate cancer by inhibiting androgen receptor-CDC6-ATR-Chk1 signaling. *Cell Rep* (2017) 18(8):1970–81. doi: 10.1016/j.celrep.2017.01.072

30. Bridges KA, Hirai H, Buser CA, Brooks C, Liu H, Buchholz TA, et al. MK-1775, a novel Wee1 kinase inhibitor, radiosensitizes p53-defective human tumor cells. *Clin Cancer Res* (2011) 17(17):5638–48. doi: 10.1158/1078-0432.CCR-11-0650

frontiers | Frontiers in Endocrinology

TYPE Systematic Review
PUBLISHED 22 March 2023
DOI 10.3389/fendo.2023.1138114

OPEN ACCESS

EDITED BY
Yuxuan Song,
Peking University People's Hospital, China

REVIEWED BY
Ruizhi Xue,
First Hospital of Shanxi Medical University, China
Andreas G. Moraitis,
Corcept, United States
Ana Valea,
Iuliu Hatieganu University of Medicine and Pharmacy Cluj-Napoca, Romania
Xiang Chen,
Xiangya Hospital, Central South University, China

*CORRESPONDENCE
Yushi Zhang
pumchzhangyushi@126.com

SPECIALTY SECTION
This article was submitted to Adrenal Endocrinology, a section of the journal Frontiers in Endocrinology

RECEIVED 05 January 2023
ACCEPTED 01 March 2023
PUBLISHED 22 March 2023

CITATION
Liao Z, Gao Y, Zhao Y, Wang Z, Wang X, Zhou J and Zhang Y (2023) Pure androgen-secreting adrenal tumor (PASAT): A rare case report of bilateral PASATs and a systematic review. *Front. Endocrinol.* 14:1138114. doi: 10.3389/fendo.2023.1138114

Pure androgen-secreting adrenal tumor (PASAT): A rare case report of bilateral PASATs and a systematic review

Zhangcheng Liao[1], Yuting Gao[2], Yang Zhao[1], Zhan Wang[1], Xu Wang[1], Jiaquan Zhou[3] and Yushi Zhang[1]*

[1]Department of Urology, Peking Union Medical College Hospital, Chinese Academy of Medical Science and Peking Union Medical College, Beijing, China, [2]Department of Endocrinology, Peking Union Medical College Hospital, Chinese Academy of Medical Science and Peking Union Medical College, Beijing, China, [3]Department of Urology, Hainan General Hospital, Haikou, China

Background: Adult pure androgen–secreting adrenal tumors (PASATs) are extremely rare, and their characteristics are largely unknown.

Methods: A rare case of adult bilateral PASATs was reported, and a systematic literature review of adult PASATs was conducted to summarize the characteristics of PASATs.

Results: In total, 48 studies, including 40 case reports and 8 articles, were identified in this review. Analysis based on data of 42 patients (including current case and 41 patients from 40 case reports) showed that average age was 40.48 ± 15.80 years (range of 18-76). The incidence of adult PASAT peaked at 21-30 years old, while that of malignant PASAT peaked at 41-50 years old. Most PASAT patients were female (40/42, 95.23%), and hirsutism was the most common symptom (37/39, 94.87%). Testosterone (T) was the most commonly elevated androgen (36/42, 85.71%), and 26 of 32 tested patients presented increased dehydroepiandrosterone sulfate (DS) levels. In malignancy cases, disease duration was significantly decreased (1.96 vs. 4.51 years, P=0.025), and tumor diameter was significantly increased (8.9 vs. 4.9 cm, p=0.011). Moreover, the androgen levels, namely, T/upper normal range limit (UNRL) (11.94 vs. 4.943, P=0.770) and DS/UNRL (16.5 vs. 5.28, P=0.625), were higher in patients with malignancy. In total, 5 out of 7 patients showed an increase in DS or T in the human chorionic gonadotropin (HCG) stimulation test. Overall, 41 out of 42 patients (including current case) underwent adrenal surgery, and recurrence, metastasis, or death was reported in 5 out of 11 malignant patients even with adjuvant or rescue mitotane chemotherapy.

Conclusion: Adult PASAT, which is predominant in women, is characterized by virilism and menstrual dysfunction, especially hirsutism. Elevated T and DS may contribute to the diagnosis of adult PASAT, and HCG stimulation test might also be of help in diagnosis. Patients with malignant PASAT have a shorter disease duration, larger tumor sizes and relatively higher androgen levels. Surgery is recommended for all local PASATs, and Malignancy of PASAT should be fully considered due to the high risk of malignancy, poor prognosis and limited effective approaches.

KEYWORDS

pure androgen-secreting adrenal tumor (PASAT), clinical characteristics, diagnosis and treatment, adrenal venous sampling (AVS), ovarian venous sampling (OVS)

Introduction

The adrenal gland is a complex structure consisting of an inner adrenal medulla and an outer adrenal cortex. Adrenal steroid hormones are synthesized in the following three zones: aldosterone in the zona glomerulosa (ZG); glucocorticoids (particularly cortisol) in the zona fasciculata (ZF); and androgens and estrogens in the zona reticularis (ZR). Aldosterone production is regulated by the renin–angiotensin–aldosterone system, while the synthesis of cortisol and androgens is modulated by the hypothalamic–pituitary–adrenal (HPA) axis (1). The primary function of adrenocorticotropic hormone (ACTH) is to stimulate cortisol and adrenal androgen secretion by increasing their synthesis. The negative feedback from circulating cortisol suppresses the release of corticotropin-releasing hormone (CRH) and ACTH, but adrenal androgens do not have similar suppressive effects on the HPA axis. Compared to cortisol- and aldosterone-secreting tumors, androgen-secreting adrenocortical tumors are less common. Adrenocortical tumors, including androgen-secreting tumors, in children have been investigated in previous studies (2–4), but androgen-secreting adrenal tumors in adults, especially pure androgen–secreting adrenal tumors (PASATs), which are usually reported as case reports or case series, are rare. In the present study, we report a rare case of adult bilateral PASATs and conduct a systematic review of adult PASATs.

Case presentation

A 28-year-old woman was admitted to our hospital in 2022 due to oligomenorrhea and then amenorrhea. The patient (menarche at 13 years) had regular menstruation with a menstrual cycle of 30-40 days and a menstrual period of 6-7 days. The patient's menstrual cycle then shortened, and her menstrual bleeding gradually decreased from 2012. At that time, her testosterone (T) level was within the normal range according to her statement. Finally, amenorrhea occurred despite the administration of estrogen and progesterone drugs. In 2015, the T level increased to 0.91 ng/ml (normal: 0.10-0.75) despite dydrogesterone administration, and ultrasound indicated polycystic morphology in bilateral ovaries. Polycystic ovary syndrome (PCOS) was considered by physicians of other hospitals, and contraceptive drugs were prescribed. During 2019-2020, the patient presented with clitoromegaly, mild hirsutism (Ferriman–Gallwey score of 9) and amenorrhea. At the same time, bilateral adrenal tumors were reported incidentally by computed tomography (CT) in a health examination.

An endocrine investigation in 2021 showed that the patient's T levels continued to increase to 1.61 ng/ml (Table 1). In addition, androstenedione (AND), dehydroepiandrosterone sulfate (DS) and 17α-hydroxypregnenolone (17OHP) also increased to 25.67 ng/mL (normal: 0.30-2.00 ng/mL), 12,260 ng/mL (normal: 830-3,770 ng/mL) and 2.49 ng/ml (normal: 0.10-2.30 ng/ml), respectively, in the patient. The ACTH level (8 am) of this patient was 28.9 pg/ml (normal: 7.2-63.3). Both the cortisol level (10.0 μg/dl, normal: 4-22) and 24-h urinary free cortisol level (52.0 μg/24 hr, normal: 12.3-103) were normal. The cortisol level was suppressed (<1.8 μg/dl) by the 48-h low-dose dexamethasone-suppression test (0.5 mg orally every 6 hours for a total of eight doses). In addition, the levels of plasma aldosterone, catecholamine and sexual hormones, including follicle-stimulating hormone (FSH), luteinizing hormone (LH) and oestradiol, were normal. The patient underwent ACTH stimulation test, and the 17OHP level was 3.89 ng/ml at 60 minutes after administering cosyntropin (0.25 mg), which basically excluded classic and nonclassic congenital adrenal hyperplasia (CAH) according to the endocrine society clinical practice guidelines (17OHP <10 ng/ml) (5, 6). The patient's bilateral adrenal tumors were gradually enlarged (Figure 1A) and were considered to be responsible for hyperandrogenism. The patient's right adrenal tumor was removed by laparoscopic partial adrenalectomy at another hospital, and adrenocortical adenoma was identified according to pathological findings.

Because the patient's amenorrhea was not relieved, she was admitted to our hospital and underwent further endocrine and imageological examination (Figure 1B). The patient's testosterone (T), androstenedione (ADN) and dehydroepiandrosterone sulfate (DS) levels were partly decreased but still above the normal range (Table 1). Adrenal steroid hormone tests indicated that pregnenolone and dehydroepiandrosterone (DHEA) were also elevated in addition to T, DS, AND and 17OHP, while the levels of steroids located in the cortisol and aldosterone synthesis pathways were normal (Figure 2). Bilateral ovarian venous sampling (OVS) and left adrenal venous sampling (AVS) were conducted (Figure 3). The left selectivity index (SI, defined as the ratio of cortisol concentration for each adrenal vein and infra-adrenal inferior vena cava or a peripheral vein) was 5.02, which indicated successful catheterization (more than 2:1 without stimulation cosyntropin use) (7). The levels of androgens, including T, ADN, DS and DHEA, in the left adrenal vein were higher (Figure 3), which indicated that excessive androgens were produced by the left adrenal gland rather than the ovaries. The patient underwent left laparoscopic adrenalectomy in our hospital, and the surgical specimen was showed in Figure 1C. The histopathologic

TABLE 1 Changes of androgens before and after two surgeries.

	T (ng/mL)	AND (ng/mL)	DHEA (ng/mL)	DS (ng/mL)
Before surgery	1.61	25.67	ND	12260
After right adrenal tumorectomy	1.01	6.44	23.8	11802
After left adrenalectomy	0.09	0.42	2.4	124
Reference range	0.08-0.60	0.30-2.00	<13	830-3770

T, testosterone; AND, androstenedione; DHEA, dehydroepiandrosterone; DS, dehydroepiandrosterone sulfate; ND, not detected.

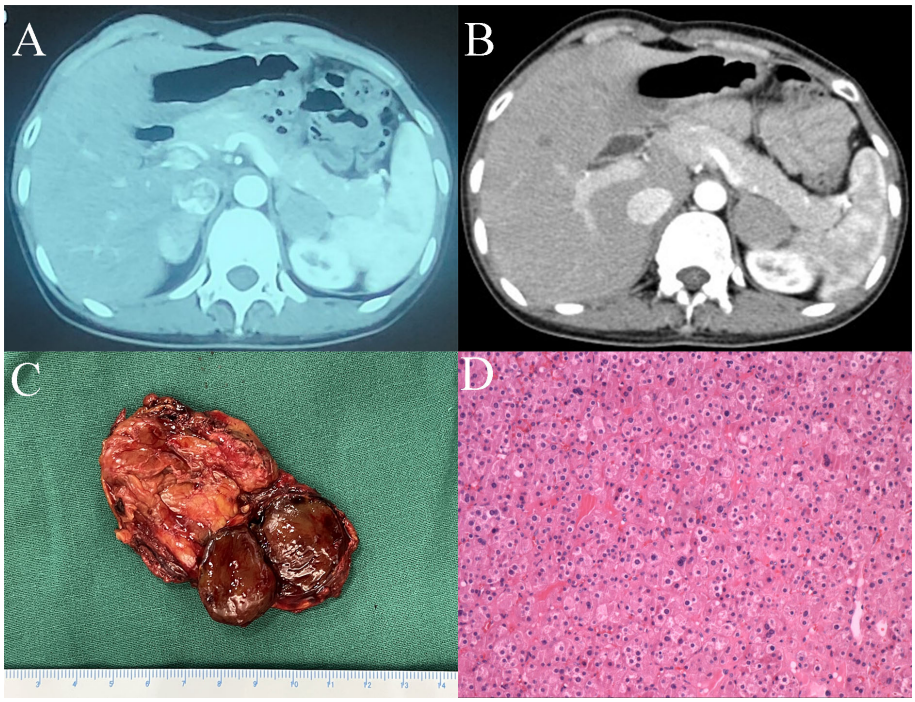

FIGURE 1
(A) CT image of bilateral adrenal tumors. **(B)** CT image of the left adrenal tumor after right adrenal tumorectomy. **(C)** Surgical specimen of the left adrenal tumor. **(D)** Haematoxylin and eosin staining of the left adrenal tumor (magnification×20).

examination confirmed the diagnosis of adrenocortical adenoma (Figure 1D). Two weeks after surgery, the levels of T, ADN and DHEA decreased to within the normal range, and the DS level decreased to below the normal level (Table 1). Then DS level returned to the normal range within 3 months. The patient's menstruation recovered to normal in 2 months after surgery, and no recurrence or metastasis was detected nearly one year after surgery.

Methods

A systematic review of the literature was performed in accordance with the Preferred Reporting Items for Systematic Reviews and Meta-Analyses (PRISMA) guidelines (Figure 4). The following search strategy was used in the PubMed online database until December 2022: ("androgen"[Title/Abstract] OR "hyperandrogenism"[Title/Abstract] OR "virilism"[Title/Abstract]) AND ("adrenocortical"[Title/Abstract] OR "adrenal"[Title/Abstract]) AND ("tumor"[Title/Abstract] OR "carcinoma"[Title/Abstract] OR "adenoma"[Title/Abstract]) NOT ("children"[Title/Abstract] OR "child"[Title/Abstract] "childhood"[Title/Abstract] OR "paediatric"[Title/Abstract] OR "peripubertal"[Title/Abstract]). Only confirmed cases of adrenal tumors exclusively secreting androgens were included in this review. The exclusion criteria for studies were as follows: (1) age < 18 years; (2) excessive secretion of cortisol, aldosterone and catecholamine, especially cortisol, because cortisol and androgen are usually produced simultaneously in certain adrenal carcinomas or adenomas (only studies with evidence to show normal cortisol in the blood or urine were included); (3) hyperandrogenic status partly or completely caused by nonadrenal factors, including polycystic ovary syndrome (PCOS), idiopathic hyperandrogenism, hyperandrogenic insulin-resistant acanthosis nigricans syndrome (HAIRAN) and ovarian androgen-secreting neoplasms; (4) congenital adrenal hyperplasia (CAH); (5) basic science or animal experiments; (6) editorials, letters and consensus reports; (7) unavailable full text article; or (8) non-English studies.

The clinical data from the included studies were analyzed using GraphPad Prism (version 9; GraphPad Software, San Diego, California, USA).

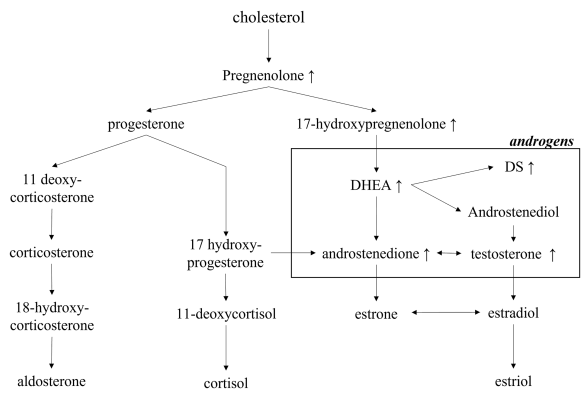

FIGURE 2
Exclusively increased steroid hormones in the androgen-producing pathway in the patient. DHEA, dehydroepiandrosterone; DS, dehydroepiandrosterone sulfate.

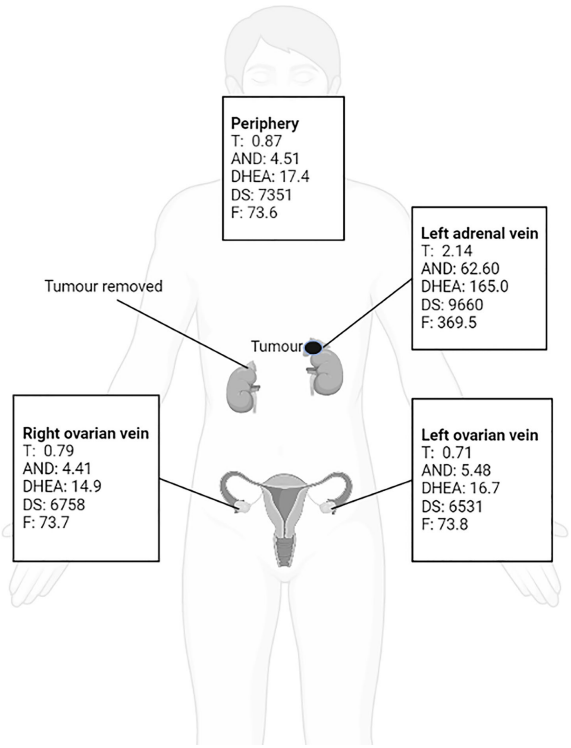

FIGURE 3
Bilateral ovarian venous sampling (OVS) and left adrenal venous sampling (AVS).

Continuous data are presented as the mean ± standard deviation (SD), and Student's t-test or the Mann–Whitney U test was utilized to compare the differences between the malignant and benign groups. A value of P<0.05 was considered statistically significant.

Results

In total, 48 studies met the inclusion criteria, including 40 case reports (8–47) and 8 articles (48–55). Forty case reports including 41 adult PASAT cases are summarized in Table 2, and 8 articles containing adult PASAT patients are summarized in Table 3.

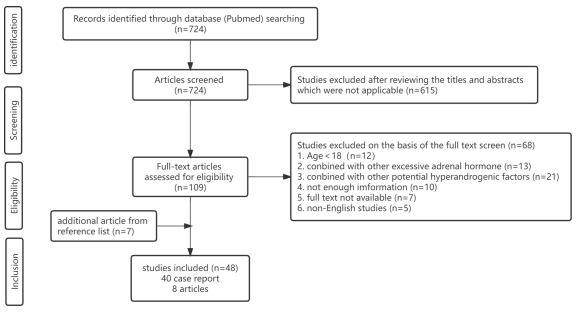

FIGURE 4
PRISMA flow diagram.

Statistical analysis was conducted on the data of 42 PASAT adult patients (including the present case) (Figures 5, 6).

The average ages of all patients, the malignant group and the benign group were 40.48 ± 15.80, 38.64 ± 10.62 and 43.17 ± 16.73 years, respectively. The incidence of adult PASAT peaked at 21-30 years old, followed by 41-50 years old, while the incidence of malignant PASAT peaked at 41-50 years old (Figure 5A). In addition, PASATs were predominantly found in women (40/42, 95.23%; Figure 5B).

Hirsutism was the most common symptom, and almost all female PASAT patients (37/39, 94.87%) presented with hirsutism (one patient's virilism was not described in detail), followed by clitoral enlargement, alopecia, voice deepening and acne (Figure 5C). Menstrual dysfunction, including oligomenorrhea, irregularity and even amenorrhea, was reported in 42.5% of female patients, while 15% of female patients showed normal menstruation (Figure 5D). There was no difference in tumor location (left or right side) (Figure 5E), but there were only two bilateral PASATs, including the present case. Tumors showing benign or malignant biological behavior accounted for 71.43% and 26.19%, respectively, with 2 uncertain tumors (Figure 5F).

The age differences between the malignant and benign groups were not significant (Figure 6A). The duration in the malignant group was significantly shorter (Figure 6B) than that in the benign group (1.96 vs. 4.51 years, P=0.025), while the tumor diameter in the malignant group was significantly increased (8.9 vs. 4.9 cm, p=0.011) (Figure 6C). For comparison, the androgen level was demonstrated as androgen concentration/upper normal range limit (UNRL). T was elevated in 36 adult PASAT patients (85.71%). The androgen levels, shown as T/UNRL (11.94 vs. 4.943, P=0.770) and DS/UNRL (16.5 vs. 5.28, P=0.625), in the malignant group were much higher than those in the benign group, but the differences were not significant (Figure 6D).

The responses of T and DS to the endocrine test are shown in Table 4. In the ACTH/synacthen test, the androgen levels increased in two patients but did not change in two patients. In another patient, the level of DS increased, but T was unresponsive. In the current patient, T decreased, but DS increased. The androgen response to the low-dose or high-dose dexamethasone test was not coordinated in different patients, and there were also paradoxical T and DS responses in the same patient. Regarding HCG (human chorionic gonadotropin) stimulation, most patients (5/7) showed an increase in DS or T. Furthermore, T and DS were slightly increased in the gonadotropin-releasing hormone (GnRH) test in two patients.

The androgen level decreased in 36 patients in a short time after surgery, and virilism symptoms were also partly or completely relieved. However, details regarding androgens after surgery were not reported in six patients. All ten patient with malignancy underwent surgery, except for one patient with nonresectable disease with multiple metastases at diagnosis (Table 2). Mitotane was applied to seven malignant patients (5 post-surgically, 1 with nonresectable disease and 1 after recurrence). Five patients with malignancy (including the one with nonresectable disease) were reported to have experienced recurrence, metastasis, or death.

TABLE 2 Characteristics of adult PASAT: summary of case reports (including current case).

case	year	1st author	Sex	Age (y)	Duration (y)	Hirsutism	Clitoromegaly	acne	voice deepening	alopecia	Menstruation	T/ UNRL	DHEA/ UNRL	DS/ UNRL
1	1975	Blichert-Toft M	F	27	2	yes	–	yes	–	yes	normal	1.15	–	–
2	1976	Larson BA	F	76	3	yes	yes	–	–	yes	menopause (GS)	11.41	–	–
3	1977	Nogeire C	M	23	–	–	–	–	–	–	–	0.44	10.50	5.20
4	1978	Smith HC	F	50	5	yes	yes	yes	yes	yes	menopause (aged)	4.35	–	–
5	1980	Stephen W	F	62	3	yes	–	–	–	yes	menopause (aged)	5.49	–	–
6	1981	Trost BN	F	60	3	yes	–	yes	yes	–	menopause (aged)	11.54	–	–
7	1983	Vancouver	F	29	3	yes	yes	yes	yes	–	amenorrhea	2.47	–	1.95
8	1983	Fuller PJ	F	33	7	yes	yes	–	yes	–	normal	1.06	1.36	4.58
9	1983	Aguirre P	F	58	10	yes	yes	yes	yes	yes	menopause (aged)	3.35	–	–
10	1984	Faggiano M	F	20	–	yes	yes	yes	–	–	normal	1.39	–	2.54
11	1985	Vasiloff J	F	49	7	yes	–	–	yes	yes	menopause (GS)	14.08	0.15	–
12	1986	O'leary TJ	F	30	–	yes	yes	–	–	yes	normal	2.23	–	4.29
13	1986	Pollock WJ	F	60	4	yes	–	–	yes	–	menopause (GS)	8.13	0.21	–
14	1987	Guillausseau PJ	F	41	15	yes	–	–	–	–	amenorrhea	normal	increased	increased
15	1989	Clouston WM	F	45	7	yes	yes	–	–	yes	menopause (GS)	2.18	–	3.57
16	1991	Jeffrey A	F	64	8	yes	yes	–	–	yes	menopause (aged)	2.21	–	7.54
17-L	1992	Micić D	F	22	5	yes	–	–	–	–	amenorrhea	4.11	–	1.43
17-R														
18	1992	Ruutiainen K-patient 1	F	30	1	yes	yes	–	yes	–	normal	2.76	–	3.51
19	1992	Ruutiainen K-patient 2	F	41	1	yes	–	–	yes	yes	oligomenorrhea	2.28	–	0.49
20	1995	Coonrod DV	F	24	2	yes	yes	yes	–	–	normal	increased	–	normal
21	2000	Bozbora A	F	23	0.25	yes	–	–	–	–	amenorrhea	42.86	–	125.71
22	2007	Mavroudis K	F	45	2	yes	yes	–	yes	yes	–	1.78	–	0.66
23	2011	Amano T	F	31	0.16	virilism (no details provided)					amenorrhea	increased	–	–
24	2012	Surrey LF	F	55	–	yes	–	–	–	yes	–	14.11	–	1.58

(Continued)

10.3389/fendo.2023.1138114

TABLE 2 Continued

case	year	1st author	Sex	Age (y)	Duration (y)	Hirsutism	Clitoromegaly	acne	voice deepening	alopecia	Menstruation	T/ UNRL	DHEA/ UNRL	DS/ UNRL
25	2013	Rodríguez-Gutiérrez R	F	18	10	yes	yes	–	yes	–	amenorrhea	5.28	–	2.33
26	2013	Varma T	F	42	7	yes	yes	–	–	yes	amenorrhea	5.28	–	2.94
27	2013	Galketiya KP	F	47	–	yes	–	–	–	yes	irregular	3.40	–	1.90
28	2015	Tetsi Nomigni M	F	34	3	yes	–	–	–	–	irregular	2.70	–	0.17
29	2015	Uruc F	F	48	–	–	–	–	–	yes	–	1.19	–	5.30
30	2016	Ghorayeb NE	M	50	–	–	–	–	–	–	–	–	–	1.80
31	2016	Carré J	F	50	–	yes	yes	–	–	–	menopause (GS)	2.35	–	0.38
32	2018	LaVoie M	F	26	0.75	yes	–	yes	yes	–	amenorrhea	6.12	–	1.33
33	2019	Karimi F	F	26	1.5	yes	–	–	–	–	–	–	–	3.29
34	2019	Zhou WB	F	28	3	yes	yes	–	yes	–	amenorrhea	0.35	–	23.06
35	2019	Dotto RS	F	67	0.42	yes	yes	–	–	–	menopause (aged)	12.76	–	0.32
36	2020	Sailo SL	F	20	5	yes	yes	–	yes	–	amenorrhea	increased	–	–
37	2020	Pinge SR	F	57	–	–	–	–	–	yes	menopause (aged)	0.61	0.42	3.53
38	2021	Prachi	F	29	3	yes	–	–	–	–	irregular, amenorrhea	8.85	–	37.39
39	2021	Correia DN	F	41	0.83	yes	yes	–	yes	–	irregular	28.05	–	2.44
40	2022	Bao ZZ	F	23	2	yes	–	yes	–	–	irregular, oligomenorrhea	7.28	–	1.79
41	2022	Gopinath C	F	68	1.50	yes	–	–	–	yes	menopause (GS)	3.44	–	5.62
42-L	current case		F	28	7	yes	yes	–	–	–	amenorrhea	2.21	–	3.14
42-R	current case													

case	year	1st author	AND/ UNRL	location	Side	Tumor size (cm)	surgery	Pathology	biobehavioral	Outcome	Follow-up time
1	1975	Blichert-Toft M	–	US, angiography	R	8	tumor resection	adenoma	benign	well	3m
2	1976	Larson BA	normal	AVS, OVS	R	4	adrenalectomy	adenoma	benign	well	2m
3	1977	Nogeire C	–	abdominal exploration	R	–	tumor resection	carcinoma	malignant	recurrence, metastasis, dead	–

(Continued)

10.3389/fendo.2023.1138114

TABLE 2 Continued

case	year	1st author	AND/ UNRL	location	Side	Tumor size (cm)	surgery	Pathology	biobehavioral	Outcome	Follow-up time
4	1978	Smith HC	–	–	R	3.5	adrenalectomy	adenoma	benign	–	–
5	1980	Stephen W	–	–	R	1	adrenalectomy	adenoma	benign	–	–
6	1981	Trost BN	–	AVS	R	3	adrenalectomy	adenoma	benign	well	2y
7	1983	Vancouver	0.88	CT	L	3	adrenalectomy	adenoma	benign	well	17m
8	1983	Fuller PJ	1.66	CT	R	5	tumor resection	adenoma	benign	–	–
9	1983	Aguirre P	–	abdominal exploration	R	3	adrenalectomy	ganglioneuroma	benign	–	–
10	1984	Faggiano M	0.86	X-ray, angiography	L	4	adrenalectomy	adenoma	benign	–	–
11	1985	Vasiloff J	0.46	CT	R	3	adrenalectomy	adenoma	benign	–	–
12	1986	O'leary TJ	–	CT	R	7.8	tumor resection	adenoma	benign	–	–
13	1986	Pollock WJ	–	CT	R	1.2	adrenalectomy	adenoma	benign	well	2y
14	1987	Guillausseau PJ	–	CT, AVS	L	10	adrenalectomy	adenoma	benign	well	6y
15	1989	Clouston WM	6.00	CT	L	6	tumor resection	adenoma	benign	well	3y
16	1991	Jeffrey A	–	CT	L	6	adrenalectomy	adenoma	benign	–	–
17-L	1992	Micić D	3.47	MRI, AVS, OVS	L	5.5	adrenalectomy	adenoma	benign	well	6m
17-R			–		R	5.4	adrenalectomy	adenoma			
18	1992	Ruutiainen	–	angiography	R	10.5	adrenalectomy	adenoma	benign	well	10m
19	1992	Ruutiainen	–	angiography	R	3.5	adrenalectomy	adenoma	benign	well	2.5y
20	1995	Coonrod DV	–	CT	R	6.4	adrenalectomy	carcinoma	malignant	well	8y
21	2000	Bozbora A	2.29	CT	R	9	adrenalectomy	carcinoma	malignant	metastasis, dead	8m
22	2007	Mavroudis K	1.21	MRI	L	2.5	tumor resection	adenoma	benign	–	–
23	2011	Amano T	–	CT, SPE-CT, PET-CT	L	5.8	adrenalectomy	carcinoma	malignant	well	1y
24	2012	Surrey LF	–	CT, MRI	L	7	tumor resection	oncocytoma, myelolipoma	benign	–	–
25	2013	Rodríguez-Gutiérrez R	3.70	CT	L	9.5	adrenalectomy	adenoma	benign	well	2m
26	2013	Varma T	–	CT	L	9.6	tumor resection	carcinoma	malignant	well	3m

(Continued)

10.3389/fendo.2023.1138114

TABLE 2 Continued

case	year	1st author	AND/ UNRL	location	Side	Tumor size (cm)	surgery	Pathology	biobehavioral	Outcome	Follow-up time
27	2013	Galketiya KP	–	CT, PET-CT	R	10	adrenalectomy	carcinoma	malignant	well	1y
28	2015	Tetsi Nomigni M	3.47	CT, AVS, OVS	R	2.6	Laparoscopic adrenalectomy	oncocytoma	benign	well	3y
29	2015	Uruc F	–	US, MRI, PET-CT	L	1.7	tumor resection	carcinoma	malignant	mitotane ongoing.	–
30	2016	Ghorayeb NE	–	MRI	L	14.9	tumor resection	carcinoma	malignant	metastasis, dead	3y
31	2016	Carré J	5.84	CT	L	3.5	adrenalectomy	oncocytic carcinoma	malignant	well	4y
32	2018	LaVoie M	2.17	MRI	L	2.5	laparoscopic adrenalectomy	adenoma	benign	well	1y
33	2019	Karimi F	–	CT	L	15	non-resectable	carcinoma	malignant	metastasis, dead	–
34	2019	Zhou WB	–	CT	L	7.1	tumor resection	myelolipoma	benign	well	1.5m
35	2019	Dotto RS	0.73	ultrasound, CT, PET-CT	L	1.5	laparoscopic tumor resection	adenoma	benign	–	–
36	2020	Sailo SL	–	CT	R	7.1	adrenalectomy	adenoma	uncertain	well	2m
37	2020	Pinge SR	0.65	CT	R	3.8	adrenalectomy	adenoma	benign	well	11m
38	2021	Prachi	–	US, CT, PET-CT	R	8.1	laparoscopic adrenalectomy	oncocytoma	benign	–	–
39	2021	Correia DN	–	CT, PET-CT	L	13.2	extensive surgery	oncocytic carcinoma	malignant	metastasis, progressing	1m
40	2022	Bao ZZ	2.86	CT	L	10	adrenalectomy	oncocytic neoplasm	uncertain	well	4y
41	2022	Gopinath C	–	CT, PET-CT	L	7.3	laparoscopic adrenalectomy	adenoma	benign	well	7y
42-L	current case		7.78	CT, AVS, OVS	L	3.1	adrenalectomy	adenoma	benign	well	1y
42-R	current case				R	2.5	tumor resection	adenoma	benign		

T, testosterone; AND, androstenedione; DHEA, dehydroepiandrosterone; DS, dehydroepiandrosterone sulfate; UNRL: upper normal range limit; GS: gynecological surgery. US, ultrasound; AVS, adrenal venous sampling; OVS, ovarian venous sampling; CT, computed tomography; PET-CT, Positron emissiontomography–computed tomography. R, right; L, left.

10.3389/fendo.2023.1138114

TABLE 3 Summary of articles containing adult PASAT.

year	1st author	Time span(y)	Measured androgens	Adult PASAT (total subjects)	average age	Female (number)	average size	Bio behavior	Outcome
1988	Naganuma H	–	–	2 (19)	48.5	2	–	2 (B)	–
1993	Gaudio AD	1960-1990	T, DS, AND, 17-KS	8 (190)	41.6	–	–	6 (M)/2 (B)	4D, 2W (M)/ 2W (B)
1998	Filipponi S	1994-1997	–	1 (50)	–	–	–	1 (B)	–
2000	Wajchenberg BL	1982-1999	–	4 (47)	–	–	–	4 (M)	–
2003	Gordera F	1946-2002	T, DS, AND, 17-KS	7 (11)	24.6(M)/ 38.8(B)	7	10.7 (M)/ 4.2(B)	3 (M)/4 (B)	1D, 2W (M)/ 4 W (B)
2004	Moreno S	1970-2003	T, DHEA, DS, AND, 17-KS	Unknown*(21)	45(M)/ 34.5(B)	21	14 (M)/ 9 (B)	10 (M)/11 (B)	5D, 3R&MS, 2 W (M)/ 11W (B)
2011	Sarfati J	1995-2009	T, DS, AND	1 (22)	–	–	–	1 (M)	–
2017	Tong A	2002-2015	T, DS, AND	6 (9)	66(M)/ 32.2(B)	6	15 (M)/ 5.3 (B)	1 (M)/5 (B)	1 MS (M)/ 4W(B)

T, testosterone; AND, androstenedione; DHEA, dehydroepiandrosterone; DS, dehydroepiandrosterone sulfate; 17-KS; 17-ketosteroid; R, reoccurrence, M, malignant group; B benign group; MS, metastasis; W, well (no recurrence or metastasis observed in the following time or till death).
*the adult and preadult patients can't be distinguished in this article and the youngest age of patient is 15 years old.

The articles containing adult PASAT were summarized Table 3. T and DS were the most frequent androgens used for hormone evaluation, and urinary 17-ketosteroid was a significant indicator of hyperandrogenism in the earlier studies. The age distribution of the patients with malignant or benign tumors varied among the different studies. The age of the malignant group was younger than that of the benign group in the study by Gordera F but older in the study by Moreno S. The average size of the malignant tumors was larger than that of the benign tumors. Most malignancy patients (14/20) had a negative outcome (recurrence, metastasis or death), while no patient with benign conditions were reported to have a negative outcome during the follow-up period.

Discussion

Androgen-secreting adrenal tumors are rare. A recent population-based study of 1287 patients diagnosed with adrenal tumors reported only one androgen-excess adrenal tumor (0.1%) (56). In another study of 1205 patients with androgen excess, 20 (1.7%) individuals were identified as having androgen-secreting adrenal tumors (57). Androgen-secreting adrenocortical tumors, especially adult PASATs, remain a challenge in clinical diagnosis and treatment due to their rarity. Here, we report a rare case of adult bilateral PASATs, and to our knowledge, only one other case of bilateral PASATs has been reported since 1970. Furthermore, we conducted a systematic review of adult PASATs to increase the understanding of adult PASATs and provide guidelines for the diagnosis and treatment of adult PASATs.

The incidence peak for adult PASAT occurred at 21-30 years of age, while the incidence peak for malignant PASAT occurred at 41-50 years of age. Hirsutism, as one of the initial complaints, was the most common symptom found in the present review and other PASAT studies (53, 55, 58). Young females might focus more on their appearance, and they may notice hirsutism once it occurs, prompting them to visit doctors and undergo medical screening for virilism-causing adrenal tumors. This may contribute to the peak incidence of adult PASAT at 21-30 years of age. The incidence of malignant PASAT peaked at 41-50 years of age, which is close to the age of incidence peak of adult adrenocortical carcinoma in a previous study (51). Several factors may be responsible for this. Above all, the incidence peak of malignant PASAT may be associated with age because the risk of malignant tumors is higher in older people (59). It may also be associated with menstrual dysfunction. It was indicated that the occurrence of menstrual dysfunction is associated with higher androgen levels in women with hirsutism (60), and our data analysis demonstrated that patients with malignant PASAT presented with higher androgen levels, which indicates that malignant PASAT might lead to more menstrual disorders. It is well known that females aged 41-50 years usually begin to suffer menstrual problems due to perimenopause, prompting them to seek medical advice and hormone evaluation. Therefore, androgen abnormalities that are related to potential virilism-causing malignant adrenal tumors are more likely to be diagnosed in patients aged 41-50 years. However, the potential factors responsible for the age distribution of PASAT need to be identified in further research.

In the present review, PASAT was predominant (40/42) in women. The low incidence of PASAT in men may be associated with clinical ignorance. It is difficult to ascertain the onset of androgen-excess symptoms in males, which are usually clinically ignored until the presence of a consistent peripheral androgen-to-estrogen conversion is determined (61). In addition to hirsutism and menstrual dysfunction, other virilism manifestations, such as clitoral enlargement, alopecia, voice deepening and acne, were found to be important signs for screening and diagnosis.

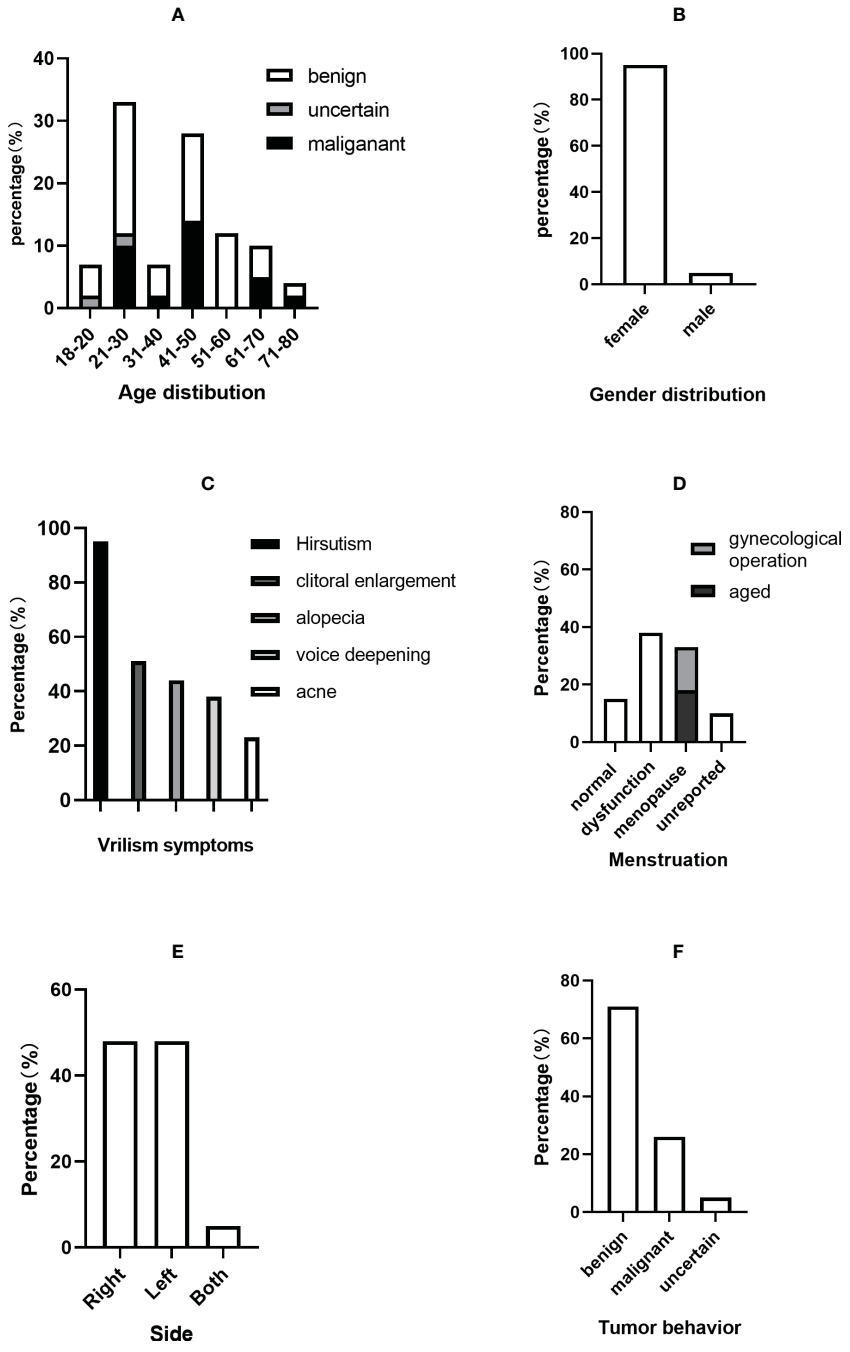

FIGURE 5
Clinical characteristics of PASAT cases. **(A)** Age distribution. **(B)** Sex distribution. **(C)** Virilism symptoms. **(D)** Menstruation change. **(E)** Tumor side. **(F)** Tumor behavior.

Malignant adrenal neoplasms were identified in 26% of adult PASAT patients, which was significantly higher than the incidence (8.6%) of malignant adrenal tumors in an adrenal tumor population (56). The average duration before diagnosis in the malignant group was significantly shorter than that in the benign group, which may be related to the rapid progression of the malignant adrenocortical tumor. The malignant adrenal tumor size was significantly larger than that of benign tumors, consistent with various studies on adrenal tumors. Testosterone is the most sensitive marker in the hormone evaluation of PASAT, as it is elevated in almost all PASAT patients and is the only increased androgen in certain patients (41, 62, 63). Some studies (64, 65) have demonstrated that increased DS (produced uniquely by the adrenal zona reticularis) and DHEA (produced mainly by the adrenal zona reticularis) are indicators of adrenal etiology, especially DS. In the current review, however, the DS level was normal in 6/32 patients, and the DHEA levels was normal in 3/6 patients. The levels of T and DS, which are presented as androgen levels/upper normal range limit in Table 2, were much higher in malignant cases, but these differences were not significant and the potential differences in androgens between malignant and

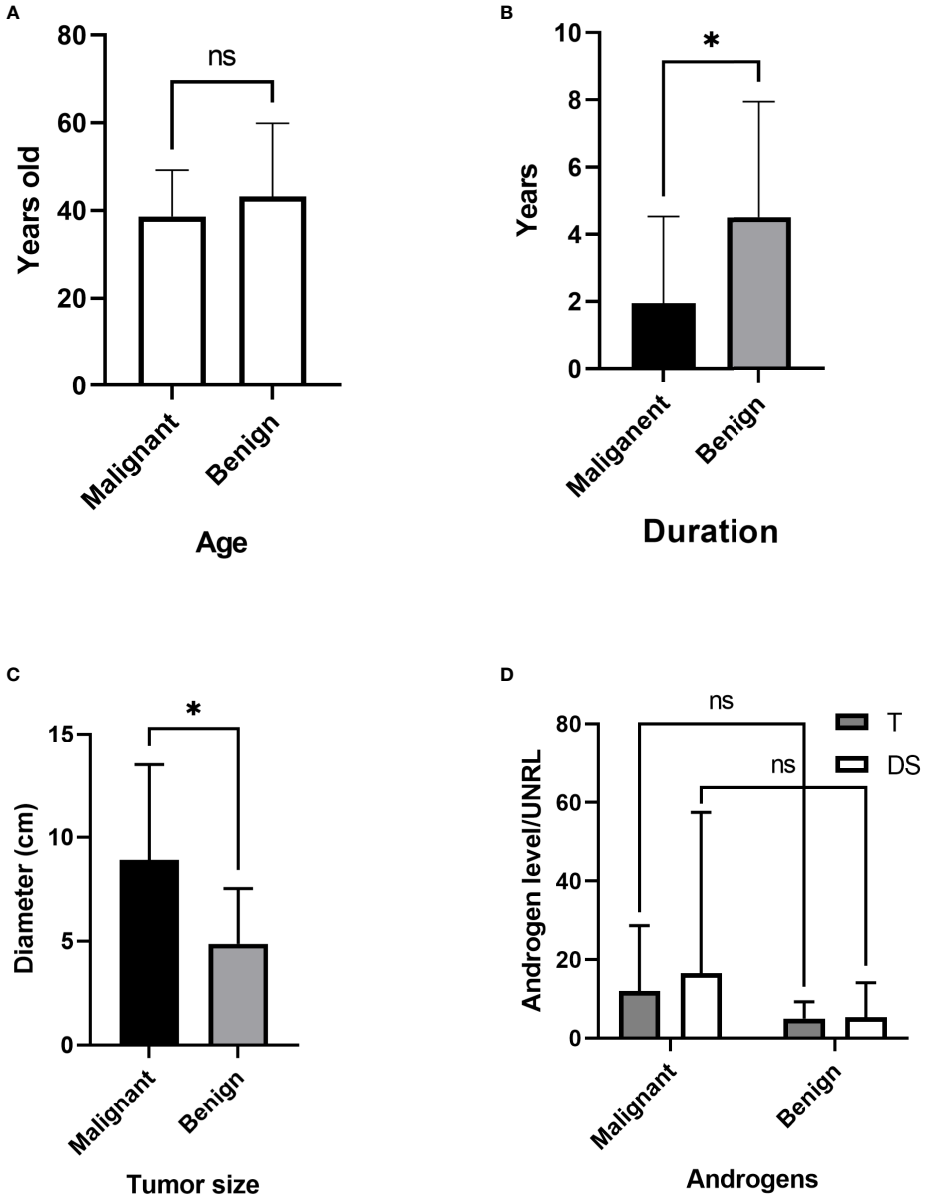

FIGURE 6
Comparison of malignant and benign tumors. **(A)** Age differences. **(B)** Duration before diagnosis. **(C)** Tumor size. **(D)** Androgen level. T, testosterone; DS, dehydroepiandrosterone sulfate; UNRL, upper normal range limit. ns, not significant; * P<0.05.

benign PASAT need to be identified in future studies due to the limited number of cases in the present review.

The contribution of the ACTH/synacthen test and dexamethasone test (low dose or high dose) to the diagnosis of PASAT may have been limited because the T and DS responses varied among different patients. However, most female patients showed an increased T and DS level in the HCG test, which may potentially contribute to the diagnosis of PASAT. Leydig cells or features related to Leydig cells, which could increase testosterone secretion under the stimulation of HCG, have been reported in the pathological findings of PASAT neoplasm (11, 13, 16, 18), and this may be the possible reason why PASAT responds actively respond to HCG.

A previous study indicated that as many as 45% of female patients with androgen-producing adrenal neoplasms underwent needless ovarian surgical treatment before obtaining the correct diagnosis (66). Polycystic ovarian morphology, a potential factor in hyperandrogenemia, has been reported in several PASAT patients (11, 24, 28, 38, 39) and was present in the current case, but it was identified as an irrelevant factor. Unfortunately, two PASAT patients included in the current review also underwent an unnecessary oophorectomy (11, 28). It is unclear whether polycystic ovarian morphology is caused by hyperandrogenemia itself, but it does lead to difficulties in identifying the source of hyperandrogenism in terms of location. Notably, adrenal venous sampling (AVS) or ovarian venous sampling (OVS) played a

10.3389/fendo.2023.1138114

TABLE 4 Endocrine test summary of PASAT.

year	1st author	Age	Androgen (unit)	basal line	ACTH test	DXM test		HCG test	GnRH test
1975	Blichert-Toft M	27	T (ng/ml)	0.98	unresponsive	unresponsive (Low dose)	unresponsive (high dose)	Increased to 1.53 (5d, under DXM)	–
1978	Smith HC	54	T (ng/ml)	6.1-8	4.3→5.4(0.25mg over 8h, after DXM)	6.1 (2mgx7d)	4.4 (8mgx7d)	Increased to 10 (3000IUx4d)	–
1981	Trost BN	60	T (nmol/l)	22.2-27.7	–	29.8 (2mgx7d)	–	–	–
1983	Vancouver	29	T (ng/ml)	173	–	–	108 (8mgx3d)	–	–
			DS (ng/ml)	6600	–	–	6850 (8mgx3d)	–	–
1983	Fuller PJ	33	T (nmol/l)	–	–	unresponsive (dose unknown)	–	2.64→3.64 (5000IU over 16h)	4.4→5.6 (100mins)
1984	Faggiano M	20	T (ng/dl)	–	unresponsive (0.25mg)	decrease slightly (2mgx4d)	–	Increase (3000IUx3d, under DXM)	–
			DS (ng/ml)	–	unresponsive (0.25mg)	unresponsive (2mgx4d)	–	Increase (3000IUx3d, under DXM)	–
1986	O'leary TJ	30	T (nmol/l)	4.9	–	–	9.8 (8mgx2d)	unresponsive (5000IU)	–
			DS (nmol/l)	39.5	–	–	99.5 (8mgx2d)	unresponsive (5000IU)	–
1987	Guillausseau PJ	41	T (ng/ml)	0.56	1.98 (1mgx2d)	0.6 (2mgx2d, after HCG)	0.75 (8mgx2d, after low DXM)	0.9 (5000IUx3d, after ACTH)	–
			DS (ng/ml)	5100	13000	10000	8700	7400(5000IUx3d)	–
1989	Clouston WM	45	T (nmol/l)	6.6-8.7	–	9.4	14	–	–
			DS (µmol/l)	20-25	–	35	71	–	–
1992	Ruutiainen (case 1)	41	T (nmol/l)	–	–	–	unresponsive	–	–
			DS (µmol/l)	–	–	–	decrease slightly	–	–
1992	Ruutiainen (case 2)	30	T (nmol/l)	–	–	–	unresponsive (10mg injection)	–	–
			DS (µmol/l)	–	–	–	decrease slightly (10mg injection)	–	–
1992	Micić D	22	T (nmol/l)	–	–	20.2→15.2 (2mgx7d)	–	16.0→15.8 (3000IUx3d)	–
2007	Mavroudis K	45	T (pmol/l)	–	Unresponsive (0.25mg)	4.8→7 (0.5mgx7d)	–	–	–
			DS (µg/dl)	–	increased by 44%	2650→2200 (0.5mgx7d)	–	–	–
current case			T (nmol/l)	–	5.82→4.33 (0.25mg over 1h)	–	5.55→6.45 (2mgx2d)	–	6.66 (over 24h, after DXM)
			DS (µmol/l)	–	23.5→36 (0.25mg over 1h)	–	36.2→47.7 (2mgx2d)	–	66.4 (over 24h, after DXM)

ACTH, adrenocorticotropic hormone; DXM, dexamethasone; HCG, human chorionic gonadotropin; GnRH, gonadotropin-releasing hormone; T, testosterone; DHEAS, dehydroepiandrosterone sulfate.

significant role in accurately identifying the aetiological location in some PASAT patients (9, 13, 21, 24, 34) and in the current case. Thus, AVS and OVS are recommended for the identification of the location of hyperandrogenemia aetiology, especially when clinical findings are inconclusive.

Conclusion

Adult PASATs are extremely rare, and their characteristics are largely unknown. The diagnosis and treatment of adult PASATs remain a clinical challenge. Adult PASATs are predominant in women and most frequently characterized by hirsutism symptoms and other virilism signs. Serum testosterone is the most sensitive indicator, and elevated DS could contribute to the diagnosis of PASAT specifically. HCG stimulation test might also be of help in diagnosis. Individuals with malignant PASATs have a shorter disease duration before diagnosis, larger tumor sizes and relatively higher androgen levels. AVS and OVS may be important approaches for the location diagnosis. Surgery is recommended for all patients with local PASATs, whether benign or malignant. Tumor malignancy should be fully considered in patients PASATs due to the high risk of malignancy, poor prognosis and limited effective treatment approaches.

Data availability statement

The raw data supporting the conclusions of this article will be made available by the authors, without undue reservation.

Author contributions

Conceptualization, ZL, YG, and YSZ. Methodology, ZL and YZ. Validation, ZW and XW. Data analysis, ZL, YG, and JZ. Writing—original draft preparation, ZL. Writing—review and editing, YSZ. All authors contributed to the article and approved the submitted version.

Funding

The research was supported by the National Natural Science Foundation of China (81670611).

Conflict of interest

The authors declare that the research was conducted in the absence of any commercial or financial relationships that could be construed as a potential conflict of interest.

Publisher's note

References

1. Lyraki R, Schedl A. Adrenal cortex renewal in health and disease. *Nat Rev Endocrinol* (2021) 17(7):421–34. doi: 10.1038/s41574-021-00491-4

2. Bonfig W, Bittmann I, Bechtold S, Kammer B, Noelle V, Arleth S, et al. Virilising adrenocortical tumours in children. *Eur J Pediatr* (2003) 162(9):623–8. doi: 10.1007/s00431-003-1230-y

3. Ribeiro R, Figueiredo B. Childhood adrenocortical tumours. *Eur J Cancer* (2004) 40(8):1117–26. doi: 10.1016/j.ejca.2004.01.031

4. Honour J, Price D, Taylor N, Marsden H, Grant D. Steroid biochemistry of virilising adrenal tumours in childhood. *Eur J Pediatr* (1984) 142(3):165–9. doi: 10.1007/BF00442442

5. Speiser PW, Azziz R, Baskin LS, Ghizzoni L, Hensle TW, Merke DP, et al. Congenital adrenal hyperplasia due to steroid 21-hydroxylase deficiency: An endocrine society clinical practice guideline. *J Clin Endocrinol Metab* (2010) 95(9):4133–60. doi: 10.1210/jc.2009-2631

6. Speiser PW, Arlt W, Auchus RJ, Baskin LS, Conway GS, Merke DP, et al. Congenital adrenal hyperplasia due to steroid 21-hydroxylase deficiency: An endocrine society clinical practice guideline. *J Clin Endocrinol Metab* (2018) 103(11):4043–88. doi: 10.1210/jc.2018-01865

7. Funder JW, Carey RM, Mantero F, Murad MH, Reincke M, Shibata H, et al. The management of primary aldosteronism: Case detection, diagnosis, and treatment: An endocrine society clinical practice guideline. *J Clin Endocrinol Metab* (2016) 101(5):1889–916. doi: 10.1210/jc.2015-4061

8. Blichert-Toft M, Vejlsted H, Hehlet H, Albrechtsen R. Virilizing adrenocortical adenoma responsive to gonadotrophin. *Acta Endocrinol (Copenh)* (1975) 78(1):77–85. doi: 10.1530/acta.0.0780077

9. Larson BA, Vanderlaan WP, Judd HL, McCullough DL. A testosterone-producing adrenal cortical adenoma in an elderly woman. *J Clin Endocrinol Metab* (1976) 42(5):882–7. doi: 10.1210/jcem-42-5-882

10. Nogeire C, Fukushima DK, Hellman L, Boyar RM. Virilizing adrenal cortical carcinoma. *Cancer* (1977) 40(1):307–13. doi: 10.1002/1097-0142(197707)40:1<307::aid-cncr2820400143>3.0.co;2-2

11. Smith HC, Posen S, Clifton-Bligh P, Casey J. A testosterone-secreting adrenal cortical adenoma. *Aust N Z J Med* (1978) 8(2):171–5. doi: 10.1111/j.1445-5994.1978.tb04506.x

12. Spaulding SW, Masuda T, Osawa Y. Increased 17 beta-hydroxysteroid dehydrogenase activity in a masculinizing adrenal adenoma in a patient with isolated testosterone overproduction. *J Clin Endocrinol Metab* (1980) 50(3):537–40. doi: 10.1210/jcem-50-3-537

13. Trost BN, Koenig MP, Zimmermann A, Zachmann M, Müller J. Virilization of a post-menopausal woman by a testosterone-secreting leydig cell type adrenal adenoma. *Acta Endocrinol (Copenh)* (1981) 98(2):274–82. doi: 10.1530/acta.0.0980274

14. Ho Yuen B, Moon YS, Mincey EK, Li D. Adrenal and sex steroid hormone production by a virilizing adrenal adenoma and its diagnosis with computerized tomography. *Am J Obstet Gynecol* (1983) 145(2):164–9. doi: 10.1016/0002-9378(83)90484-2

15. Fuller PJ, Pettigrew IG, Pike JW, Stockigt JR. An adrenal adenoma causing virilization of mother and infant. *Clin Endocrinol (Oxf)* (1983) 18(2):143–53. doi: 10.1111/j.1365-2265.1983.tb03197.x

16. Aguirre P, Scully RE. Testosterone-secreting adrenal ganglioneuroma containing leydig cells. *Am J Surg Pathol* (1983) 7(7):699–705. doi: 10.1097/00000478-198310000-00010

17. Faggiano M, Criscuolo T, Sinisi AA, Scialdone A, Bellastella A, Cuccurullo L. Virilization syndrome in a young woman due to an androgen-secreting adenoma. *J endocrinological Invest* (1984) 7(1):41–5. doi: 10.1007/bf03348374

18. Vasiloff J, Chideckel EW, Boyd CB, Foshag LJ. Testosterone-secreting adrenal adenoma containing crystalloids characteristic of leydig cells. *Am J Med* (1985) 79(6):772–6. doi: 10.1016/0002-9343(85)90531-5

19. O'Leary TJ, Ooi TC, Miller JD, Branchaud CL, Kalra J. Virilization of two siblings by maternal androgen-secreting adrenal adenoma. *J Pediatr* (1986) 109(5):840–2. doi: 10.1016/s0022-3476(86)80707-7

20. Pollock WJ, McConnell CF, Hilton C, Lavine RL. Virilizing leydig cell adenoma of adrenal gland. *Am J Surg Pathol* (1986) 10(11):816–22. doi: 10.1097/00000478-198611000-00009

21. Guillausseau PJ, Boitard C, Le Charpentier Y, Cedard L, Nahoul K, Blacker C, et al. Androgen producing adrenal adenoma. *Rep Case associated hyperparathyroidism. J Endocrinol Invest* (1987) 10(6):593–9. doi: 10.1007/bf03347005

22. Clouston WM, Cannell GC, Fryar BG, Searle JW, Martin NI, Mortimer RH. Virilizing adrenal adenoma in an adult with the beckwith-wiedemann syndrome: paradoxical response to dexamethasone. *Clin Endocrinol (Oxf)* (1989) 31(4):467–73. doi: 10.1111/j.1365-2265.1989.tb01270.x

23. Jackson JA, Mellinger RC. Hyperandrogenemia and virilization with simultaneous pituitary and adrenal adenomas. *Henry Ford Hosp Med J* (1991) 39 (1):22–4.

24. Micić D, Zorić S, Popović V, Janković R, Jancić M, Han R, et al. Androgen-producing bilateral large cortical adrenal adenomas associated with polycystic ovaries in a young female. *Postgrad Med J* (1992) 68(797):219–22. doi: 10.1136/pgmj.68.797.219

25. Ruutiainen K, Satokari K, Anttila L, Erkkola R. Adrenal- and ovarian-vein steroids and LH response to GnRH in two patients with virilizing adrenocortical adenoma studied by selective catheterizations. *Horm Res* (1992) 37(1-2):49–53. doi: 10.1159/000182281

26. Coonrod DV, Rizkallah TH. Virilizing adrenal carcinoma in a woman of reproductive age: a case presentation and literature review. *Am J Obstet Gynecol* (1995) 172(6):1912–1914; discussion 1914-1915. doi: 10.1016/0002-9378(95)91431-5

27. Bozbora A, Erbil Y, Ozbey N, Kapran Y, Ozarmagan S, Berber E, et al. A young female patient with an androgen-secreting tumor: A rare malignant disease. *Tumori* (2000) 86(6):487–8. doi: 10.1177/030089160008600612

28. Mavroudis K, Aloumanis K, Papapetrou PD, Voros D, Spanos I. Virilization caused by an ectopic adrenal tumor located behind the iliopsoas muscle. *Fertil Steril* (2007) 87(6):1468.e1413–1466. doi: 10.1016/j.fertnstert.2006.08.106

29. Amano T, Imao T, Seki M, Takemae K, Yamauchi K, Hata S. Normal delivery following resection of an androgen-secreting adrenal carcinoma. *Reprod Med Biol* (2011) 10(1):55–8. doi: 10.1007/s12522-010-0071-4

30. Surrey LF, Thaker AA, Zhang PJ, Karakousis G, Feldman MD. Ectopic functioning adrenocortical oncocytic adenoma (oncocytoma) with myelolipoma causing virilization. *Case Rep Pathol* (2012) 2012(326418). doi: 10.1155/2012/326418

31. Rodríguez-Gutiérrez R, Bautista-Medina MA, Teniente-Sanchez AE, Zapata-Rivera MA, Montes-Villarreal J. Pure androgen-secreting adrenal adenoma associated with resistant hypertension. *Case Rep Endocrinol* (2013) 2013(356086). doi: 10.1155/2013/356086

32. Varma T, Panchani R, Goyal A, Maskey R. A case of androgen-secreting adrenal carcinoma with non-classical congenital adrenal hyperplasia. *Indian J Endocrinol Metab* (2013) 17(Suppl 1):S243–245. doi: 10.4103/2230-8210.119585

33. Galketiya KP, Ranjikumar S, Majeed U. Androgen-secreting adrenocortical carcinoma. *Lancet Diabetes Endocrinol* (2013) 1(1):e10. doi: 10.1016/s2213-8587(13)70005-6

34. Tetsi Nomigni M, Ouzounian S, Benoit A, Vadrot J, Tissier F, Renouf S, et al. Steroidogenic enzyme profile in an androgen-secreting adrenocortical oncocytoma associated with hirsustism. *Endocr Connect* (2015) 4(2):117–27. doi: 10.1530/ec-15-0014

35. Uruc F, Urkmez A, Yuksel OH, Sahin A, Verit A. Androgen secreting giant adrenocortical carcinoma with no metastases: A case report and review of the literature. *Can Urol Assoc J* (2015) 9(9-10):E644–647. doi: 10.5489/cuaj.2867

36. El Ghorayeb N, Grunenwald S, Nolet S, Primeau V, Côté S, Maugard CM, et al. First case report of an adrenocortical carcinoma caused by a BRCA2 mutation. *Med (Baltimore)* (2016) 95(36):e4756. doi: 10.1097/md.0000000000004756

37. Carré J, Grunenwald S, Vezzosi D, Mazerolles C, Bennet A, Meduri G, et al. Virilizing oncocytic adrenocortical carcinoma: Clinical and immunohistochemical studies. *Gynecol Endocrinol* (2016) 32(8):662–6. doi: 10.3109/09513590.2016.1149811

38. LaVoie M, Constantinides V, Robin N, Kyriacou A. Florid hyperandrogenism due to a benign adrenocortical adenoma. *BMJ Case Rep* (2018) 2018. doi: 10.1136/bcr-2018-224804

39. Karimi F, Dehghanian A, Fallahi M, Dalfardi B. Pure androgen-secreting adrenocortical carcinoma presenting with hypoglycemia. *Arch Iran Med* (2019) 22 (9):527–30.

40. Dotto RS, Marx G, Bastos M, Machado JL, Glufke V, de Oliveira Freitas DM. A rare case of virilizing adult ectopic adrenal tumor. *Urol Case Rep* (2019) 27(100907). doi: 10.1016/j.eucr.2019.100907

41. Zhou WB, Chen N, Li CJ. A rare case of pure testosterone-secreting adrenal adenoma in a postmenopausal elderly woman. *BMC endocrine Disord* (2019) 19(1):14. doi: 10.1186/s12902-019-0342-y

42. Sailo SL, Sailo L. Primary amenorrhoea & virilization induced by pure testosterone-secreting adrenocortical adenoma. *Indian J Med Res* (2020) 152(Suppl 1):S53–s54. doi: 10.4103/ijmr.IJMR_1852_19

43. Pingle SR, Jalil F, Millar D, Malchoff CD, Ristau BT. Isolated DHEAS production by an adrenal neoplasm: Clinical, biochemical and pathologic characteristics. *Urol Case Rep* (2020) 31(101148). doi: 10.1016/j.eucr.2020.101148

44. Prachi, Aiyer HM, Jain V. Adrenocortical oncocytoma associated with androgen excess: A rare cause of hirsutism. *Indian J Urol* (2021) 37(3):277–80. doi: 10.4103/iju.IJU_636_20

45. Correia DN, Carvalho IR, Mangi JA. Virilising adrenocortical carcinoma. *BMJ Case Rep* (2021) 14(6). doi: 10.1136/bcr-2021-242895

46. Bao Z, He W, Di W, Gao H. Hyperandrogenism caused by a rare adrenocortical oncocytic neoplasm with uncertain malignant potential: A case report and review of the literature. *Endocr J* (2022). doi: 10.1507/endocrj.EJ22-0277

47. Gopinath C, Shekar S, Acharya M, Pattan V, Sundaresh V. Pure androgen-secreting radiologically suspicious adrenal mass: Benign or malignant? *Cureus* (2022) 14(6):e26234. doi: 10.7759/cureus.26234

48. Naganuma H, Ojima M, Sasano N. 11 beta-hydroxylase in mitochondrial fractions of functioning and non-functioning adrenocortical tumors. *Tohoku J Exp Med* (1988) 155(1):81–96. doi: 10.1620/tjem.155.81

49. Del Gaudio AD, Del Gaudio GA. Virilizing adrenocortical tumors in adult women. report of 10 patients, 2 of whom each had a tumor secreting only testosterone. *Cancer* (1993) 72(6):1997–2003. doi: 10.1002/1097-0142(19930915)72:6<1997::aid-cncr2820720634>3.0.co;2-1

50. Filipponi S, Guerrieri M, Arnaldi G, Giovagnetti M, Masini AM, Lezoche E, et al. Laparoscopic adrenalectomy: A report on 50 operations. *Eur J Endocrinol* (1998) 138 (5):548–53. doi: 10.1530/eje.0.1380548

51. Wajchenberg BL, Albergaria Pereira MA, Medonca BB, Latronico AC, Campos Carneiro P, Alves VA, et al. Adrenocortical carcinoma: clinical and laboratory observations. *Cancer* (2000) 88(4):711–36.

52. Cordera F, Grant C, van Heerden J, Thompson G, Young W. Androgen-secreting adrenal tumors. *Surgery* (2003) 134(6):874–880; discussion 880. doi: 10.1016/s0039-6060(03)00410-0

53. Moreno S, Montoya G, Armstrong J, Leteurtre E, Aubert S, Vantyghem MC, et al. Profile and outcome of pure androgen-secreting adrenal tumors in women: Experience of 21 cases. *Surgery* (2004) 136(6):1192–8. doi: 10.1016/j.surg.2004.06.046

54. Sarfati J, Bachelot A, Coussieu C, Meduri G, Touraine P. Impact of clinical, hormonal, radiological, and immunohistochemical studies on the diagnosis of postmenopausal hyperandrogenism. *Eur J Endocrinol* (2011) 165(5):779–88. doi: 10.1530/eje-11-0542

55. Tong A, Jiang J, Wang F, Li C, Zhang Y, Wu X. Pure androgen-producing adrenal tumor: Clinical features and pathogenesis. *Endocrine Pract* (2017) 23(4):399–407. doi: 10.4158/ep161580.or

56. Ebbehoj A, Li D, Kaur RJ, Zhang C, Singh S, Li T, et al. Epidemiology of adrenal tumours in Olmsted county, Minnesota, USA: A population-based cohort study. *Lancet Diabetes Endocrinol* (2020) 8(11):894–902. doi: 10.1016/s2213-8587(20)30314-4

57. Elhassan YS, Idkowiak J, Smith K, Asia M, Gleeson H, Webster R, et al. Causes, patterns, and severity of androgen excess in 1205 consecutively recruited women. *J Clin Endocrinol Metab* (2018) 103(3):1214–23. doi: 10.1210/jc.2017-02426

58. Sciarra F, Tosti-Croce C, Toscano V. Androgen-secreting adrenal tumors. *Minerva endocrinologica* (1995) 20(1):63–8.

59. Doll R. The age distribution of cancer: Implications for models of carcinogenesis. *J R Stat Society: Series A (General)* (1971) 134(2):133–55. doi: 10.2307/2343871

60. Redmond GP, Bergfeld W, Gupta M, Bedocs NM, Skibinski C, Gidwani G. Menstrual dysfunction in hirsute women. *J Am Acad Dermatol* (1990) 22(1):76–8. doi: 10.1016/0190-9622(90)70011-6

61. Di Dalmazi G. Hyperandrogenism and adrenocortical tumors. *Front Horm Res* (2019) 53(92-99). doi: 10.1159/000494905

62. Kamilaris TC, DeBold CR, Manolas KJ, Hoursanidis A, Panageas S, Yiannatos J. Testosterone-secreting adrenal adenoma in a peripubertal girl. *Jama* (1987) 258 (18):2558–61. doi: 10.1001/jama.1987.03400180092034

63. Sorgo W, Meyer D, Rodens K, Homoki J, Heinze E, Heymer B, et al. Testosterone-secreting adrenocortical tumor in a pubertal girl. case report and review of the literature. *Horm Res* (1988) 30(6):217–23. doi: 10.1159/000181067

64. Witchel SF, Pinto B, Burghard AC, Oberfield SE. Update on adrenarche. *Curr Opin Pediatr* (2020) 32(4):574–81. doi: 10.1097/mop.0000000000000928

65. Burger HG. Androgen production in women. *Fertility sterility* (2002) 77(3-5). doi: 10.1016/s0015-0282(02)02985-0

66. Mattox JH, Phelan S. The evaluation of adult females with testosterone producing neoplasms of the adrenal cortex. *Surg Gynecol Obstet* (1987) 164(2):98–101.

frontiers | Frontiers in Endocrinology

TYPE Original Research
PUBLISHED 24 March 2023
DOI 10.3389/fendo.2023.1148117

OPEN ACCESS

EDITED BY
Hu Han,
Beijing Chaoyang Hospital, Capital Medical University, China

REVIEWED BY
Yafeng Li,
The Fifth Hospital of Shanxi Medical University, China
Luigi Napolitano,
University of Naples Federico II, Italy

*CORRESPONDENCE
Xiaoqiang Liu
xiaoqiangliu1@163.com

SPECIALTY SECTION
This article was submitted to Reproduction, a section of the journal Frontiers in Endocrinology

RECEIVED 19 January 2023
ACCEPTED 14 March 2023
PUBLISHED 24 March 2023

CITATION
Ren C, Wang Q, Wang S, Zhou H, Xu M, Li H, Li Y, Chen X and Liu X (2023) Metabolic syndrome-related prognostic index: Predicting biochemical recurrence and differentiating between cold and hot tumors in prostate cancer.
Front. Endocrinol. 14:1148117.
doi: 10.3389/fendo.2023.1148117

Metabolic syndrome-related prognostic index: Predicting biochemical recurrence and differentiating between cold and hot tumors in prostate cancer

Congzhe Ren[1], Qihua Wang[1], Shangren Wang[1], Hang Zhou[1], Mingming Xu[1], Hu Li[1,2], Yuezheng Li[1], Xiangyu Chen[1] and Xiaoqiang Liu[1]*

[1]Department of Urology, Tianjin Medical University General Hospital, Tianjin, China, [2]Department of Urology, Shanxian Central Hospital (Affiliated Huxi Hospital of Jining Medical University), Heze, China

Background: The prostate, as an endocrine and reproductive organ, undergoes complex hormonal and metabolic changes. Recent studies have shown a potential relationship between metabolic syndrome and the progression and recurrence of prostate cancer (PCa). This study aimed to construct a metabolic syndrome-related prognostic index (MSRPI) to predict biochemical recurrence-free survival (BFS) in patients with PCa and to identify cold and hot tumors to improve individualized treatment for patients with PCa.

Methods: The Cancer Genome Atlas database provided training and test data, and the Gene Expression Omnibus database provided validation data. We extracted prognostic differentially expressed metabolic syndrome-related genes (DEMSRGs) related to BFS using univariate Cox analysis and identified potential tumor subtypes by consensus clustering. The least absolute shrinkage and selection operator (LASSO) algorithm and multivariate Cox regression were used to construct the MSRPI. We further validated the predictive power of the MSRPI using KaplanMeier survival analysis and receiver operating characteristic (ROC) curves, both internally and externally. Drug sensitivity was predicted using the half-maximal inhibitory concentration (IC50). Finally, we explored the landscape of somatic mutations in the risk groups.

Results: Forty-six prognostic DEMSRGs and two metabolic syndrome-associated molecular clusters were identified. Cluster 2 was more immunogenic. Seven metabolic syndrome-related genes (*CSF3R*, *TMEM132A*, *STAB1*, *VIM*, *DUOXA1*, *PILRB*, and *SLC2A4*) were used to construct risk equations. The high-risk index was significantly associated with a poor BFS, which was also validated in the validation cohort. The area under the ROC curve (AUC) for BFS at 1-, 3-, and 5- year in the entire cohort was 0.819, 0.785, and 0.772, respectively, demonstrating the excellent predictive power of the MSRPI. Additionally, the MSRPI was found to be an independent prognostic factor for BFS in PCa. More importantly, MSRPI helped differentiate between cold and hot tumors. Hot tumors were associated with the high-risk group. Multiple drugs demonstrated

significantly lower IC50 values in the high-risk group, offering the prospect of precision therapy for patients with PCa.

Conclusion: The MSRPI developed in this study was able to predict biochemical recurrence in patients with PCa and identify cold and hot tumors. MSRPI has the potential to improve personalized precision treatment.

KEYWORDS

metabolic syndrome, prostate cancer, biochemical recurrence, prognostic model, immune microenvironment

1 Introduction

Prostate cancer (PCa) is the second most common cancer in men worldwide (1). There were more than 1,400,000 new cases of PCa worldwide and more than 370,000 deaths as a result in 2020 (2). The incidence and mortality of PCa is positively correlated with age, with a mean age at diagnosis of 66 years (3). In addition, there are significant geographic differences in the incidence and mortality of PCa, which is particularly common in developed countries. In the United States, PCa is the leading cause of cancer events and the second most common cause of cancer death in men (4). In comparison, Asia has the lowest incidence and mortality rates. However, with economic development and westernization of lifestyle, the incidence of PCa is rapidly increasing (5).

Radical prostatectomy (RP) is the primary treatment option for localized PCa. Nevertheless, owing to persistently elevated prostate-specific antigen (PSA) levels, nearly 50% of patients still experience biochemical recurrence (BCR) after surgery, suggesting a proclivity for poor prognosis (6). Nonetheless, it is not the case that every patient undergoing BCR will suffer from progressive disease (7). The impact of BCR on survival was mainly observed in patients with specific clinical risk factors such as a high Gleason score after RP (8). Long-term follow-up of patients with PCa often spans decades, and many patients do not die from PCa, making it difficult to reach the endpoint of overall survival (OS) in clinical trials. Thus, BCR serves as an intermediate clinical endpoint that can indicate clinical progression when the disease is at a low load (9, 10). Currently, there are no accepted molecular clusters and personalized scoring criteria associated with BCR, despite efforts to identify biomarkers or subtypes of PCa for BCR prediction (11).

The metabolic syndrome (MetS) is a set of combined clinical risk factors, primarily including obesity, insulin resistance, dyslipidemia and hypertension, and is significantly associated with an increased risk of type 2 diabetes and cardiovascular disease. The WHO definition for MetS includes insulin resistance as an essential component. However, the National Cholesterol Education Program Adult Treatment Panel III (NCEP ATP III) does not require that criterion. In contrast, the NCEP ATP III considers patients who meet three of the five criteria of obesity, hyperlipidemia, hypertension, elevated blood glucose levels and reduced HDL cholesterol levels to be diagnosed with MetS, which is considered by clinicians to be more applicable to clinical practice (12). The prevalence of MetS is highly correlated with age. In France, the prevalence is 5.6% and 17.5% in people aged 30-39 years and 60-64 years, respectively. Furthermore, in the US population, the prevalence rises from 7% in participants aged 20–29 years to 44% in those aged 60–69 years (13). From 2015 to 2017, the prevalence of MetS among Chinese residents aged 20 years and older was 31.1%. In addition, due to the unique urban-rural differences in China, the prevalence of MetS is relatively higher in urban areas than in rural areas (14). In recent years, the prevalence of MetS has increased significantly with the increase in obesity rates among adolescents (13). This particular syndrome is the result of the interaction between multiple genes and the environment. Similarly, cancer, as a group of multifactorial diseases, is thought to be correlated with genetic and metabolic abnormalities (15). Consistent with the original theory of Otto Warburg, there is growing evidence that cancer is principally a metabolic disease (16). In the past few years, the association of MetS with cancer has been documented, including PCa, but the exact mechanism underlying the relationship remains unclear (17, 18). According to studies published to date, obesity and insulin resistance (IR), the central clinical features of MetS, are associated with a high risk of cancer at multiple sites (18). Generally, obesity can promote IR (19), subsequently leading to hyperinsulinemia and hyperglycemia. Hyperinsulinemia contributes to cell mitosis. Overproduction of reactive oxygen species (ROS) by hyperglycemia causes oncogenic mutations and carcinogenesis. In addition, hyperglycemia decreases sex hormone binding globulin, leading to elevated insulin-like growth factor-1 (IGF-1) and suppressed apoptosis. Overall, this process leads to tumorigenesis (20).

As a male-specific endocrine and reproductive organ, the prostate harbors complex hormonal and metabolic variations. Therefore, MetS and PCa may be linked intrinsically (21). It has been investigated that the presence of MetS is correlated with malignant outcomes of PCa, especially BCR (22). An et al. reported in a real-world study that metastatic prostate cancer (mPCa) patients with MetS traits were more likely to progress to castration-resistant prostate cancer (CRPC) and had lower PSA remission rates and shorter survival times (23). However, to the best of our knowledge, studies addressing MetS and BCR in PCa are limited.

In this era of immune-targeted therapies, the concept of hot and cold tumors has been proposed, laying the foundation for precise patient stratification and individualized treatment (24). PCa has been portrayed as an immunological desert, and the majority of PCa patients respond weakly to checkpoint inhibitors, such as anti-PD1 or anti-CTLA-4 (25). Therefore, our purpose was to identify prognostic metabolic syndrome-related genes associated with BCR in PCa. These genes may be involved in the metabolic process of PCa progression and may be potential targets for controlling disease progression and recurrence. We then constructed a metabolic syndrome-related prognostic index (MSRPI) using seven genes to stratify patients and effectively identify hot tumors to provide a basis for establishing individualized treatment regimens and drug choices.

2 Materials and methods

2.1 Data collection and processing

We downloaded the transcriptomic and clinical data of PCa patients from The Cancer Genome Atlas (TCGA) (https://portal.gdc.cancer.gov/) (26). In this study, we combined the data types of "biochemical recurrence" and "new tumor event after initial treatment" to define the state of BCR. In addition, "days to first biochemical recurrence" or "days to new tumor event after initial treatment" was identified as the time to BCR. For the samples with the data of "biochemical recurrence" and "days to first biochemical recurrence", we considered them as the state of BCR and the time to BCR, respectively. In those with data of "biochemical recurrence" but no "days to first biochemical recurrence," we consider "new tumor event after initial treatment" and "days to new tumor event after initial treatment" as the state of BCR and the time to BCR, respectively; in those with data of "days to first biochemical recurrence" but no "biochemical recurrence," we utilized "new tumor event after initial treatment" as the state of BCR. BCR-free survival (BFS) was defined as the interval from radical treatment to the first BCR or death. Finally, we screened 400 PCa samples with the state of BCR and the time to BCR, which were randomly divided into training (n = 200) and test cohorts (n = 200). The validation cohort was the dataset GSE70769 extracted from the Gene Expression Omnibus (GEO) database (http://www.ncbi.nlm.nih.gov/geo/).

Differentially expressed genes (DEGs) for PCa were obtained from Gene Expression Profiling Interactive Analysis (GEPIA) (http://gepia2.cancer-pku.cn/) using the Limma differential method (|log2FC| >1, padj <0.01) (Supplementary Data sheet 1) (27). The metabolic syndrome network containing 1,243 genes was acquired from the Molecular Signatures Database (MsigDB) (http://www.broad.mit.edu/gsea/msigdb/) (Supplementary Data sheet 2) (28, 29). We screened for differentially expressed metabolic syndrome-related genes (DEMSRGs) associated with BFS in the training cohort using univariate Cox regression analysis.

2.2 Functional enrichment

By uploading 208 DEMSRGs into the Database for Annotation, Visualization, and Integrated Discovery (DAVID) (30), we obtained the results of Gene Ontology (GO) analysis. The first ten results are displayed in ascending order of p-values. Gene set enrichment analysis (GSEA) was used for Kyoto Encyclopedia of Genes and Genomes (KEGG) pathways using GSEA software (28). $P < 0.05$ was considered statistically significant.

2.3 Clusters based on 46 prognostic DEMSRGs

Based on the prognostic DEMSRGs, potential molecular clusters were explored using the ConsensusClusterPlus R package (31). Principal component analysis (PCA) was performed using the Rtsne R package.

2.4 A novel metabolic syndrome-related prognostic index for BCR-free survival

We performed least absolute shrinkage and selection operator (LASSO) on the 46 prognostic DEMSRGs and extracted 13 DEMSRGs at the appearance of minimal partial likelihood deviance. Seven of these 13 DEMSRGs were subsequently screened using multivariate Cox regression analysis to participate in the construction of the MSRPI.

The MSRPI was calculated using the following formula:

$$\begin{aligned}\text{MSRPI} = {} & \text{gene (A) expression}*\text{coef (A)} \\ & + \text{gene (B) expression}*\text{coef (B)} + \ldots \\ & + \text{gene (i) expression}*\text{coef (i)} .\end{aligned}$$

Patients in the training cohort, test cohort, and entire cohort were divided into high- and low-risk groups based on the median MSRPI of the training cohort. KaplanMeier survival analysis was performed using the survival and survminer R packages. $P < 0.05$ was considered statistically significant. Time-dependent receiver operating characteristic (ROC) curves were generated using the timeROC R package to verify the predictive power of different factors on BFS.

2.5 A predictive nomogram and calibration

The patient data for constructing the nomogram were derived from the entire TCGA cohort. Using the rms R package, the nomogram was constructed using age, Gleason score, T stage, N stage and risk to predict 1-, 3-, and 5-year BFS. The calibration curve demonstrates the accuracy of the prediction.

2.6 Immune infiltrating cells and activation of immune checkpoints

Using the gsva R package, single-sample gene set enrichment analysis (ssGSEA) was used to calculate the scores of immune-infiltrating cells and immune function. Using the "infiltration estimation for tcga" file from the TIMER2.0 (http://timer.cistrome.org/) (32), relying on limma, scales, ggplot2, ggtext and pheatmap R packages, the immune infiltration analysis was performed using different methods and the results were visualized using a bubble chart and a heat map. In addition, we compared the tumor microenvironment (TME) scores (including stromal score, immune score, and estimate score) by estimating the R package and the activation of immune checkpoints using the ggpubr R package between different subgroups.

2.7 Drug sensitivity and landscape of somatic mutation

To evaluate the treatment response, we used the pRRophetic R package to calculate half-maximal inhibitory concentrations (IC50) for each patient using the Genomics of Drug Sensitivity in Cancer (GDSC) (https://www.cancerrxgene.org/) (33). Finally, we explored the landscape of somatic mutations and calculated the tumor mutational burden (TMB) of patients in the risk groups using the maftools R package. Single-nucleotide mutation data of the patients were obtained from TCGA database.

3 Results

3.1 Functional enrichment and cox regression analysis

The flow of this study is presented in Figure 1. The clinical characteristics of the training cohort and the testing cohort are showed in Table 1. We identified 208 DEMSRGs (Figure 2A) and the results of their functional enrichment analysis are presented in Figures 2B–D. Based on the results of GO enrichment analysis, the most relevant biological processes (BP) were angiogenesis, extracellular matrix organization, and collagen biosynthetic process (Figure 2B), and the most relevant cellular components (CC) were the extracellular matrix, plasma membrane, and endoplasmic reticulum lumen (Figure 2C). The most relevant molecular functions (MF) were extracellular matrix structural constituent, extracellular matrix structural constituent conferring tensile strength, and transforming growth factor beta binding (Figure 2D). Subsequently, 46 prognostic DEMSRGs related to BFS were screened using univariate Cox regression analysis ($P < 0.05$) (Figure 2E). The correlation network of the 46 DEMSRGs is shown in Figure 2F.

3.2 Identification of two metabolic syndrome-associated molecular clusters

Based on these 46 genes, consensus clustering analysis was performed to classify patients into two clusters (Figure 3A). We then

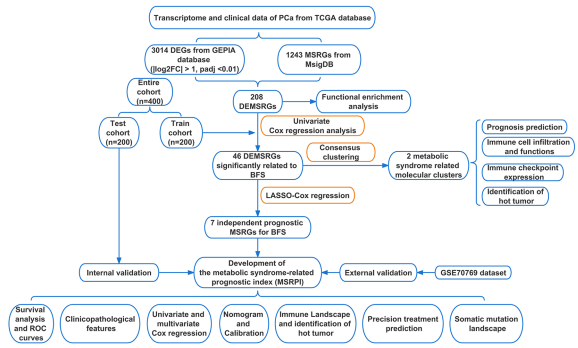

FIGURE 1
Flow chart of this study. TCGA, The Cancer Genome Atlas; DEGs, differentially expressed genes; GEPIA, Gene Expression Profiling Interactive Analysis; MSRGs, metabolic syndrome-related genes; MsigDB, molecular signatures database; DEMSRGs, differentially expressed metabolic syndrome-related genes; BFS, BCR-free survival; LASSO, least absolute shrinkage and selection operator; ROC, receiver operating characteristics.

performed a principal component analysis (PCA) to clearly distinguish the two clusters (Figure 3B). There was no significant difference in the BFS between the two clusters (Figure 3C). However, according to the analyses of the different platforms, cluster 2 was infiltrated more by immune cells (Figure 3D). In addition, immune checkpoints, such as CD274, CD40, CD44, and LAG-3, showed a greater degree of activation in cluster 2 (Figure 3E). Single-sample GSEA (ssGSEA) was used to score immune cell infiltration and function. The results showed that cluster 2 had a higher percentage of infiltrating B cells, CD8+ T cells, dendritic cells (DCs), T helper cells, and regulatory T (Treg) cells than cluster 1 (Figure 3F). The results also revealed that cluster 2 had a higher score for a series of immune functions, such as parainflammation, T-cell co-stimulation, and type II IFN response (Figure 3G). Consistently, the stromal, immune, and Estimation of STromal and Immune cells in MAlignant Tumor tissues using Expression data (ESTIMATE) scores in cluster 2 were markedly higher than those in cluster 1 (Figures 3H–J). Additionally, we further analyzed the correlation coefficients of each DEMSRGs with immune cell infiltration in the two clusters (Supplementary Figure 1). Overall, cluster 2 was more immunogenic, indicating that cluster 2 was hotter than cluster 1.

3.3 Construction and validation of MSRPI

First, we performed LASSO regression on the 46 DEMSRGs in the training cohort, extracting 13 DEMSRGs (Figures 4A, B). Subsequently, multivariate Cox regression was performed on these 13 DEMSRGs, seven of which were screened for the construction of the MSRPI (including *CSF3R*, *TMEM132A*, *STAB1*, *VIM*, *DUOXA1*, *PILRB*, and *SLC2A4*).

We calculated MSRPI with the formula:

$$\mathrm{MSRPI} = (1.405977046)*CSF3R + (0.69687348)*TMEM132A + (0.898243278)*STAB1 + (0.594172062)*VIM + (-1.073071594)*DUOXA1 + (0.508225585)*PILRB + (-0.956336578)*SLC2A4\,.$$

The MSRPI was calculated for each patient in the training, test, entire cohort, and validation cohorts. As shown in Figure 4C, the

TABLE 1 The clinical characteristics of PCa patients in the training and testing cohorts.

Characteristics	Training cohort	Testing cohort
Sample	200	200
Age	–	–
<=60	90	94
>60	110	106
Gender	–	–
Male	200	200
T stage	–	–
T2a	3	5
T2b	8	1
T2c	52	82
T3a	72	55
T3b	55	55
T4	5	2
Unknown	5	0
N stage	–	–
N0	144	142
N1	32	28
Unknown	24	30
M stage	–	–
M0	190	185
M1	0	2
Unknown	10	13
Gleason score	–	–
GS=6	17	21
GS=7	103	95
GS=8	28	22
GS=9	50	61
GS=10	2	1

principal component analysis (PCA) was able to distinguish high-risk samples from low-risk samples. Patients in the training, test, and entire cohorts were divided into high- and low-risk groups (Figure 4D). The BFS status and expression heat map of the seven DEMSRGs of the training, testing, and entire cohort are shown in Figures 4E, F, respectively. The Sankey diagram presented the relationship between the clusters and risk groups (Figure 4G).

The BFS of high-risk patients in the training (Figure 5A), test (Figure 5C), entire (Figure 5E), and validation cohorts (Figure 5G) was significantly lower than that of the low-risk patients. We utilized ROC curves to evaluate the sensitivity and specificity of the MSRPI for biochemical recurrence. The area under the ROC curve (AUC) represents the outcome of the ROC. The 1-, 3-, and 5-year AUC of the training cohort were 0.883, 0.835, and 0.877, respectively (Figure 5B). Those of the test cohort were 0.770, 0.762, and 0.702 (Figure 5D), respectively. The 1-, 3-, and 5-year AUC for the entire cohort were 0.819, 0.785, and 0.772 (Figure 5F), and those of the validation cohort were 0.622, 0.653, and 0.626, respectively (Figure 5H). The risk level based on the MSRPI showed remarkable predictive power compared to clinical factors (Figure 5I). BFS remained lower in the high-risk group in the subgroups of age (Figures 6A, E), clinical T (Figures 6B, F), Gleason score (Figures 6C, G), pathologic T (Figures 6D, H), clusters (Figures 6I, J), and pathologic N0 (Figure 6K). In the pathological N1 subgroup, the difference in BFS between the risk groups was not statistically significant (Figure 6L). Moreover, we found a significant positive correlation between the MSRPI and several staging indicators (pathologic T, pathologic N, clinical T, and Gleason score) of PCa ($P < 0.05$) (Figures 6M–P). In contrast, the MSRPI did not show a significant correlation with age (Figure 6Q) or race (Figure 6R).

3.4 Construction of a nomogram predicting the 1-, 3- and 5-year BFS

We performed univariate and multivariate Cox regression analyses on the MSRPI and clinical factors in TCGA (Figures 7A, B) and validation cohorts (Figures 7C, D), respectively. The MSRPI was an independent predictor of BFS in PCa patients in both cohorts (TCGA: univariate: HR = 1.019, $P < 0.001$; multivariate: HR = 1.013, $P = 0.002$; GSE70769: univariate: HR = 2.041, $P = 0.005$; multivariate: HR = 1.752, $P = 0.040$). In addition, we found that Gleason score was also an independent prognostic parameter (TCGA: univariate: HR = 2.325, $P < 0.001$; multivariate: HR = 1.901, $P < 0.001$; GSE70769: univariate: HR = 2.349, $P < 0.001$; multivariate: HR = 2.105, $P < 0.001$) (Figures 7A–D).

According to age, Gleason score, T stage, N stage and risk level based on the MSRPI, we constructed a nomogram to predict the 1-, 3-, and 5-year BFS of patients with PCa (Figure 7E). The calibration plot showed the excellent predictive power of the nomogram for 1-, 3-, and 5-year BFS (Figure 7F).

3.5 Differentiating between cold and hot tumors and precision treatment in risk groups

GSEA was conducted for KEGG functional enrichment analysis in the high-risk group. Glycosaminoglycan biosynthesis, chondroitin sulfate, glycosylphosphatidylinositol (GPI) anchor biosynthesis, N-glycan biosynthesis, nod-like receptor signaling pathway, spliceosome, T cell receptor signaling pathway, and ubiquitin-mediated proteolysis were the main KEGG enriched pathways in the high-risk group (Figure 8A). In addition, we found that almost all immune checkpoints were highly activated in the high-risk group, including CD276, CTLA4, HAVCR2 (TIM3), and NRP1 (Figure 8B). In addition, the landscape of immune infiltration based on different platforms demonstrated that the high-risk group possessed a richer immune abundance (Figure 8C). We further explored the correlation between the

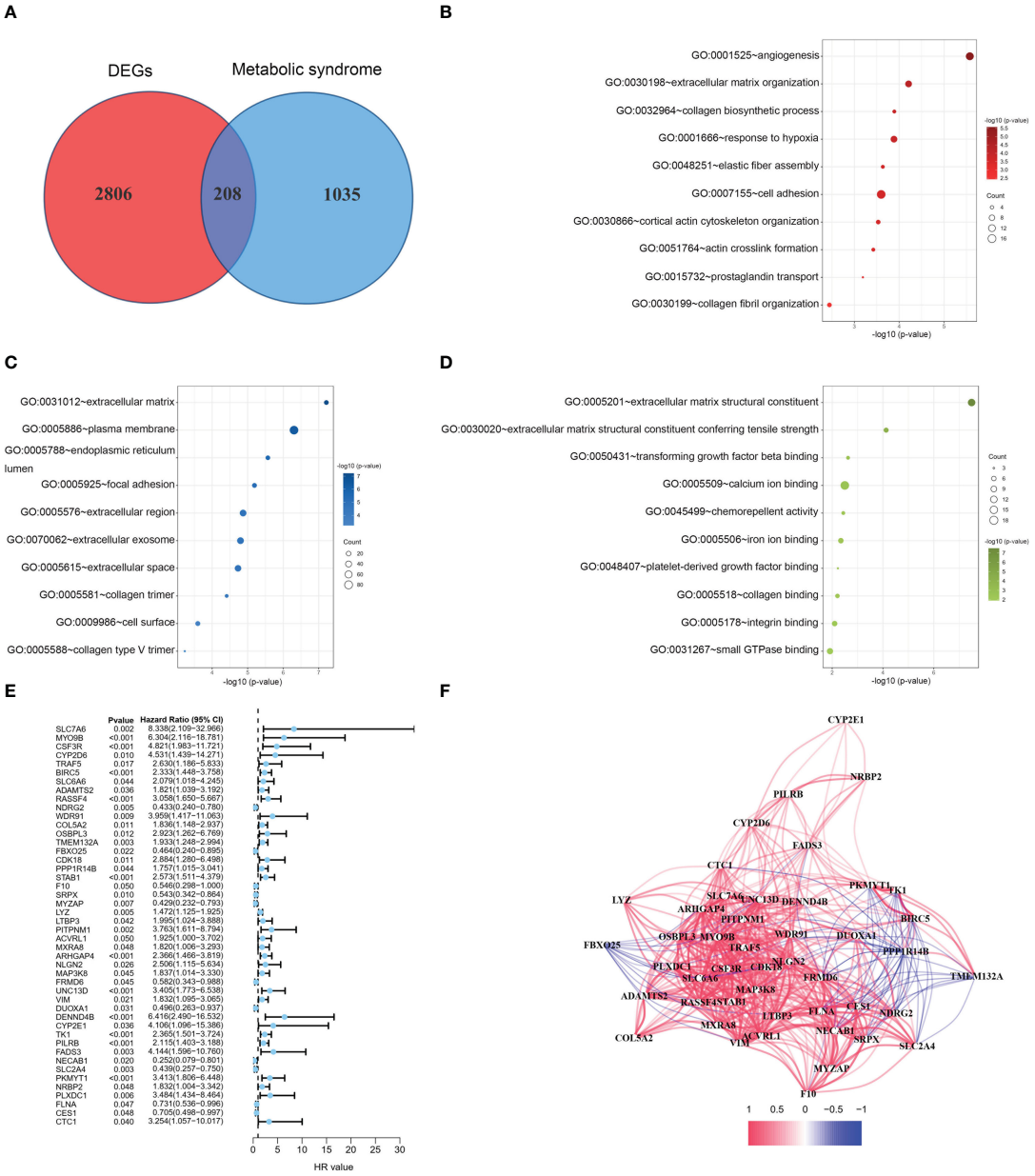

FIGURE 2
GO analyses and identification of prognostic DEMSRGs. **(A)** Venn diagram of DEGs and MSRGs. **(B–D)** BP, CC and MF of 208 DEMSRGs. **(E)** Univariable Cox regression to identify 46 DEMSRGs related to BFS in the train cohort. **(F)** Correlation network of 46 DEMSRGs.

MSRPI and immune cell infiltration. According to the results of the analysis employing different software platforms, more immune cells were significantly and positively associated with the MSRPI (Figure 8D), such as cancer-associated fibroblasts in EPIC, macrophages and myeloid dendritic cells in XCELL, and Tregs and T cell follicular helper in CIBERSORT-ABS (Figure 8E). The stromal, immune, and ESTIMATE scores were also higher in the high-risk group (Figure 8F). In summary, these indicate that the high-risk group has immunologically hot tumors and are more likely to benefit from immunotherapy. We screened 34 targeted agents that showed lower IC50 values in the high-risk group in the treatment of PCa, 12 of which were displayed, such as AMG706 (motesanib) and rapamycin (Figure 8G).

3.6 Landscape of somatic mutation in risk groups

To explore the difference in somatic mutations in the risk groups, we calculated the proportion and type of mutation for each patient and

10.3389/fendo.2023.1148117

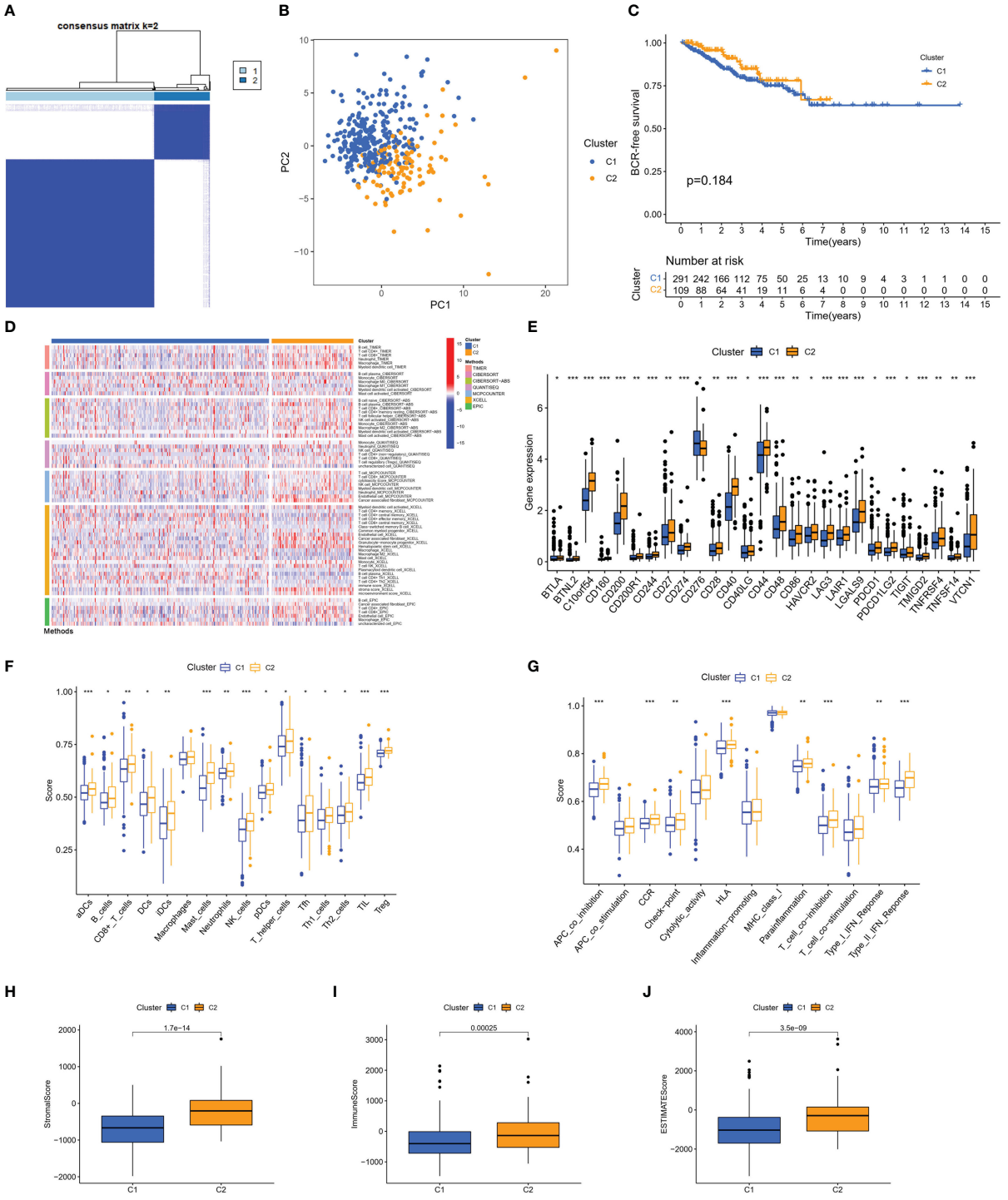

FIGURE 3
Identification of two metabolic syndrome-associated clusters. **(A)** Consensus clustering. **(B)** PCA. **(C)** KM survival analysis of clusters. **(D)** Immune infiltration analysis of the different platforms. **(E)** Expression of immune checkpoints. **(F, G)** SsGSEA of immune infiltrating cells and immune function. **(H–J)** Stromal score, immune score, and ESTIMATE score for two clusters. *p<0.05, **p<0.01, ***p<0.001.

the tumor mutational burden (TMB) of both groups. Figures 9A–D shows the landscape of mutations in the high- and low-risk groups, respectively. The top five genes with the highest mutation rates in the high-risk group were *TP53* (19%), *TTN* (14%), *SPOP* (10%), *FOXA1* (8%), and *KMT2D* (8%). *SPOP* (11%), *TTN* (6%), *TP53* (5%), *KDM6A* (4%), and *KMT2D* (4%) showed the highest mutation rates in the low-risk group. TP53 and TTN had a higher proportion of mutations in the high-risk group, whereas SPOP had a higher proportion of mutations in the low-risk group. Moreover, TMB was higher in the high-risk group than in the low-risk group (Figure 9E).

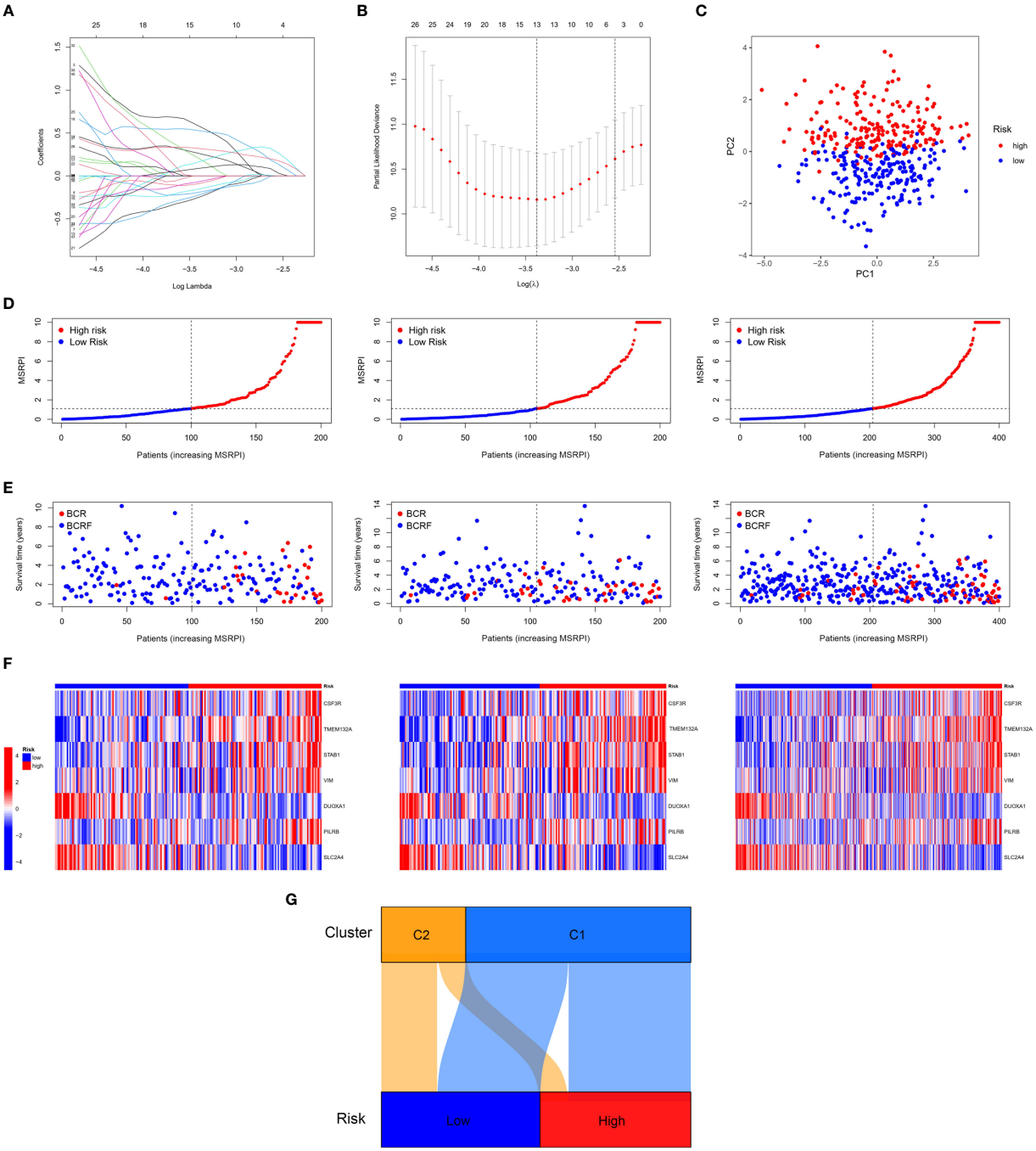

FIGURE 4
Construction of the MSRPI. **(A, B)** LASSO regression analysis **(C)** and PCA. The distribution of **(D)** MSRPI, **(E)** survival status and **(F)** gene expression of the train, test, and entire TCGA cohort. **(G)** The Sankey diagram of clusters and risk groups.

4 Discussion

Despite tremendous progress in recent years in oncologic therapeutic strategies targeting immune checkpoints, therapeutic efficacy is not satisfactory in a wide range of PCa patients owing to the immunosuppressive tumor microenvironment of PCa. Therefore, we introduce the concept of hot and cold tumors, a classification based on the type and density of immune cells inside the tumor, which can predict tumor prognosis more accurately than the traditional TNM system and guide the choice of immunotherapy for PCa (24). High-infiltration tumors with a high immune score are usually referred to as hot tumors, while low-infiltration tumors are referred to as cold tumors. BCR, a key intermediate event after RP, is suggestive of clinical recurrence or

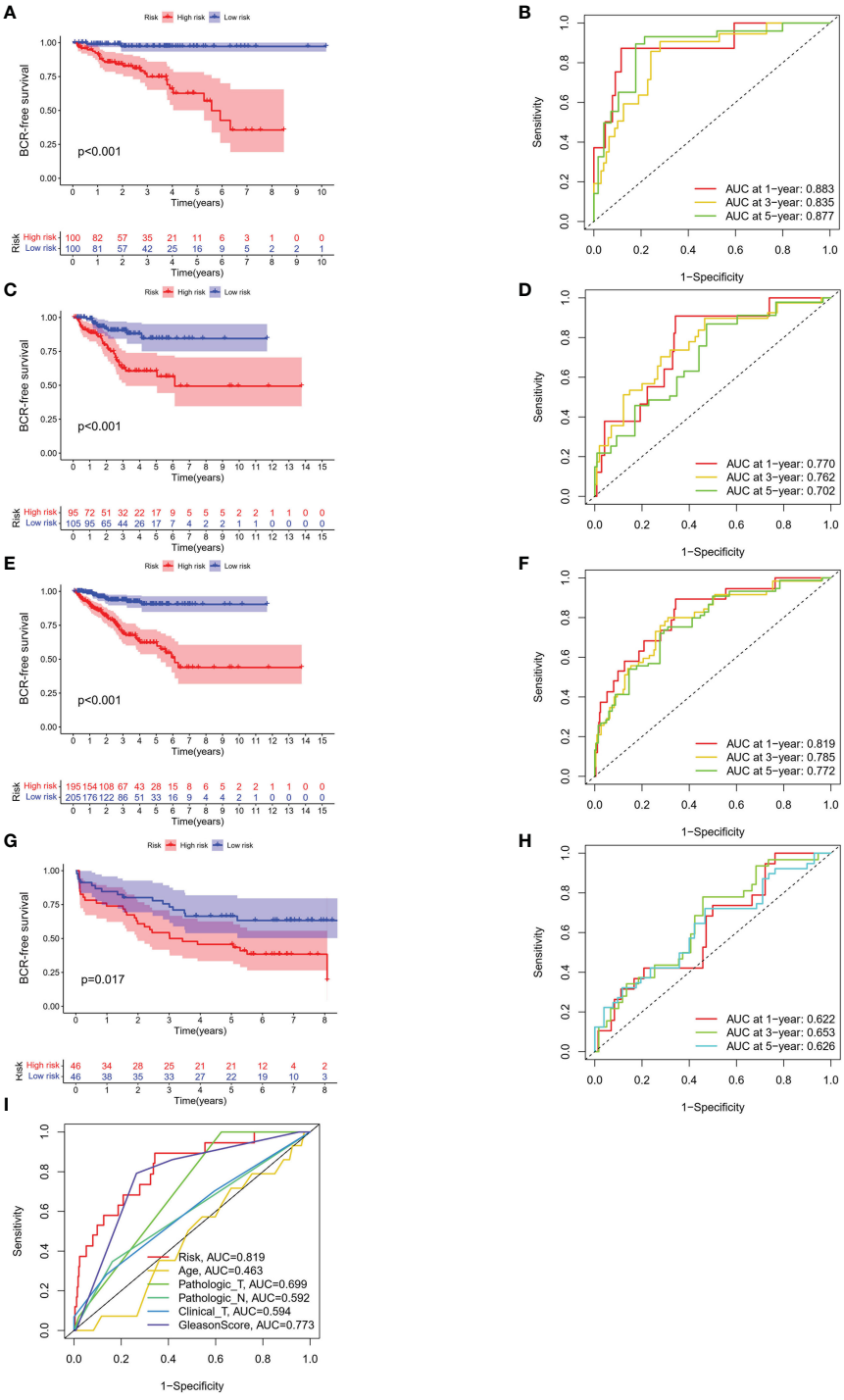

FIGURE 5
Survival analyses of different cohorts. KM analyses of BFS and 1-, 3- and 5-year ROC curves in the **(A, B)** train, **(C, D)** test, **(E, F)** entire and **(G, H)** validation cohort. **(I)** The ROC curve of risk and other clinical factors.

metastasis of PCa (34). Through this study, for the very first time, a recurrence risk signature at the polygenic level from the standpoint of MetS was constructed and validated to provide a reference for treatment decisions in clinical practice.

In this study, we first identified two MetS-related molecular clusters using consensus clustering. The two clusters had different tumor immune microenvironments. Unfortunately, there was no significant difference in BFS between the two clusters. Subsequently, we constructed the MSRPI using the LASSO multivariate Cox regression model. In the training cohort, test cohort, entire cohort, and validation cohort, the high-risk group was associated with poor BFS compared to the low-risk group. In the entire cohort,

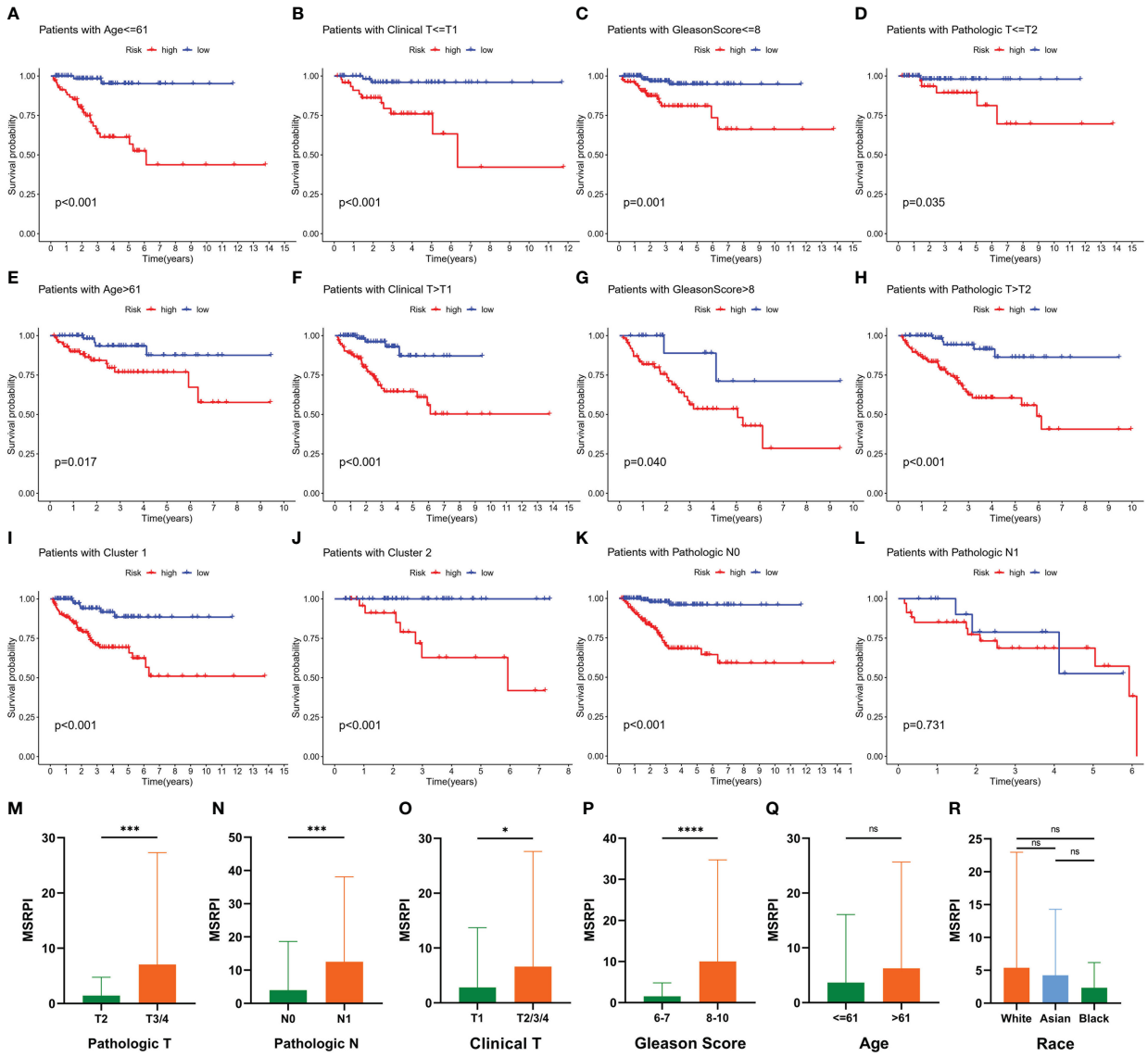

FIGURE 6
Prognostic value of MSRPI and its relationship with clinicopathological factors. KM curves of BFS in patients stratified by **(A, E)** age, **(B, F)** clinical T, **(C, G)** Gleason score, **(D, H)** pathologic T, **(K, L)** pathologic N, **(I, J)** and cluster. Relationships between MSRPI and other factors including **(M)** pathologic T, **(N)** pathologic N, **(O)** clinical T, **(P)** Gleason score, **(Q)** age and **(R)** race. *p < 0.05, **p < 0.01, ***p < 0.001, ****p < 0.0001 and "ns" means not statistically significant.

the area under the ROC curve for the MSRPI was 0.819 versus 0.773 for the Gleason score, demonstrating the outstanding predictive performance of this index for BFS. Multivariate Cox regression analysis revealed that the BFS-related MSRPI was an independent predictor of PCa. More importantly, the high- and low-risk groups exhibited distinctly different immune landscapes. The high-risk group featured more CD8+ and CD4+ T cell infiltration, higher immune scores, greater activation of immune checkpoints, and stronger sensitivity to immunotherapy, which are characteristic of hot tumors.

The MSRPI consists of seven metabolic syndrome-related genes (MSRGs), including *CSF3R*, *TMEM132A*, *STAB1*, *VIM*, *DUOXA1*, *PILRB*, and *SLC2A4*. Of these MSRGs, abnormal colony-stimulating factor receptor (CSFR) expression plays an oncogenic role in many hematologic and solid tumors, such as nasopharyngeal, breast, and ovarian cancers (35–37), but its role in PCa remains unclear. Transmembrane protein 132A (*TMEM132A*), a novel cellular pathway regulator, activates the Wnt pathway (38), the dysregulation of which underlies the metabolic traits of MetS (39). In addition, Wang et al. revealed that Wnt regulation drives prostate cancer bone metastasis and invasion (40). Stabilin-1 (*STAB1*) and triggering receptor expressed on myeloid cell 2 (*TREM2*) are expressed in a lipid-associated macrophage subset, which supports a tumor immunosuppressive

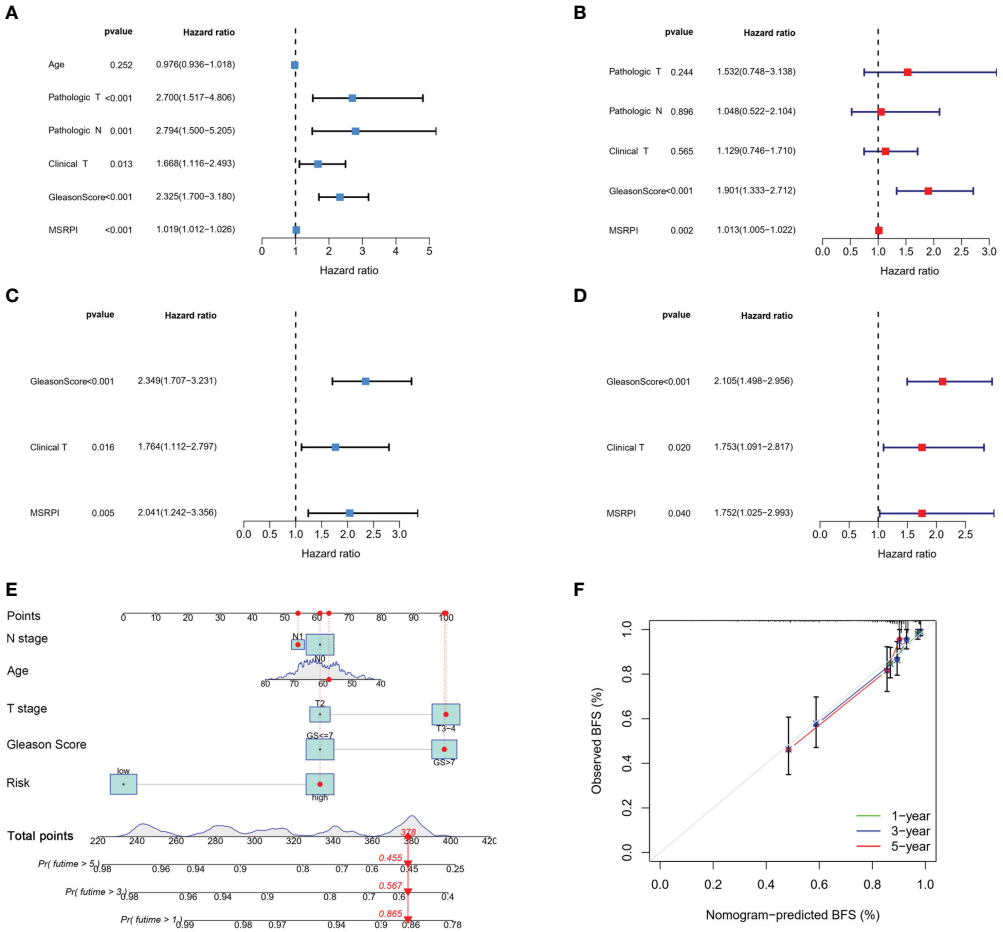

FIGURE 7
Cox regression analysis and construction of the nomogram. Univariate and multivariate Cox regression of MSRPI and other clinical parameters in the **(A, B)** entire TCGA and **(C, D)** validation cohorts. **(E)** Nomogram based on T stage, N stage, age, Gleason score and risk level. **(F)** Calibration plot of nomogram.

microenvironment and is involved in the progression of obesity and its metabolic complications (41, 42). Cheaito et al. demonstrated that vimentin (*VIM*) could serve as a biomarker of epithelial-to-mesenchymal transition (EMT) to predict BFS in PCa (43). Ostrakhovitch et al. reported that cell proliferation inhibition associated with p21 upregulation occurs after transfection of the dual oxidase 1 (*DUOXA1*) and low expression of *DUOXA1* correlates with tumor aggressiveness (44). Moreover, the oxygen radicals produced by *DUOXA1* are associated with intravascular plaque formation, which is a critical risk factor for atherosclerosis (45). Using bioinformatics and immunohistochemistry approaches, Che et al. indicated that *PILRB* was enriched in high-risk PCa patients and could serve as a predictor of recurrence-free survival (46). Solute carrier family-2-member-4-gene (*SLC2A4*) is an insulin-sensitive glucose transporter protein that plays a key regulatory role in the pathogenesis of type 2 diabetes (47). Given that accelerated glycolysis initiated by glucose transport is essential for rapid proliferation in oncogenesis, it has been suggested that *SLC2A4* may serve as a prospective biomarker for a variety of tumors (48–50). Interestingly, although there have been few studies on the role of *SLC2A4* in PCa in recent years, Gonzalez-Menendez et al. revealed that *SLC2A4* appears to be more important for glucose uptake in androgen-insensitive PCa than in androgen-sensitive PCa (51).

We explored the somatic mutation landscape of patients with PCa in the TCGA cohort, where *TP53*, *TTN*, and *SPOP* were three of the high-frequency mutated genes. Mutations in *TP53*, a widely known and prominent tumor suppressor gene, can upregulate Twist1 expression and promote the epithelial-to-mesenchymal transition and recurrence in advanced PCa (52). Furthermore, mutant p53 proteins can aggregate, resulting in a negative effect on wild-type p53 proteins. Zhang et al. demonstrated the therapeutic potential of targeting mutant p53 proteins in PCa cells using a peptide inhibitor of p53 aggregation (53). There is a strong positive correlation between the number of Titin (*TTN*) mutations and TMB. Several studies have indicated that increased

10.3389/fendo.2023.1148117

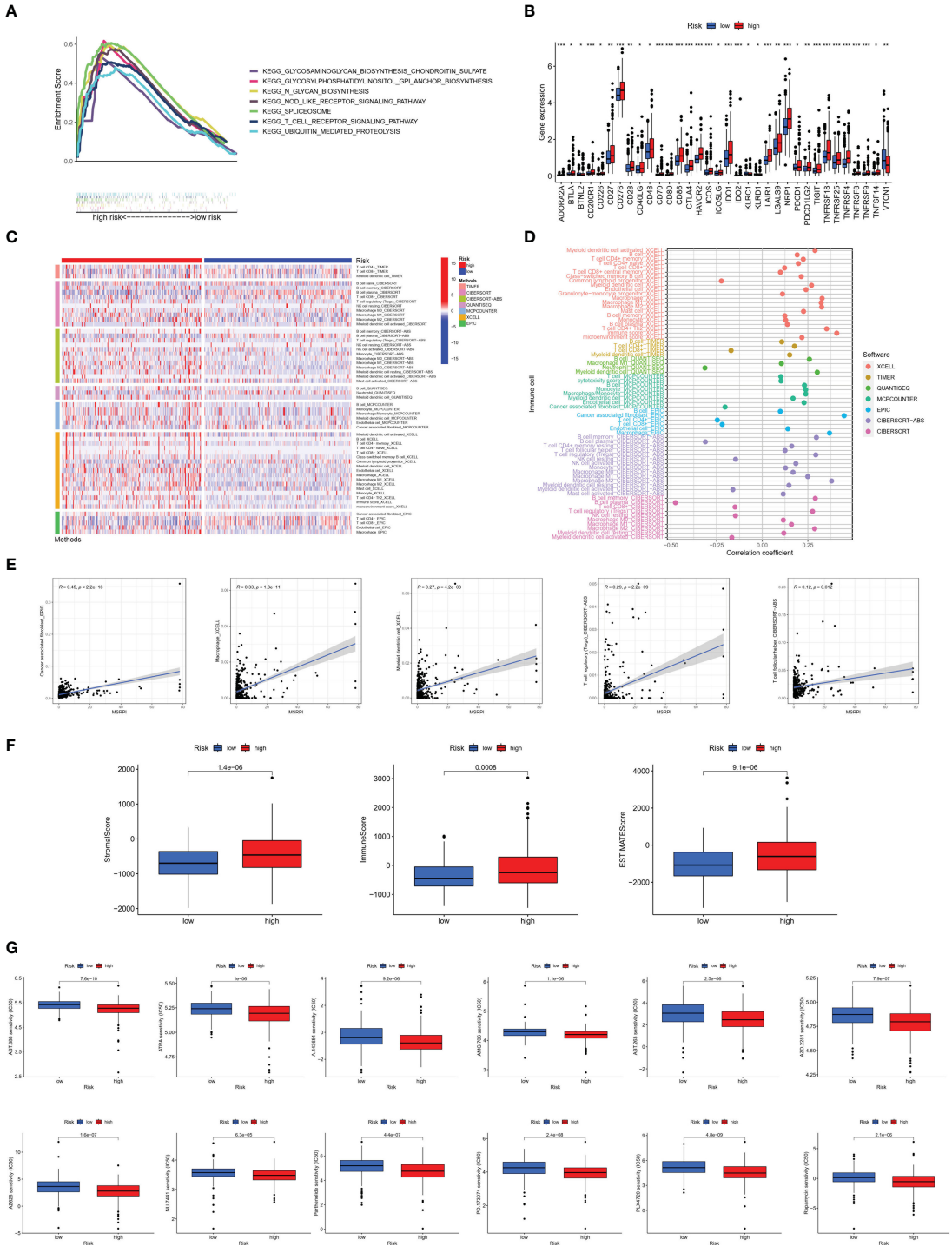

FIGURE 8
Immune infiltration analysis between the high- and low-risk groups. **(A)** Main results of GSEA in high-risk group. **(B)** Immune checkpoints activation. **(C)** Heat map of immune infiltration. **(D, E)** Association of infiltrating immune cells with MSRPI based on different software platforms. **(F)** Stromal score, immune score, and ESTIMATE score for two risk groups. **(G)** Drug sensitivity prediction in risk groups. *p<0.05, **p<0.01, ***p<0.001.

TMB correlates with improved response rates and survival benefits of immune checkpoint blockade therapy (54, 55). In our study, the high-risk group with more *TTN* mutations and higher TMB was associated with poor BFS and was more sensitive to immunotherapeutic agents, which was consistent with previous reports. Missense mutations in speckle-type POZ protein (*SPOP*) are one of the most common genetic mutations in PCa. Shi et al. showed that *SPOP* mutations prolonged the survival of PCa cells by

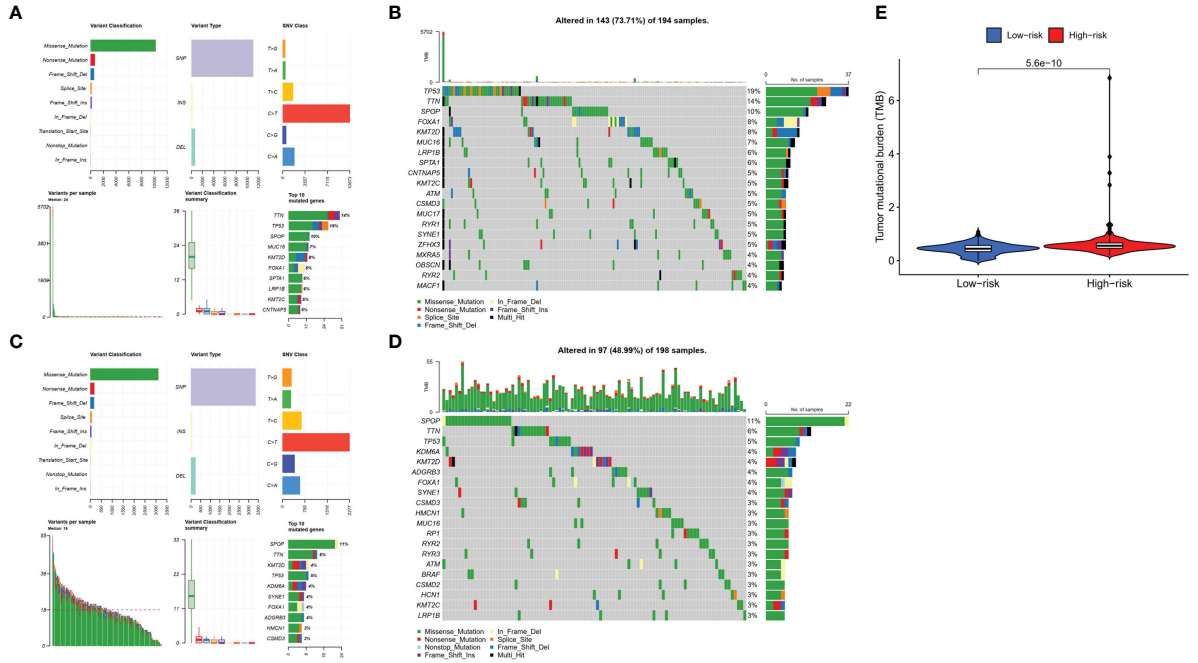

FIGURE 9
Tumor mutations diagram in risk groups. Mutational landscape in the **(A, B)** high- and **(C, D)** low-risk groups. **(E)** TMB in the high- and low-risk groups.

upregulating cell cycle-associated protein 1 (Caprin1)-dependent stress granule assembly (56). It has also been reported that PCa-related *SPOP* mutants fail to ubiquitinate *SQSTM1*, promoting *SQSTM1*-dependent autophagy and exerting tumorigenic effects (57).

In this study, we constructed and externally validated a metabolic syndrome-associated risk model using seven genes. This risk formula contains fewer genes than similar studies, making its application simpler and easier. However, this study has some limitations. Firstly, we were not able to identify metabolic differences between the two clusters of PCa patients due to limitations of patient information in public databases. Basic experiments on the potential biological mechanisms of DEMSRGs are needed in the future. In addition, we need more real-world samples to verify the stability of the model.

5 Conclusion

In this study, 46 DEMSRGs were significantly associated with BFS, and two metabolic syndrome-associated molecular clusters were identified. The MSRPI is a potent and promising biochemical marker for PCa recurrence. Although PCa tends to have a barren tumor immune microenvironment, we were still able to categorize PCa tumors into hot and cold through MSRPI. Hot tumors appear to be more sensitive to immunotherapy and consequently, patients with hot tumors can benefit from this, providing a basis for personalized treatment options for PCa.

Data availability statement

The original contributions presented in the study are included in the article/Supplementary Material. Further inquiries can be directed to the corresponding author.

Author contributions

CR and XL designed the research. HL, YL and XC collected the data. CR, QW and SW performed the bioinformatics analysis. HZ and MX wrote the manuscript. All authors contributed to the article and approved the submitted version.

Acknowledgments

We would like to thank the Cancer Genome Atlas, the Gene Expression Omnibus, GEPIA and the Molecular Signatures Database for data availability.

Conflict of interest

The authors declare that the research was conducted in the absence of any commercial or financial relationships that could be construed as a potential conflict of interest.

Publisher's note

Supplementary material

The Supplementary Material for this article can be found online at: https://www.frontiersin.org/articles/10.3389/fendo.2023.1148117/full#supplementary-material

SUPPLEMENTARY DATA SHEET 1
Differentially expressed genes in PCa from GEPIA2 database.

SUPPLEMENTARY DATA SHEET 2
Metabolic syndrome-related gene network from MsigDB.

SUPPLEMENTARY FIGURE 1
Correlation test of 46 DEMSRGs with immune cell infiltration. *p < 0.05, **p < 0.01, ***p < 0.001, ****p < 0.0001.

References

1. Licitra F, Giovannelli P, Di Donato M, Monaco A, Galasso G, Migliaccio A, et al. New insights and emerging therapeutic approaches in prostate cancer. *Front Endocrinol (Lausanne)* (2022) 13:840787. doi: 10.3389/fendo.2022.840787

2. Sung H, Ferlay J, Siegel RL, Laversanne M, Soerjomataram I, Jemal A, et al. Global cancer statistics 2020: GLOBOCAN estimates of incidence and mortality worldwide for 36 cancers in 185 countries. *CA-Cancer J Clin* (2021) 71(3):209–49. doi: 10.3322/caac.21660

3. Capece M, Creta M, Calogero A, La Rocca R, Napolitano L, Barone B, et al. Does physical activity regulate prostate carcinogenesis and prostate cancer outcomes? a narrative review. *Int J Environ Res Public Health* (2020) 17(4). doi: 10.3390/ijerph17041441

4. Pernar CH, Ebot EM, Wilson KM, Mucci LA. The epidemiology of prostate cancer. *Cold Spring Harb Perspect Med* (2018) 8(12). doi: 10.1101/cshperspect.a030361

5. Zhu Y, Mo M, Wei Y, Wu J, Pan J, Freedland SJ, et al. Epidemiology and genomics of prostate cancer in Asian men. *Nat Rev Urol* (2021) 18(5):282–301. doi: 10.1038/s41585-021-00442-8

6. Suardi N, Porter CR, Reuther AM, Walz J, Kodama K, Gibbons RP, et al. A nomogram predicting long-term biochemical recurrence after radical prostatectomy. *Cancer* (2008) 112(6):1254–63. doi: 10.1002/cncr.23293

7. Van den Broeck T, van den Bergh RCN, Briers E, Cornford P, Cumberbatch M, Tilki D, et al. Biochemical recurrence in prostate cancer: The European association of urology prostate cancer guidelines panel recommendations. *Eur Urol Focus* (2020) 6 (2):231–4. doi: 10.1016/j.euf.2019.06.004

8. Van den Broeck T, van den Bergh RCN, Arfi N, Gross T, Moris L, Briers E, et al. Prognostic value of biochemical recurrence following treatment with curative intent for prostate cancer: A systematic review. *Eur Urol* (2019) 75(6):967–87. doi: 10.1016/j.eururo.2018.10.011

9. Mottet N, van den Bergh RCN, Briers E, Van den Broeck T, Cumberbatch MG, De Santis M, et al. EAU-EANM-ESTRO-ESUR-SIOG guidelines on prostate cancer-2020 update. part 1: Screening, diagnosis, and local treatment with curative intent. *Eur Urol* (2021) 79(2):243–62. doi: 10.1016/j.eururo.2020.09.042

10. Sweeney C, Nakabayashi M, Regan M, Xie W, Hayes J, Keating N, et al. The development of intermediate clinical endpoints in cancer of the prostate (ICECaP). *J Natl Cancer Inst* (2015) 107(12):djv261. doi: 10.1093/jnci/djv261

11. Wang X, Jordahl KM, Zhu C, Livingstone J, Rhie SK, Wright JL, et al. Methylation subtypes of primary prostate cancer predict poor prognosis. *Cancer Epidemiol Biomarkers Prev* (2022) 31(7):1473–82. doi: 10.1158/1055-9965.EPI-22-0007

12. Alberti KG, Zimmet P, Shaw J. Metabolic syndrome–a new world-wide definition. a consensus statement from the international diabetes federation. *Diabetes Med* (2006) 23(5):469–80. doi: 10.1111/j.1464-5491.2006.01858.x

13. Eckel RH, Grundy SM, Zimmet PZ. The metabolic syndrome. *Lancet* (2005) 365 (9468):1415–28. doi: 10.1016/S0140-6736(05)66378-7

14. Yao F, Bo Y, Zhao L, Li Y, Ju L, Fang H, et al. Prevalence and influencing factors of metabolic syndrome among adults in China from 2015 to 2017. *Nutrients* (2021) 13 (12). doi: 10.3390/nu13124475

15. Batra S, Adekola KU, Rosen ST, Shanmugam M. Cancer metabolism as a therapeutic target. *Oncol (Williston Park)* (2013) 27(5):460–7.

16. Seyfried TN. Cancer as a mitochondrial metabolic disease. *Front Cell Dev Biol* (2015) 3:43. doi: 10.3389/fcell.2015.00043

17. Esposito K, Chiodini P, Colao A, Lenzi A, Giugliano D. Metabolic syndrome and risk of cancer: a systematic review and meta-analysis. *Diabetes Care* (2012) 35 (11):2402–11. doi: 10.2337/dc12-0336

18. O'Neill S, O'Driscoll L. Metabolic syndrome: a closer look at the growing epidemic and its associated pathologies. *Obes Rev* (2015) 16(1):1–12. doi: 10.1111/obr.12229

19. Pothiwala P, Jain SK, Yaturu S. Metabolic syndrome and cancer. *Metab Syndr Relat Disord* (2009) 7(4):279–88. doi: 10.1089/met.2008.0065

20. Arcidiacono B, Iiritano S, Nocera A, Possidente K, Nevolo MT, Ventura V, et al. Insulin resistance and cancer risk: an overview of the pathogenetic mechanisms. *Exp Diabetes Res* (2012) 2012:789174. doi: 10.1155/2012/789174

21. Morlacco A, Zattoni F, Soligo M, Lami V, Iafrate M, Zanovello N, et al. Metabolic syndrome and prostate cancer treatment. *Panminerva Med* (2022) 64 (3):359–64. doi: 10.23736/S0031-0808.21.04511-0

22. Gacci M, Russo GI, De Nunzio C, Sebastianelli A, Salvi M, Vignozzi L, et al. Meta-analysis of metabolic syndrome and prostate cancer. *Prostate Cancer Prostatic Dis* (2017) 20(2):146–55. doi: 10.1038/pcan.2017.1

23. An H, Ma D, Mei Y, Wang L, Maimaitiyiming A, Zhuo T, et al. Metabolic syndrome and metastatic prostate cancer correlation study, a real-world study in a prostate cancer clinical research center, xinjiang, China. *Front Endocrinol (Lausanne)* (2022) 13:1090763. doi: 10.3389/fendo.2022.1090763

24. Galon J, Bruni D. Approaches to treat immune hot, altered and cold tumours with combination immunotherapies. *Nat Rev Drug Discovery* (2019) 18(3):197–218. doi: 10.1038/s41573-018-0007-y

25. Galustian C, Dalgleish A, Bodman-Smith M, Kusmartsev S, Dasgupta P. Editorial: Immunotherapy for prostate cancer - turning the immunological desert into an oasis of hope. *Front Oncol* (2022) 12:1021870. doi: 10.3389/fonc.2022.1021870

26. Tomczak K, Czerwinska P, Wiznerowicz M. The cancer genome atlas (TCGA): an immeasurable source of knowledge. *Contemp Oncol (Poznan Poland)* (2015) 19(1A): A68–77. doi: 10.5114/wo.2014.47136

27. Tang Z, Kang B, Li C, Chen T, Zhang Z. GEPIA2: an enhanced web server for large-scale expression profiling and interactive analysis. *Nucleic Acids Res* (2019) 47 (W1):W556–w60. doi: 10.1093/nar/gkz430

28. Subramanian A, Tamayo P, Mootha VK, Mukherjee S, Ebert BL, Gillette MA, et al. Gene set enrichment analysis: A knowledge-based approach for interpreting genome-wide expression profiles. *Proc Natl Acad Sci U S A* (2005) 102(43):15545–50. doi: 10.1073/pnas.0506580102

29. Chen Y, Zhu J, Lum PY, Yang X, Pinto S, MacNeil DJ, et al. Variations in DNA elucidate molecular networks that cause disease. *Nature* (2008) 452(7186):429–35. doi: 10.1038/nature06757

30. Huang DW, Sherman BT, Tan Q, Collins JR, Alvord WG, Roayaei J, et al. The DAVID gene functional classification tool: a novel biological module-centric algorithm to functionally analyze large gene lists. *Genome Biol* (2007) 8(9):16. doi: 10.1186/gb-2007-8-9-r183

31. Wilkerson MD, Hayes DN. ConsensusClusterPlus: a class discovery tool with confidence assessments and item tracking. *Bioinformatics* (2010) 26(12):1572–3. doi: 10.1093/bioinformatics/btq170

32. Li TW, Fu JX, Zeng ZX, Cohen D, Li J, Chen QM, et al. TIMER2.0 for analysis of tumor-infiltrating immune cells. *Nucleic Acids Res* (2020) 48(W1):W509–W14. doi: 10.1093/nar/gkaa407

33. Yang W, Soares J, Greninger P, Edelman EJ, Lightfoot H, Forbes S, et al. Genomics of drug sensitivity in cancer (GDSC): a resource for therapeutic biomarker discovery in cancer cells. *Nucleic Acids Res* (2013) 41(Database issue):D955–61. doi: 10.1093/nar/gks1111

34. Artibani W, Porcaro AB, De Marco V, Cerruto MA, Siracusano S. Management of biochemical recurrence after primary curative treatment for prostate cancer: A review. *Urol Int* (2018) 100(3):251–62. doi: 10.1159/000481438

35. Agarwal S, Lakoma A, Chen Z, Hicks J, Metelitsa LS, Kim ES, et al. G-CSF promotes neuroblastoma tumorigenicity and metastasis *via* STAT3-dependent cancer stem cell activation. *Cancer Res* (2015) 75(12):2566–79. doi: 10.1158/0008-5472.CAN-14-2946

36. Touw IP, van de Geijn GJ. Granulocyte colony-stimulating factor and its receptor in normal myeloid cell development, leukemia and related blood cell disorders. *Front Biosci* (2007) 12:800–15. doi: 10.2741/2103

37. Wojtukiewicz MZ, Sierko E, Skalij P, Kamińska M, Zimnoch L, Brekken RA, et al. Granulocyte-colony stimulating factor receptor, tissue factor, and VEGF-r bound VEGF in human breast cancer in loco. *Adv Clin Exp Med* (2016) 25(3):505–11. doi: 10.17219/acem/62398

38. Li B, Niswander LA. TMEM132A, a novel wnt signaling pathway regulator through wntless (WLS) interaction. *Front Cell Dev Biol* (2020) 8:599890. doi: 10.3389/fcell.2020.599890

39. Abou Ziki MD, Mani A. The interplay of canonical and noncanonical wnt signaling in metabolic syndrome. *Nutr Res* (2019) 70:18–25. doi: 10.1016/j.nutres.2018.06.009

40. Wang Y, Singhal U, Qiao Y, Kasputis T, Chung JS, Zhao H, et al. Wnt signaling drives prostate cancer bone metastatic tropism and invasion. *Transl Oncol* (2020) 13 (4):100747. doi: 10.1016/j.tranon.2020.100747

41. Jaitin DA, Adlung L, Thaiss CA, Weiner A, Li B, Descamps H, et al. Lipid-associated macrophages control metabolic homeostasis in a Trem2-dependent manner. *Cell* (2019) 178(3):686–98.e14. doi: 10.1016/j.cell.2019.05.054

42. Timperi E, Gueguen P, Molgora M, Magagna I, Kieffer Y, Lopez-Lastra S, et al. Lipid-associated macrophages are induced by cancer-associated fibroblasts and mediate immune suppression in breast cancer. *Cancer Res* (2022) 82(18):3291–306. doi: 10.1158/0008-5472.CAN-22-1427

43. Cheaito KA, Bahmad HF, Hadadeh O, Saleh E, Dagher C, Hammoud MS, et al. EMT markers in locally-advanced prostate cancer: Predicting recurrence? *Front Oncol* (2019) 9:131. doi: 10.3389/fonc.2019.00131

44. Ostrakhovitch EA, Li SS. NIP1/DUOXA1 expression in epithelial breast cancer cells: regulation of cell adhesion and actin dynamics. *Breast Cancer Res Treat* (2010) 119(3):773–86. doi: 10.1007/s10549-009-0372-7

45. Aslam N, Faisal MN, Khan JA, Majeed W. Opuntia ficus indica (L.) fruit extract alleviates oxidative stress through activation of dual oxidases and Keap1/Nrf2 signaling cascades in high-fat-diet associated atherosclerosis rats. *Toxicol Res (Camb)* (2022) 11 (6):920–30. doi: 10.1093/toxres/tfac070

46. Che H, Liu Y, Zhang M, Meng J, Feng X, Zhou J, et al. Integrated analysis revealed prognostic factors for prostate cancer patients. *Med Sci Monit* (2019) 25:9991–10007. doi: 10.12659/MSM.918045

47. Aruleba RT, Adekiya TA, Oyinloye BE, Kappo AP. Structural studies of predicted ligand binding sites and molecular docking analysis of Slc2a4 as a therapeutic target for the treatment of cancer. *Int J Mol Sci* (2018) 19(2). doi: 10.3390/ijms19020386

48. Garrido P, Osorio FG, Morán J, Cabello E, Alonso A, Freije JM, et al. Loss of GLUT4 induces metabolic reprogramming and impairs viability of breast cancer cells. *J Cell Physiol* (2015) 230(1):191–8. doi: 10.1002/jcp.24698

49. Ito T, Noguchi Y, Satoh S, Hayashi H, Inayama Y, Kitamura H. Expression of facilitative glucose transporter isoforms in lung carcinomas: its relation to histologic type, differentiation grade, and tumor stage. *Mod Pathol* (1998) 11(5):437–43.

50. Liu J, Wen D, Fang X, Wang X, Liu T, Zhu J. p38MAPK signaling enhances glycolysis through the up-regulation of the glucose transporter GLUT-4 in gastric cancer cells. *Cell Physiol Biochem* (2015) 36(1):155–65. doi: 10.1159/000374060

51. Gonzalez-Menendez P, Hevia D, Rodriguez-Garcia A, Mayo JC, Sainz RM. Regulation of GLUT transporters by flavonoids in androgen-sensitive and -insensitive prostate cancer cells. *Endocrinology* (2014) 155(9):3238–50. doi: 10.1210/en.2014-1260

52. Kogan-Sakin I, Tabach Y, Buganim Y, Molchadsky A, Solomon H, Madar S, et al. Mutant p53(R175H) upregulates Twist1 expression and promotes epithelial-mesenchymal transition in immortalized prostate cells. *Cell Death Differ* (2011) 18 (2):271–81. doi: 10.1038/cdd.2010.94

53. Zhang Y, Xu L, Chang Y, Li Y, Butler W, Jin E, et al. Therapeutic potential of ReACp53 targeting mutant p53 protein in CRPC. *Prostate Cancer Prostatic Dis* (2020) 23(1):160–71. doi: 10.1038/s41391-019-0172-z

54. Samstein RM, Lee CH, Shoushtari AN, Hellmann MD, Shen R, Janjigian YY, et al. Tumor mutational load predicts survival after immunotherapy across multiple cancer types. *Nat Genet* (2019) 51(2):202–6. doi: 10.1038/s41588-018-0312-8

55. Yarchoan M, Hopkins A, Jaffee EM. Tumor mutational burden and response rate to PD-1 inhibition. *N Engl J Med* (2017) 377(25):2500–1. doi: 10.1056/NEJMc1713444

56. Shi Q, Zhu Y, Ma J, Chang K, Ding D, Bai Y, et al. Prostate cancer-associated SPOP mutations enhance cancer cell survival and docetaxel resistance by upregulating Caprin1-dependent stress granule assembly. *Mol Cancer* (2019) 18(1):170. doi: 10.1186/s12943-019-1096-x

57. Gao K, Shi Q, Liu Y, Wang C. Enhanced autophagy and NFE2L2/NRF2 pathway activation in SPOP mutation-driven prostate cancer. *Autophagy* (2022) 18(8):2013–5. doi: 10.1080/15548627.2022.2062873

frontiers | Frontiers in Endocrinology

TYPE Original Research
PUBLISHED 30 March 2023
DOI 10.3389/fendo.2023.1159241

OPEN ACCESS

EDITED BY
Xiao-qiang Liu,
Tianjin Medical University General Hospital, China

REVIEWED BY
Zihou Cao,
Second Affiliated Hospital of Soochow University, China
Qiaocheng Zhai,
Soochow University, China

*CORRESPONDENCE
Zhen Liu
rachelly520@163.com

SPECIALTY SECTION
This article was submitted to Reproduction, a section of the journal Frontiers in Endocrinology

RECEIVED 05 February 2023
ACCEPTED 01 March 2023
PUBLISHED 30 March 2023

CITATION
Du Y, Xie B, Wang M, Zhong Y, Lv Z, Luo Y, He Q and Liu Z (2023) Roles of sex hormones in mediating the causal effect of vitamin D on osteoporosis: A two-step Mendelian randomization study. *Front. Endocrinol.* 14:1159241. doi: 10.3389/fendo.2023.1159241

Roles of sex hormones in mediating the causal effect of vitamin D on osteoporosis: A two-step Mendelian randomization study

Yongwei Du[1], Baohui Xie[2], Maoyuan Wang[3], Yanbiao Zhong[3], Zhimai Lv[4], Yun Luo[3], Qiwei He[5] and Zhen Liu[3]*

[1]Department of Orthopedics, First Affiliated Hospital of Gannan Medical University, Ganzhou, China, [2]Department of Orthopedics, Shangyou Hospital of Traditional Chinese Medicine, Ganzhou, China, [3]Department of Rehabilitation, First Affiliated Hospital of Gannan Medical University, Ganzhou, China, [4]Department of Internal Medicine-Neurology, First Affiliated Hospital of Gannan Medical University, Ganzhou, China, [5]Ganzhou Polytechnic, Ganzhou, China

Background: Although 25-hydroxyvitamin D [25(OH)D] is a risk factor for osteoporosis, it is not clear whether sex hormones mediate this casual association. We aimed to explore how sex hormones affect the association between 25(OH)D and osteoporosis to provide meaningful insights on the underlying mechanisms from a genetic perspective.

Methods: Genetic variations in 25(OH)D, total testosterone (TT), androstenedione (A4), estradiol (E2), and testosterone/17β-estradiol (T/E2) were determined through summary statistics. Taking osteoporosis as the outcome (FinnGen biobank, 332,020 samples), we conducted a Mendelian randomization (MR) analysis to establish the association between 25(OH)D and these sex hormones. The two-step MR analysis quantified the mediatory effects of sex hormones on osteoporosis. The results were further verified by pleiotropy and heterogeneity analyses.

Results: MR results showed that 25(OH)D (OR= 1.27, p = 0.04) and TT (OR= 1.25, p = 0.04) had a causal effect on osteoporosis. No significant associations were observed between the other sex hormones (A4, E2, and T/E2) and osteoporosis (p>0.05). Sensitivity analysis (p>0.05) confirmed the robustness of the MR results. The two-step MR analysis provided evidence that the mediatory effect of TT was 0.014 (the percentage of TT mediation was 5.91%). Moreover, the direct effect of 25(OH)D on osteoporosis was 0.221. A4, E2, and T/E2 were not considered as potential mediators of the role of 25(OH)D as a risk factor for OP.

Conclusion: This study, through MR analysis, showed that TT mediates the causal effect of 25(OH)D on osteoporosis. Interventions targeting TT, therefore, have the potential to substantially reduce the burden of osteoporosis attributable to high 25(OH)D.

KEYWORDS

osteoporosis, vitamin D, sex hormone, Mendelian randomization, causality

1 Introduction

Osteoporosis (OP) is currently the most prevalent metabolic bone disorder, characterized by low bone mass and microarchitecture deterioration (1). According to epidemiological estimates, OP affects more than 30% of men and 50% of women (2). In addition, a substantial rise in the prevalence of OP is anticipated due to the increasing aging population, presenting a significant global health burden (3, 4). Therefore, it is meaningful to identify risk factors for OP and explore the in-depth relationship between risk/protective factors.

Vitamin D (VD) affects bone health by regulating calcium absorption and plays a crucial role in OP (5). Notably, 25-hydroxyvitamin D [25(OH)D] can be used as a marker of VD levels, allowing for its effect on OP to be evaluated (6). However, some studies have shown that the intake of VD supplements does not affect the levels of 25(OH)D (7). Additionally, it was reported that VD supplements alone did not give satisfactory results in controlling the risk of OP or fractures (8). Nonetheless, some experts in the field argue that the elderly should continue to supplement for VD (9). Considering the short duration of intervention and follow-up in randomized controlled trials, the long-term effects of 25(OH)D might have been underestimated in these previous studies.

Furthermore, it has been shown that VD exerts its effect on bone health by interacting with sex hormones. For instance, Al-Daghri et al. reported that the level of VD was positively correlated with testosterone (TT) levels (10). Androgens also play a direct and indirect role in bone metabolism. In their research using mouse experiments, Kristine et al. showed that androgens can affect bone resorption (11). Moreover, *in vitro* studies have shown that estrogen can induce osteoclast apoptosis by upregulating the Fas ligand, thus preventing bone loss caused by OP (12). Notably, Srivastava et al. (13) showed that estrogen can reduce the response of osteoclast precursors to RANKL, thus preventing bone loss. However, the metabolism of sex hormones in the human body is a complex and dynamic process, and their effect on bone health is affected by many factors. Therefore, it is difficult to directly determine the relationship between sex hormones and osteoporosis.

Most biases due to acquired confounding factors affect the assessment of OP risk mediated by the interaction of VD and sex hormones. To avoid such effects, Mendelian randomization (MR) can effectively be used to analyze causality from the perspective of genetic variation. Therefore, we performed a two-step MR analysis to examine the contribution of 25(OH)D and sex hormones in the progression of osteoporosis. Additionally, a two-step MR analysis was further used to evaluate the mediatory effect of specific sex hormones. This provides new insights on the prevention and treatment of osteoporosis.

2 Methods

2.1 Study design

This was a two-step MR study aimed at investigating the effect of 25(OH)D on the risk of osteoporosis. Sex hormones including total TT, androstenedione (A4), estradiol (E2), and testosterone/17β-estradiol (T/E2) were analyzed as mediators. The specific causal analysis included the following steps (1): exploring the effects of 25(OH)D and sex hormones on the risk of osteoporosis (2), assessment of the causal relationship between 25(OH)D and sex hormones, and (3) investigating how sex hormones mediate the role of 25(OH)D as a risk factor for osteoporosis.

2.2 Exposure: 25(OH)D GWAS data

25(OH)D data were obtained from a genome-wide association study (GWAS), based on a linear mixed model, consisting of 496,946 UK Biobank (UKB) participants (40–69 years old) (14). The Diasorin Liason® was used for the quantitative determination of 25(OH)D (range, 10–375 nmol L^{-1}). After adjusting for the fit age, sex, genotyping batch, and the first 40 ancestry principal components (PCs), 6,896,093 single nucleotide polymorphisms (SNPs) were obtained.

2.3 Mediators: Sex hormone GWAS data

Data on TT and E2 were obtained from a GWAS consisting of 194,453 European samples (15). These GWAS data, obtained from "v3" release of the UK Biobank (16) applied the K-means clustering method to the first four principal components. After adjusting for the genotyping chip, age, BMI, and 10 generically derived PCs, 16,131,612 (TT) and 16,136,413 (E2) genetic loci were obtained. The genetic structure in the cohort was explained using the genetic relationship matrix.

Data on A4 and T/E2 were obtained from a GWAS (17) consisting of 3,549 European samples from LIFE-Adult (18) and LIFE-Heart (19). This GWAS used liquid chromatography–tandem mass spectrometry to quantitatively determine A4 levels and employed the electrochemiluminescence immunoassay to quantitatively study both T and E2. After adjusting for age, sex, and log-transformed BMI, 8,783,995 (A4) and 8,822,708 (T/E2) SNPs were obtained.

2.4 Outcome: Osteoporosis GWAS data

To explore how sex hormones mediate the role of 25(OH)D as a risk factor for osteoporosis, the FinnGen biobank (sample size: 190,879 women and 151,620 men) (20) was selected as the source of OP GWAS data. A total of 2,202 disease endpoints were included, and 20,175,454 variants were analyzed in FinnGen (Release 8) (20). The GWAS data for OP were obtained from the FinnGen database (Release 8), which included 6,303 OP patients and 325,717 controls.

2.5 Quality control of SNPs

In order to obtain reliable instrument variables (IVs), three assumptions for MR were made (1): each IV was associated with 25(OH)D/sex hormone (2); all IVs for 25(OH)D/sex hormones that

had passed quality control were not associated with confounders (excluding mediators); and (3) the influence of the IVs for 25(OH)D/sex hormones on the risk of osteoporosis was only mediated by 25(OH)D and sex hormones.

A p-value $<5\times10^{-8}$ was selected as the threshold for IVs for 25(OH)D, TT, and E2. On the other hand, $p<1\times10^{-5}$ was selected as the threshold for IVs for A4 and T/E2 due to the relatively few IVs (21). Linkage disequilibrium was set to $R^2 < 0.001$ (22), and palindrome SNPs were deleted.

2.6 Mendelian randomization and statistical analysis

We used the R software (version 2.22) and package "TwoSampleMR" to complete the MR analysis. The Wald ratio (WR) method is used to evaluate the causal effect of a single IV, while the inverse variance weighted (IVW) approach was mainly employed to evaluate the causal effect of multiple IVs (23). MR-Egger (24) and the weighted median (WM) (25) were used to verify causality. In addition, Odds ratios (ORs) and 95% CI were used to indicate the impact on the risk of osteoporosis. For MR results, $p < 0.05$ was considered a potential association. In addition, mediation analysis was conducted on the mediators (sex hormones) with potential correlation. The effect of 25(OH)D on TT was multiplied by the effect of TT on osteoporosis to obtain the mediatory effect of TT. The causal effect of TT was subtracted from the total effect of 25(OH)D on OP to obtain the direct effect of 25(OH)D on osteoporosis. Moreover, the mediatory effect was divided by the total effect of 25(OH)D on OP to obtain the proportion of mediation by TT. Sensitivity analysis was further used to verify the robustness of the results, and the Cochrane's Q-test was employed to test for heterogeneity. Finally, the MR Egger intercept and MR-PRESSO (26) were used to test for pleiotropy.

3 Results

3.1 IVs after quality control

After ruling out SNPs that did not meet the standards ($p<1\times10^{-8}$, $R^2<0.001$, F>10) for quality control, 45 SNPs were selected as IVs to evaluate the causal relationship between 25(OH)D and OP (Table 1). For each sex hormone, 50 (TT), 16 (A4), 11 (E2), and 11 (T/E2) SNPs were selected as IVs to evaluate causality between 25(OH)D and OP (Table 1). All IVs were not weak (F>10) and passed the MR Steiger filtering step. More details are presented in Supplementary Table S1.

3.2 Effect of 25(OH)D on osteoporosis

The IVW results revealed a positive association between 25(OH)D and OP (OR=1.27, p=0.04) (Figure 1). However, the WM (OR=1.18, p=0.32) and MR Egger (OR=1.022, p=0.24) results showed no association between 25(OH)D and OP (Figure 1A). Results from the Cochran's Q-test confirmed that there was no heterogeneity (IVW, Q=35.73, p=0.81; MR Egger, Q=35.65, p=0.78). Additionally, the pleiotropy test verified that there was no pleiotropy in the causal relationship between 25(OH)D and OP (intercept=1.40×10^{-3}, p=0.78, Figure 1B). We further used MR-PRESSO to verify the results of pleiotropy (p=0.761).

3.3 Effect of sex hormones on osteoporosis

Figure 2 shows estimates of the causal effect of each sex hormone on osteoporosis. MR analysis of IVW indicated that TT was associated with a high risk of OP (OR= 1.25; CI, 1.01–1.54; p=0.04). However, the causal effect of A4 (OR= 0.98; CI, 0.83–1.15; p=0.78), E2 (OR= 0.77; CI, 0.16–3.83; p=0.75), and T/E2 (OR= 0.87; CI, 0.76–1.00; p=0.05) on osteoporosis was not established. More details of the MR results are shown in the Supplementary Table S2.

3.4 Mediating effect between 25(OH)D and osteoporosis

Since A4, E2, and T/E2 had no causal effect on osteoporosis, they were not considered as potential mediators of the role of 25(OH)D as a risk factor for OP. Therefore, only TT was subjected to mediation analysis. The findings showed that an increase in TT was positively correlated with the level of 25(OH)D (OR= 1.06; CI, 1.01–1.13; p=0.03). Regarding the causal effect of 25(OH)D on osteoporosis, the mediatory effect of TT was 0.014 (the percentage of TT mediation was 5.91%). Moreover, the direct effect of 25(OH)D on osteoporosis was 0.221.

TABLE 1 Selection of IVs after quality control.

Exposure	Samples	IVs	F
25(OH)D	496,946	45	29.77–1455.88
TT	194,453	50	26.17–257.56
A4	3,549	16	19.59–85.15
E2	206,927	11	31.48–319.98
T/E2	5,696	11	19.60–23.04

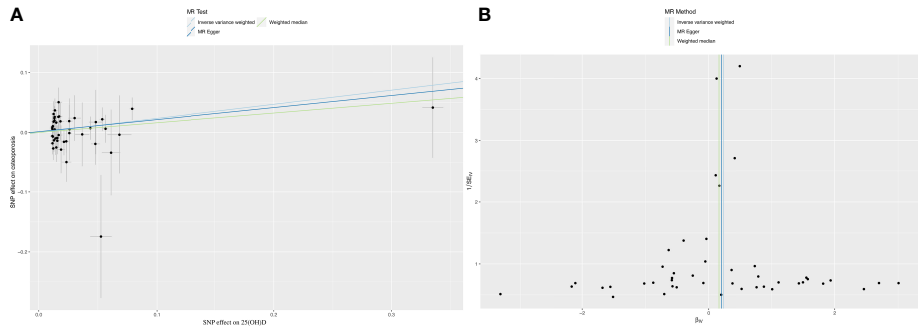

FIGURE 1
Mendelian randomization analysis between 25(OH)D and osteoporosis. **(A)** The causality between 25 (OH) D and osteoporosis. **(B)** Funnel plot: sensitivity analysis between VD and osteoporosis.

4 Discussion

Osteoporosis is one of the most common chronic diseases of the bone that affects older individuals by increasing the risk of fractures, subsequently resulting in a range of complications (27). It is characterized by a substantial reduction in bone quality, caused by deterioration of the bone micro-architecture and low bone mass (28). Moreover, epidemiological data show that more than 200 million individuals worldwide suffer from OP (29). In the aging population, osteoporotic fractures cause significant morbidity and huge cost implications to individuals and the society (30). There are several risk factors for OP, with the most common being age, lifestyle factors, diet, estrogen deficiency, and genetics (31). Furthermore, in both men and women, vitamin D deficiency and sex hormone disorders are the leading causes of OP (32). Given the high prevalence of OP in the elderly, especially post-menopausal OP in elderly women, more research is needed on the causal link between TT, 25(OH)D, and osteoporosis.

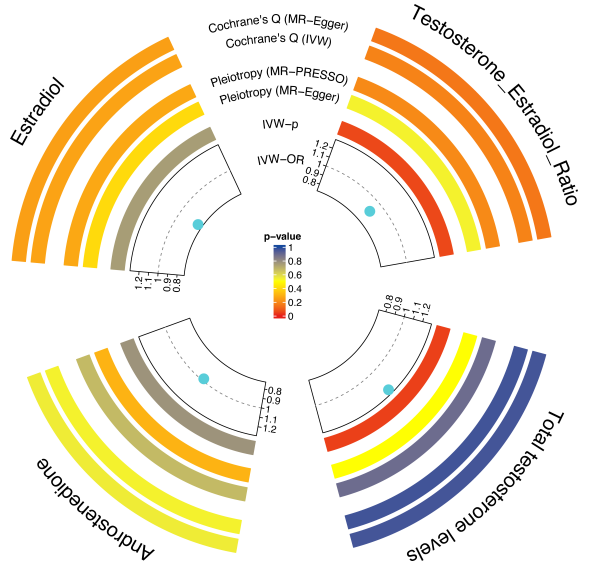

FIGURE 2
The causal effect of each sex hormone (TT, A4, E2, and T/E2) on osteoporosis. Gray dotted line: OR=1. TT, total testosterone; A4, androstenedione; E2, estradiol; T/E2, testosterone/17β-estradiol.

Vitamin D is a fat-soluble vitamin that may be obtained through diet and is synthesized endogenously when sunshine stimulates skin production (33). Vitamin D has been linked to bone growth and development and calcium/phosphorus metabolism (34). Vitamin D, in addition to its endocrine role, promotes innate immunity (35). It has been claimed that vitamin D may help to control blood pressure (36). 25-Hydroxyvitamin D is derived from vitamin D and is the final metabolite of vitamin D (37). It is predominantly generated through the hydroxylation of 25-hydroxyvitamin D (25(OH)D) under the supervision of parathyroid hormone (38). Clinically, 25(OH)D is often used to evaluate the intake and utilization of VD. Additionally, 25(OH)D is an essential condition for healthy bones and participates in the secretion and activation of hormones, maintaining the normal level of calcium ions in the blood (39). Vitamin D aids in bone mineralization by facilitating osteoblast derivatization of bone marrow mesenchymal stem cells (BMMSCs). BMMSCs play an essential role in the action of 1,25(OH)2D, which stimulates their differentiation into osteoblasts (40). 25(OH)D induces the differentiation of BMMSCs into osteoblasts at a concentration of 250 nM, and in some cases, this concentration can reach 500 nM (41, 42). According to a previous study, leptin improved the potential of 25(OH)D to stimulate osteoblast differentiation (43). Nonetheless, high levels of serum 25(OH)D3 are considered to be toxic to the body (44, 45). Additionally, there have been several reports on the association between 25(OH)D and biochemical markers of OP (46–48). These studies are consistent with our IVW results, which showed that 25(OH)D had a causal association with osteoporosis. Overall, 25(OH)D is a potential risk factor for OP.

Furthermore, testosterone can act directly on osteoblasts *via* androgen receptors to promote bone formation. It can also have an indirect effect on bone metabolism through its action on different cytokines (49). Notably, the androgen receptor (AR) mediates the action of testosterone on osteoblasts. AR is found in osteoblasts and chondrocytes and can therefore induce bone formation (50). Moreover, testosterone promotes cell differentiation and apoptosis in osteoblasts and chondrocytes (50), and the aromatase enzyme

converts TT to estradiol, which prevents osteoporosis (51). Testosterone deficiency further leads to activation of the nuclear factor kappa-B ligand (RANKL) from osteoblasts, although this also helps in promoting osteoclast differentiation (52). Additionally, a number of observational surveys have investigated the link between TT and OP and found a positive correlation between the two (50, 53–55). Here, through MR analysis of IVW, we observed that TT was associated with a high risk of OP.

Compared to observational studies, MR analyses are less susceptible to reverse causality or other potential confounding effects. Therefore, MR analysis may be more beneficial in determining causality. Human Leydig cells express the CYP2R1 gene and vitamin D receptor (VDR) (56). Intriguingly, patients with testiculopathies have lower testicular CYP2R1 gene expression, and 25(OH)D levels significantly decreased in patients after bilateral orchiectomy (56). Both VD and TT increase sperm motility and activity by not only inducing the survival of human spermatozoa but also inducing estrogen secretion from osteoblasts, thus synergistically promoting bone formation. Moreover, D'Andrea et al. (57) reported a positive relationship between total testosterone levels and 25(OH)D, suggesting that hyperandrogenemia can prevent future incidence of osteoporosis, similar to our findings. We subjected TT to mediation analysis and observed that an increase in the levels of TT was positively correlated with the levels of 25(OH)D. Additionally, the causal effect of 25(OH)D on OP was partly mediated by TT.

Although more reliable conclusions can be drawn using the large-scale genetic variation data presented herein, some limitations of the study still need to be considered. First, since all genetic variants were from European populations, the generalization of our findings to other settings needs further validation. Second, MR analysis of T/E2 and OP showed possible causality (p=0.05), which may have been due to the small sample size in the T/E2 GWAS study. In future studies, we aim to further explore the intrinsic link between VD, sex hormones, and OP based on individual-level data to provide more theoretical evidence for the prevention and treatment of osteoporosis.

In conclusion, our study provides insights on the role and effects of VD on OP, mediated by sex hormones, and broadens the understanding of the link between VD and osteoporosis. From a clinical perspective, the prevention and control of OP may need to focus on the regulation of sex hormones (especially TT).

Data availability statement

The original contributions presented in the study are included in the article/Supplementary Material. Further inquiries can be directed to the corresponding author.

Ethics statement

The data involved in this study are from public summary data. The ethical approval of each study can be found in the original publications. All studies followed the ethical guidelines of the Declaration of Helsinki.

Author contributions

YD and ZLi designed the study, analyzed the data, and drew the figures. All authors critically revised the manuscript. All authors contributed to the article and approved the submitted version.

Funding

This work was supported by grants from the Jiangxi Key R&D Plan Project (20203BBGL73145), the Jiangxi Provincial Department of Education Science and Technology Plan (GJJ190809), and the Ganzhou Guiding Science and Technology Plan (GZ2021ZSF001) to YD. The funders had no role in the study design, data collection, data analysis, interpretation, or writing of the report.

Acknowledgments

We want to acknowledge the participants and investigators of the FinnGen study (https://finngen.gitbook.io/documentation/) (OP data source), LIFE-Adult (sex hormone data source) and LIFE-Heart (sex hormone data source), and the GWAS from Revez et al. (25(OH)D data source) (14) and Ruth et al. (sex hormone data source) (15) for sharing the genetic data. We thank Home for Researchers editorial team (www.home-for-researchers.com) for language editing service.

Conflict of interest

The authors declare that the research was conducted in the absence of any commercial or financial relationships that could be construed as a potential conflict of interest.

Publisher's note

Supplementary material

The Supplementary Material for this article can be found online at: https://www.frontiersin.org/articles/10.3389/fendo.2023.1159241/full#supplementary-material

References

1. Reid IR, Billington EO. Drug therapy for osteoporosis in older adults. *Lancet* (2022) 399(10329):1080–92. doi: 10.1016/S0140-6736(21)02646-5

2. Wright NC, Looker AC, Saag KG, Curtis JR, Delzell ES, Randall S, et al. The recent prevalence of osteoporosis and low bone mass in the united states based on bone mineral density at the femoral neck or lumbar spine. *J Bone Miner Res* (2014) 29 (11):2520–6. doi: 10.1002/jbmr.2269

3. LeBoff MS, Greenspan SL, Insogna KL, Lewiecki EM, Saag KG, Singer AJ, et al. The clinician's guide to prevention and treatment of osteoporosis. *Osteoporos Int* (2022) 33(10):2049–102. doi: 10.1007/s00198-021-05900-y

4. Coughlan T, Dockery F. Osteoporosis and fracture risk in older people. *Clin Med (Lond)* (2014) 14(2):187–91. doi: 10.7861/clinmedicine.14-2-187

5. Burrows M, Nevill AM, Bird S, Simpson D. Physiological factors associated with low bone mineral density in female endurance runners. *Br J Sports Med* (2003) 37 (1):67–71. doi: 10.1136/bjsm.37.1.67

6. Reid IR, Bolland MJ, Grey A. Effects of vitamin d supplements on bone mineral density: a systematic review and meta-analysis. *Lancet* (2014) 383:146–55. doi: 10.1016/S0140-6736(13)61647-5

7. Gallagher JC, Jindal PS, Smith LM. Vitamin d does not increase calcium absorption in young women: A randomized clinical trial. *J Bone Miner Res* (2014) 29 (5):1081–7. doi: 10.1002/jbmr.2121

8. Avenell A, Mak JC, O'Connell D. Vitamin d and vitamin d analogues for preventing fractures in post-menopausal women and older men. *Cochrane Database systematic Rev* (2014) 2014(4):Cd000227. doi: 10.1038/s41467-020-15421-7

9. Grant WB, Whiting SJ, Schwalfenberg GK, Genuis SJ, Kimball SM. Estimated economic benefit of increasing 25-hydroxyvitamin d concentrations of canadians to or above 100 nmol/L. *Dermatoendocrinol* (2016) 8(1):e1248324. doi: 10.1080/19381980.2016.1248324

10. Al-Daghri NM, Yakout SM, Ansari MGA, Hussain SD, Wani KA, Sabico S. Vitamin d metabolites and sex steroid indices in postmenopausal women with and without low bone mass. *Metabolites* (2021) 11(2):86. doi: 10.3390/metabo11020086

11. Wiren KM, Zhang XW, Olson DA, Turner RT, Iwaniec UT. Androgen prevents hypogonadal bone loss *via* inhibition of resorption mediated by mature osteoblasts/osteocytes. *Bone* (2012) 51(5):835–46. doi: 10.1016/j.bone.2012.08.111

12. Nakamura T, Imai Y, Matsumoto T, Sato S, Takeuchi K, Igarashi K, et al. et al: Estrogen prevents bone loss *via* estrogen receptor alpha and induction of fas ligand in osteoclasts. *Cell* (2007) 130(5):811–23. doi: 10.1016/j.cell.2007.07.025

13. Srivastava S, Toraldo G, Weitzmann MN, Cenci S, Ross FP, Pacifici R. Estrogen decreases osteoclast formation by down-regulating receptor activator of NF-kappa b ligand (RANKL)-induced JNK activation. *J Biol Chem* (2001) 276(12):8836–40. doi: 10.1074/jbc.M010764200

14. Revez JA, Lin T, Qiao Z, Xue A, Holtz Y, Zhu Z, et al. et al: Genome-wide association study identifies 143 loci associated with 25 hydroxyvitamin d concentration. *Nat Commun* (2020) 11(1):1647.

15. Ruth KS, Day FR, Tyrrell J, Thompson DJ, Wood AR, Mahajan A, et al. et al: Using human genetics to understand the disease impacts of testosterone in men and women. *Nat Med* (2020) 26(2):252–8. doi: 10.1038/s41591-020-0751-5

16. Bycroft C, Freeman C, Petkova D, Band G, Elliott LT, Sharp K, et al. et al: The UK biobank resource with deep phenotyping and genomic data. *Nature* (2018) 562 (7726):203–9. doi: 10.1038/s41586-018-0579-z

17. Pott J, Horn K, Zeidler R, Kirsten H, Ahnert P, Kratzsch J, et al. Sex-specific causal relations between steroid hormones and obesity-a mendelian randomization study. *Metabolites* (2021) 11(11):738. doi: 10.3390/metabo11110738

18. Loeffler M, Engel C, Ahnert P, Alfermann D, Arelin K, Baber R, et al. et al: The LIFE-Adult-Study: Objectives and design of a population-based cohort study with 10,000 deeply phenotyped adults in Germany. *BMC Public Health* (2015) 15:691. doi: 10.1186/s12889-015-1983-z

19. Scholz M, Henger S, Beutner F, Teren A, Baber R, Willenberg A, et al. Cohort profile: The Leipzig research center for civilization diseases-heart study (LIFE-heart). *Int J Epidemiol* (2020) 49(5):1439–1440h. doi: 10.1093/ije/dyaa075

20. Kurki MI, Karjalainen J, Palta P, Sipilä TP, Kristiansson K, Donner K, et al. et al: FinnGen: Unique genetic insights from combining isolated population and national health register data. *medRxiv* (2022) 20, 22271360. doi: 10.1101/2022.03.03.22271360

21. Liu K, Fan H, Hu H, Cheng Y, Liu J, You Z. Genetic variation reveals the influence of steroid hormones on the risk of retinal neurodegenerative diseases. *Front Endocrinol (Lausanne)* (2022) 13:1088557. doi: 10.3389/fendo.2022.1088557

22. Hemani G, Tilling K, Davey Smith G. Orienting the causal relationship between imprecisely measured traits using GWAS summary data. *PloS Genet* (2017) 13(11): e1007081. doi: 10.1371/journal.pgen.1007081

23. Burgess S, Scott RA, Timpson NJ, Davey Smith G, Thompson SG. Using published data in mendelian randomization: A blueprint for efficient identification of causal risk factors. *Eur J Epidemiol* (2015) 30(7):543–52. doi: 10.1007/s10654-015-0011-z

24. Bowden J, Del Greco MF, Minelli C, Davey Smith G, Sheehan NA, Thompson JR. Assessing the suitability of summary data for two-sample mendelian randomization analyses using MR-egger regression: The role of the I2 statistic. *Int J Epidemiol* (2016) 45(6):1961–74. doi: 10.1093/ije/dyw220

25. Bowden J, Davey Smith G, Haycock PC, Burgess S. Consistent estimation in mendelian randomization with some invalid instruments using a weighted median estimator. *Genet Epidemiol* (2016) 40(4):304–14. doi: 10.1002/gepi.21965

26. Verbanck M, Chen CY, Neale B, Do R. Detection of widespread horizontal pleiotropy in causal relationships inferred from mendelian randomization between complex traits and diseases. *Nat Genet* (2018) 50(5):693–8. doi: 10.1038/s41588-018-0099-7

27. Salari N, Darvishi N, Bartina Y, Larti M, Kiaei A, Hemmati M, et al. Global prevalence of osteoporosis among the world older adults: A comprehensive systematic review and meta-analysis. *J Orthopaedic Surg Res* (2021) 16(1):669. doi: 10.1186/s13018-021-02821-8

28. Kanis JA. Diagnosis of osteoporosis. *Osteoporosis Int J established as result cooperation between Eur Foundation Osteoporosis Natl Osteoporosis Foundation USA* (1997) 7 Suppl 3:S108–116. doi: 10.1007/BF03194355

29. Fukuda M, Yoshizawa T, Karim MF, Sobuz SU, Korogi W, Kobayasi D, et al. et al: SIRT7 has a critical role in bone formation by regulating lysine acylation of SP7/Osterix. *Nat Commun* (2018) 9(1):2833. doi: 10.1038/s41467-018-05187-4

30. Sugiyama T, Oda H. Osteoporosis therapy: Bone modeling during growth and aging. *Front Endocrinol* (2017) 8:46. doi: 10.3389/fendo.2017.00046

31. Tabatabaei-Malazy O, Salari P, Khashayar P, Larijani B. New horizons in treatment of osteoporosis. *Daru J Faculty Pharmacy Tehran Univ Med Sci* (2017) 25 (1):2. doi: 10.1186/s40199-017-0167-z

32. Prentice A, Goldberg GR, Schoenmakers I. Vitamin d across the lifecycle: Physiology and biomarkers. *Am J Clin Nutr* (2008) 88(2):500s–6s. doi: 10.1093/ajcn/88.2.500S

33. Yuan C, Qian ZR, Babic A, Morales-Oyarvide V, Rubinson DA, Kraft P, et al. et al: Prediagnostic plasma 25-hydroxyvitamin d and pancreatic cancer survival. *J Clin Oncol Off J Am Soc Clin Oncol* (2016) 34(24):2899–905. doi: 10.1200/JCO.2015.66.3005

34. Wang L, Lv S, Li F, Yu X, Bai E, Yang X. Vitamin d deficiency is associated with metabolic risk factors in women with polycystic ovary syndrome: A cross-sectional study in shaanxi China. *Front Endocrinol* (2020) 11:171. doi: 10.3389/fendo.2020.00171

35. Dai J, Liang Y, Li H, Zhou W, Wang B, Gong A, et al. Vitamin d enhances resistance to aspergillus fumigatus in mice *via* inhibition of excessive autophagy. *Am J Trans Res* (2018) 10(2):381–91.

36. Subramanian A, Korsiak J, Murphy KE, Al Mahmud A, Roth DE, Gernand AD. Effect of vitamin d supplementation during pregnancy on mid-to-late gestational blood pressure in a randomized controlled trial in Bangladesh. *J hypertension* (2021) 39 (1):135–42. doi: 10.1097/HJH.0000000000002609

37. Nguyen TPH, Yong HEJ, Chollangi T, Brennecke SP, Fisher SJ, Wallace EM, et al. Altered downstream target gene expression of the placental vitamin d receptor in human idiopathic fetal growth restriction. *Cell Cycle (Georgetown Tex)* (2018) 17 (2):182–90. doi: 10.1080/15384101.2017.1405193

38. Ibrahim MK, Zambruni M, Melby CL, Melby PC. Impact of childhood malnutrition on host defense and infection. *Clin Microbiol Rev* (2017) 30(4):919–71. doi: 10.1128/CMR.00119-16

39. Vieth R. Vitamin D supplementation, 25-hydroxyvitamin D concentrations, and safety. *Am J Clin Nutr* (1999) 69(5):842–56. doi: 10.1093/ajcn/69.5.842

40. D'Ippolito G, Schiller PC, Perez-stable C, Balkan W, Roos BA, Howard GA. Cooperative actions of hepatocyte growth factor and 1,25-dihydroxyvitamin D3 in osteoblastic differentiation of human vertebral bone marrow stromal cells. *Bone* (2002) 31(2):269–75. doi: 10.1016/S8756-3282(02)00820-7

41. Lou YR, Toh TC, Tee YH, Yu H. 25-hydroxyvitamin D(3) induces osteogenic differentiation of human mesenchymal stem cells. *Sci Rep* (2017) 7:42816. doi: 10.1038/srep42816

42. Zarei A, Hulley PA, Sabokbar A, Javaid MK, Morovat A. 25-hydroxy- and 1α,25-dihydroxycholecalciferol have greater potencies than 25-hydroxy- and 1α,25-dihydroxyergocalciferol in modulating cultured human and mouse osteoblast activities. *PloS One* (2016) 11(11):e0165462. doi: 10.1371/journal.pone.0165462

43. He Q, Qin R, Glowacki J, Zhou S, Shi J, Wang S, et al. Synergistic stimulation of osteoblast differentiation of rat mesenchymal stem cells by leptin and 25(OH)D(3) is mediated by inhibition of chaperone-mediated autophagy. *Stem Cell Res Ther* (2021) 12 (1):557. doi: 10.1186/s13287-021-02623-z

44. Holick MF, Binkley NC, Bischoff-Ferrari HA, Gordon CM, Hanley DA, Heaney RP, et al. Evaluation, treatment, and prevention of vitamin d deficiency: An endocrine society clinical practice guideline. *J Clin Endocrinol Metab* (2011) 96(7):1911–30. doi: 10.1210/jc.2011-0385

45. Sempos CT, Heijboer AC, Bikle DD, Bollerslev J, Bouillon R, Brannon PM, et al. Vitamin d assays and the definition of hypovitaminosis d: results from the first international conference on controversies in vitamin d. *Br J Clin Pharmacol* (2018) 84(10):2194–207. doi: 10.1111/bcp.13652

46. Gao C, Qiao J, Li SS, Yu WJ, He JW, Fu WZ, et al. The levels of bone turnover markers 25(OH)D and PTH and their relationship with bone mineral density in

postmenopausal women in a suburban district in China. *Osteoporosis Int J established as result cooperation between Eur Foundation Osteoporosis Natl Osteoporosis Foundation USA* (2017) 28(1):211–8. doi: 10.1007/s00198-016-3692-6

47. Zhao J, Xia W, Nie M, Zheng X, Wang Q, Wang X, et al. et al: The levels of bone turnover markers in Chinese postmenopausal women: Peking vertebral fracture study. *Menopause (New York NY)* (2011) 18(11):1237–43. doi: 10.1097/gme.0b013e31821d7ff7

48. Kharroubi A, Saba E, Smoom R, Bader K, Darwish H. Serum 25-hydroxyvitamin d and bone turnover markers in Palestinian postmenopausal osteoporosis and normal women. *Arch osteoporosis* (2017) 12(1):13. doi: 10.1007/s11657-017-0306-7

49. Shigehara K, Izumi K, Kadono Y, Mizokami A. Testosterone and bone health in men: A narrative review. *J Clin Med* (2021) 10(3):530. doi: 10.3390/jcm10030530

50. Mohamad NV, Soelaiman IN, Chin KY. A concise review of testosterone and bone health. *Clin Interventions Aging* (2016) 11:1317–24. doi: 10.2147/CIA.S115472

51. Almeida M, Laurent MR, Dubois V, Claessens F, O'Brien CA, Bouillon R, et al. Estrogens and androgens in skeletal physiology and pathophysiology. *Physiol Rev* (2017) 97(1):135–87. doi: 10.1152/physrev.00033.2015

52. Chin KY, Ima-Nirwana S. The effects of orchidectomy and supraphysiological testosterone administration on trabecular bone structure and gene expression in rats. *Aging male Off J Int Soc Study Aging Male* (2015) 18(1):60–6. doi: 10.3109/13685538.2014.954995

53. Ye J, Zhai X, Yang J, Zhu Z. Association between serum testosterone levels and body composition among men 20-59 years of age. *Int J Endocrinol* (2021) 2021:7523996. doi: 10.1155/2021/7523996

54. Yang J, Kong G, Yao X, Zhu Z. Association between serum total testosterone level and bone mineral density in middle-aged postmenopausal women. *Int J Endocrinol* (2022) 2022:4228740. doi: 10.1155/2022/4228740

55. Snyder PJ, Kopperdahl DL, Stephens-Shields AJ, Ellenberg SS, Cauley JA, Ensrud KE, et al. et al: Effect of testosterone treatment on volumetric bone density and strength in older men with low testosterone: A controlled clinical trial. *JAMA Internal Med* (2017) 177(4):471–9. doi: 10.1001/jamainternmed.2016.9539

56. Blomberg Jensen M, Nielsen JE, Jørgensen A, Rajpert-De Meyts E, Kristensen DM, Jørgensen N, et al. Vitamin d receptor and vitamin d metabolizing enzymes are expressed in the human male reproductive tract. *Hum Reprod (Oxford England)* (2010) 25(5):1303–11. doi: 10.1093/humrep/deq024

57. D'Andrea S, Martorella A, Coccia F, Castellini C, Minaldi E, Totaro M, et al. Relationship of vitamin d status with testosterone levels: A systematic review and meta-analysis. *Endocrine* (2021) 72(1):49–61. doi: 10.1007/s12020-020-02482-3

frontiers | Frontiers in Endocrinology

TYPE Review
PUBLISHED 11 April 2023
DOI 10.3389/fendo.2023.1163787

OPEN ACCESS

EDITED BY
Yuxuan Song,
Peking University People's Hospital, China

REVIEWED BY
Xiaoyao Liao,
University of Glasgow, United Kingdom
Yan Huang,
Tianjin Medical University, China

*CORRESPONDENCE
Zhipeng You
yzp74@sina.com

†These authors have contributed equally to this work

SPECIALTY SECTION
This article was submitted to Adrenal Endocrinology, a section of the journal Frontiers in Endocrinology

RECEIVED 11 February 2023
ACCEPTED 21 March 2023
PUBLISHED 11 April 2023

CITATION
Liu K, Zou H, Fan H, Hu H, Cheng Y, Liu J, Wu X, Chen B and You Z (2023) The role of aldosterone in the pathogenesis of diabetic retinopathy. *Front. Endocrinol.* 14:1163787. doi: 10.3389/fendo.2023.1163787

The role of aldosterone in the pathogenesis of diabetic retinopathy

Kangcheng Liu[1†], Hua Zou[1†], Huimin Fan[1], Hanying Hu[1], Yanhua Cheng[1], Jingying Liu[1], Xiaojian Wu[1], Bolin Chen[2] and Zhipeng You[1*]

[1]Jiangxi Clinical Research Center for Ophthalmic Disease, Jiangxi Research Institute of Ophthalmology and Visual Science, Affiliated Eye Hospital of Nanchang University, Nanchang, China, [2]Hunan Key Laboratory of Ophthalmology, Eye Center of Xiangya Hospital, Central South University, Changsha, Hunan, China

Aldosterone, as a mineralocorticoid of adrenal origin, has effects that are not limited to the urinary tract. As an important regulator in Vasoactive hormone pathways, aldosterone may play an effect in the pathogenesis of diabetic retinopathy (DR) through the regulation of oxidative stress, vascular regulation, and inflammatory mechanisms. This implies that mineralocorticoids, including aldosterone, have great potential and value for the diagnosis and treatment of DR. Because early studies did not focus on the intrinsic association between mineralocorticoids and DR, targeted research is still in its infancy and there are still many obstacles to its application in the clinical setting. Recent studies have improved the understanding of the effects of aldosterone on DR, and we review them with the aim of exploring possible mechanisms for the treatment and prevention of DR.

KEYWORDS

aldosterone, mineralocorticoid, diabetic retinopathy, inflammation, angiogenesis

1 Introduction

Diabetic retinopathy (DR) is a serious complication of diabetes that often present with no symptoms in the initial stages. However, if left untreated, hyperglycemia-induced retinal damage can lead to irreversible vision loss, which poses a serious threat to global health. Epidemiological studies reveal that up to 33% of diabetic patients suffer from diabetic retinopathy, with 18.89% of patients progressing to proliferative diabetic retinopathy (PDR), while 23.33% experience diabetic macular edema (1). Notably, these two conditions are the primary causes of irreversible blindness among working-age individuals.

Mechanistically, diabetic macular edema is induced by the high glucose environment, which not only destroys pericytes but also damages the blood-retinal barrier, causing retinal hemorrhage, protein leakage, and hard exudation (2). This persistent damage can further lead to the accumulation of leukocytes in acellular capillaries and microvessels, resulting in tissue ischemia and non-perfusion, which in turn promote retinal neovascularization (3). As diabetic

retinopathy advances, patients' vision may continue to decline, significantly impacting their overall well-being and quality of life (4, 5). Although anti-VEGF drugs and corticosteroids have shown some therapeutic benefits for DR treatment, they cannot halt disease progression. Therefore, current research should focus on the regulation of systemic factors (6).

Mineralocorticoids, including aldosterone and deoxycorticosterone, are primarily secreted by cells in the zona glomerulosa of the adrenal cortex. Importantly, they regulate the concentration of potassium and sodium in the body through mineralocorticoid receptors (MRs) to maintain water and electrolyte homeostasis. The renin-angiotensin-aldosterone system (RAAS) is a critical part of the vasoactive hormone pathway, in which aldosterone plays a key role. When RAAS is stimulated and activated, angiotensin II stimulates adrenal glomerular cells to release aldosterone, which then causes a series of pathophysiological changes such as tissue inflammation (7), fibrosis (8) cell proliferation (9), oxidative stress (10) and neovascularization (11–13) (Figure 1). Based on these findings, researchers confirmed that aldosterone is critical in the pathological mechanism of cardiovascular disease and chronic kidney disease (14). It is worth noting that glucocorticoid receptors are widely present in the retina (15). Wilkinson-BerkaJL et al. (15) previously found that activation of the glucocorticoid receptor adversely affects the retina by promoting inflammation and fibrosis. Allingham et al. (16) also uncovered that RAAS has a local effect on the retina, contributing to the occurrence and progression of DR. Meanwhile, Lovshin et al. (17) discovered that retinal vascular hardness could increase in DR patients after RAAS activation, implying that RAAS components have a fibrotic effect. Collectively, these studies provide theoretical support for aldosterone as a target for the treatment of DR.

Nonetheless, upon reviewing previous studies on the relationship between mineralocorticoids and DR, few investigations have specifically focused on aldosterone and DR pathogenesis. Therefore, this review will primarily focus on the significance of aldosterone as a mineralocorticoid in the onset and progression of diabetic retinopathy, aiming to provide direction for future DR prophylaxis and treatment strategies.

2 Effect of aldosterone-mediated blood pressure changes on diabetic retinopathy

The effect of RAAS was discovered and described earlier in the study about the urinary system. In the study of Ames et al. (18), components of the RAAS signaling pathway were found not only in the kidney but also in the heart, brain, lung and eyes, and various cells of the retina. Interestingly, Lai et al. (19) previously surmised a relationship in terms of common pathogenic mechanisms between kidney and eye diseases. The key link between kidney and eye diseases lies in inflammation, oxidative stress and other injuries caused by RAAS disorder. Lai et al. (19) observed that RAAS affects both the glomeruli and retina in similar ways. In the eye, RAAS plays a role in neovascularization and maintaining aqueous humor circulation stability. Additionally, RAAS can influence the blood flow in the ciliary body, iris, and retina, and strictly regulate intraocular pressure by modulating the production and excretion of aqueous humor. Furthermore, RAAS also participates in the development of retinal exudation and macular edema.

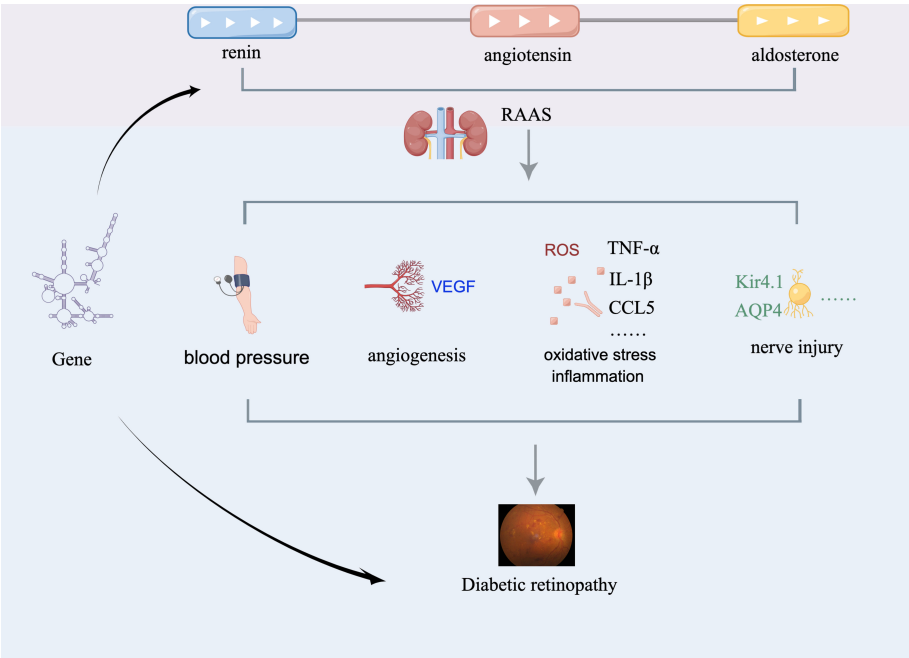

FIGURE 1
Putative mechanism whereby aldosterone affects DR. RAAS, renin-angiotensin-aldosterone system; AQP4, aquaporin-4; Kir4.1, inward rectifier potassium channel 4.1.

In a case-control study conducted by Senanayake et al. (20), the retina of diabetic patients was found to have a higher level of angiotensin II compared to nondiabetic patients. The study also detected higher levels of angiotensin II in the vitreous fluid of DR patients compared to non-diabetic patients (21), indicating that RAAS plays a critical role as a mediator of DR occurrence and progression. In a study by Lovshin et al. (17) involving long-term observation of 75 patients with type 1 diabetes, it was revealed that the angiosclerosis process in patients with PDR might trigger the continuous activation of the renin-angiotensin-aldosterone system. Notably, the positive role of RAAS in the regulation of blood pressure (BP) is well established. Pathological changes in RAAS can result in elevated BP, which is a significant risk factor for diabetic retinopathy. Some researchers suggest that patients using RAAS antagonists may lower their BP and thus reduce the risk of DR, primarily through the use of angiotensin-converting enzyme inhibitors and angiotensin receptor blockers (22). This observation is consistent with findings from rodent models, whereby RAAS antagonists were found to prevent retinal capillary leakage and reduce the risk of DR in diabetic animal models (23). These benefits were likely mediated indirectly by lowering blood pressure.

Aldosterone plays a role in the development of diabetic retinopathy by regulating blood pressure changes. Although most studies on this topic are still based on animal models, some inhibitors of RAAS components have shown promise in treating DR in such models. However, the safety and efficacy of aldosterone antagonists in the clinical therapy of DR need to be further investigated in human subjects.

3 Effect of aldosterone-mediated angiogenesis on diabetic retinopathy

It is worth noting that current studies have found that aldosterone has a certain effect on neovascularization. As a key molecule of RAAS, aldosterone binds to its corresponding MR to promote angiogenesis. Zhao et al. (24) observed an increase in endothelial growth factor mRNA and neovascularization in rat that received aldosterone injections, suggesting a potential role of aldosterone in promoting DR progression by elevating vascular endothelial growth factor (VEGF) levels and retinal neovascularization. Although the underlying mechanism is not fully understood, other research results support this finding.

Müller cells express high levels of mineralocorticoid receptors and secrete large amounts of VEGF, which contributes to neovascularization in DR (25). In a study investigating the effect of aldosterone on retinopathy of prematurity, researchers found that aldosterone could aggravate retinal neovascularization. However, interventions with spironolactone (an MR inhibitor) and an aldosterone synthase inhibitor were shown to effectively reduce retinal angiopathy and inflammation, as well as prevent retinal neovascularization by reducing VEGF levels and inflammatory factors (26).

The increase in VEGF is a well-known factor leading to diseases such as DR and retinopathy of prematurity (27). Feng et al. (28) observed the effects of KCTD10 on DR and animal models and discovered that reducing VEGF improved cell vitality and alleviated DR symptoms in rats. This finding further supports the critical role of VEGF in the development of DR. Furthermore, studies have shown that RAAS antagonists can attenuate the endothelial cell barrier dysfunction induced by VEGF, suggesting that these agents may enhance the response of DR patients to VEGF (29). It is interesting to note that aldosterone may be involved in the expression of VEGF and contribute to the development and progression of DR. Additionally, previous studies have highlighted the significant involvement of advanced glycation end products (AGEs), receptors for AGE, and nuclear factor erythroid 2-related factor 2 (NRF2) in the pathogenesis and progression of DR (30, 31). Kang et al. (32) demonstrated that AGE significantly increases VEGF mRNA expression in cells, indicating a positive correlation between AGE and VEGF levels. Moreover, recent research on diabetic nephropathy revealed that blocking receptors for AGE reduces aldosterone's negative impact on NRF2 signal mediators in renal cells, suggesting that aldosterone may block the binding of AGE and RAGE to reduce VEGF production and affect NRF2, leading to corresponding harm to the retina (33). Therefore, aldosterone may play a role in regulating angiogenesis through its effect on VEGF, thus playing a therapeutic role in DR.

MR has been identified in various retinal cells, such as vascular endothelial cells, pericytes, neurons, ganglion cells, and retinal pigment epithelial cells, indicating that aldosterone can activate MR in these target tissues (34). However, the exact mechanism of this activation remains elusive. Notably, although cortisol levels in the serum are 100 times higher than aldosterone levels, MR has a similar affinity for both hormones. Indeed, the specific binding ability of aldosterone to MR and its downstream signaling pathways are important issues that warrant further investigation. Some researchers have postulated that aldosterone may express an enzyme that inactivates cortisol, allowing it to bind to MR (16). However, the exact mechanism by which aldosterone specifically binds to MR and its downstream effects in diabetic retinopathy remain poorly understood. Despite some progress in understanding its role in angiogenesis, further investigation is needed to elucidate the specific contribution of aldosterone in the development and progression of diabetic retinopathy.

4 Effects of aldosterone-mediated oxidative stress and vascular inflammation on diabetic retinopathy

In patients with diabetes, Kang Q et al. found that the excessive production of reactive oxygen species (ROS) in the retina, and the accumulation of ROS due to insufficient clearance by the antioxidant defense system, are key factors in the development of diabetic retinopathy (35). RanaI et al. demonstrated that reducing aldosterone synthase and mineralocorticoid receptors in retinal microglia resulted in reduced intracellular ROS, indicating that local aldosterone in the retina may stimulate the overproduction of

ROS, leading to oxidative stress and retinal injury (36). These findings suggest that targeting aldosterone and MR may be a potential therapeutic strategy for preventing or treating diabetic retinopathy. In addition to promoting the accumulation of intracellular ROS, persistent elevation of aldosterone can also block the synthesis of nitric oxide and activate cyclooxygenase-2 (37, 38). While some kidney-focused clinical studies suggest a deeper perspective, Higashide T et al. found that ROS accumulation can also promote the increase of aldosterone in patients with aldosteronism and eye diseases (39). However, Reina-Couto et al. (40) suggested that a high level of aldosterone in the blood may inhibit the contraction of retinal veins due to the high inflammatory response of blood vessels. As the specific mechanism has not been fully elucidated, further studies are required to confirm these findings.

Nevertheless, aldosterone has been found to promote inflammatory damage to the retina by inducing the production of pro-inflammatory factors such as interleukin (IL)-1β, CCL5, and TNF-α. Studies by Dong et al. (41) have demonstrated the up-regulated expression of adhesion molecules in the retina of diabetic rats, including vascular cell adhesion molecule-1 in retinal endothelium, which leads to leukocyte adhesion and plays a critical role in retinal angiogenesis and the development of proliferative diabetic retinopathy. Inhibition of aldosterone synthase by FAD286 has been shown to effectively reduce the expression of pro-inflammatory factors such as TNF-α and vascular cell adhesion molecule-1 in the retina (26). Studies by Tang et al. (42) and Kong et al. (43) have also revealed increased expression of inflammatory cytokines such as IL-1β and TNF-α in DR, leading to an inflammatory response that promotes the development of DR. Thus, aldosterone may mediate the expression of cell adhesion molecules and TNF-α, to exacerbate retinal vascular inflammation. Therefore, understanding the regulation of aldosterone on inflammation has potential therapeutic value and research significance in the prevention and treatment of DR.

5 Effect of aldosterone-mediated nerve injury on diabetic retinopathy

The pathophysiology of DR involves not only angiogenesis and inflammatory injury but also neurodegeneration. Müller cells are present throughout the retina and surround the neurons and microvessels, playing a crucial role in maintaining retinal structure and homeostasis. In addition, müller cells secrete neurotrophic factors that protect retinal nerve cells, making them vital for retinal health (44, 45).

Hyperglycemia-induced stimulation of retinal müller cells leads to an increase in intracellular inflammatory factors, VEGF, and chemokines, which promote the development and progression of DR. Interestingly, müller cell activation has varying effects on the retina depending on the stage of DR. During the non-PDR phase, activation of müller cells can protect retinal nerve cells, reduce edema and maintain the integrity of the retina (44). However, in the PDR stage, müller cell activation can promote retinal cell apoptosis, weaken the blood-retinal barrier and increase the production of inflammatory factors (46). These findings highlight the important role of müller cells as the main mediator of retinal inflammation and vascular leakage in DR.

Zhao et al. (34) have previously conducted studies that show that aldosterone can regulate the ion/water pathway of retinal Müller cells, thereby maintaining normal retinal function. This finding is further supported by Allingham et al., who suggested that aldosterone can influence the expression and localization of aquaporin-4 (AQP4) and inward rectifier potassium channel 4.1 (Kir4.1) in müller cells, leading to the accumulation of glial fibrillary acidic protein (GFAP), a marker of müller cell damage (47). AQP4 and Kir4.1 are responsible for the entry and exit of water and potassium ions in müller cells, mediate the humoral transport of müller cells and maintain the balance of water and electrolytes in müller cells (48, 49). Similarly, the accumulation of water and potassium in müller cells will lead to DR aggravating retinal degeneration. The upregulation of AQP4 and downregulation of Kir4.1 can disrupt the balance of water and electrolytes in müller cells, leading to the accumulation of water and potassium, which exacerbates retinal degeneration and promotes the development of DR. In addition, these changes can stimulate the release of inflammatory factors like IL-1 β, IL-6, IL-17, and TNF- α, as well as the production of growth factors such as VEGF, further promoting the occurrence and progression of DR (50). Deliyanti et al. (26) conducted studies that confirmed the presence of aldosterone synthase, mineralocorticoid receptor, and 11-hydroxysteroid dehydrogenase type 2 in müller cells, indicating that aldosterone can specifically react with müller cells in DR patients. As a result, aldosterone inhibitors can be used to target the water and electrolyte transport pathways in müller cells. However, further research is required to validate the feasibility of this approach.

6 Evaluation of the effect of aldosterone on DR from the perspective of gene

From the perspective of genetics, many scholars have also evaluated the association between aldosterone and DR at the genetic level. Ohashi et al. (51) treated müller cells with high glucose. MR inhibitors inhibited aldosterone-induced cell swelling and up-regulated MR target genes. Younas et al. (52) conducted a genetic polymorphism study on G8790A related to RAAS, and found that A genotype (male) and AG/AA genotype (female) are risk factors for diabetes, which did not confirm the association with DR. However, in the study of Egyptian cases, MTHFR 677 TT, MTHFR 1298 CC, AC and ACE DD genotype were found to be related to DR (53). It is worth noting that the conclusion of the study is relatively limited due to the interference of race, sex, age and other factors in the study of gene level. There are many difficulties in the research of large samples and multi-ethnic. Therefore, to explore the effect of aldosterone on DR from the perspective of genetics, it is still necessary to balance more and more confounders in order to obtain more reliable conclusions.

7 Conclusion and prospect

With an increased understanding of the role of aldosterone in DR, treatments targeting various pathways and molecules have emerged. Aldosterone, as a component of RAAS, can induce retinal neovascularization and inflammation, both of which are linked to the development of DR. The use of aldosterone and its inhibitors in the treatment of diabetes and its complications has garnered significant interest, and many studies have explored various methods of aldosterone inhibition in DR treatment. However, there is still limited knowledge regarding the mechanisms underlying these effects. Further investigation into the role and mechanisms of aldosterone in DR could have significant clinical implications.

Currently, the impact of aldosterone on retinal damage is not fully understood in the field of ophthalmology. It remains unclear whether the damage is caused mainly by local or systemic factors, which limits the clinical use of aldosterone. Nevertheless, aldosterone antagonists have demonstrated some signs of efficacy in treating retinal diseases (24). Future research should use human eye tissues to determine the physiological and pathological role of aldosterone in DR, giving full play to the role of aldosterone antagonists in the treatment of patients with DR. Furthermore, the impact of different concentrations of aldosterone on the retina at different stages of DR needs to be explored, adding further complexity to the study of aldosterone, and opening up opportunities to discover new therapeutic targets.

Author contributions

KL, HZ and ZY contributed to the conception of the review, and wrote the manuscript. All authors critically revised the manuscript. All authors contributed to the article and approved the submitted version.

Funding

This work was supported by grants from the National Natural Science Foundation of China (82260212) and Science and Technology Innovation Base Construction - Clinical Medicine Research Centre Project (20221ZDG02012) to ZY; the postgraduates innovation special fund project of Jiangxi province (YC2022—B051) and a grant from the Talent Development project of the Affiliated Eye Hospital of Nanchang University (No.2022X05) and to KL. The funders had no role in the study design, data collection, data analysis, interpretation, or writing of the report.

Acknowledgments

We thank Home for Researchers editorial team (www.home-for-researchers.com) for language editing service. We thank Figdraw (www.figdraw.com) for expert assistance in Figure 1.

Conflict of interest

The authors declare that the research was conducted in the absence of any commercial or financial relationships that could be construed as a potential conflict of interest.

Publisher's note

References

1. Bain SC, Klufas MA, Ho A, Matthews DR. Worsening of diabetic retinopathy with rapid improvement in systemic glucose control: A review. *Diabetes Obes Metab* (2019) 21(3):454–66. doi: 10.1111/dom.13538

2. Mounirou BAM, Adam ND, Yakoura AKH, Aminou MSM, Liu YT, Tan LY. Diabetic retinopathy: An overview of treatments. *Indian J Endocrinol Metab* (2022) 26 (2):111–8. doi: 10.4103/ijem.ijem_480_21

3. Gonzalez-Cortes JH, Martinez-Pacheco VA, Gonzalez-Cantu JE, Bilgic A, de Ribot FM, Sudhalkar A, et al. Current treatments and innovations in diabetic retinopathy and diabetic macular edema. *Pharmaceutics* (2022) 15(1):122. doi: 10.3390/pharmaceutics15010122

4. Huang L, Liang W, Zhou K, Wassel RA, Ridge ZD, Ma JX, et al. Therapeutic effects of fenofibrate nano-emulsion eye drops on retinal vascular leakage and neovascularization. *Biol (Basel).* (2021) 10(12):1328 doi: 10.3390/biology10121328

5. Putta S, Yarla NS, Kilari EK, Surekha C, Aliev G, Divakara MB, et al. Therapeutic potentials of triterpenes in diabetes and its associated complications. *Curr Top Med Chem* (2016) 16(23):2532–42. doi: 10.2174/1568026616666160414123343

6. Qureshi I, Ma J, Abbas Q. Recent development on detection methods for the diagnosis of diabetic retinopathy. *Symmetry* (2019) 11(6):749. doi: 10.3390/sym11060749

7. Liu K, Zou J, Fan H, Hu H, You Z. Causal effects of gut microbiota on diabetic retinopathy: A mendelian randomization study. *Front Immunol* (2022) 13:930318. doi: 10.3389/fimmu.2022.930318

8. Ferreira NS, Tostes RC, Paradis P, Schiffrin EL. Aldosterone, inflammation, immune system, and hypertension. *Am J Hypertens* (2021) 34(1):15–27. doi: 10.1093/ajh/hpaa137

9. Alqudah M, Hale TM, Czubryt MP. Targeting the renin-Angiotensin-Aldosterone system in fibrosis. *Matrix Biol* (2020), 91–2:92–108. doi: 10.1016/j.matbio.2020.04.005

10. Gekle M, Mildenberger S. Glomerular mesangial cell pH homeostasis mediates mineralocorticoid receptor-induced cell proliferation. *Biomedicines* (2021) 9(9):1117. doi: 10.3390/biomedicines9091117

11. Oravcova H, Katrencikova B, Garaiova I, Durackova Z, Trebaticka J, Jezova D. Stress hormones cortisol and aldosterone, and selected markers of oxidative stress in response to long-term supplementation with omega-3 fatty acids in adolescent children with depression. *Antioxidants (Basel)* (2022) 11(8):1546. doi: 10.3390/antiox11081546

12. Kanda A, Ishida S. (Pro)renin receptor: Involvement in diabetic retinopathy and development of molecular targeted therapy. *J Diabetes Investig* (2019) 10(1):6–17. doi: 10.1111/jdi.12842

13. Barrera-Chimal J, Girerd S, Jaisser F. Mineralocorticoid receptor antagonists and kidney diseases: Pathophysiological basis. *Kidney Int* (2019) 96(2):302–19. doi: 10.1016/j.kint.2019.02.030

14. Dhaybi OA, Bakris G. Mineralocorticoid antagonists in chronic kidney disease. *Curr Opin Nephrol Hypertens* (2017) 26(1):50–5. doi: 10.1097/mnh.0000000000000290

15. Wilkinson-Berka JL, Suphapimol V, Jerome JR, Deliyanti D, Allingham MJ. Angiotensin II and aldosterone in retinal vasculopathy and inflammation. *Exp Eye Res* (2019) 187:107766. doi: 10.1016/j.exer.2019.107766

16. Allingham MJ, Mettu PS, Cousins SW. Aldosterone as a mediator of severity in retinal vascular disease: Evidence and potential mechanisms. *Exp Eye Res* (2019) 188:107788. doi: 10.1016/j.exer.2019.107788

17. Lovshin JA, Lytvyn Y, Lovblom LE, Katz A, Boulet G, Bjornstad P, et al. Retinopathy and RAAS activation: Results from the Canadian study of longevity in type 1 diabetes. *Diabetes Care* (2019) 42(2):273–80. doi: 10.2337/dc18-1809

18. Ames MK, Atkins CE, Pitt B. The renin-angiotensin-aldosterone system and its suppression. *J Vet Intern Med* (2019) 33(2):363–82. doi: 10.1111/jvim.15454

19. Lai S, Perrotta AM, Bagordo D, Mazzaferro S, Menè P, Errigo F, et al. Literature review on the cross-link between ocular and renal disease: Renin angiotensin aldosterone system is a main actor. *Eur Rev Med Pharmacol Sci* (2022) 26(13):4774–88. doi: 10.26355/eurrev_202207_29203

20. Senanayake P, Drazba J, Shadrach K, Milsted A, Rungger-Brandle E, Nishiyama K, et al. Angiotensin II and its receptor subtypes in the human retina. *Invest Ophthalmol Vis Sci* (2007) 48(7):3301–11. doi: 10.1167/iovs.06-1024

21. Chen S, Zhong H, Wang Y, Wang Z, Liang X, Li S, et al. The clinical significance of long non-coding RNA ANRIL level in diabetic retinopathy. *Acta Diabetol* (2020) 57 (4):409–18. doi: 10.1007/s00592-019-01442-2

22. Wang B, Wang F, Zhang Y, Zhao SH, Zhao WJ, Yan SL, et al. Effects of RAS inhibitors on diabetic retinopathy: A systematic review and meta-analysis. *Lancet Diabetes Endocrinol* (2015) 3(4):263–74. doi: 10.1016/s2213-8587(14)70256-6

23. Jerome JR, Deliyanti D, Suphapimol V, Kolkhof P, Wilkinson-Berka JL. Finerenone, a non-steroidal mineralocorticoid receptor antagonist, reduces vascular injury and increases regulatory T-cells: Studies in rodents with diabetic and neovascular retinopathy. *Int J Mol Sci* (2023) 24(3):2334. doi: 10.3390/ijms24032334

24. Zhao M, Mantel I, Gelize E, Li X, Xie X, Arboleda A, et al. Mineralocorticoid receptor antagonism limits experimental choroidal neovascularization and structural changes associated with neovascular age-related macular degeneration. *Nat Commun* (2019) 10(1):369. doi: 10.1038/s41467-018-08125-6

25. Liu Y, Yang Q, Fu H, Wang J, Yuan S, Li X, et al. Müller glia-derived exosomal miR-9-3p promotes angiogenesis by restricting sphingosine-1-phosphate receptor S1P (1) in diabetic retinopathy. *Mol Ther Nucleic Acids* (2022) 27:491–504. doi: 10.1016/j.omtn.2021.12.019

26. Deliyanti D, Miller AG, Tan G, Binger KJ, Samson AL, Wilkinson-Berka JL. Neovascularization is attenuated with aldosterone synthase inhibition in rats with retinopathy. *Hypertension* (2012) 59(3):607–13. doi: 10.1161/hypertensionaha.111.188136

27. Zehden JA, Mortensen XM, Reddy A, Zhang AY. Systemic and ocular adverse events with intravitreal anti-VEGF therapy used in the treatment of diabetic retinopathy: A review. *Curr Diabetes Rep* (2022) 22(10):525–36. doi: 10.1007/s11892-022-01491-y

28. Feng Y, Wang C, Wang G. Inhibition of KCTD10 affects diabetic retinopathy progression by reducing VEGF and affecting angiogenesis. *Genet Res (Camb).* (2022) 2022:4112307. doi: 10.1155/2022/4112307

29. Li Y, Yan Z, Chaudhry K, Kazlauskas A. The renin-Angiotensin-Aldosterone system (RAAS) is one of the effectors by which vascular endothelial growth factor (VEGF)/Anti-VEGF controls the endothelial cell barrier. *Am J Pathol* (2020) 190 (9):1971–81. doi: 10.1016/j.ajpath.2020.06.004

30. Oshitari T. Advanced glycation end-products and diabetic neuropathy of the retina. *Int J Mol Sci* (2023) 24(3):2927. doi: 10.3390/ijms24032927

31. Sun Z, Wang Y, Xu R, Zhang S, Yang H, Song J, et al. Hydroxysafflor yellow a improved retinopathy *via* Nrf2/HO-1 pathway in rats. *Open Life Sci* (2022) 17(1):284–92. doi: 10.1515/biol-2022-0030

32. Kang Q, Dai H, Jiang S, Yu L. Advanced glycation end products in diabetic retinopathy and phytochemical therapy. *Front Nutr* (2022) 9:1037186. doi: 10.3389/fnut.2022.1037186

33. Gaikwad DD, Bangar NS, Apte MM, Gvalani A, Tupe RS. Mineralocorticoid interaction with glycated albumin downregulates NRF - 2 signaling pathway in renal cells: Insights into diabetic nephropathy. *Int J Biol Macromol.* (2022) 220:837–51. doi: 10.1016/j.ijbiomac.2022.08.095

34. Zhao M, Valamanesh F, Celerier I, Savoldelli M, Jonet L, Jeanny JC, et al. The neuroretina is a novel mineralocorticoid target: Aldosterone up-regulates ion and water channels in müller glial cells. *FASEB J* (2010) 24(9):3405–15. doi: 10.1096/fj.09-154344

35. Kang Q, Yang C. Oxidative stress and diabetic retinopathy: Molecular mechanisms, pathogenetic role and therapeutic implications. *Redox Biol* (2020) 37:101799. doi: 10.1016/j.redox.2020.101799

36. Rana I, Suphapimol V, Jerome JR, Talia DM, Deliyanti D, Wilkinson-Berka JL. Angiotensin II and aldosterone activate retinal microglia. *Exp Eye Res* (2020) 191:107902. doi: 10.1016/j.exer.2019.107902

37. Chen ZW, Tsai CH, Pan CT, Chou CH, Liao CW, Hung CS, et al. Endothelial dysfunction in primary aldosteronism. *Int J Mol Sci* (2019) 20(20):5214. doi: 10.3390/ijms20205214

38. Bioletto F, Bollati M, Lopez C, Arata S, Procopio M, Ponzetto F, et al. Primary aldosteronism and resistant hypertension: A pathophysiological insight. *Int J Mol Sci* (2022) 23(9):4803. doi: 10.3390/ijms23094803

39. Tomomi H, Kazuyuki H, Mitsuhiro K, Kazuhisa S. Aldosterone as a possible contributor to eye diseases. *Endocrinology* (2022) 2):2. doi: 10.1210/endocr/bqac201

40. Reina-Couto M, Afonso J, Carvalho J, Morgado L, Ronchi FA, de Oliveira Leite AP, et al. Interrelationship between renin-angiotensin-aldosterone system and oxidative stress in chronic heart failure patients with or without renal impairment. *BioMed Pharmacother.* (2021) 133:110938. doi: 10.1016/j.biopha.2020.110938

41. Dong Y, Wan G, Yan P, Qian C, Li F, Peng G. Fabrication of resveratrol coated gold nanoparticles and investigation of their effect on diabetic retinopathy in streptozotocin induced diabetic rats. *J Photochem Photobiol B* (2019) 195:51–7. doi: 10.1016/j.jphotobiol.2019.04.012

42. Tang L, Xu GT, Zhang JF. Inflammation in diabetic retinopathy: possible roles in pathogenesis and potential implications for therapy. *Neural Regener Res* (2023) 18 (5):976–82. doi: 10.4103/1673-5374.355743

43. Kong H, Zhao H, Chen T, Song Y, Cui Y. Targeted P2X7/NLRP3 signaling pathway against inflammation, apoptosis, and pyroptosis of retinal endothelial cells in diabetic retinopathy. *Cell Death Dis* (2022) 13(4):336. doi: 10.1038/s41419-022-04786-w

44. Ou K, Copland DA, Theodoropoulou S, Mertsch S, Li Y, Liu J, et al. Treatment of diabetic retinopathy through neuropeptide y-mediated enhancement of neurovascular microenvironment. *J Cell Mol Med* (2020) 24(7):3958–70. doi: 10.1111/jcmm.15016

45. Singh C, Tran V, McCollum L, Bolok Y, Allan K, Yuan A, et al. Hyperoxia induces glutamine-fuelled anaplerosis in retinal müller cells. *Nat Commun* (2020) 11 (1):1277. doi: 10.1038/s41467-020-15066-6

46. Becker K, Klein H, Simon E, Viollet C, Haslinger C, Leparc G, et al. In-depth transcriptomic analysis of human retina reveals molecular mechanisms underlying diabetic retinopathy. *Sci Rep* (2021) 11(1):10494. doi: 10.1038/s41598-021-88698-3

47. Sanchez MC, Chiabrando GA. Multitarget activities of müller glial cells and low-density lipoprotein receptor-related protein 1 in proliferative retinopathies. *ASN Neuro.* (2022) 14:17590914221136365. doi: 10.1177/17590914221136365

48. Allingham MJ, Tserentsoodol N, Saloupis P, Mettu PS, Cousins SW. Aldosterone exposure causes increased retinal edema and severe retinopathy following laser-induced retinal vein occlusion in mice. *Invest Ophthalmol Vis Sci* (2018) 59(8):3355–65. doi: 10.1167/iovs.17-23073

49. Wang T, Zhang C, Xie H, Jiang M, Tian H, Lu L, et al. Anti-VEGF therapy prevents müller intracellular edema by decreasing VEGF-a in diabetic retinopathy. *Eye Vis (Lond).* (2021) 8(1):13. doi: 10.1186/s40662-021-00237-3

50. Yang S, Qi S, Wang C. The role of retinal müller cells in diabetic retinopathy and related therapeutic advances. *Front Cell Dev Biol* (2022) 10:1047487. doi: 10.3389/fcell.2022.1047487

51. Ohashi K, Hayashi T, Utsunomiya K, Nishimura R. The mineralocorticoid receptor signal could be a new molecular target for the treatment of diabetic retinal complication. *Expert Opin Ther Targets.* (2022) 26(5):479–86. doi: 10.1080/14728222.2022.2072730

52. Younas H, Ijaz T, Choudhry N. Investigation of angiotensin-1 converting enzyme 2 gene (G8790A) polymorphism in patients of type 2 diabetes mellitus with diabetic nephropathy in Pakistani population. *PloS One* (2022) 17(2):e0264038. doi: 10.1371/journal.pone.0264038

53. Settin A, El-Baz R, Ismaeel A, Tolba W, Allah WA. Association of ACE and MTHFR genetic polymorphisms with type 2 diabetes mellitus: Susceptibility and complications. *J Renin Angiotensin Aldosterone Syst* (2015) 16(4):838–43. doi: 10.1177/1470320313516172

frontiers | Frontiers in Endocrinology

TYPE Original Research
PUBLISHED 11 April 2023
DOI 10.3389/fendo.2022.1125838

OPEN ACCESS

EDITED BY
Xiao-qiang Liu,
Tianjin Medical University General Hospital, China

REVIEWED BY
DK Gong,
The First Affiliated Hospital of Soochow University, China
Aiming Xu,
The First Affiliated Hospital of Nanjing Medical University, China

*CORRESPONDENCE
Zhendong Xiang
zhendong@ctgu.edu.cn
Chengdang Xu
xuchengdang1990@163.com

†These authors have contributed equally to this work and share first authorship

SPECIALTY SECTION
This article was submitted to Adrenal Endocrinology, a section of the journal Frontiers in Endocrinology

RECEIVED 16 December 2022
ACCEPTED 28 December 2022
PUBLISHED 11 April 2023

CITATION
You X, Huang S, Wang X'a, Yi C, Gong N, Yu J, Xu C and Xiang Z (2023) Efficacy and safety of bipolar androgen therapy in castration-resistant prostate cancer following abiraterone or enzalutamide resistance: A systematic review.
Front. Endocrinol. 13:1125838.
doi: 10.3389/fendo.2022.1125838

Efficacy and safety of bipolar androgen therapy in castration-resistant prostate cancer following abiraterone or enzalutamide resistance: A systematic review

Xiangyun You[1†], Shan Huang[1†], Xin'an Wang[2], Cheng Yi[1], Niandong Gong[1], Junfeng Yu[1], Chengdang Xu[2*] and Zhendong Xiang[1*]

[1]Department of Urology, The People's Hospital of China Three Gorges University, The First People's Hospital of Yichang, Yichang, China, [2]Department of Urology, Tongji Hospital, School of Medicine, Tongji University, Shanghai, China

Bipolar androgen therapy (BAT) is a new endocrinologic treatment for castration-resistant prostate cancer (CRPC) that can restore some patients' sensitivity to drugs such as abiraterone (Abi) and enzalutamide (Enz). We performed a meta-analysis using STATA16. Sensitivity analyses were performed by examining the effects of individual studies using different effect models and detecting any publication bias using the Harbord test. In a total of 108 unique records, ten studies were included in the final meta-analysis. Participants who underwent BAT achieved a PSA50 response rate of 27% (95%CI [0.22,0.31], I2=17.98%), ORR of 34% (95%CI [0.24,0.43], I2=0), and incidence of AEs (grade≥3) of 14% (95%CI [0.09,0.19], I2=0). Patients who completed BAT proceeded to AR-targeted therapy (Abi or Enz) and achieved a PSA50 response rate of 57% (95% CI [0.36,0.78], I2=0). Patients with prior Enz resistance had a stronger impact on the PSA50 of AR-target therapy rechallenge. The results of this meta-analysis indicate that BAT is a safe and effective treatment for patients who have progressed after Abi or Enz. BAT can trigger the resensitization of patients with CRPC to subsequent endocrine therapy and improve the overall survival of patients and their quality of life.

KEYWORDS

bipolar androgen therapy, testosterone, castration-resistant prostate cancer, abiraterone, enzalutamide

1 Introduction

Prostate cancer (PCa) is one of the most common malignant tumors in men. With the continuous improvement in living standards and the aggravation of population aging, its incidence ranks second globally (1). Mortality ranks first in men, and fatality is lower than that in lung and colorectal cancers (2). In Asia, the incidence of prostate cancer is increasing every year (3). Some patients are in the middle and advanced stages of the disease when they are first diagnosed. As prostate cancer is an androgen-dependent tumor, androgen deprivation therapy (ADT) and inhibition of the androgen receptor signaling pathway are the main endocrinologic treatments for patients with metastatic prostate cancer (4). However, almost all patients eventually develop castration-resistant prostate cancer (CRPC) 14-30 months after ADT (5). Enzalutamide (Enz), abiraterone (Abi), and other new-generation anti-androgen drugs are more effective. However, most patients will still become resistant to new-generation anti-androgen drugs in the short term. For patients in this period, chemotherapy (such as docetaxel), molecular targeted drugs (such as sunitinib), and DNA damage repair-related poly ADP ribose polymerase inhibitors (such as olaparib) can only delay disease progression to a certain extent. There are currently no breakthrough treatments for CRPC (6, 7).

Bipolar androgen therapy (BAT) is a new treatment for patients with CRPC proposed by the Johns Hopkins University School of Medicine in recent years. The regulation of testosterone (T) between castration and supraphysiological levels suppresses cancer cell growth, thereby reducing prostate-specific antigen (PSA) and delaying castration-resistant prostate cancer progression (8). The opinion that SPA inhibits prostate cancer growth contradicts the mainstream treatment method of ADT. However, its therapeutic effect has often been verified both *in vitro* and *in vivo* in animal experiments (9–11). Clinical investigations have shown that BAT is effective (12–14). Thus, BAT is safer and more effective than cytotoxic drugs (15). BAT can restore some patients' sensitivity to drugs, such as Abi and Enz, showing significant advantages in treating CRPC patients (16). However, there are few BAT clinical trials at present, and most are phase I and phase II clinical trials and a few case reports. There are no large phase III prospective randomized controlled trials on BAT. However, the mechanism of BAT has not yet been fully elucidated. The effectiveness and safety of BAT in clinical settings need to be further verified; there is no clear international consensus or guidance on how and when to use BAT.

Based on the above problems, we systematically analyzed the efficacy and safety of BAT in treating Abi- or Enz-resistant CRPC using a meta-analysis. We explored the best combination or sequence of BAT and current mainstream CRPC treatment drugs to provide reference and guidance for better clinical applications of BAT in the future.

2 Material and methods

2.1 Inclusion and exclusion criteria

Inclusion criteria: ① patients diagnosed with CRPC; ②Patients who failed treatment with Abi or Enz; ③ Used BAT before; ④ reported outcome indicators, such as efficacy indicators: PSA50, PSA50 response, ORR, etc. Safety indicators: AEs. Exclusion criteria: ① Documents with repeated reports; ② documents for which the full text could not be obtained or data could not be extracted.

2.2 Search strategy

We searched the PubMed, Embase, and Cochrane Library databases for clinical trials on BAT. The search time limit was from the establishment of the database to November 2022. In addition, the references of the included literature were traced, and the relevant literature was supplemented. The following terms were searched: "Bipolar Androgen Therapy" OR "BAT" OR "Supraphysiological Testosterone" AND "Prostate Cancer".

2.3 Literature screening and data extraction

When screening the literature, the title and abstract were first read, and after excluding irrelevant literature, the full text was further read to determine whether it was finally included. The content of data extraction mainly includes ① basic information of included studies, including research title, first author, and publication time; ② baseline characteristics of research subjects, including the number of samples in each group, age of patients, etc.; ③ specific details of intervention measures, follow-up time, etc.; ④ key elements of the risk of bias assessment; ⑤ outcome indicators of concern and outcome measurement data.

2.4 Statistical analysis

Two researchers counted the number of participants in each study and calculated the ratio of PSA50, ORR, AEs(grade ≥3) after BAT, and PSA50 response to Abi or Enz after BAT in each study. Stata16 was used for the statistical analysis. The heterogeneity among the relevant data included in the research results was analyzed using the χ^2 test (the test level was a=0.1), and the heterogeneity was quantitatively judged in combination with I^2. If there was no statistical heterogeneity among the research results, the fixed-effect model was used for meta-analysis, and if there was statistical heterogeneity among the

research results, the random-effect model was used for meta-analysis.

3 Results

3.1 Literature screening process and results

A total of 108 BAT-related studies were obtained through the primary screening. After the primary screening of titles and abstracts and rescreening of the full text, ten studies on BAT (Figure 1) that met the criteria were finally included in the analysis. A total of 353 patients with CRPC participated in BAT treatment.

3.2 Basic characteristics and results summary of the included studies

The characteristics of the included studies of BAT are summarized here (Table 1), such as the type of study, sample size enrolled, time of BAT treatment, and disease stage of the enrolled patients; the baseline characteristics of the included patients (Table 2), such as baseline PSA level, bone metastasis, ECOG score, and Gleason score at the time of pathological diagnosis of the patients enrolled in each study.

3.3 PSA50, ORR and PSA50 response after BAT

3.3.1 Results of PSA50

Among the ten included studies, we found no significant difference in the heterogeneity of the data between these studies ($p > 0.05$, $I^2 < 90\%$). Therefore, the fixed-effect model was more appropriate than the random-effect model. PSA50 is defined as the PSA level of the patient after receiving BAT compared with the baseline, and the PSA level of the participant dropped by ≥50%, which is key data for evaluating the effect of BAT treatment. This was due to the heterogeneity of the enrolled patients and the unequal sample size. In these ten studies, PSA50 ranged from 14% in the study by Laura A. Sena et al (17)to 100% in the report by Senji Hoshi et al (18). Shown in Figure 2, a total of 353 patients were included, and the overall PSA50 response rate was 27% (95%CI [0.22,0.31], $I^2 = 17.98\%$). This means that nearly one-third of the patients were effectively treated with BAT, which also shows that BAT has a certain effect in clinical research.

3.3.2 Results of ORR

In clinical practice, PSA is an important indicator for prostate cancer treatment and follow-up, which doctors and patients pay great attention to. An increase in this value often indicates disease progression. The value of PSA did not increase significantly when distant metastases were detected by radiology; therefore, imaging progress and response are also key indicators for evaluating the efficacy of prostate cancer drug therapy (19). In these ten studies, patients' objective tumor response rate (ORR) was assessed according to the Response Evaluation Criteria in Solid Tumors (RECIST), mainly through imaging examinations. ORR specifically includes partial response (PR) and complete response (CR). We found that the results of the meta-analysis in these ten studies (as shown in Figure 3) suggest that the overall ORR after BAT was 34% (95%CI [0.24,0.43], $I^2 = 0\%$). BAT has a certain effect on PSA relief and is also effective in ORR defined by imaging, which further proves the efficacy of BAT.

3.3.3 Results of PSA50 response

As early as 2015, Schweizer et al (13) discovered and reported that 7 out of 10 CRPC patients who were originally resistant to Abi or Enz after completing the BAT cycle could respond to the new anti-Abi or Enz again. Sensitivity to androgen drug treatment: The PSA50 response rate of the ten studies included in this study (as shown in Figure 4) was 57% (95% CI [0.36,0.78], $I^2 = 0\%$). In other words, two-thirds of patients with CRPC who received BAT could become sensitive to antiandrogen drugs. The fact that BAT reverses the resistance of CRPC patients to Abi or Enz has undoubtedly brought new hope to patients with Abi- or Enz-resistant advanced CRPC.

3.4 Safety of BAT

Since androgens also have a certain effect on promoting cell growth, the issue we are most concerned about in BAT is safety, mainly including the impact of androgens, such as hot flashes, breast tenderness, breast dysplasia, and the risk of disease progression after BAT. The related AEs of the ten studies included in this study are summarized in Table 3, and the meta-analysis results (Figure 5) show that the incidence of AEs (grade ≥3) was 14% (95%CI [0.09,0.19], $I2 = 0\%$).

3.5 Results of survival data after the BAT

Survival data of BAT mainly include time to PSA progression (TPP), no radiographic progression-free survival (rPFS), PFS2 (progression-free survival 2), and radiographic progression-free survival (crPFS). The number of studies on data completeness varies greatly, as summarized in Table 4.

4 Discussion

Prostate cancer progression depends on androgens, therefore, reducing androgen levels or blocking the androgen

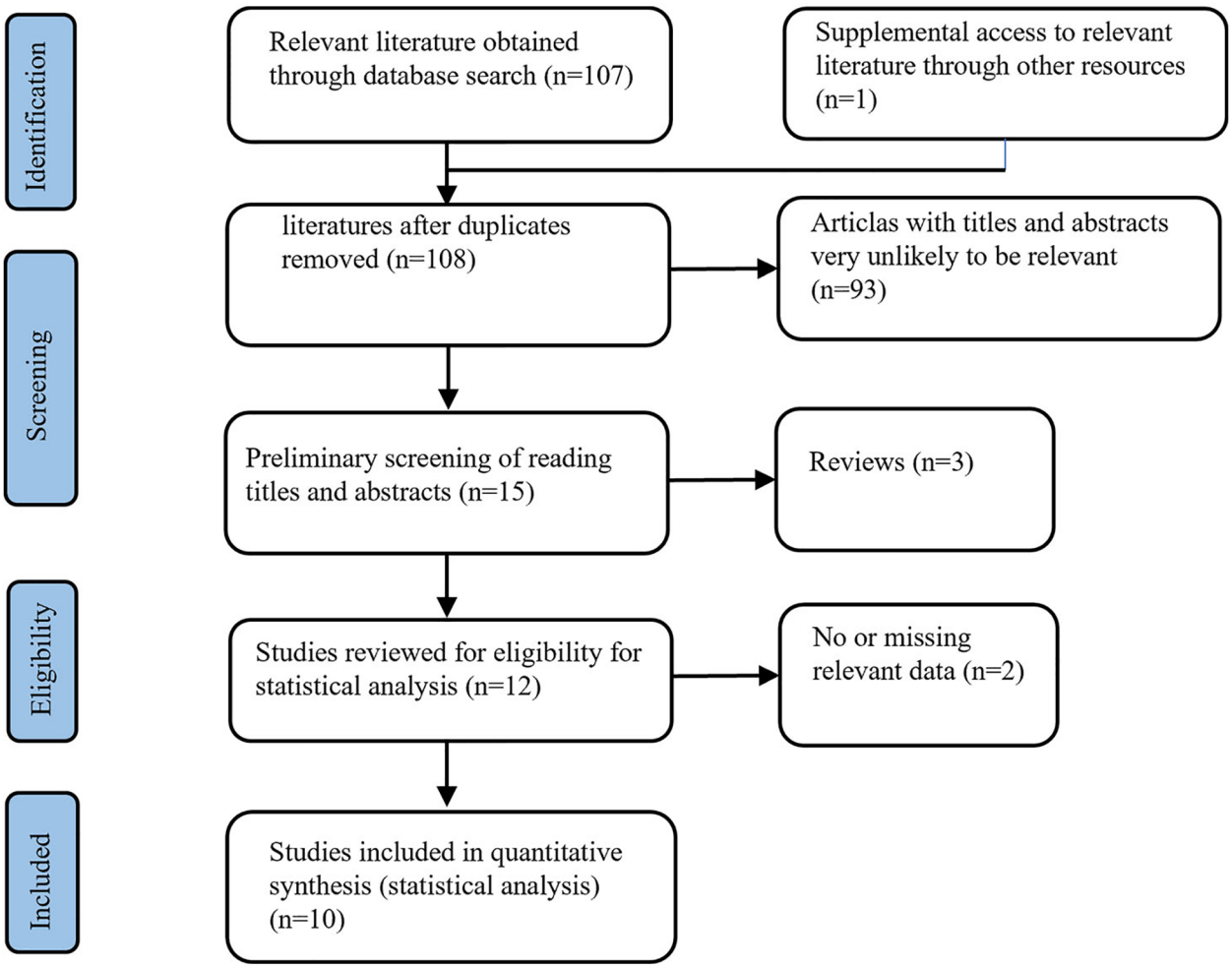

FIGURE 1
Flow chart for literature screening.

receptor (AR) can inhibit prostate cancer (20). During ADT, prostate cancer cells can regulate AR activity through AR gene amplifications, mutations, and post-translational modifications to adapt to the chronic androgen deprivation environment. However, the castration level of androgens and overexpression of AR leads to increased sensitivity of CRPC cells to supraphysiological levels of androgens, further inhibiting DNA replications and inducing double-strand DNA breaks, inhibiting tumor cell growth, and promoting apoptosis. Based on the different responses of prostate cancer cells to different levels of androgens, BAT inhibits CRPC cells through the sudden rise and fall of androgen levels and rapid alternation and delays the disease progression in the CRPC stage. The results of our meta-analysis also confirmed the effectiveness and safety of BAT for CRPC patients who progressed after Abi or Enz, with a PSA50 rate of 27% and an ORR of 34%. BAT can also trigger the resensitization of CRPC patients to subsequent endocrine therapy; the PSA50 response rate was 67%, and the incidence of AEs (grade ≥3) after BAT treatment was 14%.

Xiong et al (8) proved the safety and effectiveness of this therapy in a previous meta-analysis, which played a guiding role in the promotion and application of BAT. However, the included clinical studies and the total number of people were not many; with the increase in BAT clinical trials, we updated the included BAT clinical studies. There have been a few case reports of BAT performed in individual clinical research centers. The results showed that the PSA50 response rate was significantly increased (67% vs. 54%), and the overall safety and effectiveness were better, further demonstrating the possibility, safety, and effectiveness of BAT in optimizing traditional endocrine therapy.

TABLE 1 Characteristics of included studies.

reference	Michael T Schweizer (13)	Benjamin A Teply (12)	Payel Chatterjee (17)	Marcus Moses (18)	Laura A Sena (17)	Samuel R Denmeade (19)	Mark C Markowski 1 (18)	Mark C Markowski 2 (18)	Senji Hoshi (20)	Liu SJ (21)	Mark C Markowski (22)
year	2015	2018	2019	2020	2021	2021	2021	2021	2022	2022	2022
journal	Sci Transl Med	Lancet Oncol	J Clin Invest	Oncotarget	Eur J Cancer	J Clin Oncol	Eur Urol	Eur Urol	Clin Case Rep	BDXXBYXB	Eur Urol Open Sci
Number of patients	16	30	62	33	29	94	29	30	4	4	22
Study type	Pilot	Prospective	Prospective	Retrospective	Prospective	Prospective	Prospective	Prospective	Case report	Case report	Prospective
BAT time, median (range)	NR	6(1-26) cycle	NR	5(2-26) cycle	NR	NR	5(1-25) cycle	NR	NR	NR	NR
PSA assessment interval	Every 2 wk	Every 4 wk	NR	NR	Every 4 wk	Every 4 wk	Every 4 wk	Every 4 wk	NR	Every 1 wk	NR
Bone/CT scans	NR	Every 12 wk	NR	NR	NR	Every 12 wk	Every 12 wk	Every 12 wk	NR	NR	NR
Type of patients	Asymptomatic mCRPC	Asymptomatic or minimally symptomatic mCRPC	NR	Asymptomatic mCRPC	Asymptomatic nmCRPC or mCRPC	Asymptomatic mCRPC	Asymptomatic mCRPC	Asymptomatic mCRPC	Asymptomatic mCRPC	Asymptomatic mCRPC	Asymptomatic mCRPC

BAT, bipolar androgen therapy; CT, computed tomography; mCRPC, metastatic castration-resistant prostate cancer; NR, not reported; PSA, prostate-specific antigen; T, testosterone; Mark C Markowski 1: post Abi; Mark C MarkowskI 2: post Enz.

10.3389/fendo.2022.1125838

TABLE 2 Baseline characteristics for patients of included studies.

reference	Michael T Schweizer	Benjamin A Teply	Payel Chatterjee	Marcus Moses (18)	Laura A Sena	Samuel R Denmeade	Mark C Markowski1	Mark C Markowski2	Senji Hoshi (20)	Liu SJ	Mark C Markowski
Median age, years (range)	71 (56-87)	74 (50-89)	NR	73 (60–88)	69 (41-84)	71 (45-87)	71 (49–85)	74 (50–89)	62.5 (59-71)	74 (68-82)	NR
Median PSA, ng/ml (range)	20 (1.4-90)	39.8 (2.4-245.3)	NR	29.3 (0.04-845)	9.5 (0.5-81.1)	44.3 (1.1-323.3)	27.7 (2.8-367.9)	39.8 (3.4-245.3)	33.63 (1.4-197)	18.655 (9.939-36)	NR
Gleason score≥8,n (%)	5 (31.2)	20 (67)	NR	15 (46)	NR	60 (63.8)	16 (55)	20 (67)	3 (75)	2 (50)	NR
Bone metastasis, n (%)	3 (18.8)	21 (70)	NR	20 (61)	15 (52)	NR	NR	NR	2 (50)	3 (75)	NR
ECOG 0 (%)	15 (93.8)	22 (73)	NR	24 (73)	29 (100)	53 (56.4)	NR	NR	NR	NR	NR
Previous therapy Bicalutamide, n (%)	11 (68.8)	0	NR	0	7 (24)	NR	NR	NR	NR	4 (100)	NR
Previous therapy Abiraterone, n (%)	1 (6.3)	30 (100)	NR	16 (48)	NR	NR	NR	NR	1 (25)	1 (25)	NR
Previous therapy Enzalutamide, n (%)	3 (18.8)	13 (43.3)	NR	7 (21)	NR	NR	NR	NR	3 (75)	1 (25)	NR
Previous therapy Docetaxel, n (%)	0	0	NR	NR	6 (21)	13 (13.8)	NR	NR	0	0	NR

BAT, bipolar androgen therapy; ECOG, Eastern Cooperative Oncology Group Performance Status; GS, Gleason score; PSA, prostate-specific antigen.

10.3389/fendo.2022.1125838

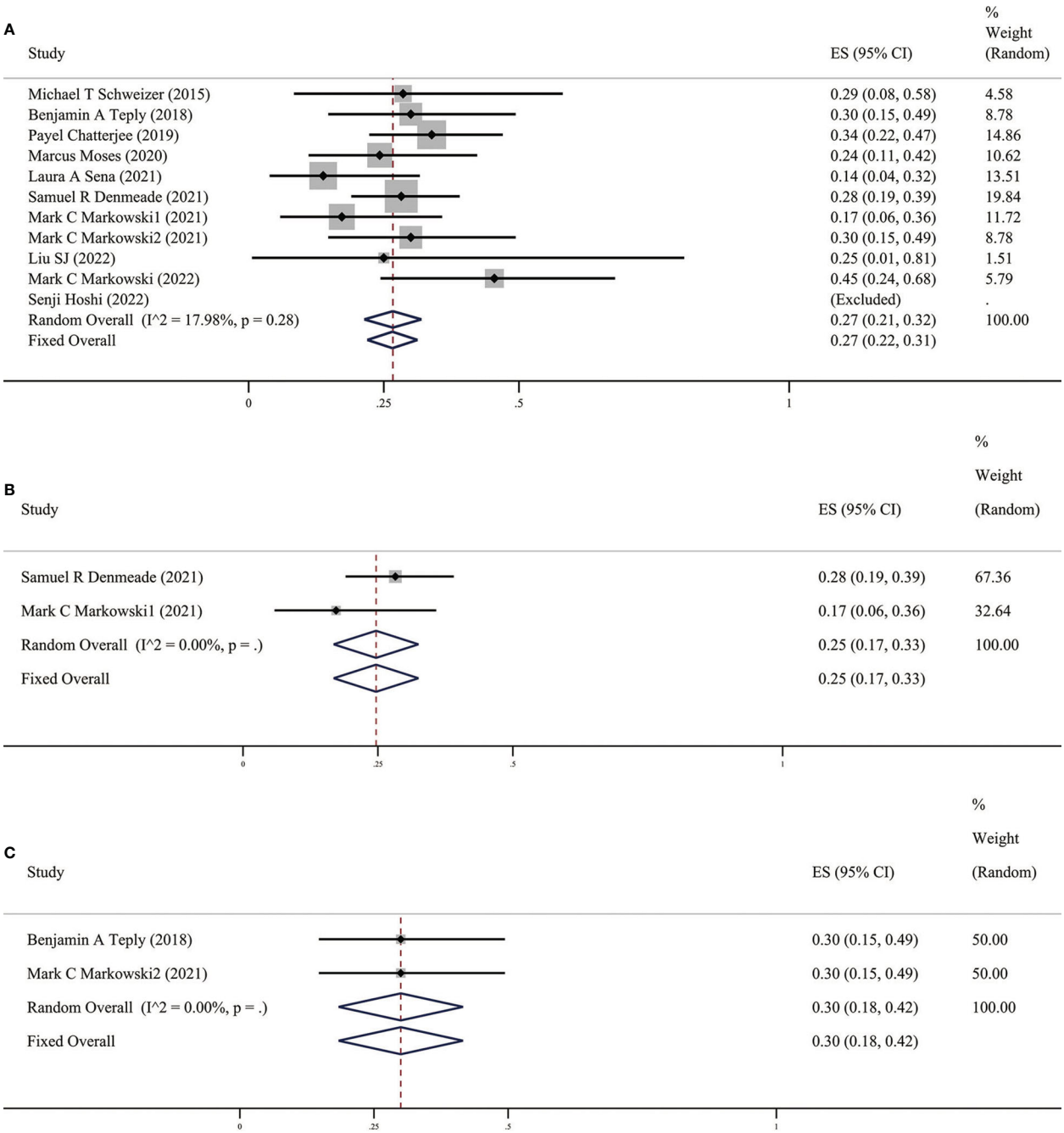

FIGURE 2
(A) Prevalence of PSA50 in all patients. **(B)** Prevalence of PSA50 in patients with previous Abi. **(C)** Prevalence of PSA50 in patients with previous Enz. CI, Confidence interval.

It is interesting that there are differences in BAT treatment efficacy in patients with previous Abi or Enz, therefore, we grouped the earlier BAT treatment studies with Abi or Enz treatment. We found that the PSA50 rate of patients with previous Abi was 25% (as shown in Figure 2B), ORR was 25% (as shown in Figure 3B), the PSA50 response rate was 53% (as shown in Figure 4B). But in the Enz group, the PSA50 rate of patients was 30% (as shown in Figure 2C), the ORR was 50% (as shown in Figure 3C), and the PSA50 response rate increased to 70% (as shown in Figure 4C) in patients continued to receive Enz after progression. According to the above results, re-sensitivity to novel hormonal therapy (NHA) can be achieved through BAT, thus prolonging the effectiveness of NHA. BAT resulted in a higher PSA50 and ORR in patients treated with Enz

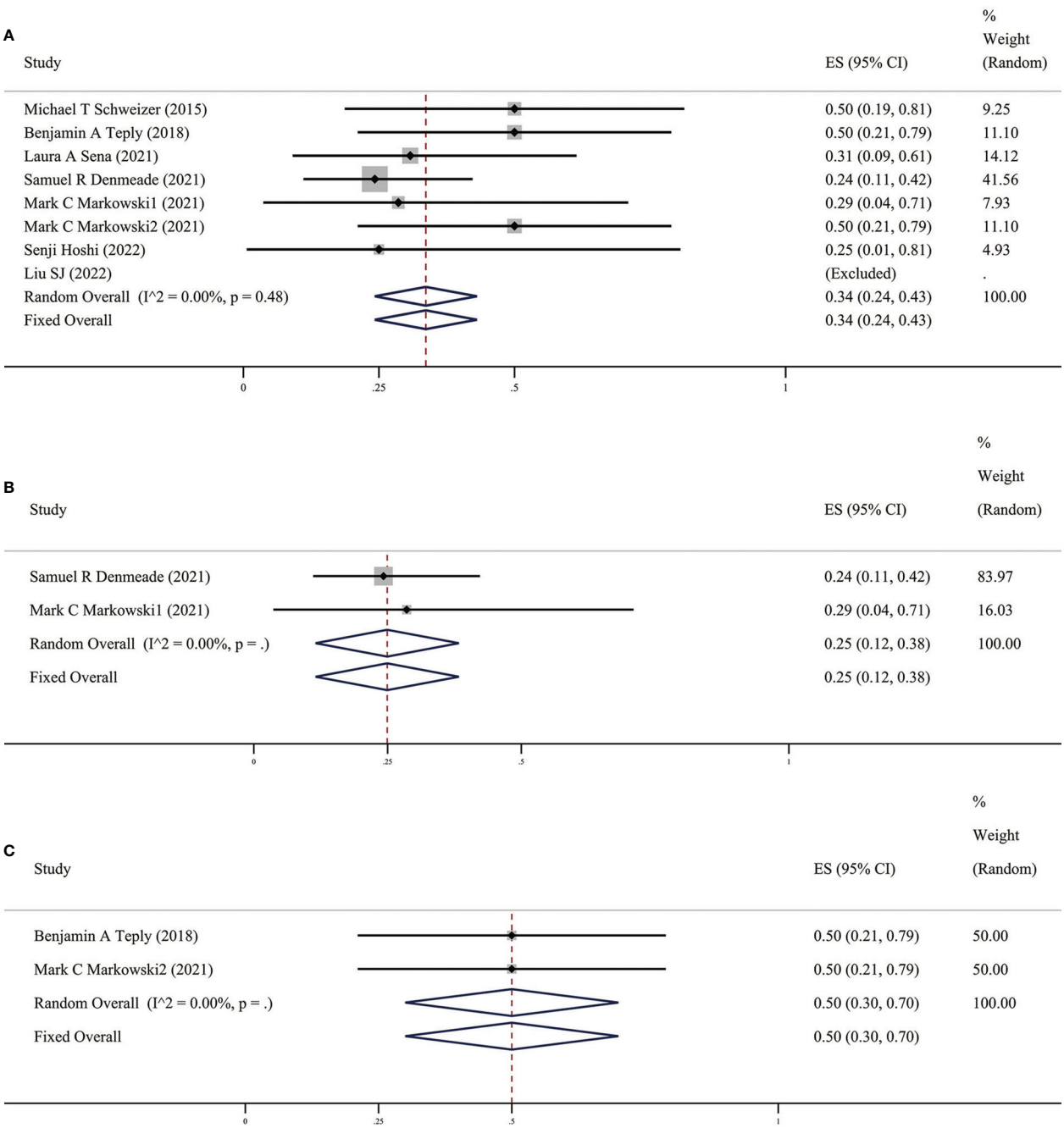

FIGURE 3
(A) Prevalence of ORR in all patients. **(B)** Prevalence of ORR in patients with previous Abi. **(C)** Prevalence of ORR in patients with previous Enz. CI, Confidence interval.

than in those treated with Abi. BAT is a better choice for patients and doctors and can be added to the NHA treatment base, in particular, BAT sequential Enz can further improve the curative effect.

In terms of safety, most of the AEs of BAT are grade 1-2, including fatigues, generalized pains, and lower extremity edema (8). Our results suggest that the incidence of AEs (grade≥3) was 14%. Compared to the incidence of AEs corresponding to Enz or Abi (21), BAT can significantly improve a patient's quality of life. This shows that the BAT regimen can be reasonably applied in patients with advanced CRPC resistant to Abi or Enz.

Simultaneously, BAT can be used to predict patient prognosis. Denmeade et al (22) showed that a peak PSA level of less than 9 ng/ml after BAT treatment was associated with a

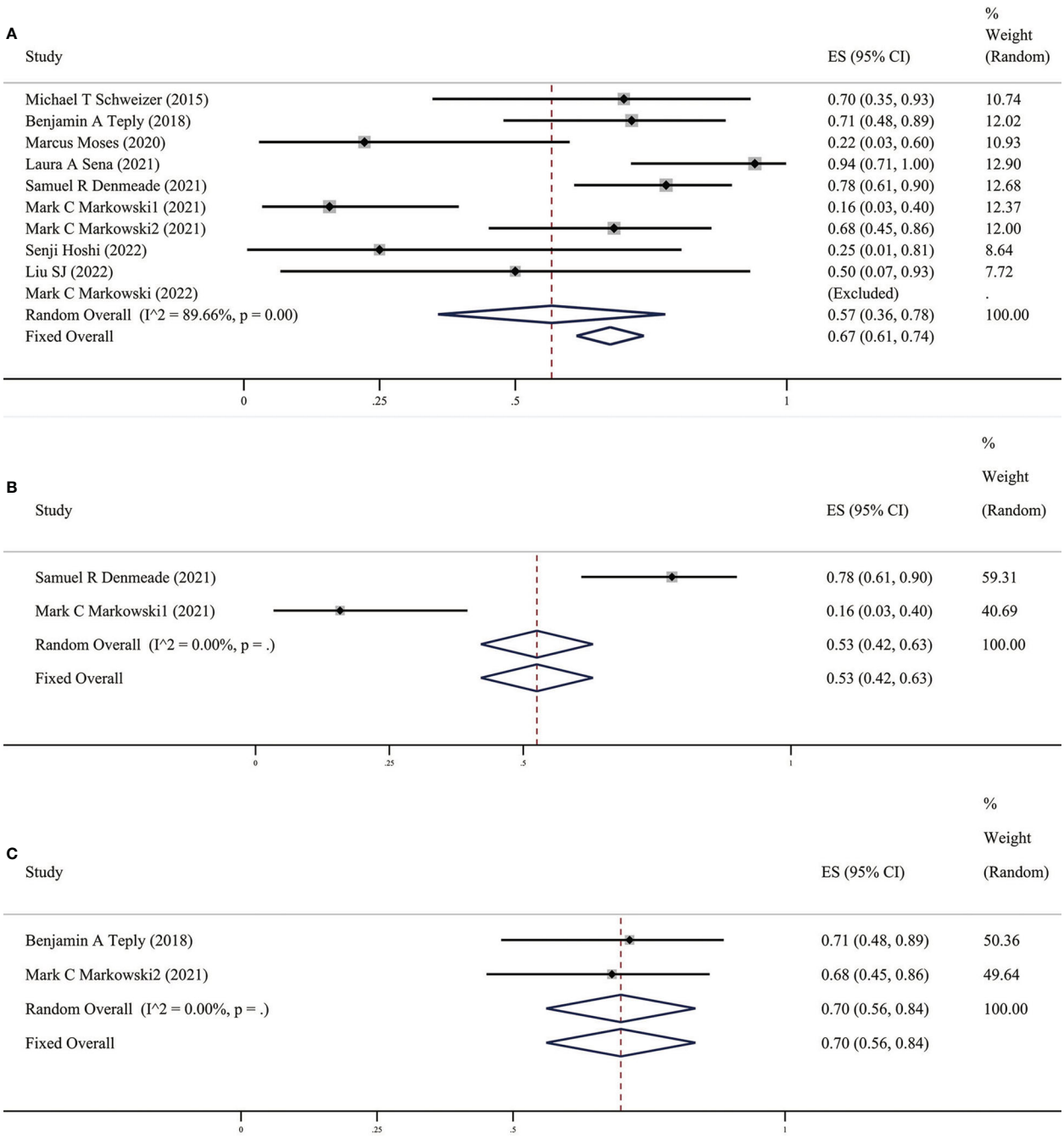

FIGURE 4
(A) Prevalence of PSA50 response in all patients. **(B)** Prevalence of PSA50 response in patients with previous Abi. **(C)** Prevalence of PSA50 response in patients with previous Enz. CI, Confidence interval.

longer duration of ADT response; PSA≥9 ng/ml (n=16) patients had a median progression-free survival of 20.6 months, while the median overall survival of patients with peak PSA <9 ng/ml was 79.6 months. In current clinical trials, it was also found that not all patients were sensitive to BAT treatment. It is important to identify suitable biomarkers to distinguish BAT responders from non-responders. With the current results, markers of response to BAT are still being explored (23), which is also the direction of our future research.

However, some studies included in this study (such as the case reports of Senji et al (18) and Liu et al (24) may have an impact on the results of this study due to the small number of cases.

TABLE 3 AEs (Grade ≥3) adverse events in included studies.

study	Michael T Schweizer	Benjamin A Teply	Payel Chatterjee	Marcus Moses	Laura A Sena	Samuel R Denmeade	Mark C Markowski1	Mark C Markowski2	Senji Hoshi	Liu SJ	Mark C Markowski
No. of Patients	16	30	62	33	29	94	29	30	4	4	22
Hypertension	0	3	NR	NR	2	0	0	NR	0	0	NR
Pulmonary embolism	2	0	NR	NR	1	0	0	NR	0	0	NR
Back pain	0	0	NR	NR	0	3	0	NR	0	0	NR
Fatigue	0	0	NR	NR	0	0	0	NR	0	0	NR
Musculoskeletal pain	0	0	NR	NR	1	4	1	NR	0	0	NR
Urinary obstruction	0	1	NR	NR	1	0	0	NR	0	0	NR
Neutropenia	1	0	NR	NR	0	0	0	NR	0	0	NR
Elevated Alk Phos	0	0	NR	NR	0	0	1	NR	0	0	NR
DIC	0	0	NR	NR	0	0	1	NR	0	0	NR
Bowel obstruction	0	0	NR	NR	0	0	1	NR	0	0	NR
Gallstone	0	0	NR	NR	0	0	0	NR	0	0	NR
Sepsis	0	1	NR	NR	0	0	0	NR	0	0	NR
NSTSEMI	0	0	NR	NR	0	0	0	NR	0	0	NR
Death	1	0	NR	NR	0	0	0	NR	0	0	NR
Stroke	0	0	NR	NR	1	0	0	NR	0	0	NR
Thrombocytopenia	0	0	NR	NR	0	0	0	NR	0	0	NR
Myocardial infarction	0	0	NR	NR	1	0	0	NR	0	0	NR
Edema limbs	0	0	NR	NR	0	1	0	NR	0	0	NR
Nausea	0	0	NR	NR	0	1	0	NR	0	0	NR
Hematuria	0	0	NR	NR	0	1	0	NR	0	0	NR

NR, not reported; DIC, disseminated Intravascular Coagulation.

10.3389/fendo.2022.1125838

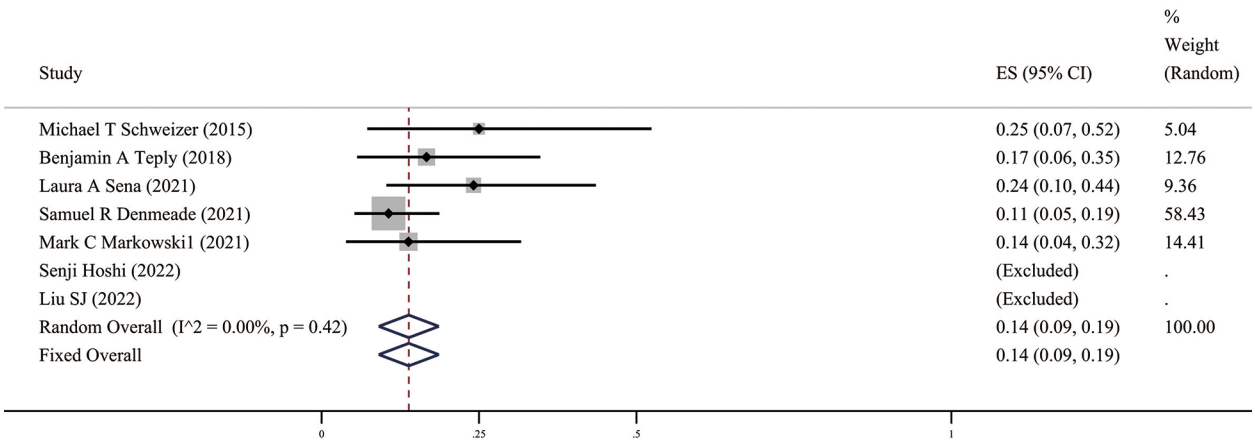

FIGURE 5
Prevalence of AEs (Grade ≥3) in patients. CI, Confidence interval.

TABLE 4 Descriptive results of survival data.

study	TPP, median (95% CI/range), mo	rPFS, median (95% CI/range), mo	crPFS, median (95% CI/range), mo	PFS2
Michael T Schweizer	7.37 (3.17-15.13)	NR	NR	12.8 (7.3-16.3)
Benjamin A Teply	3.3 (2.7-5.5)	NR	6.5 (4.3-8.0)	
Payel Chatterjee	NR	NR	NR	
Marcus Moses	0.9 (95% CI, 0.3–1.4)	NR	NR	
Laura A Sena	not been reached	8.5 (95% CI, 6.9-15.1)	NR	
Samuel R Denmeade	2.79 (95% CI, 1.81-4.5)	5.75 (5.55–8.41)	5.62 (4.76-5.91)	28.2 (23.6-NR)
Mark C Markowski	NR	5.0 (3.3-9.3)	4.3 (3.3-5.3)	8.1 (6.1-9.5)
Senji Hoshi	NR	NR	NR	
Liu SJ	NR	NR	NR	

TPP, time to PSA progression; rPFS, radiographic progression-free survival; crPFS, clinical or radiographic progression-free survival; PFS2, progression-free survival 2; NR, not reported.

5 Conclusions

The results of this meta-analysis indicate that BAT is a safe and effective treatment for patients who have progressed after Abi or Enz. BAT can trigger the resensitization of patients with CRPC to subsequent endocrine therapy and improve the overall survival of patients and their quality of life. However, biomarkers that can predict the efficacy of BAT still need to be identified.

Data availability statement

The original contributions presented in the study are included in the article/Supplementary Material. Further inquiries can be directed to the corresponding authors.

Author contributions

XY, SH: Protocol development, Data collection or management, Data analysis, Manuscript writing and editing. CY, XW: Manuscript writing and editing. JY, NG: Data collection and management. ZX, CX: Protocol development, Data analysis, Manuscript editing. All authors contributed to the article and approved the submitted version.

Funding

This work was supported by the National Natural Science Foundation of China (No. 82203408), the Natural Science Foundation of Hubei Province (No. 2020CFB378), Yichang

Medical and Health Research Project (No. A20-2-021, No. A22-2-036), Natural Science Foundation of Shanghai Municipal Science and Technology Committee (NO.22ZR1456800) and Clinical Research Plan of SHDC (NO. SHDC2020CR3074B).

Acknowledgments

We would like to thank Editage for English language editing.

Conflict of interest

The authors declare that the research was conducted in the absence of any commercial or financial relationships that could be construed as a potential conflict of interest.

Publisher's note

Supplementary material

The Supplementary Material for this article can be found online at: https://www.frontiersin.org/articles/10.3389/fendo.2022.1125838/full#supplementary-material

References

1. Global Burden of Disease Cancer C, Fitzmaurice C, Akinyemiju TF, Al Lami FH, Alam T, Alizadeh-Navaei R, et al. Global, regional, and national cancer incidence, mortality, years of life lost, years lived with disability, and disability-adjusted life-years for 29 cancer groups, 1990 to 2016: A systematic analysis for the global burden of disease study. *JAMA Oncol* (2018) 4(11):1553–68. doi: 10.1001/jamaoncol.2018.2706

2. Siegel RL, Miller KD, Jemal A. Cancer statistics, 2020. *CA Cancer J Clin* (2020) 70(1):7–30. doi: 10.3322/caac.21590

3. Bray F, Ferlay J, Soerjomataram I, Siegel RL, Torre LA, Jemal A. Global cancer statistics 2018: GLOBOCAN estimates of incidence and mortality worldwide for 36 cancers in 185 countries. *CA: Cancer J Clin* (2018) 68(6):394–424. doi: 10.3322/caac.21492

4. Battaglia A, De Meerleer G, Tosco L, Moris L, Van den Broeck T, Devos G, et al. Novel insights into the management of oligometastatic prostate cancer: A comprehensive review. *Eur Urol Oncol* (2019) 2(2):174–88. doi: 10.1016/j.euo.2018.09.005

5. El-Amm J, Aragon-Ching JB. The current landscape of treatment in non-metastatic castration-resistant prostate cancer. *Clin Med Insights Oncol* (2019) 13:1179554919833927. doi: 10.1177/1179554919833927

6. Thomas L, Baratchian M, Sharifi N. Supraphysiologic testosterone solutions for enzalutamide-resistant prostate cancer. *Eur Urol* (2020) 77(2):156–7. doi: 10.1016/j.eururo.2019.07.037

7. Lam HM, Nguyen HM, Labrecque MP, Brown LG, Coleman IM, Gulati R, et al. Durable response of enzalutamide-resistant prostate cancer to supraphysiological testosterone is associated with a multifaceted growth suppression and impaired DNA damage response transcriptomic program in patient-derived xenografts. *Eur Urol* (2020) 77(2):144–55. doi: 10.1016/j.eururo.2019.05.042

8. Xiong X, Qiu S, Yi X, Xu H, Lei H, Liao D, et al. Efficacy and safety of bipolar androgen therapy in mCRPC after progression on abiraterone or enzalutamide: A systematic review. *Urol Oncol* (2022) 40(1):4.e19–28. doi: 10.1016/j.urolonc.2021.08.014

9. Markowski MC, Shenderov E, Eisenberger MA, Kachhap S, Pardoll DM, Denmeade SR, et al. Extreme responses to immune checkpoint blockade following bipolar androgen therapy and enzalutamide in patients with metastatic castration resistant prostate cancer. *Prostate* (2020) 80(5):407–11. doi: 10.1002/pros.23955

10. Mohammad OS, Nyquist MD, Schweizer MT, Balk SP, Corey E, Plymate S, et al. Supraphysiologic testosterone therapy in the treatment of prostate cancer: Models, mechanisms and questions. *Cancers (Basel)* (2017) 9(12):166. doi: 10.3390/cancers9120166

11. Roediger J, Hessenkemper W, Bartsch S, Manvelyan M, Huettner SS, Liehr T, et al. Supraphysiological androgen levels induce cellular senescence in human prostate cancer cells through the src-akt pathway. *Mol Cancer* (2014) 13:214. doi: 10.1186/1476-4598-13-214

12. Teply BA, Wang H, Luber B, Sullivan R, Rifkind I, Bruns A, et al. Bipolar androgen therapy in men with metastatic castration-resistant prostate cancer after progression on enzalutamide: an open-label, phase 2, multicohort study. *Lancet Oncol* (2018) 19(1):76–86. doi: 10.1016/S1470-2045(17)30906-3

13. Schweizer MT, Antonarakis ES, Wang H, Ajiboye AS, Spitz A, Cao H, et al. Effect of bipolar androgen therapy for asymptomatic men with castration-resistant prostate cancer: results from a pilot clinical study. *Sci Trans Med* (2015) 7 (269):269ra2. doi: 10.1126/scitranslmed.3010563

14. Schweizer MT, Wang H, Luber B, Nadal R, Spitz A, Rosen DM, et al. Bipolar androgen therapy for men with androgen ablation naive prostate cancer: Results from the phase II BATMAN study. *Prostate* (2016) 76(13):1218–26. doi: 10.1002/pros.23209

15. Sena LA, Kumar R, Sanin DE, Thompson EA, Rosen DM, Dalrymple SL, et al. Prostate cancer androgen receptor activity dictates efficacy of bipolar androgen therapy through MYC. *J Clin Invest* (2022) 132(23):e162396. doi: 10.1101/2022.04.26.22274275

16. Denmeade SR. Bipolar androgen therapy in the treatment of prostate cancer. *Clin Adv Hematol Oncol* (2018) 16(6):408–11.

17. Sena LA, Wang H, Lim ScM SJ, Rifkind I, Ngomba N, Isaacs JT, et al. Bipolar androgen therapy sensitizes castration-resistant prostate cancer to subsequent androgen receptor ablative therapy. *Eur J Cancer* (2021) 144:302–9. doi: 10.1016/j.ejca.2020.11.043

18. Hoshi S, Bilim V, Hoshi K, Nakagawa T, Sato S, Sakagami R, et al. Clinical response in metastatic castration-resistant prostate cancer (mCRPC) cases treated with supra-physiological doses of testosterone: Bipolar androgen therapy. *Clin Case Rep* (2022) 10(2):e05433. doi: 10.1002/ccr3.5433

19. Markowski MC, Kachhap S, De Marzo AM, Sena LA, Luo J, Denmeade SR, et al. Molecular and clinical characterization of patients with metastatic castration resistant prostate cancer achieving deep responses to bipolar androgen therapy. *Clin Genitourin Cancer* (2022) 20(2):97–101. doi: 10.1016/j.clgc.2021.08.001

20. Marshall CH, Tunacao J, Danda V, Tsai HL, Barber J, Gawande R, et al. Reversing the effects of androgen-deprivation therapy in men with metastatic castration-resistant prostate cancer. *BJU Int* (2021) 128(3):366–73. doi: 10.1111/bju.15408

21. Zheng X, Zhao X, Xu H, Han X, Xu H, Dong X, et al. Efficacy and safety of abiraterone and enzalutamide for castration-resistant prostate cancer: A systematic review and meta-analysis of randomized controlled trials. *Med (Baltimore)* (2019) 98(44):e17748. doi: 10.1097/MD.0000000000017748

22. Denmeade S, Lim SJ, Isaaccson Velho P, Wang H. PSA provocation by bipolar androgen therapy may predict duration of response to first-line androgen deprivation: Updated results from the BATMAN study. *Prostate* (2022) 82 (16):1529–36. doi: 10.1002/pros.24426

23. Denmeade SR, Wang H, Agarwal N, Smith DC, Schweizer MT, Stein MN, et al. TRANSFORMER: A randomized phase II study comparing bipolar androgen therapy versus enzalutamide in asymptomatic men with castration-resistant metastatic prostate cancer. *J Clin Oncol Off J Am Soc Clin Oncol* (2021) 39 (12):1371–82. doi: 10.1200/JCO.20.02759

24. Liu SJ, Hou HM, Lv ZT, Ding X, Wang L, Zhang L, et al. Bipolar androgen therapy followed by immune checkpoint inhibitors in metastatic castration resistant prostate cancer: A report of 4 cases. *Beijing Da Xue Xue Bao Yi Xue Ban* (2022) 54(4):766–9. doi: 10.19723/j.issn.1671-167X.2022.04.030

frontiers | Frontiers in Endocrinology

TYPE Original Research
PUBLISHED 17 April 2023
DOI 10.3389/fendo.2023.1163586

OPEN ACCESS

EDITED BY
Yuxuan Song,
Peking University People's Hospital, China

REVIEWED BY
Wei-de Zhong,
Guangzhou First People's Hospital, China
Wen-Qing Shi,
Fudan University, China
Zhen Liu,
First Affiliated Hospital of Gannan Medical University, China

*CORRESPONDENCE
Pingping Xia
310132585@qq.com

SPECIALTY SECTION
This article was submitted to Reproduction, a section of the journal Frontiers in Endocrinology

RECEIVED 11 February 2023
ACCEPTED 08 March 2023
PUBLISHED 17 April 2023

CITATION
Huang Y, Chen C, Zhou W, Zhang Q, Zhao Y, He D, Ye Z and Xia P (2023) Genetically predicted alterations in thyroid function are associated with the risk of benign prostatic disease.
Front. Endocrinol. 14:1163586.
doi: 10.3389/fendo.2023.1163586

Genetically predicted alterations in thyroid function are associated with the risk of benign prostatic disease

Yan Huang[1], Cheng Chen[1], Wanqing Zhou[1], Qian Zhang[1], Yanfei Zhao[1], Dehao He[1], Zhi Ye[1,2] and Pingping Xia[1,2]*

[1]Department of Anesthesiology, Xiangya Hospital of Central South University, Changsha, Hunan, China, [2]National Clinical Research Center for Geriatric Disorders, Central South University, Changsha, Hunan, China

Background: Benign prostatic diseases (BPDs), such as benign prostate hyperplasia (BPH) and prostatitis, harm the quality of life of affected patients. However, observational studies exploring the association between thyroid function and BPDs have hitherto yielded inconsistent results. In this study, we explored whether there is a causal genetic association between them using Mendelian randomization (MR) analysis.

Methods: We used publicly available summary statistics from the Thyroidomics Consortium and 23andMe on thyrotropin (TSH; 54,288 participants), thyroxine [free tetraiodothyronine (FT4); 49,269 participants], subclinical hypothyroidism (3,440 cases and 49,983 controls), overt hypothyroidism (8,000 cases and 117,000 controls), and subclinical hyperthyroidism (1,840 cases and 49,983 controls) to screen for instrumental variables of thyroid function. Results for BPD such as prostatic hyperplasia (13,118 cases and 72,799 controls) and prostatitis (1,859 cases and 72,799 controls) were obtained from the FinnGen study. The causal relationship between thyroid function and BPD was primarily assessed using MR with an inverse variance weighted approach. In addition, sensitivity analyses were performed to test the robustness of the results.

Results: We found that TSH [OR (95% CI) = 0.912(0.845-0.984), p =1.8 x 10^{-2}], subclinical hypothyroidism [OR (95% CI) = 0.864(0.810-0.922), p =1.04 x 10^{-5}], and overt hypothyroidism [OR (95% CI) = 0.885 (0.831-0. 944), p =2 x 10^{-4}] had a significant effect on genetic susceptibility to BPH, unlike hyperthyroidism [OR (95% CI) = 1.049(0.990-1.111), p =1.05 x 10^{-1}] and FT4 [OR (95% CI) = 0.979(0.857-1.119), p = 7.59 x 10^{-1}] had no effect. We also found that TSH [OR (95% CI) =0.823(0.700-0.967), p = 1.8 x 10^{-2}] and overt hypothyroidism [OR (95% CI) = 0.853(0.730-0.997), p = 4.6 x 10^{-2}] significantly influenced the prostatitis, whereas FT4 levels [OR (95% CI) = 1.141(0.901-1.444), p = 2.75 x 10^{-1}], subclinical hypothyroidism [OR (95% CI) =0. 897(0.784- 1.026), p = 1.12 x 10^{-1}], and hyperthyroidism [OR (95% CI) = 1.069(0.947-1.206), p = 2.79 x 10^{-1}] did not have a significant effect.

10.3389/fendo.2023.1163586

Conclusion: Overall, our study results suggest that hypothyroidism and TSH levels influence the risk of genetically predicted BPH and prostatitis, providing new insights into the causal relationship between thyroid function and BPD.

KEYWORDS

thyroid function, benign prostatic diseases, Mendelian randomization, genome-wide association study, causality

Introduction

Benign prostatic diseases (BPDs), such as benign prostatic hyperplasia (BPH) and prostatitis, significantly impact men's quality of life. It is now understood that BPH may lead to the development of prostate cancer (1). However, the etiology of BPH remains unclear. The possible influencing factors are inflammation, bacterial infection, and endocrine hormones (2). From an endocrinological perspective, several studies (3, 4) have been performed to investigate the unique role of endocrine hormones, including testosterone, estrogen, vitamin D, and sex hormone–binding protein. However, the relationship between thyroid function and BPH has been largely understudied.

Thyroid hormones (THs) are extensively involved in cell growth, metabolism, and differentiation. Current evidence suggests that THs activate the TH response element (TRE) in the promoter of TH target genes by binding to nuclear TH receptors (THRs) (5). The thyroid-stimulating hormone (TSH) is secreted by the pituitary gland, promotes the secretion of THs, and is regulated by THs' feedback control. Hyperthyroidism and hypothyroidism are the most direct manifestations of dysregulated TH secretion. It has been reported that THRs are mainly present in the epithelial cells of the prostate (6), suggesting that nuclear THRs can regulate glandular activity. In the most extensive observational study to date (5,708 Korean men), prostate volume was associated with FT4 but not with TSH (7). However, the data were taken from a single institution cross-sectional study and may have some limitations in causal inference. BPH and urinary retention have been associated with a poor prognosis in prostatitis (8). It is well established that patients with prostatitis are more susceptible to BPH (9), suggesting a possible relationship between prostate enlargement and prostatitis. Furthermore, the mechanisms underlying prostate enlargement may participate in the pathogenesis of prostatitis. However, no relevant studies have demonstrated a direct association between thyroid hormones and the risk of prostatitis. In addition, traditional observational studies may be subject to inherent confounding or selection bias, which prompted us to use new methods to explore the true picture.

We hypothesized that thyroid function (THs and thyroid disease) is causally related to the occurrence of BPD (BPH and prostatitis) in the general population, and Mendelian randomization (MR) analysis could be used to address these unmet research needs. In MR, genetic variation is used as an instrumental variable to estimate the causal effect of the exposure (thyroid function) on the outcome (BPD). Due to the random assignment of variance, MR is not susceptible to confounding, measurement error, and reverse causality (10). The present study used a two-sample MR approach to investigate whether thyrotropin (TSH), thyroxine [free tetraiodothyronine (FT4)], hypothyroidism (subclinical and overt), and hyperthyroidism are associated with BPH and prostatitis using publicly available summary-level data from the Genome-Wide Association Study (GWAS).

Methods

Data source and study population

Our study was conducted using publicly available summary-level GWAS data. The design of this study was informed by the Strengthening the Reporting of Observational Studies in Epidemiology Using Mendelian Randomization (STROBE-MR) checklist (11). Detailed information on study characteristics, participants, and ethical statements for each dataset were extracted from the original publication or website. We selected TSH, FT4, subclinical hypothyroidism, and subclinical hyperthyroidism–related GWAS from the Thyroidomics Consortium (12, 13), all within the cohort-specific reference range and without significant thyroid disease (thyroid surgery or medication use). Overt hypothyroidism–related GWAS cases from 23andMe included subclinical and overt hypothyroidism. The GWAS associated with BPD was obtained from FinnGen. The FinnGen study is a unique study that combines genomic information with digital healthcare data from participants aged 18 years and older living in Finland (14). All participants were of European ancestry, and there was no overlap between the exposure (thyroid function) and outcome (BPH) samples. Single-nucleotide polymorphism (SNP) locations are based on Genome Reference Consortium Human Build 37 (GRCh37). All detailed descriptions are included in the table (Supplementary Table S1).

Genetic variants

Valid MR is based on three assumptions (15), and the detailed principles are shown in Figure 1. First, genetic variation is significantly associated with thyroid function; second, as an instrumental variable (IV) for exposure, the data should not be

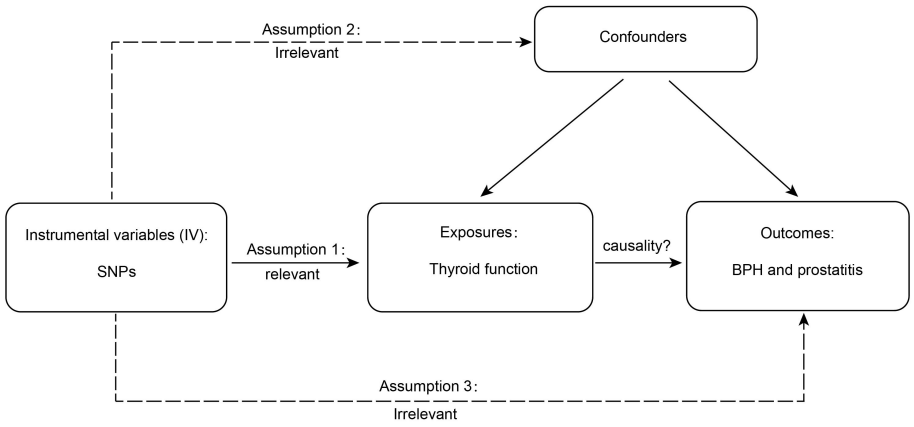

FIGURE 1
The detailed principles of Mendelian randomization study. BPH, benign prostatic hyperplasia.

associated with the confounders of thyroid function and BPD; and, finally, BPD should only be influenced by genetic variation through thyroid function. SNPs are commonly used as independent genetic predictors and are IVs if they meet stringent assumptions (16). For quality control, we screened SNPs with a genome-wide significance threshold ($p < 5 \times 10^{-8}$). SNPs with linkage dependence and excessively short genetic distance ($r^2 < 1 \times 10^{-3}$ and $kb > 1 - 10^4$) were excluded. We also removed variants with F values <10 as an indicator of IV strength. SNPs with mismatching alleles were also removed to reduce potential bias from weak instrumentation (10).

Mendelian randomization analysis

We used a two-sample MR approach to determine the association between thyroid function and BPD. The effect of exposure on the outcome can be estimated from the ratio of the genetic outcome and genetic exposure association estimates. In addition, if the genetic variants are not in linkage disequilibrium, the ratio estimates for each genetic variant can be combined into an overall estimate using a formula from the literature known as inverse variance weighted (IVW) methods (17). When all SNPs met the requirement for valid instrumental variables, causality was mainly assessed by IVW methods. Furthermore, MR–Egger regression, weighted median, weighted mode, and simple mode can provide complementary effects for additional evaluation in the presence of outliers (18). If there were no weak IV, we used IVW as the primary outcome and the other methods as secondary outcomes (19). If the Mendelian Randomization Pleiotropy RESidual Sum and Outlier (MR-PRESSO) method detected significant horizontal pleiotropy, we removed outlier variants and repeated the MR analysis (20). We used the leave-one-out test to identify the effect of individual SNP effects (21). Cochran's Q test was used to calculate heterogeneity, and $p < 0.05$ indicated the presence of considerable heterogeneity and the need to exclude SNPs (21). The MR–Egger method provided the estimates of horizontal multiplicity from the intercepts of linear regressions of SNP-outcome and SNP-exposure association estimates (22). $p < 0.05$ indicated the presence of nominal significance (23). We used TwoSampleMR 0.5.6 and the MR-PRESSO 1.0 package in R version 4.2.1 for the analysis.

Results

We found that 59 SNPs, 31 SNPs, 8 SNPs, 18 SNPs, and 7 SNPs from the Thyroidomics Consortium with 23andMe were associated with TSH, FT4, subclinical hypothyroidism, overt hypothyroidism, and subclinical hyperthyroidism, respectively. Due to the concordance of the outcomes, some SNPs were eliminated after harmonization. All F-statistics reached the threshold value (F > 10) (Supplementary Table S2). The detailed data for all five methods we used are provided in the Supplementary Material (Supplementary Table 3).

Thyroid hormones and benign prostatic diseases

Our MR-IVW analysis suggested a causal relationship between thyroid hormones and BPD (Figure 2 and Supplementary Figures 1, 2). Genetically predicted elevated TSH levels were potentially associated with a reduced risk of BPH [OR (95% CI) = 0.912 (0.845–0.984); $p = 1.8 \times 10^{-2}$] and prostatitis [OR (95% CI) = 0.823 (0.700–0.967); $p = 1.8 \times 10^{-2}$]. However, genetically predicted FT4 levels were not significantly associated with either BPH or prostatitis risk [BPH OR (95% CI) = 0.979 (0.857–1.119), $p = 7.59 \times 10^{-1}$; prostatitis OR (95% CI) =1.141(0.901–1.444), $p = 2.75 \times 10^{-1}$)].

No significant heterogeneity was found between TSH and BPD during Cochran's Q test ($p > 0.05$) (Table 1). The MR–Egger test [BPH ($p = 0.762$); prostatitis ($p = 0.608$)] or the MR-PRESSO global test [BPH ($p = 0.605$); prostatitis ($p = 0.625$)] showed no pleiotropy (Table 2). The sensitivity analysis of FT4 and BPH indicated the presence of aberrant SNPs. After excluding rs4149056 by the MR-PRESSO test, no heterogeneity or pleiotropy was found (Table 2). There was no heterogeneity between FT4 and prostatitis ($p > 0.05$)

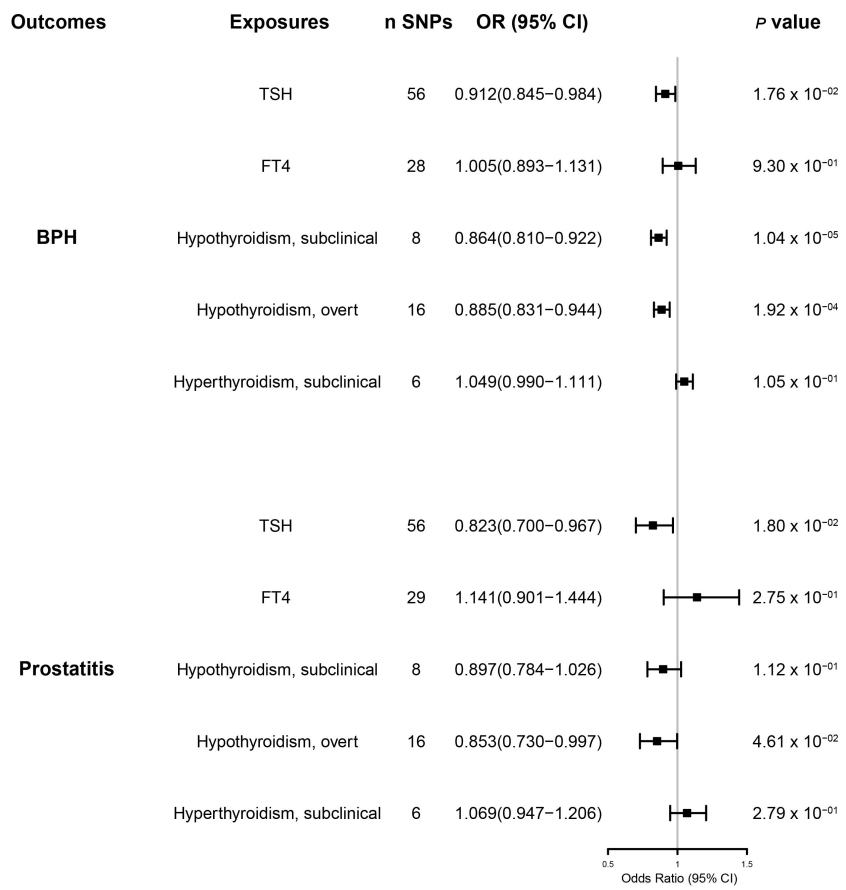

FIGURE 2
The results of the inverse variance weighted method to assess the causal role of thyroid function in the risk of benign prostatic hyperplasia and prostatitis. BPH, benign prostatic hyperplasia; CI, confidence interval; SNPs, single-nucleotide polymorphisms.

(Table 1). The MR–Egger test ($p = 0.338$) or the MR-PRESSO global test ($p = 0.468$) showed no pleiotropy (Table 2). No single genetic variant that strongly drove the overall effect of TSH or FT4 on BPD was identified in the leave-one-out analysis (Supplementary Figures 3, 4).

Hypothyroidism and benign prostatic diseases

Subclinical and overt hypothyroidism predicted primarily by the IVW method was associated with a reduced risk of BPH [subclinical hypothyroidism OR (95% CI) = 0.864(0.810–0.922), $p = 1.04 \times 10^{-5}$; overt hypothyroidism OR (95% CI) = 0.885(0.831–0.944), $p = 2 \times 10^{-4}$)] (Figure 2 and Supplementary Figure 1). Genetically predicted overt hypothyroidism was associated with a reduced risk of prostatitis [OR (95% CI) = 0.853(0.730–0.997), $p = 4.6 \times 10^{-2}$)], whereas subclinical hypothyroidism was not related to prostatitis [OR (95% CI) = 0.897 (0.784–1.026)], $p = 1.12 \times 10^{-1}$)] (Figure 2 and Supplementary Figure 2).

For BPH, Cochran's Q test showed no significant heterogeneity ($p > 0.05$) for hypothyroidism (subclinical and overt) (Table 1). The MR–Egger test [subclinical hypothyroidism (intercept = -0.005, $p = 0.862$); overt hypothyroidism ($p = 0.198$)] or the MR-PRESSO global test [subclinical hypothyroidism ($p = 0.471$); overt hypothyroidism ($p = 0.554$)] showed no pleiotropy (Table 2). Leave-one-out analysis revealed no specific genetic variation (Supplementary Figure 3). For prostatitis, Cochran's Q test and leave-one-out analysis both demonstrated the robustness of this association ($p > 0.05$) (Table 1 and Supplementary Figure 4). The MR–Egger test [subclinical hypothyroidism ($p = 0.784$); overt hypothyroidism ($p = 0.888$)] or the MR-PRESSO global test [subclinical hypothyroidism ($p = 0.943$); overt hypothyroidism ($p = 0.252$)] indicated low pleiotropy (Table 2).

Hyperthyroidism and benign prostatic diseases

Genetic susceptibility to subclinical hyperthyroidism was not correlated with the risk of BPH and prostatitis, according to the IVW results [BPH OR (95% CI) = 1.049(0.990–1.111), $p = 1.05 \times 10^{-1}$; prostatitis OR (95% CI) = 1.069(0.947–1.206), $p = 2.79 \times 10^{-1}$)] (Figure 2 and Supplementary Figures 1, 2). Cochran's Q test showed no significant heterogeneity ($p > 0.05$) (Table 1). The MR–Egger test [BPH ($p = 0.888$); prostatitis ($p = 0.485$)] or MR-PRESSO global test [BPH ($p = 0.252$); prostatitis ($p = 0.772$)] did not indicate

10.3389/fendo.2023.1163586

TABLE 1 Heterogeneity tests in the causality of thyroid function and benign prostatic diseases.

	Benign prostate hyperplasia				Prostatitis			
	Method	Q	df	*p* value	Method	Q	df	*p* value
TSH	IVW	51.895	55	0.594	IVW	51.150	55	0.622
	MR–Egger	51.802	54	0.560	MR–Egger	50.884	54	0.595
FT4 (before correction)	IVW	42.169	28	0.042	IVW	29.227	28	0.401
	MR–Egger	42.131	27	0.032	MR–Egger	28.233	27	0.399
FT4 (after correction)	IVW	31.202	27	0.263	–	–	–	–
	MR–Egger	31.135	26	0.223	–	–	–	–
Hypothyroidism, overt	IVW	12.591	15	0.634	IVW	19.832	15	0.178
	MR–Egger	10.768	14	0.704	MR–Egger	19.803	14	0.136
Hypothyroidism, subclinical	IVW	7.343	7	0.394	IVW	2.374	7	0.936
	MR–Egger	7.303	6	0.294	MR–Egger	2.292	6	0.891
Hyperthyroidism, subclinical	IVW	5.094	5	0.405	IVW	2.221	5	0.818
	MR–Egger	4.320	4	0.364	MR–Egger	1.629	4	0.804

Q, Cochran's Q statistic; df, degrees of freedom; IVW, inverse variance weighted.

any evidence of pleiotropy (Table 2). In addition, the leave-one-out test suggests that there is no overwhelming IV interference on the reliability of the results (Supplementary Figures 3, 4).

Discussion

The present study investigated the relationship between thyroid function and BPH. We found that TSH levels and the occurrence of subclinical and overt hypothyroidism were potentially associated with the risk of developing BPH. TSH and overt hypothyroidism significantly affected the risk of prostatitis. Interestingly, FT4 levels and the occurrence of subclinical hyperthyroidism did not have a significant effect on BPH.

Although the relationship between TSH or FT4 and BPH has been studied, the exact association remains unclear. In an observational study of 40 patients with confirmed BPH and 40 age-matched non-patients, TSH was negatively associated with prostate size (24). However, no association was observed in another study (7). A positive correlation was observed between prostate volume and elevated FT4 levels among patients with documented BPH (n = 5,708) (7). A small case–control study (40 cases *vs.* 40 controls) found a significant increase in serum FT3 and FT4 in patients with BPH (24). However, another prospective study reported no association between the thyroid status (total T4 or FT4) and BPH risk (25). There is an association between BPH and prostatitis (26, 27). Therefore, although no direct relationship between TSH or FT4 and prostatitis has been reported, we can seek an explanation from BPH-related studies. The most common cause of prostatitis is the reflux of infected urine into the prostatic ducts (episodic urethral infection), and the incidence of prostatic hyperplasia is associated with the chance of reflux, thus influencing the risk of prostatitis (8). In the data from those who underwent transurethral resection of the prostate (TURP) (n = 374), 70% of

TABLE 2 Pleiotropy test in the causality of thyroid function and benign prostatic diseases.

	Benign prostate hyperplasia					Prostatitis				
	MR–Egger			MR-PRESSO		MR–Egger			MR-PRESSO	
	Egger Intercept	SE	*p* value	Global test	*p* value	Egger Intercept	SE	*p* value	Global test	*p* value
TSH	0.002	0.006	0.762	53.739	0.605	-0.007	0.014	0.608	53.16	0.625
FT4 (before correction)	-0.002	0.011	0.877	50.526	0.026	-0.018	0.018	0.338	32.435	0.468
FT4 (after correction)	0.002	0.009	0.814	38.765	0.167	–	–	–	–	–
Hypothyroidism, subclinical	-0.005	0.028	0.862	9.409	0.471	-0.015	0.054	0.784	3.094	0.943
Hypothyroidism, overt	0.014	0.011	0.198	16.789	0.554	-0.004	0.027	0.888	22.376	0.252
Hyperthyroidism, subclinical	0.031	0.037	0.445	6.934	0.471	0.058	0.075	0.485	3.992	0.772

patients with urinary retention and 45% of patients with lower urinary tract symptoms (LUTS) had acute and/or chronic intraprostatic inflammation (ACI) (28). Another study revealed that among patients with self-reported prostatitis, 57% had a history of BPH (29). These findings inspired us to re-examine TSH and FT4 in prostatitis.

Chronic inflammation reportedly plays an important role in the pathogenesis and progression of BPH. It may lead to altered growth patterns of prostate stromal cells (PSCs) and fibromuscular tissue in BPH, resulting in wound-healing-like changes that drive local growth factor production and angiogenesis in the tissue (30, 31). It has been found that, in BPH specimens with a low inflammatory response, the immune response is predominantly type 1, whereas, in nodular BPH with chronic inflammatory infiltration, it is mainly type 0 or 2 (32). In the Reduction by Dutasteride of Prostate Cancer Events trial, among 4,109 men receiving a placebo (non-androgen), men with chronic prostate inflammation at baseline had a more significant increase in prostate volume (33). This suggests that BPH and prostatitis may be interchangeable. It has been established that THs directly affect inflammation. Several studies have shown that THs mediate many inflammatory pathways, including regulating xanthine oxidase production, *via* the Toll-like receptors 4/nuclear factor kappa beta (TLR4/ NF-κβ) pathway (34) and controlling Interleukin 6 (IL-6) signaling during toxemia (35). THs attach to the integrin αvβ3 and reactive the PI3K-AKT signaling pathway, generating large amounts of eactive oxygen species (ROS) and triggering the release of pro-inflammatory cytokines from the NLR Family Pyrin Domain Containing 3 (NLRP3) complex (36). THs have been shown to increase prostate cell proliferation and the activation of inflammatory signaling in primary fibroblasts from human BPH samples (37). The above studies overlap in their assertion that inflammation and oxidative stress represent potential mechanisms by which thyroid hormones act in BPD.

Interestingly, our study revealed an inconsistent association between genetically predicted TSH and FT4 in BPH. One possible explanation for this inconsistency is that biologically active T3 acts directly on receptors in the prostate. Although FT4 represents an accurate indicator of thyroid function, it may not reflect localized T3 levels acting on the prostate. Current evidence suggests that the binding of T3 mediates the direct classical effect of THs on nuclear receptors (38). Landmark studies in adult rats with normal thyroid function have shown that approximately 20% of prostate T3 content is derived from T4 deiodination, with the rest derived from native plasma T3 (39). Some observational studies have shown increased T3 levels (40) and no change in T4 levels in patients with BPH. Another possible mechanism is that the direct action of thyroid hormones on the prostate receptors may not be predominant and other non-direct actions may be more critical. A seminal study showed that physiological T4 supplementation during the postnatal period (days 1–35) decreased prostate weight in prepubertal rats (41), whereas an increase in prostate weight was observed in T4-treated castrated rats (42). Although these two early studies did not measure TSH, FT4, and T3 levels, preventing us from determining the relationship between the thyroid functional status and prostate volume, their findings suggest the existence of a thyroid–sex hormone–prostate axis. We speculate that this indirect action may act through TSH released by the pituitary gland, which may determine prostate function through sex hormone levels. A recent MR study showed that TSH, but not FT4 levels, correlated with total serum testosterone concentrations (12). Interestingly, it has been shown that androgens stimulate prostate epithelial and mesenchymal cell differentiation and proliferation (43). Epidemiological studies have shown that circulating serum levels of endogenous sex hormones correlate with prostate volume and may influence the natural course of BPH (44). Elevated TSH levels and symptomatic improvement have been observed in patients with BPH treated with testosterone inhibitors (43). Given the previously mentioned, our findings do not exclude an association between thyroid hormones and BPH.

The relationship between hypothyroidism and the prostate has been reported previously in related studies. Hypothyroidism reduces luteinizing hormone and testosterone levels in adult rats, as well as indirectly reducing prostate weight (45). A prospective analysis (326 cases/9,981 participants) revealed that subclinical and overt hypothyroidism were not linked to an increased risk of prostate cancer (46). In contrast, although confounding cannot be completely ruled out, a decreased risk was reported in smoking men with overt hypothyroidism (20 cases/total 75) (46), suggesting that hypothyroidism may be associated with prostate cell proliferation. Subclinical and overt hypothyroidism were both associated with a reduced risk of BPH, further strengthening the credibility of the present study results. However, for prostatitis, only overt hypothyroidism was significantly associated, which may be attributed to the fact that patients with overt hypothyroidism have significantly higher TSH levels than patients with subclinical hypothyroidism, exerting a greater impact on prostate volume and thus on prostatitis (47).

A retrospective study demonstrated that hyperthyroidism significantly increased the odds of BPH (191 cases/832 patients), but the association was no longer significant when the data were corrected for age and other metabolic diseases (48). However, studies have also shown an association between hyperthyroidism and BPH (7). In the studies of prostate cancer, hyperthyroidism was significantly associated with increased cancer risk (46, 49). In contrast, this association was not significant in other studies (50–52), revealing a complex hyperthyroid-prostate cell proliferation profile. From a genetic correlation perspective, our study confirms the absence of a causal relationship between subclinical hyperthyroidism and BPH. However, this association cannot be excluded because the subjects were from a single cohort and had a single phenotype.

A strength of our study is the MR design that could simulate a randomized controlled trial. Our instrumental variable SNP was randomly assigned at conception, avoiding confounding bias. MR also avoids reverse causal effects compared with other observational studies. Moreover, large sample-based population studies on the relationship between thyroid function and prostatitis have yet to be reported. Indeed, our finding of an inconsistent association between the severity of hypothyroidism and prostatitis may inspire future studies. The limitations of the present study should be acknowledged. First, all GWAS data come from people of European ancestry, and whether our findings can be generalized

to other populations remains to be investigated. In addition, sample sets from Europe may be shared, which could lead to the overuse of genetic data. Furthermore, since we only examined the effect of the subclinical phenotype on hyperthyroidism, our findings do not necessarily extend to more severe conditions. Therefore, we cannot exclude that overt hyperthyroidism is associated with BPD.

Conclusion

Overall, the present study substantiated that elevated TSH levels and the development of hypothyroidism reduce the risk of prostate enlargement and prostatitis, suggesting an association between thyroid disease and BPH at the endocrine level. Our findings suggest that TSH may be a better predictor of BPH than FT4 levels and that the euthyroid status may have a preventive and therapeutic effect on BPH.

Data availability statement

The original contributions presented in the study are included in the article/Supplementary Material. Further inquiries can be directed to the corresponding author.

Ethics statement

All summary level data are from de-identified genome-wide association studies (GWAS) and are available for download. These studies were conducted in accordance with the Declaration of Helsinki and approved by the relevant institutional ethics committees.

Author contributions

PX and YH conceived the research and determined the structure and layout of the paper. YH, CC, WZ, QZ, and DH collected and interpreted the data. CC, WZ, and YZ helped to analyze the results of this Mendelian randomization study. ZY and PX contributed to revising and finalizing the article. All authors contributed to the article and approved the submitted version.

Acknowledgments

We are grateful to the investigators of the GWAS included in our study for sharing summary data.

Conflict of interest

The authors declare that the research was conducted in the absence of any commercial or financial relationships that could be construed as a potential conflict of interest.

Publisher's note

All claims expressed in this article are solely those of the authors and do not necessarily represent those of their affiliated organizations, or those of the publisher, the editors and the reviewers. Any product that may be evaluated in this article, or claim that may be made by its manufacturer, is not guaranteed or endorsed by the publisher.

Supplementary material

The Supplementary Material for this article can be found online at: https://www.frontiersin.org/articles/10.3389/fendo.2023.1163586/full#supplementary-material

References

1. De Nunzio C, Kramer G, Marberger M, Montironi R, Nelson W, Schröder F, et al. The controversial relationship between benign prostatic hyperplasia and prostate cancer: the role of inflammation. *Eur Urol* (2011) 60:106–17. doi: 10.1016/j.eururo.2011.03.055

2. La Vignera S, Condorelli RA, Russo GI, Morgia G, Calogero AE. Endocrine control of benign prostatic hyperplasia. *Andrology* (2016) 4:404–11. doi: 10.1111/andr.12186

3. Ma H DM, Cj B, Je D, HJ MK, et al. Low 25-OH vitamin d is associated with benign prostatic hyperplasia. *J Urol* (2013) 190(2):608–14. doi: 10.1016/j.juro.2013.01.104

4. Rył A, Rotter I, Miazgowski T, Słojewski M, Dołęgowska B, Lubkowska A, et al. Metabolic syndrome and benign prostatic hyperplasia: association or coincidence? *Diabetol Metab Syndr* (2015) 7:94. doi: 10.1186/s13098-015-0089-1

5. Gauthier BR, Sola-García A, Cáliz-Molina MÁ, Lorenzo PI, Cobo-Vuilleumier N, Capilla-González V, et al. Thyroid hormones in diabetes, cancer, and aging. *Aging Cell* (2020) 19:e13260. doi: 10.1111/acel.13260

6. Sánchez-Tusie A, Montes de Oca C, Rodríguez-Castelán J, Delgado-González E, Ortiz Z, Álvarez L, et al. A rise in T3/T4 ratio reduces the growth of prostate tumors in a murine model. *J Endocrinol* (2020) 247:225–38. doi: 10.1530/JOE-20-0310

7. Lee JH, Park YW, Lee SW. The relationships between thyroid hormone levels and lower urinary tract Symptoms/Benign prostatic hyperplasia. *World J Mens Health* (2019) 37:364–71. doi: 10.5534/wjmh.180084

8. Coker TJ, Dierfeldt DM. Acute bacterial prostatitis: diagnosis and management. *Am Fam Physician* (2016) 93:114–20.

9. Hung S-C, Lai S-W, Tsai P-Y, Chen P-C, Wu H-C, Lin W-H, et al. Synergistic interaction of benign prostatic hyperplasia and prostatitis on prostate cancer risk. *Br J Cancer* (2013) 108:1778–83. doi: 10.1038/bjc.2013.184

10. Davies NM, Holmes MV, Davey Smith G. Reading mendelian randomisation studies: a guide, glossary, and checklist for clinicians. *BMJ* (2018) 362:k601. doi: 10.1136/bmj.k601

11. Skrivankova VW, Richmond RC, Woolf BAR, Yarmolinsky J, Davies NM, Swanson SA, et al. Strengthening the reporting of observational studies in epidemiology using mendelian randomization: the STROBE-MR statement. *JAMA* (2021) 326:1614–21. doi: 10.1001/jama.2021.18236

12. Kjaergaard AD, Marouli E, Papadopoulou A, Deloukas P, Kuś A, Sterenborg R, et al. Thyroid function, sex hormones and sexual function: a mendelian randomization study. *Eur J Epidemiol* (2021) 36:335–44. doi: 10.1007/s10654-021-00721-z

13. Teumer A, Chaker L, Groeneweg S, Li Y, Di Munno C, Barbieri C, et al. Genome-wide analyses identify a role for SLC17A4 and AADAT in thyroid hormone regulation. *Nat Commun* (2018) 9:4455. doi: 10.1038/s41467-018-06356-1

14. Kurki MI, Karjalainen J, Palta P, Sipilä TP, Kristiansson K, Donner K, et al. FinnGen: Unique genetic insights from combining isolated population and national health register data. *midRxiv* (2022) 2022:03.03.22271360. doi: 10.1101/2022.03.03.22271360

15. Liu K, Wu P, Zou J, Fan H, Hu H, Cheng Y, et al. Mendelian randomization analysis reveals causal relationships between gut microbiome and optic neuritis. *Hum Genet* (2022). doi: 10.1007/s00439-022-02514-0

16. Burgess S, Small DS, Thompson SG. A review of instrumental variable estimators for mendelian randomization. *Stat Methods Med Res* (2017) 26:2333–55. doi: 10.1177/0962280215597579

17. Bowden J, Davey Smith G, Haycock PC, Burgess S. Consistent estimation in mendelian randomization with some invalid instruments using a weighted median estimator. *Genet Epidemiol* (2016) 40:304–14. doi: 10.1002/gepi.21965

18. Wang R. Mendelian randomization study updates the effect of 25-hydroxyvitamin d levels on the risk of multiple sclerosis. *J Transl Med* (2022) 20:3. doi: 10.1186/s12967-021-03205-6

19. Jones HJ, Borges MC, Carnegie R, Mongan D, Rogers PJ, Lewis SJ, et al. Associations between plasma fatty acid concentrations and schizophrenia: A two-sample mendelian randomisation study. *Lancet Psychiatry* (2021) 8:1062–70. doi: 10.1016/S2215-0366(21)00286-8

20. Verbanck M, Chen C-Y, Neale B, Do R. Detection of widespread horizontal pleiotropy in causal relationships inferred from mendelian randomization between complex traits and diseases. *Nat Genet* (2018) 50:693–8. doi: 10.1038/s41588-018-0099-7

21. Wu F, Huang Y, Hu J, Shao Z. Mendelian randomization study of inflammatory bowel disease and bone mineral density. *BMC Med* (2020) 18:312. doi: 10.1186/s12916-020-01778-5

22. Burgess S, Thompson SG. Interpreting findings from mendelian randomization using the MR-egger method. *Eur J Epidemiol* (2017) 32:377–89. doi: 10.1007/s10654-017-0255-x

23. Georgakis MK, Harshfield EL, Malik R, Franceschini N, Langenberg C, Wareham NJ, et al. Diabetes mellitus, glycemic traits, and cerebrovascular disease: A mendelian randomization study. *Neurology* (2021) 96:e1732–42. doi: 10.1212/WNL.0000000000011555

24. Eldhose A, Nandeesha H, Dorairajan LN, Sreenivasulu K, Arul Vijaya Vani S. Thyroid and parathyroid hormones in benign prostatic hyperplasia. *Br J BioMed Sci* (2016) 73:94–6. doi: 10.1080/09674845.2016.1173333

25. Gupta A, Gupta S, Pavuk M, Roehrborn CG. Anthropometric and metabolic factors and risk of benign prostatic hyperplasia: A prospective cohort study of air force veterans. *Urology* (2006) 68:1198–205. doi: 10.1016/j.urology.2006.09.034

26. Azzouni F, Mohler J. Role of 5α-reductase inhibitors in benign prostatic diseases. *Prostate Cancer Prostatic Dis* (2012) 15:222–30. doi: 10.1038/pcan.2012.1

27. Freeman MR, Solomon KR. Cholesterol and benign prostate disease. *Differentiation* (2011) 82:244–52. doi: 10.1016/j.diff.2011.04.005

28. Mishra VC, Allen DJ, Nicolaou C, Sharif H, Hudd C, Karim OMA, et al. Does intraprostatic inflammation have a role in the pathogenesis and progression of benign prostatic hyperplasia? *BJU Int* (2007) 100:327–31. doi: 10.1111/j.1464-410X.2007.06910.x

29. Sciarra A, Mariotti G, Salciccia S, Autran Gomez A, Monti S, Toscano V, et al. Prostate growth and inflammation. *J Steroid Biochem Mol Biol* (2008) 108:254–60. doi: 10.1016/j.jsbmb.2007.09.013

30. Kramer G, Steiner GE, Handisurya A, Stix U, Haitel A, Knerer B, et al. Increased expression of lymphocyte-derived cytokines in benign hyperplastic prostate tissue, identification of the producing cell types, and effect of differentially expressed cytokines on stromal cell proliferation. *Prostate* (2002) 52:43–58. doi: 10.1002/pros.10084

31. Lucia MS, Lambert JR. Growth factors in benign prostatic hyperplasia: Basic science implications. *Curr Urol Rep* (2008) 9:272–8. doi: 10.1007/s11934-008-0048-6

32. Steiner GE, Stix U, Handisurya A, Willheim M, Haitel A, Reithmayr F, et al. Cytokine expression pattern in benign prostatic hyperplasia infiltrating T cells and impact of lymphocytic infiltration on cytokine mRNA profile in prostatic tissue. *Lab Invest* (2003) 83:1131–46. doi: 10.1097/01.lab.0000081388.40145.65

33. Nickel JC, Roehrborn CG, Castro-Santamaria R, Freedland SJ, Moreira DM. Chronic prostate inflammation is associated with severity and progression of benign prostatic hyperplasia, lower urinary tract symptoms and risk of acute urinary retention. *J Urol* (2016) 196:1493–8. doi: 10.1016/j.juro.2016.06.090

34. de Castro AL, Fernandes RO, Ortiz VD, Campos C, Bonetto JHP, Fernandes TRG, et al. Thyroid hormones decrease the proinflammatory TLR4/NF-κβ pathway and improve functional parameters of the left ventricle of infarcted rats. *Mol Cell Endocrinol* (2018) 461:132–42. doi: 10.1016/j.mce.2017.09.003

35. Contreras-Jurado C, Alonso-Merino E, Saiz-Ladera C, Valiño AJ, Regadera J, Alemany S, et al. The thyroid hormone receptors inhibit hepatic interleukin-6 signaling during endotoxemia. *Sci Rep* (2016) 6:30990. doi: 10.1038/srep30990

36. De Luca R, Davis PJ, Lin H-Y, Gionfra F, Percario ZA, Affabris E, et al. Thyroid hormones interaction with immune response, inflammation and non-thyroidal illness syndrome. *Front Cell Dev Biol* (2020) 8:614030. doi: 10.3389/fcell.2020.614030

37. Miro C, Di Giovanni A, Murolo M, Cicatiello AG, Nappi A, Sagliocchi S, et al. Thyroid hormone and androgen signals mutually interplay and enhance inflammation and tumorigenic activation of tumor microenvironment in prostate cancer. *Cancer Lett* (2022) 532:215581. doi: 10.1016/j.canlet.2022.215581

38. Bianco AC, Dumitrescu A, Gereben B, Ribeiro MO, Fonseca TL, Fernandes GW, et al. Paradigms of dynamic control of thyroid hormone signaling. *Endocr Rev* (2019) 40:1000–47. doi: 10.1210/er.2018-00275

39. van Doorn J, Roelfsema F, van der Heide D. Concentrations of thyroxine and 3,5,3'-triiodothyronine at 34 different sites in euthyroid rats as determined by an isotopic equilibrium technique. *Endocrinology* (1985) 117:1201–8. doi: 10.1210/endo-117-3-1201

40. Lehrer S, Diamond EJ, Stone NN, Droller MJ, Stock RG. Serum triiodothyronine is increased in men with prostate cancer and benign prostatic hyperplasia. *J Urol* (2002) 168:2431–3. doi: 10.1097/01.ju.0000032178.16280.e0

41. Talbert GB. Effect of thyroxine on maturation of the testes and proxtate gland of the rat. *Proc Soc Exp Biol Med* (1962) 111:290–2. doi: 10.3181/00379727-111-27770

42. Das RP, Perrault MJ. The androgenic response of the genital accessory organs of thyroxine-treated and castrated rats exposed to cold. *J Endocrinol* (1971) 49:591–8. doi: 10.1677/joe.0.0490591

43. Rastrelli G, Vignozzi L, Corona G, Maggi M. Testosterone and benign prostatic hyperplasia. *Sex Med Rev* (2019) 7:259–71. doi: 10.1016/j.sxmr.2018.10.006

44. Joseph MA, Wei JT, Harlow SD, Cooney KA, Dunn RL, Jaffe CA, et al. Relationship of serum sex-steroid hormones and prostate volume in African American men. *Prostate* (2002) 53:322–9. doi: 10.1002/pros.10154

45. Choudhury S, Chainy GBN, Mishro MM. Experimentally induced hypo- and hyper-thyroidism influence on the antioxidant defence system in adult rat testis. *Andrologia* (2003) 35:131–40. doi: 10.1046/j.1439-0272.2003.00548.x

46. Hellevik AI, Asvold BO, Bjøro T, Romundstad PR, Nilsen TIL, Vatten LJ. Thyroid function and cancer risk: A prospective population study. *Cancer Epidemiol Biomarkers Prev* (2009) 18:570–4. doi: 10.1158/1055-9965.EPI-08-0911

47. Sharma LK, Sharma N, Gadpayle AK, Dutta D. Prevalence and predictors of hyperprolactinemia in subclinical hypothyroidism. *Eur J Intern Med* (2016) 35:106–10. doi: 10.1016/j.ejim.2016.07.012

48. Man K-M, Chen K-B, Chen H-Y, Chiang J-H, Su Y-C, Man SS, et al. Hyperthyroidism is not a significant risk of benign prostatic hyperplasia: A nationwide population-based study. *Med (Baltimore)* (2018) 97:e12459. doi: 10.1097/MD.0000000000012459

49. Krashin E, Silverman B, Steinberg DM, Yekutieli D, Giveon S, Fabian O, et al. Opposing effects of thyroid hormones on cancer risk: A population-based study. *Eur J Endocrinol* (2021) 184:477–86. doi: 10.1530/EJE-20-1123

50. Mellemgaard A, From G, Jørgensen T, Johansen C, Olsen JH, Perrild H. Cancer risk in individuals with benign thyroid disorders. *Thyroid* (1998) 8:751–4. doi: 10.1089/thy.1998.8.751

51. Metso S, Auvinen A, Huhtala H, Salmi J, Oksala H, Jaatinen P. Increased cancer incidence after radioiodine treatment for hyperthyroidism. *Cancer* (2007) 109:1972–9. doi: 10.1002/cncr.22635

52. Chen Y-K, Lin C-L, Chang Y-J, Cheng FT-F, Peng C-L, Sung F-C, et al. Cancer risk in patients with graves' disease: a nationwide cohort study. *Thyroid* (2013) 23:879–84. doi: 10.1089/thy.2012.0568

frontiers | Frontiers in Endocrinology

TYPE Original Research
PUBLISHED 18 April 2023
DOI 10.3389/fendo.2023.1125299

OPEN ACCESS

EDITED BY
Fred Sinowatz,
Ludwig Maximilian University of Munich, Germany

REVIEWED BY
Luigi Napolitano,
University of Naples Federico II, Italy
Xiaoling Du,
Nankai University, China

*CORRESPONDENCE
Xiaoqiang Liu
xiaoqiangliu1@163.com

†These authors have contributed equally to this work and share first authorship

SPECIALTY SECTION
This article was submitted to Reproduction, a section of the journal Frontiers in Endocrinology

RECEIVED 16 December 2022
ACCEPTED 30 March 2023
PUBLISHED 18 April 2023

CITATION
Li Y, Wang H, Pan Y, Wang S, Zhang Z, Zhou H, Xu M and Liu X (2023) Identification of bicalutamide resistance-related genes and prognosis prediction in patients with prostate cancer. *Front. Endocrinol.* 14:1125299. doi: 10.3389/fendo.2023.1125299

Identification of bicalutamide resistance-related genes and prognosis prediction in patients with prostate cancer

Yuezheng Li†, Haoyu Wang†, Yang Pan†, Shangren Wang, Zhexin Zhang, Hang Zhou, Mingming Xu and Xiaoqiang Liu*

Department of Urology, Tianjin Medical University General Hospital, Tianjin, China

Background: Prostate cancer (PCa) is the second most common type of cancer and the fifth leading cause of cancer-related death in men. Androgen deprivation therapy (ADT) has become the first-line therapy for inhibiting PCa progression; however, nearly all patients receiving ADT eventually progress to castrate-resistant prostate cancer. Therefore, this study aimed to identify hub genes related to bicalutamide resistance in PCa and provide new insights into endocrine therapy resistance.

Methods: The data were obtained from public databases. Weighted correlation network analysis was used to identify the gene modules related to bicalutamide resistance, and the relationship between the samples and disease-free survival was analyzed. Gene Ontology and Kyoto Encyclopedia of Genes and Genomes analyses were performed, and hub genes were identified. The LASSO algorithm was used to develop a bicalutamide resistance prognostic model in patients with PCa, which was then verified. Finally, we analyzed the tumor mutational heterogeneity and immune microenvironment in both groups.

Results: Two drug resistance gene modules were identified. Gene Ontology and Kyoto Encyclopedia of Genes and Genomes analyses revealed that both modules are involved in RNA splicing. The protein–protein interaction network identified 10 hub genes in the brown module *LUC7L3*, *SNRNP70*, *PRPF3*, *LUC7L*, *CLASRP*, *CLK1*, *CLK2*, *U2AF1L4*, *NXF1*, and *THOC1*) and 13 in the yellow module (*PNN*, *PPWD1*, *SRRM2*, *DHX35*, *DMTF1*, *SALL4*, *MTA1*, *HDAC7*, *PHC1*, *ACIN1*, *HNRNPH1*, *DDX17*, and *HDAC6*). The prognostic model composed of *RNF207*, *REC8*, *DFNB59*, *HOXA2*, *EPOR*, *PILRB*, *LSMEM1*, *TCIRG1*, *ABTB1*, *ZNF276*, *ZNF540*, and *DPY19L2* could effectively predict patient prognosis. Genomic analysis revealed that the high- and low-risk groups had different mutation maps. Immune infiltration analysis showed a statistically significant difference in immune infiltration between the high- and low-risk groups, and that the high-risk group may benefit from immunotherapy.

Conclusion: In this study, bicalutamide resistance genes and hub genes were identified in PCa, a risk model for predicting the prognosis of patients with PCa was constructed, and the tumor mutation heterogeneity and immune infiltration in high- and low-risk groups were analyzed. These findings offer new insights into ADT resistance targets and prognostic prediction in patients with PCa.

KEYWORDS

prostate cancer, androgen deprivation therapy, bicalutamide, immune infiltration, prognostic model

1 Introduction

Prostate cancer (PCa) is the second most common cancer and the fifth leading cause of cancer-related death in men. In 2022, approximately 1,414,259 new cases of PCa were diagnosed worldwide, and 375,304 deaths were reported (1). It is expected that the number of new cases of PCa worldwide and that of deaths will increase to approximately 1.7 million and 499,000, respectively, by 2030 (2). The growth and development of the prostate depend on androgens, which play a predominant role in the development of PCa (3). Therefore, androgen deprivation therapy (ADT) is the first-line therapy for inhibiting PCa progression. Despite an 80–90% initial efficacy, virtually all patients receiving ADT eventually develop castrate-resistant prostate cancer (CRPC) (4). The data indicate that the median survival of patients with CRPC is about 14 months (range 9–30). Moreover, about 15–33% of patients with non-metastatic CRPC would develop metastases within 2 years, contributing to the mortality load of PCa (5). Thus, it is crucial to understand the mechanism of ADT resistance and identify related therapeutic targets to help improve the prognosis of patients with PCa.

Among ADTs, bicalutamide belongs to the first generation of non-steroidal antiandrogen drugs, which can effectively block androgen receptor (AR) activity and tumor invasion in androgen-responsive PCa and has been widely used in clinical practice (6). Over time, drug resistance has emerged in patients with PCa. Recent studies have found that AR mutations, protocadherin B9, and the microtubule-associated protein tau contribute to bicalutamide resistance (7–9). However, the underlying mechanisms remain unclear. Therefore, identifying biomarkers of bicalutamide resistance and potential therapeutic targets may greatly contribute to choosing treatment options.

With the advent of high-throughput sequencing and bioinformatics, researchers can classify and analyze a large number of samples, explore tumor characteristics and heterogeneity, and find new personalized markers. Based on these methods, hub genes associated with PCa progression and recurrence and CRPC have been identified (10, 11). However, only a few studies have used bioinformatics to explore the key genes and mechanisms underlying ADT resistance in PCa.

In the present study, our purpose is identifying hub genes related to bicalutamide resistance in PCa. These genes may be related to endocrine therapy resistance in patients with PCa and may be potential targets for reversing such resistance. Later we constructed a risk model to predict the prognosis of patients with PCa based on samples and analyzed tumor mutational heterogeneity and immune infiltration in high- and low-risk patient groups. Altogether, our findings provide new insights into ADT resistance and prognostic prediction in patients with PCa, which will help establish personalized treatment regimens and drug choice.

2 Materials and methods

2.1 Data acquisition

Transcriptome and clinical data from The Cancer Genome Atlas - Prostate Adenocarcinoma (TCGA-PRAD) dataset were downloaded from the Xena database (https://xena.ucsc.edu/). After excluding samples without disease-free survival (DFS), Gleason score, and T stage, 483 samples were included in this study. RNA-seq data were converted to transcripts per million to remove the effect of sequencing depth. TCGA-PRAD single nucleotide mutation data were downloaded from the Genomic Data Commons - The Cancer Genome Atlas website (https://portal.gdc.cancer.gov/). A total of 1832 differentially expressed genes in PCa were obtained from the GEPIA2 database (http://gepia.cancer-pku.cn/detail.php?clicktag=degenes).

2.2 Weighted correlation network analysis and predictive analysis of drugs

The pRRophetic package (12) was used to analyze the transcriptome data of the 483 samples to predict the bicalutamide resistance of each sample. Subsequently, we performed WGCNA (13) to further identify the gene modules related to drug resistance. We set a soft threshold of 10, and each gene module included at least 30 genes. Finally, 49 samples were discarded owing to outliers, and 6 gene modules were obtained. Univariate Cox regression

analysis was used to predict the relationship with DFS in the sample modules.

2.3 Gene ontology and Kyoto encyclopedia of genes and genomes pathway enrichment analyses

GO and KEGG analyses of the brown (218) and yellow modules (163) were annotated using the Metascape (14) website (http://metascape.org/gp/index.html#/main/step1). Concomitantly, the key hub genes in these modules were identified *via* the protein–protein interaction network (PPI). These key hub genes were identified with the MCODE plugin of Cytoscape, and statistical significance was set at $p < 0.05$.

2.4 Prognostic model establishment

To further determine the prognostic model for drug resistance genes, univariate Cox regression analysis was used for all genes in the brown and yellow modules, and 89 prognostic genes were identified. We included these genes in the prognostic model, which consisted of 12 genes and was constructed using the LASSO algorithm. The risk score was calculated as (risk coefficient × gene expression level). Subsequently, the samples were divided into a training set and a validation set at a 1:1 ratio, and the low- and high-risk groups were divided by the median risk score. The Kaplan–Meier (KM) curve was used to describe the DFS of the low- and high-risk groups, and statistical significance was set at $p < 0.05$. Receiver-operating characteristic (ROC) curves were used to demonstrate the predictive efficacy of the training and validation sets for 1, 3, and 5 years.

2.5 Mutational landscape diagram

The single-nucleotide mutation data of TCGA-PRAD were processed using the maftools package (15). The 10 most mutated genes were determined for the high- and low-risk groups.

2.6 Immunoassay

Twenty-eight tumor immune cell markers were obtained from published articles and seventeen immune pathways were obtained from the IMMPORT website (https://www.immport.org/home). The ssGSEA algorithm (16) was used to calculate the enrichment scores of the 28 immune cells and 17 immune pathways in the sample. The Wilcoxon test was used to identify the difference between the immune cell fractions and pathway scores of the high- and low-risk groups. Furthermore, the expression of 39 immune checkpoint molecules was also examined for differences between these two groups using the Wilcoxon test, and statistical significance was set at $p < 0.05$.

2.7 Statistical analysis

All statistical analyses were performed using R version 4.1.1. Specific statistical methods are referred to in the above Methods subsections.

3 Results

3.1 Identification of gene modules associated with bicalutamide resistance

Identification of bicalutamide resistance-related genes can help urologists personalize drug choice for patients with PCa. To identify key genes, we calculated the half-maximal inhibitory concentration (IC50) of bicalutamide for each sample in the TCGA-PRAD dataset. WGCNA was constructed based on 1832 differentially expressed genes in PCa. A total of 434 samples were included in subsequent analyses, while 49 were excluded (Figure 1A). In the scale-free network, the soft threshold was set to 10 (Figure 1B). The gene matrix was transformed into an adjacency matrix and an adjacency topology matrix. At least 30 genes were identified in each module. The characteristic genes of each module were calculated and the close modules were integrated into a new module. WGCNA identified six gene modules, as shown in Figure 1C. Subsequently, we calculated the correlation between each module, each sample, and the IC50 values for bicalutamide (Figure 1D and Supplementary Table 1). The brown and yellow modules displayed strong positive correlations with the IC50 values for bicalutamide ($r = 0.5$, $p = 2e{-}29$; $r = 0.27$, $p = 7e{-}09$). The brown and yellow genes are shown in Supplementary Tables 2, 3, respectively. Subsequently, we used univariate Cox regression to analyze the correlation between the gene expression of each module and DFS. The brown and yellow gene modules were highly correlated with the prognosis of patients with PCa (HR > 1, Figure 1E). In summary, we identified brown and yellow gene modules that were closely associated with the IC50 values of bicalutamide and DFS, suggesting that these two gene modules may be associated with resistance to endocrine therapy.

3.2 GO and KEGG analyses

To further identify the biological processes in which genes in the brown and yellow modules are involved, GO and KEGG enrichment analyses were carried out. As shown in Figure 2A, the genes in the brown module were mainly involved in mRNA processing, RNA splicing, XBP1(S) activation of chaperone genes, and microtubule-based movement. PPI analysis showed that 10 genes (*LUC7L3, SNRNP70, PRPF3, LUC7L, CLASRP, CLK1, CLK2, U2AF1L4, NXF1*, and *THOC1*) are hub genes of the brown module (Figure 2B). Conversely, the genes in the yellow module were mainly related to mRNA processing, cilium organization, protein modification by small protein conjugation, and herpes simplex virus 1 (HSV-1) infection (Figure 2C). The 13 hub genes in the

10.3389/fendo.2023.1125299

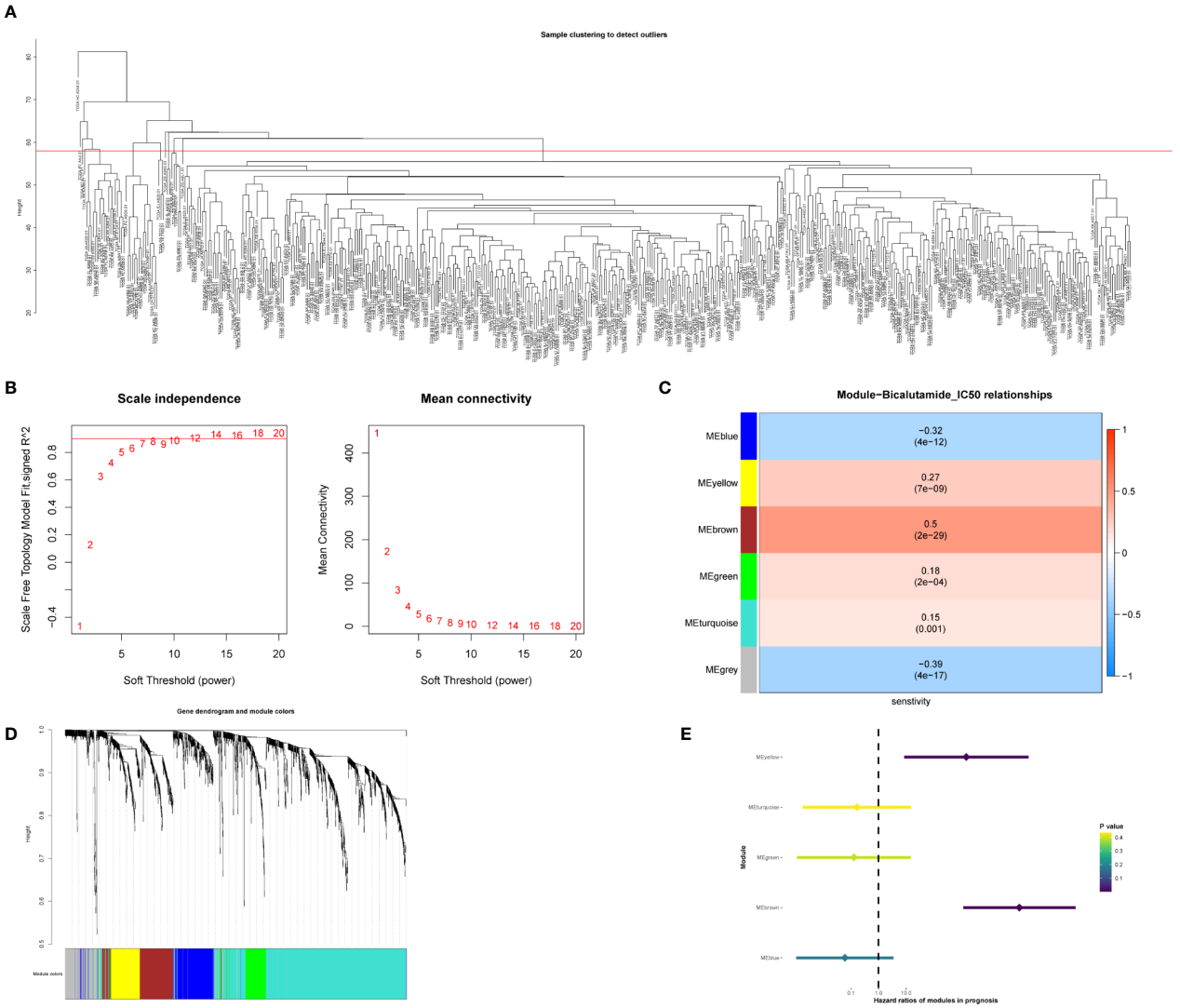

FIGURE 1
Identification of gene modules associated with bicalutamide resistance. **(A)** Sample clustering. **(B)** Scale-free fit index for various soft-thresholding powers. Mean connectivity for various soft-thresholding powers. **(C)** Dendrogram of all differentially expressed genes clustered based on dissimilarity. **(D)** Correlation between the 6 gene modules with the bicalutamide IC50 values. **(E)** Forest plot of univariate survival analysis for the 6 modules.

yellow module include were *PNN, PPWD1, SRRM2, DHX35, DMTF1, SALL4, MTA1, HDAC7, PHC1, ACIN1, HNRNPH1, DDX17*, and *HDAC6* (Figure 2D). Taken together, both brown and yellow module genes are involved in RNA splicing, suggesting that RNA splicing may be an important factor in endocrine resistance. These hub genes may be potential targets for reversing resistance to endocrine therapy.

3.3 Establishing a prognostic risk model

Univariate Cox regression analysis was used to calculate the prognostic risk of the brown and yellow module genes (Supplementary Table 4), which yielded 204 genes with survival values. A prognostic model was constructed using LASSO regression analysis (Figures 3A, B). The obtained prognostic model comprised *RNF207, REC8, DFNB59, HOXA2, EPOR, PILRB, LSMEM1, TCIRG1, ABTB1, ZNF276, ZNF540*, and *DPY19L*. All the included samples were randomly divided into a training cohort and a test cohort (242:241), and the training cohort was divided into low- and high-risk groups according to the median risk score (121:121) (Figure 3C). The KM curve in the training cohort showed that high-risk patients had a worse prognosis than low-risk patients ($p = 0.011$, Figure 3D). More patients in the high-risk group suffered recurrence or death, and a shorter survival period (Figure 3E). Heat map analysis revealed elevated expression levels of the 12 risk genes in high-risk patients (Figure 3F). Subsequently, ROC curves were used to evaluate the prognostic efficacy of the 12-gene in patients with PCa. As shown in Figure 3G, the area under the curve (AUC) scores of the 12 genes prognostic model in the training cohort for 1-, 3-, and 5-year survival prediction were 0.582, 0.635, and 0.671, respectively.

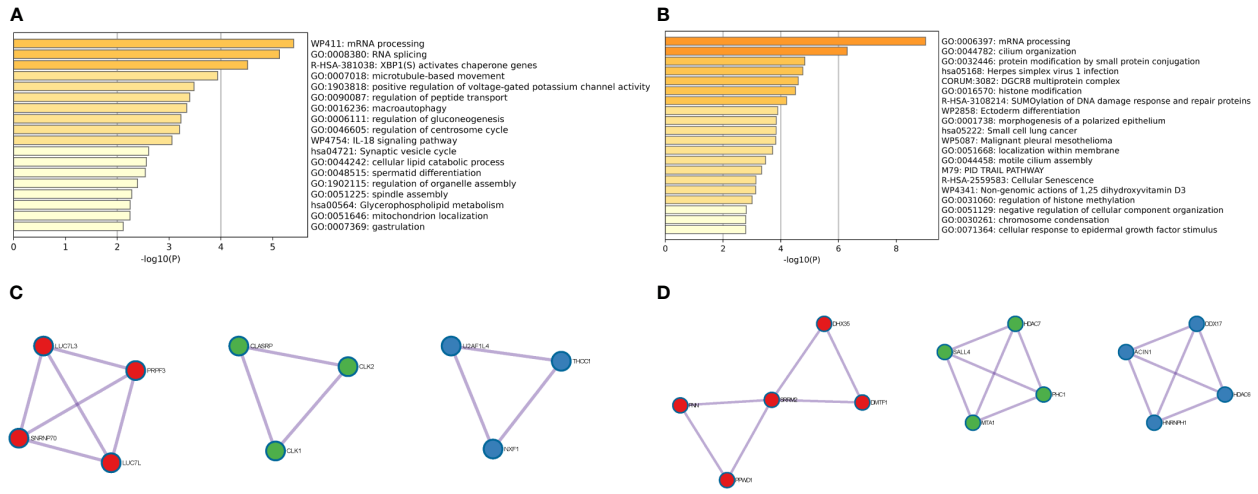

FIGURE 2
GO and KEGG enrichment analyses of bicalutamide-resistance genes and hub gene identification. **(A)** GO and KEGG analyses of the brown module. **(B)** Hub genes of the brown module. **(C)** GO and KEGG analyses of the yellow module. **(D)** Hub genes of the yellow module.

3.4 Validation of the prognostic model

The same results were validated in the test cohort, which was divided into low and high-risk groups according to the median risk score (121:120; Figure 4A). The KM curves for the test cohort are shown in Figure 4B ($p = 0.0052$). The high-risk group tended to have a worse prognosis (recurrence or death) and higher risk of gene expression (Figures 4C, D). The AUC scores of the prognostic model for predicting 1-, 3-, and 5-year survival in the test cohort were 0.632, 0.681, and 0.681, respectively (Figure 4E). In conclusion, the prognostic model we constructed can predict the prognosis of patients with PCa.

3.5 Mutational landscape diagram

To determine the heterogeneity between the high- and low-risk groups in patients with PCa, we studied the mutation landscape

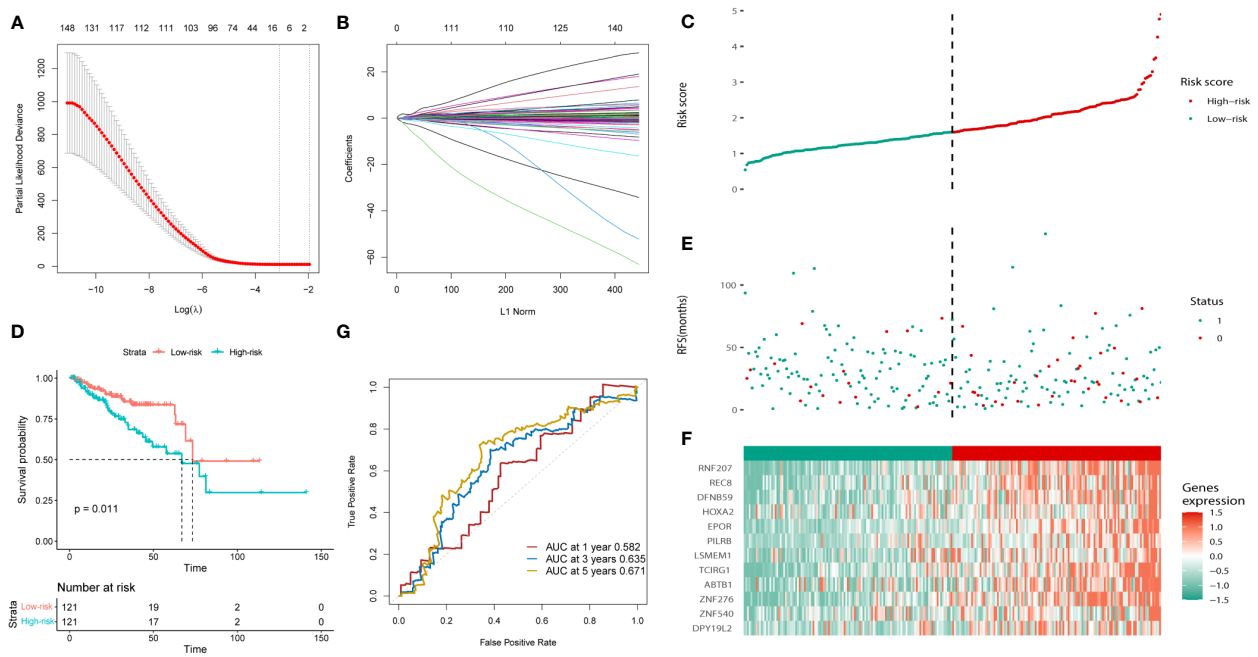

FIGURE 3
Construction of the bicalutamide-resistance gene-based risk prognostic model in the training cohort. **(A, B)** Construction of the LASSO regression model based on the 12 predictive genes. **(C)** Distribution of the risk scores. **(D)** The KM analysis of PFS in the high- and low-risk groups. **(E)** Survival status. **(F)** Expression of the 12 predictive genes. **(G)** ROC analysis to evaluate the predictive efficiency.

10.3389/fendo.2023.1125299

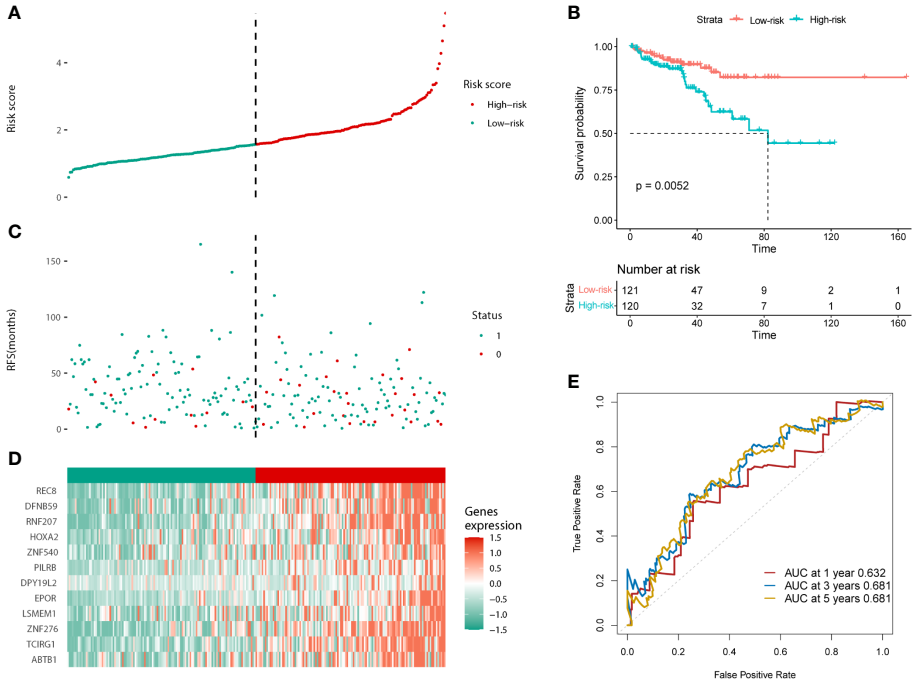

FIGURE 4
Validation of the prognostic model in the test cohort. **(A)** Distribution of the risk scores. **(B)** The KM analysis of PFS in the high and low-risk groups. **(C)** Survival status. **(D)** Expression of the 12 predictive genes. **(E)** ROC analysis to evaluate the predictive efficiency.

diagram of the two groups. By displaying the 10 most mutated genes in the identified PRAD database, we observed a significantly different landscape between the high- and low-risk groups (Figures 5A, B). The frequencies of *SPOP* and *TP53* mutations were significantly higher in the high-risk group than in the low-risk group (13% vs. 10% and 12% vs. 10%, respectively), while the *TTN* mutation rate was significantly lower (8% vs. 14%). The high-risk group also presented mutations in *KMT2D, FOXA1*, and *RYR1* (8%, 6%, and 6%, respectively). Conversely the low-risk group presented *MUC16, SYNE1*, and *FOXA1* mutations (9%, 7%, and 7%, respectively). In summary, genomic heterogeneity was identified between the low- and high-risk populations.

3.6 Immune infiltration analysis

In tumors, the immune microenvironment is closely related to endocrine resistance (17). Therefore, we assessed the presence of 28 immune cell types in TCGA-PRAD samples (Figure 6A). Violin plots showed that the high-risk group had a higher immune infiltration (Figure 6B). Activated B cells, activated CD8 T cells, CD56dim natural killer (NK) cells, central memory CD4 T cells, and plasmacytoid dendritic cells were significantly increased in the high-risk group. We also assessed the presence of 17 immune-related signaling pathways (Figure 6C). The violin plot shows that antimicrobials, chemokines, cytokines, and TNF family members receptors are increased in the high-risk group (Figure 6D). Finally, we analyzed the expression levels of immune checkpoints in the two groups (Figure 6E). CD200, CD200R1, CD86, LAG3, LAIR1, LGALS9, NRP1, TIGIT, TNFRSF18, TNFRSF25, and TNFSF14 were significantly upregulated in the high-risk group. In summary, the high- and low-risk groups showed different immune infiltration, and the high expression of immune checkpoint molecules in the high-risk group suggests that the high-risk group may benefit from immune checkpoint blockade.

4 Discussion

PCa is a solid malignant tumor in males with high morbidity, mortality, and heterogeneity (18). ADT is the treatment of choice for PCa at virtually all stages (19). Nonetheless, almost all patients receiving ADT eventually develop CRPC (4), thereby hindering the therapeutic efficacy of the initial ADT plan. Consequently, it is crucial to identify genes related to ADT resistance in PCa and explore the mechanisms of this resistance. To date, only a few studies have been conducted in this direction.

In this study, through a comprehensive analysis of transcriptome data and bicalutamide IC50 values of samples from the TCGA-PRAD dataset, we identified two gene modules, brown and yellow, that are associated with bicalutamide treatment resistance. To explore how these genes are involved in bicalutamide resistance in patients with PCa, GO and KEGG enrichment analyses were performed. The results showed that these genes are mainly involved in mRNA processing and RNA splicing, and are also involved in the XBP1(S) activates chaperone genes, microtubule-based movement, positive regulation of voltage-gated potassium channel activity, macroautophagy, protein modification by small

10.3389/fendo.2023.1125299

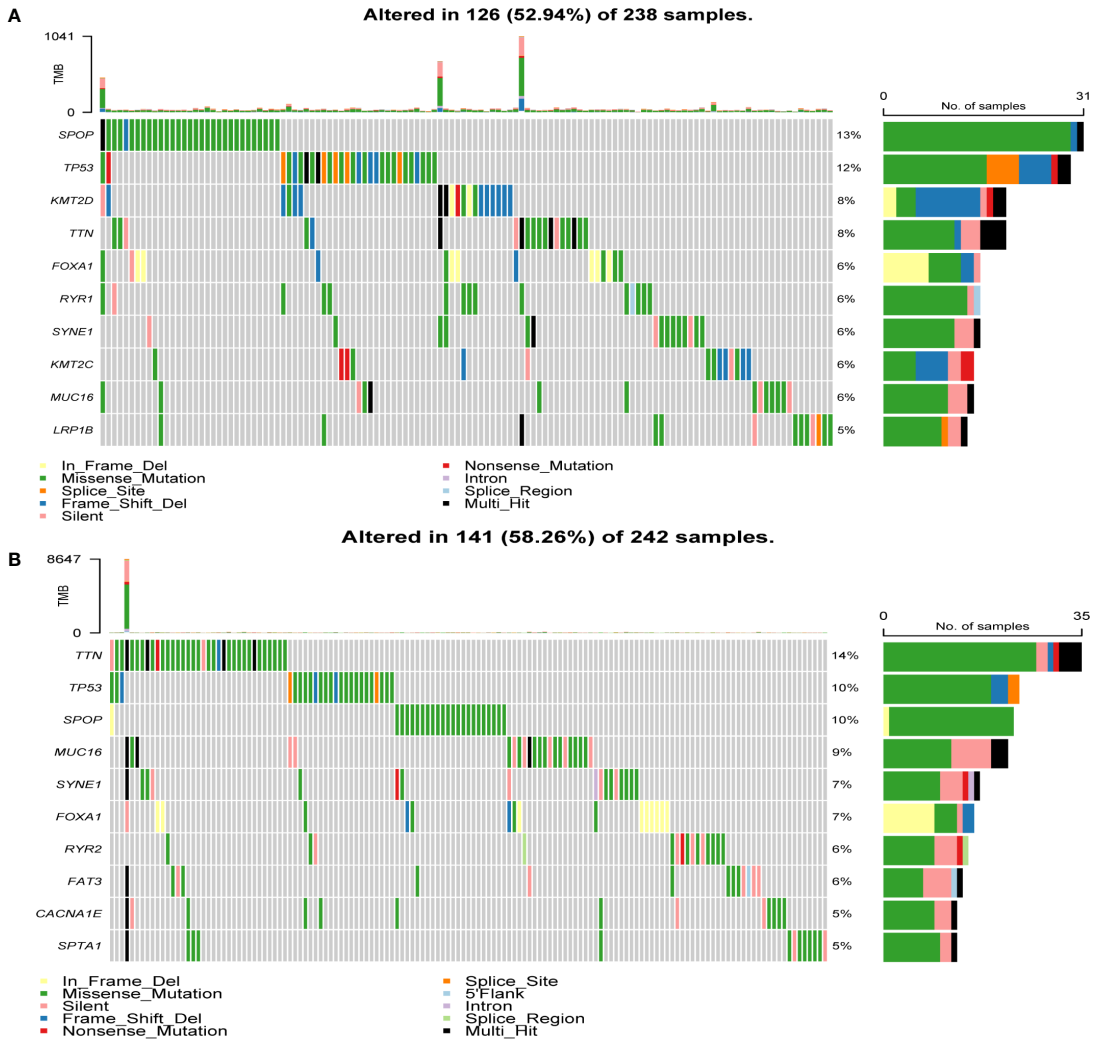

FIGURE 5
Heterogeneity of tumor mutations between the high and low-risk groups. **(A)** Mutational landscape diagram in the high-risk group. **(B)** Mutational landscape diagram in the low-risk group.

protein conjugation, and HSV-1 infection. Previous studies have found that many aberrant mRNA splice variants are upregulated in PCa, which further aggravates the disease by promoting proliferation, metastasis, tumor growth, anti-apoptosis, and drug resistance (20). Selective cleavage of AR is an important mechanism of drug resistance in PCa. Among the 20 different AR splice variants identified, Arv7 is the most common (21). ARv7 mRNA levels in patients with PCa have been shown to help predict responsiveness to ADTs, such as enzalutamide and abiraterone (22). C-MYC signaling is highly activated in the progression of PCa, which needs XBP1(S). Expression of XBP1(S) is strongly correlated with PCa prognosis (23). Zucchini et al. found that nine functional groups associated with high liver/bone/kidney alkaline phosphatase activity, including microtubule movement, are strongly associated with tumor aggressiveness (24). Voltage-gated potassium channels can regulate cancer cell proliferation, and their inhibition *via* piperine can have a therapeutic effect in PCa (25). Nguyen et al. found that autophagy is an important mechanism of CRPC resistance to AR inhibitors (such as bicalutamide and enzalutamide), and blocking autophagy significantly reduced the survival of PCa cells *in vitro* and *in vivo*, suggesting the great potential of autophagy inhibitors in the treatment of patients with CRPC (26). Tokarz et al. developed inhibitors of small ubiquitin related modified protein (SUMO) specific proteases (SENPs). *In vitro* and *in vivo* experiments have shown that SENPs are a suitable target for anti-tumor therapy (27). HSV-1 is also involved in tumorigenesis (28). Therefore, we speculate that the brown and yellow module genes play an important role in drug resistance and PCa progression through these pathways.

We performed PPI analysis of the two resistance-related gene modules separately, and identified 23 hub genes (*LUC7L3, SNRNP70, PRPF3, LUC7L, CLASRP, CLK1, CLK2, U2AF1L4, NXF1, THOC1, PNN, PPWD1, SRRM2, DHX35, DMTF1, SALL4, MTA1, HDAC7, PHC1, ACIN1, HNRNPH1, DDX17*, and *HDAC6*). *HNRNPH1* knockdown has been shown to reduce the expression of AR and its splice variant AR-V7 (or AR3). Small interfering RNA silencing of *HNRNPH1* sensitizes PCa cells to bicalutamide and inhibits prostate tumorigenesis *in vivo* (29). HDAC6 deacetylates

10.3389/fendo.2023.1125299

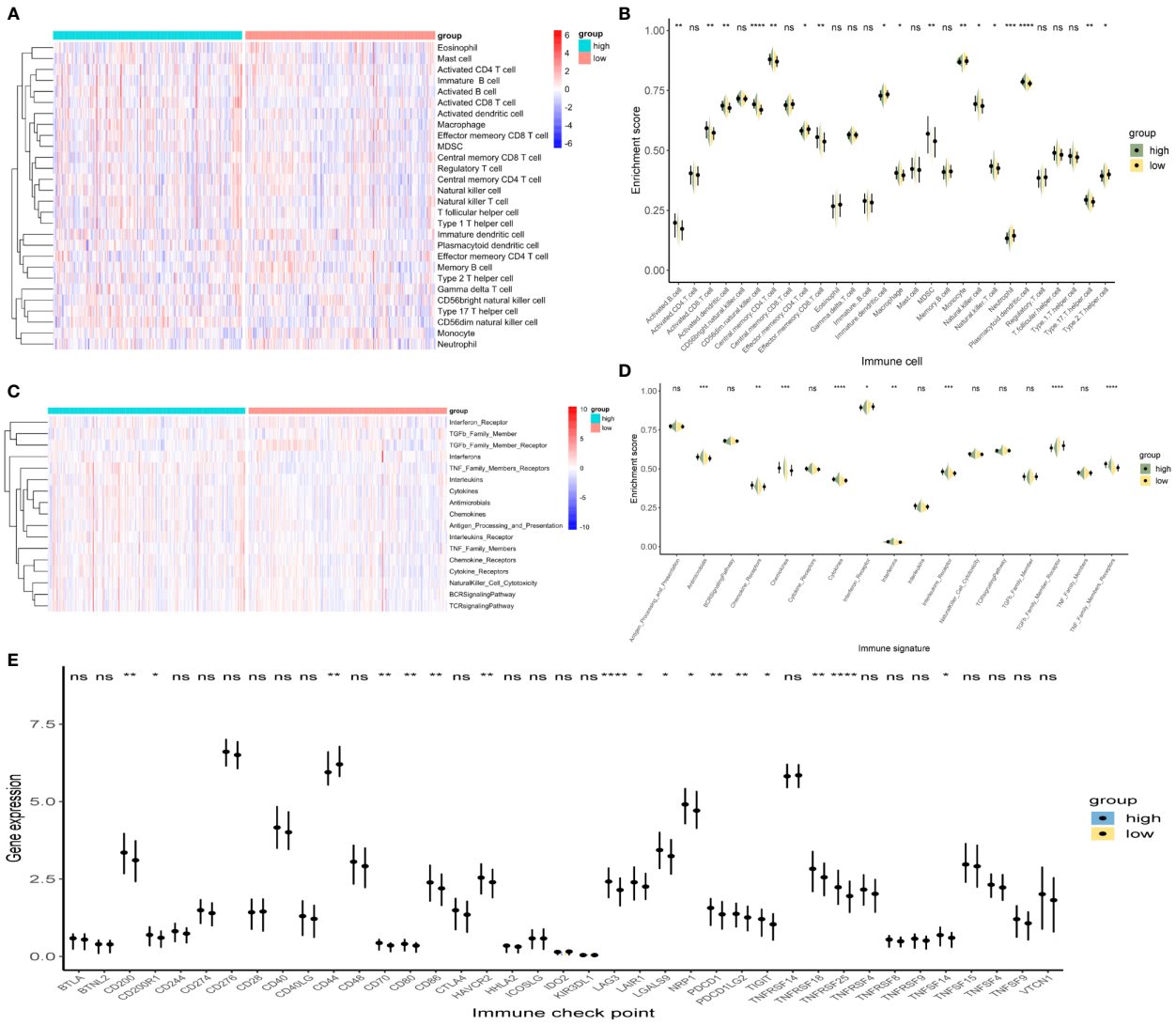

FIGURE 6
Immune infiltration analysis between the high- and low-risk groups. **(A, B)** Heat map and violin plot of 28 immune cells. **(C, D)** Heat map and violin plot resulting from the enrichment analysis of 17 immune-related signaling pathways. **(E)** Expression levels of immune checkpoints. *p < 0.05, **p < 0.01, ***p < 0.001, ****p < 0.0001, whereas 'ns' is non-significant.

various cytoplasmic proteins and participates in protein degradation, protein transport, cell migration, and metastasis. Zhou et al. studied a novel AR/HDAC6 dual inhibitor, which showed a more potent anti-proliferative effect on PCa cells than an AR antagonist (MDV3100) (30). High expression levels of *THOC1* (31), *PNN* (32), *MTA1* (33), *DDX17* (34), and *CLK1* (35) have been shown to promote PCa progression. Niklaus et al. found that *DMTF1* expression is related to increased cisplatin resistance in breast cancer (36). Therefore, we believe that these 23 hub genes may be important targets for reversing ADT resistance in patients with PCa, and that part of these can also improve the sensitivity of patients to chemotherapy.

Patients with PCa with castration resistance present a shorter survival time and higher risk of progression (4). For survival prediction, we analyzed the prognostic risk of the brown and yellow gene modules, and finally established a prognostic model consisting of *RNF207, REC8, DFNB59, HOXA2, EPOR, PILRB, LSMEM1, TCIRG1, ABTB1, ZNF276, ZNF540*, and *DPY19L2*. According to the median risk score, the patients were divided into high- and low-risk groups. The results showed that the high-risk group had a higher number of recurrences or deaths and shorter survival than the low-risk group. A high expression of these 12 genes is related to a worse prognosis. *RNF207* was found to predict lymph node involvement in patients with obesity and endometrial cancer (37). By targeting the PKA pathway, *REC8* can promote tumor migration, invasion, and angiogenesis in hepatocellular carcinoma (38). *PILRB* (39) and *TCIRG1* (40) are associated with clear cell renal cell carcinoma prognosis. Huang et al. found that targeted downregulation of *ABTB1* expression *via* miR-4319 can inhibit colorectal cancer progression (41). *ZNF276*

can promote the malignant phenotype of breast cancer by activating the CYP1B1-mediated Wnt/β-catenin pathway (42). Subsequently, we used the test cohort to validate the model, and the results were highly consistent with the training cohort, implying that our prognostic model can predict the prognosis of patients with PCa.

Tumor mutation burden is closely associated with tumor heterogeneity (43). To determine the heterogeneity of the high- and low-risk groups in patients with PCa, we studied the mutation landscape diagram in both groups; the most frequently mutated genes were *SPOP* and *TTN* in the high- and low-risk groups, respectively, which may indicate that patients with a high *SPOP* mutation rate have a worse prognosis, whereas those with a high *TTN* mutation rate have a relatively better prognosis. *TP53* was the second most frequent mutation in both groups. *SPOP* mutations can promote PCa progression by promoting autophagy and Nrf2 activation (44). However, *SPOP* mutation can increase the sensitivity of PCa cells to ADT (45). Studies have shown that patients with metastatic CRPC and *SPOP* mutations and/or CHD1 deletions are more sensitive to abiraterone treatment (46). Notably, *SPOP* mutations lead to PCa resistance to cellular stress induced by chemotherapeutic agents such as docetaxel (47). *TP53* is the most prominent gene in pan-cancer studies, and its somatic alterations are independently associated with the rapid emergence of drug resistance in patients with metastatic CRPC (48). Mutations or deletions in *TP53* and *RB1* can transform PCa AR-dependent luminal epithelial cells into AR-independent basal-like cells, which are resistant to ADT (49). These genes may be potential targets for the prognosis of PCa, and the different gene mutation frequencies between the high- and low-risk groups may provide new therapeutic strategies for PCa endocrine resistance.

Further research, has shown that the tumor immune microenvironment is closely associated with endocrine therapy resistance (17). Therefore, we assessed the abundance of immune cells and immune-related signaling pathways in the high- and low-risk groups as well as the level of immune checkpoint expression. In the high-risk group, we found that activated B cells, activated CD8 T cells, macrophages, and NK cells were highly expressed, and antimicrobials, chemokines, cytokines, and TNF family members receptors were up-regulated. Loss of NK cell activity has a significant correlation with PCa progression and the lethal phenotype of metastatic CRPC (50). NK cells inhibit enzalutamide resistance and cell invasion in CRPC by targeting ARv7 (51). Prostate tumor-associated macrophages can promote the growth of PCa, and secreted Gas6 can further enhance the activation of RON and AXL receptors in PCa cells, thereby driving CRPC. Targeting RON and macrophages promotes CRPC sensitivity to ADT (52). Targeting the CSF1 receptor can also reverse macrophage-mediated resistance to androgen blockade in PCa (53). IL-23 produced by myeloid-derived suppressor cells (MDSCs) can activate the AR pathway in PCa cells, and promote cell survival and proliferation under androgen-deprived conditions. Treatment that blocks IL-23 antagonizes MDSC-mediated castration resistance in PCa (54). CXCR7 activates MAPK/ERK signaling, which contributes to enzalutamide resistance in PCa (55). The combination of enzalutamide and a CXCR7 inhibitor can reduce pro-angiogenic signaling and macro-angiogenesis in PCa, and its therapeutic effect is significantly better than that of enzalutamide monotherapy (56). IL-6 can induce the castration-resistant growth of androgen-dependent human PCa cells and increase the bicalutamide resistance of PCa cells through TIF2 (57). These results also showed that the high- and low-risk groups had a different immune status.

After immune checkpoint expression analysis, we found that CD200, CD200R1, CD70, CD80, CD86, HAVCR2, LAG3, LAIR1, LGALS9, NRP1, PDCD1, PDCD1LG2, TIGIT, TNFRSF18, TNFRSF25, and TNFSF14 were highly expressed in the high-risk group. Based on the inflammation and immune imbalance in various tumor microenvironments, the CD200–CD200R pathway is differentially regulated (58). In liver metastases from primary pancreatic ductal adenocarcinoma, CD200 and BTLA pathways can drive macrophage-mediated adaptive immune tolerance. Targeting CD200/BTLA can enhance the immunogenicity of macrophages and T cells and enhance the immunotherapeutic effect on liver metastases (59). Allogeneic CAR-T cells targeting CD70 have shown efficacy in the treatment of renal cell carcinoma and have entered phase I clinical trials (60). Cis-PD-L1 interacts with CD80 to obtain an optimal T-cell response to destroy the tumor (61). LAG3 can be used as a target for cancer immunotherapy, targeting LAG3/GAL-3 to overcome immunosuppression and enhances the antitumor immune response in multiple myeloma (62). Blockade of Sema3A/Nrp1 signaling prevents macrophages from entering hypoxic tumor regions, inhibits angiogenesis and restores anti-tumor immunity (63). Inhibition of TIGIT enhances the functional activity of NK cells against CRPC cells (64). These studies suggest that patients in high-risk groups may benefit from immunotherapy targeting these checkpoints.

Notably, this study has some strengths. Firstly, 23 hub genes associated with bicalutamide resistance were identified. These genes may be potential targets for reversing bicalutamide resistance or even other endocrine therapies resistance in PCa. Then, we constructed a prognostic model consisting of 12 genes, showing a high predictive value. Besides, we found differential tumor mutation burden and immune status in high- and low-risk groups. Therefore, our study has greater clinical implications for the prognostic assessment and selection of treatment options for patients with PCa. Yet, our study presents certain limitations. First of all, it's a retrospective study with relatively small sample sizes in the training and test cohorts, so further studies with larger cohorts are necessary to confirm our results. Moreover, *in vivo* and *in vitro* experiments are required, and the function of drug resistance genes needs to be further explored.

5 Conclusion

In summary, using public databases, we identified genes and hub genes associated with bicalutamide resistance in PCa. These genes may be related to endocrine therapy resistance in PCa, and may be potential targets for reversing endocrine therapy resistance. Concomitantly, we constructed an effective risk model to predict the

prognosis of patients with PCa and analyzed tumor mutation heterogeneity and immune infiltration in high- and low-risk groups. In conclusion, this study provides new insights for the exploration of ADT resistance targets and prognosis prediction in patients with PCa, which will help establish personalized treatment options and drug choice.

Data availability statement

Publicly available datasets were analyzed in this study. This data can be found here: https://xena.ucsc.edu/, the Xena database https://portal.gdc.cancer.gov/, the Genomic Data Commons - The Cancer Genome Atlas http://gepia.cancer-pku.cn/detail.php?clicktag=degenes, the GEPIA2 database.

Author contributions

YL and XL designed the study. YL, YP, and ZZ performed the bioinformatics analysis. HW, HZ, and MX wrote the manuscript. SW and XL supervised the study. All authors have read and approved the final manuscript. All authors contributed to the article and approved the submitted version.

Acknowledgments

The authors would like to thank Xena, Genomic Data Commons - The Cancer Genome Atlas, and GEPIA2 databases for data availability.

Conflict of interest

The authors declare that the research was conducted in the absence of any commercial or financial relationships that could be construed as a potential conflict of interest.

Publisher's note

Supplementary material

The Supplementary Material for this article can be found online at: https://www.frontiersin.org/articles/10.3389/fendo.2023.1125299/full#supplementary-material

SUPPLEMENTARY TABLE 1
The correlation analysis between each sample and IC50 values for bicalutamide.

SUPPLEMENTARY TABLE 2
List of genes in the brown module.

SUPPLEMENTARY TABLE 3
List of genes in the yellow module.

SUPPLEMENTARY TABLE 4
Univariate Cox regression analysis of prognostic risk for genes in the brown and yellow modules.

References

1. Sung H, Ferlay J, Siegel RL, Laversanne M, Soerjomataram I, Jemal A, et al. Global cancer statistics 2020: GLOBOCAN estimates of incidence and mortality worldwide for 36 cancers in 185 countries. *CA: Cancer J Clin* (2021) 71(3):209–49. doi: 10.3322/caac.21660

2. Taitt HE. Global trends and prostate cancer: a review of incidence, detection, and mortality as influenced by race, ethnicity, and geographic location. *Am J men's Health* (2018) 12(6):1807–23. doi: 10.1177/1557988318798279

3. Hsing AW, Chu LW, Stanczyk FZ. Androgen and prostate cancer: is the hypothesis dead? *Cancer epidemiology Biomarkers Prev* (2008) 17(10):2525–30. doi: 10.1158/1055-9965.EPI-08-0448

4. Wang Y, Chen J, Wu Z, Ding W, Gao S, Gao Y, et al. Mechanisms of enzalutamide resistance in castration-resistant prostate cancer and therapeutic strategies to overcome it. *Br J Pharmacol* (2021) 178(2):239–61. doi: 10.1111/bph.15300

5. Mansinho A, Macedo D, Fernandes I, Costa L. Castration-resistant prostate cancer: mechanisms, targets and treatment. *Adv Exp Med Biol* (2018) 1096:117–33. doi: 10.1007/978-3-319-99286-0_7

6. Liu C, Armstrong CM, Lou W, Lombard AP, Cucchiara V, Gu X, et al. Niclosamide and bicalutamide combination treatment overcomes enzalutamide- and bicalutamide-resistant prostate cancer. *Mol Cancer Ther* (2017) 16(8):1521–30. doi: 10.1158/1535-7163.MCT-16-0912

7. Bohl CE, Gao W, Miller DD, Bell CE, Dalton JT. Structural basis for antagonism and resistance of bicalutamide in prostate cancer. *Proc Natl Acad Sci United States America.* (2005) 102(17):6201–6. doi: 10.1073/pnas.0500381102

8. Sekino Y, Oue N, Mukai S, Shigematsu Y, Goto K, Sakamoto N, et al. Protocadherin B9 promotes resistance to bicalutamide and is associated with the survival of prostate cancer patients. *Prostate.* (2019) 79(2):234–42. doi: 10.1002/pros.23728

9. Sekino Y, Han X, Babasaki T, Goto K, Inoue S, Hayashi T, et al. Microtubule-associated protein tau (MAPT) promotes bicalutamide resistance and is associated with survival in prostate cancer. *Urologic Oncol* (2020) 38(10):795.e1–.e8. doi: 10.1016/j.urolonc.2020.04.032

10. Wu YP, Ke ZB, Lin F, Wen YA, Chen S, Li XD, et al. Identification of key genes and pathways in castrate-resistant prostate cancer by integrated bioinformatics analysis. *Pathology Res practice.* (2020) 216(10):153109. doi: 10.1016/j.prp.2020.153109

11. Li S, Hou J, Xu W. Screening and identification of key biomarkers in prostate cancer using bioinformatics. *Mol Med Rep* (2020) 21(1):311–9. doi: 10.3892/mmr.2019.10799

12. Geeleher P, Cox N, Huang RS. pRRophetic: an r package for prediction of clinical chemotherapeutic response from tumor gene expression levels. *PloS One* (2014) 9(9):e107468. doi: 10.1371/journal.pone.0107468

13. Langfelder P, Horvath S. WGCNA: an r package for weighted correlation network analysis. *BMC Bioinf* (2008) 9:559. doi: 10.1186/1471-2105-9-559

14. Zhou Y, Zhou B, Pache L, Chang M, Khodabakhshi AH, Tanaseichuk O, et al. Metascape provides a biologist-oriented resource for the analysis of systems-level datasets. *Nat Commun* (2019) 10(1):1523. doi: 10.1038/s41467-019-09234-6

15. Mayakonda A, Lin DC, Assenov Y, Plass C, Koeffler HP. Maftools: efficient and comprehensive analysis of somatic variants in cancer. *Genome Res* (2018) 28(11):1747–56. doi: 10.1101/gr.239244.118

16. Hänzelmann S, Castelo R, Guinney J. GSVA: gene set variation analysis for microarray and RNA-seq data. *BMC Bioinf* (2013) 14:7. doi: 10.1186/1471-2105-14-7

17. Ruan H, Bao L, Tao Z, Chen K. Flightless I homolog reverses enzalutamide resistance through PD-L1-Mediated immune evasion in prostate cancer. *Cancer Immunol Res* (2021) 9(7):838–52. doi: 10.1158/2326-6066.CIR-20-0729

18. Desai K, McManus JM, Sharifi N. Hormonal therapy for prostate cancer. *Endocr Rev* (2021) 42(3):354–73. doi: 10.1210/endrev/bnab002

19. Yu EM, Aragon-Ching JB. Advances with androgen deprivation therapy for prostate cancer. *Expert Opin Pharmacother.* (2022) 23(9):1015–33. doi: 10.1080/14656566.2022.2033210

20. Calderon-Aparicio A, Wang BD. Prostate cancer: alternatively spliced mRNA transcripts in tumor progression and their uses as therapeutic targets. *Int J Biochem Cell Biol* (2021) 141:106096. doi: 10.1016/j.biocel.2021.106096

21. Olender J, Lee NH. Role of alternative splicing in prostate cancer aggressiveness and drug resistance in African americans. *Adv Exp Med Biol* (2019) 1164:119–39. doi: 10.1007/978-3-030-22254-3_10

22. Antonarakis ES, Lu C, Wang H, Luber B, Nakazawa M, Roeser JC, et al. AR-V7 and resistance to enzalutamide and abiraterone in prostate cancer. *New Engl J Med* (2014) 371(11):1028–38. doi: 10.1056/NEJMoa1315815

23. Sheng X, Nenseth HZ, Qu S, Kuzu OF, Frahnow T, Simon L, et al. IRE1α-XBP1s pathway promotes prostate cancer by activating c-MYC signaling. *Nat Commun* (2019) 10(1):323. doi: 10.1038/s41467-018-08152-3

24. Zucchini C, Bianchini M, Valvassori L, Perdichizzi S, Benini S, Manara MC, et al. Identification of candidate genes involved in the reversal of malignant phenotype of osteosarcoma cells transfected with the liver/bone/kidney alkaline phosphatase gene. *Bone.* (2004) 34(4):672–9. doi: 10.1016/j.bone.2003.12.008

25. George K, Thomas NS, Malathi R. Piperine blocks voltage gated k(+) current and inhibits proliferation in androgen sensitive and insensitive human prostate cancer cell lines. *Arch Biochem biophysics.* (2019) 667:36–48. doi: 10.1016/j.abb.2019.04.007

26. Nguyen HG, Yang JC, Kung HJ, Shi XB, Tilki D, Lara PNJr., et al. Targeting autophagy overcomes enzalutamide resistance in castration-resistant prostate cancer cells and improves therapeutic response in a xenograft model. *Oncogene.* (2014) 33 (36):4521–30. doi: 10.1038/onc.2014.25

27. Tokarz P, Woźniak K. SENP proteases as potential targets for cancer therapy. *Cancers (Basel)* (2021) 13(9):2059. doi: 10.3390/cancers13092059

28. Golais F, Mrázová V. Human alpha and beta herpesviruses and cancer: passengers or foes? *Folia microbiologica* (2020) 65(3):439–49. doi: 10.1007/s12223-020-00780-x

29. Yang Y, Jia D, Kim H, Abd Elmageed ZY, Datta A, Davis R, et al. Dysregulation of miR-212 promotes castration resistance through hnRNPH1-mediated regulation of AR and AR-V7: implications for racial disparity of prostate cancer. *Clin Cancer Res* (2016) 22(7):1744–56. doi: 10.1158/1078-0432.CCR-15-1606

30. Zhou M, Zheng H, Li Y, Huang H, Min X, Dai S, et al. Discovery of a novel AR/HDAC6 dual inhibitor for prostate cancer treatment. *Aging.* (2021) 13(5):6982–98. doi: 10.18632/aging.202554

31. Chinnam M, Wang Y, Zhang X, Gold DL, Khoury T, Nikitin AY, et al. The Thoc1 ribonucleoprotein and prostate cancer progression. *J Natl Cancer Inst* (2014) 106(11):dju306. doi: 10.1093/jnci/dju306

32. Meng XY, Zhang HZ, Ren YY, Wang KJ, Chen JF, Su R, et al. Pinin promotes tumor progression *via* activating CREB through PI3K/AKT and ERK/MAPK pathway in prostate cancer. *Am J Cancer Res* (2021) 11(4):1286–303. doi: 10.1093/jnci/dju306

33. Ma J, Li C, Qian H, Zhang Y. MTA1: a vital modulator in prostate cancer. *Curr Protein Pept science.* (2022) 23(7):456–64. doi: 10.2174/1389203723666220705152713

34. Wu XC, Yan WG, Ji ZG, Zheng GY, Liu GH. Long noncoding RNA SNHG20 promotes prostate cancer progression *via* upregulating DDX17. *Arch Med Sci AMS* (2021) 17(6):1752–65. doi: 10.5114/aoms.2019.85653

35. Uzor S, Porazinski SR, Li L, Clark B, Ajiro M, Iida K, et al. CDC2-like (CLK) protein kinase inhibition as a novel targeted therapeutic strategy in prostate cancer. *Sci Rep* (2021) 11(1):7963. doi: 10.1038/s41598-021-86908-6

36. Niklaus NJ, Humbert M, Tschan MP. Cisplatin sensitivity in breast cancer cells is associated with particular DMTF1 splice variant expression. *Biochem Biophys Res Commun* (2018) 503(4):2800–6. doi: 10.1016/j.bbrc.2018.08.042

37. López-Ozuna VM, Kogan L, Hachim MY, Matanes E, Hachim IY, Mitric C, et al. Identification of predictive biomarkers for lymph node involvement in obese women with endometrial cancer. *Front Oncol* (2021) 11:695404. doi: 10.3389/fonc.2021.695404

38. Han J, Bai Y, Wang J, Xie XL, Li AD, Ding Q, et al. REC8 promotes tumor migration, invasion and angiogenesis by targeting the PKA pathway in hepatocellular carcinoma. *Clin Exp Med* (2021) 21(3):479–92. doi: 10.1007/s10238-021-00698-9

39. Chen Y, Liang Y, Chen Y, Ouyang S, Liu K, Yin W. Identification of prognostic metabolism-related genes in clear cell renal cell carcinoma. *J Oncol* (2021) 2021:2042114. doi: 10.1155/2021/2042114

40. Xu C, Jia B, Yang Z, Han Z, Wang Z, Liu W, et al. Integrative analysis identifies TCIRG1 as a potential prognostic and immunotherapy-relevant biomarker associated with malignant cell migration in clear cell renal cell carcinoma. *Cancers (Basel)* (2022) 14(19):4583. doi: 10.3390/cancers14194583

41. Huang L, Zhang Y, Li Z, Zhao X, Xi Z, Chen H, et al. MiR-4319 suppresses colorectal cancer progression by targeting ABTB1. *United Eur Gastroenterol J* (2019) 7 (4):517–28. doi: 10.1177/2050640619837440

42. Lei T, Zhang W, He Y, Wei S, Song X, Zhu Y, et al. ZNF276 promotes the malignant phenotype of breast carcinoma by activating the CYP1B1-mediated wnt/β-catenin pathway. *Cell Death disease.* (2022) 13(9):781. doi: 10.1038/s41419-022-05223-8

43. Salem ME, Bodor JN, Puccini A, Xiu J, Goldberg RM, Grothey A, et al. Relationship between MLH1, PMS2, MSH2 and MSH6 gene-specific alterations and tumor mutational burden in 1057 microsatellite instability-high solid tumors. *Int J cancer.* (2020) 147(10):2948–56. doi: 10.1002/ijc.33115

44. Shi Q, Jin X, Zhang P, Li Q, Lv Z, Ding Y, et al. SPOP mutations promote p62/SQSTM1-dependent autophagy and Nrf2 activation in prostate cancer. *Cell Death differentiation.* (2022) 29(6):1228–39. doi: 10.1038/s41418-021-00913-w

45. Bernasocchi T, El Tekle G, Bolis M, Mutti A, Vallerga A, Brandt LP, et al. Dual functions of SPOP and ERG dictate androgen therapy responses in prostate cancer. *Nat Commun* (2021) 12(1):734. doi: 10.1038/s41467-020-20820-x

46. Boysen G, Rodrigues DN, Rescigno P, Seed G, Dolling D, Riisnaes R, et al. SPOP-Mutated/CHD1-Deleted lethal prostate cancer and abiraterone sensitivity. *Clin Cancer Res* (2018) 24(22):5585–93. doi: 10.1158/1078-0432.CCR-18-0937

47. Shi Q, Zhu Y, Ma J, Chang K, Ding D, Bai Y, et al. Prostate cancer-associated SPOP mutations enhance cancer cell survival and docetaxel resistance by upregulating Caprin1-dependent stress granule assembly. *Mol cancer.* (2019) 18(1):170. doi: 10.1186/s12943-019-1096-x

48. Annala M, Vandekerkhove G, Khalaf D, Taavitsainen S, Beja K, Warner EW, et al. Circulating tumor DNA genomics correlate with resistance to abiraterone and enzalutamide in prostate cancer. *Cancer discovery.* (2018) 8(4):444–57. doi: 10.1158/2159-8290.CD-17-0937

49. Mu P, Zhang Z, Benelli M, Karthaus WR, Hoover E, Chen CC, et al. SOX2 promotes lineage plasticity and antiandrogen resistance in TP53- and RB1-deficient prostate cancer. *Sci (New York NY).* (2017) 355(6320):84–8. doi: 10.1126/science.aah4307

50. Wu J. Could harnessing natural killer cell activity be a promising therapy for prostate cancer? *Crit Rev Immunol* (2021) 41(2):101–6. doi: 10.1615/CritRevImmunol.2021037614

51. Lin SJ, Chou FJ, Li L, Lin CY, Yeh S, Chang C. Natural killer cells suppress enzalutamide resistance and cell invasion in the castration resistant prostate cancer *via* targeting the androgen receptor splicing variant 7 (ARv7). *Cancer letters.* (2017) 398:62–9. doi: 10.1016/j.canlet.2017.03.035

52. Brown NE, Jones A, Hunt BG, Waltz SE. Prostate tumor RON receptor signaling mediates macrophage recruitment to drive androgen deprivation therapy resistance through Gas6-mediated axl and RON signaling. *Prostate.* (2022) 82(15):1422–37. doi: 10.1002/pros.24416

53. Escamilla J, Schokrpur S, Liu C, Priceman SJ, Moughon D, Jiang Z, et al. CSF1 receptor targeting in prostate cancer reverses macrophage-mediated resistance to androgen blockade therapy. *Cancer Res* (2015) 75(6):950–62. doi: 10.1158/0008-5472.CAN-14-0992

54. Calcinotto A, Spataro C, Zagato E, Di Mitri D, Gil V, Crespo M, et al. IL-23 secreted by myeloid cells drives castration-resistant prostate cancer. *Nature.* (2018) 559 (7714):363–9. doi: 10.1038/s41586-018-0266-0

55. Li S, Fong KW, Gritsina G, Zhang A, Zhao JC, Kim J, et al. Activation of MAPK signaling by CXCR7 leads to enzalutamide resistance in prostate cancer. *Cancer Res* (2019) 79(10):2580–92. doi: 10.1158/0008-5472.CAN-18-2812

56. Luo Y, Azad AK, Karanika S, Basourakos SP, Zuo X, Wang J, et al. Enzalutamide and CXCR7 inhibitor combination treatment suppresses cell growth and angiogenic signaling in castration-resistant prostate cancer models. *Int J cancer.* (2018) 142 (10):2163–74. doi: 10.1002/ijc.31237

57. Feng S, Tang Q, Sun M, Chun JY, Evans CP, Gao AC. Interleukin-6 increases prostate cancer cells resistance to bicalutamide *via* TIF2. *Mol Cancer Ther* (2009) 8 (3):665–71. doi: 10.1158/1535-7163.MCT-08-0823

58. Liu JQ, Hu A, Zhu J, Yu J, Talebian F, Bai XF. CD200-CD200R pathway in the regulation of tumor immune microenvironment and immunotherapy. *Adv Exp Med Biol* (2020) 1223:155–65. doi: 10.1007/978-3-030-35582-1_8

59. Diskin B, Adam S, Soto GS, Liria M, Aykut B, Sundberg B, et al. BTLA(+)CD200 (+) b cells dictate the divergent immune landscape and immunotherapeutic resistance in metastatic vs. primary pancreatic cancer. *Oncogene.* (2022) 41(38):4349–60. doi: 10.1038/s41388-022-02425-4

60. Panowski SH, Srinivasan S, Tan N, Tacheva-Grigorova SK, Smith B, Mak YSL, et al. Preclinical development and evaluation of allogeneic CAR T cells targeting CD70 for the treatment of renal cell carcinoma. *Cancer Res* (2022) 82(14):2610–24. doi: 10.1158/0008-5472.CAN-21-2931

61. Sugiura D, Maruhashi T, Okazaki IM, Shimizu K, Maeda TK, Takemoto T, et al. Restriction of PD-1 function by cis-PD-L1/CD80 interactions is required for optimal T cell responses. *Sci (New York NY).* (2019) 364(6440):558–66. doi: 10.1126/science.aav7062

62. Bae J, Accardi F, Hideshima T, Tai YT, Prabhala R, Shambley A, et al. Targeting LAG3/GAL-3 to overcome immunosuppression and enhance anti-tumor immune responses in multiple myeloma. *Leukemia.* (2022) 36(1):138–54. doi: 10.1038/s41375-021-01301-6

63. Casazza A, Laoui D, Wenes M, Rizzolio S, Bassani N, Mambretti M, et al. Impeding macrophage entry into hypoxic tumor areas by Sema3A/Nrp1 signaling blockade inhibits angiogenesis and restores antitumor immunity. *Cancer Cell* (2013) 24 (6):695–709. doi: 10.1016/j.ccr.2013.11.007

64. González-Ochoa S, Tellez-Bañuelos MC, Méndez-Clemente AS, Bravo-Cuellar A, Hernández Flores G, Palafox-Mariscal LA, et al. Combination blockade of the IL6R/STAT-3 axis with TIGIT and its impact on the functional activity of NK cells against prostate cancer cells. *J Immunol Res* (2022) 2022:1810804. doi: 10.1155/2022/1810804

frontiers | Frontiers in Endocrinology

TYPE Original Research
PUBLISHED 21 April 2023
DOI 10.3389/fendo.2023.1131564

OPEN ACCESS

EDITED BY
Yuxuan Song,
Peking University People's Hospital, China

REVIEWED BY
Zhenquan Wu,
First People's Hospital of Foshan, China
Ramakanth Bhargav Panchangam
BGH (Bhargav Endocrine Hospital), India

*CORRESPONDENCE
Kun-wu Yan
1749200794@qq.com

SPECIALTY SECTION
This article was submitted to Adrenal Endocrinology, a section of the journal Frontiers in Endocrinology

RECEIVED 25 December 2022
ACCEPTED 11 April 2023
PUBLISHED 21 April 2023

CITATION
Yan K-w, Tian X-f, Wu Y-n, Cai M and Guo M-t (2023) Abandonment of intravenous volume expansion after preoperative receipt of α-blockers in patients with adrenal pheochromocytoma was not an independent risk factor for intraoperative hemodynamic instability. *Front. Endocrinol.* 14:1131564. doi: 10.3389/fendo.2023.1131564

Abandonment of intravenous volume expansion after preoperative receipt of α-blockers in patients with adrenal pheochromocytoma was not an independent risk factor for intraoperative hemodynamic instability

Kun-wu Yan[1*], Xiao-fei Tian[2], Yan-ni Wu[3], Meng Cai[4] and Ming-tao Guo[1]

[1]Department of Urology, Handan First Hospital, Handan, China, [2]Department of General Surgery, Handan First Hospital, Handan, China, [3]Department of Pharmaceutical Technology, Faculty of Pharmacy, Heze Domestic Professional College, Heze, China, [4]Department of Oncology, Handan First Hospital, Handan, China

Background: There is no consensus on whether intravenous rehydration must be added after preoperative phenoxybenzamine (PXB) administration for pheochromocytoma. The aim of this study is to investigate whether abandonment of intravenous volume expansion after PXB administration is associated with intraoperative hemodynamic instability.

Methods: 83 Patients with pheochromocytoma received surgical treatment in the Department of Urology, Handan First Hospital, between October 2014 and July 2022. All patients were subclassified into either the hemodynamic stability group (HS group) or the hemodynamic instability group (HU group) according to whether intraoperative hemodynamic instability occurred, with 51 cases in HS group and 32 cases in HU group. Differences in data between the two groups were examined, and the risk factors for intraoperative hemodynamic instability were analyzed using logistic regression.

Results: The results of the analysis showed no statistically significant differences in age, sex, location of the tumor, surgical method, body mass index (BMI) $\geq$ 24 kg/m^2, blood and urine catecholamine test results, preoperative oral PXB followed by combined intravenous volume expansion, proportion of patients with hypertension or diabetes mellitus or coronary heart disease between the two groups (P>0.05). The size of the tumor in the HS group was smaller than that in the HU group (5.3 $\pm$ 1.9 cm vs 6.2 $\pm$ 2.4 cm P=0.010). Multivariate analyses demonstrated that abandonment of intravenous volume expansion after

preoperative receipt of α-blockers in patients with adrenal pheochromocytoma was not an independent risk factor for intraoperative hemodynamic instability. Only the tumor size (P=0.025) was an independent risk factor for intraoperative hemodynamic instability.

Conclusion: The purpose of general preoperative intravenous fluid expansion is to prevent hypotension after the tumor has been resected. In the current study, we indicated that preoperative management of pheochromocytomas using the α-blocker PXB in combination with intravenous volume expansion does not further reduce the risk of intraoperative hemodynamic instability or postoperative complications compared with oral PXB alone. Therefore, our study supports preoperative management of pheochromocytoma with a single α-blocker, PXB, as sufficient.

KEYWORDS

intravenous volume, expansion, α-blockers, adrenal pheochromocytoma, hemodynamic

Introduction

Pheochromocytoma is a rare catecholamine-producing neuroendocrine tumor that originates from chromophores in the adrenal medulla, and can cause a variety of clinical symptoms (1). In mild cases, the symptoms may be silent, localized, or nonspecific; in typical cases, the symptoms may be paroxysmal hypertension with headache, palpitations, and excessive sweating, while in severe cases, they may cause hemodynamic instability and end-organ damage or insufficiency (2). The release of catecholamines from pheochromocytoma can cause a range of clinical manifestations, including hypertension, sweating, and tachycardia (3). Currently, surgical removal of the tumor is the only available radical approach for its treatment; unfortunately, intraoperative management of the tumor can lead to uncontrolled release of catecholamine, which may result in unstable intraoperative hemodynamic changes, including fatal hypertensive crisis and arrhythmias (4). Therefore, patients with a suspected or confirmed diagnosis of pheochromocytoma should undergo adequate preoperative preparation to improve the safety of the procedure. Bihain et al. found that, after reviewing nearly 50 years of literature on the use of antihypertensive drugs in patients with pheochromocytoma, the proportion of patients suffering with perioperative complications decreased from 69% to 3% (5). Buitenwerf et al. used α-blockers for preoperative management of 134 patients with pheochromocytoma (6). The 30-day cardiovascular complication rate was 8.8% and 6.9% and there was no mortality after 30 days. The consensus recommendation is that all patients with pheochromocytoma should receive appropriate preoperative medical management to block the effects of circulating catecholamines.

Currently, the main preoperative preparatory drugs for pheochromocytoma include α-blockers for blood pressure control and beta-blockers for heart rate stabilization. Although α-blockers were first administered to patients in the middle of the last century, they are administered before pheochromocytoma resection (7) and have been recommended for reducing the risk of intraoperative hypertension since their introduction. Blockade with α-blockers is currently the first choice for preoperative blockade in patients with functional pheochromocytoma (1). α-blockers are divided into two categories: selective and non-selective. Zawadzka et al. reported that non-selective α-blockade was more effective in preventing intraoperative blood pressure fluctuations while maintaining comparable risk of both intraoperative and postoperative hypotension (8). The American College of Endocrinology Clinical Practice Guidelines recommend that all pheochromocytoma patients receive α-adrenergic receptor blockers for 7-14 days preoperatively to reduce surgical mortality and postoperative complication rates. The results of another study provided evidence of more complete preoperative preparation, patients should consume fluids and be instructed to eat foods high in sodium and to increase blood volume as soon as they are on α-blockers (9). Continuous use of phenoxybenzamine along with intravenous saline until 1 day before surgery has also been reported (6, 10). At present, the effect of oral α-blockers combined with intravenous volume expansion on perioperative hemodynamics is inconclusive, and it is worth exploring whether intravenous fluid expansion is necessary after preoperative oral phenoxybenzamine. Therefore, in our medical center, we use phenoxybenzamine (PXB) as a preoperative preparation drug for

Abbreviations: PXB, Phenoxybenzamine; BMI, body mass index; HS, hemodynamic stability; HI, hemodynamic instability; BB, β-blockers; CCB, calcium channel blockers; ACEI, angiotensin-converting enzyme inhibitors; ARB, angiotensin receptor blockers.

pheochromocytoma patients; therefore, the aim of this study is to investigate whether perioperative hemodynamics are associated with preoperative oral phenoxybenzamine followed by intravenous volume expansion.

Patients and methods

This study was a retrospective analysis and included patients with pheochromocytoma who were hospitalized at Handan First Hospital from October 2014 to July 2022. A total of 89 patients were treated surgically, of whom 6 were excluded, including 4 patients with incomplete data, 1 patient with tumor recurrence, and 1 patient with an extra-adrenal tumor. A total of 83 patients were finally screened. pheochromocytoma was considered by qualitative diagnosis (24-hour urinary catecholamines, plasma catecholamines, 24-hour urinary fractionated metanephrines, plasma metanephrines) and local diagnosis (CT plain + enhanced, MRI), and was supported by postoperative pathology. patients with a postoperative pathological diagnosis not supporting pheochromocytoma. The ethical review committee approved the study at Handan First Hospital, and the requirement for informed consent was waived due to the retrospective design.

Before 2018, patients undergoing pheochromocytoma resection were treated with the α-blocker PXB 14 days prior to surgery and intravenous volume expansion 3 days prior to surgery. Since 2018, we are gradually using α-blocker PXB alone and discontinuing preoperative intravenous volume expansion in patients undergoing pheochromocytoma resection. 41 of the 83 patients did not receive intravenous volume expansion. Before surgery, all patients completed at least one catecholamine test, such as for norepinephrine, epinephrine, and dopamine. Since 2017, we have performed blood and urine metanephrines tests in patients with suspected pheochromocytoma. Therefore, 37 of the 83 patients did not receive metanephrines testing. The patients were considered to have tested positive for catecholamines if one of their tests for norepinephrine, epinephrine and dopamine was above the normal range, If all of them were within the normal range, the test is considered negative. Of the 83 cases we collected, 54 patients tested positive for catecholamines (65.1%) and 29 patients tested negative for catecholamines (34.9%).

Preoperative medications

All patients received non-selective α-blockade PXB as part of preoperative medical preparation for at least 2 weeks. The initial dose of PXB was 10 mg orally twice daily, and the maximum dose was 10 mg orally five times daily. Patients were hospitalized in our endocrinology department or followed up regularly in outpatient clinics to regulate their blood pressure. Clinicians increased or decreased the dose of PXB intake depending on the patient's daily blood pressure fluctuations. Hypertension defined as systolic blood pressure (SBP) > 140 mmHg or diastolic blood pressure (DBP) > 90 mmHg. In accordance with the 2022 Endocrine Society recommendations, the preoperative patient's target blood pressure was controlled to less than 130/80 mmHg and the target heart rate to approximately 60-70 beats per minute when sitting (1). and changes in peripheral circulation, such as warmth in the extremities, were observed. Other drugs for hypertension, such as β-blockers (BB), calcium channel blockers (CCB), angiotensin-converting enzyme inhibitors (ACEI), and angiotensin receptor blockers (ARB), were considered when needed. All patients were admitted to the urology department 3 days before surgery. Patients who needed combined intravenous volume expansion were given 1000-2000 ml of saline intravenously 1 day before the procedure.

Surgical techniques

All patients underwent adrenal tumor resection under general anesthesia. The surgical approach (open versus laparoscopic) was determined based on tumor size, relationship to adjacent organs, and history of previous abdominal surgery. The anesthesiologist routinely inserted an arterial catheter into the patient's radial artery after anesthesia induction to monitor arterial pressure. The computer automatically recorded blood pressure measurements every 10 seconds. Haemodynamic variables, including BP and HR, were collected from the electronic anaesthetic chart, the intraoperative hemodynamic instabilities were defined as an intraoperative mean arterial pressure <60 mmHg (11). The main observation was whether there was intraoperative hemodynamic stability, followed by complications directly related to hemodynamic stability, including new-onset arrhythmias, postoperative hypotension, and need for antihypertensive drugs (12). Patients were divided into the hemodynamically stable group (HS group) and the hemodynamically unstable group (HU group) according to whether they were hemodynamically stable intraoperatively (Figure 1).

Statistical analysis

IBM SPSS statistics v26.0. Software was used to analyze the data. Continuous variables were presented as means and standard deviations. Group comparisons for continuous variables were performed by the t-test for approximately normally distributed data or the Mann-Whitney U-test for non-normally distributed data. Category variables were presented as numbers and percentages. Group comparisons for categorical variables were performed by the χ^2-test. Binary logistic regression analysis was used to determine predictive risk factors of hemodynamic instability. $P < 0.05$ (two-tailed tests) was defined as a statistically significant difference.

Results

This study included 30 men and 53 women with a mean age of 45 at the time of surgery. The patient characteristics in the two groups were comparable as shown in Table 1. The tumor size in the HS group [(5.3 ± 1.9) cm] was smaller than that in the HU group

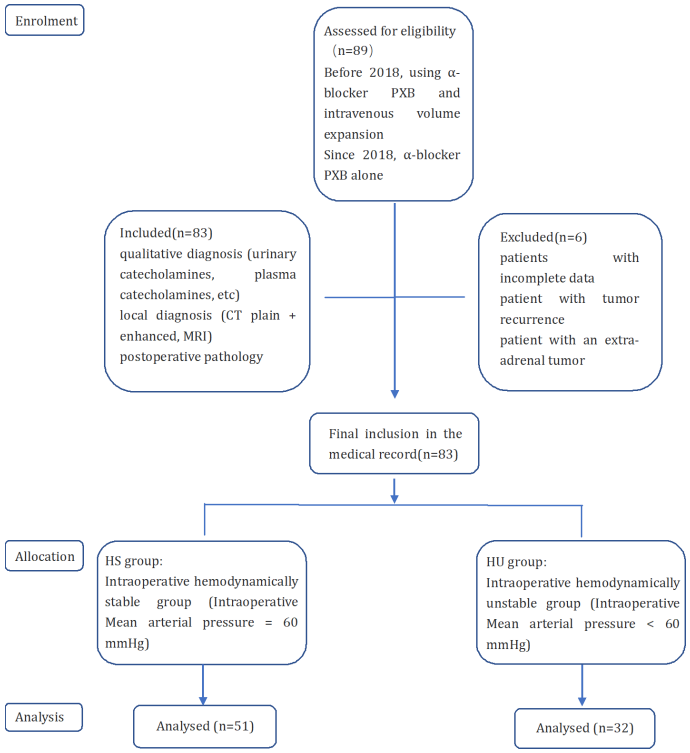

FIGURE 1
Flow chart of the study grouped according to hemodynamic stability or not.

TABLE 1 Clinical characteristics of patients with adrenal pheochromocytoma.

	Overall (n = 83)	HS group (n = 51)	HU group (n = 32)	P value
Age, years (mean ± SD)	45.2 ± 8.5	44.5 ± 8.1	46.7 ± 9.2	0.546
Sex, n (%)				0.790
Male	30 (36.1)	19 (37.3)	11 (34.4)	
Female	53 (63.9)	32 (62.7)	21 (65.6)	
Size of tumor, cm (mean ± SD)	5.6 ± 2.2	5.3 ± 1.9	6.2 ± 2.4	0.010
Location of tumor, n (%)				0.710
Left	24 (28.9)	14 (27.5)	10 (31.2)	
Right	59 (71.1)	37 (72.5)	22 (68.8)	
Surgery method, n (%)				0.625
Open	31 (37.3)	18 (35.3)	13 (40.6)	
Laparoscopy	52 (62.7)	33 (64.7)	19 (59.4)	
Catecholamine test, n (%)				0.390
Positive	54 (65.1)	35 (68.6)	19 (59.4)	
negative	29 (34.9)	16 (31.4)	13 (40.6)	
Preoperative oral PXB followed by combined intravenous volume expansion, n (%)	42 (50.6)	27 (52.9)	15 (46.9)	0.591
BMI ≥ 24 kg/m^2, n (%)	49 (59.0)	31 (60.8)	18 (56.2)	0.683
Comorbidities				

(Continued)

TABLE 1 Continued

	Overall (n = 83)	HS group (n = 51)	HU group (n = 32)	P value
Previous hypertension history, n (%)	67 (81.0)	42 (82.3)	25 (78.1)	0.635
Diabetes mellitus history, n (%)	14 (16.9)	8 (16.7)	6 (18.8)	0.717
Coronary artery disease, n (%)	7 (8.4)	5 (9.8)	2 (6.2)	0.571
Urine norepinephrine, nmol/24h	298 ± 59	281 ± 53	323 ± 67	0.620
Urine epinephrine, nmol/24h	34 ± 15	31 ± 12	38 ± 18	0.172
Urine dopamine, nmol/24h	2138 ± 348	2076 ± 299	2232 ± 392	0.283
Blood norepinephrine, pmol/L	2672 ± 487	2458 ± 437	2814 ± 543	0.664
Blood epinephrine, pmol/L	95 ± 19	94 ± 17	97 ± 22	0.322
Blood dopamine, pmol/L	67 ± 27	62 ± 24	74 ± 30	0.401

Data are presented as the mean standard deviation, median (interquartile range), or number (percentages).
BMI, body mass index; PXB, phenoxybenzamine (mg/d).

[(6.2 ± 2.4) cm], and the difference between the two groups was statistically significant (P=0.010). There were no significant differences in age, tumor size, tumor location, surgical method, preoperative oral PXB followed by combined intravenous volume expansion, BMI ≥ 24 kg/m^2, hypertension history, mellitus history, coronary artery disease history, blood catecholamines and urine catecholamines in the two groups.

We further compared the preoperative application of α-blockers and other medications in the two groups (Table 2). The differences in medicinal use between the two groups of patients were not statistically significant. Moreover, age, tumor size, tumor location, surgical method, preoperative oral PXB followed by combined intravenous volume expansion, BMI ≥ 24 kg/m^2, hypertension history, mellitus history, coronary artery disease history, blood catecholamines and urine catecholamines were subjected to multifactorial logistic regression analysis. Only tumor size was an independent risk factor for intraoperative hemodynamic instability (Table 3).

There were 2 postoperative complications in the HS group (both were postoperative fat liquefaction of the wound) and 2 postoperative complications in the HU group (1 postoperative subcutaneous hematoma and 1 poor wound healing due to infection), and all patients had no tumor recurrence or metastasis at the 3-month postoperative follow-up. The difference was not statistically significant (χ^2 = 0.323, P=0.614).

Discussion

The main risk for patients with pheochromocytoma is intraoperative hemodynamic instability. Different studies have adopted reference standards for determining intraoperative hemodynamic stability. A common reference standard is the presence of mean arterial pressure less than a certain value, such as a mean arterial pressure < 60 mmHg. By analyzing the electronic medical records of 114 patients with pheochromocytoma, Kim et al. found that one or more episodes of mean blood pressure < 60 mmHg or systolic blood pressure > 200 mmHg during surgery was a high-risk factor for postoperative cardiovascular events (11). The reason for this condition is the increase of systolic blood pressure due to the release of catecholamines from the tumor into the bloodstream caused by compression of the tumor during surgery, and the decrease of mean arterial pressure due to insufficient establishment of collateral circulation after tumor removal. Combining the literature and clinical experience (13, 14), In our study, after initial sample size estimation, we included a total of 83 patients, intraoperative mean arterial pressure <60 mmHg is considered to be hemodynamically unstable.

According to reports, Huang had collected clinical data of 136 patients with pheochromocytoma who underwent laparoscopic adrenalectomy, and found that tumor size and previous history of hypertension were associated with intraoperative hemodynamic

TABLE 2 Preoperative medication for patients with adrenal pheochromocytoma.

	Overall (n = 83)	HS group (n = 51)	HU group (n = 32)	P Value
Average dose of PXB (mean ± SD)	32.6 ± 9.4	31.3 ± 9.1	33.7 ± 9.8	0.127
Patients taking β-blockers, n (%)	14 (16.9%)	9 (17.6%)	5 (15.6%)	0.685
Patients taking ACEIs[a], n (%)	5 (6.0%)	4 (7.8%)	1 (3.1%)	0.685
Patients taking ARBs[b], n (%)	1 (1.2%)	0 (0.0%)	1 (3.1%)	0.813
Patients taking CCBs, n (%)	21 (25.3%)	15 (29.4%)	6 (18.8%)	0.277

Data are presented as the mean standard deviation, median (interquartile range), or number (percentages).
PXB, phenoxybenzamine (mg/d); ACEIs, angiotensin-converting enzyme inhibitors; ARBs, angiotensin receptor blockers; CCBs, calcium channel blockers.
[a]Continuity Correction was used for analysis.
[b]Fisher's Exact Test was used for analysis.

TABLE 3 Multifactorial logistic regression analysis of intraoperative hemodynamic instability in patients with adrenal pheochromocytoma.

	B	S.E.	Wald	P	OR	95% CI
Age	-0.141	0.158	0.789	0.374	0.869	0.637~1.185
Sex (1=male)	-0.451	1.341	0.113	0.737	0.637	0.046~8.829
Size of tumor	1.490	0.677	4.847	0.028	4.439	1.178~16.731
Location of tumor (1=left)	-0.778	1.596	0.238	0.626	0.459	0.020~10.491
Surgery method (1=open)	-0.268	1.286	0.044	0.835	0.765	0.061~9.511
Preoperative oral PXB alone	0.630	1.312	0.230	0.631	1.878	0.143~24.592
BMI ≥ 24 kg/m^2	-0.051	0.599	0.007	0.932	0.950	0.294~3.075
Previous hypertension history	-0.505	0.671	0.566	0.452	0.604	0.162~2.248
Diabetes mellitus history	0.938	0.843	1.240	0.266	2.556	0.490~13.329
Coronary artery disease	-1.282	1.141	1.264	0.261	0.277	0.030~2.594
Urine norepinephrine	0.024	0.016	2.238	0.135	1.025	0.993~1.058
Urine epinephrine	0.144	0.104	1.899	0.168	1.154	0.941~1.416
Urine dopamine	0.003	0.003	1.339	0.247	1.003	0.998~1.008
Blood norepinephrine	0.005	0.003	3.119	0.077	1.005	0.999~1.012
Blood epinephrine	0.076	0.072	1.134	0.287	1.079	0.938~1.242
Blood dopamine	-0.094	0.063	2.193	0.139	0.911	0.804~1.031

BMI, body mass index; PXB, phenoxybenzamine (mg/d).

instability by multivariate logistic regression analysis (15). Pisarska-Adamczyk retrospectively analyzed data from 96 patients undergoing laparoscopic adrenalectomy and found that adrenal tumor size and diabetes mellitus were associated with hemodynamic instability during pheochromocytoma resection (16). Ma evaluated the relationship between preoperative parameters and the incidence of intraoperative hemodynamic instability in 428 patients with pheochromocytoma and found that tumor size and high urinary epinephrine levels were tumor-related factors for intraoperative hemodynamic instability (17). History of hypertension and diabetes mellitus and urinary epinephrine levels were not found to be associated with intraoperative hemodynamic stability in patients in our study. Larger tumours have been shown to significantly release catecholamines during pheochromocytoma removal and as a result to increase the number of intraoperative hypertensive episodes. Also as tumor size increases, the potential for intraoperative blood loss increases (16, 18). It is therefore not surprising that larger tumors are more prone to intraoperative hemodynamic fluctuations.

The 2022 year of Personalized Management of Pheochromocytoma and Paraganglioma published by The Endocrine Society (TES) recommends preoperative α-blockers for patients with secretory pheochromocytoma to reduce the incidence of perioperative complications, including intraoperative hemodynamic crises (1). PXB is a nonselective α-blocker that has been widely used in the clinic to help minimize intraoperative hemodynamic instability and to help control intraoperative catecholamine fluctuations (19).

Previous studies on this issue did not include the important factor of whether intravenous rehydration was available before the operation (18). This is probably because, in the past, such patients were usually started on intravenous saline after a period of preoperative oral α-blockers (6, 9). Currently, the duration of preoperative intravenous rehydration is based on previous experience and varies by institution. The earliest intravenous saline administration as preoperative management at our center was 3 days prior to surgery. some studies have reported the duration of preoperative intravenous rehydration as 1 week or even 2 weeks (6, 10). Preoperative intravenous rehydration was widely used in many medical centers, however its usefulness has not been well evaluated. Hao found that in patients with pheochromocytoma, preoperative intravenous rehydration did not optimize perioperative hemodynamics or improve early outcomes (20). Preoperative intravenous rehydration failed to optimize perioperative hemodynamics or improve early outcome and this approach may increase the burden on the kidneys and heart. In this study, we collected data from 83 patients with pheochromocytoma and subclassified them into two groups according to intraoperative hemodynamics. Comparing the data between the two groups, we found no significant differences in intraoperative hemodynamic changes or incidence of postoperative hypotension between patients with pheochromocytoma receiving preoperative α-blockers alone and those receiving α-blockers combined with intravenous volume expansion. The binary logistic regression shows that it did not show any association between hemodynamic instability and preoperative intravenous rehydration.

Of course, there were some limitations in this study. First, this study was a retrospective analysis of data from a single center. Related selectivity and recall bias may have been influential, and further external validation (especially from non-Chinese teams)

would be significant. Second, our study did not consider using other types of α-blockers in the perioperative period and the anesthesiologists did not follow a uniform protocol to control intraoperative hemodynamic instability. Finally, Some scholars have used the LASSO regression model for bioinformatics articles and achieved good effects (21, 22), which warrants the application of this model to better predict the risk factors for hemodynamic instability.

Conclusions

In conclusion, during the preoperative preparation of patients with pheochromocytoma, oral α-blockers plus intravenous volume expansion did not further reduce the incidence of intraoperative hemodynamic instability compared with oral α-blockers alone. Therefore, patients with adrenal pheochromocytoma are advised to take α-blockers alone preoperatively, with the addition of other antihypertensive agents to help stabilize blood pressure and expand blood volume if necessary. Since this study is a single-center retrospective study, selection bias exists, and the conclusions need to be further validated in a large sample of prospective randomized controlled studies.

Data availability statement

The raw data supporting the conclusions of this article will be made available by the authors, without undue reservation.

Ethics statement

Ethical review and approval was not required for the study on human participants in accordance with the local legislation and institutional requirements. Written informed consent from the patients was not required to participate in this study in accordance with the national legislation and the institutional requirements.

Author contributions

K-WY and X-FT: first author. Y-NW, MC, M-TG: Senior authorship. All authors contributed to the article and approved the submitted version.

Conflict of interest

The authors declare that the research was conducted in the absence of any commercial or financial relationships that could be construed as a potential conflict of interest.

Publisher's note

All claims expressed in this article are solely those of the authors and do not necessarily represent those of their affiliated organizations, or those of the publisher, the editors and the reviewers. Any product that may be evaluated in this article, or claim that may be made by its manufacturer, is not guaranteed or endorsed by the publisher.

References

1. Nölting S, Bechmann N, Taieb D, Beuschlein F, Fassnacht M, Kroiss M, et al. Personalized management of pheochromocytoma and paraganglioma. *Endocr Rev* (2022) 43(2):199–239. doi: 10.1210/endrev/bnab019

2. Meijs AC, Snel M, Corssmit EPM. Pheochromocytoma/paraganglioma crisis: Case series from a tertiary referral center for pheochromocytomas and paragangliomas. *Hormones (Athens)* (2021) 20(2):395–403. doi: 10.1007/s42000-021-00274-6

3. Fang F, Ding L, He Q, Liu M. Preoperative management of pheochromocytoma and paraganglioma. *Front Endocrinol (Lausanne)* (2020) 11:586795. doi: 10.3389/fendo.2020.586795

4. Ugleholdt R, Rasmussen AK, Haderslev PAH, Kromann-Andersen B, Feltoft CL. Preoperative blood pressure targets and effect on hemodynamics in pheochromocytoma and paraganglioma. *Endocr Connect* (2022) 11(5):e210539. doi: 10.1530/EC-21-0539

5. Bihain F, Nomine-Criqui C, Guerci P, Gasman S, Klein M, Brunaud L. Management of patients with treatment of pheochromocytoma: A critical appraisal. *Cancers (Basel)* (2022) 14(16):3845. doi: 10.3390/cancers14163845

6. Buitenwerf E, Osinga TE, Timmers HJLM, Lenders JWM, Feelders RA, Eekhoff EMW, et al. Efficacy of α-blockers on hemodynamic control during pheochromocytoma resection: A randomized controlled trial. *J Clin Endocrinol Metab* (2020) 105(7):2381–91. doi: 10.1210/clinem/dgz188

7. Grimson KS, Longino FH, Kernodle CE, O'Rear HB. Treatment of a patient with a pheochromocytoma; use of an adrenolytic drug before and during operation. *J Am Med Assoc* (1949) 140(16):1273. doi: 10.1001/jama

8. Zawadzka K, Więckowski K, Małczak P, Wysocki M, Major P, Pędziwiatr M, et al. Selective vs non-selective alpha-blockade prior to adrenalectomy for pheochromocytoma: Systematic review and meta-analysis. *Eur J Endocrinol* (2021) 184(6):751–60. doi: 10.1530/EJE-20-1301

9. Yang Y, Zhang J, Fang L, Jia X, Zhang W. Non-selective alpha-blockers provide more stable intraoperative hemodynamic control compared with selective Alpha1-blockers in patients with pheochromocytoma and paraganglioma: A single-center retrospective cohort study with a propensity score-matched analysis from China. *Drug Des Devel Ther* (2022) 16:3599–608. doi: 10.2147/DDDT.S378796

10. Kong H, Li N, Tian J, Bao Z, Liu L, Wu K, et al. The use of doxazosin before adrenalectomy for pheochromocytoma: Is the duration related to intraoperative hemodynamics and postoperative complications? *Int Urol Nephrol* (2020) 52 (11):2079–85. doi: 10.1007/s11255-020-02539-2

11. Kim JH, Lee HC, Kim SJ, Yoon SB, Kong SH, Yu HW, et al. Perioperative hemodynamic instability in pheochromocytoma and sympathetic paraganglioma patients. *Sci Rep* (2021) 11(1):18574. doi: 10.1038/s41598-021-97964-3

12. Urabe F, Kimura S, Iwatani K, Takahashi K, Ito K, Tashiro K, et al. Risk factors for perioperative hemodynamic instability in pheochromocytoma: A systematic review and meta-analysis. *J Clin Med* (2021) 10(19):4531. doi: 10.3390/jcm10194531

13. Godoroja-Diarto D, Moldovan C, Tomulescu V. Actualities in the anaesthetic management of pheochromocytoma/ paraganglioma. *Acta Endocrinol (Buchar)* (2021) 17(4):557–64. doi: 10.4183/aeb.2021.557

14. Patel D, Phay JE, Yen TWF, Dickson PV, Wang TS, Garcia R, et al. Update on pheochromocytoma and paraganglioma from the SSO endocrine and head and neck disease site working group, part 2 of 2: Perioperative management and outcomes of pheochromocytoma and paraganglioma. *Ann Surg Oncol* (2020) 27(5):1338–47. doi: 10.1245/s10434-020-08221-2

15. Li N, Kong H, Li SL, Zhu SN, Zhang Z, Wang DX. Intraoperative hypotension is associated with increased postoperative complications in patients undergoing surgery for pheochromocytoma-paraganglioma: A retrospective cohort study. *BMC Anesthesiol* (2020) 20(1):147. doi: 10.1186/s12871-020-01066-y

16. Huang YS, Yan L, Li ZY, Fang ZQ, Liu Z, Xu ZH, et al. Risk factors for hemodynamic instability during laparoscopic resection of pheochromocytoma. *BMC Urol* (2022) 22(1):158. doi: 10.1186/s12894-022-01109-1

17. Ma L, Shen L, Zhang X, Huang Y. Predictors of hemodynamic instability in patients with pheochromocytoma and paraganglioma. *J Surg Oncol* (2020) 122(4):803–8. doi: 10.1002/jso.26079

18. Pisarska-Adamczyk M, Zawadzka K, Więckowski K, Przęczek K, Major P, Wysocki M, et al. Risk factors for hemodynamic instability during laparoscopic pheochromocytoma resection: A retrospective cohort study. *Gland Surg* (2021) 10 (3):892–900. doi: 10.21037/gs-20-783

19. Iglesias P, Santacruz E, García-Sancho P, Marengo AP, Guerrero-Pérez F, Pian H, et al. Pheochromocytoma: A three-decade clinical experience in a multicenter study. *Rev Clin Esp (Barc)* (2021) 221(1):18–25. doi: 10.1016/j.rceng.2019.12.011

20. Kong H, Yang JN, Tian J, Li N, Zhang YX, Ye PC, et al. Preoperative intravenous rehydration for patients with pheochromocytomas and paragangliomas: Is it necessary? a propensity score matching analysis. *BMC Anesthesiol* (2020) 20(1):294. doi: 10.1186/s12871-020-01212-6

21. Lai C, Wu Z, Li Z, Yu H, Li K, Tang Z, et al. A robust signature of immune-related long non-coding RNA to predict the prognosis of bladder cancer. *Cancer Med* (2021) 10(18):6534–45. doi: 10.1002/cam4.4167

22. Wu Z, Wang Y, Yan M, Liang Q, Li B, Hou G, et al. Comprehensive analysis of the endoplasmic reticulum stress-related long non-coding RNA in bladder cancer. *Front Oncol* (2022) 12:951631. doi: 10.3389/fonc.2022.951631

frontiers | Frontiers in Endocrinology

TYPE Original Research
PUBLISHED 21 April 2023
DOI 10.3389/fendo.2023.1129622

OPEN ACCESS

EDITED BY
Xiao-qiang Liu,
Tianjin Medical University General Hospital, China

REVIEWED BY
Luigi Petramala,
Sapienza University of Rome, Italy
Jia-quan Zhou,
Hainan General Hospital, China

*CORRESPONDENCE
Yushi Zhang
beijingzhangyushi@126.com

SPECIALTY SECTION
This article was submitted to Adrenal Endocrinology, a section of the journal Frontiers in Endocrinology

RECEIVED 22 December 2022
ACCEPTED 04 April 2023
PUBLISHED 21 April 2023

CITATION
Wang X, Zhao Y, Liao Z and Zhang Y (2023) Surgical strategies of complicated pheochromocytomas/paragangliomas and literature review.
Front. Endocrinol. 14:1129622.
doi: 10.3389/fendo.2023.1129622

Surgical strategies of complicated pheochromocytomas/paragangliomas and literature review

Xu Wang, Yang Zhao, Zhangcheng Liao and Yushi Zhang*

Department of Urology, Peking Union Medical College Hospital, Chinese Academy of Medical Sciences and Peking Union Medical College, Beijing, China

Pheochromocytomas (PCC)/paragangliomas (PGL) are catecholamine (CA) -secreting neuroendocrine tumors, which are known as PPGL due to their histological and pathophysiological similarities. In addition to the typical triad of paroxysmal headache, palpitation, and sweating, PPGL may also be accompanied by symptoms and signs involving multiple organs and systems such as the cardiovascular system, digestive system, endocrine system, and nervous system. Currently, surgical resection is the first choice for PPGL. Safe and effective surgical management of complicated PPGL is the goal of clinical work. In this paper, we discuss this hot issue based on complicated PPGL cases, aiming to share our experience of the surgical management strategy of PPGL.

KEYWORDS

pheochromocytomas, paragangliomas, catecholamine, surgery, multidisciplinary treatment

1 Introduction

Pheochromocytomas arise from chromaffin cells, which can produce CAs in the adrenal medulla, whereas paragangliomas arise from the extra-adrenal region (1). Sympathetic paragangliomas can produce CAs, which are generally distributed in paravertebral and pelvic areas, while non -CA-secreting-parasympathetic paragangliomas are usually located in the skull base and neck. Pheochromocytoma and paraganglioma are referred to as PPGL due to the similarity of histological features and physiological effects (2). Pheochromocytomas account for about 80% of PPGL and the rest are paragangliomas (3). The typical triad of PPGL is paroxysmal headache, palpitations, and heavy sweating. Other systemic signs and symptoms may also occur (4). Diagnosis of PPGL requires evidence of excessive CAs and localization of the tumor by imaging. Generally, the biochemical tests include CAs and intermediate metabolites of CAs in plasma or urine (5). In most cases, computed tomography (CT) should be the first choice for detecting tumors. Functional imaging, such as metaiodobenzylguanidine (MIBG) and

somatostatin receptor(SSTR) scintigraphy, has advantages in detecting potential and metastatic lesions in PPGL (6). In 2017, the World Health Organization (WHO) replaced the previous concept of "malignant PPGL" with "metastatic PPGL" in the classification of neuroendocrine tumors. It is believed that all PPGLs have metastatic potential, and the concept of malignancy and benign was disregarded (7). In this paper, the complexity of PPGLs depends on the surgical difficulty. Therefore, PPGLs without surgical indications were excluded. The definition of complicated PPGLs in this paper is as follows: 1. The tumor is located in a complicated region (e.g. close to important blood vessels and organs), which can easily cause surgical collateral damage. 2. The tumor size is larger than 6cm with an obvious occupying effect (6, 8). 3. PPGL with unclear boundary with surrounding tissues and suspected invasion of adjacent tissues and organs. All the above conditions may significantly increase the difficulty of the operation. If any of the above conditions are met, it can be considered as complicated PPGLs.

2 Surgical region

The surgical treatment of PPGL is closely related to the anatomic location of paraganglia. Pheochromocytoma originates only from the adrenal medulla. In comparison, paraganglia is derived from embryonic neural crest cells and distributed in clusters throughout the body, mainly along the great vessels. Paraganglia is named for its location adjacent to the sympathetic and parasympathetic ganglia. Studies have shown that about 21% of paragangliomas are located in the abdominal cavity, which is often accompanied by the paraspinal sympathetic trunk and other less common sites, including the neck, chest, and bladder (9). Three operative areas were identified for a better surgical strategy according to important vascular routes such as the abdominal aorta, inferior vena cava, renal pedicle vessels, and iliac vessels: Zone 1 (central vascular area) originates from the aortic hiatus and descends to the bifurcation of the iliac vessels, including the abdominal aorta and the origin of its main branches (abdominal trunk, renal artery, superior/inferior mesenteric artery) and inferior vena cava. Zone 2 (Perirenal area) mainly contains the kidneys and adrenal glands. According to the different anatomical structures, Zone 2 is further divided into the left(L) and right(R) perirenal areas. First, adrenal venous reflux is different. The left adrenal central vein is longer and generally flows into the left renal vein. In comparison, the right one is concise and runs in front of the adrenal apex until it flows directly into the inferior vena cava (10). Besides, the left perirenal area is adjacent to the tail of the pancreas, spleen, and abdominal aorta, while the right perirenal area is adjacent to the duodenum, the head of the pancreas, the inferior vena cava, and portal vein. Clinical studies have shown that PPGL tends to occur in the perirenal area, especially near the hilum of the kidney. The tumors seem more likely to present on the left side, which may be related to the left-sided location of the abdominal aorta (11, 12). Zone 3 (Pelvic area) mainly involves the bladder and its surrounding area (Figure 1).

3 Surgical treatment strategy

After determining the qualitative and locational diagnosis of PPGL, the tumor should be surgically removed as soon as possible. Most PCCs are feasible for minimally invasive laparoscopic surgery, which has significant advantages in decreasing blood loss and pain, accurate dissection, shortening hospital stay, and reducing postoperative complications. Several surgical approaches are available for minimally invasive surgery. It mainly includes the transabdominal approach and retroperitoneal approach (13). The transabdominal approach provides the surgeon with a broader field of view and a larger operating space, and it is convenient to remove bilateral tumors. The transperitoneal lateral approach can achieve good therapeutic effects (14). The retroperitoneal approach has unique advantages in resecting the unilateral PCC at a shorter distance, which can effectively avoid abdominal organ injury (15). Both minimally invasive methods can be finished with robot assistance (16, 17). The Endocrine Society Guidelines recommended minimally invasive adrenalectomy (e.g. laparoscopic) for most pheochromocytomas(<6cm) (6). This cut-off was determined by several clinical studies that laparoscopic surgery for PCCs < 6cm means less intraoperative bleeding, shorter

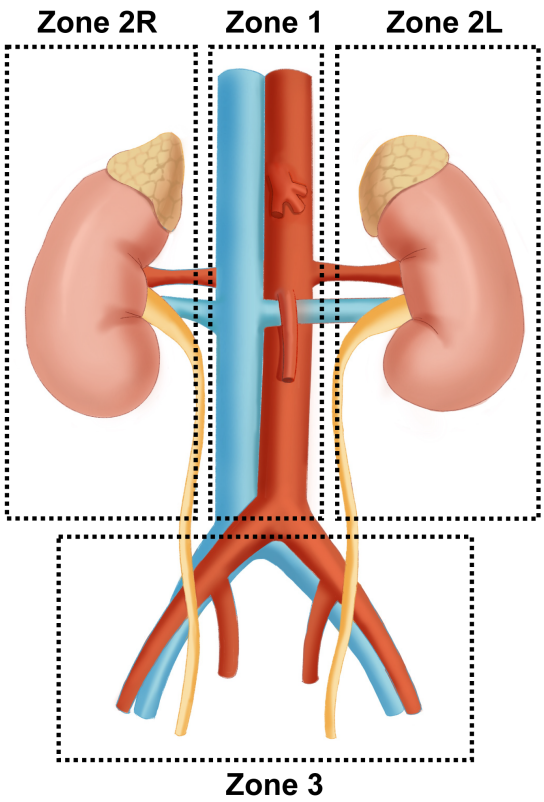

FIGURE 1
Surgical region of complicated PPGL Zone 1 (central vascular area) originates from the aortic hiatus and descends to the bifurcation of the iliac vessels, including the abdominal aorta, its main branches, and inferior vena cava. Zone 2 (Perirenal area) mainly contains bilateral kidneys and adrenal glands. Zone 3 (Pelvic area) mainly involves the bladder and its surrounding area (Figure 1).

operating time, and less frequent hypertensive crises (18, 19). Although studies have shown that for experienced surgeons, laparoscopic adrenalectomy is superior to open adrenalectomy in reducing bleeding, hospitalization, and blood pressure management for selected PCCs larger than 6cm (20). However, as a risk factor affecting prognosis, tumor size (<6cm) is regarded as an important reference for surgical method selection (8). For large (e.g., >6 cm) or suspected invasive PCC, open surgery is recommended to ensure complete resection, prevent tumor rupture, and local recurrence (6).

The selection of surgical method and approach should be based on the principle of complete resection of the tumor. In addition to the standard open surgery, laparoscopic resection is feasible for small and non-invasive PGL by guidelines (6).

The choice of surgical approach for abdominal PGL mainly depends on the tumor location. In addition, since most of the supplying arteries of abdominal PGL originate from the abdominal aorta or its branches directly or indirectly, several factors such as tumor dissociation and vascular ligation also need to be considered (21). The retroperitoneal approach can also achieve good surgical efficacy for experienced surgeons (11, 22). And the safety and prognosis of retroperitoneal PGL with the retroperitoneoscopic and transperitoneoscopic approaches were proved no significant difference based on studies with large sample numbers (23). Therefore, surgeons can choose the most appropriate surgical procedure in combination with the guidelines, tumor conditions, and their own experience.

There are various factors contributing to the difficulty of PPGL surgery, which can be mainly attributed to the following points. First, the location of the tumor is complicated, such as the tumor surrounding the abdominal aorta and/or the inferior vena cava. There is a very high risk of vascular injury during surgical resection under these conditions. Second, PPGL can expand gradually with a size of more than 10cm in the retroperitoneal cavity. The occupying effect caused by the huge tumor and the unclear boundary with the surrounding tissue increases the surgical difficulty greatly. Therefore, PPGL surgery may involve multiple zones mentioned above, and we identified the zone with more than 50% tumor as the main surgical area for the convenience of summary. We share surgical treatment strategies based on several typical complicated PPGL cases.

3.1 PPGL in central vascular area

Patient A is a 43-year-old female admitted for a 2-month paroxysmal headache, palpitations, and sweating. The diagnosis of abdominal para-aortic paraganglioma was considered by biochemical tests and radionuclide scintigraphy. Enhanced CT showed a 3.6cm×3.3cm retroperitoneal tumor with significant enhancement and unclear demarcation with the left renal vein, inferior vena cava, and abdominal aorta (Figure 2).

It is very challenging to manage PPGL embedded between the inferior vena cava and the abdominal aorta. First, the tumor was covered by the pancreas and pushed the inferior vena cava and the abdominal aorta laterally. The narrow space made both exposure and resection very troublesome. Second, the tumor was tightly restricted by the left renal vein and right renal artery, which increased the risk of intraoperative vascular injury. Besides, the pulsation of the abdominal aorta affects the tumor, leading to difficulty in the operation and higher requirements for precision. Finally, strong secretion of CA may cause hemodynamic instability.

The laparoscopic transabdominal approach was finally considered to dissociate precisely and reduce tumor irritation during operation. The lateral peritoneum was opened along the right paracolic sulcus. The ascending colon, duodenum, and the head of the pancreas were dissociated towards the midline to expose the tumor gradually. At the same time, assistants should carefully retract peritumor tissues and blood vessels to expand the operating space as much as possible. Since the tumor was located on the upper right side of the abdominal aorta, the ventral and vascularless sides of the tumor were explored at the beginning for simple dissociation. In addition, the tumor was adjacent to several important blood vessels and should be isolated along the surface carefully to avoid vascular injury. Gentle movement was necessary throughout the operation to reduce tumor irritation and avoid sharp fluctuations in blood pressure.

3.2 PCC in left perirenal area

Patient B was a 49-year-old female who suffered sudden palpitations and severe headaches with the highest blood pressure

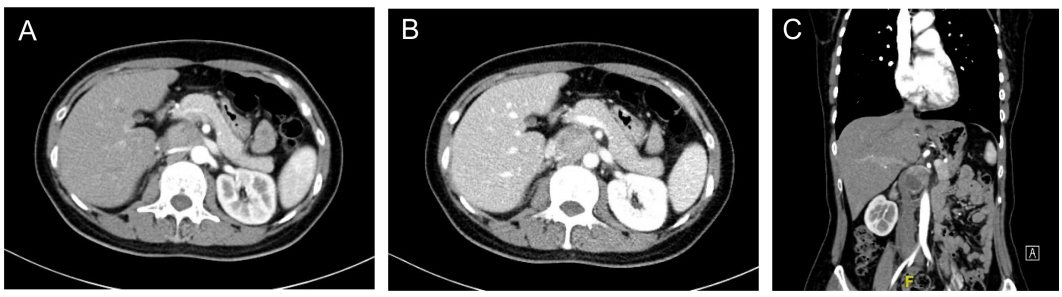

FIGURE 2
Enhanced CT of retroperitoneal PGL **(A)** Arterial phase of the PGL. The tumor was located behind the pancreas, pushing the right renal artery dorsally and adjacent to the abdominal aorta **(B)** Portal phase of the PGL. The inferior vena cava was pushed to the right and the left renal vein ran in front of the tumor. **(C)** Coronary position of the PGL.

of 188/90 mmHg two months ago. The diagnosis of PCC was considered by biochemical tests and radionuclide scintigraphy. Enhanced CT showed a giant mass in the left upper abdomen with a cross-section size of 14.4cm×12.5cm. The low-density focus in the liver was hepatic cysts confirmed by enhanced CT (Figure 3).

The difficulty of this case was how to remove the entire tumor and avoid accidental injury. This giant tumor was mainly composed of cystic components with apparent occupying effects: the upper part of the tumor pressed against the spleen and stomach. The middle part was not demarcated from the tail of the pancreas and was close to the abdominal aorta and celiac trunk. The lower part pressed against the left kidney, which elongated the kidney pedicle significantly.

Generally, there is no fixed surgical approach for open surgery of massive retroperitoneal tumors, and the incision selection is usually based on total exposure and convenient operation. Open surgical treatment was performed through an arc incision 3cm below the costal margin to ensure complete resection. The tumor was fully exposed after the posterior peritoneum was opened through the left paracolic sulcus. The surface of giant PCC was coated with an envelope, which was separated from the surrounding tissue by a combination of blunt and sharp separation. The surgical plane should be accurately found, which could improve the dissociation efficiency and reduce bleeding. The cooperation of assistants was also essential. The tissue needed to be pulled away from the tumor as much as possible to expand the surgical space. The PCC was isolated from the opposite side of the abdominal aorta and left renal pedicle vessels to avoid injury. Tortuous vessels on the surface of the tumor were electrocoagulated, ligated, and dissected. Finally, the tumor was removed entirely after the blood supply vessels were tightly ligated with relatively stable hemodynamics.

3.3 PCC in right perirenal area

Patient C was a 20-year-old female admitted for obvious palpitations, breath shortness, chest tightness, and dizziness during running for two years. The diagnosis of PCC was considered by biochemical tests and radionuclide scintigraphy. Enhanced CT showed a huge mass (10.9cm×9.0cm×10.7cm) in the right adrenal area, with uneven density and poorly defined boundary. There was a tortuous and thickened vessel in the tumor with multiple aneurysmal-like dilatations. It was considered the blood supply artery from the right adrenal artery (Figure 4).

The strategy of treating the right giant PCC is similar to the left one but still has its particularity. First, the right liver naturally occludes the PCC, so the surgical incision should be appropriately designed. Second, the space-occupying effect of the tumor pushed the pancreatic head, duodenum, inferior vena cava, and portal veins, resulting in a high risk of intraoperative organ and blood vessel injury. Besides, the malformed supply vessel ran longitudinally through the entire tumor, with multiple arteries originating from the abdominal aorta, which increased the difficulty of ligation and the potential risk of bleeding.

A "Y-shaped" incision was selected at the right side of the mid-abdomen for the convenience of exposure and dissociation. The

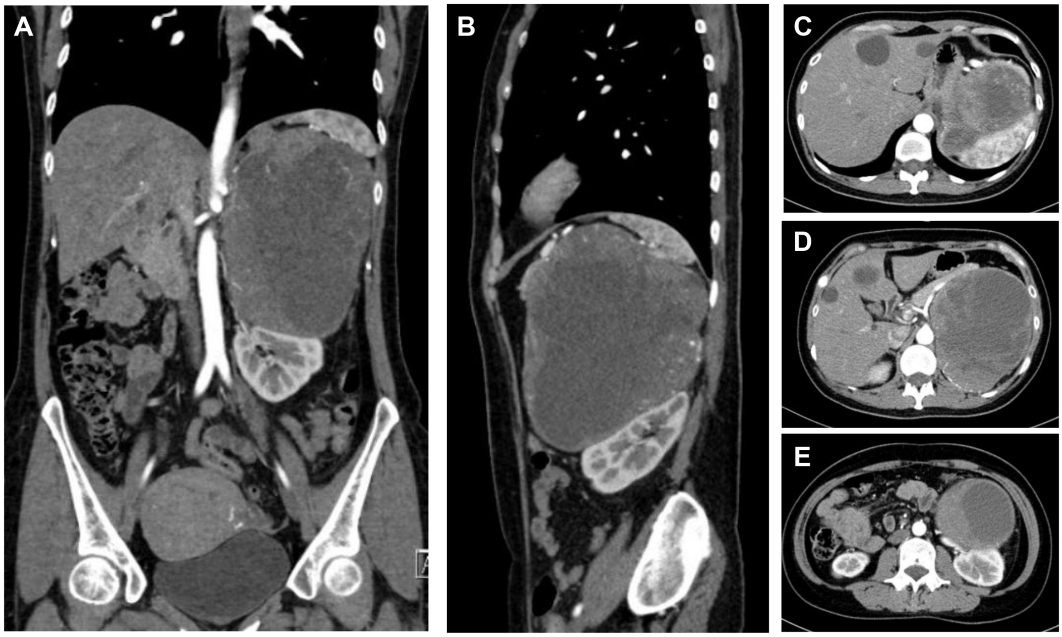

FIGURE 3
CT of a giant PCC in the left perirenal area. **(A)** Coronary position of the PCC. A mass of mixed density, with approximately 14.4cm×12.5cm in size, had significantly enhanced solid components. **(B)** Sagittal position of the PCC. The tumor pushed against the spleen and the left kidney. **(C)** The upper part of the PCC compressed the stomach. **(D)** The middle part of the PCC was not well demarcated with the tail of the pancreas and was close to the celiac trunk and the abdominal aorta. **(E)** The lower part of the PCC pressed on the left kidney and was close to the left renal pedicle.

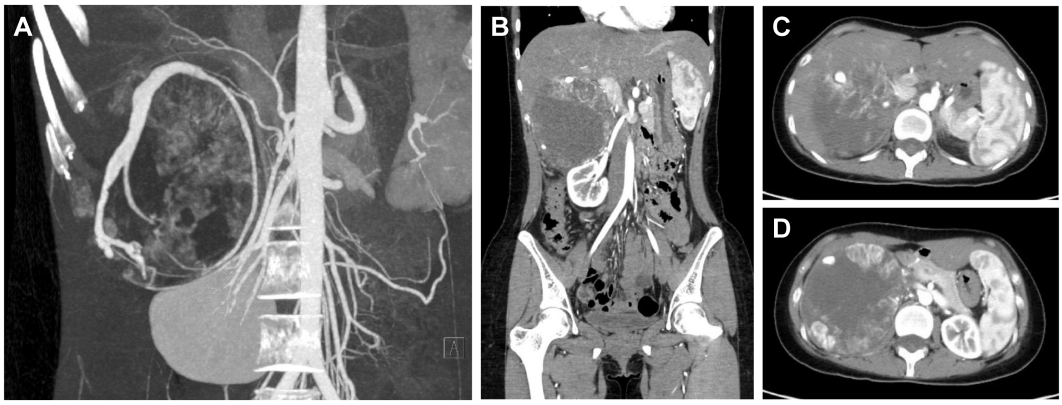

FIGURE 4
CT of a giant PCC in the right perirenal area. **(A)** CT of PCC angiography. Tortuous vessels with multiple aneurysmal-like dilatations were seen around the tumor. **(B)** Coronary position of the PCC. The tumor had a vague boundary with the liver and was close to the right renal pedicle. 10.9cm×9.0cm×10.7cm in size. **(C)** The upper part of the PCC was close to the inferior vena cava. **(D)** The maximum cross-section of the PCC was about 10.9cm×10.7cm.

right lobe of the liver was freed at the beginning. A giant PCC was shown after opening the posterior peritoneum through the right paracolic sulcus. Extra attention should be taken to avoid injury and severe complications near the pancreatic head and duodenum. Since the location of the blood supply artery was clear and shallow, it was ligated and cut off first. On the side near the abdominal aorta, all suspected small supply arteries were carefully ligated in case of postoperative hemorrhage. The inferior vena cava and portal vein were protected adequately during the operation due to the occupying effect of the considerable PCC. The tumor was finally removed with no extra injury.

3.4 PPGL in pelvic area

Patient D, a 26-year-old female, was admitted due to hypertension, paroxysmal headache, and palpitations for 2 years. The diagnosis of PCC was considered by biochemical tests and radionuclide scintigraphy. CT and MRI identified a mass that was located above the uterus at the S1-S3 level, about 5.4cm×6.0cm×6.1cm in size, with uneven enhancement (Figure 5).

Surgical resection of pelvic PPGL is a challenge. The difficulty lies in that presacral tumors are often located deep, close to internal organs and blood vessels in the pelvic cavity. The narrow space of the pelvis will lead to an unclear surgical field and cause accidental injuries. Especially the presacral venous plexus bleeding will often cause relatively severe consequences (24). With several factors such as tumor size, location, and surgeon's experience considered, the approach of transabdominal laparoscopic surgery was chosen with the Trendelenburg position. The tumor was exposed above the uterus and to the right of the sigmoid colon. First, the ventral side of the tumor was carefully dissociated. During the operation, the assistants needed to immobilize the tumor. Extra Trocar should be available if necessary. The surgeon was supposed to carefully separate the plane between the tumor surface and the sacrum to reduce irritation and accidental injury. The endoscopic gauze was

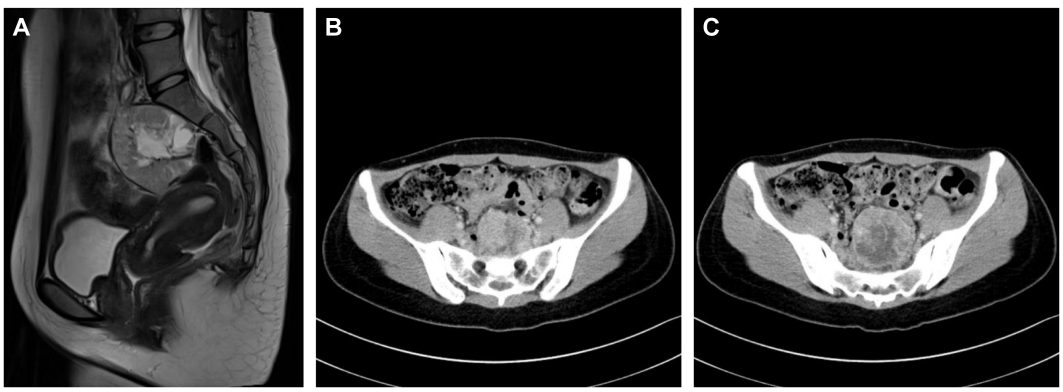

FIGURE 5
Imaging of a pelvic PGL **(A)** MRI of the sagittal position of the PGL. **(B)** The upper part of the PGL was close to the sacrum. **(C)** The maximum cross-section of the PCC was about 6.0cm×6.1cm.

packed appropriately to protect the presacral venous plexus. The action should be gentle and avoid scratching. The presacral venous plexus should be carefully checked before the end of the procedure in case of hemorrhage after closing the pneumoperitoneum.

4 Multidisciplinary treatment of PPGL

Pheochromocytoma/paraganglioma are neuroendocrine-related tumors with varied clinical symptoms and pathophysiological features due to the excessive secretion of CAs. Multidisciplinary treatment (MDT) has gradually become a routine process for PPGL because of the complexity of preoperative diagnosis, treatment, and postoperative care. After integrating the various opinions, the MDT model can develop the best strategies for patients, significantly improving the efficiency and quality of treatment (25, 26).

The Endocrine Society Guidelines indicated that imaging examination should be performed in potential PPGL patients with positive biochemical evidence. CT is considered the preferred method for its excellent spatial resolution in conventional imaging (6). On unenhanced CT, PPGL could show various appearances. The density of PPGL may be homogeneous or heterogeneous. About two-thirds of PPGLs are solid with soft-tissue density, and the rest are cystic or solid-cystic (27). As a neuroendocrine tumor associated with a genetic background, there were some significant differences between hereditary and sporadic PCC. Chung et al found that sporadic PCCs were larger in size with more cystic or necrotic components than the hereditary ones (28). Enhanced CT has a higher sensitivity for locating PPGL as small as about 5 mm. Almost 100% PPGLs showed a mean attenuation of more than 10 Hounsfield units (HU) and more than 60% washout in a 15-minute delay (29). MRI was applied in certain populations such as children, pregnant women, and patients who have recently been overexposed to radiation or are allergic to contrast (6). Relatively high signal intensity on T2-weighted images was shown in most PPGLs (30).

Since the definition of potential metastasis risk of PPGL was confirmed in 2017, molecular imaging has played an important role in diagnosis. Compared with conventional CT/MRI, positron emission tomography (PET)/CT with radiopharmaceuticals has more advantages in evaluating metastatic/multifocal PPGL and adjacent organ infiltration. ^{18}F-fluorodeoxyglucose (^{18}F-FDG) is one of the most widely used PET/CT markers in clinics. An amount of glucose was needed by tumor tissues due to the rapid growth and anaerobic metabolism, and ^{18}F-FDG is transported into the cell but does not participate in metabolism, and eventually marks tumor tissues (31). A clinical study involving 216 patients with PPGL compared the sensitivity and specificity of ^{18}F-FDG-PET/CT with CT, MRI, and ^{123}I-MIBG. The results showed that the sensitivity of ^{18}F-FDG-PET/CT was similar to that of ^{123}I-MIBG (76.8% vs 75.0%) and its specificity was similar to that of ^{123}I-MIBG and CT/MRI for non-metastatic tumors (90.2% vs 91.8% vs 90.2%). For metastatic PPGL, the sensitivity of ^{18}F-FDG-PET/CT was significantly higher than that of ^{123}I-MIBG and CT/MRI (82.5% vs 50.0% vs 74.4%) (32). In recent years, ^{68}Ga-DOTA (0)-Tyr (3)-octreotate (^{68}Ga-DOTATATE) PET/CT has attracted more attention. Several clinical researches reported that the lesion detection sensitivity for ^{68}Ga-DOTATATE PET/CT was significantly higher than that of ^{18}F-FDG PET/CT, CT/MR, and ^{131}I-MIBG scintigraphy especially in pediatric PPGL cohort (33, 34). The application of ^{68}Ga-DOTATATE was approved by the US Food and Drug Administration (33).

Due to the complexity of PPGL, it is often tricky for the department of urology to manage alone. For example, vascular surgery strongly supports vessel dissociation, ligation, repairment, and thrombotic events management (35). Hepatic surgery supports liver dissociation and portal vessel protection (36). General surgery provides essential help in abdominal organ dissociation and multiple organ resection (37). Because of the MDT system, surgical protocols are made to fulfill individual needs, which eventually benefits patients.

PPGL is a kind of tumor with metastatic potential, and there is a risk of local or metastatic recurrence even after the tumor is completely removed. Therefore, it is necessary to maintain postoperative follow-up and surveillance (25). The test of intermediate metabolites of catecholamine — metanephrine(MN) and normetanephrine(NMN) in plasma has been widely used in clinical with good sensitivity and specificity (38, 39). For the short-term postoperative follow-up, the monitoring of MN and NMN was recommended after recovery from surgery in 2–6 weeks. All the postoperative patients with PPGLs are supposed to keep at least a 10-year follow-up to monitor recurrences or new tumors, especially with High-risk factors (young ages, heredity, large size, and/or a paraganglioma) (40). In general, annual routine physical examinations and clinical follow-ups are recommended for PPGL patients. Imaging examinations are necessary among suspected cases. Functional imaging (e.g.^{123}I-MIBG scintigraphy) has an advantage in diagnosing metastasis or recurrence. ^{18} F-FDG PET/CT is suitable for definite metastatic cases (6). For patients who have developed metastases or whose tumors cannot be completely removed by surgery, although the efficacy of systematic treatment is limited, it can still relieve symptoms and control the disease to a certain extent. Individualized therapy plans require multidisciplinary collaboration (41).

In addition to the surgical department, several other departments play an essential role in PPGL-MDT. The endocrinology department plays a vital role in regulating blood pressure and managing PPGL-related complications, dramatically improving patients' quality of life, and laying the foundation for surgery. Excessive CAs secreted by PPGL may cause a hypertensive crisis, low blood volume, arrhythmias, myocardial ischemia, pulmonary edema, stroke et al. (42). Before medical treatment became widespread in the 1950s, the risk of perioperative death in adults was nearly 45%. This rate could be reduced to less than 2% via systematic preoperative blood pressure monitoring by medicine therapy (α-adrenergic antagonists, calcium channel blockers, and β-receptor blockers) (25, 43).

α-adrenergic receptor (AR) antagonists are recommended by the guidelines for PPGL complications. Phenoxybenzamine is a non-selective AR antagonist commonly used for perioperative blood pressure control. In general, phenoxybenzamine should be initiated at least 7-14 days before surgery to ensure adequate

blocking of α-receptors. The initial dose of phenoxybenzamine is 10mg twice a day, which can be increased or decreased depending on symptoms until the patient has normal blood pressure and no sudden tachycardia. The maximum daily dose can reach 1mg/kg (42). According to our clinical experience, for complicated PPGLs or PPGLs with the strong secretion of catecholamine, an appropriate extension of phenoxybenzamine administration time can better control PPGL symptoms. We generally extend the duration of phenoxybenzamine to at least 1 month. Some side effects of phenoxybenzamine can also be indicators of preoperative preparation besides blood pressure. In general, the blood pressure of PPGL patients with adequate medication preparation is generally less than 140/90 mmHg. Patients may have mild postural hypotension or nasal congestion. In addition, the antagonistic effect of phenoxybenzamine on α receptors will cause vasodilation and increase blood volume. Hematocrit is generally less than 40%, and the patient will gain weight and the fingertips become warm from cold.

Selective AR antagonists such as doxazosin can also achieve ideal clinical efficacy. Studies have shown that there is no statistical difference in efficacy between selective AR antagonists and non-selective AR antagonists (44, 45). When hypertension is not well controlled by α-AR antagonists alone, calcium channel blockers (CCBs) are often combined to further improve blood pressure control in PPGL patients. CCBs inhibit the norepinephrine-induced transmembrane calcium influx of vascular smooth muscle, thereby reducing peripheral vascular resistance and blood pressure (46). Multiple studies have demonstrated that CCBs have similar effects to α-AR antagonists on hemodynamic stability during the perioperative period (47, 48). PPGL-related tachycardia can be effectively controlled by β-AR antagonists (6). It is noticeable that β-AR antagonists are contraindicated in patients with PPGL alone or before α-AR is adequately treated. Because β-AR antagonists may cause loss of vasodilation before α-AR is adequately blocked, resulting in a sharp increase in blood pressure, and even hypertensive crisis (49).

Secondary hypertension and hemodynamic instability are common complications of PPGL. Patients with excessive CA secretion of PPGL often have a paroxysmal headache, secondary hypertension, large blood pressure fluctuation, and severe postural hypotension. In clinical practice, blood pressure is an important indicator to reflect PPGL patients' medical preparation and physical conditions and it is generally considered that patients with PPGL should control their blood pressure at 140/90 mmHg, and the ideal value is 120/80 mmHg without obvious postural hypotension (46). Therefore, ambulatory blood pressure monitoring (ABPM) is an important method of evaluation. Increasing studies identified that ABPM plays an indispensable role in the routine of secondary hypertension, which revealed the blood pressure pattern of PPGLs (50, 51). Although 24h-ABPM is not currently a routine blood pressure monitoring method in our hospital, its clinical value is widely recognized. Therefore, the anesthesiologist will pay attention to the fluctuation of patients' blood pressure and the conditions of vital organs during the intraoperative period of high risk, such as endotracheal intubation, operation on a tumor, and ligation of essential blood vessels (52). In our hospital, a PPGL-related group of anesthesiologists has been established to have a complete and detailed pre-anesthetic evaluation. Under the guidance of experienced anesthesiologists, personalized anesthesia protocols are made based on the surgical procedure and physical conditions, which makes the surgical procedures run smoothly.

The ICU provides a solid guarantee for the postoperative treatment of PPGL. Some studies have shown that ICU monitoring is unnecessary when the patient is hemodynamically stable during surgery (46). However, postoperative complications should not be underestimated. The most common is persistent hypotension due to loss of blood, impaired vascular compliance, or residual effects of the preoperative adrenergic blockade. Other complications, such as hypertensive crisis, severe arrhythmia, and hemorrhagic shock, could endanger life in severe conditions (53). Therefore, patients with the risk for potential hemodynamic instability still need to have closely cared in the ICU during the first 24-48 hours after surgery (54). In combination with our clinical experience, all these complicated PPGL cases were transferred to the ICU due to the long-time operation and high risk of postoperative hemodynamic instability. They were transferred back 24 or 48 hours later with vital signs in the normal range.

According to Toniato et al, PPGL surgery is not more difficult than the laparoscopic adrenalectomy for incidentaloma, Conn's disease, and Cushing's disease (55). So surgical treatment of common PPGL is feasible for most hospitals. However, in complicated PPGL cases (e.g., large tumor size, tumor compressing important blood vessels or organs, PPGL-induced hemodynamic instability), experienced surgeons and anesthesiologists, proper perioperative monitoring, and a well-cooperated multidisciplinary team can maximize the safety and postoperative recovery of patients. Therefore, complicated PPGL patients should be treated in general hospitals with specialized PPGL surgical teams.

In conclusion, PPGL has diverse clinical manifestations and complex complications, which may involve multiple organs and systems. The MDT-PPGL model can effectively evaluate the tumor, formulate the treatment plan, and complete the postoperative monitoring, which fully guarantees efficacy and safety. We will continue to summarize the surgical management strategy of PPGL in future clinical work so that more patients can benefit from it.

Data availability statement

The raw data supporting the conclusions of this article will be made available by the authors, without undue reservation.

Ethics statement

The studies involving human participants were reviewed and approved by Ethic committee of Peking Union Medical College Hospital. The patients/participants provided their written informed consent to participate in this study.

Author contributions

YSZ led the operation team. XW, YZ and ZL took part in the operation. XW acquired the data and prepared the first draft. YSZ, YZ and ZL reviewed critically and contributed to the final revision. All authors read and approved the final manuscript. All authors contributed to the article and approved the submitted version.

Funding

This study was funded by the National High Level Hospital Clinical Research Funding (2022-PUMCH-B-010).

Conflict of interest

The authors declare that the research was conducted in the absence of any commercial or financial relationships that could be construed as a potential conflict of interest.

Publisher's note

Supplementary material

The Supplementary Material for this article can be found online at: https://www.frontiersin.org/articles/10.3389/fendo.2023.1129622/full#supplementary-material

SUPPLEMENTARY FIGURE 1
Intraoperative gross images of the PPGLs A–D represents the gross PPGL of patients **(A–D)** respectively.

References

1. Tevosian SG, Ghayee HK. Pheochromocytomas and paragangliomas. *Endocrinol Metab Clin North Am* (2019) 48:727–50. doi: 10.1016/j.ecl.2019.08.006

2. Fang F, Ding L, He Q, Liu M. Preoperative management of pheochromocytoma and paraganglioma. *Front Endocrinol* (2020) 11:586795. doi: 10.3389/fendo.2020.586795

3. Lenders JWM, Eisenhofer G, Mannelli M, Pacak K. Phaeochromocytoma. *Lancet Lond Engl* (2005) 366:665–75. doi: 10.1016/S0140-6736(05)67139-5

4. Jain A, Baracco R, Kapur G. Pheochromocytoma and paraganglioma-an update on diagnosis, evaluation, and management. *Pediatr Nephrol Berl Ger* (2020) 35:581–94. doi: 10.1007/s00467-018-4181-2

5. Neumann HPH, Young WF, Eng C. Pheochromocytoma and paraganglioma. *N Engl J Med* (2019) 381:552–65. doi: 10.1056/NEJMra1806651

6. Lenders JWM, Duh Q-Y, Eisenhofer G, Gimenez-Roqueplo A-P, Grebe SKG, Murad MH, et al. Endocrine society. pheochromocytoma and paraganglioma: an endocrine society clinical practice guideline. *J Clin Endocrinol Metab* (2014) 99:1915–42. doi: 10.1210/jc.2014-1498

7. Lam AK-Y. Update on adrenal tumours in 2017 world health organization (WHO) of endocrine tumours. *Endocr Pathol* (2017) 28:213–27. doi: 10.1007/s12022-017-9484-5

8. Bittner JG, Gershuni VM, Matthews BD, Moley JF, Brunt LM. Risk factors affecting operative approach, conversion, and morbidity for adrenalectomy: a single-institution series of 402 patients. *Surg Endosc* (2013) 27:2342–50. doi: 10.1007/s00464-013-2789-7

9. Fischer T, Gaitonde S, Jones M, Bandera B, Goldfarb M. Anatomic location is the primary determinant of survival for paragangliomas. *Am Surg* (2017) 83:1132–6. doi: 10.1177/000313481708301024

10. Cesmebasi A, Du Plessis M, Iannatuono M, Shah S, Tubbs RS, Loukas M. A review of the anatomy and clinical significance of adrenal veins. *Clin Anat N Y N* (2014) 27:1253–63. doi: 10.1002/ca.22374

11. Xu W, Li H, Ji Z, Yan W, Zhang Y, Zhang X, et al. Retroperitoneal laparoscopic management of paraganglioma: a single institute experience. *PloS One* (2016) 11:e0149433. doi: 10.1371/journal.pone.0149433

12. Ji X-K, Zheng X-W, Wu X-L, Yu Z-P, Shan Y-F, Zhang Q-Y, et al. Diagnosis and surgical treatment of retroperitoneal paraganglioma: a single-institution experience of 34 cases. *Oncol Lett* (2017) 14:2268–80. doi: 10.3892/ol.2017.6468

13. Patel D. Surgical approach to patients with pheochromocytoma. *Gland Surg* (2020) 9:32–42. doi: 10.21037/gs.2019.10.20

14. Tarallo M, Crocetti D, Cavallaro G, Caruso D, Chiappini A, Petramala L, et al. Surgical treatment and management of syndromic paraganglioma. the experience of a referral center. *Ann Ital Chir* (2021) 92:465–70.

15. Paganini AM, Balla A, Guerrieri M, Lezoche G, Campagnacci R, D'Ambrosio G, et al. Laparoscopic transperitoneal anterior adrenalectomy in pheochromocytoma: experience in 62 patients. *Surg Endosc* (2014) 28:2683–9. doi: 10.1007/s00464-014-3528-4

16. Hassan T, de la Taille A, Ingels A. Right robot-assisted partial adrenalectomy for pheochromocytoma with video. *J Visc Surg* (2020) 157:259–60. doi: 10.1016/j.jviscsurg.2020.02.008

17. Xia L, Xu T, Wang X, Qin L, Zhang X, Zhang X, et al. Robot-assisted laparoscopic resection of large retroperitoneal paraganglioma - initial experience from China. *Int J Med Robot Comput Assist Surg MRCAS* (2016) 12:686–93. doi: 10.1002/rcs.1701

18. Toniato A, Boschin IM, Opocher G, Guolo A, Pelizzo M, Mantero F. Is the laparoscopic adrenalectomy for pheochromocytoma the best treatment? *Surgery* (2007) 141:723–7. doi: 10.1016/j.surg.2006.10.012

19. Conzo G, Musella M, Corcione F, De Palma M, Avenia N, Milone M, et al. Laparoscopic treatment of pheochromocytomas smaller or larger than 6 cm. a clinical retrospective study on 44 patients. laparoscopic adrenalectomy for pheochromocytoma. *Ann Ital Chir* (2013) 84:417–22.

20. Wang W, Li P, Wang Y, Wang Y, Ma Z, Wang G, et al. Effectiveness and safety of laparoscopic adrenalectomy of large pheochromocytoma: a prospective, nonrandomized, controlled study. *Am J Surg* (2015) 210:230–5. doi: 10.1016/j.amjsurg.2014.11.012

21. Renard J, Clerici T, Licker M, Triponez F. Pheochromocytoma and abdominal paraganglioma. *J Visc Surg* (2011) 148:e409–416. doi: 10.1016/j.jviscsurg.2011.07.003

22. Wang J, Li Y, Xiao N, Duan J, Yang N, Bao J, et al. Retroperitoneoscopic resection of primary paraganglioma: single-center clinical experience and literature review. *J Endourol* (2014) 28:1345–51. doi: 10.1089/end.2014.0345

23. Xu W, Li H, Ji Z, Yan W, Zhang Y, Xiao H, et al. Comparison of retroperitoneoscopic versus transperitoneoscopic resection of retroperitoneal paraganglioma: a control study of 74 cases at a single institution. *Med (Baltimore)* (2015) 94:e538. doi: 10.1097/MD.0000000000000538

24. Celentano V, Ausobsky JR, Vowden P. Surgical management of presacral bleeding. *Ann R Coll Surg Engl* (2014) 96:261–5. doi: 10.1308/003588414X13814021679951

25. Lenders JWM, Kerstens MN, Amar L, Prejbisz A, Robledo M, Taieb D, et al. Genetics, diagnosis, management and future directions of research of phaeochromocytoma and paraganglioma: a position statement and consensus of the working group on endocrine hypertension of the European society of hypertension. *J Hypertens* (2020) 38:1443–56. doi: 10.1097/HJH.0000000000002438

26. Taberna M, Gil Moncayo F, Jané-Salas E, Antonio M, Arribas L, Vilajosana E, et al. The multidisciplinary team (MDT) approach and quality of care. *Front Oncol* (2020) 10:85. doi: 10.3389/fonc.2020.00085

27. Leung K, Stamm M, Raja A, Low G. Pheochromocytoma: the range of appearances on ultrasound, CT, MRI, and functional imaging. *AJR Am J Roentgenol* (2013) 200:370–8. doi: 10.2214/AJR.12.9126

28. Chung R, O'Shea A, Sweeney AT, Mercaldo ND, McDermott S, Blake MA. Hereditary and sporadic pheochromocytoma: comparison of imaging, clinical, and laboratory features. *AJR Am J Roentgenol* (2022) 219:97–109. doi: 10.2214/AJR.21.26918

29. Sbardella E, Grossman AB. Pheochromocytoma: an approach to diagnosis. *Best Pract Res Clin Endocrinol Metab* (2020) 34:101346. doi: 10.1016/j.beem.2019.101346

30. Blake MA, Cronin CG, Boland GW. Adrenal imaging. *AJR Am J Roentgenol* (2010) 194:1450–60. doi: 10.2214/AJR.10.4547

31. Patel HV, Srivastava A, Becker MD, Beninato T, Laird AM, Singer EA. From diagnosis to therapy-PET imaging for pheochromocytomas and paragangliomas. *Curr Urol Rep* (2021) 22:2. doi: 10.1007/s11934-020-01021-x

32. Timmers HJLM, Chen CC, Carrasquillo JA, Whatley M, Ling A, Eisenhofer G, et al. Staging and functional characterization of pheochromocytoma and paraganglioma by 18F-fluorodeoxyglucose (18F-FDG) positron emission tomography. *J Natl Cancer Inst* (2012) 104:700–8. doi: 10.1093/jnci/djs188

33. Krokhmal AA, Kwatra N, Drubach L, Weldon CB, Janeway KA, DuBois SG, et al. 68 Ga-DOTATATE PET and functional imaging in pediatric pheochromocytoma and paraganglioma. *Pediatr Blood Cancer* (2022) 69:e29740. doi: 10.1002/pbc.29740

34. Jha A, Ling A, Millo C, Gupta G, Viana B, Lin FI, et al. Superiority of 68Ga-DOTATATE over 18F-FDG and anatomic imaging in the detection of succinate dehydrogenase mutation (SDHx)-related pheochromocytoma and paraganglioma in the pediatric population. *Eur J Nucl Med Mol Imaging* (2018) 45:787–97. doi: 10.1007/s00259-017-3896-9

35. Veith FJ, Stanley JC. Vascular surgery's identity. *J Vasc Surg* (2020) 72:293–7. doi: 10.1016/j.jvs.2020.02.023

36. Geller DA, Tohme S. Liver anatomy quiz: test your knowledge. *J Gastrointest Surg Off J Soc Surg Aliment Tract* (2021) 25:1093–104. doi: 10.1007/s11605-020-04582-x

37. Williams MD, Grunvald MW, Skertich NJ, Hayden DM, O'Donoghue C, Torquati A, et al. Disruption in general surgery: randomized controlled trials and changing paradigms. *Surgery* (2021) 170:1862–6. doi: 10.1016/j.surg.2021.05.011

38. Lee SM, Lee MN, Oh HJ, Cho YY, Kim JH, Woo HI, et al. Development and validation of liquid chromatography-tandem mass spectrometry method for quantification of plasma metanephrines for differential diagnosis of adrenal incidentaloma. *Ann Lab Med* (2015) 35:519–22. doi: 10.3343/alm.2015.35.5.519

39. Jian M, Huang H, Li K, Chuan L, Li L, Jiang L. A 3-min UPLC-MS/MS method for the simultaneous determination of plasma catecholamines and their metabolites: method verification and diagnostic efficiency. *Clin Biochem* (2021) 87:67–73. doi: 10.1016/j.clinbiochem.2020.10.009

40. Plouin PF, Amar L, Dekkers OM, Fassnacht M, Gimenez-Roqueplo AP, Lenders JWM, et al. European Society of endocrinology clinical practice guideline for long-term follow-up of patients operated on for a phaeochromocytoma or a paraganglioma. *Eur J Endocrinol* (2016) 174:G1–G10. doi: 10.1530/EJE-16-0033

41. Garcia-Carbonero R, Matute Teresa F, Mercader-Cidoncha E, Mitjavila-Casanovas M, Robledo M, Tena I, et al. Multidisciplinary practice guidelines for the diagnosis, genetic counseling and treatment of pheochromocytomas and paragangliomas. *Clin Transl Oncol Off Publ Fed Span Oncol Soc Natl Cancer Inst Mex* (2021) 23:1995–2019. doi: 10.1007/s12094-021-02622-9

42. Gunawardane PTK, Grossman A. Phaeochromocytoma and paraganglioma. *Adv Exp Med Biol* (2017) 956:239–59. doi: 10.1007/5584_2016_76

43. Livingstone M, Duttchen K, Thompson J, Sunderani Z, Hawboldt G, Sarah Rose M, et al. Hemodynamic stability during pheochromocytoma resection: lessons learned over the last two decades. *Ann Surg Oncol* (2015) 22:4175–80. doi: 10.1245/s10434-015-4519-y

44. Malec K, Miśkiewicz P, Witkowska A, Krajewska E, Toutounchi S, Gałązka Z, et al. Comparison of phenoxybenzamine and doxazosin in perioperative management of patients with pheochromocytoma. *Kardiol Pol* (2017) 75:1192–8. doi: 10.5603/KP.a2017.0147

45. van der Zee PA, de Boer A. Pheochromocytoma: a review on preoperative treatment with phenoxybenzamine or doxazosin. *Neth J Med* (2014) 72:190–201.

46. Naranjo J, Dodd S, Martin YN. Perioperative management of pheochromocytoma. *J Cardiothorac Vasc Anesth* (2017) 31:1427–39. doi: 10.1053/j.jvca.2017.02.023

47. Brunaud L, Boutami M, Nguyen-Thi P-L, Finnerty B, Germain A, Weryha G, et al. Both preoperative alpha and calcium channel blockade impact intraoperative hemodynamic stability similarly in the management of pheochromocytoma. *Surgery* (2014) 156:1410–7. doi: 10.1016/j.surg.2014.08.022

48. Jaiswal SK, Memon SS, Lila A, Sarathi V, Goroshi M, Garg R, et al. Preoperative amlodipine is efficacious in preventing intraoperative HDI in pheochromocytoma: pilot RCT. *J Clin Endocrinol Metab* (2021) 106:e2907–18. doi: 10.1210/clinem/dgab231

49. Farrugia F-A, Charalampopoulos A. Pheochromocytoma. *Endocr Regul* (2019) 53:191–212. doi: 10.2478/enr-2019-0020

50. Rimoldi SF, Scherrer U, Messerli FH. Secondary arterial hypertension: when, who, and how to screen? *Eur Heart J* (2014) 35:1245–54. doi: 10.1093/eurheartj/eht534

51. Ceruti M, Petramala L, Cotesta D, Cerci S, Serra V, Caliumi C, et al. Ambulatory blood pressure monitoring in secondary arterial hypertension due to adrenal diseases. *J Clin Hypertens Greenwich Conn* (2006) 8:642–8. doi: 10.1111/j.1524-6175.2006.05712.x

52. Araujo-Castro M, Pascual-Corrales E, Nattero Chavez L, Martínez Lorca A, Alonso-Gordoa T, Molina-Cerrillo J, et al. Protocol for presurgical and anesthetic management of pheochromocytomas and sympathetic paragangliomas: a multidisciplinary approach. *J Endocrinol Invest* (2021) 44:2545–55. doi: 10.1007/s40618-021-01649-7

53. Riester A, Weismann D, Quinkler M, Lichtenauer UD, Sommerey S, Halbritter R, et al. Life-threatening events in patients with pheochromocytoma. *Eur J Endocrinol* (2015) 173:757–64. doi: 10.1530/EJE-15-0483

54. Papachristos AJ, Cherry TJ, Nyandoro MG, Lisewski D, Stevenson S-J, Mercer P, et al. Bi-national review of phaeochromocytoma care: is ICU admission always necessary? *World J Surg* (2021) 45:790–6. doi: 10.1007/s00268-020-05866-8

55. Toniato A, Boschin I, Bernante P, Opocher G, Guolo AM, Pelizzo MR, et al. Laparoscopic adrenalectomy for pheochromocytoma: is it really more difficult? *Surg Endosc* (2007) 21:1323–6. doi: 10.1007/s00464-006-9190-8

frontiers | Frontiers in Endocrinology

TYPE Review
PUBLISHED 21 April 2023
DOI 10.3389/fendo.2023.1164067

OPEN ACCESS

EDITED BY
Xiao-qiang Liu,
Tianjin Medical University General Hospital, China

REVIEWED BY
Yafeng Li,
The Fifth Hospital of Shanxi Medical University, China
Durai Sellegounder,
Buck Institute for Research on Aging, United States

*CORRESPONDENCE
Xin Yao
yaoxin@tjmuch.com

SPECIALTY SECTION
This article was submitted to Adrenal Endocrinology, a section of the journal Frontiers in Endocrinology

RECEIVED 12 February 2023
ACCEPTED 03 April 2023
PUBLISHED 21 April 2023

CITATION
Zhang Z, Diao L, Zhang C, Wang F, Guan X and Yao X (2023) Use of PARP inhibitors in prostate cancer: from specific to broader application.
Front. Endocrinol. 14:1164067.
doi: 10.3389/fendo.2023.1164067

Use of PARP inhibitors in prostate cancer: from specific to broader application

Zhenting Zhang[1], Lei Diao[1], Chao Zhang[1], Feifei Wang[2], Xin Guan[2] and Xin Yao[1]*

[1]Department of Genitourinary Oncology, Tianjin Medical University Cancer Institute and Hospital, Tianjin, China, [2]PBG China Medical, Pfizer Inc, Shanghai, China

Prostate cancer (PC) is one of the major health issues of elderly men in the word. It is showed that there were approximately 1.414 million patients with PC in 2020 worldwide, with a high mortality rate in metastatic cases. In the present choices of treatment in PC, androgen deprivation therapy has long been as a backbone of them. But the clinical outcomes of patients with metastatic castration-resistant prostate cancer (mCRPC) were not ideal because of their poor prognosis, more effective therapeutic approaches are still necessary to further improve this problem. Poly (ADP-ribose) polymerase (PARP) inhibitors lead to the single-strand DNA breaks and/or double-strand DNA breaks, and result in synthetic lethality in cancer cells with impaired homologous recombination genes. It is estimated that approximately 20~25% of patients with mCRPC have a somatic or germinal DNA damage repair gene mutation. Furthermore, in "*BRCA*ness" cases, which has been used to describe as tumors that have not arisen from a germline *BRCA1* or *BRCA2* mutation, there were also a number of studies sought to extend these promising results of PARP inhibitors. It is worth noting that an interaction between androgen receptor signaling and synthetic lethality with PARP inhibitors has been proposed. In this review, we discussed the mechanism of action and clinical research of PARP inhibitors, which may benefit population from "specific" to the "all-comer" in patients with PC when combined with novel hormonal therapies.

KEYWORDS

prostate cancer, PARP inhibitor, DNA damage response and repair, novel hormonal therapy, metastatic prostate cancer

1 Introduction

GLOBOCAN-2020 estimated that there were approximately 1.414 million total prostate cancer (PC) patients and 30.7/100,000 incidences worldwide (1). PC became the second most common malignancy in men, with a mortality of 6.8% (1). The prognosis of metastatic PC remains poor compared to the favorable clinical outcome of localized PC

under today's advanced healthcare system (2). Metastatic PC causes over 400 thousand deaths annually, and the number of deaths is expected to be more than doubled by 2040, according to the Global Burden of Disease study in 2016 (3).

PC can be categorized into hormone-sensitive prostate cancer (HSPC) and castration-resistant prostate cancer (CRPC) based on its response to hormonal therapy. Usually cancer progression to CRPC results in the death of the patients. In addition to androgen deprivation therapy (ADT), the existing management strategies for CRPC include the administration of PC vaccine, chemotherapy, anti-androgen therapy, radionuclide therapy, immunotherapy and targeted therapies such as poly (ADP-ribose) polymerase (PARP) inhibitors (2). Novel hormonal therapies (NHTs) have been tried in the treatment of metastatic HSPC (mHSPC) for many years, but no additional efficacious drugs against metastatic CRPC (mCRPC) are currently available, leaving the largest unmet treatment need for metastatic PC. Therefore, new drugs are eagerly sought for mCRPC to improve the clinical outcome of mCRPC.

PARP inhibitors are a new class of targeted drugs developed recently, which are used in the treatment of various tumors such as mCRPC, and they mainly inhibit tumor cells proliferation by damaging DNA. These drugs were initially approved for the treatment of breast or ovarian cancer and subsequently were used in the clinical management of PC. Globally, olaparib and rucaparib are presently available approved PARP inhibitors for the treatment of PC.

As clinical research advances, PARP inhibitors have not been limited to managing PC patients with *BRCA1/2* gene mutation and have been implemented in a wider range of patients with homologous recombination repair (HRR)-associated gene mutation. Notably, PARP inhibitors when combined with NHTs might further improve the efficacy of treatment against mCRPC. In this manuscript, the clinical progress of PARP inhibitors and their mechanism of action are described to explore their potential application in a wider type of mCRPC.

2 The action of PARP on cellular DNA

The two ways of cellular DNA damages are single-strand breaks (SSBs) and double-strand breaks (DSBs). DNA damage response and repair (DDR) mechanisms can rapidly detect DNA damage and repair cells from intrinsic and extrinsic injuries. The SSBs are restored by nucleotide excision repair, base excision repair, and base mismatch repair, whereas DSBs are repaired by HRR and non-homologous end joining (4). During the S-phase of the cell cycle, the DNA replication phase, homologous recombination (HR) uses sister chromatids as a reference to restore the nucleotides damaged in the replication fork arrest (5). Therefore, targeting the DDR process may provide valuable therapeutic options for certain conditions promoting carcinogenesis through DDR gene mutation. When tumor cells already have genomic defects, targeted tumor therapies probably address both the genetic defect and tumor effect, like a "double hit" (6).

PARP is a group of enzymes participate in the synthesis of poly (ADP-ribose) (PAR), which involved in several cellular processes. Among them, PARP-1 is the most widely expressed and abundantly found enzyme, and it is regarded as a key sensor protein for DNA damage. With its increased catalytic activity (500-fold) while responding to the damaged DNA (7), PARP-1 induces poly ADP-ribosylation (PARylation), i.e., cleaving nicotinamide adenine dinucleotide (NAD+) and moving the resulting ADP ribose to itself (autoPARylization) or other targeted proteins (PARylation). These post-translational modifications automatically activate PARP and other DNA repair enzymes, mediating DNA repair by modifying chromatin structure and by localizing DNA repair effectors (8, 9). PARP-1 and/or PARP-2 proteins can repair SSBs, and PARP-1 can also repair DSBs and replication damage (10).

BRCA2 gene mutation is considered a high-risk factor for developing PC in men. About 20% of mCRPC patients displayed DDR-associated genetic variants, including *BRCA1/2* and *ATM* mutations. HRR is a *BRCA1/2* gene-dependent repair mechanism (11), and therefore, tumor cells carrying *BRCA1/2*-deficient genes cannot repair DNA damage through the HRR, and requiring PARP proteins for the restoration of SSBs (12). If PARP protein is inhibited by PARP inhibitors, DNA will not be repaired, and tumor cells will die subsequently.

3 Mechanism of action of PARP inhibitors

PC patients carrying *BRCA2* mutation have showed more effectively responded to carboplatin-based chemotherapy regimens than PC patients without *BRCA2* mutation (13). Carboplatin-based chemotherapy in the presence of DNA strand breaks caused by HRR-damage may produce synergistic lethal effects in tumor cells. These findings may help to understand the mechanisms of PARP inhibitors.

PARP inhibitors exert a pharmaceutically similar function to nicotinamide. They act primarily through two mechanisms (Figure 1) (1); inhibiting the catalytic activity of PARP by competitive binding to the active site against NAD+, hindering the repair of SSBs and thereby transforming into DSBs (10); (2) trapping PARP-1 into the damaged DNA through preventing PARP-1 release from DNA by inhibiting autoPARylization or enhancing DNA affinity to the catalytic site by creating allosteric PARP-1 structure (9). Further, PARP-1 delays the progression of replication forks, blocking the DSBs repair, and ultimately leading to cell death (12). PARP trapping does not occur independently of catalytic inhibition of PARylation. Since PARP-1 and PARP-2 cannot be isolated from DNA until PARP inhibitors dissociate from the active site following effective capture (10). Based on these mechanisms, *BRCA1/2* gene deficiency causing and PARP inhibition may synergistically prompt death in tumor cells, known as synthetic lethality (14).

BRCA mutated tumor cells are 1000-fold more sensitive to PARP inhibitors than *BRCA* wild-type cells (15). Hence, the development of PARP inhibitors initially emphasized the population with *BRCA1/2* gene mutation. However, with the advancement of molecular biological research, PARP inhibitor therapy has been gradually adopted for DDRs with mutations of

10.3389/fendo.2023.1164067

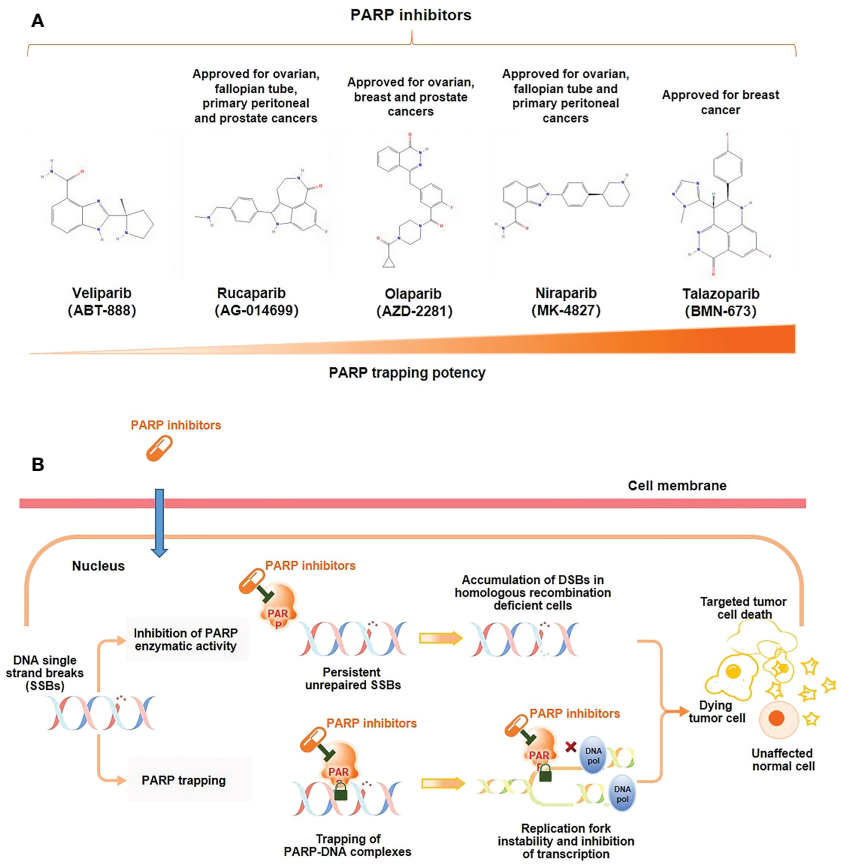

FIGURE 1
Mechanism of action of PARP inhibitors. **(A)** Molecular structure of PARP inhibitors and their capacity of trapping PARP; **(B)** PARP inhibitors lead to tumor cell death through two distinct mechanisms: the inhibition of the PARylation or trapping the PARP.

ATM, ATR, CHK1, CHK2, DSS1, RPA1, NBSI, FANCD2, FANCA, CDK12, PALB2, BRIP1, RAD51B, RAD51C, RAD51D, and RAD54, in addition to *BRCA1/2* gene variants (16). PARP inhibitors also prolonged the survival in some cancer patients without HRR-associated genetic alterations as demonstrated in the PRIMA trial (17). In patients with advanced ovarian cancer responding to platinum-based chemotherapy, regardless of their HRR biomarker state, niraparib as a first-line maintenance therapy prolonged the progression-free survival (PFS), prompting the U.S. Food and Drug Administration (FDA) to approve the first PARP inhibitor therapy in April 2020 for the population without *BRCA* mutation (17). Nevertheless, the application potential of PARP inhibitors in tumor therapy needs to be comprehensively explored.

4 Pharmaceutical development and preclinical evaluation of PARP inhibitors for PC

PARP inhibitors that have been used clinically in the treatment of mCRPC are olaparib, rucaparib, niraparib, and talazoparib, and all of them can cause tumor cell death, but the mechanism of action varies between drugs.

No clinical trials have directly compared different PARP inhibitors, but preclinical studies have shown that PARP trapping capacity by different PARP inhibitors varies from strong to weak in a variety of tumor cells, including PC cells, talazoparib > niraparib > olaparib = rucaparib > veliparib (Figure 1) (18, 19). In human PC cells (DU145 cells), the levels of PARP-DNA complexes induced by talazoparib with concentration of 0.1 μM were comparable to those induced by olaparib with 10 μM (18). In human ovarian cancer cells (HeyA8 cells), talazoparib also showed the strongest activity of trapping PARP-1, and could be detected at subnanomolar concentrations, while olaparib showed significant capture of PARP-1 at its concentrations as low as 10 to 100 nM, which had a moderate trapping capacity (20). In addition, the capacity of trapping PARP-2 varies among PARP inhibitors, with more potent of niraparib and talazoparib than olapari (21, 22). Of these PARP inhibitors, current evidence suggests that talazoparib has the strongest trapping capacity for PARP, with about 100-fold higher than olaparib and rucaparib (18).

The ranking of trapping potency of PARP inhibitors described above is consistent with their cytotoxic potential. For instance, in

most tumor cell lines, veliparib is still ineffective at concentrations up to 100 μM, while talazoparib is of potent cytotoxicity which showing effect even at nanomolar concentrations (18). The results from an indirect comparative analysis showed that the dissociation constant (Kd) to PARP of various PARP inhibitors and their monotherapy dose were not the same for similar efficacy (23). Among them, niraparib had the highest Kd for both PARP-1 and PARP-2, indicating its worst affinity for PARP. The dose of talazoparib as monotherapy was only 1 mg (od), while the doses of niraparib, olaparib, and rucaparib were hundreds of folds higher than that of talazoparib (300~600 mg, od/bd) (23). These may partially explain the close correlation between the clinical efficacy and safety of different PARP inhibitors and their trapping capacity.

The strong trapping potency of talazoparib for PARP may be related to its chemical structure. Among available PARP inhibitors at present, talazoparib has the most stable molecular structure with two racemic centers, reducing the occurrence of allosteric effects due to this unique stereostructure (10, 18, 24). The pharmacokinetic data of talazoparib showed a lower maximum concentration (C_{max}), suggesting that it has a lower drug exposure compared to olaparib, niraparib and rucaparib *in vivo*. And talazoparib was found to have a relatively low half maximal inhibitory concentration (IC_{50}) in PC cells. In addition, its relatively longer half-life is conducive to reducing the administration frequency (18, 24, 25) (Table 1). Together, talazoparib has shown certain advantages in preclinical studies in terms of both its trapping capacity and the inhibition against PARP enzymes.

5 Clinical development of PARP inhibitor monotherapies in PC

About 10% to 20% of PC patients develop mCRPC within 5 to 7 years of diagnosis (26). Metastatic PC is incurable, patients with metastatic PC have short survival, and the treatment goal is to prolong the survival of patients. Although today's therapeutic advancement in hormonal therapy, chemotherapy and other healthcare provision are outstanding for mCRPC, the prognosis of patients remains unsatisfied and new therapeutic strategies are sought. PARP inhibitors have provided new treatment options for mCRPC in recent years.

PROfound phase III study based on two Phase II clinical trials, TOPARP-A (NCT01682772) and TOPARP-B (NCT01682772), elucidated mCRPC patients with HRR gene mutation and disease progression after prior treatment with enzalutamide or abiraterone acetate plus prednisone (AA). The results (data as of June 04, 2019) showed that, compared with the patients of the control group that treated with enzalutamide or AA, the patients treated with olaparib displayed longer radiographic progression-free survival (rPFS) (5.8 vs. 3.5 months, $P<0.001$) and better objective response rate (ORR) (22% vs. 4%; odds ratio 5.93, 95% CI: 2.01 -25.40). The incidence of grade ≥3 adverse events (AEs) was higher in the olaparib group than in the control group (27). Based on the outcomes of this study, the FDA approved the drug in May 2020 for the treatment of mCRPC harboring deleterious or suspected deleterious germline/somatic HRR gene mutation with disease progression after treatment with enzalutamide or AA in adult patients. The PROfound study is currently completed, but with detailed data analysis ongoing. Its final results would hopefully further confirm the benefits of olaparib in mCRPC.

GALAHAD (28) was a phase II clinical study with a single-arm design, which aimed to investigate the efficacy and safety of niraparib in patients with disease progression after prior paclitaxel and androgen receptor (AR)-targeted therapy. Its provisional results (as of May 23, 2019) showed that niraparib treatment gave rise to an ORR of 41%, a complete response rate (CRR) of 63%, a median rPFS and OS of 8.2 and 12.6 months in the *BRCA1/2* mutant population. At the same time, for the non-*BRCA* mutant cohort, a CRR of 17% was reported when treated by niraparib (28). The drug was then designated as a breakthrough therapy by the FDA in October 2019 for the treatment of mCRPC patients with a *BRCA1/2* mutation who have previously been treated with paclitaxel chemotherapy and AR-targeted therapy. The final results demonstrated niraparib's significant anti-tumor activity in patients with DNA repair gene defect (DRD)-PC who had cancer progression after androgen signaling inhibitors and paclitaxel administration, particularly in patients with *BRCA* mutation, with controllable adverse events (29).

In the single-arm phase II TRITON-2 study (30) of rucaparib, patients with mCRPC, HRR-related gene mutations, and disease progression after 1-2 novel AR-targeted therapy and paclitaxel chemotherapy, the ORR was 43.5% and the prostate-specific antigen (PSA) response rate was 54.8% in the *BRCA1/2* mutation cohort. Anemia (25.2%) was the most common grade ≥3 adverse event. Rucaparib exhibited considerable anti-tumor activity and acceptable safety in treating patients with mCRPC harboring deleterious *BRCA* gene mutation (30). Consequently, the FDA accelerated the approval of rucaparib for the treatment of adult

TABLE 1 Pharmacodynamic/pharmacokinetic parameters of PARP inhibitors in solid tumors.

Drug	C_{max} (ng/mL)(25)	AUC (ng/mL·h)(25)	Mean $T_{1/2}$ (h)(25)	PARP-1 Inhibition IC_{50} (nM)(24)	PARP Inhibition IC_{50}* (nM) in PC(18)
Olaparib	5700~9500	33300~62100	6.52~11.9	1.94	18
Niraparib	1399~2071	19540~27852	36.2~36.45	/	/
Rucaparib	1940~2650	16900~47507	12.6	1.98	18
Talazoparib	16.4~32.84	208~244	50.0~50.73	0.57	11

* PARP inhibition in DU145 PC cell line.

patients with mCRPC associated with deleterious *BRCA* mutation (germline and/or somatic) who have previously received AR-targeted therapy and paclitaxel chemotherapy in May 2020. The phase III randomized controlled trial (RCT) TRITON-3 study (NCT02975934), is currently in progress, substantiating the efficacy of rucaparib, and the outcome is yet to be published.

Although talazoparib has not been approved yet for PC, the phase II TALAPRO-1 study (31) evaluated its efficacy and safety. In mCRPC patients with DDR-HRR alterations and at least 1 prior dose of paclitaxel-based chemotherapy, talazoparib treatment achieved an ORR of 29.8% and a median follow-up of 16.4 months, with a significantly higher ORR in patients with *BRCA1/2* gene mutations (46%) than in those without *BRCA* gene mutations (25% for *PALB2* mutations, 12% for *ATM* mutations, and 0% for other mutations); the most common grades 3-4 AEs requiring emergency treatment were anemia (31%), thrombocytopenia (9%), and neutropenia (8%) (31). Suggestively, talazoparib showed durable anti-tumor activity in advanced mCRPC patients with DDR-HRR genetic alterations who have failed multi-line therapy, offering a new potential treatment option for patients with mCRPC (31).

PARP inhibitors treatment is generally considered safe, non-hematological toxicities such as fatigue, diarrhea, and nausea is common, but several grade 3-4 AEs may leading to limitations in treatment adherence. As shown in the previous trials, PARP inhibitors are associated with a significant increase in the risk of hematologic toxicities cancer patients (32). According to the results of a meta-analysis aimed at analyzing the adverse events in castration-resistant prostate cancer patients receiving PARP inhibitors, anemia was the most frequently observed grade 3-4 toxicity (24.1%), followed by thrombocytopenia (6.7%), neutropenia (5.2%), fatigue (4.9%), leukopenia (3.4%). And the incidence of treatment-related dose reduction and treatment discontinuation due to adverse events in mCRPC patients above was 26.9% and 14.1%, respectively (33). Therefore, frequent clinical monitoring still should be emphasized during PARP inhibitors administration.

Currently approved PARP inhibitors used as a monotherapy are only effective in PC patients with mutations in the *BRCA1/2* gene or HRR-related genes, but the incidence of these mutations is small with the rate of *BRCA1/2* mutations of 8.8% in mCRPC patients (34). Therefore, it is highly desirable to confirm the efficacy of PARP inhibitors in more PC populations without *BRCA1/2* mutation. In addition, patients with advanced PC may also become resistant to PARP inhibitors, as like other targeted therapies. Combination therapy with PARP inhibitors may be an important strategy for improving efficacy or resistance.

6 Mechanism of PARP inhibitors when combined with NHTs and their clinical development for PC

The results of clinical trials on olaparib, niraparib, rucaparib, and talazoparib have fully demonstrated that PARP inhibitors can benefit patients with mCRPC who carrying *BRCA1/2* gene or HRR-related gene mutation, and showed manageable safety (27, 29–31). The benefit populations from these medications include mCRPC patients with prior AR-based targeted therapy. Further, considering their mechanisms of action, AR inhibitors and PARP inhibitors may synergize in the treatment of mCRPC (35, 36). The efficacy of PARP inhibitors may also not limited to PC with *BRCA1/2* mutation (16, 17). Based on this, the combination of PARP inhibitors and inhibiting androgens by NHTs is considered to be a potential treatment strategy for the broader PC population, prompting extensive preclinical and clinical exploration by researchers.

6.1 Preclinical exploration of PARP inhibitors when combined with NHTs

AR signaling induces posttranslational modifications. AR contains >20 sites for modifications, such as phosphorylation, acetylation, SUMOylation, and ubiquitination, which involve in the development of PC (37). AR signaling regulates the expression levels of genes, such as *TMPRSS2* and *PSA* in normal prostate cells or PC cells (38). Therefore, repression of AR signaling is an important purpose of PC therapy. Androgen deprivation and anti-androgen therapy suppress the AR signaling and cause damage to the HR gene (e.g., *BRCA1/2* and *ATM*). Enzalutamide has been reported to induce a *BRCA*ness state (35). In addition to PARP1/2 enzymes, recent studies also found that ADP-ribosylation regulated AR signaling through PARP7-mediated nuclear pathways (37), and AR signaling also controlled PARP7 post-transcriptional regulation in PC cells (39). Based on this finding, a certain interaction between AR signaling and synthetic lethality caused by PARP inhibitors was proposed.

6.1.1 Mechanisms of PARP affecting AR signaling

Polkinghorn et al. (40) found that approximately 32 direct target genes of AR, including PARP-1 and many DDR-related genes, were found in ChIP-sequencing analysis of AR in LNCaP cells, a human PC cell line, supporting the interaction of PARP inhibitors with AR signaling. *TMPRSS2*, an androgen-regulated gene and a product of repeated *ETS* gene fusion, is the driver of various cancers, including PC, with a *TMPRSS2* gene fusion to *ETS* transcription factors of 50% in PC[37]. PARP-1 interacted with *ERG* and inhibition of PARP-1 caused *ERG* overexpression-induced DSBs and inhibited the growth of ERG-positive PC cells (41). Schiewer et al. (42) also proposed that PARP-1 may contribute to PC progression through a dual role of DNA damage repair and transcription factor regulation, and clarified the following points (42) (1). PARP-1 can be recruited to the site of AR and can regulate the AR function; PARP-1 activity is increased in CRPC and can regulate the AR activity in castration-resistant states; (2) PARP inhibition can suppress the AR function, increase the sensitivity of PC cells to genotoxic damage, and synergize with anti-androgen therapy to inhibit cell proliferation, thereby suppressing tumor

growth and delaying the development of the castration-resistant state. FOXA1 protein binds to chromatin and regulates AR transactivation by interacting with AR, Gui et al. (43)found that PARP-2 enhanced the AR activity through its interaction with FOXA1. In contrast, inhibition of PARP decreased AR gene expression and inhibited the AR-positive PC cellsgrowth (43). PARP promoted the recruitment of AR to the nucleus and the AR activity was decreased in PARP knockdown cells upon stimulation with the androgen dihydrotestosterone and restored following PARP-1 supplementation (42). Gui et al. (43) also found that targeted PARP blockade impaired the AR function through interaction with the transcriptional activator FOXA1. Hence, PARP has the potential to enhance AR activity and inhibition of PARP decreases AR activity, provoking NHTs to benefit further.

6.1.2 Mechanism of NHTs affecting PARP activity

Genes involved in DNA damage repair may be downregulated following AR knockdown (36), demonstrating that NHTs has the potential to induce a phenotype resembling HRR deficiency and enhance the inhibiting efficacy of PARP-1. PARP-1 activity was significantly increased in PC patients after initiation of ADT compared with pre-treatment (36), also suggesting that inhibition of AR is associated with the up-regulation of PARP. PARylation, representing the PARP-1 activity, was elevated in the ADT-resistant PC cells compared with ADT-sensitive PC cells (42). Codeletion of *BRCA2* and *RB1* was found in approximately 10% to 50% of PC patients, and the codeletion might be one of the resistance mechanisms in NHTs (44); the sensitivity to PARP inhibition was increased in this state, and the inhibition of PARP might have weakened the growth of mCRPC cells (44). Therefore, early intervention using combined PARP inhibition and NHTs may delay the prospective resistance in patients with metastatic PC.

6.1.3 Translational studies of PARP inhibitors when combined with anti-neoplastic drugs

Li et al. (35) showed that enzalutamide, olaparib, and their combination downregulated the HR-related genes (*BRCA1, RAD51AP1, RAD51C, RAD54L*, and *RMI2*) in AR-positive PC cells, using the strategy of synergizing enzalutamide and olaparib activities in increasing PC cell apoptosis and inhibiting cell growth (35). Further, olaparib plus enzalutamide treatment inhibited PC tumor growth in subcutaneous patient-derived xenograft tumor models (MDA PCa 133-4, AR-positive) as well as in two orthotopic PC cell lines (AR-positive VCaP and CWR22Rv1)[34]. In a study by Asim et al. (36), the cell viability was significantly reduced in AR-positive PC cell lines, C4-2 and LN3, after olaparib plus bicalutamide/enzalutamide treatment. Combined inhibition of AR and PARP by olaparib plus enzalutamide decreased the proliferation of PC cells in xenograft PC model mice after 1 week of treatment, suggesting that the combination may synergistically inhibit tumor growth (36).

6.2 Clinical research progress of PARP inhibitors when combined with NHTs

In 2018, the phase II NCI 9012 study (45) showed negative results with the PARP inhibitor veliparib plus AA regimen initially, but on further analysis, this combination regimen resulted in a significantly higher PSA response (90% vs. 56.7%, P=0.007) and longer PFS (14.5 vs. 8.1 months, P=0.025) compared with the control group without veliparib in patients with DRD-mutated mCRPC. Although this is a feasible combination regimen, the complexity and biological context of mCRPC patients should be considered in future clinical trial designs (45). Another phase II RCT study evaluated the olaparib plus AA in patients with mCRPC and found that this regimen prolonged the median rPFS compared with the placebo plus AA group (13.8 months vs. 8.2 months, P=0.034), proposing that this regimen may provide additional clinical benefit to a wider range of patients with mCRPC (46). These patients were not selected on the basis of biomarker criteria, suggested that they might benefit from the combination treatment irrespective of HRR mutation status (46). The PROpel study (47) presented at the 2022 annual meeting of the American Society of Clinical Oncology (ASCO) further demonstrated that olaparib plus AA, as the first-line therapy for mCRPC (including patients with HRR mutated and HRR-non-mutated), significantly prolonged rPFS in patients compared with the placebo plus AA group (24.8 vs. 16.6 months, P<0.0001). Preliminary results from the MAGNITUDE study (48) reported that niraparib plus AA significantly improved rPFS (relative risk 0.53, 95% CI: 0.36-0.79, P=0.0014) and reduced the risk of disease progression/death (47% vs. 27%) in the *BRCA1/2* mutation subgroup of mCRPC.

The success of the olaparib/niraparib plus AA regimen may have been attributed to the more potent PARP trapping ability of olaparib/niraparib compared with veliparib plus AA (16), suggesting that it is critical to select suitable PARP inhibitors when designing combination therapies. Talazoparib is a PARP inhibitor exhibiting a dual mechanism of action that may synergize with NHTs activity (24). On the one hand, talazoparib inhibited PARP catalytic activity and displayed potent PARP trapping ability. On the other hand, talazoparib monotherapy demonstrated potent anti-tumor activity in HRR-deficient mCRPC patients. Recent studies demonstrated that enzalutamide not only inhibited the androgen binding to AR but also suppressed the AR nuclear translocation, as well as AR-mediated DNA binding in anti-androgen treatments (49–51). Enzalutamide showed improved efficacy compared with abiraterone as the first-line treatment in patients with mCRPC (52, 53). Therefore, enzalutamide is a preferred drug for NHTs when combined with a PARP inhibitor. As of January 2023, several ongoing clinical trials using this combination strategy were identified in the *ClinicalTrials.gov* database, and their results are anticipated (Table 2). It has been found that HRR gene alterations are associated with the worse outcomes in mHSPC patients, with significantly shorter time to mCRPC (54). The results supported the possibility that using

10.3389/fendo.2023.1164067

TABLE 2 Ongoing clinical trials with the combination of PARP inhibitors and NHTs in PC.

Drug	Subjects	Study Registration No./ Title	Study Design	Study Phase	Treatment & Grouping	Primary Outcomes	Study Progress
Olaparib	mHSPC (carry deleterious germline or HRR mutations)	NCT05167175/ PROact	Single Group Assignment	Phase II	Olaparib+AA	rPFS	Recruiting
	mCRPC	NCT01972217/ D081DC00008	RCT	Phase II	Olaparib+AA vs Placebo+AA	rPFS; Percentage of Patients with Progression Events or Death	Active, not recruiting
	mCRPC	NCT03012321/ NU_16U05	RCT	Phase II	AA vs. Olaparib vs. Olaparib+AA	Objective PFS	Recruiting
	mCRPC	NCT05171816/ D081SC00001Sub	RCT	Phase III	Olaparib + AA vs. Placebo+ AA	rPFS	Active, not recruiting
	mCRPC	NCT03732820/ PROpel	RCT	Phase III	Olaparib+AA vs. Placebo+AA	rPFS	Active, not recruiting
Niraparib	PC	NCT04194554/ ASCLEPIuS	Single Group Assignment	Phase I, II	AA+Leuprolide+100 mg/200mg Niraparib but held for 5 days (+/- 2 days) prior to RT, during SBRT, and 5 days (+/- 2 days) after last fraction of SBRT AA+Leuprolide+200 mg Niraparib without breaks during SBRT until completion of 6 cycles	DLT; Proportion of patients experiencing biochemical failure	Recruiting
	deleterious germline or somatic HRR gene-mutated mHSPC	NCT04497844/ AMPLITUDE	RCT	Phase III	Niraparib+AA vs. Placebo+ AA	rPFS	Recruiting
	mCRPC	NCT04577833/ CR108783	RCT	Phase I	Treatment: Niraparib Formulation 1: A; Niraparib Formulation 2: B; Niraparib Formulation 3: C; Niraparib Formulation 4: D; Cohort: AA+Treatment ABD; AA+Treatment ADB; AA+Treatment CBD; AA+Treatment CDB	$C_{max,ss}$; $AUC_{(0\text{-}24h),ss}$; Ratio of Individual $C_{max,ss}$ Values; Ratio of individual $AUC_{(0\text{-}24h),ss}$ Values	Active, not recruiting
	mCRPC	NCT03748641/ MAGNITUDE	RCT	Phase III	Treatment: Phase RCT: Niraparib+AA vs. Placebo+ AA; Phase OLE:all receive Niraparib+AA Cohort 1: Participants with mCRPC and HRR Gene Alteration; Cohort 2: Participants with mCRPC and No HRR Gene Alteration; Cohort 3 (Open-label): Participants with mCRPC	rPFS	Active, not recruiting
Rucaparib	CRPC and mPA and phase IV/ IVA/IVB PC	NCT04455750/ CASPAR	RCT	Phase III	Rucaparib+Enzalutamide vs. Placebo +Enzalutamide	rPFS;OS	Recruiting
	mCRPC	NCT04179396/ RAMP	Non-Randomized, Parallel Assignment	Phase Ib	Rucaparib+Enzalutamide vs. Rucaparib+AA	PK; treatment-related AEs/SAEs	Active, not recruiting
Talazoparib	HSPC	NCT04734730/ 20476	Single Group Assignment	Phase II	Talazoparib+AA+ADT	PSA nadir<0.2	Recruiting
	mHSPC		RCT	Phase II		PSA-CR	Recruiting

(Continued)

TABLE 2 Continued

Drug	Subjects	Study Registration No./ Title	Study Design	Study Phase	Treatment & Grouping	Primary Outcomes	Study Progress
		NCT04332744/ ZZ-First			Talazoparib+Enzalutamide+ADT vs. Enzalutamide+ADT		
	DDR-deficient mHSPC	NCT04821622/ TALAPRO-3	RCT	Phase III	Talazoparib + Enzalutamide vs. Placebo + Enzalutamide	rPFS	Recruiting
	mCRPC	NCT03395197/ TALAPRO-2	RCT	Phase III	Talazoparib+Enzalutamide vs. Placebo +Ezalutamide	Confirm the dose of Talazoparib (part 1); rPFS (part 2)	Active, not recruiting

RCT: Randomized controlled trial; OLE, Open label extension; PC, Prostate cancer; mCRPC, Metastatic castration resistant prostate cancer; mHSPC, Metastatic hormone-sensitive prostate cancer; AA, Abiraterone Acetate plus Prednisone; rPFS, Radiographic progression-free survival; OS, Overall survival; ADT, Androgen deprivation therapy; SBRT, Stereotactic body radiotherapy; DLT, Dose Limiting toxicities; MTD, Maximum Tolerated dose; RP2D, Recommended Phase 2 Dose; PPSA, Prostate specific antigen; CR, Complete response.

PARP inhibitors earlier in the clinical course for PC patients. And as shown in Table 2, the regimen of PARP inhibitors in combination with NHTs may bring promising results for HSPC or PC patients.

7 Mechanisms of PARP inhibitor actions when combined with other personalized therapies and their clinical development for PC

7.1 PARP inhibitors when combined with immunotherapies

In preclinical studies, PARP inhibitors upregulated the programmed cell death 1 ligand 1 (PD-L1) expression and enhanced the tumor-associated immunosuppression, but PARP inhibitors when combined with anti-PD-L1 therapy were more effective (55). In a non-randomized phase I/II clinical trial, olaparib when combined with the immune checkpoint inhibitor durvalumab achieved an rPFS of 16.1 months in patients with mCRPC, with an rPFS rate of 51.5% within 1 year. Further, most patients with *BRCA2* mutation showed a good response (rPFS rate of 83.3% within 1 year) (56). Based on the interim results of another phase Ib/II KEYNOTE-365 study, the combination therapeutic regimen improved response in patients with mCRPC (regardless of HRR state) compared with olaparib or pembrolizumab monotherapy, with ORRs of 33% and PSA response rates of 50% in *BRCA*-mutated patients (57). And in the *BRCA*-non-mutated cohort, patients have likewise obtained a certain response, with ORRs of 6% and PSA response of 14% (57).

7.2 PARP inhibitors when combined with other targeted therapies

PARP inhibitors were combined with therapies against vascular endothelial growth factor (VEGF). PARP inhibitors exerted some anti-angiogenic effects in invasive PC cells *in vitro*, downregulated VEGF expression, and induced PC cell apoptosis (58). A phase II RCT further confirmed a significant increase in median rPFS in patients with mCRPC who received olaparib plus cediranib compared with olaparib monotherapy (8.5 vs. 4.0 months, P=0.033) (59). In addition, combinations of PARP inhibitors and PI3K/AKT inhibitors also improved the treatment efficacy, in which PI3K signaling promoted the DNA double-strand repair through interaction with HRR complexes and inhibition of PI3K enhanced the anti-tumor effect of PARP inhibitors (60). An ongoing Phase Ib clinical trial is evaluating rucaparib plus AKT inhibitor ipatasertib (NCT03840200), and its results will provide a reference regarding this regimen.

7.3 Other combinatory regimens at the clinical trial phase

In addition to drug therapies, clinical studies investigated PARP inhibitors combined with other treatment modalities. The NADIR study (NCT04037254) combined the radiotherapy and the LuPARP study (NCT03874884) and the COMRADE study (NCT03317392) incorporated the radionuclide therapy. The outcomes of these studies will support wider application strategies of PARP inhibitors.

8 Looking into the future

In recent years, evidence-based elucidations demonstrated the efficacy and safety of PARP inhibitors as monotherapy in mCRPC with *BRCA 1/2* gene mutation or HRR-related gene mutation. A comprehensive investigation of PARP inhibitors has not been paused, and over 80 PARP inhibitor treatment studies in PC patients, including a variety of monotherapies or combination regimens, are found in the database of *ClinicalTrials.gov*. The research and development of combination therapies will enhance treatment efficacy, improve drug resistance, and address other issues. Notably, PARP inhibitors combined with NHTs are expected to provide benefits to a wider population with PC.

The following directions specific to PARP inhibitors are worthy of further exploration: (1) exploring potential response biomarkers to PARP inhibitor treatment to determine the precise indicative population; (2) selecting different PARP inhibitors in combination

therapies may have different resistance mechanisms and further exploration to overcome resistance is needed; (3) novel hormonal therapy is very effective in both mHSPC and mCRPC, and adding PARP inhibitors may further improve the cancer prognosis; (4) translating preclinical results into clinical applications should be focused. When these issues are addressed, adding PARP inhibitors to the treatment protocols could provide better survival in patients with PC and other cancers in the future.

Author contributions

ZZ and XY contributed to the conception, design, and final approval of the submitted version. LD and CZ contributed to completing the Figure, writing the paper. All authors contributed to the article and approved the submitted version.

Funding

The work was supported by PBG China Medical, Pfizer Inc, China. The funder was not involved in the study design, analysis, interpretation of data, the writing of this article or the decision to submit it for publication.

Acknowledgments

Medical writing support was provided by Yi Wang at Shanghai Meisi Medical Technology Co,Ltd and was funded by Pfizer. Editorial support was provided by Chunyan Wang at Pfizer.

Conflict of interest

Authors FW and XG were employed by Pfizer Inc.

The remaining authors declare that the research was conducted in the absence of any commercial or financial relationships that could be construed as a potential conflict of interest.

Publisher's note

References

1. World Health Organization. *Global cancer obsearvatory. estimated number of new cases in 2020, world, both sexes, all ages* (2020). Available at: https://gco.iarc.fr/today/home.

2. Powers E, Karachaliou GS, Kao C, Harrison MR, Hoimes CJ, George DJ, et al. Novel therapies are changing treatment paradigms in metastatic prostate cancer. *J Hematol Oncol* (2020) 13:144. doi: 10.1186/s13045-020-00978-z

3. Foreman KJ, Marquez N, Dolgert A, Fukutaki K, Fullman N, McGaughey M, et al. Forecasting life expectancy, years of life lost, and all-cause and cause-specific mortality for 250 causes of death: reference and alternative scenarios for 2016-40 for 195 countries and territories. *Lancet* (2018) 392:2052–90. doi: 10.1016/S0140-6736(18)31694-5

4. McNevin CS, Cadoo K, Baird AM, Finn SP, McDermott R. PARP inhibitors in advanced prostate cancer in tumors with DNA damage signatures. *Cancers (Basel)* (2022) 14:4751. doi: 10.3390/cancers14194751

5. Lundin C, Erixon K, Arnaudeau C, Schultz N, Jenssen D, Meuth M, et al. Different roles for nonhomologous end joining and homologous recombination following replication arrest in mammalian cells. *Mol Cell Biol* (2002) 22:5869–78. doi: 10.1128/MCB.22.16.5869-5878.2002

6. Bryant HE, Schultz N, Thomas HD, Parker KM, Flower D, Lopez E, et al. Specific killing of BRCA2-deficient tumours with inhibitors of poly(ADP-ribose) polymerase. *Nature* (2005) 434:913–7. doi: 10.1038/nature03443

7. Francica P, Rottenberg S. Mechanisms of PARP inhibitor resistance in cancer and insights into the DNA damage response. *Genome Med* (2018) 10:101. doi: 10.1186/s13073-018-0612-8

8. Rao A, Moka N, Hamstra DA, Ryan CJ. Co-Inhibition of androgen receptor and PARP as a novel treatment paradigm in prostate cancer-where are we now? *Cancers (Basel)* (2022) 14:801. doi: 10.3390/cancers14030801

9. Mateo J, Lord CJ, Serra V, Tutt A, Balmaña J, Castroviejo-Bermejo M, et al. A decade of clinical development of PARP inhibitors in perspective. *Ann Oncol* (2019) 30:1437–47. doi: 10.1093/annonc/mdz192

10. Pommier Y, O'Connor MJ, de Bono J. Laying a trap to kill cancer cells: PARP inhibitors and their mechanisms of action. *Sci Transl Med* (2016) 8:362ps17. doi: 10.1126/scitranslmed.aaf9246

11. Stok C, Kok YP, van den Tempel N, van Vugt M. Shaping the BRCAness mutational landscape by alternative double-strand break repair, replication stress and mitotic aberrancies. *Nucleic Acids Res* (2021) 49:4239–57. doi: 10.1093/nar/gkab151

12. Rose M, Burgess JT, O'Byrne K, Richard DJ, Bolderson E. PARP inhibitors: clinical relevance, mechanisms of action and tumor resistance. *Front Cell Dev Biol* (2020) 8:564601. doi: 10.3389/fcell.2020.564601

13. Pomerantz MM, Spisák S, Jia L, Cronin AM, Csabai I, Ledet E, et al. The association between germline BRCA2 variants and sensitivity to platinum-based chemotherapy among men with metastatic prostate cancer. *Cancer* (2017) 123:3532–9. doi: 10.1002/cncr.30808

14. Neiger HE, Siegler EL, Shi Y. Breast cancer predisposition genes and synthetic lethality. *Int J Mol Sci* (2021) 22:5614. doi: 10.3390/ijms22115614

15. Congregado B, Rivero I, Osmán I, Sáez C, Medina López R. PARP inhibitors: a new horizon for patients with prostate cancer. *Biomedicines* (2022) 10:1416. doi: 10.3390/biomedicines10061416

16. Adashek JJ, Jain RK, Zhang J. Clinical development of PARP inhibitors in treating metastatic castration-resistant prostate cancer. *Cells* (2019) 8:860. doi: 10.3390/cells8080860

17. González-Martín A, Pothuri B, Vergote I, DePont Christensen R, Graybill W, Mirza MR, et al. Niraparib in patients with newly diagnosed advanced ovarian cancer. *N Engl J Med* (2019) 381:2391–402. doi: 10.1056/NEJMoa1910962

18. Murai J, Huang SY, Renaud A, Zhang Y, Ji J, Takeda S, et al. Stereospecific PARP trapping by BMN 673 and comparison with olaparib and rucaparib. *Mol Cancer Ther* (2014) 13:433–43. doi: 10.1158/1535-7163.MCT-13-0803

19. Murai J, Huang SY, Das BB, Renaud A, Zhang Y, Doroshow JH, et al. Trapping of PARP1 and PARP2 by clinical PARP inhibitors. *Cancer Res* (2012) 72:5588–99. doi: 10.1158/0008-5472.CAN-12-2753

20. Hopkins TA, Shi Y, Rodriguez LE, Solomon LR, Donawho CK, DiGiammarino EL, et al. Mechanistic dissection of PARP1 trapping and the impact on *In vivo* tolerability and efficacy of PARP inhibitors. *Mol Cancer Res* (2015) 13:1465–77. doi: 10.1158/1541-7786.MCR-15-0191-T

21. Zhang H, Lin X, Zha S. Revisiting PARP2 and PARP1 trapping through quantitative live-cell imaging. *Biochem Soc Trans* (2022) 50:1169–77. doi: 10.1042/BST20220366

22. Lin X, Jiang W, Rudolph J, Lee BJ, Luger K, Zha S. PARP inhibitors trap PARP2 and alter the mode of recruitment of PARP2 at DNA damage sites. *Nucleic Acids Res* (2022) 50:3958–73. doi: 10.1093/nar/gkac188

23. Leo E, Johannes J, Illuzzi G, Zhang A, Hemsley P, Bista MJ, et al. Abstract LB-273: a head-to-head comparison of the properties of five clinical PARP inhibitors identifies new insights that can explain both the observed clinical efficacy and safety profiles. *Cancer Res* (2018) 78:LB–273. doi: 10.1158/1538-7445.AM2018-LB-273

24. Shen Y, Rehman FL, Feng Y, Boshuizen J, Bajrami I, Elliott R, et al. BMN 673, a novel and highly potent PARP1/2 inhibitor for the treatment of human cancers with DNA repair deficiency. *Clin Cancer Res* (2013) 19:5003–15. doi: 10.1158/1078-0432.CCR-13-1391

25. Bruin MAC, Sonke GS, Beijnen JH, Huitema ADR. Pharmacokinetics and pharmacodynamics of PARP inhibitors in oncology. *Clin Pharmacokinet* (2022) 61:1649–167. doi: 10.1007/s40262-022-01167-6

26. Kirby M, Hirst C, Crawford ED. Characterising the castration-resistant prostate cancer population: a systematic review. *Int J Clin Pract* (2011) 65:1180–92. doi: 10.1111/j.1742-1241.2011.02799.x

27. de Bono J, Mateo J, Fizazi K, Saad F, Shore N, Sandhu S, et al. Olaparib for metastatic castration-resistant prostate cancer. *N Engl J Med* (2020) 382:2091–102. doi: 10.1056/NEJMoa1911440

28. Smith MR, Sandhu SK, Kelly WK, Scher HI. Pre-specified interim analysis of GALAHAD: a phase 2 study of niraparib in patients (pts) with metastatic castration-resistant prostate cancer (mCRPC) and biallelic DNA-repair gene defects. *Ann Oncol* (2019) 30:v851–934. doi: 10.1093/annonc/mdz394.043

29. Smith MR, Scher HI, Sandhu S, Efstathiou E, Lara PNJr., Yu EY, et al. Niraparib in patients with metastatic castration-resistant prostate cancer and DNA repair gene defects (GALAHAD): a multicentre, open-label, phase 2 trial. *Lancet Oncol* (2022) 23:362–73. doi: 10.1016/S1470-2045(21)00757-9

30. Abida W, Patnaik A, Campbell D, Shapiro J, Bryce AH, McDermott R, et al. Rucaparib in men with metastatic castration-resistant prostate cancer harboring a BRCA1 or BRCA2 gene alteration. *J Clin Oncol* (2020) 38:3763–72. doi: 10.1200/JCO.20.01035

31. de Bono JS, Mehra N, Scagliotti GV, Castro E, Dorff T, Stirling A, et al. Talazoparib monotherapy in metastatic castration-resistant prostate cancer with DNA repair alterations (TALAPRO-1): an open-label, phase 2 trial. *Lancet Oncol* (2021) 22:1250–64. doi: 10.1016/S1470-2045(21)00376-4

32. Zhou JX, Feng LJ, Zhang X. Risk of severe hematologic toxicities in cancer patients treated with PARP inhibitors: a meta-analysis of randomized controlled trials. *Drug Des Devel Ther* (2017) 11:3009–17. doi: 10.2147/DDDT.S147726

33. Rizzo A, Mollica V, Merler S, Morelli F, Sorgentoni G, Oderda M, et al. Incidence of grade 3-4 adverse events, dose reduction, and treatment discontinuation in castration-resistant prostate cancer patients receiving PARP inhibitors: a meta-analysis. *Expert Opin Drug Metab Toxicol* (2022) 18:235–40. doi: 10.1080/17425255.2022.2072727

34. Tukachinsky H, Madison RW, Chung JH, Gjoerup OV, Severson EA, Dennis L, et al. Genomic analysis of circulating tumor DNA in 3,334 patients with advanced prostate cancer identifies targetable BRCA alterations and AR resistance mechanisms. *Clin Cancer Res* (2021) 27:3094–105. doi: 10.1158/1078-0432.CCR-20-4805

35. Li L, Karanika S, Yang G, Wang J, Park S, Broom BM, et al. Androgen receptor inhibitor-induced "BRCAness" and PARP inhibition are synthetically lethal for castration-resistant prostate cancer. *Sci Signal* (2017) 10:eaam7479. doi: 10.1126/scisignal.aam7479

36. Asim M, Tarish F, Zecchini HI, Sanjiv K, Gelali E, Massie CE, et al. Synthetic lethality between androgen receptor signalling and the PARP pathway in prostate cancer. *Nat Commun* (2017) 8:374. doi: 10.1038/s41467-017-00393-y

37. Yang CS, Jividen K, Kamata T, Dworak N, Oostdyk L, Remlein B, et al. Androgen signaling uses a writer and a reader of ADP-ribosylation to regulate protein complex assembly. *Nat Commun* (2021) 12:2705. doi: 10.1038/s41467-021-23055-6

38. Fujita K, Nonomura N. Role of androgen receptor in prostate cancer: a review. *World J Mens Health* (2019) 37:288–95. doi: 10.5534/wjmh.180040

39. Kamata T, Yang CS, Melhuish TA, Frierson HFJr., Wotton D, Paschal BM. Post-transcriptional regulation of PARP7 protein stability is controlled by androgen signaling. *Cells* (2021) 10:363. doi: 10.3390/cells10020363

40. Polkinghorn WR, Parker JS, Lee MX, Kass EM, Spratt DE, Iaquinta PJ, et al. Androgen receptor signaling regulates DNA repair in prostate cancers. *Cancer Discovery* (2013) 3:1245–53. doi: 10.1158/2159-8290.CD-13-0172

41. Brenner JC, Ateeq B, Li Y, Yocum AK, Cao Q, Asangani IA, et al. Mechanistic rationale for inhibition of poly(ADP-ribose) polymerase in ETS gene fusion-positive prostate cancer. *Cancer Cell* (2011) 19:664–78. doi: 10.1016/j.ccr.2011.04.010

42. Schiewer MJ, Goodwin JF, Han S, Brenner JC, Augello MA, Dean JL, et al. Dual roles of PARP-1 promote cancer growth and progression. *Cancer Discovery* (2012) 2:1134–49. doi: 10.1158/2159-8290.CD-12-0120

43. Gui B, Gui F, Takai T, Feng C, Bai X, Fazli L, et al. Selective targeting of PARP-2 inhibits androgen receptor signaling and prostate cancer growth through disruption of FOXA1 function. *Proc Natl Acad Sci USA* (2019) 116:14573–82. doi: 10.1073/pnas.1908547116

44. Chakraborty G, Armenia J, Mazzu YZ, Nandakumar S, Stopsack KH, Atiq MO, et al. Significance of BRCA2 and RB1 Co-loss in aggressive prostate cancer progression. *Clin Cancer Res* (2020) 26:2047–64. doi: 10.1158/1078-0432.CCR-19-1570

45. Hussain M, Daignault-Newton S, Twardowski PW, Albany C, Stein MN, Kunju LP, et al. Targeting androgen receptor and DNA repair in metastatic castration-resistant prostate cancer: results from NCI 9012. *J Clin Oncol* (2018) 36:991–9. doi: 10.1200/JCO.2017.75.7310

46. Clarke N, Wiechno P, Alekseev B, Sala N, Jones R, Kocak I, et al. Olaparib combined with abiraterone in patients with metastatic castration-resistant prostate cancer: a randomised, double-blind, placebo-controlled, phase 2 trial. *Lancet Oncol* (2018) 19:975–86. doi: 10.1016/S1470-2045(18)30365-6

47. Thiery-Vuillemin A, Saad F, Armstrong AJ, Oya M, Vianna KCM, Özgüroğlu M, et al. Tolerability of abiraterone (abi) combined with olaparib (ola) in patients (pts) with metastatic castration-resistant prostate cancer (mCRPC): further results from the phase III PROpel trial. *J Clin Oncol* (2022) 40:5019. doi: 10.1200/JCO.2022.40.16_suppl.5019

48. Chi KN, Rathkopf DE, Smith MR, Efstathiou E, Attard G, Olmos D, et al. Phase 3 MAGNITUDE study: first results of niraparib (NIRA) with abiraterone acetate and prednisone (AAP) as first-line therapy in patients (pts) with metastatic castration-resistant prostate cancer (mCRPC) with and without homologous recombination repair (HRR) gene alterations. *J Clin Oncol* (2022) 40:12. doi: 10.1200/JCO.2022.40.6_suppl.012

49. Pinto-Bazurco Mendieta MA, Negri M, Jagusch C, Müller-Vieira U, Lauterbach T, Hartmann RW. Synthesis, biological evaluation, and molecular modeling of abiraterone analogues: novel CYP17 inhibitors for the treatment of prostate cancer. *J Med Chem* (2008) 51:5009–18. doi: 10.1021/jm800355c

50. Tran C, Ouk S, Clegg NJ, Chen Y, Watson PA, Arora V, et al. Development of a second-generation antiandrogen for treatment of advanced prostate cancer. *Science* (2009) 324:787–90. doi: 10.1126/science.1168175

51. Watson PA, Chen YF, Balbas MD, Wongvipat J, Socci ND, Viale A, et al. Constitutively active androgen receptor splice variants expressed in castration-resistant prostate cancer require full-length androgen receptor. *Proc Natl Acad Sci USA* (2010) 107:16759–65. doi: 10.1073/pnas.1012443107

52. McCool R, Fleetwood K, Glanville J, Arber M, Goodall H, Naidoo S. Systematic review and network meta-analysis of treatments for chemotherapy-naive patients with Asymptomatic/Mildly symptomatic metastatic castration-resistant prostate cancer. *Value Health* (2018) 21:1259–68. doi: 10.1016/j.jval.2018.03.012

53. Fang M, Nakazawa M, Antonarakis ES, Li C. Efficacy of abiraterone and enzalutamide in pre- and postdocetaxel castration-resistant prostate cancer: a trial-level meta-analysis. *Prostate Cancer* (2017) 2017:8560827. doi: 10.1155/2017/8560827

54. Lee AM, Saidian A, Shaya J, Nonato T, Cabal A, Randall JM, et al. The prognostic significance of homologous recombination repair pathway alterations in metastatic hormone sensitive prostate cancer. *Clin Genitourin Cancer* (2022) 20:515–23. doi: 10.1016/j.clgc.2022.06.016

55. Jiao S, Xia W, Yamaguchi H, Wei Y, Chen MK, Hsu JM, et al. PARP inhibitor upregulates PD-L1 expression and enhances cancer-associated immunosuppression. *Clin Cancer Res* (2017) 23:3711–20. doi: 10.1158/1078-0432.CCR-16-3215

56. Karzai F, VanderWeele D, Madan RA, Owens H, Cordes LM, Hankin A, et al. Activity of durvalumab plus olaparib in metastatic castration-resistant prostate cancer in men with and without DNA damage repair mutations. *J Immunother Cancer* (2018) 6:141. doi: 10.1186/s40425-018-0463-2

57. Yu E, Piulats JM, Gravis G, Fong P, Todenhöfer T, Laguerre B, et al. 73P association between homologous recombination repair mutations and response to pembrolizumab (pembro) plus olaparib (ola) in metastatic castration-resistant prostate cancer (mCRPC): KEYNOTE-365 cohort a biomarker analysis. *Ann Oncol* (2021) 32:S387. doi: 10.1016/j.annonc.2021.08.353

58. Sargazi S, Saravani R, Zavar Reza J, Zarei Jaliani H, Galavi H, Moudi M, et al. Novel Poly(Adenosine diphosphate-ribose) polymerase (PARP) inhibitor, AZD2461, down-regulates VEGF and induces apoptosis in prostate cancer cells. *Iran BioMed J* (2019) 23:312–23. doi: 10.29252/ibj.23.5.2

59. McKay RR, Radke MR, Shyr Y, Zhao S, Taplin M-E, Davis NB, et al. Biomarker analysis from a randomized phase II study of olaparib with or without cediranib in men with metastatic castration-resistant prostate cancer (mCRPC). *J Clin Oncol* (2021) 39:7. doi: 10.1200/JCO.2021.39.6_suppl.7

60. Zhou S, Dai Z, Wang L, Gao X, Yang L, Wang Z, et al. MET inhibition enhances PARP inhibitor efficacy in castration-resistant prostate cancer by suppressing the ATM/ATR and PI3K/AKT pathways. *J Cell Mol Med* (2021) 25:11157–69. doi: 10.1111/jcmm.17037

frontiers | Frontiers in Endocrinology

TYPE Original Research
PUBLISHED 16 May 2023
DOI 10.3389/fendo.2023.1158573

OPEN ACCESS

EDITED BY
Yuxuan Song,
Peking University People's Hospital, China

REVIEWED BY
Adriana G. Ioachimescu,
Emory University, United States
Ana Valea,
Iuliu Hatieganu University of Medicine and Pharmacy Cluj-Napoca, Romania

*CORRESPONDENCE
Qing He
hech69@163.com
Ming Liu
mingliu@tmu.edu.cn

†These authors have contributed equally to this work and share first authorship

SPECIALTY SECTION
RECEIVED 04 February 2023
ACCEPTED 25 April 2023
PUBLISHED 16 May 2023

CITATION
Gao C, Ding L, Zhang X, Yuan M, Tang S, Li W, Ye Y, Liu M and He Q (2023) Distinct serum steroid profiles between adrenal Cushing syndrome and Cushing disease. *Front. Endocrinol.* 14:1158573. doi: 10.3389/fendo.2023.1158573

Distinct serum steroid profiles between adrenal Cushing syndrome and Cushing disease

Chang Gao[1†], Li Ding[1†], Xiaona Zhang[1†], Menghua Yuan[1], Shaofang Tang[1], Wei Li[2], Yuanyuan Ye[1], Ming Liu[1*] and Qing He[1*]

[1]Department of Endocrinology and Metabolism, Tianjin Medical University General Hospital, Tianjin, China, [2]Department of Endocrinology, Wuhan No.1 Hospital, Tongji Medical College, Huazhong University of Science and Technology, Wuhan, China

Background: Differentiating between adrenal Cushing syndrome (adrenal CS) and Cushing disease (CD) can be challenging if there are equivocal or falsely elevated adrenocorticotropic hormone (ACTH) values. We aim to investigate the diagnostic value of serum steroid profiles in differentiating adrenal CS from CD.

Method: A total of 11 serum steroids in adrenal CS (n = 13) and CD (n = 15) were analyzed by liquid chromatography with tandem mass spectrometry (LC-MS/MS). Age- and gender-specific steroid ratios were generated by dividing the actual steroid concentration by the upper limit of the relevant reference range. A principal component analysis (PCA) and an orthogonal partial least squares discriminant analysis (OPLS-DA) were performed.

Results: The PCA and OPLS-DA analyses showed distinct serum steroid profiles between adrenal CS and CD. Dehydroepiandrosterone sulfate (DHEA-S), dehydroepiandrosterone (DHEA), and androstenedione ratios were identified as biomarkers for discrimination by variable importance in projection (VIP) in combination with t-tests. The sensitivity and specificity of DHEA-S ratios <0.40 were 92.31% (95% CI 64.0%–99.8%) and 93.33% (95% CI 68.1%–99.8%), respectively, in identifying adrenal CS. The sensitivity and specificity of DHEA ratios <0.18 were 100% (95% CI 75.3%–100.0%) and 100% (95% CI 78.2%–100.0%), respectively, in identifying adrenal CS.

Conclusion: Our data support the clinical use of the DHEA-S and DHEA ratios in the differential diagnosis of adrenal CS and CD, especially when falsely elevated ACTH is suspected.

KEYWORDS

dehydroepiandrosterone sulfate (DHEA-S), serum steroids, mass spectrometry, orthogonal partial least squares discriminant analysis (OPLS-DA), Cushing syndrome

1 Introduction

Cushing syndrome (CS) is a disease characterized by endogenous hypercortisolism. It can be adrenocorticotropic hormone (ACTH) dependent when it results from excessive ACTH production by a pituitary corticotroph adenoma (Cushing disease, CD), or by an extrapituitary tumor secreting ACTH (ectopic ACTH syndrome) or CRH (ectopic CRH syndrome). CS can also be ACTH-independent when it results from cortisol overproduction by adrenocortical tumors (adrenal CS). As surgery is the primary treatment, after a diagnosis of CS is confirmed, further diagnostic tests to determine the exact etiology should be performed.

Plasma ACTH is the first diagnostic test in differentiating between ACTH-dependent CS and ACTH-independent CS (1, 2). Lower levels of plasma ACTH are indicative of ACTH-independent CS, and an ACTH level of < 2.2 pmol/L (10 pg/mL) can usually exclude the diagnosis of ACTH-dependent CS. However, previous studies have reported ACTH values that are not fully suppressed in adrenal CS patients (3, 4), leading to difficulties in differentiating between ACTH-dependent CS and ACTH-independent CS. Moreover, spurious elevated ACTH results due to heterophile antibody interference led to misdiagnosis or unnecessary testing (5, 6). Owing to the impact of plasma ACTH values on clinical practice, the results must be interpreted with caution (4).

The adrenal gland produces multiple steroids and the latest research suggests distinct steroid profiles between CS subtypes. Using simultaneous liquid chromatography and tandem mass spectrometry (LC-MS/MS) measurements of 15 adrenal steroids in plasma, Graeme Eisenhofer et al. generated a 10-steroid panel that could provide optimal discrimination of three subtypes of CS (7). We analyzed serum steroids in CS patients based on CD or adrenal CS grouping, aiming to unearth steroids that contributed to the differentiation of adrenal CS from CD and evaluate their diagnostic utility in differentiating adrenal CS from CD.

2 Materials and methods

2.1 Subjects

We retrieved records of patients diagnosed consecutively with Cushing syndrome between October 2020 and August 2022 at the Department of Endocrinology and Metabolism at Tianjin Medical University General Hospital. The diagnosis and differential diagnosis between Cushing syndrome subtypes were made by hormone evaluations such as 24-h urinary free cortisol (UFC), ACTH, low-dose dexamethasone suppression test (LDDST), high-dose dexamethasone suppression test (HDDST), desmopressin (DDAVP) stimulation test, and bilateral inferior petrosal sinus sampling (BIPSS) measurements, and radiological imaging findings in accordance with current guidelines (8). Patients with excess cortisol with an unconfirmed cause and patients with subclinical CS, ectopic CS, iatrogenic CS, or CS due to bilateral macronodular adrenal hyperplasia were not included. We did not include the two ectopic CS patients because one patient had undergone adrenal gland surgery before steroid measurement and one patient did not achieve total tumor resection and clinical remission and was therefore on medical therapy. The diagnosis of adrenal CS or CD was confirmed by postsurgical pathological examination. One patient who did not undergo surgery and one patient without postoperative relief and pathological confirmation of CD were excluded. Patients with a history of steroid intake in the previous 5 years and patients lacking steroid measurement results were also excluded. Finally, 28 patients, including 15 patients with CD and 13 patients with adrenal CS, were enrolled (Figure 1). This study was approved by the Institutional Review Board of Tianjin Medical University General Hospital with a waiver of individual patient consent.

2.2 Methods

To evaluate the clinical usefulness of the differential diagnoses of adrenal CS and CD, we estimated the following serum steroid hormones: progesterone, 17-OH-progesterone, dehydroepiandrosterone (DHEA), DHEA-S, androstenedione (A4), testosterone, 11-deoxycorticosterone (DOC), 11-deoxycortisol (11-DOC), cortisol, corticosterone, and cortisone. Blood samples for steroid measurement were taken in the morning after at least 8 h of fasting. A steroid testing kit (Hangzhou Calibra Diagnostics Co., Ltd., Zhejiang, China) was used for sample preparation. A volume of 100 µL of EHA extractant was added to 100 µL of serum. After vortexing for 10 min, the mixture was centrifuged at 14,000 g and 4°C for 10 min. A volume of 100 µL of supernatant was analyzed by a Jasper™ high-performance liquid chromatography system connected to an AB SCIEX Triple Quad™ 4500 MD mass spectrometer with a heated nebulizer ionization source in positive ion mode. The MultiQuant™ MD 3.0.3 software was used to quantify the data. Six calibration standards and two quality control samples were included for each set of samples. Using linear regression with $1/x^2$

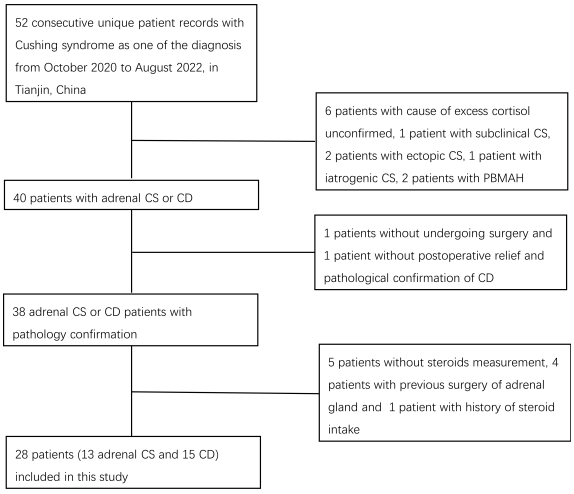

FIGURE 1
Flow chart of identification of study population.

weighting, the correlation coefficients of the peak intensities of analytes to the internal standards were all greater than 0.99.

Plasma ACTH, cortisol (besides the sample measured by LC-MS/MS), and 24-h urinary free cortisol were measured by chemiluminescent enzyme immunoassay (Siemens Healthcare Diagnostics Inc., Erlangen, Germany). Renin and aldosterone were measured by chemiluminescence immunoassay (DiaSorin, Saluggia, Italy).

2.3 Statistical analysis

Chi-squared tests were used for categorical variables and Mann–Whitney *U*-tests were used for quantitative variables. To rule out the influence of sex and age on steroid measurements, steroid data were divided by sex- and/or age-specific upper cutoff values established elsewhere (9) to generate steroid ratios. Steroid ratios were introduced into the SIMCA software (version 14.1; Umetrics, Sweden) for principal component analysis (PCA) and orthogonal partial least squares discriminant analysis (OPLS-DA) analysis. Data were logarithmically transformed, and Pareto scaling was conducted before model construction. R^2 and Q^2 were utilized to evaluate goodness of fit and the predictive ability of the constructed model, respectively. A permutation test with 200 permutations was conducted to evaluate the over-fitness of the model. S-plots, variable importance in the projection (VIP) scores, and *t*-tests were used to select potential biomarkers.

A receiver operating characteristic (ROC) curve analysis was performed to test the usefulness of DHEA-S, DHEA, androstenedione, and their ratios as markers for differentiating between adrenal CS and CD. The optimal cutoff values were determined using the Youden index (sensitivity + specificity − 1). The sensitivity and specificity for each marker were derived from the optimal cutoff value. Statistical analyses were performed using SPSS, version 25, and the MedCalc statistical software (version 20.022). A p-value <0.05 was considered statistically significant.

3 Results

3.1 Patient characteristics

No significant differences in sex and age were observed between the adrenal CS and CD groups (Table 1). Compared with the adrenal CS patients, those with CD exhibited higher basal serum cortisol (median, 37.40 μg/dL vs. 27.90 μg/dL; p = 0.005), basal plasma ACTH (median, 115.00 pg/mL vs. 5.00 pg/mL; p < 0.001), and 24-h UFC (median, 579.60 μg/24 h vs. 226.60 μg/24 h; p = 0.003). No significant differences in aldosterone and renin were observed. No significant differences in body mass index were observed, and patients with Cushing disease had nominally higher fasting blood glucose [5.00 (4.20–14.50) mmol/L vs. 4.50 (3.50–6.60) mmol/L; p = 0.060]. There was no significant difference in the percentages of patients with hypertension, diabetes mellitus, or smoking between the two groups.

ACTH levels < 10 pg/mL, identified in 11 out of 13 patients with adrenal CS, corresponded to a sensitivity and specificity of 84.6% and 100%, respectively.

TABLE 1 Baseline characteristics and biochemical test results of patients with adrenal Cushing syndrome and Cushing disease.

Characteristic	Adrenal Cushing syndrome (n = 13)	Cushing disease (n = 15)	p-value
Gender (F/M)	12/1	12/3	0.600
Age	36 (25–67)	36 (21–69)	0.683
Basal serum cortisol (μg/dL) (normal range 5.00–25.00 μg/dL)	27.90 (11.30–46.40)	37.40 (26.90–69.50)	0.005
Basal plasma ACTH 8:00 (pg/mL) (normal range 0.00–46.00 pg/mL)	5.00 (5.00–143.00)	115.00 (23.20–211.00)	< 0.001
24-h UFC (μg/24 h)	226.60 (56.24–597.50)	579.60 (111.60–1,550.00)	0.003
Serum cortisol after 1 mg of DST (μg/dL)	26.60 (11.70–40.20)	27.60 (3.35–50.00)	0.830
Serum cortisol after LDDST (μg/dL)	28.10 (16.70–38.80)	26.05 (2.13–59.90)	1.000
Serum cortisol after HDDST (μg/dL)	24.60 (15.70–29.70)	13.90 (1.38–50.00)	0.087
Aldosterone (ng/dL) (normal range 3.0–23.6 ng/dL)	4.30 (1.60–24.30)	4.00 (2.80–8.30)	0.314
Renin (μIU/mL) (normal range 2.8–39.9 μIU/mL)	5.10 (0.70–56.70)	4.85 (0.80–22.30)	0.512
Fasting glucose (mmol/L)	4.50 (3.50–6.60)	5.00 (4.20–14.50)	0.060
Body mass index (kg/m^2)	24.15 (20.31–39.52)	24.44 (17.42–39.84)	0.728
Hypertension (%)	9 (69.2%)	10 (66.7%)	1.000
DM (%)	6 (46.2%) : 7 (53.8%)	7 (46.7%) : 8 (53.3%)	1.000
Smoking (%)	2 (15.4%)	3 (20%)	1.000

Data are expressed as a median (minimum–maximum) or number (%).
ACTH, adrenocorticotropic hormone; UFC, urinary free cortisol; LDDST: low-dose dexamethasone suppression test; HDDST, high-dose dexamethasone suppression test; DM, diabetes mellitus.

3.2 Steroid profiles and pattern recognition of adrenal Cushing syndrome and Cushing disease

Plasma concentrations of 11 steroids in patients with adrenal Cushing syndrome and Cushing disease are shown in Table 2. Serum steroid levels of testosterone ($p = 0.037$), dehydroepiandrosterone ($p < 0.001$), cortisol ($p = 0.005$), androstenedione ($p < 0.001$), dehydroepiandrosterone-sulfate ($p < 0.001$), and corticosterone ($p = 0.019$) were significantly lower in the adrenal CS group than in the CD group. There were no significant differences in serum levels of progesterone, 17-OH-progesterone, 11-deoxycorticosterone, 11-deoxycortisol, and cortisone between the two groups.

The unsupervised PCA method was applied to sex- and age-adjusted basal serum steroids of the adrenal CS and CD patients. The score plot ($R^2X = 0.79$ and $Q^2 = 0.36$; Figure 2) showed some separation of the adrenal CS patients and CD patients. The samples are dispersed, reflecting the heterogeneity of steroid profiles of CS patients. There were no strong outliers.

To further study the underlying differences between the adrenal CS and CD groups, OPLS-DA was applied. An OPLS-DA model was established with one predictive and three orthogonal components ($R^2X = 0.788$, $R^2Y = 0.899$, and $Q^2Y = 0.807$). The adrenal CS and CD groups exhibited a clear distinction, as shown in Figure 3A. The Q^2Y value indicated the good predictability and good quality of the model. The results of statistical validation of the OPLS-DA model by permutation analysis using 200 different model permutations showed that the built model is valid (Figure 3B).

As shown in the P1 loading plot, DHEA-S, DHEA, and androstenedione were positively correlated with CD (Figure 4A). An S-plot (Figure 4B) and VIP were employed to reflect the importance of variables. Steroid biomarkers were selected based on the criterion VIP score > 1 and validated using *t*-tests. DHEA-S, DHEA, and androstenedione were identified as potential markers enabling differentiation between adrenal CS and CD (Table 3). DHEA-S and DHEA provided the best discrimination, followed by androstenedione.

3.3 Sensitivity and specificity of the diagnosis of adrenal Cushing syndrome

A receiver operating characteristic curve analysis was used to assess the diagnostic power of plasma ACTH, serum DHEA-S, DHEA, A4, and its ratios in differentiating adrenal CS from CD (Table 4). The optimal cutoff value for ACTH from our patients was 12.6 pg/mL, with a sensitivity of 92.31% and a specificity of 100%. After excluding the patient with spuriously elevated ACTH, the range for ACTH was 5–12.6 pg/mL. The optimal cutoff value for ACTH remained at 12.6 pg/mL, with a sensitivity of 100% and a specificity of 100%. The DHEA-S ratio had a sensitivity of 92.31% and a specificity of 93.33%, with a cutoff value of 0.3971 and an area under the curve (AUC) of 0.979. The DHEA ratio had a sensitivity of 100% and a specificity of 100%, with a cutoff value of 0.1798 and an AUC of 1. The androstenedione ratio had a sensitivity of 92.31% and a specificity of 93.33%, with a cutoff value of 0.3752 and an AUC of 0.944. Their exact serum steroid concentrations showed similar diagnostic performances. A ROC analysis demonstrated that a DHEA-S ratio < 0.3971 (DHEA ratio < 0.1798) was sensitive and specific for the diagnosis of adrenal CS.

4 Discussion

The result of the PCA indicated that serum steroid profiles of adrenal CS patients were differentiated from that of CD patients. OPLS-DA is a multivariate statistical method, which was first proposed by Johan Trygg et al. in 2002, that identifies differences between two groups. It concentrates categorical information in one principal component while other data variations that have nothing

TABLE 2 Plasma concentrations of 11 steroids in patients with adrenal Cushing syndrome and Cushing disease.

Steroid	Adrenal Cushing syndrome	Cushing disease	p-value
T	152.02 (25.42–533.54)	218.50 (78.00–946.73)	0.037
DHEA	536.00 (111.25–907.47)	4,313.22 (1,252.00–8,610.71)	< 0.001
P	100.00 (8.00–5,858.72)	100.00 (8.00–262.47)	0.717
Cortisol	163,283.36 (91,838.13–243,000.00)	246,827.91 (86,980.52–398,047.00)	0.005
17-OHP	242.12 (72.41–1,644.37)	450.96 (138.61–1,080.92)	0.118
A4	437.46 (136.10–1,356.26)	1143.00 (489.00–3,050.45)	< 0.001
DOC	80.00 (35.00–276.45)	80.00 (15.22–127.52)	0.440
11-DOC	981.02 (386.51–3,543.56)	613.05 (179.89–1,859.94)	0.118
DHEA-S	0.30×10^6 (0.07×10^6–1.99×10^6)	3.59×10^6 (0.73×10^6–7.05×10^6)	< 0.001
Cortisone	16,701.13 (11,141.08–23,100.00)	21,268.13 (15,282.90–35,736.22)	0.118
Corticosterone	2,880.00 (885.66–5,951.02)	4,995.36 (1,060.00–13,226.76)	0.019

Data are expressed as medians and ranges in pg/mL.
T, testosterone; DHEA, dehydroepiandrosterone; P, progesterone; 17-OHP, 17-OH-progesterone, A4, androstenedione; DOC, 11-deoxycorticosterone; 11-DOC, 11-deoxycortisol; DHEA-S, dehydroepiandrosterone-sulphate.

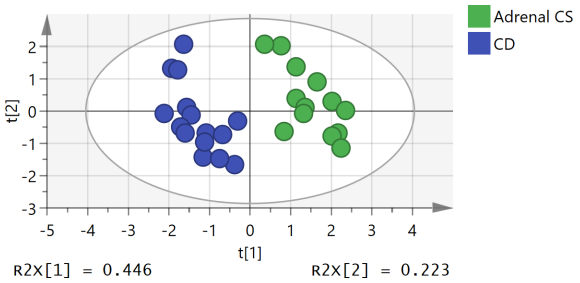

FIGURE 2
Principal component analysis (PCA) score plot of adrenal Cushing syndrome (adrenal CS) group and Cushing disease (CD) group. The *x*- and *y*-axes represent the first principal component and the second principal component after PCA, respectively. The model parameters were R^2X = 0.79 and Q^2 = 0.36. PCA, principal component analysis.

to do with categorical variables or orthogonal variables are removed so that the model is easy and simple to explain. OPLS-DA showed obvious group discrimination and selected several steroids to discriminate adrenal CS from CD. DHEA-S, DHEA, and androstenedione were shown to be related to group separation, which is consistent with previous studies. Previous studies have found that serum DHEA-S and DHEA levels varied among different CS subtypes. Serum DHEA-S levels in Cushing syndrome patients due to adrenal adenoma were lower than that of patients with non-functional adrenal adenoma (10–12), whereas DHEA-S levels in CD patients were significantly higher than in the reference group (7, 13, 14). Significantly higher serum DHEA-S levels were confirmed in Cushing disease than in adrenal Cushing syndrome (7). Reduced DHEA-S levels were also described in patients with subclinical Cushing syndrome due to adrenal incidentalomas (11, 15–19). Steroid profiling by LC-MS revealed lower levels of DHEA and androstenedione in patients with subclinical CS than in patients with non-secreting adenomas and lower levels of DHEA in patients with non-secreting adenomas than in the control group in the basal condition (20). A retrospective study by Yener et al. suggested that a low DHEA-S value could be advantageous for distinguishing patients with subclinical CS. They retrospectively collected data from 249 subjects with adrenal incidentalomas, and 15.2% of participants met the criteria for subclinical CS after excluding overt CS and other adrenal gland diseases (16). DHEA-S levels were significantly reduced in subclinical CS patients compared with patients with non-functional adrenal adenomas. They reported that a DHEA-S value of 40.0 μg/dL was the best cutoff value for detecting subclinical CS (sensitivity = 68%; specificity = 75%; positive predictive value = 43%; negative predictive value = 90%; AUC = 0.788, and $p < 0.001$). Logistic regression showed DHEA-

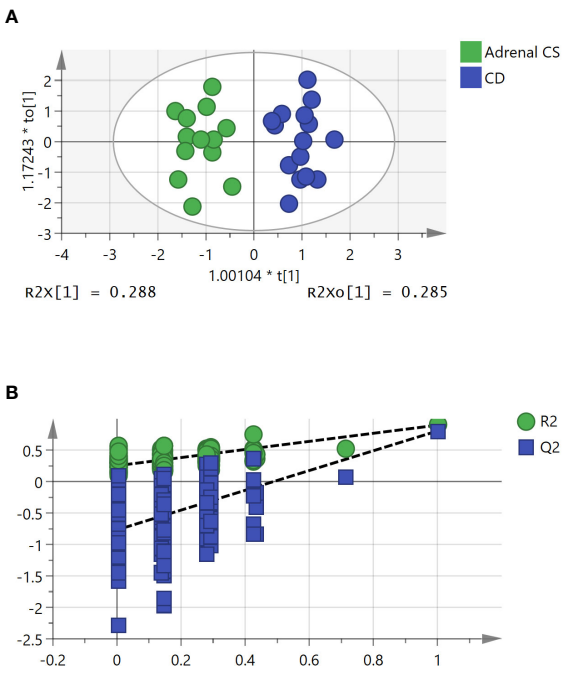

FIGURE 3
The orthogonal partial least squares discriminant analysis (OPLS-DA) model for the classification of adrenal Cushing syndrome (adrenal CS) and Cushing disease (CD). **(A)** Score plot of first predictive component (t[1]) vs. first orthogonal component (to[1]) of established OPLS-DA model based on the adrenal CS vs. CD dataset. The model parameters were as follows: R^2X = 0.788, R^2Y = 0.899, and Q^2Y = 0.807. **(B)** Permutation test of 200 permutations of the OPLS-DA model. OPLS-DA, orthogonal partial least squares discriminant analysis.

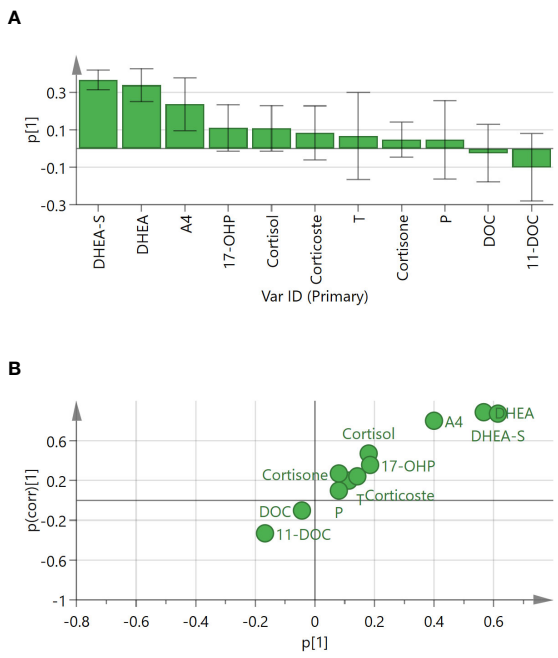

FIGURE 4
Loading plot and S-plot for identifying putative steroid biomarkers between adrenal Cushing syndrome (adrenal CS) and Cushing disease (CD). **(A)** P1 loading plot of the OPLS-DA model. p[1] provided confidence intervals of each loading value. **(B)** S-plot of OPLS-DA for adrenal CS and CD. The p[1]-axis describes the magnitude of each variable. The p(corr)[1]-axis represents the reliability of each variable. Ideal steroid biomarkers have high magnitude and high reliability. T, testosterone; DHEA, dehydroepiandrosterone; P, progesterone; 17-OHP, 17-OH-progesterone; A4, androstenedione; DOC, 11-deoxycorticosterone; 11-DOC, 11-deoxycortisol; DHEA-S, dehydroepiandrosterone-sulfate.

TABLE 3 Summary of steroid biomarkers derived from the OPLS-DA model.

Biomarkers	VIP	AUC	p-value
DHEA-S ratio	2.03837	0.979	$4.12062e^{-8}$
DHEA ratio	1.88414	1	$5.79024e^{-9}$
A4 ratio	1.31677	0.944	$9.51022e^{-6}$
17-OHP ratio	0.613463	0.667	0.126915
Cortisol ratio	0.598739	0.805	0.0150976
11-DOC ratio	0.558519	0.667	0.0685968
Corticosterone ratio	0.464982	0.621	0.141944
T ratio	0.373418	0.631	0.472274
Cortisone ratio	0.264856	0.595	0.141944
P ratio	0.262561	0.585	0.646301
DOC ratio	0.140212	0.505	0.703713

OPLS-DA, orthogonal partial least squares discriminant analysis; VIP, variable importance in the projection; AUC, area under the curve; T, testosterone; DHEA, dehydroepiandrosterone; P, progesterone; 17-OHP, 17-OH-progesterone, A4, androstenedione; DOC, 11-deoxycorticosterone; 11-DOC, 11-deoxycortisol; DHEA-S, dehydroepiandrosterone-sulphate.
A p-value < 0.05 was considered significant.

S (< 40.0 μg/dL) as the strongest predictor of the likelihood of having subclinical CS, with an odds ratio of 9.41.

Significantly reduced expression of dehydroepiandrosterone sulfotransferase in surgically removed attached non-neoplastic adrenal tissues in patients with subclinical CS and adrenal CS was described (11, 21), which was considered to represent the degree of suppression of the hypothalamus–pituitary–adrenal (HPA) axis. In patients with adrenal incidentalomas, a negative rank correlation between post-LDDST cortisol concentrations and serum DHEA-S was found, suggesting DHEA-S as a potential index in assessing subtle cortisol autonomy (22). It is also reasonable to find a lower level of DHEA-S in adrenal Cushing syndrome than in subclinical Cushing syndrome (23). A strong positive correlation between levels of DHEA-S and levels of ACTH and cortisol was detected in CD patients (24), supporting DHEA-S as a possible marker for the diagnosis of CD. Consistent with a previous study (7), CS patients had higher plasma levels of 11-deoxycorticosterone and 11-deoxycortisol than normal, whereas there were no differences for those steroids between patients with adrenal CS and CD. There were no differences in serum levels of progesterone, 17-OH-progesterone, and cortisone between the two groups, which is also consistent with previous study results (7). In contrast to a previous study (25), cortisol was shown to be significantly higher in CD than in adrenal CS in our study; however, the previous study found that the sum of cortisol metabolites and tetrahydrocortisol were significantly higher in CD than in adrenal CS, although this might only reflect a baseline difference of 24 h urinary free cortisol (25). Corticosterone tended to be higher in CD patients in a previous study (7), whereas in our study there was a significant difference. Of the 11 steroids analyzed, only DHEA-S, DHEA, and androstenedione showed a distinction between adrenal CS and CD after OPLS-DA.

Our results showed that the cutoff value of the DHEA-S ratio (DHEA-S concentration divided by the upper limit of the relevant reference range) for discriminating adrenal CS and CD was 0.40 and that the cutoff value for the DHEA ratio (DHEA concentration divided by the upper limit of the relevant reference range) was 0.18, with relatively high sensitivity and specificity. The result provided great insight into discrimination between adrenal CS and CD in respect of steroid profiles and the role it may play in clinical practice. One patient in our sample with falsely increased ACTH levels ultimately had a diagnosis of adrenal CS. She had repeated elevated plasma ACTH measurements of over 100 pg/mL (reference range: 0–46 pg/mL) and, combining results of other diagnostic tests, was considered to have

TABLE 4 Accuracy of steroid biomarkers for diagnosing adrenal Cushing syndrome.

	AUC (95% CI)	Sensitivity (%)	Specificity (%)	Youden index	Accuracy (%)
DHEA-S ratio < 0.3971	0.979 (0.841–1.000)	92.31 (64.0–99.8)	93.33 (68.1–99.8)	0.8564	92.86
DHEA-S ≤ 800,129.2737 pg/mL	0.974 (0.832–1.000)	92.31 (64.0–99.8)	93.33 (68.1–99.8)	0.8564	92.86
DHEA ratio < 0.1798	1 (0.877–1.000)	100 (75.3–100.0)	100 (78.2–100.0)	1	100
DHEA < 907.4740 pg/mL	1 (0.877–1.000)	100 (75.3–100.0)	100 (78.2–100.0)	1	100
A4 ratio < 0.3752	0.944 (0.786–0.995)	92.31 (64.0–99.8)	93.33 (68.1–99.8)	0.8564	92.86
A4 ≤ 913.6404 pg/mL	0.918 (0.751–0.988)	92.31 (64.0–99.8)	86.67 (59.5–98.3)	0.7897	89.29
ACTH ≤ 12.6 pg/mL	0.938 (0.779–0.994)	92.31 (64.0–99.8)	100 (78.2–100.0)	0.9231	96.43

AUC, area under the curve; CI, confidence interval; ACTH, adrenocorticotropic hormone; DHEA-S, dehydroepiandrosterone-sulphate; DHEA, dehydroepiandrosterone; A4, androstenedione.

ACTH-dependent Cushing syndrome. But after pituitary surgery her symptoms were not relieved. Her plasma ACTH level and 24-h urinary free cortisol were still high. Adrenal Cushing syndrome was her final diagnosis and was confirmed after unilateral adrenalectomy and pathological examination. Elevated ACTH levels were confirmed to be caused by heterophile antibodies. The DHEA and DHEA-S ratios were 0.0958 and 0.1553, respectively, below the diagnostic cutoff values in the current study. A recent study assessed the utility of DHEA-S to differentiate adrenal CS from CD, in which they only included patients with DHEA-S levels within the reference interval, and reported that a DHEA-S percentile rank of 19.5% had a sensitivity of 80.8% and specificity of 81.5% for the differential diagnoses of CD and adrenal CS (26). Hána et al. generated a prediction model of ACTH-dependent compared with ACTH-independent CS, finding that DHEA could best differentiate ACTH-dependent CS from ACTH-independent CS (27).

Although plasma ACTH level is used first to discriminate between adrenal CS and CD, the overlap in values between adrenal CS and CD (4) and falsely elevated ACTH levels (5) could mislead the direction of differential diagnoses. Falsely elevated ACTH levels lead to the consideration of ACTH-dependent CS, also leading to screening for pituitary adenoma or ectopic ACTH-secreting adenoma. In addition, incidental pituitary tumors were found to be disclosed on MRI in 10% of the general population (2) and patients with adrenal CS could harbor a pituitary adenoma simultaneously (4), making it more obscure to find the real etiology in CS patients. It is important to realize that healthy volunteers could have increased inferior petrosal sinus-to-peripheral ratios, as they can have ACTH responses to CRH (5), that is, a positive inferior petrosal sinus sampling (IPSS) result is not sufficient to suggest that a pituitary adenoma is the etiology. As a seemingly "positive" IPSS may present in patients without a pituitary source of ACTH (5), an elevated ACTH result may converge to cause misdiagnosis or result in unnecessary pituitary surgery. With more cases with the ACTH assay problem being reported, Greene believed these cases to represent a group of cases that are unrecognized or unreported (5). The possibility of spurious elevated ACTH results should be considered in clinical practice and adjuvant diagnostic information could be helpful.

The results revealed that DHEA-S and DHEA were the most prominent steroids for differentiating adrenal CS from CD. Owing to the relationship between DHEA-S and ACTH, if DHEA-S and DHEA do not match the result of spuriously elevated ACTH, ACTH test accuracy and ACTH-independent CS should be highly suspected. A further differential diagnosis of ACTH-dependent CS may be unnecessary. We thought that DHEA-S and DHEA tests could be useful to help rule out the consideration of ACTH-dependent CS when serum ACTH and DHEA-S (DHEA) mismatch, especially when ACTH is spuriously elevated and/or both a pituitary lesion and adrenal adenoma are present in one patient. Owing to the small sample size of our study, more accurate cutoff values of DHEA-S and DHEA for differentiating adrenal CS from CD should be confirmed in prospective large sample size studies and various ethnicities. We did not include ectopic ACTH syndrome cases; the diagnostic utility of DHEA-S and DHEA in differentiating adrenal CS from ectopic ACTH syndrome should be validated in future studies. In addition, we did not include primary bilateral macronodular adrenal hyperplasia (PBMAH) cases in this study. It is well established that ACTH can be produced by some adrenocortical cells, influencing steroid production directly and indirectly (28, 29). The level of DHEA-S might be influenced consequently, and whether the levels of DHEA-S and DHEA in PBMAH are in accord with that of hypercortisolism due to adrenocortical adenomas should be verified.

DHEA-S has a long half-life and is relatively stable throughout the day (17), making its measurement a useful additional test to confirm the source of etiology in cases with falsely elevated ACTH results. In conclusion, the study suggested that DHEA-S, DHEA, and androstenedione were the steroids differing between adrenal CS and CD and their measurement might serve as an additional diagnostic test, especially when the ACTH test result is high.

Data availability statement

The raw data supporting the conclusions of this article will be made available by the authors, without undue reservation.

Ethics statement

The studies involving human participants were reviewed and approved by Institutional Review Board of Tianjin Medical University General Hospital. The ethics committee waived the requirement for written informed consent for participation.

Author contributions

CG, LD, and XZ designed research, analyzed the data, and wrote the manuscript. MY, ST, WL, and YY researched the data. QH and ML designed the study, and revised and edited the manuscript paper. All authors contributed to the article and approved the submitted version.

Funding

This work was supported by the Major Project of Tianjin Municipal Science and Technology Bureau 21ZXJBSY00060, Project of Tianjin Municipal Health Commission ZC20210 and Tianjin Key Medical Discipline (Specialty) Construction Project (TJYXZDXK-030A).

Acknowledgments

We thank all participants from the Department of Endocrinology and Metabolism at Tianjin Medical University General Hospital.

Conflict of interest

The authors declare that the research was conducted in the absence of any commercial or financial relationships that could be construed as a potential conflict of interest.

Publisher's note

References

1. Klose M, Kofoed-Enevoldsen A, Ostergaard Kristensen L. Single determination of plasma ACTH using an immunoradiometric assay with high detectability differentiates between ACTH-dependent and -independent cushing's syndrome. *Scandinavian J Clin Lab Invest* (2002) 62(1):33–7. doi: 10.1080/003655102753517181

2. Arnaldi G, Angeli A, Atkinson AB, Bertagna X, Cavagnini F, Chrousos GP, et al. Diagnosis and complications of cushing's syndrome: a consensus statement. *J Clin Endocrinol Metab* (2003) 88(12):5593–602. doi: 10.1210/jc.2003-030871

3. Pecori Giraldi F, Saccani A, Cavagnini F. Assessment of ACTH assay variability: a multicenter study. *Eur J endocrinology* (2011) 164(4):505–12. doi: 10.1530/EJE-10-0962

4. Hong AR, Kim JH, Hong ES, Kim IK, Park KS, Ahn CH, et al. Limited diagnostic utility of plasma adrenocorticotropic hormone for differentiation between adrenal cushing syndrome and cushing disease. *Endocrinol Metab (Seoul Korea)* (2015) 30 (3):297–304. doi: 10.3803/EnM.2015.30.3.297

5. Greene LW, Geer EB, Page-Wilson G, Findling JW, Raff H. Assay-specific spurious ACTH results lead to misdiagnosis, unnecessary testing, and surgical misadventure-a case series. *J Endocrine Society* (2019) 3(4):763–72. doi: 10.1210/js.2019-00027

6. Morton A, Dover T. Heterophile antibody to adrenocorticotropin hormone interfering with the investigation of cushing's syndrome. *Indian J Clin Biochem IJCB* (2019) 34(2):234–6. doi: 10.1007/s12291-018-0770-x

7. Eisenhofer G, Masjkur J, Peitzsch M, Di Dalmazi G, Bidlingmaier M, Gruber M, et al. Plasma steroid metabolome profiling for diagnosis and subtyping patients with cushing syndrome. *Clin Chem* (2018) 64(3):586–96. doi: 10.1373/clinchem.2017.282582

8. Gilbert R, Lim EM. The diagnosis of cushing's syndrome: an endocrine society clinical practice guideline. *Clin biochemist Rev* (2008) 29(3):103–6.

9. Eisenhofer G, Peitzsch M, Kaden D, Langton K, Pamporaki C, Masjkur J, et al. Reference intervals for plasma concentrations of adrenal steroids measured by LC-MS/MS: impact of gender, age, oral contraceptives, body mass index and blood pressure status. *Clinica chimica acta; Int J Clin Chem* (2017) 470:115–24. doi: 10.1016/j.cca.2017.05.002

10. Arnaldi G, Martino M. Androgens in cushing's syndrome. *Front hormone Res* (2019) 53:77–91. doi: 10.1159/000494904

11. Morio H, Terano T, Yamamoto K, Tomizuka T, Oeda T, Saito Y, et al. Serum levels of dehydroepiandrosterone sulfate in patients with asymptomatic cortisol producing adrenal adenoma: comparison with adrenal cushing's syndrome and non-functional adrenal tumor. *Endocrine J* (1996) 43(4):387–96. doi: 10.1507/endocrj.43.387

12. Khawandanah D, ElAsmar N, Arafah BM. Alterations in hypothalamic-pituitary-adrenal function immediately after resection of adrenal adenomas in patients with cushing's syndrome and others with incidentalomas and subclinical hypercortisolism. *Endocrine.* (2019) 63(1):140–8. doi: 10.1007/s12020-018-1769-z

13. Yamaji T, Ishibashi M, Sekihara H, Itabashi A, Yanaihara T. Serum dehydroepiandrosterone sulfate in cushing's syndrome. *J Clin Endocrinol Metab* (1984) 59(6):1164–8. doi: 10.1210/jcem-59-6-1164

14. Barbetta L, Dall'Asta C, Re T, Colombo P, Travaglini P, Ambrosi B. Androgen secretion in ectopic ACTH syndrome and in cushing's disease: modifications before and after surgery. *Hormone Metab Res = Hormon- und Stoffwechselforschung = Hormones metabolisme* (2001) 33(10):596–601. doi: 10.1055/s-2001-17906

15. Hana V, Jezkova J, Kosak M, Krsek M, Hana V, Hill M. Novel GC-MS/MS technique reveals a complex steroid fingerprint of subclinical hypercortisolism in adrenal incidentalomas. *J Clin Endocrinol Metab* (2019) 104(8):3545–56. doi: 10.1210/jc.2018-01926

16. Yener S, Yilmaz H, Demir T, Secil M, Comlekci A. DHEAS for the prediction of subclinical cushing's syndrome: perplexing or advantageous? *Endocrine* (2015) 48 (2):669–76. doi: 10.1007/s12020-014-0387-7

17. Dennedy MC, Annamalai AK, Prankerd-Smith O, Freeman N, Vengopal K, Graggaber J, et al. Low DHEAS: a sensitive and specific test for the detection of subclinical hypercortisolism in adrenal incidentalomas. *J Clin Endocrinol Metab* (2017) 102(3):786–92. doi: 10.1210/jc.2016-2718

18. Taylor DR, Ghataore L, Couchman L, Vincent RP, Whitelaw B, Lewis D, et al. A 13-steroid serum panel based on LC-MS/MS: use in detection of adrenocortical carcinoma. *Clin Chem* (2017) 63(12):1836–46. doi: 10.1373/clinchem.2017.277624

19. Podbregar A, Janez A, Goricar K, Jensterle M. The prevalence and characteristics of non-functioning and autonomous cortisol secreting adrenal incidentaloma after patients' stratification by body mass index and age. *BMC endocrine Disord* (2020) 20 (1):118. doi: 10.1186/s12902-020-00599-0

20. Di Dalmazi G, Fanelli F, Mezzullo M, Casadio E, Rinaldi E, Garelli S, et al. Steroid profiling by LC-MS/MS in nonsecreting and subclinical cortisol- secreting adrenocortical adenomas. *J Clin Endocrinol Metab* (2015) 100(9):3529–38. doi: 10.1210/JC.2015-1992

21. Kamenicky P, Houdoin L, Ferlicot S, Salenave S, Brailly S, Droupy S, et al. Benign cortisol-secreting adrenocortical adenomas produce small amounts of androgens. *Clin endocrinology* (2007) 66(6):778–88. doi: 10.1111/j.1365-2265.2007.02810.x

22. Tsagarakis S, Roboti C, Kokkoris P, Vasiliou V, Alevizaki C, Thalassinos N. Elevated post-dexamethasone suppression cortisol concentrations correlate with hormonal alterations of the hypothalamo-pituitary adrenal axis in patients with adrenal incidentalomas. *Clin endocrinology* (1998) 49(2):165–71. doi: 10.1046/j.1365-2265.1998.00509.x

23. Masjkur J, Gruber M, Peitzsch M, Kaden D, Di Dalmazi G, Bidlingmaier M, et al. Plasma steroid profiles in subclinical compared with overt adrenal cushing syndrome. *J Clin Endocrinol Metab* (2019) 104(10):4331–40. doi: 10.1210/jc.2018-02349

24. Burkhardt T, Schmidt NO, Vettorazzi E, Aberle J, Mengel M, Flitsch J. DHEA (S)–a novel marker in cushing's disease. *Acta neurochirurgica* (2013) 155(3):479–84; discussion 84. doi: 10.1007/s00701-012-1596-6

25. Ahn CH, Lee C, Shim J, Kong SH, Kim SJ, Kim YH, et al. Metabolic changes in serum steroids for diagnosing and subtyping cushing's syndrome. *J Steroid Biochem Mol Biol* (2021) 210:105856. doi: 10.1016/j.jsbmb.2021.105856

26. Ciftci S, Soyluk O, Selek A, Erol S, Hekimsoy Z, Esen A, et al. The importance of DHEA-s levels in cushing's syndrome; is there a cut-off value in the differential diagnosis? *Hormone Metab Res = Hormon- und Stoffwechselforschung = Hormones metabolisme* (2022) 54(4):232–7. doi: 10.1055/a-1783-7901

27. Hana VJr., Jezkova J, Kosak M, Krsek M, Hana V, Hill M. Serum steroid profiling in cushing's syndrome patients. *J Steroid Biochem Mol Biol* (2019) 192:105410. doi: 10.1016/j.jsbmb.2019.105410

28. Lefebvre H, Thomas M, Duparc C, Bertherat J, Louiset E. Role of ACTH in the Interactive/Paracrine regulation of adrenal steroid secretion in physiological and pathophysiological conditions. *Front endocrinology* (2016) 7:98. doi: 10.3389/fendo.2016.00098

29. Louiset E, Duparc C, Young J, Renouf S, Tetsi Nomigni M, Boutelet I, et al. Intraadrenal corticotropin in bilateral macronodular adrenal hyperplasia. *New Engl J Med* (2013) 369(22):2115–25. doi: 10.1056/NEJMoa1215245

Frontiers in Endocrinology

Explores the endocrine system to find new therapies for key health issues

The second most-cited endocrinology and metabolism journal, which advances our understanding of the endocrine system. It uncovers new therapies for prevalent health issues such as obesity, diabetes, reproduction, and aging.

Discover the latest Research Topics

See more →

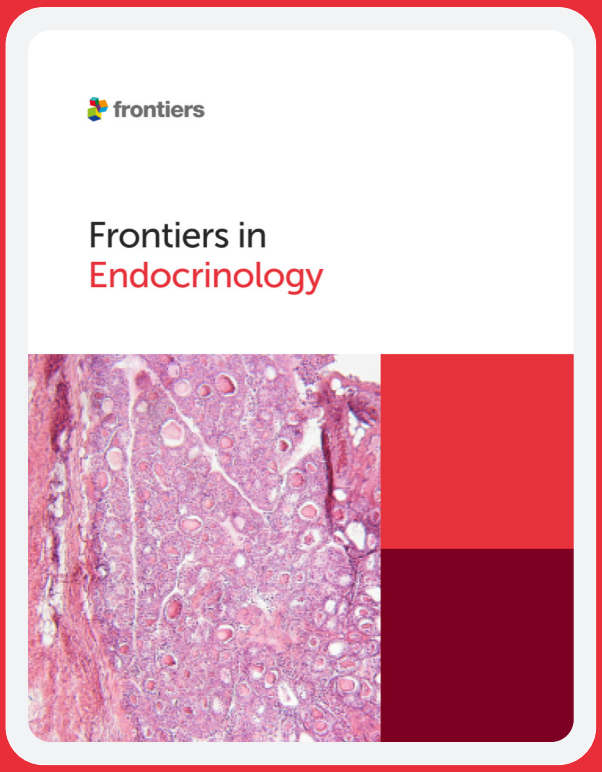

Frontiers

Avenue du Tribunal-Fédéral 34
1005 Lausanne, Switzerland
frontiersin.org

Contact us

+41 (0)21 510 17 00
frontiersin.org/about/contact